ISSN 0021-9673

VOL. 462 JANUARY 13, 1989
COMPLETE IN ONE ISSUE

JOURNAL OF CHROMATOGRAPHY

INTERNATIONAL JOURNAL ON CHROMATOGRAPHY, ELECTROPHORESIS AND RELATED METHODS

ELSEVIER

JOURNAL OF CHROMATOGRAPHY

Scope. The *Journal of Chromatography* publishes papers on all aspects of chromatography, electrophoresis and related methods. Contributions consist mainly of research papers dealing with chromatographic theory, instrumental development and their applications. The section *Biomedical Applications*, which is under separate editorship, deals with the following aspects: developments in and applications of chromatographic and electrophoretic techniques related to clinical diagnosis or alterations during medical treatment; screening and profiling of body fluids or tissues with special reference to metabolic disorders; results from basic medical research with direct consequences in clinical practice; drug level monitoring and pharmacokinetic studies; clinical toxicology; analytical studies in occupational medicine.

Submission of Papers. Papers in English, French and German may be submitted, in three copies. Manuscripts should be submitted to: The Editor of *Journal of Chromatography*, P.O. Box 681, 1000 AR Amsterdam, The Netherlands, or to: The Editor of *Journal of Chromatography, Biomedical Applications*, P.O. Box 681, 1000 AR Amsterdam, The Netherlands. Review articles are invited or proposed by letter to the Editors. An outline of the proposed review should first be forwarded to the Editors for preliminary discussion prior to preparation. Submission of an article is understood to imply that the article is original and unpublished and is not being considered for publication elsewhere. For copyright regulations, see below.

Subscription Orders. Subscription orders should be sent to: Elsevier Science Publishers B.V., P.O. Box 211, 1000 AE Amsterdam, The Netherlands, Tel. 5803 911, Telex 18582 ESPA NL. The *Journal of Chromatography* and the *Biomedical Applications* section can be subscribed to separately.

Publication. The *Journal of Chromatography* (incl. *Biomedical Applications*) has 37 volumes in 1989. The subscription prices for 1989 are:

J. Chromatogr. + *Biomed. Appl.* (Vols. 461–497):
Dfl. 6475.00 plus Dfl. 999.00 (p.p.h.) (total *ca.* US$ 3933.75)

J. Chromatogr. only (Vols. 461–486):
Dfl. 5200.00 plus Dfl. 702.00 (p.p.h.) (total *ca.* US$ 3106.25)

Biomed. Appl. only (Vols. 487–497):
Dfl. 2200.00 plus Dfl. 297.00 (p.p.h.) (total *ca.* US$ 1314.25).

Our p.p.h. (postage, package and handling) charge includes surface delivery of all issues, except to subscribers in Argentina, Australia, Brasil, Canada, China, Hong Kong, India, Israel, Malaysia, Mexico, New Zealand, Pakistan, Singapore, South Africa, South Korea, Taiwan, Thailand and the U.S.A. who receive all issues by air delivery (S.A.L. — Surface Air Lifted) at no extra cost. For Japan, air delivery requires 50% additional charge; for all other countries airmail and S.A.L. charges are available upon request. Back volumes of the *Journal of Chromatography* (Vols. 1–460)are available at Dfl. 230.00 (plus postage). Claims for missing issues will be honoured, free of charge, within three months after publication of the issue. Customers in the U.S.A. and Canada wishing information on this and other Elsevier journals, please contact Journal Information Center, Elsevier Science Publishing Co. Inc., 655 Avenue of the Americas, New York, NY 10010. Tel. (212) 989-5800.

Abstracts/Contents Lists published in Analytical Abstracts, ASCA, Biochemical Abstracts, Biological Abstracts, Chemical Abstracts, Chemical Titles, Chromatography Abstracts, Current Contents/Physical, Chemical & Earth Sciences, Current Contents/Life Sciences, Deep-Sea Research/Part B: Oceanographic Literature Review, Excerpta Medica, Index Medicus, Mass Spectrometry Bulletin, PASCAL-CNRS, Referativnyi Zhurnal and Science Citation Index.

See inside back cover for Publication Schedule, Information for Authors and information on Advertisements.

0021-9673/89/$03.50

Printed in The Netherlands

CONTENTS

(Abstracts/Contents Lists published in Analytical Abstracts, ASCA, Biochemical Abstracts, Biological Abstracts, Chemical Abstracts, Chemical Titles, Chromatography Abstracts, Current Contents/Physical, Chemical & Earth Sciences, Current Contents/Life Sciences, Deep-Sea Research/Part B: Oceanographic Literature Review, Excerpta Medica, Index Medicus, Mass Spectrometry Bulletin, PASCAL-CNRS, Referativnyi Zhurnal and Science Citation Index)

(Continued overleaf)

(Continued overleaf)

In articles with more than one author, the name of the author to whom correspondence should be addressed is indicated in the article heading by a 6-pointed asterisk (*).

An authoritative review... highly recommended...

Optimization of Chromatographic Selectivity

A Guide to Method Development

by **P. Schoenmakers,** *Philips Research Laboratories, Eindhoven, The Netherlands*

(Journal of Chromatography Library, 35)

"The contents of this book have been put together with great expertise and care, and represent an authoritative review of this very timely topic... highly recommended to practising analytical chemists and to advanced students." (Jnl. of Chromatography)

"...an important contribution by a worker who has been in the field almost from its inception and who understands that field as well as anyone. If one is serious about method development, particularly for HPLC, this book will well reward a careful reading and will continue to be useful for reference purposes." (Mag. of Liquid & Gas Chromatography)

This is the first detailed description of method development in chromatography - the overall process of which may be summarized as: method selection, phase selection, selectivity optimization, and system optimization. All four aspects receive attention in this eminently readable book.

The first chapter describes chromatographic theory and nomenclature and outlines the method development process. Guidelines are then given for method selection and quantitative concepts for characterizing and classifying chromatographic phases. Selective separation methods (from both GC and LC) are given - the main parameters of each method are identified and simple, quantitative relations are sought to describe their effects. Criteria by which to judge the quality of separation are discussed with clear recommendations for different situations. The specific problems involved in the optimization of chromatographic selectivity are explained. Optimization procedures, illustrated by examples, are described and compared on the basis of a number of criteria. Suggestions are made both for the application of different procedures and for further research. The optimization of programmed analysis receives special attention, and the last chapter summarizes the optimization of the chromatographic system, including the optimization of the efficiency, sensitivity and instrumentation.

Those developing chromatographic methods or wishing to improve existing methods will value the detailed, structured way in which the subject is presented. Because optimization procedures and criteria are described as elements of a complete optimization package, the book will help the reader to understand, evaluate and select current and future commercial systems.

Contents: 1. Introduction. 2. Selection of Methods. 3. Parameters Affecting Selectivity. 4. Optimization Criteria. 5. Optimization Procedures. 6. Programmed Analysis. 7. System Optimization. Indexes.

1986 1st repr. 1987 xvi + 346 pages
US$ 110.50 / Dfl. 210.00
ISBN 0-444-42681-7

ELSEVIER SCIENCE PUBLISHERS

P.O. Box 211, 1000 AE Amsterdam, The Netherlands
P.O. Box 1663, Grand Central Station, New York, NY 10163, USA

Quantitative Gas Chromatography for Laboratory Analyses and On-line Process Control

by G. GUIOCHON and C.L. GUILLEMIN

(Journal of Chromatography Library, 42)

This is a book which no chemical analyst should be without!

It explains how quantitative gas chromatography can - or should - be used for accurate and precise analysis. All the problems involved in the achievement of quantitative analysis by GC are covered, whether in the research lab, the routine analysis lab or in process control.

The discussion of the theoretical background is restricted to essentials. It is presented in a way that is simple enough to be understood by all analytical chemists, while being complete and up-to-date.

Extensive and detailed descriptions are given of the various steps involved in the derivation of precise and accurate data. This starts with the selection of the instrumentation and column, continues with the choice of optimum experimental conditions, then calibration and ends with the use of correct procedures for data acquisition and calculations.

Finally, there is almost always a way to reduce errors and an entire chapter deals with this single issue. Numerous examples are provided.

A lexicon explaining the most important chromatographic terms and a detailed index complete the book.

This is a book which should be on the library shelf of all universities, instrument companies and any laboratory and plant where gas chromatography is used.

1988 780 pages
US$ 165.75 / Dfl. 315.00
ISBN 0-444-42857-7

A brochure describing the contents of this book in detail is available on request from the publisher

Elsevier Science Publishers

P.O. Box 211, 1000 AE Amsterdam, The Netherlands
P.O. Box 1663, Grand Central Station, New York, NY 10163, USA

JOURNAL OF CHROMATOGRAPHY

VOL. 462 (1989)

JOURNAL
of
CHROMATOGRAPHY

INTERNATIONAL JOURNAL ON CHROMATOGRAPHY,
ELECTROPHORESIS AND RELATED METHODS

ELSEVIER
AMSTERDAM — OXFORD — NEW YORK — TOKYO

0021-9673/89/$03.50

Printed in The Netherlands

Journal of Chromatography, 462 (1989) 1–2
Elsevier Science Publishers B.V., Amsterdam — Printed in The Netherlands

CHROM. 21 107

Obituary

Edgar Lederer, 1908–1988

On the 19th of October of this year Edgar Lederer died, after a short illness, in his eightieth year. Better than I could say it, a recent book states: "The foundation of chromatography was laid by M. S. Tswett in his paper published in 1906. Following this work, chromatography was neglected for about thirty years. The revival dates back to 1931 when R. Kuhn, A. Winterstein and E. Lederer isolated α- and β-carotene from raw carotene by using Tswett's technique".

May we also be permitted to cite Professor Dr. G. Ourisson in the original French text, a language that became Edgar Lederer's second and beloved mother-tongue:

EDGAR LEDERER NOUS A QUITTÉS

Le CNRS a la tristesse d'annoncer le décès d'Edgar Lederer, l'un des plus prestigieux représentants de la chimie française. L'oeuvre du professeur Lederer, dans le domaine de la détermination de structures de produits naturels, témoigne d'une rare continuité et les techniques d'analyse qu'il a mises au point et perfectionnées constituent une contribution importante au développement de la biochimie.

C'est à Heidelberg que Edgar Lederer commence sa carrière de chercheur en démontrant l'importance des applications de l'analyse chromatographique. En 1935–1936, il isole et purifie toute une série de pigments nouveaux à partir de plantes et d'intervébrés.

A Lyon pendant la guerre, il commence un travail sur les constituants odorants d'origine animale; il devait rester très longtemps fidèle à l'étude clinique des parfums, dont il put résoudre certains problèmes classiques comme la constitution de l'ambréine de l'ambre gris, celle d'autres substances à odeurs ambrées, celles du géranium Bourbon. Il initia très tôt des travaux sur la chimie des insectes alors inconnue, sur les voies utilisées par les organismes vivants pour synthétiser des stérols, la vitamine K, certains antibiotiques. Il a été l'un des principaux artisans de l'introduction en chimie organique de méthodes très variées, allant de la spectrométrie de masse des protéines à l'utilisation d'organismes comme adjoints dans des études de biosynthèse.

La pratique de la chromatographie, également introduite par Edgar Lederer, est désormais l'une des techniques les plus efficaces de la chimie organique utilisée quotidiennement par les chercheurs du monde entier.

Mais c'est surtout l'étude de la chimie de bactéries très importantes comme le bacille tuberculeux qui forme pendant une trentaine d'années l'essentiel de son oeuvre de pionnier, à l'interface de la chimie et de la biologie. De la paroi de ces bactéries, il isola et caractérisa de nombreuses substances nouvelles, dont certaines sont, en ce moment, très prometteuses en immunothérapie.

L'oeuvre d'Edgar Lederer est caractérisée par une exceptionnelle continuité dans l'originalité: il n'aborda, avec succès, que des problèmes très importants pour la compréhension du monde vivant, ou pour la santé de l'homme. Les épreuves qu'il avait traversées avant et pendant la guerre l'avaient profondément marqué, et il a con-

0021-9673/89/$03.50

stamment cherché à aider les scientifiques forcés par l'adversité à se réfugier en France, et a demandé que soit utilisée dans ce but une Fondation créée à l'Académie des Sciences à l'occasion de son 80ème anniversaire.

Edgar Lederer est né en 1908 à Vienne (Autriche). Docteur en philosophie de l'université de Vienne (1930), il était également docteur des sciences physiques de l'université de Paris (1938). Entre 1930 et 1933, Lederer séjourna à Heidelberg au Kaiser Wilhelm Institut für medizinische Forschung.

En raison des évènements politiques, il quitta l'Allemagne avec son épouse Hélène Fréchet, fille du mathématicien français Maurice Fréchet, pour venir s'installer à Paris où il travailla d'abord à l'hôpital Necker puis, de 1934 à 1935, à l'institut de biologie physico-chimique. Il a ensuite été nommé directeur du laboratoire de synthèse à l'institut des vitamines de Léningrad, où il séjourna un an.

A son retour, en 1938, il entre au CNRS, au laboratoire de zoologie de l'École normale supérieure, puis est mobilisé pendant la guerre. Après l'armistice, il poursuit sa carrière au laboratoire de chimie biologique de la faculté des sciences de Lyon et, en 1947, à l'institut de biologie physico-chimique de Paris où il est successivement maître de recherche puis directeur de recherche (1953). Edgar Lederer a été co-fondateur de l'Institut de chimie de substances naturelles à Gif-sur-Yvette dont il a assuré la direction de 1960 à 1978.

Professeur en 1956 à la faculté des sciences de Paris dont il dirigeait le laboratoire de chimie biologique, il a enseigné, depuis 1963, à la faculté des sciences d'Orsay, où il a dirigé le laboratoire de biochimie. Edgar Lederer était membre de l'Académie des Sciences depuis 1982 ainsi que de huit académies étrangères.

Médaille d'or du CNRS, il avait été également honoré par les médailles d'or Fritzsche, A. W. Von Hoffman, P. Karrer et R. Koch; il était docteur *honoris causa* de deux universités étrangères, membre d'honneur de six sociétés étrangères. Edgar Lederer était chevalier de la Légion d'Honneur, Commandeur de l'ordre national du Mérite et des Palmes Académiques.

Professor Edgar Lederer remained active almost till the end of his life. In June he celebrated his 80th birthday with a party in the *Château de Gif*, which is part of the institute he founded in the 1950s. After spending his holidays in Switzerland he went for a lecture tour to Leningrad and Moscow in September. Upon his return he fell ill and after a battle of three weeks he passed away. He was the last and perhaps the most active of the pioneers of chromatography.

MICHAEL LEDERER

Journal of Chromatography, 462 (1989) 3–12
Elsevier Science Publishers B.V., Amsterdam — Printed in The Netherlands

CHROM. 20 998

CHROMATOGRAPHIC DISPERSION CORRECTIONS UTILIZING THE GENERALIZED EXPONENTIAL FUNCTION

R. D. HESTER*, R. A. VAIDYA and J. P. DICKERSON
Department of Polymer Science, University of Southern Mississippi, Southern Station Box 10076, Hattiesburg, MS 39406-0076 (U.S.A.)
(First received March 7th, 1988; revised manuscript received September 13th, 1988)

SUMMARY

Chromatographic dispersion, sometimes referred to as band broadening or zone spreading, reduces instrument resolution especially for long analysis times. Tung has described chromatographic dispersion as resulting from the convolution of a true chromatogram with a spreading function. This convolution produces an observed chromatogram which is broader than the true chromatogram. An algorithm which uses the generalized exponential function has been developed for solving Tung's dispersion equation for the true (non-dispersed) chromatogram. Mathematical constraints and data analysis methods have been developed which enable the generation of realistic dispersion-corrected chromatograms.

INTRODUCTION

Separation of components in chromatography can occur because of retention differences produced by molecular adsorption, component size or charge character. Proper selection of packing materials and mobile phase can maximize separation. Dispersion, also referred to as zone spreading, produces signal band broadening.

Several complex mass transfer or diffusional phenomena are responsible for dispersion[1]. These are related to packing material type, mesh size, column packing efficiency, mobile phase flow-rate and macromolecular size. Therefore, dispersion is unique to the chromatographic system. Dispersion corrections for one size-exclusion chromatography system cannot be applied to a different system or to different operating conditions within the same system. Dispersion is always present in chromatography and works to decrease separation capabilities. However dispersion corrections can be performed by applying mathematical techniques.

An observed chromatogram, h, is the result of a convolution between a true chromatogram, f, and an instrument spreading function, g.

$$h = f * g \tag{1}$$

The integral form of this convolution is given by eqn. 2.

0021-9673/89/$03.50

$$h(x) = \int_{-\infty}^{\infty} f(u)\, g(x - u)\, du \tag{2}$$

As shown by eqn. 2, the value of the observed chromatogram at each elution volume x or $h(x)$ is obtained by an integration involving the true chromatogram and a shifted spreading function.

Tung[2] defined the spreading function g as a normal function of mean zero and standard deviation s.

$$g(x - u) = \frac{1}{s\sqrt{2\pi}} \exp\left[-\frac{(x - u)^2}{2s^2}\right] \tag{3}$$

The standard deviation s, usually called the spreading factor, controls the amount of dispersion produced on each element, $f(u)\, du$, of the true chromatogram. The observed chromatogram at elution volume $h(x)$ is the sum of the dispersion produced on each element of the true chromatogram evaluated at x. In exclusion chromatography, eqn. 2 is generally referred to as Tung's dispersion equation.

Observed chromatograms of standards having known or true distributions can be used to solve eqn. 2 for the unique single spreading factor associated with the instrument. By knowing the spreading factor, Tung's equation can thereafter be inverted (solved) to obtain the dispersion-corrected or true chromatogram for other samples analyzed by the instrument.

Solution of Tung's dispersion equation for function $f(u)$ is difficult and usually requires a computer program involving an algorithm which solves eqn. 1. Several algorithms have been previously developed[3-5]; however, because of the ill-conditioned nature of eqn. 1, the true chromatogram solution produced is usually unsatisfactory, especially if the observed chromatographic data contain random signal noise[6].

In this work we will estimate a solution to eqn. 1 by making the assumption that the true chromatogram $f(u)$ can be described by a modified generalized exponential (GEX) function[7]. In the past, we have used this function extensively to fit noisy chromatographic data[8]. We have shown that the GEX function is very general in nature and can fit negatively or positively skewed data with low or high kurtosis (flatness). The overall generality of the GEX makes the fixed chromatographic shape assumption less limiting. We will use constrained non-linear regression analysis to solve for the GEX function parameters which best fit Tung's dispersion equation. The best fit GEX parameters will then define an estimate of the true chromatogram.

THE GENERALIZED EXPONENTIAL FUNCTION*

The modified GEX function which will be used to define the true or dispersion corrected chromatogram is given by eqn. 4.

* For symbols, see the list at the end of the paper.

For $u > u_o$,

$$f(u) = u_h \left[\frac{u - u_o}{u_m - u_o}\right]^{B-1} \exp\left\{\frac{B-1}{A}\left(1 - \left[\frac{u - u_o}{u_m - u_o}\right]^{A}\right)\right\}$$

with $A > 0$ and $B > 1$.

For $u \leqslant u_o$,

$$f(u) = 0 \tag{4}$$

The GEX has five parameters: u_o, u_m, u_h, A and B. The values of u_o, u_m and h_m can be easily obtained from the chromatogram (see Fig. 1). The A and B parameters are related to the shape of the GEX function and define the inflection points (u_1, u_{1h}; u_2, u_{2h}). It can be shown that:

$$u_1 = u_o + (u_m - u_o)t^+ \tag{5}$$

$$u_2 = u_o + (u_m - u_o)t^- \tag{6}$$

with $t^{\pm} = \left\{\frac{3 - A - 2B \pm \sqrt{A^2 - 6A + 4AB + 1}}{2 - 2B}\right\}^{\frac{1}{A}}$

$$u_{1h} = f(u_1) \tag{7}$$

$$u_{2h} = f(u_2) \tag{8}$$

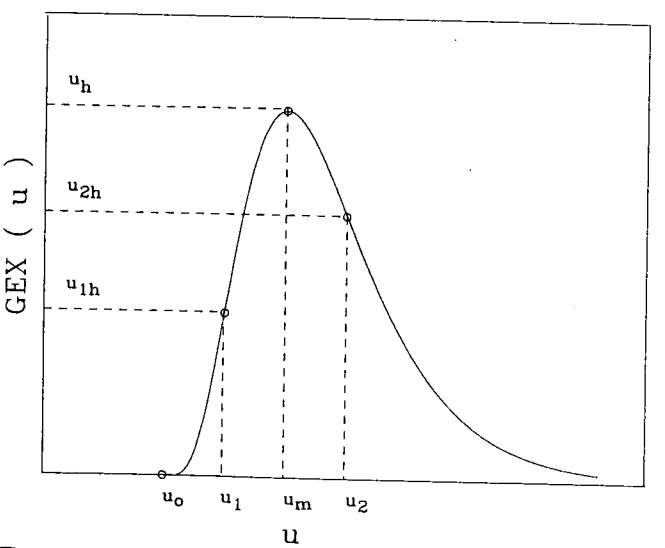

Fig. 1. Typical GEX function starting at u_o having a maximum at (u_m, u_h) and inflection points at (u_1, u_{1h}) and (u_2, u_{2h}).

Also it has been shown that the nth moment of a GEX function about an axis parallel to the ordinate at an elution volume equal to z is given by[9]:

$$\gamma_n^z = \sum_{r=0}^{n} \Theta_r \left[\frac{A}{B-1}\right]^{\frac{B+r}{A}} \Gamma\left[\frac{B+r}{A}\right] \tag{9}$$

where $\Theta_r = \frac{u_h}{A} {}^nC_r \, \beta^{r+1} \, \alpha^{n-r} \exp[(B-1)/A]$

$$\beta = u_m - u_o$$

$${}^nC_r = \frac{n!}{r!\,(n-r)!}$$

$$\alpha = u_o - z$$

Eqn. 9 can be used to determine the area within the GEX function (area $= \gamma_0^0$), the mean of the function (mean $= \gamma_1^0$/area), variance of the function (variance $= \gamma_2^{mean}$/area), and skewness of the function {skewness $= \gamma_3^{mean}$/[area (variance)$^{3/2}$]}, and kurtosis of the function {kurtosis $= \gamma_4^{mean}$/[area (variance)^2]}.

REGRESSION ANALYSIS

In regression analysis an objective function which has a set of adjustable parameters is optimized. Optimization involves maximizing or minimizing an objective function. In non-linear regression, optimization will usually converge provided that the initial start values of the parameters (first-guess values) are not too distant from the best fit parameter values. A successful regression is crucially dependent upon having an objective function that has a minimum number of parameters and also upon having "good" first guess parameter values.

To solve Tung's equation a least squares objective function of the form

$$\sum_{i=1}^{N} [h(x_i) - \int_{-\infty}^{\infty} f(u)\, g(x_i - u)\, du]^2 \tag{10}$$

was minimized by using a Levenberg–Marquardt regression algorithm[10]. The objective function is the sum of N terms each of which is the square of the difference between the observed chromatogram and the convolution integral both evaluated at elution volume x_i. x_1 and x_N are the first and last elution volumes respectively which span the total elution volume over which the observed chromatogram signal is detected.

Unfortunately there exists a large number of significantly different parameter sets each of which adequately minimize the objective function. Thus the regression is ill-conditioned and the parameter solution set found may not be realistic. To

compensate for the ill-conditioned nature of the regression, constraints must be used to limit the number of possible parameter solution sets. If the constraints are not adequate, the regression will probably find a solution which is distant from the correct solution. Therefore it is critical that regression constraints be found that are both realistic and as confining as possible.

REGRESSION CONSTRAINTS

Inherent in the GEX function are three intrinsic constraints which realistically confine the regression solution space. These are (1) continuity of signal; (2) non-negativity of signal; and (3) signal appearance over a finite range.

Most single-component chromatographic signals are continuous and smooth. The GEX function satisfies this requirement. We do not normally expect to see both negative and positive appearance of a single component at a detector. Thus the chromatographic signal should always be positive and the GEX function answers this requirement. A chromatographic signal should only deviate from non-zero vlues during the time interval over which material is eluting through a detector. The GEX function meets this condition because it is zero for elution volume values less than u_0 and also because it approaches zero as the elution volume becomes large.

Unfortunately, the above inherent constraints are usually not sufficient to restrict the regression solution space. Additional constraints are necessary to insure reasonable regression convergence to an acceptable solution.

Additional constraints can be imposed by noting that in the convolution h of two functions, g and f that[11] (1) the area of the convolution is the product of the areas of the functions g and f; (2) the mean of the convolution is the sum of the means of functions g and f; and (3) the variance of the convolution is the sum of the variances of functions g and f.

The spreading function g has unit area, zero mean, and variance s^2. Thus the true chromatogram or function f has an area and mean equal to the area and mean of the observed chromatogram or the convolution h. Also, the variance of the function f is the variance of the convolution h less the variance of the spreading function g.

We can easily calculate the area S, mean $\bar{X}$, and variance σ^2 of he observed chromatogram. By using eqn. 9, the area, mean and variance of the GEX function representing the true chromatogram can be expressed in terms of the GEX parameters. We can use this knowledge to eliminate three of the five GEX parameters. The most convenient parameters to eliminate are u_o, u_m and u_h.

$$u_o = \bar{X} - \sqrt{\sigma^2/(C - 1)} \tag{11}$$

with $C = \Gamma[B/A]\,\Gamma\,[(B + 2)/A]/\{\Gamma[(B + 1)/A]\}^2$

$$u_m = u_o + (\bar{X} - u_o)D \tag{12}$$

with $D = [(B - 1)/A]^{1/A}\,\Gamma(B/A)/\Gamma[(B + 1)/A]$

$$u_h = SE/(u_m - u_o) \tag{13}$$

with $E = A \exp[(1 - B)/A]\,[(B - 1)/A]^{B/A}/\Gamma(B/A)$

The true chromatogram function then becomes a GEX function having only two shape parameters. The regression algorithm must find the two shape parameters (A,B) which best minimize the much simplified and more constraining objective function.

Our past experience in fitting chromatograms has shown that the GEX shape parameters, A and B almost always have values that are less than ten. Also the GEX function only exists in real space when A and B have values that are greater than zero and one, respectively. Acceptable first guess values for the shape parameters are the shape parameters found by fitting a GEX function to the observed chromatogram. Table I summarizes the information needed to set up parameter first guess values and their constraints when regression is used to find an estimate of the true chromatogram.

It should be emphasized that the regression solution constraints that have been developed apply only to a Gaussian spreading function in which the spreading factor, s, is constant. If the spreading function was made to vary with the elution volume then some of the constraints would not necessarily apply.

EXPERIMENTAL

A non-linear regression routine was developed which contains the objective function (eqn. 10) and incorporates the parameter constraints previously discussed. A computer program of this regression, named "CDC" for chromatogram dispersion correction, was generated using a Pascal compiler (Turbo Pascal 3.0, Borland International) operating with a Z148 personal computer (Zenith Data Systems) having a 8087 math coprocessor. The math coprocessor enable calculations to be performed on real data with 16 digits accuracy within a range of $4.19 \cdot 10^{-307}$ to $1.67 \cdot 10^{+308}$.

Two dispersed chromatograms were produced using the convolution operator, eqn. 2. GEX functions were used to represent the true (non-dispersed) chromatograms and the normal spreading functions were defined by assigning specific spreading factors. Both dispersed chromatograms, made by the convolutions which represent the observed chromatograms, were each fitted to a GEX function so that first guess values for the shape parameters could be made for the the program CDC. The computer program CDC was then used to reverse the convolution or invert eqn. 2. Thus CDC deconvolutes the obeserved (dispersed) chromatograms and thereby should return the original GEX functions representing the true chromatograms. Using the above technique it was possible to gauge the ability of the program CDC to deconvolute typical chromatogram data.

TABLE I

TRUE CHROMATOGRAM REGRESSION SOLUTION SPACE

Δ = Small positive amount, *i.e.*, 0.01.

Parameter	*Maximum*	*Minimum*	*First guess value*
A	10	Δ	A_x
B	10	$1 + \Delta$	B_x

TABLE II

CASE 1 CHROMATOGRAMS

Information	*Symbol*	*True chromatogram*	*Observed or dispersed chromatogram, $s = 2.5$*	*CDC estimate of the true chromatogram*
Shape parameter	A	3.14	2.99	3.03
Shape parameter	B	3.45	5.62	4.73
Signal start point	u_o	36.0	30.0	34.3
Maximum of signal	u_m	45.0	45.0	45.0
Maximum height	u_h	2.06	1.61	2.07
1st Inflection point	u_1	41.6	40.9	41.7
2nd Inflection point	u_2	48.3	49.1	48.2
Area	S	0.161	0.161	0.161
Mean	$\bar{X}$	45.1	45.05	45.05
Variance	σ^2	9.00	15.4	9.15
Skewness		0.105	0.068	0.079
Kurtosis		2.74	2.85	2.82

RESULTS AND DISCUSSION

Tables II and III give information on the two cases tested. Case 1 was intended to test CDC performance when a true chromatogram is nearly Gaussian or normal in shape and is only slightly dispersed ($s = 2.5$). Case 2 was designed to evaluate CDC when a true chromatogram is skewed right and has been severely dispersed ($s = 10.0$). The three chromatogram plots associated with each test case are shown in Figs. 2 and 3.

Case 1 is a less demanding test of CDC capability than Case 2. The data in Table II and Fig. 2 show that CDC deconvoluted the dispersed chromatogram with a great

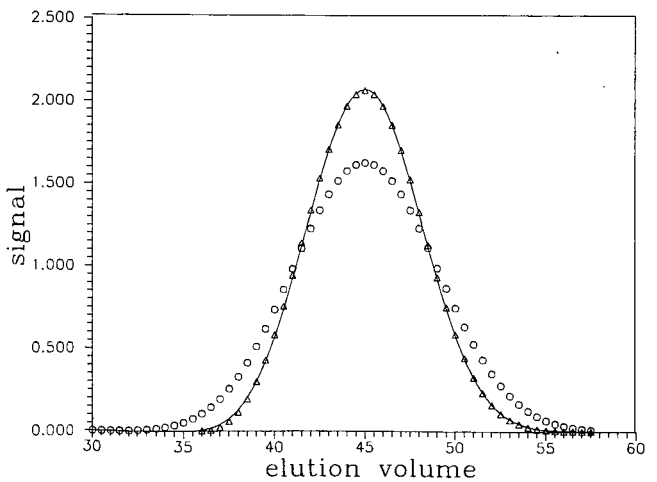

Fig. 2. Test Case 1 Chromatograms. Circles and triangles are data points for dispersed and true chromatograms, respectively. Solid line is the CDC estimate of the true chromatogram.

TABLE III

CASE 2 CHROMATOGRAMS

Information	*Symbol*	*True chromatogram*	*Observed or dispersed chromatogram* $s = 10.0$	*CDC estimate of the true chromatogram*
Shape parameter	A	0.50	2.74	0.663
Shape parameter	B	8.50	4.30	9.11
Signal start point	u_o	36.0	12.0	34.4
Maximum of signal	u_m	45.0	47.5	45.4
Maximum height	u_h	1.00	0.430	0.932
1st Inflection point	u_1	40.5	35.3	40.3
2nd Inflection point	u_2	49.6	59.4	50.5
Area	S	12.5	12.5	12.5
Mean	$\bar{X}$	48.2	48.0	48.0
Variance	σ^2	36.2	135.7	35.7
Skewness		1.26	0.162	0.962
Kurtosis		5.70	2.83	4.52

deal of accuracy. The true chromatogram and the CDC-estimated chromatogram made from inverting the dispersed chromatogram are almost identical.

Although Case 2 is a harsh and rigorous test of CDC, the computer algorithm performed much better than expected. The data in Table III and the chromatogram plots in Fig. 3 show that the estimate of the true chromatogram made by CDC is very close to the true chromatogram.

The time required for CDC to converge to a deconvolution solution was 630 and 760 s for Cases 1 and 2, respectively. Thus computer time requirements are reasonable even for a microcomputer. Computation time would have been much less (probably two orders of magnitude less) on a mainframe computer and/or if a more efficient regression algorithm was used.

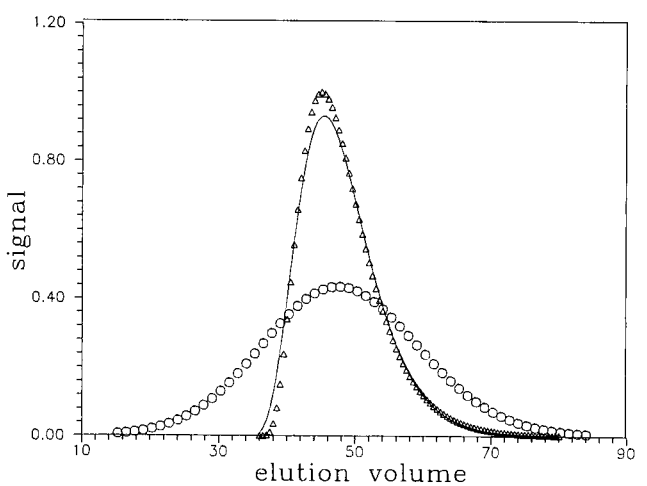

Fig. 3. Test Case 2 Chromatograms. Circles and triangles are data points for dispersed and true chromatograms respectively. Solid line is the CDC estimate of the true chromatogram.

CONCLUSIONS

The use of a GEX function and constrained non-linear regression has been shown to be a very effective in correcting the dispersion produced in chromatography. This is possible because realistic regression solution constraints have been developed which minimize the computational time required to reach a solution and simultaneously reduce the possibility of converging to a false solution. Because of the above features, the regression can be performed on a personal computer.

SYMBOLS

A	first shape parameter of the GEX function
B	second shape parameter of the GEX function
C	factor in eqn. 11
${}^nC_r$	combination of n taken r at a time, see eqn. 9
D	factor in eqn. 12
E	factor in eqn. 13
f	true chromatogram
g	spreading function
h	observed chromatogram
n	order of a moment
N	total number of data points
r	index variable
S	area
s	spreading factor, see eqn. 2
u	true chromatogram elution volume
u_o	GEX starting point
u_1	abscissa value of the first GEX inflection point
u_2	abscissa value of the second GEX inflection point
u_h	GEX function maximum signal value
u_m	abscissa point of GEX maximum signal
u_{1h}	signal value of the first GEX inflection point
u_{2h}	signal value of the second GEX inflection point
t^+, t^-	factor used in eqn. 6
x	observed chromatogram elution volume
$\bar{X}$	mean elution volume value
z	axis for a moment (axis $\equiv u = z$)
α	factor used in eqn. 9
β	factor used in eqn. 9
Γ	gamma function
γ_n^z	nth moment about axis z
Θ_r	factor used in eqn. 9
σ^2	variance

REFERENCES

1 W. W. Yau, J. J. Kirkland and D. D. Bly, *Modern Size-Exclusion Liquid Chromatography*, Wiley, New York, 1979.
2 L. H. Tung, *J. Appl. Polym. Sci.*, 10 (1966) 375.
3 M. Kubin, D. Horak and F. Svec, *Angew. Makromol. Chem.*, 71 (1978) 51.
4 J. A. M. Smit, C. J. P. Hoogervorst and A. J. Staverman, *J. Appl. Polym. Sci.*, 15 (1971) 1479.
5 P. E. Pierce and J. E. Armonas, *J. Polym. Sci.*, 21 (1968) 23.
6 K. S. Chang and R. Y. M. Huang, *J. Appl. Polym. Sci.*, 13 (1969) 1459.
7 R. A. Vaidya and R. D. Hester, *J. Liq. Chromatogr.*, 287 (1984) 231.
8 C. E. Lundy and R. D. Hester, *J. Liq. Chromatogr.*, 7(10) (1985) 1911.
9 R. A. Vaidya and R. D. Hester, *J. Chromatogr.*, 333 (1985) 152.
10 J. L. Kuester and J. H. Mize, *Optimization Techniques with Fortran*, McGraw-Hill, New York, 1973, p. 240.
11 R. N. Bracewell, *The Fourier Transform and Its Application*, McGraw-Hill, New York, 2nd ed., 1986, p. 302.

Journal of Chromatography, 462 (1989) 13–21
Elsevier Science Publishers B.V., Amsterdam — Printed in The Netherlands

CHROM. 20 990

AN INFORMATION THEORY OF CHROMATOGRAPHY

I. EVALUATION OF ANALYTICAL SYSTEMS BY MEANS OF *FUMI*

RIEKO MATSUDA, YUZURU HAYASHI*, MUMIO ISHIBASHI and YASUSHI TAKEDA
Division of Drugs, National Institute of Hygienic Sciences, 18-1, Kamiyoga 1-Chome, Setagaya-ku, Tokyo 158 (Japan)
(First received April 7th, 1988; revised manuscript received September 19th, 1988)

SUMMARY

The application of the *f*unction of *m*utual *i*nformation (*FUMI*) to the logical evaluation of methods for chromatographic quantitation is described. *FUMI* provides the Shannon mutual information of overlapped peaks with various resolutions. Hence an analytical method can be evaluated logically based on both the amount of information transmitted by overlapped peaks and the observation period of chromatography. As an example of the evaluation, a previously proposed chromatographic analysis consisting in a rapid but incomplete separation of naphthalene and diphenyl, and peak-deconvolution based on the Kalman filter, is considered. The "best" chromatogram that can transmit the maximal mutual information in unit time is given.

INTRODUCTION

A major aim in analytical chemistry is to elaborate or search for a method through which more information can be effectively transmitted from analytes (Ω) of interest. For high-performance liquid chromatography (HPLC), efforts are made towards the development of column structure, elution conditions, etc., and also data processing of signals. The development of methods often depends on trial and error, and may result from chance. Such new methods are evaluated quantitatively, even if empirically, by some chemometric strategies. A more desirable aim, however, is strict evaluation on a theoretical basis, without recourse to experience.

The aid of information theory is desirable for the above-mentioned purpose. The information on analytes Ω is quantitatively described as the Shannon information $I[\Omega]$ (ref. 1). In general, it is through observation and data processing of the raw data Ψ that we can actualy acquire knowledge about the analytes Ω. The total amount of information $I[\Omega]$ involved originally in the samples, however, cannot be obtained from the data Ψ because of inevitable noise contamination, baseline drift, interference, etc., in the measurement process. Of more analytical importance is the available information called the mutual information $I[\Omega; \Psi]$ between the analytes Ω and the data Ψ (ref.

0021-9673/89/$03.50

1). Excess peak overlap, for example, which often arises in rapid chromatography, induces a critical loss of the mutual information $I[\Omega; \Psi]$ and makes ambiguous our knowledge about the samples of interest. The amount of mutual information $I[\Omega; \Psi]$, therefore, should underlie the logical evaluation of the whole analytical system.

The simple *fu*nction of *m*utual *i*nformation (*FUMI*), which describes the mutual information of chromatography, has recently been proposed[2]. The derivation is based on information theory and the theory of the Kalman filter[2]. Given the numerically expressed shape of each chromatographic peak and the noise level in the measurement process, *FUMI* can provide mutual information about overlapped chromatographic peaks with various resolutions. The whole analytical system, therefore, can be evaluated by taking into account both the observation period of the chromatography and the information loss caused by the peak overlap. The best method is defined as one with the maximal flow of mutual information under the experinental conditions adopted, *i.e.*, one that can transmit the largest amount of information in unit time.

Our aim is to apply *FUMI* to the logical evaluation of an HPLC method for quantitation. The method adopted here as an example concerns a rapid but incomplete HPLC separation of naphthalene and diphenyl and the mathematical processing of the overlapped peaks by means of the Kalman filter[3]. We examine the problems of whether or not the data processing of the Kalman filter can outweigh the information loss caused by the peak overlap in rapid chromatography and whether the whole system can provide the maximal information flow. Logical optimization of overlapped chromatograms is treated in Part II[4].

THEORETICAL

We give a brief review of *FUMI* and some additions for its rational utilization. An approximate function $P_k^{\dagger}$ plays an important role in the derivation of *FUMI*[2]. $P_k^{\dagger}$ is derived from the strict P_k (the error variance involved in the Kalman filter algorithm) by mathematical induction[2]. It has the further theoretical importance that the correlation between the Kalman filter and the linear least-squares method can be elucidated clearly by $P_k^{\dagger}$ (ref. 2).

For a single peak, *FUMI* represents the mutual information that we can collect through the filtering of the raw data ranging from a data point $i = 1$ to k ($k = 1, \ldots, N$)[2]:

$$FUMI = -\frac{1}{2}\log\left(P_k^{\dagger}\right) \tag{1}$$

$$= \frac{1}{2}\left[\log\left(\sum_{i=1}^{k} F_i^2\right) - \log\left(\tilde{W}_c\right)\right] \tag{2}$$

where F_i denotes the signal intensity of a peak at a data point k and $\tilde{W}_c$ is the variance of the contaminating noise (= constant). We see that larger peaks provide more information and that *FUMI* increases as a new signal F_{k+1} appears, but never decreases. The mutual information for q peaks partially overlapped is given at the last

point N (the observation period of the chromatogram) and is simply described as the sum of the individual peak information[2]:

$$FUMI = \frac{1}{2}\left\{\sum_{j=1}^{q} \log\left[\sum_{i=k_c(j)+1}^{k_f(j)} F_i(j)^2\right]\right\} - \frac{1}{2} q \log(\tilde{W}_c) \tag{3}$$

where $[i = k_c(j) + 1, k_f(j)]$ denotes the region where the signals $F_i(j)$ of the jth peak contribute to *FUMI*. The cutoff point $k_c(j)$ is specified to be the point where the signal $F_i(j)$ first gains predominance over the noise $\tilde{W}_c$. The filtering-off point $k_f(j)$ is defined as the cutoff point $k_c(j + 1)$ of the following peak $j + 1$. Without peak overlap, the overall shape of every peak contributes to *FUMI*. If two peaks weakly overlap, then the virtual peak lacking the tailing edge after $k_f(1)$ $[= k_c(2)]$ is input in *FUMI*.

The efficiency of the chromatograms is given as the mutual information in unit time:

$$I_E[1, N] = \frac{FUMI}{N} \tag{4}$$

This function denotes the averaged flow of mutual information through the chromatography and the filtering of the whole data sequence F_1–F_N $[N = k_f(g)]$.

For convenience to chromatographers, we shall describe the mutual information in terms of the relative standard deviation (R.S.D.) of the filtering error $P_k^\dagger$. The error variance $P_k^\dagger$ is derived from the assumption that the amount (or concentration) indicated by the signals F_k of the peak is unity. Hence the R.S.D. of the error at a point k is given by

$$\text{R.S.D.}_{\cdot k} = (P_k^\dagger)^{1/2} \cdot 100 \tag{5}$$

$\text{R.S.D.}_{\cdot k}$ can be described by the minimum error $P_{\min}^\dagger$. Let $P_k^\dagger$ be $\alpha^2 P_{\min}^\dagger$:

$$\text{R.S.D.}_{\cdot k} = \alpha(P_{\min}^\dagger)^{1/2} \cdot 100 \tag{6}$$

The coefficient α denotes the ratio

$$\alpha = \frac{\text{R.S.D.}_{\cdot k}}{\text{R.S.D.}_{\cdot \min}} \tag{7}$$

The minimum error $\text{R.S.D.}_{\cdot \min}$ or $P_{\min}^\dagger$ corresponds to the maximum information $I_{\max}$ (see eqn. 1). Usually, the observation period N is specified to be wide compared with the peak region and taken as a point that can give the maximum information ($I_{\max} = I_N$). The information loss δI is defined as

$$\delta I = I_{\max} - I_k \tag{8}$$

$$= -\frac{1}{2}\log(P_{\min}^\dagger) + \frac{1}{2}\log(P_{\min}^\dagger \alpha^2) \tag{9}$$

$$= \log \alpha \tag{10}$$

where I_k denotes *FUMI* at k. The R.S.D. ratio α is given by the information loss:

$$\alpha = \exp(\delta I) \tag{11}$$

The filtering error R.S.D.$_k$ is described in the intelligible form

$$\text{R.S.D.}_k = \exp(\delta I) \cdot \exp(-I_{\max}) \cdot 100 \tag{12}$$

(see eqns. 1 and 6). R.S.D.$_k$ and δI denote the two measures of the excess error or the lost information when the data processing is stopped at k.

For multi-component chromatograms, let us consider the information loss or the filtering error, which depends on the degree of peak overlap, the whole data sequence is analysed. We give a convenient method covering the worst condition that the loss is concentrated on a peak: only two peaks overlap. For simplicity, it is assumed that all the peaks move along the time scale (k) of the chromatogram without any changes in shape. The maximal information $I_{\max}$ will be picked up from a chromatogram with peaks sufficiently or even well separated from each other. The error in the worst case is easily estimated by the information loss. The mean of $I_{\max}$ is defined as

$$\langle I_{\max} \rangle = I_{\max}/q \tag{13}$$

According to eqn. 12, the worst error is given by the information loss δI:

$$\langle \text{R.S.D.} \rangle = \exp(\delta I) \cdot \exp(-\langle I_{\max} \rangle) \cdot 100 \tag{14}$$

We can easily obtain, using eqn. 14, an estimate of the error $\langle$R.S.D.$\rangle$ concentrated on a peak. If $\delta I = 0$, then the error of the filtering is equal to the minimum error and may be completely negligible, indicating that the selected experimental conditions are optimal. If $\delta I = 1$, then the filtering error is e-fold more than the minimum error. It should be noted that R.S.D.$_k$, $\langle$R.S.D.$\rangle$, $P_k^{\dagger}$, etc., are not referred to the total HPLC error involving the elution process, detection process, etc., but depend only on the error in the Kalman filtering[2].

EXPERIMENTAL

All the programs were written in BASIC. A PC-9801 VX desk-top computer (NEC) equipped with an Intel-80286 compatible CPU (8 MHz), a 640-kbyte RAM and two 5-in. floppy disk drives was used. The cutoff point $k_c(i)$ was specified to be the point of the fronting edge with 0.5% signal of the peak maximum.

The chromatographic experiments were performed on a Model 655A-11 liquid chromatograph system (Hitachi) with an Inertsil ODS column (250 mm × 4.6 mm I.D.) (Gasukuro Kogyo). The details have been described previously[3].

RESULTS AND DISCUSSION

A chromatogram of naphthalene and diphenyl is shown in Fig. 1. The overlapped peaks have an apparent ratio of the height of the valley to that of the mean

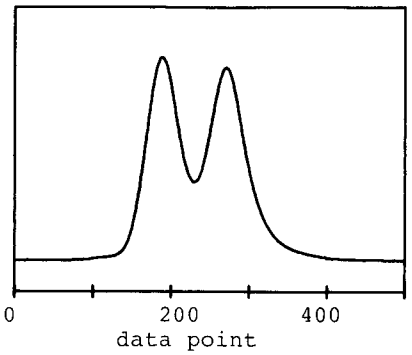

Fig. 1. Chromatogram of a mixture of naphthalene (leading) and diphenyl (trailing). The abscissa denotes the number of the data acquired by an analogue-to-digital converter at 200-ms intervals, 420 s after injection. For details, see ref. 3.

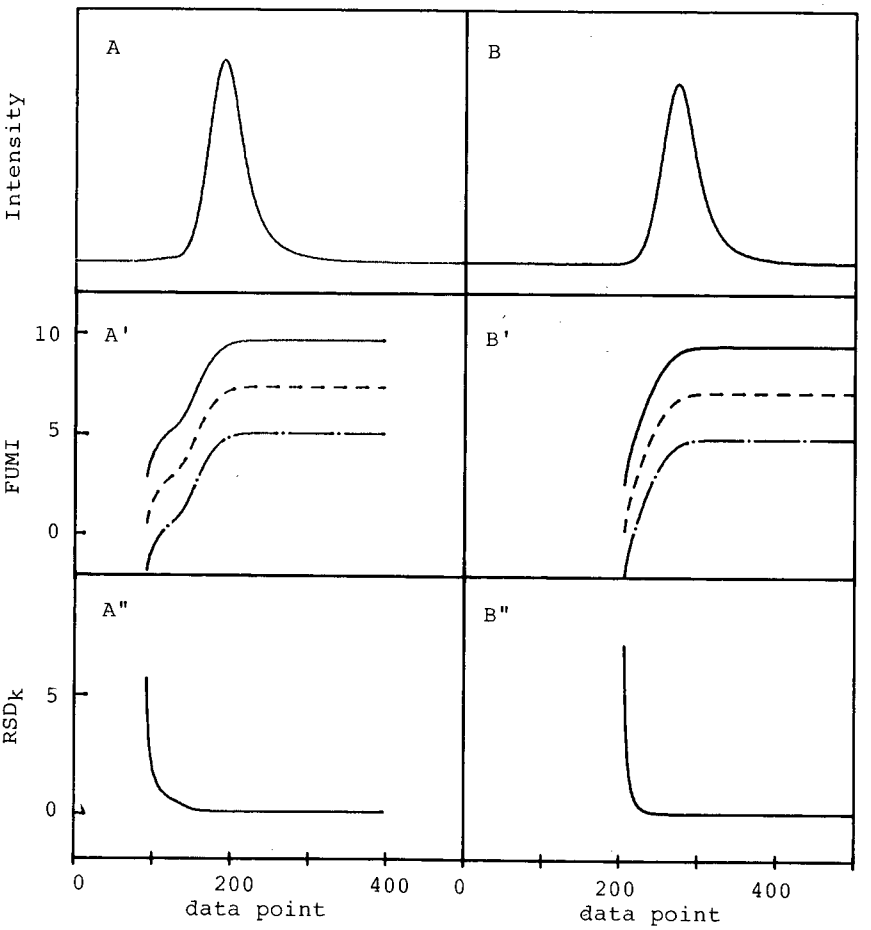

Fig. 2. Chromatograms of (A) naphthalene and (B) diphenyl, (A′ and B′) the time (k) courses of the mutual information and (A″ and B″) the filtering error. (A) $I_{max} = 9.68$; (B) $I_{max} = 9.46$. ——, $X_s = 1$; – – –, $X_s = 10$; – · – · –, $X_s = 100$. Experimental conditions as in Fig. 1.

peak maximum of *ca.* 40% and were analysed by the Kalman filter[3]. The analytical system was concluded to be satisfactory: the observed total error, obtained from five experiments, was less than 0.7% (R.S.D.) for both peaks[3]. The above system was originally evaluated quantitatively but empirically[3]; it has now been evaluated again but deductively based on *FUMI*.

Fig. 2 shows the individual peaks of (A) naphthalene and (B) diphenyl in Fig. 1, (A′ and B′) the time (k) course of *FUMI* and the (A″ and B″) R.S.D.$_k$ of the filtering error. As the observation proceeds, the mutual information increases and reaches a maximum around the peak maximum. The filtering error R.S.D.$_k$ displays the opposite behaviour to *FUMI*. In other words, our knowledge about the samples increases greatly or becomes more precise through observation and analysis until the vicinity of the peak maxima. The slight waving in the early region of *FUMI* for the

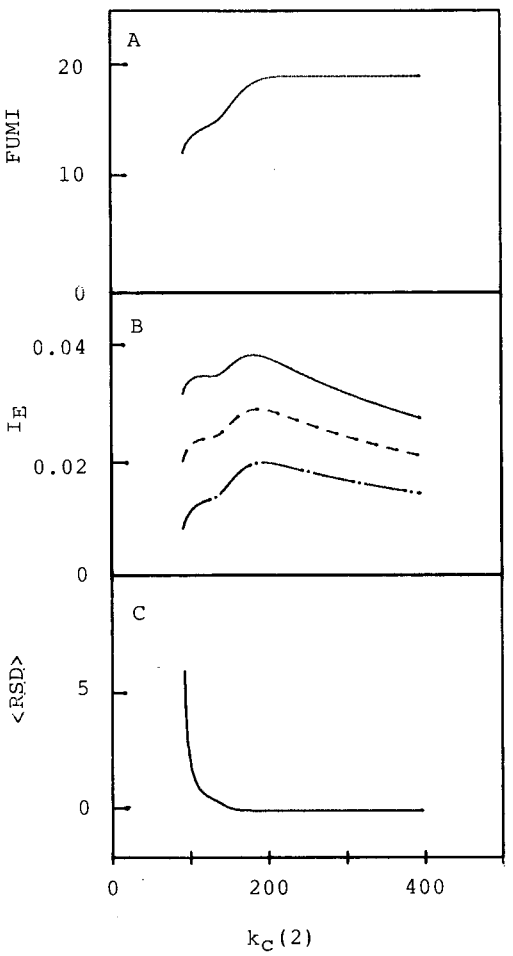

Fig. 3. Influence of the peak overlap on (A) *FUMI*, (B) $I_E[1, N]$ and (C) $\langle$R.S.D.$_k\rangle$ for a mixture of naphthalene and diphenyl. The abscissa denotes the cutoff point $k_c(2)$ of the diphenyl peak. $I_{max} = 19.14$ (= I_{max} of naphthalene + I_{max} of diphenyl). ——, $X_s = 1$; – – –, $X_s = 10$; – · – · –, $X_s = 100$. $N = k_c(2) + 282$.

naphthalene peak seems to come from the conspicuous fronting of the peak[3]. We can see that after the peak maxima, no further appreciable amount of information can be obtained from the Kalman filtering of the chromatograms. This suggests that the most efficient chromatogram must consist of overlapped peaks, and not only baseline separation.

Let us consider the relationship between the mutual information and the degree of peak overlap. In Fig. 3, (A) *FUMI*, (B) the efficiency $I_E[1, N]$ and (C) $\langle$R.S.D.$\rangle$ for the overlapped peaks are plotted as a function of the cutoff point $k_c(2)$ of the trailing peak. It is assumed that the trailing peak moves the time scale k without any changes in shape; the position of the leading peak is fixed. As the peaks are increasingly separated, the efficiency increases, reaches a maximum and decreases hyperbolically. If the peaks overlap completely $[k_c(1) = k_c(2)]$, then no information can be obtained and the efficiency takes the least value. The hyperbolic decrease in $I_E[1, N]$ is due to the saturation of the mutual information for both peaks. It should be noted that the last peak gives the saturated or maximal information according to our definition.

The most efficient chromatogram with the maximum of $I_E[1, N]$ is simulated in Fig. 4C. The input signals F_i^* $(= F_i/X_s)$ is 100-fold smaller than the actual signals F_i. The peak suppression $(X_s = 100)$ means that $I_E[1, N]$ allows for the "unexpected" small peaks (for theoretical meanings, see below). This chromatogram is the "best" in that it can transmit the mutual information in the most efficient way through observation and filtering. In other words, the flow of information through the chromatogram is maximal. Fortuitously, it corresponds to the actual chromatogram shown in Fig. 1. The total errors of the small peaks (6% concentration) of naphthalene and diphenyl

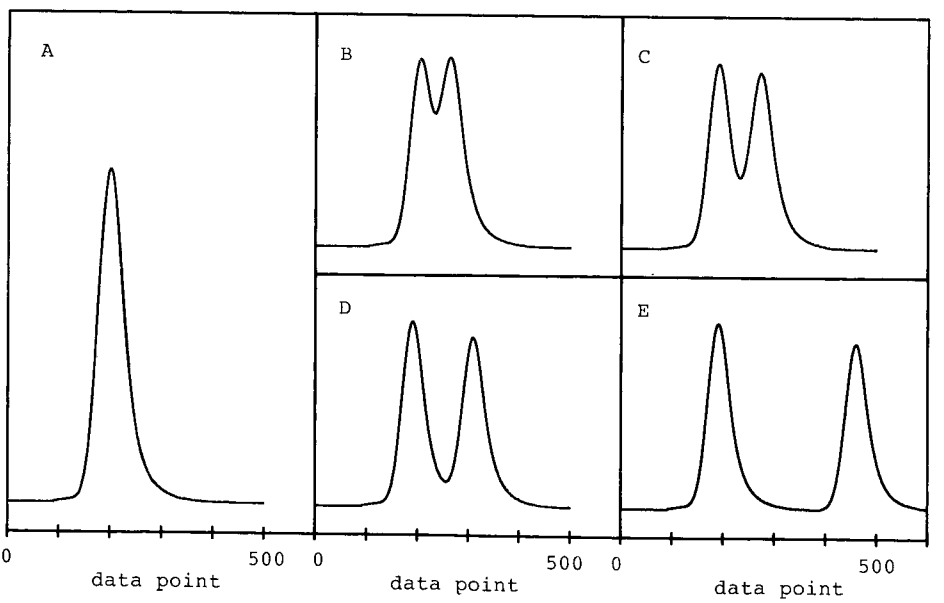

Fig. 4. Simulated chromatograms with various amounts of mutual information. (A) Peak interval $p = 19$, information loss $\delta I = 3.66$, R.S.D.$_{\cdot\text{min}} = 0.27\%$, period of the chromatogram $N = 436$; (B) $p = 61$, $\delta I = 0.60$, R.S.D.$_{\cdot\text{min}} = 0.013\%$, $N = 478$; (C) $p = 73$, $\delta I = 0.25$, R.S.D.$_{\cdot\text{min}} = 0.009\%$, $N = 490$; (D) $p = 119$, $\delta I = 0.006$, R.S.D.$_{\cdot\text{min}} = 0.007\%$, $N = 536$; (E) $p = 269$, $\delta I = 0.000$, R.S.D.$_{\cdot\text{min}} = 0.007$, $N = 686$.

were reported to be *ca.* 4% and 11% (R.S.D.), respectively, and larger than those for the 100% materials shown in Fig. 2A and B[3]. This result indicates the necessity to use the suppression factor X_s in evaluating or designing versatile determination (see below). Some chromatograms with their own information are also shown in Fig. 4. For the more strongly overlapped peaks (A and B), the observation time is relatively short, but sufficient information cannot always be obtained. For the chromatograms with weakly overlapped peaks (D and E) the opposite situation applies.

FUMI and $I_E[1, k]$ have been derived on the assumption that the data processing involved in the calculation of the mutual information is the one-dimensional Kalman filter for peak resolution[5,6]. If another type of data handling with inferior peak-resolving power such as the commonly used perpendicular dropping is utilized, then the chromatograms with the weak peak overlap (D or E) would be the most efficient. The bias for the estimates provided by the common technique was shown to be not less than 10% for the overlapped peaks, whereas the Kalman filter gave a *ca.* 0.2% bias[3]. The superior data processing with the Kalman filter can provide a faster flow of mutual information than the commonly used technique.

The information loss δI is very important as it can serve to solve the problem of whether or not the rapidity of the chromatography shown in Fig. 1 can outweigh the incomplete peak separation in the elution process[3]. The loss δI in Fig. 1 is shown to be negligibly small in comparison with the total HPLC error in the following way. The information loss of the leading peak is 0.25 and the corresponding filtering error ⟨R.S.D.⟩ is 0.009% for a 100% concentration. These values for the trailing peak are the most favourable. On the other hand, the total error in the whole HPLC system covering the elution, detection and filtering was observed to be *ca.* 0.7% (R.S.D.) for the overlapped peaks; the error or reproducibility of the whole system, measured with a solution of diphenyl, was 0.24%[3]. The filtering error is far smaller than the observed total HPLC error; the information loss δI (= 3.538) corresponding to the HPLC error (= 0.24%) is far larger than δI for the filtering (= 0.25). We therefore conclude that the rapid analysis design comprising Kalman filtering of the overlapped peaks shown in Fig. 1 is excellent if the overall HPLC errors are acceptable.

When the suppressed signals F_i^* are input in *FUMI*, the values of the mutual information and the efficiency function decrease (see Figs. 2A′, 2B′ and 3B). The position of the efficiency maximum increases slightly with increasing X_s (see Fig. 3B) and the degrees of peak overlap of the best chromatograms are varied accordingly. The factor X_s seems to remain arbitrary in the function I_E, but is closely related to the linearity of the filter involved in *FUMI* and of the signals of HPLC systems[2]. X_s can be determined as characteristic of a particular HPLC system used. Incomplete linearity of HPLC signals has been observed in special cases and interfered with the successful application of the linear filter[5,6]. This is the case for *FUMI*. If the HPLC signals completely satisfied the linearity postulate, there would be no need for the above consideration and Fig. 4B (X_s = 1) would be given as the best in the ideal HPLC system. The factor X_s, therefore, was introduced to bridge the gap between theory and practice, and should be specified according to the HPLC linearity observance[2]. The necessity to use X_s in proposing the best chromatogram (Fig. 4C) can be interpreted by the same situation: the small peaks that would give poor precision should be appropriately separated in the chromatogram for a successful determination. The relationship between the suppression factor X_s and the peak-resolving powers of the one-dimensional Kalman filter for peak resolution was described previously[2].

The best chromatogram presented here holds true for the adopted experimental conditions involving linear Kalman filtering and an HPLC system with limited linearity. Its elution pattern may vary according to the conditions adopted. If the analysis is carried out or designed under more ideal situations, then more complicated chromatograms will be provided as the best (see above). The experimental design should be performed so that the mutual information may be maximal or most efficiently transferred to real situations.

CONCLUSION

The overall analytical system shown in Fig. 1 has been logically evaluated with the aid of *FUMI* and concluded to provide the maximal information flow. Information theory and the Kalman filter underlie the procedure proposed here and no experience has been utilized. *FUMI* is a simple, quantitative description of the Shannon mutual information in chromatography and will be useful in various areas of analytical chemistry.

REFERENCES

1 S. Arimoto, *Information Theory*, Kyoritsu Shuppan, Tokyo, 1976.
2 Y. Hayashi, S. Yoshioka and Y. Takeda, submitted for publication.
3 Y. Hayashi, T. Shibazaki, R. Matsuda and M. Uchiyama, *J. Chromatogr.*, 407 (1987) 59.
4 R. Matsuda, Y. Hayashi, M. Ishibashi and Y. Takeda, *J. Chromatogr.*, 462 (1989) 23.
5 Y. Hayashi, S. Yoshioka and Y. Takeda, *Anal. Chim. Acta*, 212 (1988) 81.
6 Y. Hayashi, R. Matsuda, S. Yoshioka and Y. Takeda, *Anal. Chim. Acta*, 209 (1988) 45.

Journal of Chromatography, 462 (1989) 23–30
Elsevier Science Publishers B.V., Amsterdam — Printed in The Netherlands

CHROM. 20 987

AN INFORMATION THEORY OF CHROMATOGRAPHY

II. APPLICATION OF *FUMI* TO THE OPTIMIZATION OF OVERLAPPED CHROMATOGRAMS

RIEKO MATSUDA*, YUZURU HAYASHI, MUMIO ISHIBASHI and YASUSHI TAKEDA
Division of Drugs, National Institute of Hygienic Sciences, 18-1, Kamiyoga 1-Chome, Setagaya-ku, Tokyo 158 (Japan)
(First received April 7th, 1988; revised manuscript received September 19th, 1988)

SUMMARY

The *fu*nction of *m*utual *i*nformation (*FUMI*) was used as a quality criterion in the optimization of the injection interval in overlapped chromatograms. *FUMI*, which represents the amount of Shannon's mutual information involved in the chromatograms, was calculated for overlapped chromatograms with various injection intervals. The most efficient peak separation was selected with respect to the amount of the mutual information and the observation time. Overlapped chromatograms containing negative peaks were also optimized successfully.

INTRODUCTION

The final goal of analytical techniques is to obtain an exact knowledge of the amounts of substances of interest in a sample. Liquid chromatography is not an exception, and many chromatographers have endeavoured to achieve this goal by optimizing the chromatographic conditions. However, how can we evaluate the chromatographic separation? In reply to this question, researchers have proposed various quality criteria for chromatographic separation which can quantify the quality of the chromatograms[1]. Most of these criteria include the peak resolution (R_s) or the peak separation for each pair of adjacent peaks. In commonly used criteria, the summation of R_s for all adjacent pairs of peaks was calculated and the chromatograms were evaluated by means of this value. The efficiency of analysis was also regarded as an important factor, so some workers included the measurement time in addition to R_s in their criteria. These criteria, however, lack a theoretical base.

A versatile criterion should cover two important factors that are missing in R_s: (A) the noise level in the measurement process and (B) the mathematical formalism of data processing. It should be noted that a knowledge of the samples of interest cannot be obtained before the observation and mathematical processing of the raw data. The reliability of quantification is well known to be significantly dependent on the contamination noise levels. Point B concerns the fact that the peak-resolving power of the Kalman filter, previously proposed[2,3], was shown to be superior to the commonly

0021-9673/89/$03.50

used perpendicular dropping, and to give more reliable estimates. The criteria based on these methods of different powers cannot be the same.

A function called *FUMI* (*f*unction of *m*utual *i*nformation) has been derived on the basis of information theory and the Kalman filter theory[4]. *FUMI* represents the mutual information in chromatograms. The efficiency is represented as the ratio of *FUMI* to the observation time. In Part I[5], *FUMI* was calculated with two overlapped peaks, and the relationship between the amount of mutual information and the degree of peak overlap was discussed.

Recently we have presented overlapped chromatograms that resulted from the successive injection of samples at relatively short intervals[6–8]. The overlapped chromatograms efficiently reduced the total analysis time and improved the efficiency of the analysis.

The object of this paper is to assess the feasibility of this function as a quality criterion for multi-peak chromatograms. We demonstrate the optimization procedure for injection intervals in the overlapped chromatograms with the use of *FUMI*. The procedure presents the peak separation with sufficient precision and favourable efficiency. The advantage of overlapped chromatograms can be expanded with the aid of *FUMI*. Although we use overlapped chromatograms as a model in this study, *FUMI* is a general criterion and is applicable to the usual chromatographic separation modes.

THEORETICAL

We shall briefly review the theory developed in Part I[5]. For a single peak, *FUMI* represents the mutual information that we can retrieve through the filtering of raw data ranging from a data point $i = 1$ to k ($k = 1, \ldots, N$)[4]:

$$FUMI = \frac{1}{2}\left[\log\left(\sum_{i=1}^{k} F_i^2\right) - \log(\tilde{W}_c)\right] \tag{1}$$

where F_i denotes the signal intensity of a peak at a data point i and $\tilde{W}_c$ is the variance of the contaminating noise (= constant).

The mutual information for partially overlapped multiple peaks is[5]

$$FUMI = \frac{1}{2}\left\{\sum_{j=1}^{q} \log\left[\sum_{i=k_c(j)+1}^{k_f(j)} F_i(j)^2\right]\right\} - \frac{1}{2} q \log(\tilde{W}_c) \tag{2}$$

where q denotes the number of peaks and $[k_c(j) + 1, k_f(j)]$ the region where the signals $F_i(j)$ of the jth peak contribute to *FUMI*. The cutoff point $k_c(j)$ of the jth peak is often specified to be the first point where the peak signals predominate in noisy chromatograms. On the other hand, the filtering-off point $k_f(j)$ is variable and determined to be equal to the cutoff point $k_c(j + 1)$ of the following peak: $k_f(j) = k_c(j + 1)$. The information derived from the late region of the jth peak after $k = k_f(j)$, overlapped with the early region of the following peak, is neglected, as the filtering is always performed sequentially in a one-dimensional way from $i = 1$ to N (ref. 2). Thus, the strong peak overlap makes the region $[k_c(j) + 1, k_f(j)]$ narrow and then causes the loss of mutual information. When $k_c(j)$ coincides with $k_c(j + 1)$, no mutual information is picked up from either peak.

The efficiency of the chromatograms is given as

$$I_E[1,N] = \frac{FUMI}{N} \tag{3}$$

where N denotes the observation period of the chromatogram. This function represents the average amount of information in unit time and its maximum gives a chromatogram with the most efficient peak separation.

The information loss of a chromatogram, δI, arising from the peak overlap is defined as

$$\delta I = I_{max} - FUMI \tag{4}$$

where I_{max} denotes the maximal information obtained from a chromatogram with every peak sufficiently separated from each other. The filtering error is minimized at the maximum of $FUMI$ ($\delta I = 0$).

In the worst case, the information loss occurs only in a single peak, *i.e.*, the peak is overlapped strongly with the second peak, which is separated from the third peak. The error in this instance is easily calculated by the difference from the maximal information of the multi-component chromatogram; the relative standard deviation (R.S.D.) of the worst error is given approximately by[5]

$$\langle \text{R.S.D.} \rangle = \exp(\delta I) \cdot \exp(-\langle I_{max} \rangle) \cdot 100 \tag{5}$$

where $\langle I_{max} \rangle$ denotes the mean maximal information of q peaks ($= I_{max}/q$). This equation is useful for estimating the filtering error (R.S.D.) of a chromatogram from the information loss δI.

An additional procedure has been introduced for the practical use of the function of the information efficiency, I_E. The peak signals F_i are replaced by a small shape F_i^*($F_i = F_i^* \cdot X_s$, where X_s is the suppression factor); the calculated I_E with F_i^* presupposes the appearance of small peaks.

EXPERIMENTAL

High-performance liquid chromatographic (HPLC) data

Chromatographic measurements were made on an Inertsil ODS column (250 × 4 mm I.D.) with methanol as the eluent at a flow-rate of 0.5 ml/min. HPLC signals were converted and stored on 5-in. floppy disks. Additional experimental details can be obtained from refs. 6 and 7.

Computer simulation

All calculations were performed on a PC-9801 VM desk-top computer (NEC). Programs were written in N88BASIC. Graphics were performed using a Model MP3100 X–Y plotter (Graphtec).

Raw HPLC signals for a single chromatogram were overlapped with various injection intervals and the corresponding value of $FUMI$ was calculated. The beginning point of the ith peak, $k_c(i)$, was set at the point where the signal level reaches 0.5% of the peak maximum.

RESULTS

A methanolic solution containing four components, phenetol, diphenyl, pyrene and perylene, was injected into the HPLC system and gave the chromatogram shown in Fig. 1. When this solution is injected into the HPLC system successively at short, regular intervals, an overlapped chromatogram results. *FUMI* was calculated for the overlapped chromatograms involving 20 peaks derived from five-fold injections at various injection intervals. Fig. 2 illustrates the change of *FUMI* with injection intervals from 5 to 800 s. The maximal interval of 800 s, is equal to the chromatographic duration for one sample, and then the injection mode is the same as in the usual repeated experiments.

With short injection intervals *FUMI* shows some local maxima and minima corresponding to the complex change of the peak overlapping pattern. At an interval of about 315 s, *FUMI* is maximal and no longer increases with increasing intervals. No peak overlap occurs in the chromatograms with injection intervals longer than 315 s. Even with an interval shorter than 315 s, however, *FUMI* has an almost maximal value. To select the most efficient interval, we restricted ourselves to the satisfactory region of the injection interval where the information loss is less than unity; in the satisfactory region, the R.S.D. of the filtering error is expected to be less than 2.7 times the value of the minimum (eqn. 5), and the precision is guaranteed sufficiently. The optimal interval was searched within this region with the use of the information efficiency.

The information efficiency, I_E, was calculated with the suppression factor, X_s. When X_s is set at 100, for example, I_E is calculated with signals of 100-fold smaller intensity than the model peaks. This procedure means that I_E takes account of the case where peaks of 1% concentration of the model appear in the overlapped chromatogram. The effect of X_s was described in Part I[5]. The change in I_E is shown in Fig. 3 with suppression factors of 10, 100 and 1000. I_E decreases hyperbolically in the long interval region where *FUMI* takes a constant value. The maximum value of I_E in the

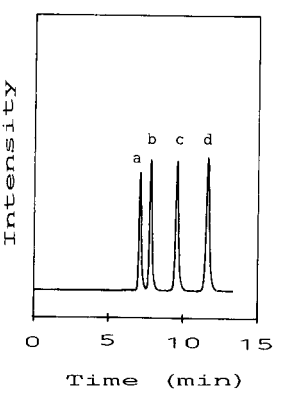

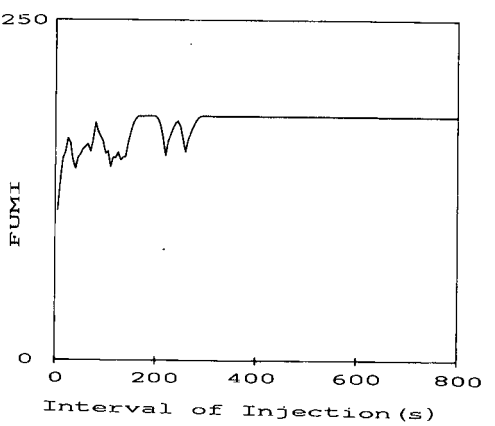

Fig. 1. Chromatogram of (a) phenetole, (b) diphenyl, (c) pyrene and (d) perylene.

Fig. 2. Variation of *FUMI* of the overlapped chromatogram derived from the single chromatogram shown in Fig. 1.

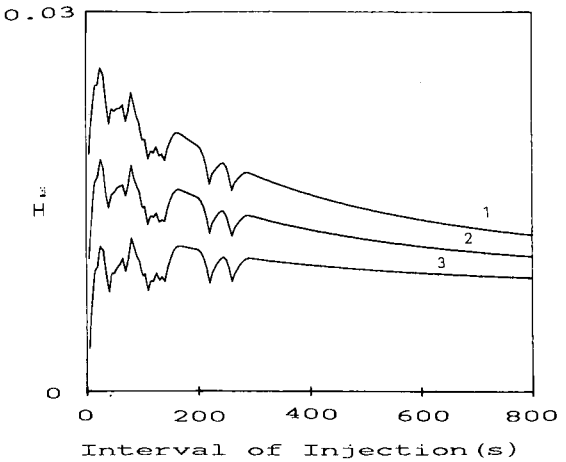

Fig. 3. Variation of I_E with suppression factors X_s of (1) 10, (2) 100 and (3) 1000.

satisfactory region defined above is obtained at an injection interval of 165 s with any X_s value, while the neighbouring local maximum of *FUMI* is at 185 s.

Fig. 4A shows the optimal overlapped chromatograms with injection intervals of 165 s. The value of *FUMI* is 179.084 and the maximum of *FUMI* is 179.46, and δI is

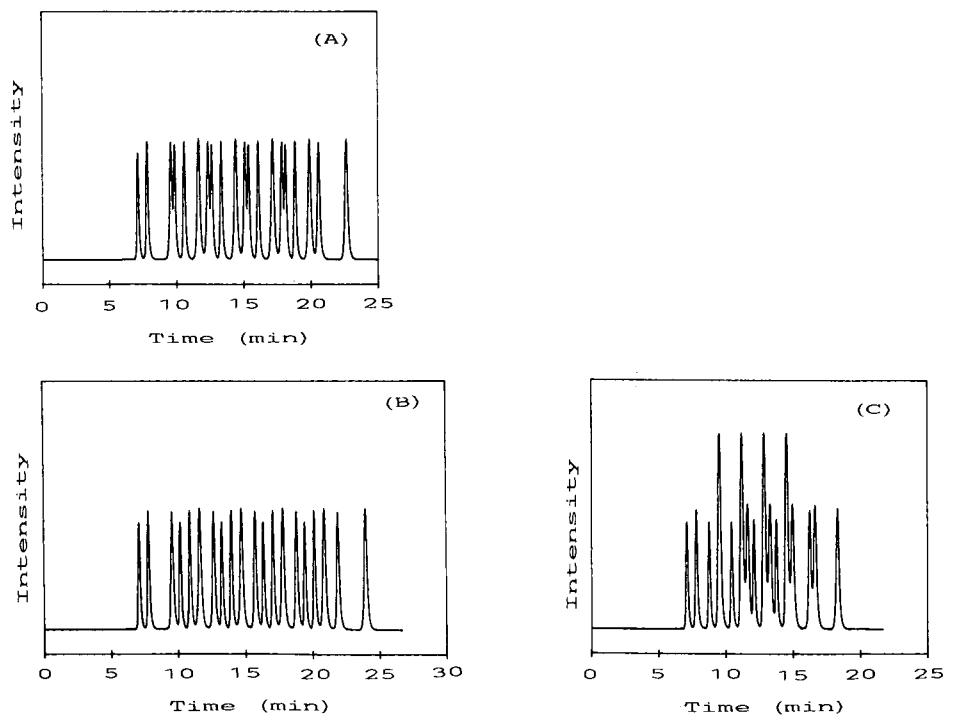

Fig. 4. Overlapped chromatograms derived from the single chromatogram shown in Fig. 1. Injection interval: (A) 165 s; (B) 180 s; (C) 80 s.

0.382. The predicted R.S.D. (0.018%) of the filtering error for the optimal chromatogram is considered satisfactory and almost the same as the minimum R.S.D. (0.012%). The overlapped chromatograms shown in Fig. 4B and C were obtained with injection intervals of 185 and 80 s, respectively. *FUMI* for the former is 179.464 and almost equivalent to the maximum, but I_E is slightly smaller than the optimal chromatogram (Fig. 4A). The shortest interval, 80 s, gives a local maximum of *FUMI*, but is outside the satisfactory region.

The suppression factor, X_s, does not influence I_E in the satisfactory region, but the effect of X_s appears in the region of short intervals. For a short observation period, the effect of X_s is greater[5].

We show another example of the optimization of overlapped chromatograms using *FUMI*. The chromatogram shown in Fig. 5 contains three component peaks that are also present in the preceding example and a small solvent peak. This chromatogram was overlapped and *FUMI* was calculated according to the procedure described above. The calculated value of *FUMI* and I_E are plotted in Fig. 6. The results reveal

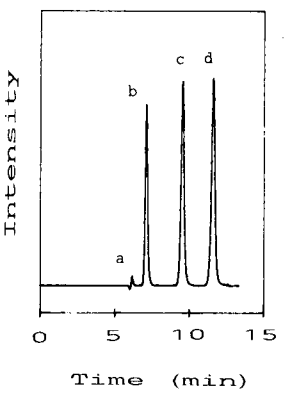

Fig. 5. Chromatogram of (a) solvent peak (10% ethanol), (b) phenetole, (c) pyrene and (d) perylene.

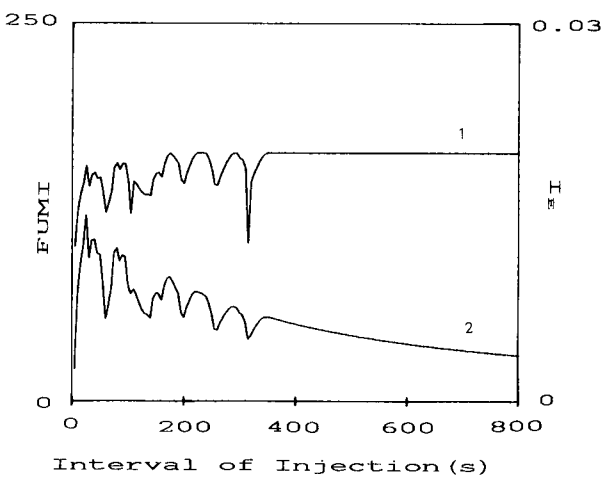

Fig. 6. Variation of (1) *FUMI* and (2) I_E (X_s = 100) of the overlapped chromatogram.

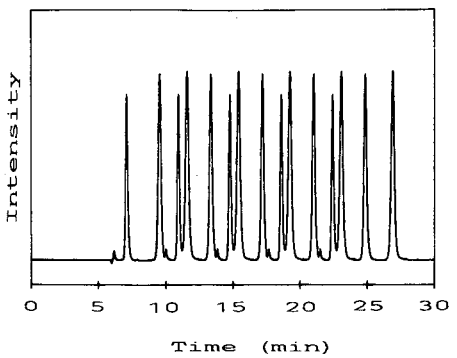

Fig. 7. Optimal overlapped chromatogram derived from the single chromatogram shown in Fig. 5.

that the small peaks and even the negative peaks are also adaptable to *FUMI*. The optimal interval was 230 s and the corresponding overlapped chromatogram is shown in Fig. 7. *FUMI* for the optimal chromatogram was 164.385, and the information loss and the R.S.D. of the error were 0.025 and 0.027%, respectively.

DISCUSSION

We have defined the quality of chromatograms with use of the mutual information or the precision of the quantification of target components. In other studies, R_s seemed to be related closely to the analytical precision and was used as the quality criterion for multi-peak chromatograms. It is obvious that the quantification error is minimized when peaks are separated completely ($R_s > 2$), and increases with decrease in R_s, but no definite relationship between the error and R_s has been given.

FUMI represents the mutual information in chromatograms and can also be connected to the R.S.D. of the filtering error, and we can estimate the precision of the filtering for various overlapped chromatograms with the aid of *FUMI*. The optimal chromatogram presented above is considered to be reasonable because the information loss or the excess filtering error is negligibly small. Practical consideration of the optimal chromatogram is given below.

We are interested in the correspondence between the filtering error and the total precision of actual chromatographic analyses. The filtering error predicted from *FUMI* is shown to describe well, although qualitatively, the change in the actual HPLC error as follows. Overlapped chromatograms with the same sample solution as that shown in Fig. 1 were analysed by the reduced Kalman filter of four dimensions[6]. The injection intervals were 200, 180, 160 and 150 s and the observed repeatability of the systems was 0.42%, 0.28%, 1.09% and 6.32%, respectively. With the shortest interval (150 s), some peaks are exceedingly overlapped and the estimated concentration was biased by *ca.* 12% at most. The calculated R.S.D.s of the filtering error with each interval are 0.017%, 0.013%, 0.17% and 2440%, respectively. The first three values for the filtering error are far smaller than the actual errors, including the errors in elution, detection and filtering. The filtering error (R.S.D. = 2440%) with an injection interval of 150 s is overestimated because of the mathematical property of the error variance P_k^+ involved in *FUMI*[4]. The overestimating property is favourable, because we can

avoid choosing the excessively overlapped chromatogram as optimal. The "visual" inspection of the optimal overlapped chromatograms described in ref. 6 is not unreliable, but *FUMI* is more useful.

Overlapping of the chromatograms with the successive injection of samples at short intervals is an effective method of reducing the analysis time and increasing the efficiency without the need for any skilful techniques. We applied this method to an automated system for the content uniformity test on pharmaceutical formulations and greatly increased the total efficiency or throughput[3,8]. The only critical parameter in this method is the injection interval, on which the precision and the efficiency of analysis depend. The injection interval, however, had been selected empirically in spite of its importance. The introduction of the mutual information is a clear solution to this problem. The R.S.D. of the filtering error can be predicted with a fairly simple function, *FUMI*, and optimal conditions can be selected with regard to both efficiency and precision. The overlapped chromatography method is shown here to be better than previously considered. The optimization method using *FUMI* must increase the reliability and applicability of overlapped chromatograms.

REFERENCES

1 H. J. G. Debets, B. L. Bajema and D. A. Doornbos, *Anal. Chim. Acta*, 151 (1983) 131, and references cited therein.
2 Y. Hayashi, S. Yoshioka and Y. Takeda, *Anal. Chim. Acta*, 212 (1988) 81.
3 Y. Hayashi, R. Matsuda, S. Yoshioka and Y. Takeda, *Anal. Chim. Acta*, 209 (1988) 45.
4 Y. Hayashi, S. Yoshioka and Y. Takeda, submitted for publication.
5 R. Matsuda, Y. Hayashi, M. Ishibashi and Y. Takeda, *J. Chromatogr.*, 462 (1989) 13.
6 Y. Hayashi, T. Shibazaki, R. Matsuda and M. Uchiyama, *Anal. Chim. Acta*, 202 (1987) 187.
7 Y. Hayashi, T. Shibazaki and M. Uchiyama, *J. Chromatogr.*, 411 (1987) 95.
8 R. Matsuda, Y. Hayashi, M. Ishibashi and Y. Takeda, *J. Chromatogr.*, 438 (1988) 319.

Journal of Chromatography, 462 (1989) 31–37
Elsevier Science Publishers B.V., Amsterdam — Printed in The Netherlands

CHROM. 20 968

DISPERSION AND SELECTIVITY INDICES IN GAS CHROMATOGRAPHY

III*. ALKYL, ω-CHLOROETHYL AND ALKENYL BENZOATE AND CHLOROBENZOATE ESTERS

M. B. EVANS*
Division of Chemical Sciences, The Hatfield Polytechnic, College Lane, Hatfield, Hertfordshire (U.K.)
and
J. K. HAKEN
Department of Polymer Science, University of New South Wales, P.O. Box 1, Kensington, N.S.W. 2033 (Australia)
(Received July 21st, 1988)

SUMMARY

The dispersion (I_M) and selectivity (I^*) indices of homologous alkyl, ω-chloroethyl and alkenyl benzoate and monochlorobenzoate esters are presented as obtained on low polarity (SE-30) and polar (OV-351) capillary columns. The effects of alkyl chain length, unsaturation and the position of chlorination are discussed and the results compared with studies of aliphatic esters. The compounds considered allow a study of the effect upon retention of chlorination in both the aromatic ring and the alkyl group.

INTRODUCTION

The division of the retention index of a solute in gas chromatography (GC) into a contribution due to apolar forces and related to molecular weight and a second contribution due to a summation of polar interactions and steric effects has been described recently[1,2]. The first communication dealt in general[1] with the development of the indices whilst the second detailed various homologous groups of carbonyl compounds. With the carboxyl compounds[2] the effects of substitution and branching in both constituent chains were considered together with carbonyl compounds, *i.e.* mono- and diketones and pyruvates, containing both a carboxyl and carbonyl functional group.

The present work considers both normal[3], ω-chloroethyl[4] and branched-chain[5] alkyl and alkenyl[6] benzoate esters and their isomeric monochlorinated derivatives examined isothermally at 160°C on low-polarity (SE-30) and polar (OV-351) capillary columns. The phase OV-351 is described as highly purified FFAP, reported to be the

* For Part II, see ref. 2.

0021-9673/89/$03.50

TABLE I

DISPERSION (I_m) AND SELECTIVITY (I^*) INDICES FOR ALKYL AND ALKENYL BENZOATE ESTERS AND THEIR MONOCHLORINATED DERIVATIVES ON SE-30 AND OV-351

Alkyl group	*SE-30*						*OV-351*			
	Benzoate esters		*o,m,p-Chlorobenzoate esters*	*o-Chloro-benzoate esters*	*m-Chloro-benzoate esters*	*p-Chloro-benzoate esters*	*Benzoate esters*	*o-Chloro-benzoate esters*	*m-Chloro-benzoate esters*	*p-Chloro-benzoate esters*
	I_M	I^*	I_M	I^*	I^*	I^*	I^*	I^*	I^*	I^*
n-C_1	956.3	140.7	1201.8	56.2	51.2	52.2	686.7	735.2	652.2	647.2
n-C_2	1056.3	107.7	1301.8	25.2	21.2	22.2	628.7	669.2	585.2	583.2
n-C_3	1156.3	107.7	1401.8	20.2	16.2	17.2	620.7	653.2	566.2	568.2
n-C_4	1256.3	103.7	1501.8	18.2	15.2	16.2	622.7	642.2	555.2	563.2
n-C_5	1356.3	101.7	1601.8	15.2	12.2	14.2	617.7	638.2	551.2	556.2
n-C_6	1456.3	101.7	1701.8	15.2	12.2	14.2	616.7	636.2	549.2	552.2
n-C_7	1556.3	100.7	1801.8	14.2	10.2	13.2	617.7	636.2	552.2	554.2
n-C_8	1656.3	99.7	1901.8	13.2	9.2	12.2	616.7	637.2	551.2	554.2
n-C_9	1756.3	99.7	2001.8	12.2	8.2	14.2	617.7	637.2	551.2	553.2
n-C_{10}	1856.3	98.7	2101.8	12.2	7.2	11.2	618.7	638.2	551.2	554.2
n-C_{11}	1956.3	98.7	2201.8	11.2	6.2	10.2	619.7	639.2	551.2	553.2
n-C_{12}	2056.3	98.7	2301.8	11.2	6.2	10.2	620.7	641.2	552.2	556.2
Methylethyl	1156.3	37.7	1301.8	−26.6	−37.6	−31.6	526.7	556.4	481.4	482.4
1-Methylpropyl	1256.3	36.7	1501.8	−41.8	−45.6	−45.8	517.7	539.2	454.2	456.2
2-Methylpropyl	1256.3	61.7	1501.8	−21.8	−26.6	−24.8	554.7	573.2	486.2	492.0
1,2-Dimethylpropyl	1356.3	10.7	1601.8	−73.3	−80.3	−76.3	476.7	499.7	403.7	410.6
1-Methylbutyl	1356.3	24.7	1601.8	−61.3	−65.3	−63.3	497.7	515.7	429.7	442.6
3-Methylbutyl	1356.3	68.7	1601.8	−23.3	−24.3	−20.3	568.7	576.7	498.7	503.6
2-Propenyl	1141.9	160.1	1387.5	22.6	16.6	16.5	694.4	716.6	632.5	631.5
2-Propynyl	1127.5	125.5	1373.1	46.9	37.9	36.9	889.5	924.9	833.9	830.9
3-Butenyl	1241.9	99.1	1487.5	17.5	10.5	12.5	675.1	698.5	613.5	614.5
1-Methyl-3-butenyl	1341.9	26.1	1587.5	−52.5	−61.5	−58.5	554.1	575.5	486.5	489.5
(*E*)-2-Butenyl	1241.9	131.1	1487.5	48.5	42.5	44.5	731.1	743.5	664.5	662.5
4-Pentyl	1341.9	105.1	1587.5	19.5	16.5	18.5	686.1	702.5	620.5	623.5
(*E*)-3-Hexenyl	1441.9	102.1	1687.5	19.5	8.5	11.5	658.1	683.5	588.5	591.5
(*Z*)-3-Hexenyl	1441.9	111.1	1687.5	24.5	18.5	21.5	674.1	601.5	610.5	613.5

esterification product of Carbowax 20M and 2-nitroterephthalic acid[7]. Various studies of the esters of interest, particularly the parent esters, have been recently reported[8] and are not repeated in this work. The influence of the various structural parameters, particularly on the selectivity indices, are discussed and some comparisons are made with earlier studies of aliphatic carboxyl compounds.

EXPERIMENTAL

The GC was conducted on a Perkin-Elmer Sigma 3 instrument using a vitreous silica SE-30 capillary column (25 m × 0.33 mm I.D.), (S.G.E., North Melbourne, Australia) and a fused-silica OV-351 column (25 m × 0.32 mm I.D.) (Orion Analytica, Espoo, Finland). The conditions were: injection and flame-ionisation detector temperature, 275°C; column temperature, 160°C; nitrogen carrier gas and a split ratio of 1:25. Retentions were measured as retention indices as previously reported[3–6].

RESULTS AND DISCUSSION

Table I shows dispersion (I_M) and selectivity (I^*) indices for the alkyl and alkenyl esters studied. The *n*-alkyl benzoate esters on the low-polarity phase show I^* values which tend to decrease slightly as the chain length is increased although the main decrease occurs with the lower alkyl esters. This is indicative of a significant methyl effect and formation of a homologous series where additional methylene groups have a truly additive effect. The values are, however, considerably higher than those of the corresponding alkyl esters, *i.e.* the *n*-alkyl hexanoates, due to the higher boiling points and the aromatic structure. As with alkyl- and alkenylbenzenes[1] an extension of the π bonding system greatly extends the selectivity.

Chlorination at all three positions on the ring produces equivalent and higher I_M values due to the increased molecular weight but lower values of I^* on the SE-30 stationary phase. It has been shown previously[1] with aliphatic compounds that the presence of polar functional groups tends toward positive I^* values whilst groups with screened electrons display strongly negative values. Here while the basic aromatic structure is of greater polarity, the addition of a halogen causes a considerable reduction.

The I^* values of the *ortho*, *meta* and *para* isomers are very similar, there being a slight decrease from *ortho* to *para* and a minimal further decrease from *para* to *meta*. The corresponding values of all compounds are greatly increased on the polar (OV-351) column. The substantial difference between the values of the parent esters and their derivatives is not evident now. The elution pattern is as demonstrated previously where maximization of the polar effects occurs with the *ortho* substituent[3,6]. This behaviour can be explained on the basis of electromerism[6]. The decrease in electron density occurring in the phenyl ring with *o*-substitution is more pronounced than that with *m*- and *p*-substitution, the increased interaction between this more electron-deficient ring and the electron-donating groups of the phase giving rise to the relatively higher retentions of the *o*-chloro isomers on OV-351. This effect with the *m*- and *p*-chloro isomers seems to be similar, *i.e.* the retention behaviour between the isomeric esters remains unchanged with increasing column polarity.

The effect of branching of the alkyl group is evident from Table I. Methylethyl

TABLE II

DISPERSION (I_m) AND SELECTIVITY (I^*) INDICES FOR ω-CHLOROETHYL BENZOATES AND THEIR MONOCHLORINATED DERIVATIVES ON SE-30 AND OV-351

Alkyl group	*SE-30*						*OV-351*			
	Benzoate esters		*o,m,p-Chlorobenzoate esters*	*o-Chloro-benzoate esters*	*m-Chloro-benzoate esters*	*p-Chloro-benzoate esters*	*Benzoate esters*	*o-Chloro-benzoate esters*	*m-Chloro-benzoate esters*	*p-Chloro-benzoate esters*
	I_M	I^*	I_M	I^*	I^*	I^*	I^*	I^*	I^*	I^*
Ethyl	1056.3	107.7	1301.8	25.2	21.2	22.2	628.7	669.2	585.2	583.2
2-Chloroethyl	130.18	78.2	1547.4	1.6	−5.4	−3.4	821.2	850.6	756.6	777.6
2,2-Dichloroethyl	1547.4	−77.4	1793.0	−154.0	−166.0	−158.0	665.6	698.0	628.0	626.0
2,2,2-Trichloroethyl	1793.0	−257.0	2038.5	−330.5	−348.5	−342.5	391.0	430.5	327.5	333.5

TABLE III

REDUCTION IN SELECTIVITY (I^*) WITH ADDITION OF INDIVIDUAL CHLORINE ATOMS IN ALKYL CHAIN AND AROMATIC RING

Alkyl substitution	*SE-30*				*Alkyl substitution*	*OV-351*			
	I^* Reduction	*Ring substitution*				*I^* Reduction*	*Ring substitution*		
		o-	*m-*	*p-*			*o-*	*m-*	*p-*
$C_2H_5 \rightarrow C_2H_4Cl$	29.5	23.6	26.6	25.6	$C_2H_5 \rightarrow C_2H_4Cl$	+192.5	+181.4	+171.4	194.4
$C_2H_4Cl \rightarrow C_2H_3Cl_2$	155.6	155.6	160.6	161.4	$C_2H_4Cl \rightarrow C_2H_3Cl_2$	156.5	152.6	138.6	151.6
$C_2H_3Cl_2 \rightarrow C_2H_2Cl_3$	179.6	176.5	182.5	184.5	$C_2H_3Cl_2 \rightarrow C_2H_2Cl_3$	274.6	267.5	300.5	292.5
$C_2H_5 \rightarrow C_2H_4Cl$	29.5	23.6	26.6	25.6	$C_2H_5 \rightarrow C_2H_4Cl$	+192.5	+181.4	+171.4	+194.4
$C_2H_5 \rightarrow C_2H_3Cl_2$	185.5	179.2	187.2	180.2	$C_2H_5 \rightarrow C_2H_3Cl_2$	+36.9	+29.8	+42.8	+42.8
$C_2H_5 \rightarrow C_2H_2Cl_3$	364.7	355.7	369.7	344.7	$C_2H_5 \rightarrow C_2H_2Cl_2$	237.7	238.7	257.7	249.7

benzoate on SE-30 has a considerably lower value of I^* than any of the *n*-alkyl benzoates, the effect of the methyl group in shielding the carbonyl being considerable as indicated previously[2]. The other five esters all follow a logical sequence, the 1-methylpropyl has a lower I^* value but this is greater than that of 2-methylpropyl ester where greater separation occurs. The 1,2-dimethylpropyl ester with further constraints has a lower I^* value. The 1-methylbutyl and 3-methylbutyl esters follow the corresponding propyl esters. With chlorination the greatest values of I^* are again shown with the *ortho* homologues, but the absolute values of I^* are very much lower than those for the saturated esters because branching on the carboxyl group reduces the polarity of this part of the compound and this in company with the aromatic moiety and the halogen atom has a marked effect.

On the polar phase the values of all four series are lower than for the straight chain esters but the trends are the same, namely

$$I^*_{o\text{-chloro}} < I^*_{\text{alkyl}} < I^*_{p\text{-chloro}} < I^*_{m\text{-chloro}}$$

The effect of unsaturation in the alkyl benzoates is evident firstly by comparison of 2-propenyl and *n*-propyl benzoate. On SE-30 slight enhancement of I^* occurs with the unsaturated ester while the three sets of chlorinated isomers have essentially equal I^* values. With increased phase polarity the I^* values of the unsaturated esters and of the chlorinated esters are expectedly increased. The 3-butenyl ester showed a reduced I^* value compared to the *n*-butyl ester on SE-30 but an increased value on OV-351. The 2-butenyl ester with closer proximity of the unsaturation to the carbonyl group shows further increased values of I^* in both phases. It is evident here as in the preceding work on alkyl esters that the 2-butenyl isomer shows greater relative I^* enhancement than the 2-propenyl ester, the significance of the terminal methyl group again being apparent. The 4-pentenyl ester shows increased values of I^* relative to the *n*-pentyl benzoates but the values are reduced compared to the shorter-chain unsaturated esters indicating further that transmission of polar effects along an alkyl chain is limited.

The ester (1-methyl-3-butenyl) with a pendant methyl group adjacent to the carboxyl group shows the lowest values of I^* of all the esters on both phases, and the effect relative to both the 3-butenyl and 4-pentenyl is quite dramatic. The moderating effect of a methyl group as a substituent adjacent to the carbonyl group has been observed previously with unsaturated aliphatic esters.

Table II shows dispersion (I_M) and selectivity (I^*) indices for the ω-chloroethyl benzoates and their monochlorinated derivatives.

Monochlorination of the aromatic ring has been shown on the non-polar phase to produce a reduction in I^*. With ethyl benzoate, a reduction in I^* in excess of 80 is evident on monochlorination of the ring while similar chlorination of the ethyl group causes a reduction of about 30. The difference in the values are due to less interference of the π bonding system by the chlorine substituent. As expected, Table II shows that the selectivity index on the same phase is reduced both with chlorination of the ethyl group and of the ring.

Table III shows the effects of di- and trichlorination of the ethyl group where very much greater reductions in I^* are evident as expected, while similarly with ring chlorination comparably large reductions also occur. In common with the other series (Table I), the *ortho* compounds (Table II) exhibit greater retention and the highest I^*

TABLE IV
ALTERNATIVE TABULATION OF REDUCTION IN SELECTIVITY (I^*) INDICES WITH ω-ETHYL AND RING CHLORINATION

Compound chlorinated	*Site of chlorination*	*I* Reduction*	
		SE-30	*OV-351*
Ethyl benzoate	Alkyl group	29.5	192.5
	Aromatic ring	82.5, 85.5, 88.5*	40.5, 43.5, 45.5
Monochloroethyl benzoate	Alkyl group	155.6	155.6
	Aromatic ring	76.6, 83.6, 81.6	29.4, 64.6, 43.6
Dichloroethyl benzoate	Alkyl group	180.0	274.6
	Aromatic ring	76.6, 88.5, 80.6	39.5, 63.5, 57.5
Trichloroethyl benzoate	Aromatic ring	73.5, 91.8, 85.5	32.4, 37.6, 39.6

* *o*-, *m*-, *p*- respectively.

values of the three isomers. The actual variations in the I^* values are shown in Table III.

The increased difference in selectivity of monochloroethyl benzoate and dichloroethyl benzoate in comparison to ethyl benzoate and monochloroethyl benzoate is observed. However, a very similar reduction in I^* occurs with ring chlorination of the two species, and the same effect is apparent with all three series with I^* decreasing expectedly with increasing chlorine content. The effect of the addition of one, two or three chlorine atoms to ethyl benzoate is shown in the lower part of Table III.

With the polar stationary phase the same trends are evident but increased I^* values are initially experienced due to the predominant effects of the donor phase but are overcome with increased chlorine content.

The effects of ring chlorination are also shown in Table IV. The effect of chlorine introduction in the alkyl chain is as indicated in Table III. Introduction of a chlorine atom at any of the ring positions produces on SE-30 similar and possibly slightly lower reductions of I^* as the polarity or chlorine content of the parent compound is increased. With the polar stationary phase a significant increase in I^* is evident with the first alkyl chlorination and much less with ring chlorination of ethyl benzoate. The results for the three isomers are very variable with the monochloroethyl compound and only slightly less so with the dichloroethyl benzoate, but significantly lower with the trichlorobenzoate derivatives.

ACKNOWLEDGEMENT

The authors wish to acknowledge the assistance of Miss Jane Fordham in the preparation of the manuscript of this paper.

REFERENCES

1 M. B. Evans, J. K. Haken and T. Tóth, *J. Chromatogr.*, 351 (1986) 155.
2 M. B. Evans and J. K. Haken, *J. Chromatogr.*, in press.
3 I. O. O. Korhonen and M. A. Lind, *J. Chromatogr.*, 322 (1985) 83.
4 I. O. O. Korhonen, *J. Chromatogr.*, 324 (1985) 192.
5 I. O. O. Korhonen and M. A. Lind, *J. Chromatogr.*, 323 (1985) 331.
6 I. O. O. Korhonen and M. A. Lind, *J. Chromatogr.*, 324 (1985) 113.
7 J. K. Haken, H. N. T. Hartley and D. Srisukh, *Chromatographia*, 17 (1983) 589.
8 K. Hammerstrand and D. R. Gerr, *Varian Aerograph Previews and Reviews*, 10 (1987) 6.

Journal of Chromatography, 462 (1989) 39–47
Elsevier Science Publishers B.V., Amsterdam — Printed in The Netherlands

CHROM. 20 964

ANALYSIS AND MOLAR MASS DISTRIBUTION OF POLYOXYETHYLENE 4-ALKYLPHENYLAMINES

MACIEJ WIŚNIEWSKI and JAN SZYMANOWSKI*
Poznań Technical University, Institute of Chemical Technology and Engineering, Pl. M. Skłodowskiej-Curie 2, 60-965 Poznań (Poland)
and
BRONISŁAW ATAMAŃCZUK
Institute of Heavy Organic Chemicals, Kędzierzyn-Koźle (Poland)
(First received June 17th, 1988; revised manuscript received August 19th, 1988)

SUMMARY

Polyoxyethylene 4-alkylphenylamines having from 1 to 16 carbon atoms in their alkyl groups and average degrees of ethoxylation from 1 to 8 were analyzed by gas chromatography and distribution coefficients were computed. Successive homologues having different numbers of oxyethylene groups were separated according to their increasing molar masses. Arithmetic retention indices were determined for separated homologues and increments for characteristic molecular fragments were calculated. They are equal to 298 and 805 for the oxyethylene group and the benzene ring, respectively. Retention indices of polyoxyethylene 4-alkylphenylamines can be estimated from the appropriate increments with an error of about 10 units. The molar mass distribution for these compounds is between those obtained for polyoxyethylene alkylamines and polyoxyethylene alcohols.

INTRODUCTION

4-Alkylphenylamines are known as extractants for noble metals[1,2]. They were also used as intermediates to obtain quaternary ammonium salts[3] and polyoxyethylene 4-alkylphenylamines[4,5]. These last surfactants were obtained in the reaction of 4-alkylphenylamines with ethylene oxide:

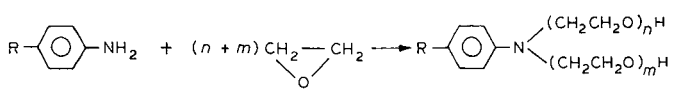

(1)

They are polydisperse mixtures and contain successive homologues having various numbers of oxyethylene groups.

The molar mass distribution of typical non-ionic surfactants, *i.e.*, polyoxyethylene alcohols and polyoxyethylene alkylphenols, was discussed in several independent

0021-9673/89/$03.50

papers and different models were proposed to calculate the molar fractions of successive homologues[6–10]. Recently, a general and mathematically improved computing technique was used and molar mass distributions were computed for polyoxyethylene alcohols and polyoxyethylene alkylphenols and also for typical polyoxyethylene alkylamines[11].

The aim of this work is to determine the composition of polyoxyethylene 4-alkylphenylamines and the retention indices of their successive homologues having different numbers of oxyethylene groups and to use these data to calculate the increments of the retention indices for characteristic molecular fragments and to compute the so-called distribution coefficients.

EXPERIMENTAL

Polydisperse polyoxyethylene 4-alkylphenylamines having 1, 6, 8, 10, 12 and 16 carbon atoms in their alkyl groups and average degrees of ethoxylation equal to 1, 3, 5 and 8 were used.

A gas–liquid chromatograph (Perkin-Elmer Model 900) with a flame ionization detector was used. The separation was carried out in stainless-steel columns (0.4 m × 2.7 mm I.D., 0.9 m × 2.7 mm I.D. or 1.8 m × 2.7 mm I.D.), Chromosorb G AW DMCS (60–80) mesh was used as the support and silicone resin OV-17 (3%) as the liquid phase.

Nitrogen was used as the carrier gas and its flow-rate was 20 cm^3/min. The analyses were started with a column temperature, depending on the product composition, of 80–170°C, which after 1 min of separation was increased at 6°C/min to 320°C, where it was maintained.

Trimethylsilyl derivatives were prepared in a glass microreaction vessel (capacity 3 cm^3) having a PTFE-lined cap (Supelco, Bellefonte, PA, U.S.A.). A sample of about 0.05 g was weighed and 0.5 cm^3 of N,O-bis(trimethylsilyl)acetamide (Applied Science Labs., State College, PA, U.S.A.) were added. The sealed reaction vessel was maintained at 70°C for 1 h and shaken from time to time.

The arithmetic retention indices[12] were determined for the homologues separated. The percentages of the components were calculated from the areas of their peaks, assuming correction coefficients of 1. The values of the peak resolutions were calculated according to

$$R = \frac{2(t_{R1} - t_{R2})}{w_1 + w_2} \tag{2}$$

where t_{R1} and t_{R2} denote the retention times of successive peaks and w_1 and w_2 the widths of these peaks measured at their bases.

RESULTS AND DISCUSSION

The chromatographic conditions were similar to those reported previously for polyoxyethylene alkylamines[14–16]. Under these conditions, successive homologues having different numbers of oxyethylene groups are eluted according to their increasing molar masses, and they can easily be identified by their retention indices.

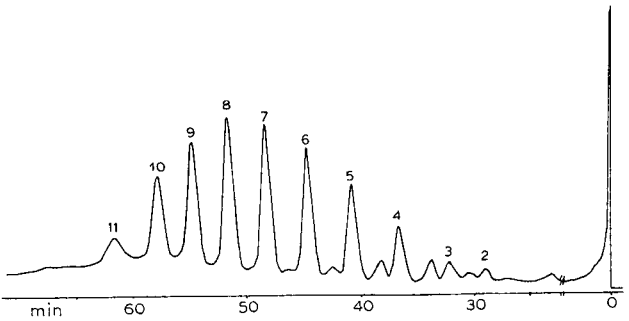

Fig. 1. Chromatogram of polyoxyethylene 4-dodecylphenylamine. Average degree of ethoxylation, 8; peak numbers denote oxyethylene groups present in the homologues separated.

Positional isomers having the same total number of oxyethylene groups but located in different ways in both the polyoxyethylene chains are not separated. An exemplary chromatogram of polyoxyethylene 4-dodecylphenylamine with an average degree of ethoxylation equal to 8 is shown in Fig. 1. The separation of polyoxyethylene 4-alkylphenylamines up to the homologues containing thirteen oxyethylene groups was achieved. Small peaks due to by-products, mainly polyoxyethylene glycols, are also observed between the main peaks of polyoxyethylene 4-alkylphenylamines.

The values of the arithmetic retention index for successive homologues of polyoxyethylene 4-alkylphenylamines and of the peak resolutions are given in Table I. The arithmetic retention index is linearly correlated with the number of oxyethylene groups. The slopes of such plots give the increments of the retention index per

TABLE I

ARITHMETIC RETENTION INDICES, I_A, AND PEAK RESOLUTIONS, R_s, FOR TRIMETHYLSILYL DERIVATIVES

No. of oxyethylene groups	*Polyoxyethylene 4-alkylphenylamines*					
	Methyl		*Hexyl*		*Dodecyl*	
	I_A	R_s	I_A	R_s	I_A	R_s
0	1390	–	1875	–	2480	–
1	1695	8.5	2170	5.6	2785	3.2
2	1955	6.7	2475	5.3	3080	3.6
3	2276	6.3	2780	5.0	3375	3.1
4	2584	5.2	3082	4.5	3670	2.6
5	2881	4.6	3380	3.6	3970	2.5
6	3180	4.2	3678	3.6	4265	2.4
7	3479	3.7	3975	2.1	4565	2.4
8	3770	3.4	4270	2.0	4860	1.7
9	4069	3.0	4565	2.0	5160	1.7
10	4366	2.6	4860	1.9	5455	1.5
11	4660	2.6	5155	1.7	5755	1.2
12	4960	2.4	5430	1.8	6050	1.3
13	5260	2.5	5750	1.7	6350	1.2

TABLE II

COMPOSITION OF POLYOXYETHYLENE 4-ALKYLPHENYLAMINES

In % (w/w); I and II denote the average degrees of ethoxylation and the number of oxyethylene groups, respectively.

II	*I*																							
	n = 1						*n* = 3						*n* = 5						*n* = 8					
	C_1	C_6	C_8	C_{10}	C_{12}	C_{16}	C_1	C_6	C_8	C_{10}	C_{12}	C_{16}	C_1	C_6	C_8	C_{10}	C_{12}	C_{16}	C_1	C_6	C_8	C_{10}	C_{12}	C_{16}
0	21.0	8.1	6.2	4.1	4.5	5.9	0	3.8	4.1	5.0	5.2	5.0	0	1.5	1.0	2.0	2.1	1.7	0	0	0	0	0	0
1	33.0	22.2	21.8	23.4	23.1	20.6	0	6.1	7.2	8.2	6.8	7.5	0	0.5	0.7	0.9	0.8	1.0	0	0.4	0.5	0.7	0.8	0.8
2	41.0	42.8	44.1	45.3	45.2	43.1	30.2	17.6	17.0	16.4	16.1	16.8	0.6	1.0	1.5	1.6	1.7	1.9	0	1.2	1.5	1.7	1.9	2.2
3		18.9	19.0	17.5	17.8	20.1	45.2	40.5	38.0	33.1	36.4	33.5	14.0	21.6	21.2	21.3	21.0	21.1	1.4	1.5	1.6	1.7	1.8	2.1
4							14.3	15.0	14.8	14.9	14.5	17.0	25.0	23.9	24.3	24.1	24.5	24.7	3.7	3.7	3.6	3.8	3.9	3.9
5							3.3	3.0	4.1	5.0	5.2	4.9	23.9	20.5	19.3	18.3	18.2	18.5	7.1	7.0	7.6	7.8	7.9	8.1
6							0	1.1	0.8	1.5	0	0.3	16.4	10.3	11.9	10.8	10.6	10.3	10.1	10.9	11.2	11.8	12.1	11.7
7													15.9	6.8	5.6	5.2	5.1	5.0	5.0	14.1	14.1	13.9	13.4	13.6
8													5.7	3.0	2.5	2.5	2.6	2.2	15.1	14.8	14.1	14.7	14.3	14.5
9													2.2	0.5	0.3	0.9	0.8	1.0	12.5	14.1	14.1	14.2	14.0	13.9
10													0.5	0.5					10.0	13.5	13.3	13.2	13.4	13.1
11																			8.6	4.3	2.0			
12																			3.8	2.1	1.9			
13																			1.0	0.9	0			
Other	4.9	8.0	7.9	9.7	9.4	10.3	9.0	12.9	14.0	15.9	15.8	15.0	5.8	9.9	11.7	12.4	12.6	12.6	12.6	12.5	14.7	16.7	16.5	16.1

oxyethylene group. The following values of this increment were obtained: 297.7, 298.1 and 297.6 for polyoxyethylene 4-alkylphenylamines having 1, 6 and 12 carbon atoms in the alkyl group, respectively. Thus, the average value is approximately equal to 298 and agrees well with the increment obtained previously for polyoxyethylene alkylamines ($\Delta I_A = 299$)[16]. Arithmetic retention indices of polyoxyethylene 4-hexylphenylamines are about 796–816 units higher than those obtained previously for polyoxyethylene hexylamines. These differences are equal to 816, 805, 808, 807, 806, 804 , 800 and 796 for appropriate homologues having 2, 3, 4, 5, 6, 7, 8 and 9 oxyethylene groups, respectively. Thus, the aromatic ring increases the retention index by about 805 units, and this effect does not depend upon the length of the polyoxyethylene chain. The increments previously determined[16] can also be used to predict the values of the retention index for polyoxyethylene 4-alkylphenylamines. The average error of such an estimation is equal to 11 units, and only in one case does the error exceed 20 units.

The peak resolutions are similar to those reported previously for other groups of non-ionic surfactants[17]. They decrease as the lengths of the polyoxyethylene chain and/or of the alkyl group increase.

The contents of the successive homologues in the products analyzed are given in Table II. They were used as initial data for further computing of the distribution coefficients. The contents of other compounds, mainly polyoxyethylene glycols, which are eluted between the main peaks, are also given in Table II. Quite significant amounts of these compounds are formed and their contents increase in a typical way as the average degree of ethoxylation increases. Polyoxyethylene 4-alkylamines obtained from 4-methylphenylamine contain less polyoxyethylene glycols in comparison to products obtained from 4-alkylphenylamines containing from 6 to 16 carbon atoms in their alkyl groups.

The reaction between an initial 4-alkylphenylamine (RXH) and ethylene oxide (EO) can be described as follows

$$\begin{aligned} &\mathrm{RXH} + \mathrm{EO} \xrightarrow{k_0} \mathrm{RXEOH} \\ &\mathrm{RXEOH} + \mathrm{EO} \xrightarrow{k_1} \mathrm{RX(EO)_2H} \\ &\vdots \\ &\mathrm{RX(EO)_{n-1}H} + \mathrm{EO} \xrightarrow{k_n} \mathrm{RX(EO)_nH} \end{aligned} \tag{3}$$

where k_0, k_1, ... k_n denote the rate constants for the successive steps of the process, X denotes N or NH and R a 4-alkylphenyl group.

The abbreviations used for 4-alkylphenylamine and its polyoxyethylene derivatives are the same as those used in our previous work[11] on polyoxyethylene alcohols, alkylphenols and alkylamines. This is possible because positional isomers having the same total number of oxyethylene groups but different distributions in the two polyoxyethylene chains are not separated, and consequently, they are not taken into consideration. In this case X denotes NH in 4-alkylphenylamines, 4-alkylphenyl-2-hydroxyethylamine and in some higher homologues having only one polyoxyethylene chain, while X is N in those typical homologues having two polyoxyethylene chains.

TABLE III

DISTRIBUTION COEFFICIENTS

Alkyl	C_1	C_2	C_3	C_4	C_5	C_6	C_7	C_8	C_9	C_{10}	C_{11}	C_{12}	*Correlation coefficient*
CH_3	–	0.564	0.567	0.701	0.874	0.725	0.738	0.712	0.710	0.383	0.224	–	0.99
C_6H_{13}	1.345	1.133	0.750	0.976	0.957	0.974	0.892	0.844	0.715	0.349	0.544	0.401	0.91
C_8H_{17}	1.165	1.043	0.726	1.009	0.936	0.987	0.884	0.803	0.333	0.404	0.863	–	0.88
$C_{10}H_{21}$	1.772	1.697	0.773	0.840	0.818	0.808	0.820	0.708	0.492	–	–	–	0.93
$C_{12}H_{25}$	1.982	1.666	0.738	0.827	0.812	0.796	0.829	0.726	0.505	–	–	–	0.92
$C_{16}H_{33}$	1.252	1.044	0.786	0.925	0.903	0.902	0.872	0.748	0.519	–	–	–	0.86
Average	1.503	1.317	0.755	0.915	0.885	0.893	0.859	0.766	0.512	0.151	0.281	0.080	0.89

By using the computing method previously described by us[11], the distribution coefficients $c_1 = k_1/k_0$, $c_2 = k_2/k_0$, ..., $c_n = k_n/k_0$, defined as the ratio of the successive rate constants to the rate constant of the first step, were determined (Table III). They demonstrate that results obtained for polyoxyethylene 4-methylphenylamines differ from those obtained for polyoxyethylene 4-alkylphenylamines having long alkyl groups (C_6–C_{16}). The distribution constants are of similar order and a sharp decrease is observed between homologues containing 8 and 9 oxyethylene groups in polyoxyethylene 4-alkylphenylamines having from 6 to 16 carbon atoms in the alkyl groups. This clearly demonstrates that homologues having 9 or more oxyethylene groups are not eluted completely from the chromatographic column. Thus, their actual contents are higher than those given in Table II.

The correlation coefficients are approximately 0.9 and the value of 0.99 was obtained only for polyoxyethylene 4-methylphenylamines. This means that some important deviations of the computed values from those experimentally determined are observed for polyoxyethylene 4-alkylphenylamines having from 6 to 16 carbon atoms in their alkyl groups. This is not caused by the errors of the chromatographic analysis, the accuracy and precision of which are the same as in analyses of other non-ionic surfactants[18]. This is a result of some differences observed in the reaction course during the syntheses of polyoxyethylene 4-alkylphenylamines.

The molar mass distribution of the successive homologues for polyoxyethylene 4-octylphenylamines is presented in Fig. 2. The numbers on the curves denote the total numbers of oxyethylene groups present in the homologue considered. Similar distributions were obtained for other products although the concentrations of the individual homologues were somewhat different.

They demonstrate that the content of 4-alkylphenylamine does not decrease so quickly to zero as in the case of polyoxyethylene alkylamines, and small amounts of it are observed in the products having an average degree of ethoxylation equal to 6. As a result, it is impossible to obtain almost pure 4-alkylphenyldi(2-hydroxyphenyl)-amines as in the case of alkylamines. This is caused by the low basicity of the nitrogen atom in 4-alkylphenylamines and, as a result, by the relatively low reaction rates of the first two steps leading to the formation of 4-alkylphenyl(2-hydroxyethyl)amine and 4-alkylphenyldi(2-hydroxyethyl)amine.

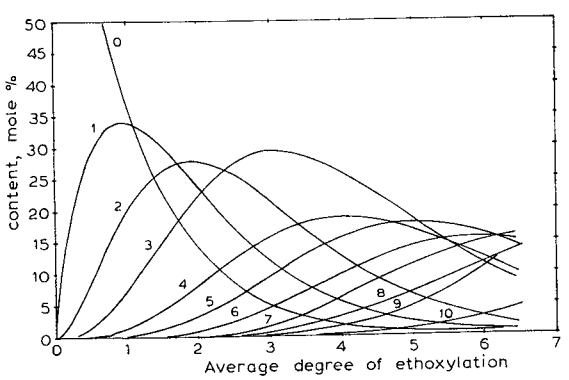

Fig. 2. Molar mass distribution for polyoxyethylene 4-octylphenylamines.

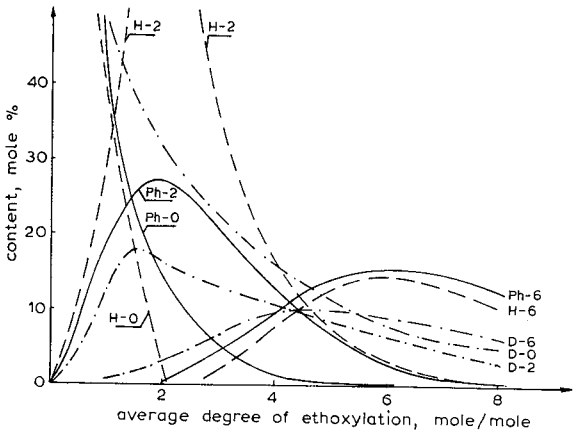

Fig. 3. Comparison of molar mass distributions for polyoxyethylene 4-octylphenylamines (Ph-0, Ph-2 and Ph-6), polyoxyethylene hexylamines (H-0, H-2 and H-6) and polyoxyethylene dodecanol (D-0, D-2 and D-6). Numbers denote the numbers of oxyethylene groups in the homologues considered.

The distribution of the successive homologues is also different in comparison to polyoxyethylene alcohols, as is demonstrated in Fig. 3. The content of 4-alkylphenylamine (Ph-O) decreases more quickly than that of dodecanol (D-O), but more slowly than that of hexylamine (H-O). The content of 4-alkylphenyldi(2-hydroxyethyl)amine (Ph-2) never reaches the high value of alkyldi(2-hydroxyethyl)hexylamine (H-2) but is higher than that of the appropriate analogue of dodecanol having two oxyethylene groups (D-2). Thus, the molar mass distribution of polyoxyethylene 4-alkylphenylamines is between those reported previously for polyoxyethylene alkylamines and polyoxyethylene alcohols[11].

CONCLUSIONS

Successive homologues of polyoxyethylene 4-alkylphenylamines having different numbers of oxyethylene groups can be separated according to their increasing molar masses and their contents can be determined by gas chromatography. The separations are similar to those reported previously for other groups of non-ionic surfactants having polyoxyethylene chains. The retention index increments are similar to those obtained previously for polyoxyethylene alkylamines. Those for the polyoxyethylene group and the aromatic benzene ring are equal to 298 and 805, respectively. Retention indices of polyoxyethylene 4-alkylphenylamines can be estimated from the appropriate increments with an error of about 10 units. The molar mass distribution of polyoxyethylene 4-alkylphenylamines is between those reported previously for polyoxyethylene alkylamines and polyoxyethylene alcohols.

ACKNOWLEDGEMENT

This work was supported by Polish Research Program CPBP No. 03.08.

REFERENCES

1 A. A. Vasileyeva, *Talanta*, 22 (1975) 745.
2 C. Pohlandt, *Talanta*, 26 (1975) 199.
3 M. Wiśniewski, B. Nowak, B. Kędzia and J. Szymanowski, *Tenside Deterg.*, 24 (1987) 46.
4 M. Wiśniewski, *Chem. Stos.*, in press.
5 M. Wiśniewski and J. Szymanowski, *J. Colloid Polym. Sci.*, in press.
6 P. I. Flory, *J. Am. Chem. Soc.*, 62 (1940) 1561.
7 B. Weibull and K. Nycander, *Acta Chem. Scand.*, 8 (1954) 847.
8 L. Gold, *Chem. Phys.*, 20 (1952) 1651.
9 L. Gold, *Chem. Phys.*, 28 (1958) 91.
10 G. Natta and E. Mantica, *J. Am. Chem. Soc.*, 74 (1952) 3152.
11 J. Szymanowski, B. Atamańczuk and H. Szewczyk, *J. Chem. Technol. Biotechnol.*, 40 (1987) 1.
12 A. G. Douglas, *J. Chromatogr. Sci.*, 7 (1969) 581.
13 C. Horvath, *The Practice of Gas Chromatography*, Wiley, New York, 1967, p. 157.
14 J. Szymanowski, H. Szewczyk and W. Jerzykiewicz, *Tenside Deterg.*, 18 (1981) 130.
15 H. Szewczyk, J. Szymanowski and W. Jerzykiewicz, *Tenside Deterg.*, 19 (1982) 287.
16 J. Szymanowski, A. Voelkel and H. Szewczyk, *J. Chromatogr.*, 360 (1986) 43.
17 J. Szymanowski, H. Szewczyk and J. Hepter, *Tenside Deterg.*, 18 (1981) 333.
18 J. Szymanowski, H. Szewczyk and B. Atamańczuk, *Tenside Deterg.*, 21 (1984) 139.

Journal of Chromatography, 462 (1989) 49–60
Elsevier Science Publishers B.V., Amsterdam — Printed in The Netherlands

CHROM. 20 976

GAS CHROMATOGRAPHIC BEHAVIOUR OF CARBOHYDRATE TRIMETHYLSILYL ETHERS

II. ALDOHEXOSES

I. MARTÍNEZ-CASTRO*, M. I. PÁEZ and J. SANZ
Instituto de Química Orgánica General (CSIC), Juan de la Cierva 3, 28006 Madrid (Spain)
and
A. GARCÍA-RASO
Departament de Química, Facultat de Cienciès, Universitat de les Illes Balears, 07071 Palma de Mallorca (Spain)
(First received March 11th, 1988; revised manuscript received August 23rd, 1988)

SUMMARY

The tautomeric forms of the eight aldohexoses were separated as their O-trimethylsilyl ethers on several packed and capillary columns. Their chromatographic behaviour was similar to that previously found for aldopentoses, but different from that of other ethers. A mathematical approach developed for aldopentoses was applied to aldohexose retention indices on several stationary phases, in an attempt to relate these values to their structural characteristics.

INTRODUCTION

The study of carbohydrates by gas chromatography (GC) requires their derivatization in order to improve the volatility. Among the derivatives which do not cause changes in the initial configuration of the molecules, the trimethylsilyl (TMS) ethers are the most used[1,2].

Although many studies have dealt with the relationships between chemical structure and chromatographic behaviour, publications on sugar derivatives are scarce and incomplete. Several rules were deduced by Sweeley *et al.*[3] and have since been confirmed[4].

In the first part of this series[5] it was found that aldopentose TMS ethers show an unusual chromatographic behaviour on stationary phases of different polarities. Some structural features were correlated with retention, the highest positive contribution corresponding to TMS groups in equatorial positions. The retention indices of aldopentose TMS ethers decreased with increasing temperature. Now this study is extended to the TMS ethers of the eight aldohexoses.

0021-9673/89/$03.50

TABLE I

CHROMATOGRAPHIC COLUMNS USED IN THE GC ANALYSIS OF TMS ETHERS OF HEXOSES

Stationary phase	*Origin*	*Type*	*Material*	*Length (m)*	*I.D. (mm)*	*Support*	*Temperature (°C)*
SE-30	Teknokroma	Packed	Stainless steel	3	3	Supelcoport	150–210
Carbowax 20M	Teknokroma	Packed	Stainless steel	3	3	Supelcoport	160
DEGS	Teknokroma	Packed	Stainless steel	3	3	Supelcoport	160–180
SE-54	Laboratory-made	Open tubular	Glass	40	0.18	–	180–200
OV-17	Chrompack	Open tubular	Fused silica	25	0.22	–	160–190
Carbowax 20M	Hewlett-Packard	Open tubular	Fused silica	25	0.22	–	160
OV-215	Laboratory-made	Open tubular	Glass	25	0.18	–	170
OV-225	Laboratory-made	Open tubular	Glass	25	0.18	–	170

MATERIALS AND METHODS

Samples

β-D-Allose and D-altrose were obtained from Fluka (Buchs, Switzerland); D-mannose, D-gulose, D-idose, D-galactose and α-D-talose from Sigma (Eisenhofen, F.R.G.), and D-glucose from Ferosa (Spain).

A 1-mg amount of crystalline sample was dissolved in water or pyridine and left to stand for 48 h at room temperature, in order to attain the anomeric equilibrium. Syrup samples (idose and gulose) were equilibrated in water. Aqueous samples were lyophilized prior to silylation.

To silylate the samples, 0.1 ml of trimethylsilylimidazole was added and the mixture heated at 65°C for 30 min[6].

GC analysis

The chromatographic equipment, carrier gas and injection and detection conditions were as described previously[5]. Columns and conditions are summarized in Table I. Chromatograms were taken in the isothermal mode: oven temperatures were equal or slightly higher than those used previously[5].

Kováts retention indices were calculated from the retention times of TMS ethers and suitable *n*-alkanes. The dead time was determined by linear regression[7].

Calculations

Retention index calculations and normal and stepwise linear regressions were carried out by using several programs written by us in BASIC for a microcomputer Olivetti M-20.

RESULTS AND DISCUSSION

The eight aldohexose TMS ethers showed in capillary GC four peaks corresponding to the four cyclic tautomers (two pyranoses and two furanoses); only two peaks were observable for most sugars when using the packed columns. Retention indices are shown in Table II. They were similar on both capillary and packed columns, with the exception of Carbowax 20M columns where the retention indices were highly variable. The aldohexose identification was carried out by GC–mass spectrometry (MS) and by comparison with NMR data[8,9]. In two cases (mannose and glucose), it was impossible for us to assign some furanose forms present in the mixtures in very small amounts.

Effect of the stationary phase polarity

Retention indices changed with the polarity of the stationary phase, but no correlation was established. In a plot of the stationary phase polarity calculated according to McReynolds[10] against the first principal component, a positive correlation is expected[5]. However, Fig. 1 shows that the overall retention decreases in the order SE-54, OV-215, OV-17, OV-225 and Carbowax 20M. Similar chromatographic behaviour was observed for the packed columns, where Carbowax 20M showed the lowest *I* values. These results agree with those found[5] for aldopentoses, and confirm that the usual criteria of stationary phase polarity are not suitable for TMS ethers of sugars.

TABLE II

RETENTION INDICES, I_x, OF ALDOHEXOSES

Stationary phase, McReynolds polarity and temperature (°C).

Component		*SE-54* *334* *180*	*OV-17* *884* *180*	*OV-215* *1545* *170*	*OV-225* *1813* *170*	*C 20M* *2308* *160*
17	α-Allofuranose	1857	1829	1849	1772	1768
18	β-Allofuranose	1896	1886	1849	1831	1843
1	α-Allopyranose	1862	1814	1849	1789	1754
2	β-Allopyranose	1879	1829	1849	1789	1778
19	α-Altrofuranose	1837	1972	1774	1699	1739
20	β-Altrofuranose	1912	1871	1739	1699	1838
3	α-Altropyranose	1830	1765	1872	1826	1703
4	β-Altropyranose	1830	1758	1777	1710	1695
21	α-Glucofuranose	–	–	1824	1783	–
22	β-Glucofuranose	–	–	1824	1800	–
5	α-Glucopyranose	1924	1908	1905	1853	1793
6	β-Glucopyranose	2022	2002	2175	1984	1972
23	α-Mannofuranose	1944	–	1915	1870	–
24	β-Mannofuranose	–	–	2032	–	–
7	α-Mannopyranose	1835	1798	1794	1729	1716
8	β-Mannopyranose	1937	1886	1963	1882	1862
25	α-Gulofuranose	1908	1867	1824	1830	1832
26	β-Gulofuranose	1982	1883	1938	1858	–
9	α-Gulopyranose	1858	1803	1826	1762	1757
10	β-Gulopyranose	1825	1789	1765	1734	1729
27	α-Idofuranose	1896	1832	1853	1796	1815
28	β-Idofuranose	1858	1816	1793	1766	1771
11	α-Idopyranose	1858	1812	1837	1784	1764
12	β-Idopyranose	1909	1865	1893	1846	1841
29	α-Galactofuranose	1941	1909	1922	1878	1869
30	β-Galactofuranose	1852	1827	1779	1759	1763
13	α-Galactopyranose	1894	1859	1874	1817	1786
14	β-Galactopyranose	1941	1902	1946	1904	1869
31	α-Talofuranose	1882	1867	1918	1816	1823
32	β-Talofuranose	1863	1836	1833	1800	1794
15	α-Talopyranose	1882	1848	1840	1813	1890
16	β-Talopyranose	1943	1900	2021	1960	1896

Effect of temperature

The retention indices of aldohexose TMS ethers decreased with increasing temperature in both packed and capillary columns. Fig. 2 shows some examples for capillary (a) and packed (b) columns. Values of $\Delta I/10°C$ for capillary columns are shown in Table III. A similar chromatographic behaviour was found[5] for aldopentoses.

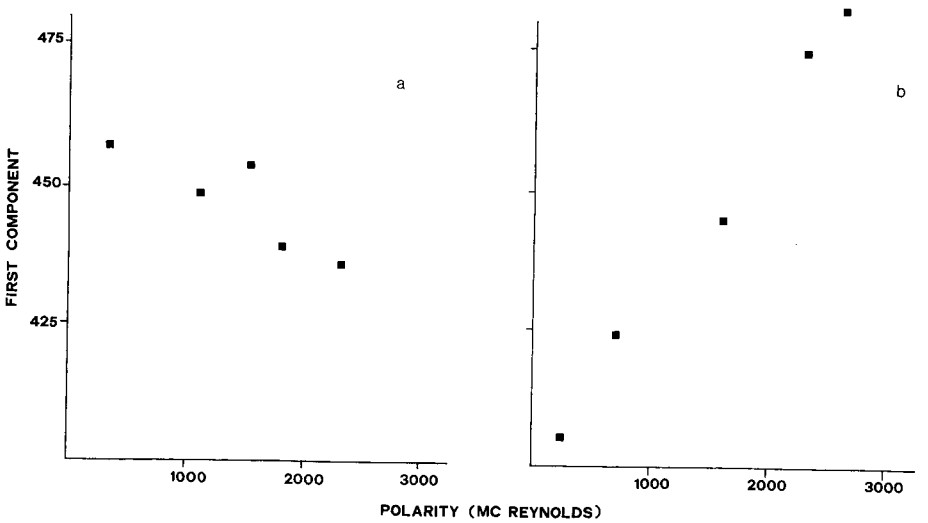

Fig. 1. (a) Values of the coefficients of the first principal component of the data matrix for aldohexose TMS ethers *versus* the polarity of the stationary phase. (b) Values obtained with thirteen ethers from McReynolds[5], given for comparison.

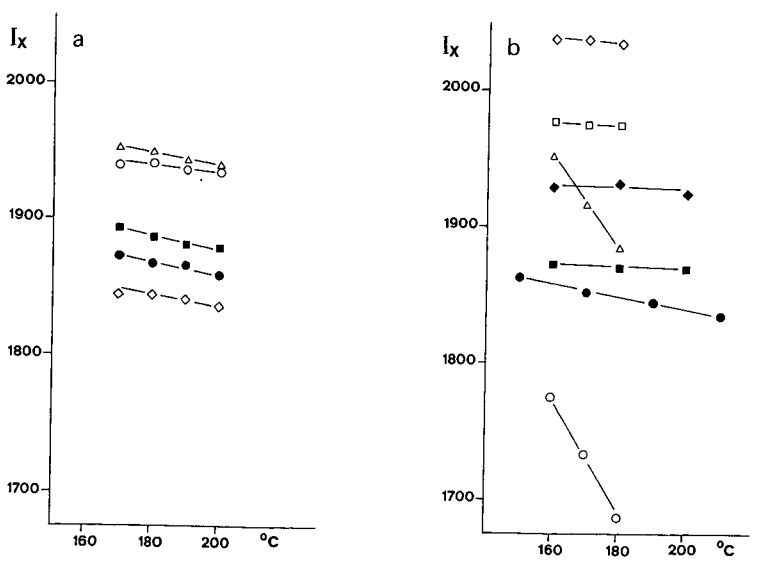

Fig. 2. Variation of I_x with temperature for several aldohexose TMS ethers. (a) Capillary column of SE-54: △, α-mannofuranose; ◇, α-mannopyranose; ○, β-mannopyranose; ■, α-talopyranose; ●, β-talofuranose. (b) Packed columns: □, α-talose (DEGS); ◇, β-talose (DEGS); ○, α-mannose (DEGS); △, β-mannose (DEGS); ■, α-talose (SE-30); ◆, β-talose (SE-30); ●, α-mannose (SE-30).

TABLE III

TEMPERATURE DEPENDENCE OF THE RETENTION INDICES, $\Delta I/10°C$, OF TMS ETHERS OF ALDOHEXOSES

Component	*SE-54* *180–200°C*	*OV-17* *160–190°C*
α-Allofuranose	−4.0	−12.3
β-Allofuranose	−5.0	−12.3
α-Allopyranose	−1.5	−7.3
β-Allopyranose	−4.5	−8.0
α-Altrofuranose	−6.5	−9.7
β-Altrofuranose	−5.0	−8.7
α-Altropyranose	−3.0	−6.3
β-Altropyranose	−3.0	−9.3
α-Glucopyranose	−3.5	−10.0
β-Glucopyranose	−7.0	−9.3
α-Mannopyranose	−4.0	−9.7
β-Mannopyranose	−0.5	−8.0
α-Gulofuranose	−7.0	−7.0
β-Gulofuranose	−3.5	−5.7
α-Gulopyranose	−4.0	−6.3
β-Gulopyranose	−6.0	−2.0
α-Idofuranose	−2.0	−6.3
β-Idofuranose	−2.5	−7.3
α-Idopyranose	−2.5	−7.3
β-Idopyranose	−4.5	−9.0
α-Galactofuranose	−1.0	−11.7
β-Galactofuranose	−5.0	−10.7
α-Galactopyranose	−1.5	−8.5
β-Galactopyranose	−1.0	−7.7
α-Talofuranose	−4.5	−9.3
β-Talofuranose	−0.5	−9.3
α-Talopyranose	−2.0	−7.7
β-Talopyranose	−2.5	−5.7

Effect of carbohydrate structure

Table II shows the retention indices of aldohexoses on five stationary phases.

For pyranose forms, except altrose and gulose, the α-anomer was eluted before the β-anomer. Sweeley *et al.*[3] explained the gulose behaviour by supposing that while β-gulose is almost certainly in the conformation $^4C_1$, α-gulose may well be in the conformation $^1C_4$ with three axial OTMS groups including the anomeric one (Scheme 1). A similar explanation would be valid for altrose, although these authors did not assign the α- and β-forms.

The planar structures are usually more strongly retained[3], as in the case of pentoses[5]. β-Glucopyranose, whose OTMS groups are all equatorial, always showed the highest retention. On the contrary, the different altrose tautomers, with many axial substituents, were the least strongly retained on most phases.

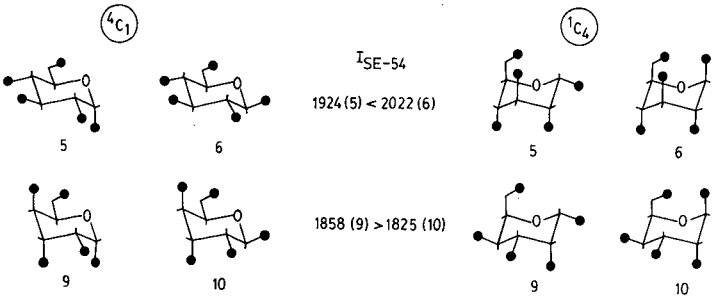

Scheme 1.

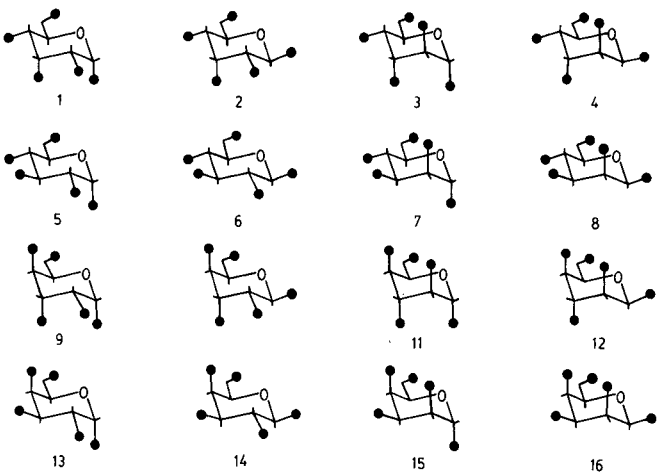

Scheme 2.

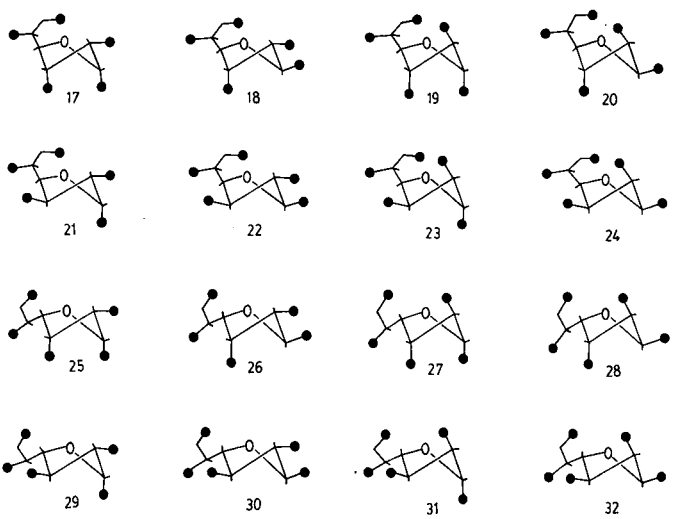

Scheme 3.

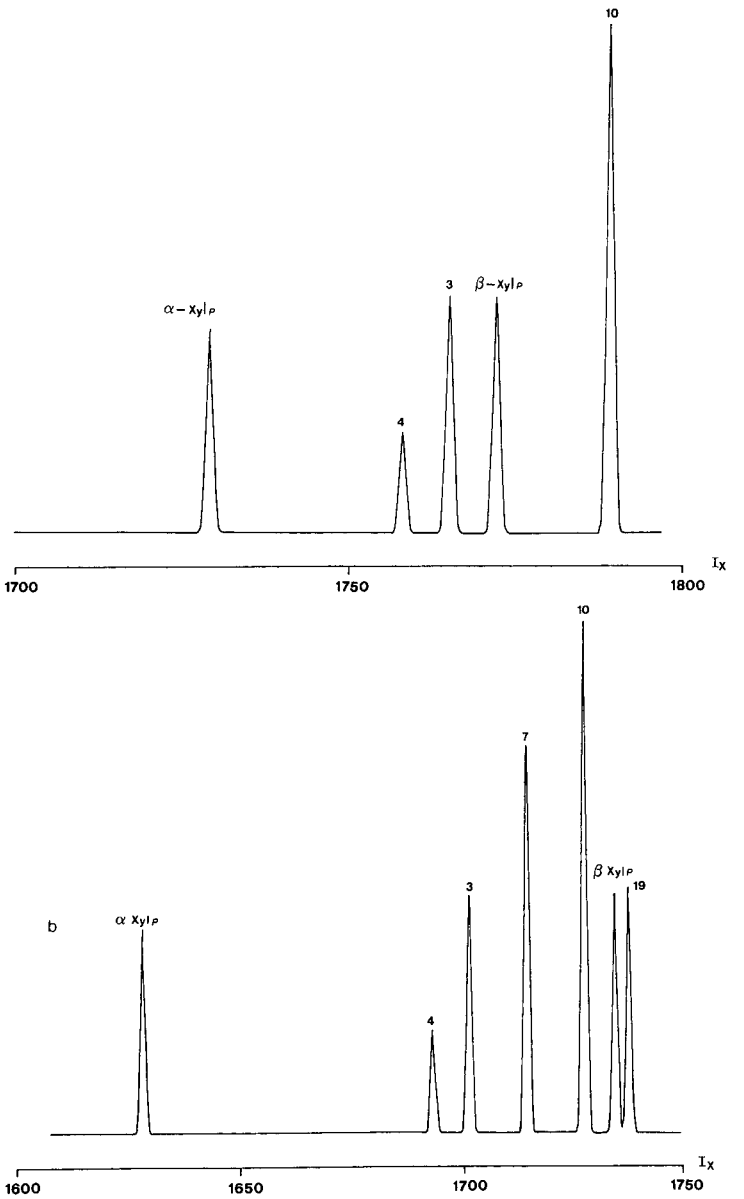

Fig. 3. Chromatographic patterns for some hexose TMS ethers eluted before β-xylopyranose on (a) OV-17 and (b) Carbowax 20M (both at 160°C). Numbers of peaks correspond to structures in Schemes 2 and 3.

The highest separation between anomeric pairs was found in glucopyranoses (179 I.U. on Carbowax 20M). The least separated were those corresponding to allose and altrose, which overlapped on some phases.

The behaviour of furanoses was opposite to that of pyranoses: the β-anomers were eluted before the α-anomers, with the exception of gulose and allose. In general,

TABLE IV

STRUCTURAL DESCRIPTORS OF HEXOSE TMS ETHERS

Code	*Range*	*Structural significance*
Eq1	0–1	OTMS group equatorial on C-1 (anomeric)
Eq2	0–1	OTMS group equatorial on C-2
Eq3	0–1	OTMS group equatorial on C-3
Eq4	0–1	OTMS group equatorial on C-4
ΣEq	0–4	Total number of equatorial OTMS groups
2c	0–4	Two OTMS groups in a *cis* disposition
2t	0–4	Two OTMS groups in a *trans* disposition
3c	0–3	Three OTMS groups in a *cis* disposition
A13	0–2	Two OTMS groups in alternate diaxial disposition
AA	0–3	Two OTMS groups in adjacent diaxial disposition
AE	0–4	Two OTMS groups in adjacent axial–equatorial disposition
EE	0–4	Two OTMS groups in adjacent diequatorial disposition

the separation range was smaller than for pyranoses. The most strongly retained compound (on three phases) was α-galactofuranose, whereas α- and β-altrose were the least strongly retained. The most easily resolved anomeric pair was α- and β-galactose (except on Carbowas 20M).

The increment in molecular weight with respect to aldopentoses produces an increase in the overall retention which averaged 200 I.U. (231 ± 31 on SE-54, 194 ± 35 on OV-17). All the aldohexoses were eluted after the aldopentose (β-xylopyranose) on SE-54, but there were several exceptions on OV-17 and Carbowax 20M (Fig. 3).

TABLE V

MULTIPLE LINEAR REGRESSION LEAST-SQUARES FIT FOR HEXOPYRANOSES ON FIVE STATIONARY PHASES

Contribution of hexopyranose descriptors (I_x units) and correlation coefficient.

Descriptor (see Table IV)	*Phase*				
	OV-17	*Carbowax 20M*	*OV-215*	*OV-225*	*SE-54*
ΣEq	78.6	75.7	249.7	221.4	98.4
Eq1	35.4	82.3	10.7	8.9	24.5
Eq2	30.9	37.9	18.1	30.3	13.1
Eq3	111.1	127.9	149.8	145.7	87.6
2c	35.6	22.8	−8.6	−14.5	35.2
3c	−61.9	−45.5	−73.9	−62.3	−62.4
A13	142.9	160.6	241.9	194.0	137.7
EE	−3.4	−13.2	−114.8	−131.4	−17.8
Ring	1507.9	1443.9	1388.9	1424.9	1558.7
Correlation coefficient	0.972	0.962	0.952	0.986	0.970
α-Allopyranose Exptl.	1814	1754	1849	1789	1862
Calc.	1818.7	1757.9	1860.3	1791.7	1869.1
β-Allopyranose Exptl.	1829	1778	1849	1789	1879
Calc.	1812.7	1765.0	1846.3	1774.3	1863.8

Correlation between structure and retention

The correlation between the retention indices and the chemical structure of aldohexose TMS ethers has been examined using the approach described[5] for pentoses. Two different models have been used.

Prediction of retention data from structural descriptors. In this model, we suppose that the retention index, I_x, of a compound x on the stationary phase p can be expressed as a sum of the contributions, c_{jp}, of their descriptors, d_{xj}:

$$I_{xp} = \sum d_{xj} c_{jp}$$

The c_{jp} values can be calculated from experimental I_{xp} retention indices and descriptor values by multiple linear regression.

We have selected as molecular descriptors several structural features related to the absolute and relative positions of the OTMS groups on the furanose and pyranose rings. Unfortunately, the conformations of many hexose TMS ethers have not been reported. Scheme 2 presents the $^4C_1$ (D) conformation of hexopyranoses, that has been shown to be the preferred one for the TMS ethers of β-allo- and β-altropyranose, and of gluco-, manno-, galacto- and talopyranose α- and β-anomers at 25°C[11,12]. There are no data for the other aldohexoses (idose, gulose and α-anomers from allose and altrose), although it may be supposed that α-gulose, α-altrose and α-idose are in a $^1C_4$ (D) conformation.

The actual conformations of hexofuranose TMS ethers have not been reported. They are presented in Scheme 3 in a twist $^2T_3$ conformation, where some extracyclic carbon atoms are neither truly axial nor equatorial.

Descriptor values were calculated from the conformations shown in Schemes 2 and 3. The furanose OTMS substituents were considered as pseudoaxial or pseudoequatorial according to the conformation in Scheme 3. The significance and range of values of the hexose descriptors is shown in Table IV.

In a first step, both furanose and pyranose forms were included in the calculations. Although up to twelve descriptors were used, the quality of fit, measured from the correlation coefficient, r, was not good (r values between 0.76 and 0.78 for the five stationary phases). For this reason, we decided to consider as different the descriptor sets for furanose and pyranose forms.

For pyranoses, sixteen experimental I_x values were available for each phase (Table II). Eight descriptors provide a reasonably good fit, the r values being between 0.95 and 0.99 (Table V). The quality of fit decreased when the descriptors of α-gulose and α-altrose were calculated from their $^1C_4$ conformation; in the case of α-idose it increased slightly. The descriptor contributions were positive, with two exceptions: three OTMS groups in a *cis*-arrangement (3c) and two equatorial OTMS groups on connected carbon atoms (EE), which take negative values for the five stationary phases used. The highest contributions corresponded, in the five phases, to the number of pairs of OTMS groups on alternate carbon atoms (A13), and to the descriptors related to the number of equatorial OTMS groups (Eq1-4). Table V shows also, as an example, the experimental and calculated retention indices of α-allopyranose and β-allopyranose on the five stationary phases. Although the quality of fit was good, the method does not allow the identification of compounds having similar retentions; nevertheless, when the problem is an equilibrated mixture (as in biological samples)

this can be accomplished by considering the chromatographic pattern of the different tautomers.

In the case of furanoses, the low number of experimental I_x values limits the number of descriptors which can be used. Even when using eight descriptors the quality of fit is not good (r values between 0.71 and 0.97). The descriptors showing higher positive contributions to the retention indices are those related to the existence of equatorial OTMS groups and also the number of pairs of axial OTMS groups on alternate carbon atoms, while the β-substitution and the existence of three OTMS groups in a *cis*-position have a negative contribution.

Although it was necessary to fit the pyranose and furanose data in separate ways, there are some relationships among the descriptor values calculated for these hexose forms. In both sets, equatorial OTMS groups (Eq1-Eq4) and pairs of axial OTMS groups on alternate carbon atoms (A13) had high positive contributions to the retention indices, and the presence of three *cis*-OTMS groups (3c) had a negative value.

The descriptor values for hexose (Table V) and pentose (Table VI from ref. 5) were also similar. Equatorial OTMS groups and pairs of axial OTMS groups had also the highest positive values in pentoses, and the only pentose descriptor showing a negative contribution was that for a pair of *cis*-OTMS groups at C-2 and C-3[5].

Although the descriptor values from different sets of compounds cannot be related in a quantitative way, these similiarities confirm their physical significance, which seems to be related[5] to the overall structure of the molecule.

Prediction of structural descriptor values from retention data. In the second model we suppose that the descriptor values for a compound can be approximated by the expression

$$d_{ix} = \sum I_{xp} c_{pi} \tag{2}$$

where d_{ix} is the value of the descriptor i in the compound x, I_{xp} is the retention index of the compound x on phase p and c_{pi} the contribution of phase p to the descriptor i. From both d_{ix} values and experimental I_{xp}, c_{pi} can be calculated by a least squares fit.

As in the first model, we grouped both furanose and pyranose forms in a first least squares fit. However, the quality of fit was poor for most of the fourteen descriptors considered; r values were lower than 0.6 except for the ring size (pyranose/furanose descriptor) which had a r value of 0.71.

For this reason, we applied eqn. 2 in a separate way to furanose and pyranose forms, as in the first model. Although the quality of fit was better (r values up to 0.92 for furanoses and 0.88 for pyranoses), it was not enough to allow the accurate prediction of descriptor values in most cases. In order to achieve a useful prediction, it was necessary to carry out different calculations for α- and β-compounds. The quality of fit improved and most descriptors provided r values higher than 0.9 for pyranoses. Calculated descriptor values were correct in 95.5% of cases. The r values were even higher for furanoses, but the number of experimental data available was lower and the results were less reliable.

Table VI shows the experimental and calculated values for the descriptors of α- and β-anomers from allo- and glucopyranose.

TABLE VI

TRUE AND CALCULATED VALUES OF ALLOSE AND GLUCOSE DESCRIPTORS

Descriptor	*α-Allopyranose*		*β-Allopyranose*		*α-Glucopyranose*		*β-Glucopyranose*	
	True	*Calc.*	*True*	*Calc.*	*True*	*Calc.*	*True*	*Calc.*
2c	3	3 (2.93)	2	2 (1.68)	1	1 (1.18)	0	0 (0.02)
2t	1	1 (1.06)	2	2 (2.31)	3	3 (2.81)	4	4 (3.97)
3c	2	1 (1.41)	1	0 (0.22)	0	0 (0.03)	0	0 (0.09)
ΣEq	2	2 (1.83)	3	3 (2.57)	3	3 (3.02)	4	4 (4.13)
Eq2	1	1 (0.85)	1	1 (0.67)	1	1 (1.01)	1	1 (1.02)
Eq3	0	0 (0.40)	0	0 (0.26)	1	1 (1.13)	1	1 (1.03)
Eq4	1	1 (0.58)	1	1 (0.64)	1	1 (0.87)	1	1 (1.07)
A13	1	1 (0.51)	0	0 (−0.03)	0	0 (−0.16)	0	0 (−0.06)
AA	0	0 (0.19)	0	1 (0.58)	0	0 (−0.11)	0	0 (−0.14)
AE	3	3 (2.93)	2	2 (1.68)	1	1 (1.18)	0	0 (0.03)
EE	1	1 (0.74)	2	2 (1.73)	3	3 (2.92)	4	4 (4.12)

ACKNOWLEDGEMENTS

This work was supported by the Comision Asesora de Investigación Cientifica y Técnica (CAICYT) (Project No. 966). The authors thank M. I. Jimenez for technical assistance.

REFERENCES

1 M. F. Laker, *J. Chromatogr.*, 184 (1980) 457.
2 D. R. Knapp, *Handbook of Analytical Derivatization Reactions*, Wiley-Interscience, New York, 1979.
3 C. C. Sweeley, R. Bentley, M. Makita and W. W. Wells, *J. Am. Chem. Soc.*, 85 (1963) 2497.
4 J. Haverkamp, J. P. Kamerling and J. F. G. Vliegenthart, *J. Chromatogr.*, 59 (1971) 281.
5 A. García-Raso, I. Martínez-Castro, M. I. Páez, J. Sanz, J. García-Raso and F. Saura-Calixto, *J. Chromatogr.*, 398 (1987) 9.
6 A. E. Pierce, *Silylation of Organic Compounds*, Pierce Chem. Co., Rockford, IL, 1977.
7 R. J. Smith, J. K. Haken and M. S. Wainwright, *J. Chromatogr.*, 334 (1985) 95.
8 M. I. Páez, I. Martínez-Castro, J. Sanz, A. García-Raso, F. Saura-Calixto and A. Olano, *Chromatographia*, 23 (1987) 43.
9 S. Angyal, *Adv. Carbohyd. Chem.*, 42 (1984) 15.
10 W. O. MacReynolds, *Gas Chromatographic Retention Data*, Preston Technical Abstracts, Evanston, IL, 1966.
11 D. G. Streefkerk, M. J. A. De Bie and J. F. G. Vliegenthart, *Tetrahedron*, 29 (1973) 833.
12 D. G. Streefkerk, M. J. A. De Bie and J. F. G. Vliegenthart, *Carbohyd. Res.*, 38 (1974) 47.

Journal of Chromatography, 462 (1989) 61–69
Elsevier Science Publishers B.V., Amsterdam — Printed in The Netherlands

CHROM. 20 975

SOLUTE–SOLVENT INTERACTIONS OF MACROPOROUS METHACRYLATE ION EXCHANGERS IN SALT FORM STUDIED BY GAS CHROMATOGRAPHY

J. HRADIL* and F. ŠVEC
Institute of Macromolecular Chemistry, Czechoslovak Academy of Sciences, 162 06 Prague 6 (Czechoslovakia)
and
N. D. KAKRIASHVILI, M. N. GOGITIDZE and T. G. ANDRONIKASHVILI
Laboratory of Chromatography, Institute of Physical and Organic Chemistry, Academy of Sciences of Georgian SSR, Jikia 5 Tbilisi (U.S.S.R.)
(First received June 21st, 1988; revised manuscript received September 7th, 1988)

SUMMARY

Interaction of macroporous methyl methacrylate copolymers carrying strongly acidic sulphopropyl groups exchanged with metal ions of the IIb, VIb, VIIIb and rare earth groups of the Periodic Table with solutes —homologous alkanes, aromatic hydrocarbons, ketones, alcohols and organic acids— were studied by gas chromatography. The results show that the sorbents belong to class 3 according to Kiselev since, in addition to interactions due to dispersion forces, they also exhibit strong specific interactions. In comparison with the original copolymers, the ion exchangers carrying sulphopropyl groups exhibit stronger specific interactions, in particular with alcohols, due to hydrogen bonding. The methacrylate-based ion exchangers in salt form exhibit weaker specific interactions than the same sorbents in H^+ form. Non-specific interactions involving dispersion forces generally predominate.

INTRODUCTION

Interactions of methacrylate copolymers carrying sulphopropyl groups in the form of salts with group Ia ions were studied previously[1–3], and the magnitudes of non-specific and specific interactions were estimated by mathematical processing of experimental data.

With the aim of generalizing the conclusions obtained, we have broadened the scope of the interactions of methacrylate ion exchangers by including also salts of elements from groups IIb, VIb and VIIIb of the Periodic Table. We have tried to determine the selectivity of these sorbents, in particular applications, and the ability to vary their polarities by exchanging with different metal ions.

0021-9673/89/$03.50

EXPERIMENTAL

Materials

Methacrylate ion exchangers were prepared from macroporous glycidyl methacrylate–ethylene dimethacrylate copolymers[4] by treating the hydrolyzed copolymer with propane-sultone in an alkaline medium[5]. The basic copolymer for the synthesis of type A ion exchanger was prepared from 85% (w/w) of the cross-linking agent and 15% (w/w) of glycidyl methacrylate in the inert solvent cyclohexanol–dodecanol (91:9). The type B ion exchanger was based on a copolymer prepared from 30% (w/w) of the cross-linking agent and 70% (w/w) of glycidyl methacrylate; the ratio of the inert solvents was 85:15. Ion exchanger A is identical with type A in ref. 3 and the present type B is identical with type C of ref. 3.

Chromatography

The ion exchangers were washed successively with 1 *M* hydrochloric acid, distilled water, a solution of the chloride or nitrate of the corresponding metal (from the group Cd^{2+}, La^{2+}, Cr^{3+}, Fe^{3+}, Co^{2+}, Ni^{2+}), distilled water and finally dried. Sorbents (particle sizes 180–250 μm) were packed into stainless-steel columns (50 cm × 0.3 cm I.D.) and activated by heating to 170°C for 24 h in a stream of helium. Retention times of homologous paraffins, aromatic hydrocarbons, ketones, organic acids and alcohols were measured at 100 or 150°C in helium at a flow-rate of 50 ml/min. The retention relative to pentane, the Kováts indices and the excess molar Gibbs energy of a methylene group[6], $\Delta G^{E}(CH_2)$, were determined from these data. The Kováts indices were calculated by interpolating the retention times, t_R, between the retention ties of adjacent paraffins, t_n, t_{n+1}. The contribution of solute–solvent interactions to the Kováts retention index was evaluated by multiple linear regression[3]

$$I = I_\alpha \alpha + I_\mu \mu + I_{c_p} c_p + I_R R \tag{1}$$

where α (Å^3) and μ (D, absolute electrostatic unit) are the solute electron polarizability and dipole moment respectively, c_p (μmol/m^2) is the surface concentration of active groups and R(Å) is the ionic radius of the cation; the coefficients I_α, I_μ, I_{c_p} and I_R characterize the magnitudes of the individual contributions.

The polarizability was evaluated from the molar refraction, R_m

$$\alpha = 3R_m/4\pi N \tag{2}$$

where N is the Avogadro number ($= 6.023 \cdot 10^{23}$). The molar refraction was evaluated from the molar mass, M, density, ρ, and refractive index, n, of the solutes:

$$R_m = \frac{n^2 - 1}{n^2 + 1} \cdot \frac{M}{\rho} \tag{3}$$

Values of the dipole moments have been published elsewhere[6].

The partial molar excess free energy of the methylene group was determined from the relative retentions of homologous paraffins, using the formula[7]

$$\Delta G^{E}(CH_2) = -RT \ln \frac{V_{g(n+1)} P^0_{(n+1)}}{V_{g(n)} P^0_{(n)}} \tag{4}$$

where R is the universal gas constant (= 8.31423 J/K · mol), T is the column temperature (K), $V_{g(n)}$ and $V_{g(n+1)}$ are the specific retention volumes (ml/g) of neighbouring paraffinic hydrocarbons and $P^0_{(n)}$ and $P^0_{(n+1)}$ are the vapour pressures of pure solutes under the given conditions.

RESULTS AND DISCUSSION

Retention times of paraffins, aromatic hydrocarbons, alkenes, ethers, alcohols and carboxylic acids were determined for fourteen columns packed with methacrylate ion exchangers of two basic types, carrying sulphopropyl groups and in the forms H^+, Cd^{2+}, La^{3+}, Cr^{3+}, Fe^{3+}, Co^{2+} and Ni^{2+} (see Table I). The polymers under investigation are sufficiently stable for gas chromatography (GC), in particular in the salt form[8] where the decomposition temperature exceeded 300°C according to differential thermogravimetry (DTG).

The retentions of individual groups of compounds of the same carbon number increase in the series: paraffins < olefins < aromatic hydrocarbons < ethers < ketones < carboxylic acids. In comparison with similar ion exchangers in the form of salts with alkali metals[1–3], retention on the above ionic forms was always larger. Sorbent B, characterized by a smaller specific surface area and higher polarity, exhibited a stronger retention for water than for methanol; in the form of salts with Cd^{2+}, Co^{2+} and Ni^{2+} the retention of water was even greater than that of ethanol. Individual organic acids can be separated on sorbent A, but some tailing was observed in this case. The retention of formic acid on sorbent B was higher than that of the next homologues and the same was true for methanol, apparently owing to the formation of hydrogen bonds with the polar sorbent.

Kováts retention indices calculated from the retention times (*cf.*, Table II) enable one to compare sorbent polarity on a more general basis. First, it is apparent that the original glycidyl methacrylate copolymers are much more polar than sulphopropyl derivatives in the salt form, as evidenced by the increased Kováts indices (by 350 units for benzene and by 200 units for methanol). In the case of ion exchangers in H^+ form the interaction with alcohols increases by 230 units, but interactions with benzene and methyl ethyl ketone decrease somewhat (by 200 and 500 units, respectively).

With the exception of interactions of ion exchangers in the form of Ag^+ salts (*cf.*, ref. 3) and of those between the original methacrylate copolymers and aromatic hydrocarbons or ketones, the interactions of ion exchangers in salt form with alcohols represent the only selective interaction in this broad spectrum of sorbents (32 types). Specific interactions were so large that the retention order was reversed as discussed below. In the series of aromatic hydrocarbons and ketones the interactions increased in the series: styrene–divinylbenzene copolymers < methacrylate ion exchangers in the form of salts with alkali metals[3] < methacrylate ion exchangers in the form of salts with heavy metals ≪ glycidyl methacrylate–ethylene dimethacrylate copolymers ≪ methacrylate ion exchangers in Ag^+ form. On the other hand, interactions with alcohols increase in the series styrene–divinylbenzene copolymers ≪ glycidyl methacrylate–ethylene dimethacrylate copolymers < methacrylate ion exchangers in the form of salts with alkali metals[3] ≈ methacrylate ion exchangers in the form of salts with heavy metals.

The statistical significance of correlation between the Kováts indices and either

TABLE I

RETENTION TIMES RELATIVE TO PENTANE OF SOLUTES ON METHACRYLATE ION EXCHANGERS AT 150°C

Solute	*Form H^+*		*Form Cd^{2+}*		*Form La^{3+}*	
	A	*B**	*A*	*B**	*A*	*B**
Hexane	2.30	1.36	2.36	1.54	2.56	1.66
Heptane	2.95	2.27	5.70	2.54	6.83	2.33
Octane	16.38	4.27	17.5	4.72	18.16	4.00
Nonane	47.18	8.00	**	9.36	39.32	7.33
Decane	109.73	15.90	***	17.72	***	15.00
Undecane	***	32.54	***	35.38	***	29.33
Benzene	3.72	3.45	4.16	2.00	4.06	2.33
Toluene	10.26	6.81	13.08	3.90	11.32	3.66
Ethylbenzene	24.18	9.81	34.25	7.45	24.89	6.00
Isopropylbenzene	***	11.54	63.25	10.45	50.00	9.33
1,2,4-Trimethylbenzene	37.43	27.27	***	14.27	79.96	13.33
o-Xylene	26.80	10.27	27.91	7.90	39.64	6.66
m-Xylene	23.72	10.18	22.07	6.81	34.19	6.66
p-Xylene	18.07	10.27	22.25	6.63	28.74	6.00
Cyclohexane	2.89	1.36	3.42	1.54	4.01	1.00
1-Hexene	2.35	1.54	2.63	1.54	3.10	1.66
1-Octene	14.87	5.00	24.44	5.18	51.28	4.33
Diethyl ether	1.53	2.72	1.47	1.54	1.73	1.00
Di-*n*-butyl ether	58.46	15.18	**	12.00	***	10.66
Acetone	2.30	32.27	2.31	11.54	3.42	4.33
Methyl ethyl ketone	4.20	15.63	5.55	6.09	6.41	3.66
Diethyl ketone	11.03	14.36	14.36	5.72	16.66	4.00
Methyl butyl ketone	4.35	41.18	**	11.63	**	8.33
Water	0.80	34.54	1.52	45.18	1.25	29.00
Methanol	1.00	22.00	3.80	20.45	1.32	16.00
Ethanol	2.12	47.00	2.41	38.18	2.85	21.00
Propanol	5.89	40.90	7.31	61.36	3.74	15.66
Isopropanol	3.84	20.00	3.97	7.54	5.03	4.33
n-Butanol	18.27	41.09	33.61	21.54	14.10	11.66
Isobutanol	11.66	11.18	16.07	9.36	18.05	6.66
sec.-Buanol	9.35	18.18	12.58	9.27	11.85	5.66
tert.-Butanol	0.64	2.09	7.50	5.72	6.85	4.00
n-Pentanol	***	26.09	55.02	29.54	46.83	22.33
2-Pentanol	***	25.00	27.41	20.72	**	11.00
n-Hexanol	***	51.54	***	53.81	***	35.66
n-Heptanol	***	38.63	***	91.63	***	68.33
n-Octanol	***	58.45	***	109.4	***	69.33
Formic acid	0.87	60.63	1.07	42.90	***	152.3
Acetic acid	11.73	32.70	1.47	52.27	**	41.00
Propionic acid	22.43	55.27	2.36	52.00	**	244.3

* At 100°C.

** No elution.

*** Data were not obtained.

Form Cr^{3+}		Form Fe^{3+}		Form Co^{2+}		Form Ni^{2+}	
A	*B**	*A*	*B**	*A*	*B**	*A*	*B**
2.29	1.54	2.39	1.36	2.35	1.46	2.72	1.62
7.20	2.72	5.66	2.27	5.79	2.46	5.02	2.50
17.74	5.00	15.88	4.09	14.56	4.80	13.19	4.45
**	8.45	43.54	8.36	35.15	9.13	37.84	9.12
***	18.00	113.2	16.36	87.26	20.2	85.02	17.25
***	41.36	***	29.54	***	38.00	***	32.25
5.10	2.09	4.94	2.00	3.92	2.20	2.31	2.25
11.82	4.27	12.96	3.45	10.13	3.80	7.38	4.12
35.75	8.45	31.13	6.18	27.50	4.00	18.86	6.50
**	12.72	59.90	9.27	43.86	10.86	***	9.37
***	17.45	60.37	12.90	59.90	16.46	***	13.12
30.82	8.45	24.90	6.54	9.75	7.46	***	7.25
27.33	7.54	21.84	6.18	7.20	6.20	***	7.25
28.49	8.18	21.00	6.09	4.86	6.66	26.73	6.87
2.96	1.36	2.67	1.18	2.50	1.46	2.31	1.62
2.68	1.54	2.35	1.36	2.35	2.09	2.36	1.62
20.69	5.18	12.98	4.27	11.54	5.00	18.75	5.25
1.34	1.54	1.47	1.54	1.47	1.13	1.34	1.50
**	14.72	47.79	10.63	1.11	11.13	42.36	11.25
2.11	9.54	2.35	13.90	2.03	14.66	2.25	10.37
5.19	5.18	4.49	5.45	4.47	7.40	5.20	4.12
16.45	5.27	12.49	4.81	12.41	7.20	12.84	4.75
**	12.09	33.96	9.27	32.20	13.33	42.81	10.25
1.62	43.18	1.28	31.54	1.37	56.86	–	61.62
1.66	22.45	2.35	17.72	2.73	21.80	1.62	22.50
5.16	47.72	2.13	35.63	2.26	48.80	2.95	36.00
13.89	38.63	5.66	31.36	5.86	44.46	9.16	38.87
5.59	4.81	3.45	5.63	3.52	9.46	3.47	5.25
28.84	12.09	16.83	13.63	14.47	22.80	13.38	14.62
15.23	6.09	12.69	6.09	11.69	10.13	12.80	7.75
10.56	5.90	8.52	6.63	9.05	10.00	8.68	6.50
3.09	3.81	5.66	3.81	5.79	5.80	5.38	4.62
***	23.00	22.49	24.27	39.05	35.33	***	30.00
***	10.27	21.28	11.54	31.13	22.80	***	21.25
***	29.09	77.35	37.72	96.54	58.33	***	53.12
***	64.63	***	61.36	***	125.5	***	107.2
***	81.09	***	64.36	***	***	***	112.5
3.60	47.72	11.09	45.72	9.96	48.86	6.56	59.37
**	37.90	23.58	40.90	15.33	68.86	9.48	112.5
**	109.1	47.16	101.4	37.41	94.46	**	110.4

TABLE II

KOVÁTS RETENTION INDICES ON METHACRYLATE ION EXCHANGERS AT 150°C

Solute	*Copolymers*		*Form* H^+		*Form* Cd^{2+}		*Form* La^{3+}	
	A	*B*	*A*	*B**	*A*	*B**	*A*	*B**
Benzene	709	956	715	767	656	655	649	700
Toluene	795	1051	773	875	775	770	753	785
Ethylbenzene	***	1136	838	931	**	867	743	869
Isopropylbenzene	***	***	908	954	**	918	**	935
1,2,4-Trimethylbenzene	***	***	879	1076	**	968	**	985
Methanol	514	809	500	1046	655	1023	529	1010
Ethanol	588	846	590	**	603	**	613	1052
Propanol	625	951	741	**	723	**	640	1009
n-Butanol	***	1083	811	**	**	1031	776	967
Isobutanol	***	***	781	950	793	900	800	886
sec.-Butanol	***	***	768	1019	771	899	758	859
tert.-Butanol	***	***	**	686	726	829	701	800
n-Pentanol	***	1169	***	1070	**	1076	***	1062
2-Pentanol	***	***	***	1037	**	1025	***	901
n-Hexanol	***	***	***	**	***	**	***	**
Diethyl ether	553	607	551	729	545	600	558	500
Di-*n*-butyl ether	***	970	926	994	***	937	***	954
Acetone	621	863	600	1099	597	934	631	814
Methyl ethyl ketone	713	950	785	**	698	838	841	695
Diethyl ketone	***	***	800	**	783	829	823	793
Methyl butyl ketone	***	1116	724	724	***	935	***	818

* At 100°C.

** Data were not calculated.

*** Data were not obtained.

the ionic radius or the molar mass of the cation was tested on the whole set of data. Significant dependences were found for methanol and methyl ethyl ketone. In the case of benzene, although the values varied over a broad interval, the correlation was not significant, because these interactions were of a different nature, involving mostly the polymer matrix. The Kováts indices in general decrease with increasing ionic radius and increasing molar mass of the cation.

To conclude, three specific interactions are typical for the investigated methacrylate ion exchangers:

(1) between the methacrylate ion exchanger in salt form and alcohols and carboxylic acids, interpreted as due to the formation of hydrogen bonds;

(2) between glycidyl methacrylate–ethylene dimethacrylate copolymers and aromatic hydrocarbons and ketones, attributed to the formation of coordinate bonds;

(3) between the methacrylate ion exchangers in Ag^+ form[3] and aromatic hydrocarbons and ketones, ascribed to the formation of coordinate compounds which involve a double bond.

Form Cr^{3+}		*Form Fe^{3+}*		*Form Co^{2+}*		*Form Ni^{2+}*	
A	*B**	*A*	*B**	*A*	*B**	*A*	*B**
670	656	685	678	657	618	584	680
757	777	781	772	761	765	740	789
**	900	868	858	874	773	810	856
***	955	935	916	926	922	***	908
***	997	936	966	959	975	***	960
561	1029	598	1015	617	1014	548	1044
672	**	587	**	595	**	634	**
774	1096	600	**	702	**	762	**
**	949	806	974	800	1021	801	977
785	841	779	856	777	913	797	880
704	835	740	868	749	913	757	856
627	758	700	789	700	830	707	808
***	1031	835	1067	913	1092	***	1089
***	928	830	949	888	1021	***	1036
***	1061	962	**	***	***	***	**
535	600	544	626	545	532	529	584
***	975	912	937	**	925	916	936
590	918	598	937	583	961	581	923
673	811	674	841	672	863	704	790
793	814	777	823	783	863	797	812
***	949	877	815	892	900	918	922

TABLE III

COEFFICIENTS CALCULATED USING EQN. 1 AND AVERAGE CONTRIBUTIONS TO THE KOVÁTS INDICES

Mean square deviations: * 35.6; ** 22.1; *** 94.8.

	Solution interaction		*Sorbent interaction*		*Average contribution (%)*			
	I_α	I_μ	I_{c_p}	I_R	$I_\alpha\bar{\alpha}$	$I_\mu\bar{\mu}$	$I_{c_p}\bar{c}_p$	$I_R\bar{R}$
Aromatic hydrocarbons*	−482	3.06	1.43	−149.5	75.2	0.1	2.4	22.3
Ethers**	−426	−56.2	2.33	−161	63.9	7.9	3.9	24.3
Alcohols***	−314	−427	14.6	−133	17.6	47.4	19.3	2.25

TABLE IV

VALUES OF PARTIAL MOLAR EXCESS GIBBS FREE ENERGY OF A METHYLENE GROUP, $\Delta G^E(CH_2)$ (kJ/mol), OF METHACRYLATE ION EXCHANGERS

Sorbent A; standard deviation ± 0.66 kJ/mol.

Form H^+	*Form* Cd^{2+}	*Form* La^{3+}	*Form* Cr^{3+}	*Form* Fe^{3+}	*Form* Co^{2+}	*Form* Ni^{2+}
−1.04	−1.42	−1.40	−1.19	−0.92	−0.80	−0.37

Multiple linear regression of Kováts indices (eqn. 1), which includes contributions of (i) the solute (characterized by electron polarizability and dipole moment) and (ii) the sorbent (characterized by the surface concentration of groups and by ionic radius), indicated that this equation is valid also for the ion exchangers containing heavy metal ions. The contribution of non-specific interactions in this case was somewhat smaller (75% as compared to 98% for aromatic hydrocarbons, Table III). Non-specific interactions involving dispersion forces further decrease to 17% for alcohols, where the contribution of dipole–dipole interactions rises to 46%. Contribution (ii) due to the sorbent remains approximately constant at 22–28%. These values and the general trends are similar to those established for the series which included salts with alkali metals[3]. Hence, the sorbents investigated belong to class 3 of the Kiselev classification[9].

Thermodynamic quantities can be used for correlating sorbent polarity. Values of the partial molar excess free energy of a methylene group, $\Delta G^E(CH_2)$, range between −0.37 and −1.04 kJ/mol for the ion exchanger based on polymer A with sulphopropyl groups in H^+ form (Table IV), and parallel the increase in polarity measured by the Kováts indices. However, $\Delta G^E(CH_2)$ is inferior to the Kováts indices in that it is not sensitive enough in reflecting the transition from the original polymer to the ion exchanger with sulphopropyl groups in different ionic forms: whilst the Kováts indices order the individual sorbents into well defined series, the overall difference in $\Delta G^E(CH_2)$ within the investigated series of sorbents (0.82 kJ/mol for series A) is comparable with the standard deviation (± 0.66 kJ/mol). Moreover, the values are complicated by inaccuracies in the heats of evaporation. The molar excess enthalpy would be more exact but less sensitive still to the variation in solvent polarity.

The values of $\Delta G^E(CH_2)$ found in this study are smaller than those determined for Porapak P and T[7] but also negative, indicating that the heats of adsorption of all solutes are larger than their heats of evaporization.

CONCLUSIONS

Because of their macroporous structure the copolymers studied can be used also in the analysis of organic compounds in aqueous solutions. They can be used for separation of hydrocarbon isomers, ketones, ethers and alcohols.

REFERENCES

1 T. G. Andronikashvili, N. M. Gogitidze, J. Hradil and F. Švec, *J. Chromatogr.*, 291 (1984) 103.
2 T. G. Andronikashivili, N. M. Gogitidze, J. Hradil and F. Švec, *Proc. Acad. Sci. Georgian SSR, Chem. Ser.*, 10 (1984) 67.
3 J. Hradil, F. Švec, N. M. Gogitidze and T. G. Androkašvili, *J. Chromatogr.*, 324 (1985) 277.
4 F. Švec, J. Hradil, J. Čoupek and J. Kálal, *Angew. Makromol. Chem.*, 48 (1975) 135.
5 C. M. A. Ribeiro, J. Hradil, F. Švec and J. Kálal, *Angew. Makromol. Chem.*, 87 (1980) 119.
6 R. C. Weast (Editor), *Handbook of Chemistry and Physics*, CRC Press, Boca Raton, FL, 1979, p. E 66.
7 J. Novák, J. Růžičková, S. Wičar and J. Janák, *Anal. Chem.*, 45 (1973) 1365.
8 J. Hradil and F. Svec, *Angew. Makromol. Chem.*, 135 (1985) 85.
9 A. V. Kiselev, *Zh. Fiz. Khim.*, 41 (1967) 2470.

Journal of Chromatography, 462 (1989) 71–84
Elsevier Science Publishers B.V., Amsterdam — Printed in The Netherlands

CHROM. 20 986

BEHAVIOR OF SIMPLE SALTS ON SILICA AND C_{18} COLUMNS

RETENTION DYNAMICS OF CATIONS, ANIONS AND ION PAIRS

LOUIS G. DAIGNAULT*, DONALD C. JACKMAN and D. PAUL RILLEMA
Department of Chemistry, The University of North Carolina at Charlotte, Charlotte, NC 28223 (U.S.A.)
(First received February 4th, 1988; revised manuscript received July 22nd, 1988)

SUMMARY

The retention behavior of simple inorganic salts on silica and ODS columns was investigated by high-performance liquid chromatography with methanol–water (80:20, v/v) as the mobile phase. Both a major (dissolved salt) and a minor (ion pair) peak were observed on the ODS columns; only the major peak was present on silica columns. The retention time of the major peak was a function of the number of moles of salt placed on the column and was sigmoidal with respect to the logarithm of the number of moles analyzed. The retention time of the minor peak was dependent upon the composition of the mobile phase. It disappeared in a mobile phase of water and was absent on a silica column. The general behavior was independent of the anion or cation being analyzed. The sigmoidal behavior of salt retention was attributed to both cationic and anionic exchange at the silica surface; the ion pair retention was attributed to solubility in the C_{18} phase of the ODS columns. The areas under the major peak and the minor peak were used to calculate ion pair formation constants. For sodium nitrate, $K = 15 \cdot 10^{-3}\ M^{-1}$; for sodium nitrite, $K = 2.0 \cdot 10^{-3}\ M^{-1}$. The ion pair formation constants were used to calculate the theoretical distance of closest approach between the ions based on Bjerrum theory. For sodium nitrate, the distance calculated between center of Na^+ and NO_3^- in the ion pair was 6.5 Å.

INTRODUCTION

Recently we used high-performance liquid chromatographic (HPLC) techniques to identify the reaction products formed in photoelectrochemical cells[1]. The retention times of all known components of the reaction were determined on a Partisil ODS-2 column using methanol–water (80:20, v/v) as mobile phase at a flow-rate of 0.7 ml/min. During the identification procedure, a 25% difference in retention time between the reference sodium EDTA solution (t_R = 3.45 min) and the sample sodium EDTA solution from the reaction cell (t_R = 4.35 min) was observed. According to existing practice, sodium EDTA should have exhibited a constant t_R rather than the observed variation. This result was unexpected and suggested that perhaps sodium EDTA was retained on ODS columns and perhaps the common practice of measuring t_m by injection of a "non-retained" ionic species[2] should be reexamined.

0021-9673/89/$03.50

In this study we have investigated the retention behavior of mono-charged salts on various ODS and silica columns. Systems peaks as well as anion peaks were observed in the absence of ion-pairing agents. The anion retention behavior is explained on the basis of competition between the cation and anion for active sites on the column. Finally, we suggest that the separation of two components, the dissolved solid and the ion pair, can be used to estimate ion pairing constants in the mobile phase.

EXPERIMENTAL

Materials

Reagent grade sodium salts were used. Methanol was HPLC grade and water was purified with a Milli-Q reagent grade water system.

HPLC systems

One HPLC apparatus consisted of a Perkin-Elmer Series 2/2 solvent delivery system equipped with a Rheodyne Model 7125 injection valve (20-μl loop), a Model LC-75 variable-wavelength detector and an autocontroller. Recordings of chromatograms were made on a Hewlett-Packard Model 3390A computing integrator. The analytical columns used were 250 × 4.6 mm I.D. Partisil 1025 ODS, ODS-2 and ODS-3. The columns were protected by a 70 × 2.1 mm I.D. guard column containing Whatman CO: PELL ODS. The inorganic anions were detected at 205 nm. The flow-rate was 0.7 ml/min.

The second HPLC system consisted of a Perkin-Elmer Series 100 pump system equipped with a Rheodyne Model 7010 injector valve (10 μl loop) and a Tri Det detector. Recordings of the chromatograms were made on a Series 5000 Fisher Recordall. The column used was a 3 × 3 Perkin-Elmer HC-3 C_{18} column.

The third system consisted of a Dionex Series 4000i system equipped with a 50-μl loop, conductivity detector and Dionex anion and cation micro-membrane suppressors. Recordings of the chromatograms and data handling were made using both a Spectra-Physics SP 4290 integrator and an Epson Equity +1 computer equipped with a Spectra-Physics Labnet software program. The columns used were HPIC-AS4A analytical with a HPIC-AG4A guard for the anions and a HPIC-CS3 with a HPIC-CG3 guard for the cations (all the columns from Dionex).

Solution conductivities were obtained in methanol–water (80:20, v/v) at 25° ± 0.1°C with a Model RC-18A Beckman conductivity bridge. The temperature was controlled with a Haake FK-2 constant-temperature bath.

The concentrations of the sodium and nitrate ions were obtained in the following manner. First, the appropriate sample, mobile phase or sample peak, was collected in an inert plastic syringe from the effluent of the Perkin-Elmer Series 2 HPLC system. The size of the peak samples ranged in size from 0.5 to 0.7 ml. The concentration of sodium and nitrate in the various samples was then measured by injecting the samples into the Dionex ion chromatography system.

RESULTS

Retention behavior of simple salts

The retention behavior studies were carried out using Partisil 1025 ODS, ODS-2 and ODS-3 reversed-phase columns and a silica A normal phase column. The specifics of these columns are shown in Table I. The general behavior on the three ODS columns is illustrated in Fig. 1. The sodium salts used in this study contained iodate, iodide, nitrite and bromide anions and the mobile phase was methanol–water (80:20, v/v). As shown in Fig. 1, the retention times of the salts on various reversed-phase ODS columns were a function of the number of moles injected onto the column. Furthermore, there was up to a 60% increase in retention time over the range $2 \cdot 10^{-9}$–$9 \cdot 10^{-6}$ mol. This behavior was independent of carbon loading, available silanol sites and whether the column was capped or uncapped. Some additional features shown in Fig. 1 are: (1) retention times of the simple salts follow a pattern grouping themselves about a line characteristic of each column; (2) in the 10^{-9}–10^{-8} mol region, the retention times on various ODS columns were fairly constant, but different for each one; (3) in the $5 \cdot 10^{-8}$–$1 \cdot 10^{-6}$ mol region, a more linear increase in retention time occurred; (4) for quantities greater than 10^{-6} mol, retention times became fairly constant which could be attributed to saturation of the column since, at this point, tailing of peaks started to occur; (5) the scatter of points for each column, especially at higher number of moles, is probably due to variations in the atomic configurations of the monovalent anions injected onto the column; and (6) the retention behavior on each column appears to be relatively independent of the salt used.

TABLE I

WHATMAN PARTISIL 1025* AND PERKIN ELMER SILICA A** COLUMN SPECIFICATIONS

Whatman columns	*Carbon loading (%)*	*Available silanols*** (%)*
ODS	5	50
ODS-2	15	25
ODS-3	10	≈ 0.5§

* Physical properties: irregular shaped; particle size, 10 μm; surface area, 350 m^2/g; pore volume, 0.85 ml/g; pore diameter, 85 Å.

** Physical properties: irregular shaped, particle size 10 μm; pore diameter, 60 Å.

*** Available silanols refers to SiOH groups on the end of the C_{18} chain attached to the surface of the silica beads.

§ "Capped" column: available silanols on end of C_{18} chain were converted to $-SiOCH_3$ groups.

Retention behavior of sodium nitrate

Sodium nitrate is recognized as a strong electrolyte and devoid of acid-base properties. Hence, it was chosen as a standard for documenting the general salt behavior observed above. Careful studies on ODS columns revealed that in addition to a major component, a minor peak for sample salts was present at longer retention

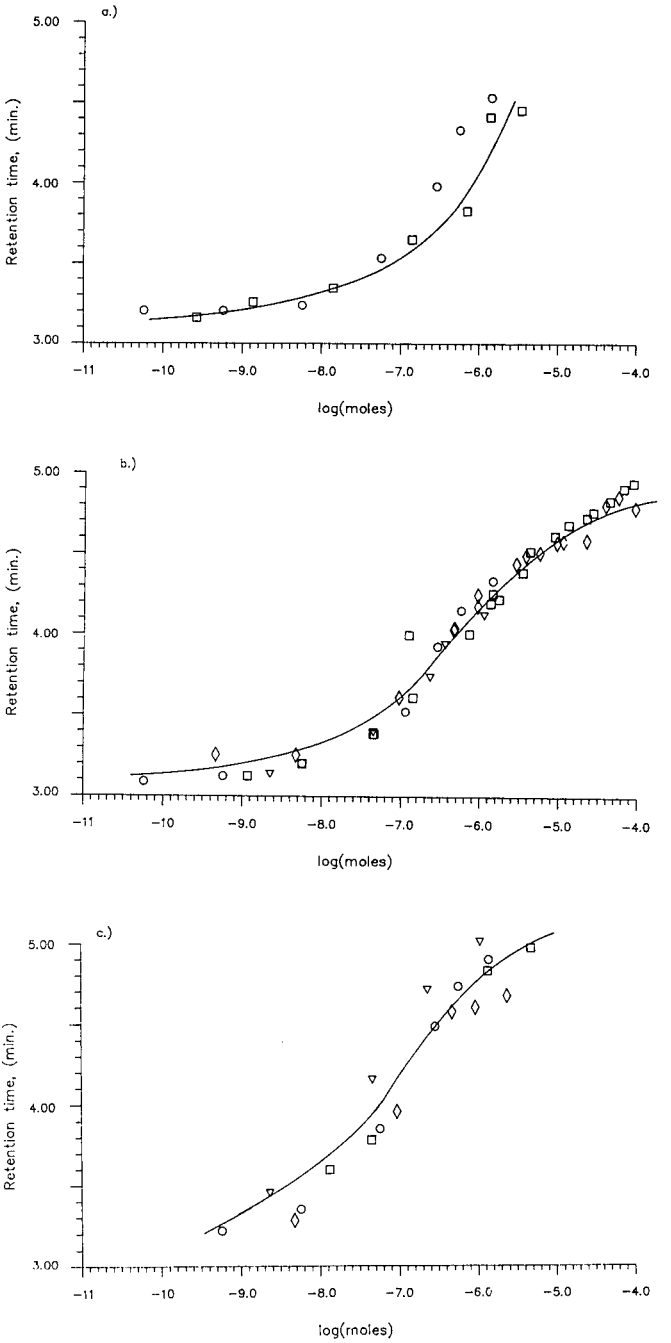

Fig. 1. Retention times (min) for sodium iodate (▽), sodium iodide (○), sodium nitrite (□), sodium bromide (◇), as a function of the logarithm of the number of moles of salt on ODS (a), ODS-2 (b) and ODS-3 (c). The mobile phase was methanol–water (80:20, v/v) (pH 7). The flow-rate was 0.7 ml/min, T = 20 ± 2°C.

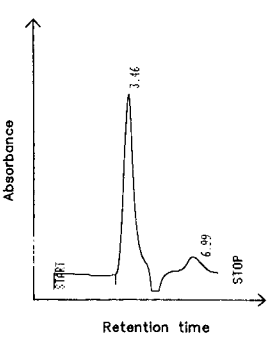

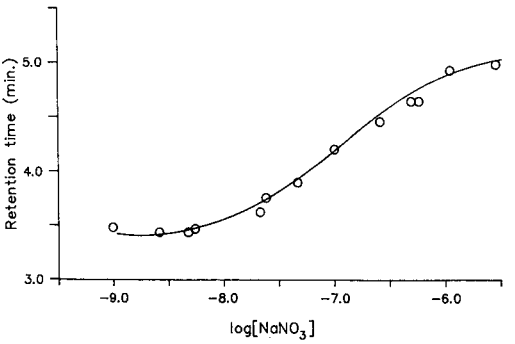

Fig. 2. Chromatogram of sodium nitrate showing the major peak (3.48 min) and the minor peak (6.96 min) on an ODS-2 column. The mobile phase of methanol–water (80:20, v/v) at a pH 6.3 and a flow-rate of 0.7 ml/min. The peak below baseline is a systems peak. These have recently been described in ref. 7.

Fig. 3. Retention time (min) for sodium nitrate as a function of the logarithm of the number of moles of sodium nitrate injected, onto an ODS-2 column. The mobile phase was methanol–water (80:20, v/v) (pH 6.8) and the flow-rate was 0.7 ml/min.

times. This is shown in Fig. 2 for sodium nitrate. The retention behavior on an ODS-2 column of the major peak as a function of column loading is shown graphically in Fig. 3.

Effect of sample concentration

Variations in retention time were studied as a function of sample concentration. Samples of 20 μl containing various concentrations of sodium nitrate were injected onto an ODS-2 column. According to the data in Table II, the retention time of the major peak decreased as the concentration decreased while the retention time of the minor peak remained constant. This data could be interpreted to mean that the retention time depended on concentration. However, the final column in Table II indicates that 2-μl injections of solutions of differing molarity gave the same retention time as those in column one. Thus, the resulting retention times correspond to those based on the total number of moles of sodium nitrate injected onto the column.

TABLE II

RETENTION TIMES OF SODIUM NITRATE AT VARIOUS CONCENTRATIONS

Sodium nitrate concentration (M)	*Retention time (min)**		*Retention time (min)***
	Major peak	*Minor peak*	*Major peak*
$1 \cdot 10^{-4}$	3.27	6.8	3.41***
$1 \cdot 10^{-3}$	3.62	6.9	3.65§
$1 \cdot 10^{-2}$	4.34	6.9	4.45§§

* Column: Partisil ODS-2; mobile phase, methanol–water (80:20, v/v) at a flow-rate of 0.7 ml/min, pH 6.8; sample size 20 μl; detection 205 nm.

** Retention time from Fig. 3 based on the number of moles of sodium nitrate in the sample.

*** 2 μl injection of 0.0010 *M* sodium nitrate.

§ 2 μl injection of 0.010 *M* sodium nitrate.

§§ 2 μl injection of 0.10 *M* sodium nitrate.

TABLE III

RETENTION TIME OF SODIUM NITRATE (0.0100 *M*): DEPENDENCE ON AMOUNT

Column: Partisil ODS-2; mobile phase, methanol–water (80:20, v/v) at a flow-rate of 0.7 ml/min, pH 6.8.

Sample size (μl)	*Retention time (min)*		*Approximate area ratio*
	Major peak	*Minor peak*	
10.0	4.15	6.81	300:1
5.0	3.95	6.85	100:1
0.5	3.58	6.88	32:1
0.1	3.38	6.91	6:1

Sample size

The injection volume was varied and the other parameters were held constant. The data in Table III indicate that the retention time of the minor peak remained constant while the retention time of the major peak decreased as the sample size decreased.

Mobile phase polarity

The polarity of the mobile phase was changed by altering the mole fraction of methanol–water from zero to one. According to the data in Table IV, the retention time of the minor peak tripled as the mole fraction of water in the mobile phase increased. In addition, the area ratio of the major to the minor peak increased as the mole fraction of water in the mobile phase increased and eventually at high levels of water the minor peak disappeared.

TABLE IV

RETENTION TIME OF SODIUM NITRATE IN VARIOUS METHANOL–WATER MOBILE PHASES

Column: Partisil ODS-2; flow-rate 0.7 ml/min, pH 6.8; sample size $4 \cdot 10^{-7}$ *M*.

Methanol (%)	*Retention time (min)*		*Approximate area ratios*
	Major peak	*Minor peak*	
100	4.00	4.97	40:1
90	4.07	5.23	30:1
80	4.13	5.55	45:1
60	4.14	7.48	50:1
40	4.12	10.58	50:1
20	4.17	14.14	100:1
0	4.14	–	–

Quantitative assessment of the sodium and nitrate-minor peak

The results of nineteen measurements on the concentration of the nitrate ion in the minor peak gave an average value of $1.858 \cdot 10^{-9}$ M, $\sigma = 2.831 \cdot 10^{-10}$. An average of six measurements on the sodium concentration resulted in an average value of $2.475 \cdot 10^{-9}$ M, $\sigma = 5.77 \cdot 10^{-10}$. These results indicate a sodium-to-nitrate ratio of approximately one to one was found in the minor peak region.

The content of sodium and nitrate in the mobile phase assessed between the major and minor peaks was $1.843 \cdot 10^{-9}$ M, $\sigma = 1.64 \cdot 10^{-10}$, for sodium and below the detection limit for nitrate. Clearly, the minor peaks components are significant compared to the background.

TABLE V

RETENTION TIMES OF TBAN AND SODIUM NITRATE ON AN ODS-2 COLUMN

Mobile phase, methanol–water (80:20, v/v), flow-rate was 0.7 ml/min, pH = 6.9.

Moles	t_R *(TBAN) (min)*	t_R *(sodium nitrate) (min)*
$1 \cdot 10^{-9}$	3.38	3.42
$5 \cdot 10^{-9}$	3.38	3.44
$5 \cdot 10^{-8}$	3.64	3.88
$1 \cdot 10^{-7}$	3.98	4.23
$5 \cdot 10^{-7}$	4.37	4.69
$1 \cdot 10^{-6}$	4.63	4.89

Comparison of cations

The retention times of the major peaks of sodium nitrate on an ODS-2 column are compared to those of *tert.*-butylammonium nitrate (TBAN) on the same column in Table V. The retention times of sodium nitrate were slightly longer than those of TBAN, but both followed the same trend of a slight increase in retention time as the column sample loading increased.

The retention times for both salts were also determined on a silica column as a function of pH after adjusting the mobile phase with a small amount of 11.6 M perchloric acid. At low pH (2.7), the retention times for TBAN and sodium nitrate were nearly constant as given in Table VI. At a pH 4.9 and 6.3, TBAN followed the same trend observed for sodium nitrate. However, the retention time change was about a factor of 2 greater for TBAN than for sodium nitrate. In addition, the retention times of TBAN and sodium nitrate are reversed; now TBAN is retained by the column longer than sodium nitrate.

Systems peaks

Systems peaks were observed for samples containing methanol–water ratios other than 80:20 (v/v). These peaks were observed between the injection peak and the minor peak. The peaks were in the positive direction for greater methanol content

TABLE VI

RETENTION TIME OF TBAN AND SODIUM NITRATE ON A SILICA COLUMN AT VARIOUS MOBILE PHASE pH VALUES

Mobile phase, methanol–water (80:20, v/v), flow-rate was 0.7 ml/min.

Moles	*TBAN*			*Sodium nitrate*		
	pH 6.3	*pH 4.9*	*pH 2.7*	*pH 6.3*	*pH 4.9*	*pH 2.7*
$1 \cdot 10^{-9}$	3.91	3.72	5.81	3.47	3.37	6.23
$5 \cdot 10^{-9}$	4.10	3.83	6.06	3.44	3.56	6.23
$5 \cdot 10^{-8}$	4.91	4.51	6.06	3.88	3.85	6.23
$1 \cdot 10^{-7}$	5.01	4.96	6.03	4.23	4.06	6.14
$5 \cdot 10^{-7}$	5.75	5.75	6.27	4.67	4.57	6.23
$1 \cdot 10^{-6}$	5.85	6.07	6.11	4.89	4.56	–

(higher absorbance) and in the negative direction for greater water content (lower absorbance).

Conductivity detection

In all the previous studies, the mobile phase was monitored with a UV–VIS detector. The generality of the results was verified with a different instrument and a different detector. Both TBAN and sodium nitrate samples were injected onto a Perkin-Elmer HS-3, C_{18}, 3 × 3, ODS column and eluted with a methanol–water (80:20, v/v) mobile phase. A major peak eluted after 0.60 min for both salts; a minor peak eluted after 2.40 min for a sodium nitrate sample and after 2.54 min for a TBAN sample. The ratio of the major component to the minor component was 29:1 for the TBAN sample and 86:1 for the sodium nitrate experiment.

Dilution conductivity

Dilution conductivity studies were effected according to the procedures of Boggess and Zatko[3]. In water, sodium nitrate was completely dissociated in the 10^{-4}–10^{-1} *M* range. However, as shown in Figs. 4 and 5, both sodium nitrate and TBAN give non-linear equivalent conductance plots indicative of ion pairs in methanol–water (80:20, v/v). This is expected in solvents of low dielectric constants.

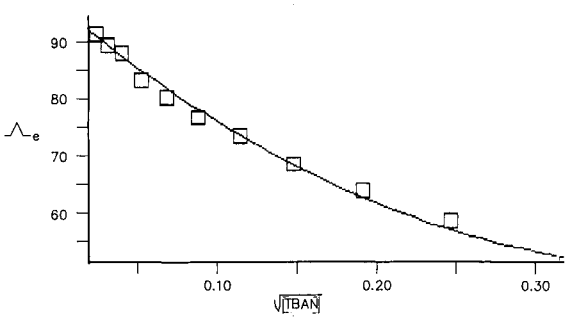

Fig. 4. Dilution conductivity profile for TBAN in methanol–water (80:20, v/v). $T = 25.0 \pm 0.1$°C.

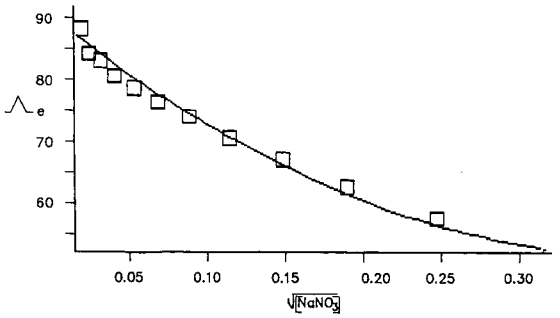

Fig. 5. Dilution conductivity profile for sodium nitrate in methanol–water (80:20, v/v). $T = 25.0 \pm 0.1$°C.

Solomon and Uchiyama[4] recently reported formation constants for ion doublets and triplets in solvents of low dielectric constants ranging from 3 to 10. The ion pairing constants reported by Solomon and Uchiyama were large, ranging from 10^4 to 10^{11} M^{-1}.

DISCUSSION

The experimental observations can be summarized as follows: (1) both a major and a minor peak were observed; (2) the major peak has the shorter retention time, the minor peak the longer one; (3) the retention time of the major peak changed as the number of moles of simple salt injected onto the column increased; (4) the retention time of the major peak remained constant as the composition of the mobile phase was varied; (5) simple salts behave similiarly on the same column; (6) a comparison of the columns, silica, ODS, ODS-2 and ODS-3 indicates that the retention behavior of simple salts follows the same trend, but retention times differ somewhat for different columns; (7) the retention time of the minor peak increased as the water composition of the mobile phase increased and disappeared after the water fraction increased to one; (8) dilution conductivity indicates that simple salts are ion paired in methanol–water (80:20, v/v); (9) systems peaks derived from the solvent were observed when the sample injected onto the column was in a solvent other than methanol–water (80:20, v/v); (10) both sodium and nitrate were observed in the minor peak in a 1:1 molar ratio.

Systems peaks in this study were expected. They are reported to appear in liquid chromatograms when the mobile phase contains more than one component[5] and the sample is dissolved in a solution different from the mobile phase[6,7]. The systems peaks observed here meet this requirement. A positive peak at $t_R = 5.1$ min is observed for samples in more concentrated methanol and a negative peak is observed at $t_R = 4.7$ min for samples containing greater water content than the methanol–water (80:20, v/v) ratio. Both of these peaks also meet another criterion for systems peaks, the areas are non-linear with respect to sample size.

The major and minor peaks, on the other hand, are linear with respect to sample size and their presence can be explained on the basis of eqn. 1,

$$M^+ + A^- \overset{K_s}{\rightleftharpoons} (M^+, A^-)_s \overset{K_c}{\rightleftharpoons} (M^+, A^-)_c \qquad (1)$$

where M^+ and A^- are the dissociated ions, $(M^+, A^-)_s$ is the ion pair in the mobile phase, $(M^+, A^-)_c$ is the ion pair on the column and K_s and K_c are the respective equilibrium constants. The major peak is associated with the dissociated salt, $M^+ + A^-$ and $(M^+, A^-)_s$; the minor peak is associated with the ion pair, $(M^+, A^-)_c$. The rationale for the assignment is as follows: dilution conductivity results in methanol–water (80:20, v/v) clearly indicate that the major species in solution is the dissociated salt, but ion pairs are also present. Thus, variation in the retention time of the major fraction as a function of column loading is related to either interaction of the dissociated cation or anion with the column. Neither the identity of the monocation, the identity of the monoanion, nor the type of column appear to play a significant role in altering the retention behavior of the major peak. The pH of the mobile phase, however, does alter the retention characteristics. At a pH of approximately 4, retention times of the major peak appear to approach an upper limit. In a separate experiment, it was found that 0.5 g silanol column material in 10 ml water lowered the pH from 6 to 4.8. This suggests that the column bears excess negative charge and perhaps behaves as a cation-exchange column. The increase in retention times as the pH is lowered, however, implies the opposite, namely, the column operates by an anion-exchange mechanism. The signoidal character of Figs. 1 and 3 suggests that at low salt concentrations the cation-exchange mechanism may predominate whereas at high salt concentrations, the anion-exchange process takes precedence.

The minor peak is associated with the ion pair. It appeared when samples were prepared with Milli-Q-Water, methanol or methanol–water and the mobile phase was methanol–water (80:20, v/v) but disappeared when the mobile phase was water. The source of the peak is believed to be the ion pair since the ion pair is present in methanol–water (80:20, v/v) but not in water as determined by dilution conductivity measurements. Ion pairs apparently are retained on the column via the equilibrium process given in eqn. 1.

The mechanism most likely responsible for retention of the ion pair on the column is solubility of the ion pair in the C_{18} component of the ODS column. This is supported by the finding that the minor peak is absent on silica columns devoid of C_{18} linkages. The assignment of the minor peak to the ion pair is reasonable given that the retention time remains constant with column loading, but changes with mobile phase content variations. Clearly as the water fraction increases, the concentration of ion pairs decreases. Hence, the magnitude of the minor peak decreases. The reason for the increase in retention time as the water content of the mobile phase increases is related to the miscibility of water in the C_{18} phase of the column. There is an increase in the hydrophilic interaction of the mobile phase with the hydrophobic character of the C_{18} phase resulting in an increase in ion pair retention times as the water content of the mobile phase increases.

The mechanism

Silicon oxide surfaces have been studied in detail by others. The surface is acidic with a pK_a value of 7.1[8]. The acidity is derived from the silanol group on the surface as illustrated in eqn. 2.

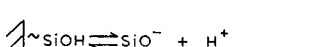

(2)

At high pH, the surface contains negatively charged groups which can behave as a cation-exchange column as illustrated in Scheme 1. According to Scheme 1, cations are retained on the column by SiO^- groups until they are eventually released from the column.

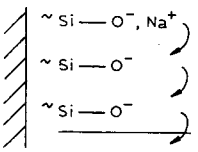

Scheme 1. A cation-exchange process observed on silica columns at low substrate concentration in methanol–water (80:20, v/v) (pH ≃ 7).

At lower pH (pH < 4), the acid sites are fully protonated. The surface would become neutral were it not for the fact that silica sorbs water[9]. The water is polarized and the partial positive end of the water molecule most likely interacts with substrates resulting in an anion-exchange column as illustrated in Scheme 2. According to this scheme, the anion is retained on the column by the water dipole until it eventually is released from the column.

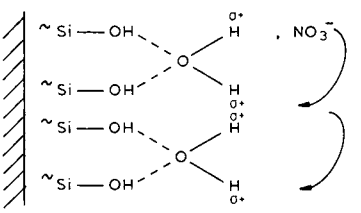

Scheme 2. An anion-exchange process observed at pH < 4 on silica columns in methanol–water (80:20, v/v).

In addition, silica columns are known to adsorb cations in the order $Cs^+ > K^+ > Na^+$ (ref. 10). The surface can then accommodate additional positive charge which is reflected in the retention time. For example, sodium nitrate has a longer retention time than TBAN as given in Table V. In this case, Na^+ is preferentially sorbed onto the silica column and the retention time of sodium nitrate is slightly longer than for TBAN.

The mechanistic situation at pH > 4 and at higher substrate concentrations is a hybrid of both Schemes 1 and 2. At higher pH and greater column loading, two effects are important. The negative sites on the column become occupied by cations and adsorbed water polarizes the column as illustrated in Scheme 3. The predominant process under these conditions appears to be anion exchange as illustrated in Scheme 3, although cation exchange cannot be ruled out. Schemes 1 and 3 account for the sigmoidal character observed in Figs. 1 and 3. At low sample loading, the primary mechanism of retention is interaction of the cations with the negative column sites; at high loading, the primary mechanism for retention involves anion exchange via interaction of the anion with the positive dipole of the adsorbed water molecule.

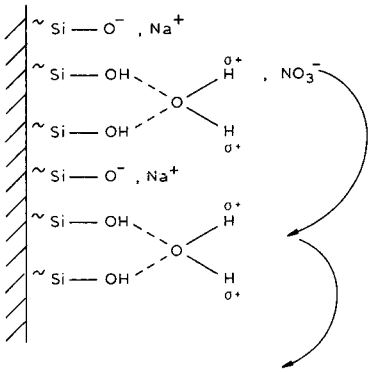

Scheme 3. The anion-exchange process observed at pH > 4 with greater substrate loading on silica columns in methanol–water (80:20, v/v).

The mechanism of retention on silica and C_{18} derivatized silica columns without an ion pairing agent present in the mobile phase is more complex than the situation where an ion pairing agent is present. In the latter case, the cation is generally a large organic molecule which is soluble in the C_{18} phase of the column and acts as a site for anion exchange[11]. Without the ion pairing agent present in the mobile phase, our results suggest that ion pairs of the original salt absorb into the C_{18} phase and are retained on the column longer than the cationic or anionic component.

Ion pairing constant determination

The area under the minor peak was taken to be indicative of the ion paired concentration; the area under the major peak was equated with the concentration of the dissociated salt. This was derived mathematically as follows:

$$\frac{(\text{area})_c}{(\text{area})_s} = \frac{(M^+, A^-)_c}{A_s^- + (M^+, A^-)_s} \approx \frac{(M, A^-)_c}{A_s} \tag{3}$$

The area of the minor peak is given by the ion pair eluted from the column $(\text{area})_c$; the area of the major peak is given by the sum of the anion and ion pair in the mobile phase $(\text{area})_s$, since the anionic component in its various forms is the species detected in the experiment. Ion pairing constants in polar solvents generally are on the order of 10^{-3} M^{-1} (see below) which means $A^- \gg (M^+, A^-)_s$ allowing eqn. 3 to be approximated as indicated.

Ion pairing constants can then be determined by eqn. 4 in the limit with $K_c = 1$.

$$K_s = \frac{[M^+, A^-]_s}{[M^+]_s[A^-]_s} = \frac{K_c[M^+, A^-]_c}{[M^+]_s[A^-]_s} \approx \frac{[M^+, A^-]_c}{[M^+]_s[A^-]_s} \approx \frac{(\text{area } M^+, A^-)_c}{(\text{area}, A^-)_s^2} \tag{4}$$

The ion pair association constant determined for an average of four samples for sodium nitrate was $15 \cdot 10^{-3}$ M^{-1} and for sodium nitrite was $2.0 \cdot 10^{-3}$ M^{-1} under similar conditions.

Fuoss and Krauss[12] reported an ion pairing constant of $2.9 \cdot 10^{-3}$ M^{-1} for sodium nitrate in liquid ammonia at $-40°C$. The ion pair formation constant they found for tetraisoamylammonium nitrate in a dioxane–water (47:53, v/v) system was 0.15 M^{-1}. The dielectric constant of this solvent mixture was 38, close to 41 for the methanol–water (80:20, v/v) mixture used in our studies.

The distance of ion separation in the ion pair was estimated using Bjerrum theory[13] of ionic association. The theory relates the ion pair formation constant to electrostatic, solvent, and distance of charge separation parameters[14]. Substitution of the appropriate parameters for sodium nitrate in methanol–water (80:20, v/v) at 20°C resulted in a distance of charge separation between the centers of sodium and nitrate of 6.7 Å. This value certainly is reasonable given that the ionic radius of sodium is 1.16 Å, nitrate is 1.65 Å (ref. 15) and the fact that the ions are solvated in solution.

The closeness of both experimental and theoretical ion pairing constants lend credibility to the assumption that $K_c \approx 1$.

CONCLUSIONS

This paper points out two important items. The first indicates that C_{18} derivatized silica columns exhibit dual functionality. The silica backbone functions as an ion exchange resin; the C_{18} component dissolves the ion pair. This allows the determination of ion pairing formation constants by a new method. The second item is related to equating t_m to t_R for simple anions on ODS columns. Clearly this is incorrect and a standard will need to be defined in order to report data for reproducibility. Sodium nitrate at low concentration ($< 10^{-8}$ M) seems to be an excellent choice.

ACKNOWLEDGEMENTS

We thank the Foundation of the University of North Carolina for support. We also express our thanks to Larry Morgan for the dilution conductivity measurements, to Laleh Dashti for some of the HPLC determinations and to John W. Burke for some of the HPLC and the ion chromatography determinations. The Dionex ion chromatography system was purchased under Grant 2-4-01015 from the U.S. Department of Education.

REFERENCES

1 D. C. Jackman, S.-L. Yau, L. G. Daignault and D. P. Rillema, *J. Membrane Sci.*, 34 (1987) 109–119.
2 L. R. Snyder and J. J. Kirkland, *Introduction to Modern Liquid Chromatography*, Wiley, New York, 1979, Ch. 2, p. 23.
3 R. K. Boggess and D. A. Zatko, *J. Chem. Ed.*, 52 (1975) 649.
4 M. Salomon and M. C. Uchiyama, *J. Solution Chem.*, 16 (1987) 21–29.
5 J. J. Stranahan and S. N. Deming, *Anal. Chem.*, 54 (1982) 1540.
6 S. Levin and E. Grushka, *Anal. Chem.*, 58 (1986) 1602.
7 S. Levin and E. Grushka, *Anal. Chem.*, 59 (1987) 1157.
8 M. L. Hair and W. Hertt, *J. Phys. Chem.*, 74 (1970) 91–94.
9 C. Clark-Monks and B. Ellis, *J. Colloid Interface Sci.*, 44 (1973) 37–49.
10 R. P. Abendroth, *J. Colloid Interface Sci.*, 34 (1970) 588–593.
11 R. L. Smith, Z. Iskandarani and D. J. Pietrzyk, *J. Liq. Chromatogr.*, 7 (1984) 1935–1959.
12 R. M. Fuoss and C. A. Kraus, *J. Am. Chem. Soc.*, 55 (1933) 1019–1028.

13 H. S. Harned and B. B. Owen, *The Physical Chemistry of Electrolytic Solutions*, Reinhold, New York, 1943, Ch. 3, p. 42.
14 H. S. Harned and B. B. Owen, *The Physical Chemistry of Electrolytic Solutions*, Reinhold, New York, 1943, Ch. 5, p. 112.
15 J. E. Huheey, *Inorganic Chemistry*, Harper and Row, New York, 1983, pp. 73–78.

Journal of Chromatography, 462 (1989) 85–94
Elsevier Science Publishers B.V., Amsterdam — Printed in The Netherlands

CHROM. 20 963

EXTERNAL RECYCLE CHROMATOGRAPHY: A PRACTICAL METHOD FOR PREPARATIVE PURIFICATIONS

JOHN R. CRARY*, KIMBERLY CAIN-JANICKI and RANMALI WIJAYARATNE
G.D. Searle & Co., 4901 Searle Parkway, Skokie, IL 60077 (U.S.A.)
(First received May 16th, 1988; revised manuscript received August 30th, 1988)

SUMMARY

This report describes a new recycle concept for use in preparative liquid chromatography (PLC). External recycle is a technique that involves the reinjection of unevaporated impure eluent fractions, as a single injection, back onto the original column to enhance the total recovery and purity of components from a separation. Results of this study indicate that resolution is more dependent upon sample load and on the weight distribution of components in the mixture than upon injection volume. The application of this technique to PLC was demonstrated using crude reaction mixtures of synthetically prepared compounds of pharmaceutical interest.

INTRODUCTION

Preparative chromatography is the application of chromatographic methods for the purpose of isolating significant amounts of pure compounds from a mixture. Generally, these methods are based on analytical high-performance liquid chromatography (HPLC) or thin-layer chromatography (TLC) systems.

The objectives for PLC separations are different from HPLC or TLC separations in that productivity should be emphasized rather than resolution[1]. To maximize productivity, (the weight of pure product resolved per gram of adsorbant), PLC columns are typically operated at sample overloaded conditions which often results in the incomplete resolution of the components.

The effect of sample overload on band broadening and resolution has been the subject of a number of investigations[2–9]. Knox and Pyper[5] discussed the effects of both injection "volume overloading" and "concentration overloading" on band broadening in preparative chromatography. "Volume overloading" for a single component is insignificant as long as the injection volume remains less than half the volume of a compound's eluting band. "Concentration overloading" is a result of applying sample concentrations that are higher than the linear portion of the adsorption isotherm.

In addition to understanding the effects of overloading on the resolution of components for single-pass separations, there are a variety of methods, such as conventional recycle chromatography[10–14], to enhance the recovery and purity of

0021-9673/89/$03.50

single-pass separations where the resolutions are not complete. In conventional recycle chromatography, the eluent is routed from the column outlet through the pump and directly back to the head of the column. The effect of recycle chromatography is that the components of a mixture are further resolved with each additional pass through the column. There are also variations on the conventional recycle method[15,16] to improve the performance of separations, however, conventional recycle systems are typically limited to the isolation of two component mixtures, and to separations where the total band width is less than the recycle volume.

This report describes an external recycle technique for preparative purifications that fills an operational gap between single-pass purifications and conventional recycle methods. This technique is useful after an initial single-pass purification, where a crude mixture has been applied to a column and eluted from the column using the appropriate solvent system. Some of the eluted fractions may still contain an impure mixture of adjacent eluting compounds. These impure mixture fractions can then be sequentially reinjected back onto the column, in a "volume overload" condition, to further resolve the desired components. Sequential reinjection of fractions refers to a process by which any number of unevaporated fractions are recycled back onto the same column, in the same order in which they had eluted from the column during the previous single-pass. This process is, in effect, a recycle rechromatography of only the unresolved portion of the initial sample. This reinjection process by itself or in conjunction with conventional recycle techniques provides another approach for improving the quality and speed of purifications.

EXPERIMENTAL

Apparatus

Preparative chromatography was performed using either a Beckman 421 controller and 100A pumping system or a Waters PrepLC/500A system. The elution profiles were monitored by either a Hitachi Model 100-10 UV–VIS detector, or a Waters 500A refractive index detector.

Chemicals

Androst-4-ene-3,17-dione (AD) and $\Delta^{1,4}$-androstene-3,17-dione (ADD) were obtained from Searle Chemical. Diastereomers of a *tert.*-butyloxy-carbonyl (Boc) protected peptide and an isoquinoline derivative were obtained as synthetic intermediates from reaction mixtures (G. D. Searle).

Methods

All resolution studies were performed using mixtures of AD and ADD on a LiChrosorb Si-60, 10 μm, 500 mm × 10 mm silica column and a mobile phase of 10% ethyl acetate in methylene chloride. The eluent was monitored by TLC, and by UV adsorption using a Hitachi Model 100-10 spectrophotometer at a wavelength of 286 nm so as to obtain equal responses for AD and ADD.

The resolution values were calculated using the standard equation

$$R_s = 2(V_{R,2} - V_{R,1})/(W_1 + W_2)$$

where R_s is the resolution, $V_{R,1}$ is the retention volume (ml) of the AD peak, $V_{R,2}$ is the retention volume (ml) of the ADD peak, W_1 and W_2 are the eluting band widths (ml) for AD and ADD. In all cases, the skewed peak retention volumes could be measured from the chromatogram that was obtained during each run. The band widths were often completely obscured due to mass overloading. For this reason the band widths for AD and ADD were determined by the number of fractions that contained each of the compounds and multiplied by 10 ml per fraction. Therefore, the base width measurements have a precision that is related to the fraction size.

Method development for the separation of the crude sample mixtures was performed using precoated Merck Kieselgel 60, F_{254}, 0.25-mm TLC plates, and the resulting separations were scaled directly to column purifications using the same mobile phases. All preparative column purifications were performed using Merck Kieselgel 60, 230–400 mesh silica dry packed into stainless-steel columns. The selection of an appropriate column size was determined by the sample weight, typically being on the order of 0.02 g sample/g silica. Columns were then preconditioned with 1–2 void volumes of mobile phase prior to sample injection. For practical considerations, a column void was determined as the volume of solvent residing in the preparative column. These provide an estimate of the amount of solvent necessary to saturate a dry packed column, or to displace a solvent previously occupying the column.

Weights of reinjected samples were not determined directly but were estimated by integrating the areas under the peaks and by the final weight of products. This is because the compounds purified during the reinjections had been combined with the same pure compound produced from the first single-pass run through each column.

Samples were typically dissolved in the appropriate mobile phases at concentrations of 0.2–0.3 g/ml, and injected onto the column. Eluent fractions ranged from 0.05 to 0.20 void volumes, with the fraction purity being determined by TLC. The wet unevaporated fractions containing the unresolved components were sequentially reinjected onto the head of the column using the solvent inlet lines to the pump. The reinjections were made from test tubes or other vessels containing the impure fractions. Generally, each vessel was washed with a small amount of mobile phase to ensure a quantitative transfer onto the column. A three-way valve was used to momentarily cavitate the pump while the solvent line was being moved between fractions to eliminate the introduction of air into the system.

RESULTS AND DISCUSSION

Fig. 1 shows the effect of sample injection volume on resolution. An amount of 16 mg of a mixture containing equal proportions of AD and ADD was applied per injection onto a column having a 28.5-ml void volume. The resolutions measured ranged from 1.33 to 0.87 when the injection volume applied to the column was varied from 0.160 to 40.0 ml. These results are difficult to compare to the Knox model for "volume overloading" since, in the present study, the sample weight was kept constant and the effect of injection volume on the resolution of a two component mixture was evaluated. It was observed that even though the 40.0-ml injection volume was equal to the elution band width for AD during the 0.16-ml injections, the resulting peak shapes were not flat, but showed only a slight increase in peak broadening. It seems that even at the sample weight used in this study, a "concentration overloading" effect was still

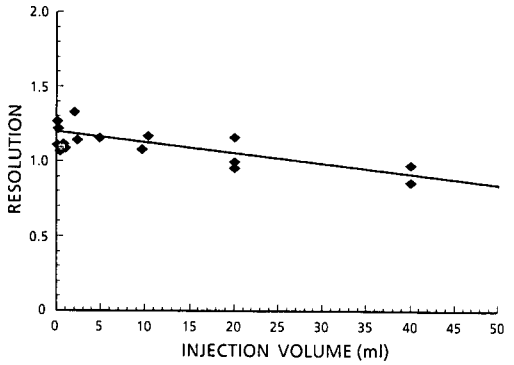

Fig. 1. Influence of injection volume on the resolution of a 50% mixture of AD and ADD. Column 50 × 1.0 cm I.D., LiChrosorb SI-60, 10 μm; column void, 28.5 ml; solvent, 10% ethyl acetate in methylene chloride; flow-rate, 8 ml/min; sample weight, 16 mg; detector, 286 nm for equal AD and ADD response. Resolutions are calculated based on detector response and TLC profile analysis.

observed. These results indicate that the injection volume may not be the most significant factor in determining the resolution of a multi-component separation as long as the total weight of sample mixture being injected remains constant.

Fig. 2 illustrates the effect of increased sample weight on resolution when a 50% mixture of AD and ADD was applied in a "concentration overloaded" condition. In this example, sample weights greater than 0.4 g reduced the yield and purity of AD and ADD to make preparative purifications of larger samples impractical on this column. Although the effect of sample weight on resolution is dependent on a number of chromatographic parameters, this example illustrates that sample load is typically the dominant factor influencing resolution. The Knox model for "concentration overloading", where the peak mass distributions are skewed toward earlier elution volumes as band spreading increases, fits the elution profiles obtained for AD and ADD during these trials.

Fig. 3 illustrates a third major factor in determining the overall resolution of a sample mixture. In this case, the sample weight ratio of AD and ADD is shown to have a major influence on the resulting resolutions. Fig. 3a shows a separation using

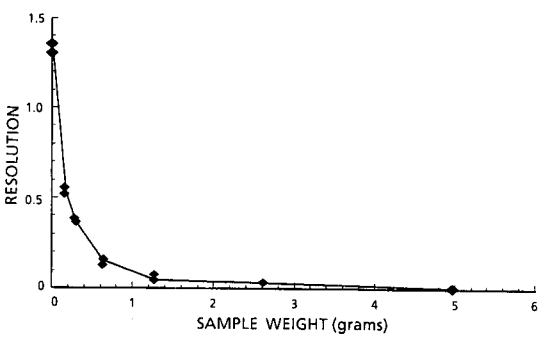

Fig. 2. Effect of sample loading weight on resolution of a 50% mixture of AD and ADD. Conditions are the same as in Fig. 1.

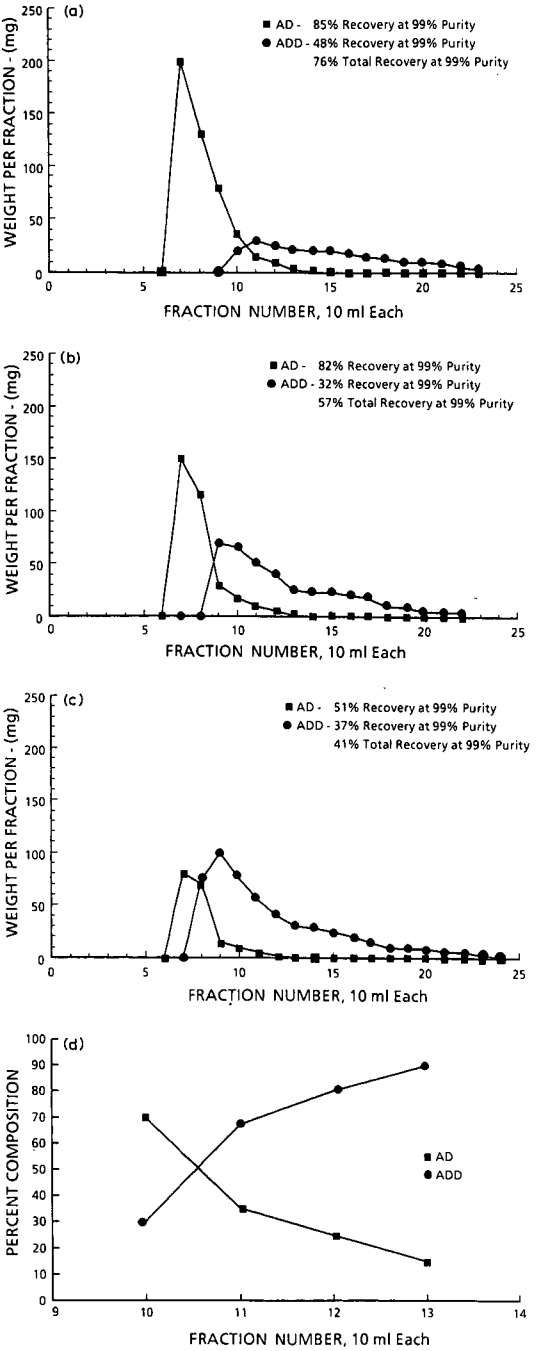

Fig. 3. Effect of weight composition of a mixture of AD and ADD on resolution. Sample: 640 mg. Conditions are the same as in Fig. 1, except the flow-rate was 2.0 ml/min. (a) 75% AD and 25% ADD; (b) 50% AD and 50% ADD; (c) 25% AD and 75% ADD; (d) percent AD (■) and ADD (●) composition of overlapping fractions 10–13 from a.

TABLE I

THE EFFECT OF AD AND ADD WEIGHT DISTRIBUTION ON RECOVERY AND RESOLUTION

*AD:ADD composition**	*Totals at 99% purity*			*Resolution*
	AD (mg)	*ADD (mg)*	*Percent***	
75:25	408	76	76	0.29
50:50	262	103	57	0.15
25:75	82	177	41	0.05

* 640 mg total weight per injection.
** Percent total recovery at 99% purity.

0.64 g of a mixture containing 75% AD and 25% ADD. Fig. 3b shows a similar profile for 0.64 g of 50% AD and 50% ADD, while Fig. 3c shows a profile for 0.64 g of 25% AD and 75% ADD. The effect of sample weight distribution on the resolution and recovery of AD and ADD is shown in Table I. This data indicates that for weight overloaded conditions the total resolution of a mixture of components can be enhanced if the component distributions are altered.

The separation of the fastest eluting component of any mixture is significantly improved as its relative weight in the sample mixture is increased. This is because the tail of each peak remains at a relatively constant tail capacity (k'_t) value that is equivalent to the same component's peak capacity (k'_p) for small analytical injections[6]. As the weight of a component in a mixture is increased, the peak capacity (k'_p) gets smaller and comes at an earlier elution volume due to greater "concentration overloading" effects[4]. This band broadening effect improves the resolution of a separation if the first eluting component of a mixture has the highest weight ratio. This is because as this band broadening occurs, it cannot spread forward to contaminate any other eluting compounds. Later eluting components can overlap the faster eluting components as their relative weight in the mixture increase, and the overall resolution of a separation decreases dramatically.

These studies indicate that injection volume, sample weight, and sample distribution all have an effect on resolution. However, the change in sample weight distribution can outweigh the disadvantages of larger injection volumes required to apply wet fractions directly back onto the column. This significantly enhances the advantages of injecting the unevaporated impure fractions directly back onto the column, as a single injection, rather than combining, drying, and rechromatographing them as a new mixture to obtain the desired purity and recovery. Fig. 3d illustrates the region of AD and ADD overlap from Fig. 3a. Although the AD and ADD contained in these fractions has not been purified to the desired level, the distribution of AD and ADD in these fractions has been changed dramatically. These fractions are ideal for reinjection because the weight distribution of AD and ADD has been altered.

Fig. 4a shows a single-pass normal phase purification of a mixture of diastereomers of a Boc protected dipeptide using a mobile phase of 3% ethanol in methylene chloride. TLC analysis of the eluted fractions indicated that fractions 28–33 still contained the first diastereomer and some of the faster eluting impurities, while fractions 45–51 contained a mixture of both diastereomers. The column was then eluted with 100% ethanol to remove any residual impurities remaining on the column,

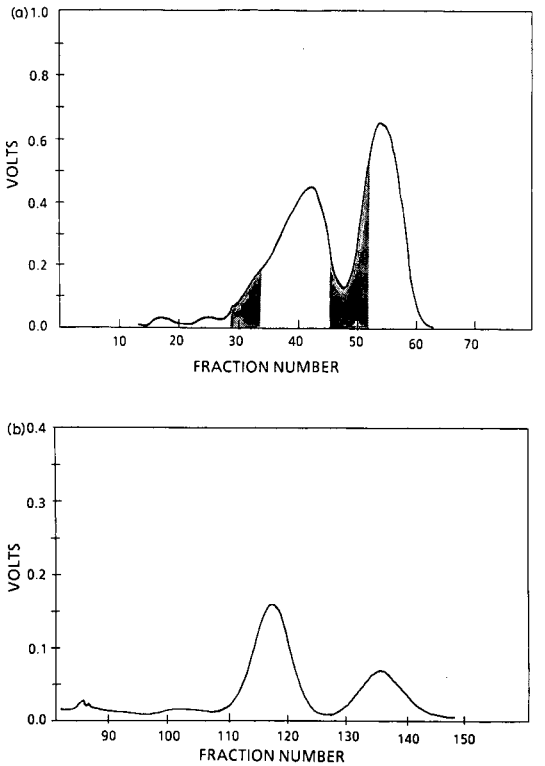

Fig. 4. (a) Single-pass separation of a crude mixture of Boc-protected dipeptide. Column: 100 × 2.5 cm I.D.; dry packed with Merck Kieselgel 60 silica; column void: 400 ml; solvent: 3% ethanol in chloroform. Sample: 5.29 g of a mixture of Boc-protected dipeptide diastereomers; flow-rate: 25.0 ml/min; fraction volume: 25.0 ml; detector: 254 nm. (b) Re-injection of fractions 28–33 and 45–51 from a onto the same column using the same conditions. Sample: 1.07 g. The purified diastereomers were found to constitute 94% of the crude sample mixture weight.

and reconditioned with the initial mobile phase. The unevaporated factions 28–33 and 45–51 were then sequentially reinjected back onto the original column as a single volume overloaded injection. Each of these 13 fractions was 25.0 ml for a total single injection volume of 325 ml or 0.81 column void volumes. It is critical that these fractions be reinjected back onto the column in the same order in which they had initially eluted, so that the faster eluting components are the first to be reinjected back onto the column. The results of this external recycle are shown in Fig. 4b, where the reinjected impure fractions were completely resolved. The final result is that instead of approximately 75% total recovery of both diastereomers after one single-pass through the column, there is now almost complete recovery at 100% purity. This technique of externally recycling fractions need not be limited to the overlap of only two adjacent components, but can be applied to any number of adjacent overlapping peaks from the same separation.

The major criteria used to decide when a reinjection of eluent fractions should be performed can best be determined by examining the tail retentions of the eluting peaks

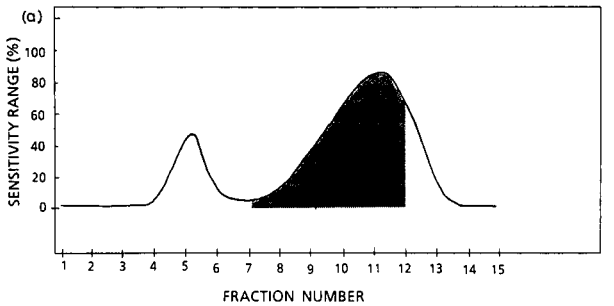

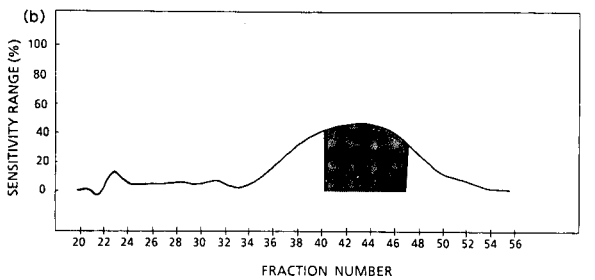

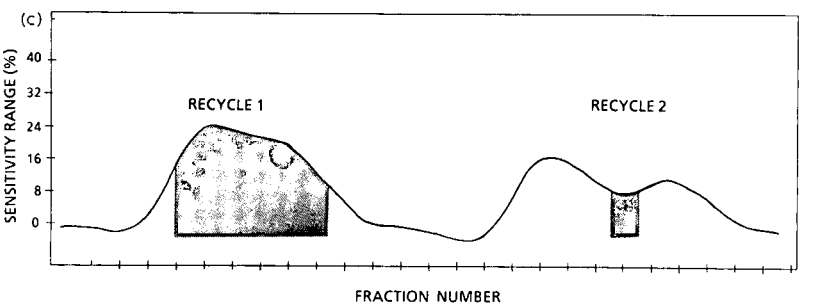

Fig. 5. (a) Single-pass separation of a crude mixture of tetrahydral isoquinoline diastereomers. Column: 150 × 5.0 cm I.D.; dry packed with Merck Kieselgel 60 silica; column void: 2400 ml; solvent: 3.0% isopropanol in hexane. Sample weight: 20.7 g; flow-rate: 500 ml/min; fraction volume: 500 ml; detector: refractive index with a range of 2. (b) Re-injection of fractions 7–11 from a onto the same column using the same conditions, except for the fraction volume being 250 ml. Sample: 11.5 g. (c) Re-injection of fractions 40–46 from b onto the same column, then recycled for two passes using the same conditions, except for the refractive index range being 5. Shaded areas were recycled or collected as a mixture. Sample: 6.5 g. The purified diastereomers were found to constitute 73.4% of the crude sample weight.

of interest. Large differences in the tail retentions of eluting compounds could indicate that a reinjection will be useful. When an initial separation has been partially successful, improvements in recovery and purity can generally be expected for all components. Reinjections are usually performed with only a portion of the initial sample weight. This reduced total sample weight does not seem to be a significant factor in determining the resolution of the components for reinjected fractions, but it appears to be more dependent on the altered weight distribution of the mixture components in the fractions.

Another example of the advantages of external recycle is shown in Fig. 5a. The initial single-pass separation isolated a mixture of tetrahydral isoquinoline diastereomers from a crude reaction mixture using a mobile phase of 3% isopropanol in hexane. The column was then eluted with 50% isopropanol in hexane to remove the more polar impurities, and reconditioned with the initial mobile phase. TLC analysis of all eluting fractions indicated that fractions 7–11 contained a mixture of both diastereomers. Fractions 7–11 were then sequentially injected back onto the same column as a single injection. The results of the reinjection in Fig. 5b indicate that a complete separation was still not obtained.

The initial injected sample weight could have been decreased, or a larger column size could have been used to give a complete separation of the mixture with one single-pass separation. The major drawback with this approach to preparative chromatography is that the amount of work and materials required to achieve the purification of the total sample increases with the number of runs and the size of the column used for the purification. Hence, in most instances, sample weight overloading is a more prudent way to maximize the throughput efficiency of preparative purifications[1].

TLC analysis of the fractions in Fig. 5b suggested that the weight distribution of the components had been altered significantly. This indicated that the reinjection process was working and only needed to be continued in order to further resolve the diastereomers. A second reinjection was made using fractions 40–47. This process of reinjecting fractions could have continued until the sample was completely resolved, however, because the band width of the two diastereomers was less than the recycle eluent volume, the system was run in a conventional recycle mode for two passes through the column. The resulting separation profiles are shown in Fig. 5c, where the pure portion of each eluting diastereomer was removed with each recycle pass through the column. The final outcome of using this technique is that a 96.4% recovery of the diastereomers at better than 95% purity was obtained in one column run using two reinjections and two conventional recycle passes.

This example illustrates how a purification can evolve from a clean-up mode into a highly efficient conventional recycle mode of operation by incorporating an external recycle operation into the process. Conventional recycle is the easiest method of performing recycle chromatography, but although it has many practical applications its use is often limited. When a mixture containing more than two components is being separated, or a two-component eluent band volume is larger than its conventional recycle eluent volume, external recycle chromatography can be more practical than conventional recycle methods.

CONCLUSION

External recycle is a technique where significant improvements can be achieved in the recovery and purity of valuable samples when an initial single-pass separation through a column does not give adequate resolution of the components of interest. This operation can be performed using multiple fractions in an eluting stream, provided they are sequentially reinjected back onto the column in the same order in which they had initially eluted. Further, reinjections can be performed in a series of cycles with most separations, to stepwise isolate the components of interest. This method is less laborious and more efficient than combining and drying the unresolved fractions to reduce the injection volume, and then rechromatographing them as a new mixture. This technique has been applied to reversed-phase systems, and should be applicable to other modes of liquid chromatography when using isocratic conditions and where the lack of resolution is due to sample weight overload on the column.

REFERENCES

1 S. Ghodbane and G. Guiochon, *J. Chromatogr.*, 444 (1988) 275.
2 B. Coq, G. Cretier and J. L. Rocca, *J. Chromatogr.*, 186 (1979) 457.
3 G. Cretier and J. L. Rocca, *Chromatographia*, 20 (1985) 461.
4 F. Eisenbeib, S. Ehrlerding, A. Wehrli and J. F. K. Huber, *Chromatographia*, 20 (1985) 657.
5 J. H. Knox and H. M. Pyper, *J. Chromatogr.*, 363 (1986) 1.
6 L. R. Snyder, G. B. Cox and P. E. Antle, *Chromatographia*, 24 (1987) 82.
7 J. E. Eble, R. L. Grob, P. E. Antle and L. R. Snyder, *J. Chromatogr.*, 384 (1987) 25.
8 J. E. Eble, R. L. Grob, P. E. Antle and L. R. Snyder, *J. Chromatogr.*, 384 (1987) 45.
9 J. E. Eble, R. L. Grob, P. E. Antle, G. B. Cox and L. R. Snyder, *J. Chromatogr.*, 405 (1987) 31.
10 B. Bidlingmeyer (Editor), *Preparative Liquid Chromatography*, Elsevier, Amsterdam, 1987.
11 G. Guiochon and A. Katti, *Chromatographia*, 24 (1987) 165.
12 M. Minarik, M. Popl and J. Mostecky, *J. Chromatogr. Sci.*, 19 (1981) 250.
13 K. J. Bombaugh and R. F. Levangie, *J. Chromatogr. Sci.*, 8 (1970) 560.
14 T. Yoshida, C. Shu and E. T. Theimer, *J. Chromatogr.*, 137 (1977) 461.
15 R. F. Sutthoff and W. J. Nelson, *U.S. Pat.*, 4022637 (1977).
16 R. A. Henry, S. H. Byrne and D. R. Hudson, *J. Chromatogr. Sci.*, 12 (1974) 197.

Journal of Chromatography, 462 (1989) 95–103
Elsevier Science Publishers B.V., Amsterdam — Printed in The Netherlands

CHROM. 20 970

EXAMPLE OF THE CONCENTRATION DEPENDENCE OF ELUTION ORDER IN THE RESOLUTION OF ENANTIOMERS ON MICROCRYSTALLINE TRIACETYLCELLULOSE CHIRAL STATIONARY PHASE

CHRISTIAN ROUSSEL*, JEAN-LOUIS STEIN, FRANÇOISE BEAUVAIS and AHMED CHEMLAL
ESIPSOI, UA CNRS 126, Rue Escadrille Normandie-Niemen, 13397 Marseille Cedex 13 (France)
(First received July 27th, 1988; revised manuscript received September 9th, 1988)

SUMMARY

The resolution of 3-(2-propylphenyl)-4-methyl-4-thiazolin-2-one atropisomers by liquid chromatography on microcrystalline triacetylcellulose shows an unprecedented inversion of the capacity factors with increasing amount of sample injected. The two enantiomers behave independently on the chiral stationary phase. The occurrence of such different isotherms for the two enantiomers is related to the presence of a propyl group and provides experimental proof of the intervention of different sites for chiral recognition in the supramolecular structure of microcrystalline triacetylcellulose.

INTRODUCTION

In recent years, the separation of enantiomers by liquid chromatography on chiral stationary phases (CSPs) and the design of new CSPs have aroused wide interest[1–15]. Among the various commercially available phases of this type, microcrystalline triacetylcellulose (MTAC)[16–20] is attractive as it has been used with success in separating various racemates on a preparative scale (Pirkle and Hamper[21] "preparative" separations as those involving the collection of the resolved materials for subsequent utilization, whether this isolation affords sub-milligram or multi-gram amounts of material).

During a systematic study of the factors that affect chiral discrimination on MTAC for a series of atropisomers of N-arylthiazolin(thi)ones, we found that 3-(2-propylphenyl)-4-methyl-4-thiazolin-2-one (3a) shows an unprecedented behaviour on MTAC; chromatography of racemic 3a with polarimetric detection indicates that the first eluted enantiomer is dextrorotatory for an analytical-scale sample (3 mg), whereas the first eluted enantiomer is laevorotatory for semi-preparative-scale injections (50 mg). We believe that this observation may open the way to a better understanding of the type of molecular recognition involved in these chiral separations.

0021-9673/89/$03.50

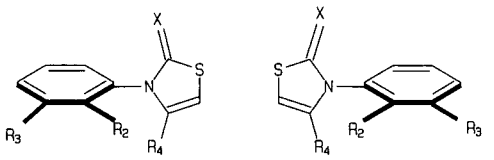

1a $R_2=C_3H_7$, $R_3=H$, $R_4=CH_3$, X=S
3a $R_2=C_3H_7$, $R_3=H$, $R_4=CH_3$, X=O
1b $R_2=CH_3$, $R_3=CH_3$, $R_4=CH_3$, X=S
3b $R_2=CH_3$, $R_3=CH_3$, $R_4=CH_3$, X=O

Scheme 1.

EXPERIMENTAL AND RESULTS

N-Arylthiazoline-2-thiones and their oxygen analogues bearing alkyl substituents in positions 4 and 2′ have a steric barrier to rotation around the N–aryl bond larger than 29 kcal mol^{-1}, giving rise to stable atropisomers which can be eventually separated at room temperature on MTAC (Scheme 1) [the lower limit was determined for thiazoline with methyl groups in the 4 and 2′ positions in diglyme; in ethanol the barriers are larger owing to the specific solvation of the (thio)carbonyl group[22,23]. For a general discussion of steric barriers in atropisomers in heterocycles, see ref. 24]. These compounds are interesting models for a study of molecular recognition on MTAC and on other CSPs because (i) a wide variety of steric requirements through alkyl substituents can be regioselectively introduced in various positions on the aryl ring and in the 4 and 5 positions on the heterocycle by unequivocal syntheses, (ii) X-ray data indicate that the two rings are almost perpendicular in the crystalline state[22–24] and the absolute configurations of the 3-(2′-alkylphenyl)-4-alkyl-4-thiazoline-2-thiones are known [the absolute configuration has been determined on optically pure (+)-3-(2′-methylphenyl)-4-*tert.*-butyl-4-thiazoline-2-thione by X-ray analysis of the salt obtained by reaction with an optically active menthyl derivative of known configuration[25]], (iii) optically pure thiazoline-2-thiones can be converted into optically pure thiazolin-2-ones without racemization at room temperature and (iv) the two parts of these compounds have very different dipolar requirements, basicities and hydrogen bonding abilities. In order to investigate the effect of the lipophilicity of the alkyl chain in the 2′ position on the aryl ring on the separation on MTAC, we prepared 3-(2-propylphenyl)-4-methyl-4-thiazoline-2-thione (1a) and its oxygen analogue (3a).

The determinations of the chromatographic parameters (capacity factors and separation coefficients) were performed on a thermostated (20°C) 200 mm × 25 mm I.D. MTAC (15–25 nm) (Merck) column eluted with 95% ethanol at a flow-rate of 138 ml/h with UV and polarimetric detection. The dead volume of the column was determined from the elution volume of 1,3,5-tri-*tert.*-butylbenzene, which was injected together with the sample in ethanol using a 5-ml injection loop[26].

In the general experimental procedure, the compounds studied were injected in an analytical run (*ca.* 2 mg) in racemic form. If baseline separation was observed, the chromatographic parameters were extracted directly from the chromatogram using either UV or polarimetric data. If partial resolution was obtained, UV detection gave

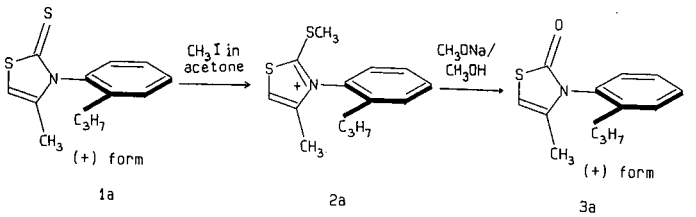

Scheme 2.

a useless single envelope whereas the polarimeter indicated the order of elution and the shape of the resulting signal. In the latter instance, a larger amount of the compound was injected in order to collect the very beginning and the very end of the peak, and this procedure was repeated until enantiomerically pure samples were obtained in milligram amounts, which could be injected separately so as to determine the chromatographic parameters.

The thiazolinethione 1a showed a baseline separation, the dextrorotatory enantiomer appearing first, whereas the thiazolinone 3a was partially resolved with again the dextrorotatory enantiomer appearing first. On applying the general procedure described above to a larger amount of 3a, we found that the first eluted enantiomer is the laevorotatory form. In order to study this unexpected behaviour,we prepared optically pure (+)-3a and (−)-3a from the corresponding thiones (+)-1a and (−)-1a after preparative separation of the latter on MTAC (Scheme 2). Known amounts of optically pure samples of (+)-3a were injected into the column and the peak shapes recorded using polarimetric detection. Digitization of the experimental curves and treatment by computer afforded the series of positive curves depicted in Fig. 1 together with the experimental area and the position of the barycentre [the barycentre (moment of mass) was determined instead of the peak maximum to account for the asymmetry of the curves] (Table I).

It appears that the capacity factor k'^{+} increased from 1.37 to 1.64 when the amount of compound injected was increased from 1.82 to 16.36 mg. The same experiments performed on the laevorotatory enantiomer (−)-3a for the same amounts gave the series of negative curves depicted in Fig. 1, and it appears that the capacity factor k'^{-} decreased when the amount of compound injected was increased.

Simultaneous treatments of the two independent curves obtained for the pure enantiomers in order to simulate the response of the corresponding racemic injections are shown in Fig. 1. They account perfectly for the observed experimental inversion of the elution order on increasing the amount of compounds injected. Fig. 1c is particularly instructive as the calculated resulting curve obtained by combination of the two separate injections of 4.55 mg of each enantiomer has a very unusual and sensitive shape owing to the contrasting shapes of the two constituent curves. Such an unusual shape with more than two maximal was obtained experimentally by injection of 9.10 mg of racemic sample. It is worth noting that the different shapes of the two curves indicate that under conditions of identical capacity factors on would still observe a signal with polarimetric detection. We were able to reproduce experimentally the calculated curves for racemic injections over the whole range of concentration, and it follows that the two enantiomers show completely independent behaviour on the

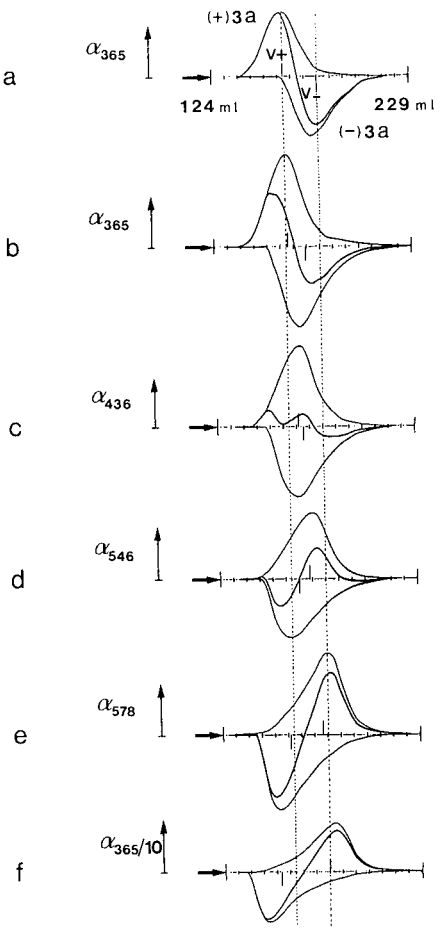

Fig. 1. Concentration dependence of elution order for 3a on MTAC (polarimetric detection). Experimental positive or negative curves were obtained by independent injections of pure (+)-3a and (−)-3a, respectively: (a) 1.82 mg; (b) 2.73 mg; (c) 4.55 mg; (d) 7.30 mg; (e) 10.45 mg; (f) 16.36 mg. The resulting curves are computer simulations of the corresponding racemic form.

column and that a displacement process is not involved in the observed phenomena.

Fig. 2 reports the variation of capacity factors with the amount of sample injected. An explanation of the behaviour of (+)-3a, which shows an increase in capacity factor with increase in the amount of sample injected, based on self-association (which is generally involved in such behaviour mainly on zeolites) seems improbable, as it should be enantioselective in order to account for the fitting of the experimental chromatogram of a racemic injection with the calculated result obtained by combination of the experimental chromatograms for each enantiomer.

It was therefore interesting to study the influence of concentration on the capacity factors of the thiazolinethione 1a. For this purpose, increasing amounts of optically pure sample were injected separately. The resulting curves do not overlap and the separation is excellent (Fig. 3 and Table I). In the same rang of concentration as for

TABLE I

CAPACITY FACTORS AND SEPARATION COEFFICIENTS FOR COMPOUNDS 1a, 3a, 1b AND 3b AS A FUNCTION OF THE AMOUNT OF SAMPLE INJECTED ON MTAC

Compound	*Fig.*	*Amount in 5 ml of ethanol (mg)*	k'^{+}*	k'^{-}	k'^{+}/k'^{-}	α**
(+)-3a	1a	1.82	1.37			
(−)-3a	1a	1.82		1.64	0.84	1.19
(+)-3a	1b	2.73	1.41			
(−)-3a	1b	2.73		1.53	0.92	1.09
(+)-3a	1c	4.55	1.43			
(−)-3a	1c	4.55		1.49	0.96	1.04
(+)-3a	1d	7.30	1.52			
(−)-3a	1d	7.30		1.44	1.06	1.06
(+)-3a	1e	10.45	1.605			
(−)-3a	1e	10.45		1.35	1.19	1.19
(+)-3a	1f	16.36	1.645			
(−)-3a	1f	16.36		1.27	1.30	1.30
(+)-1a	3a	1.82	1.04			
(−)-1a	3a	1.82		3.09	0.366	2.98
(+)-1a	3b	4.54	1.02			
(−)-1a	3b	4.54		2.88	0.354	2.82
(+)-1a	3c	9.10	1.00			
(−)-1a	3c	9.10		2.64	0.379	2.64
(+)-1a	3d	13.64	0.98			
(−)-1a	3d	13.64		2.51	0.391	2.55
(+/−)-1b	4a	3.27	0.97	3.29	0.296	3.38
(+/−)-1b	4b	24.55	0.93	3.35	0.277	3.60
(+/−)-3b	4c	3.57	0.83	2.00	0.415	2.41
(+/−)-3b	4d	25.57	0.835	1.97	0.425	2.35

* Defined by $V^{+} - V^{ref}/V^{ref}$ using barycentric calculation to account for tailing.
** Defined as the ratio of the capacity factor of the more bound to that of the less bound enantiomer.
*** Injected in racemic form.

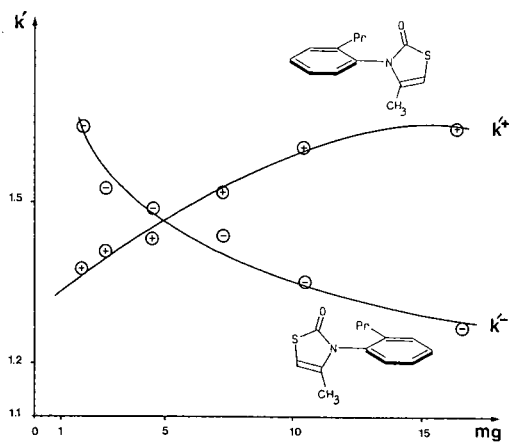

Fig. 2. Variation of the capacity factors k'^{+} and k'^{-} for 3a as a function of amount injected.

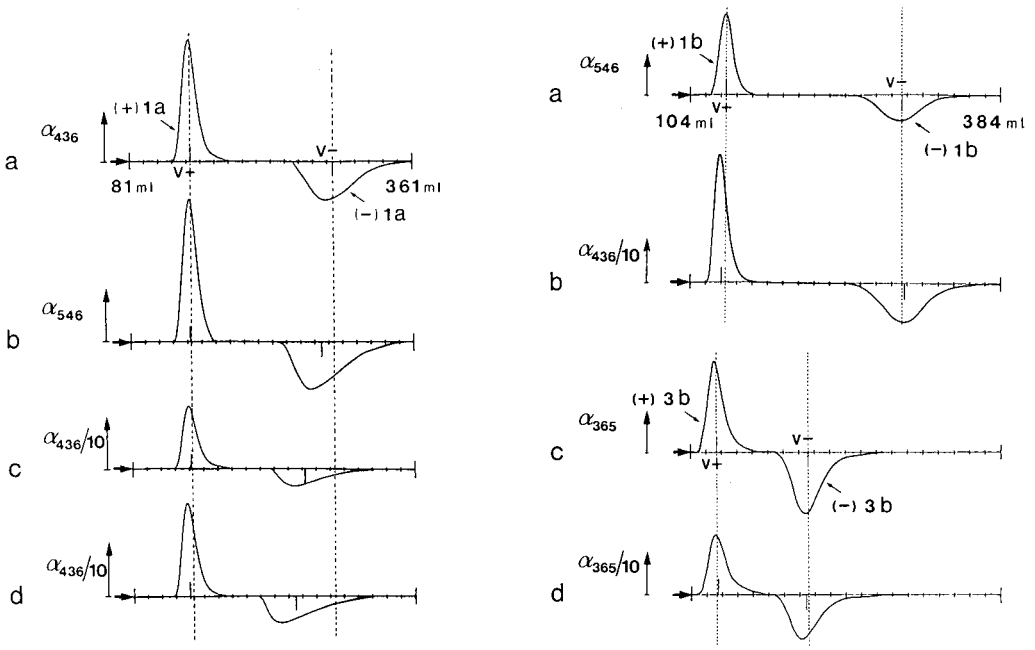

Fig. 3. Concentration dependence of the chromatographic behaviour of 1a on MTAC. Positive and negative curves were obtained by independent injections of pure (+)-1a and (−)-1a, respectively: (a) 1.82 mg; (b) 4.54 mg; (c) 9.10 mg; (d) 13.64 mg.

Fig. 4. Chromatographic behaviour of 1b [(a) and (b)] and 3b [(c) and (d)] as a function of the amount of sample injected (Table I). These curves were obtained by direct analysis of the racemic form; (a) 3.27 mg; (b) 24.55 mg; (c) 3.57 mg; (d) 25.57 mg.

3a, the capacity factor of the positive enantiomer decreases slightly whereas that of the negative enantiomer is much more dependent on concentration. In order to verify the independence of enantiomer behaviour on the CSP as already discussed for 3a, we prepared samples in wich 1.82 mg of the negative enantiomer was mixed with 13.6 mg of the positive enantiomer. The resulting capacity factors for bot enantiomers agree perfectly with those obtained in the respective separate injections.

The chromatographic behaviours of 1a and 3a are in sharp contrast with those reported in Table I for 3-(2,3-dimethylphenyl)-4-methyl-4-thiazoline-2-thione (1b) and its oxygen analogue (3b) (the syntheses of these compounds have been described elsewhere[22]). The capacity factors for these two compounds display very little dependence on the amount of sample injected in the concentration range studied (Fig. 4 and Table I). The results indicate that in the concentration range considered the number of suitable sites is large enough to prevent saturation phenomema for compounds very similar to 1a and 3b. Hence it appears that the presence of a lipophilic propyl group in 1a and 3a might account for the concentration dependence of the capacity factors.

To the best of our knowledge, very little attention has been paid to the effect of the amount of racemates injected on resolution on MTAC[27] and on other CSPs. Some

examples were provided by Soah and Cram[28,29] for the resolution of enantiomers of amino acid and ester salts in host–guest complexation studies[28,29]. No inversion of the elution order was observed but the chiral recognition was dependent on the host:guest ratio and it was suggested that "the sterically more confined sites which exhibit higher chiral recognition were engaged in binding as the amounts of guest were increased". We believe such an explanation might hold for compounds 3a. An example of the inversion of elution order with increasing sample size for achiral compounds as been reported recently and was accounted for by isotherm crossing, but in that instance both compounds exhibited a differential decrease in capacity factors with increasing sample size.[30]

We are currently extending this type of study to tailored racemates with suitable substitution to improve our knowledge of the mechanism of chiral recognition on MTAC and similar CSPs. So far our experimental results confirm the concurrence of various sites for chiral recognition in the supramolecular structure of MTAC[31,32] which are dramatically discriminatory towards the lipophilic effect.

Synthesis of compounds

3-(2-Propylphenyl)-4-methyl-4-thiazoline-2-thione (racemic) (1a). This was prepared by reaction of the corresponding ammonium dithiocarbamate with chloropropanone[33]. Yield 64%; m.p. = 75–76°C; R_F (silica gel, chloroform as eluent) = 0.53. ^{1}H NMR (C^2HCl_3): δ (ppm) 0.95 (3H,t), 1.3–1.8 (2H,m), 1.82 (3H,s), 2.39 (2H,t), 6.35 (1H,s), 7–7.6 (4H,m). ^{13}C NMR (C^2HCl_3): δ (ppm) 14.20, 15.83, 22.32, 32.78, 106.73 (C-5), 127.40, 128.23, 129.87, 130.18, 136.30, 140,03, 140.03, 189.23 (C=S). Mass spectrum, (70 eV): *m/z* (%) 249(27), 217(15), 216(100), 214(15), 206(10), 200(9), 188(10), 187(25), 91(11), 77(12), 45(8), 41(7), 39(8). UV (95% ethanol); $\lambda(\varepsilon)$ = 320 nm (15 400). Analysis: calculated for $C_{13}H_{15}NS_2$, C 62.7, H 6.0, N 5.6, S 25.7; found, C 62.65, H 6.09, N 5.62, S 25.55%.

Racemic thiazoline-2-thione (525 mg in ten injections) was separated into 235 mg of the (+)-form and 255 mg of the (−)-form. (+)-form (20.8 mg in 2 ml of 95% ethanol, 25°C): λ (nm), α, [α], Φ 436, +4.31, +414.5, +1032; 546, +1.970, +183.4, +471.6; 578, +1.667, +160.3, +399.1; 589, +1.58, +151.9, +378.2. (−)-form (23.1 mg in 2 ml of 95% ethanol, 25°C): λ (nm), α, [α], Φ 436, −4.573, −395.9, −985.8; 546, −2.088, −180.8, −450.2; 578, −1.768, −153.1, −381.2; 589, −1.677, −145.2, −361.5.

2-Methylthio-4-methyl-3-(2-propylphenyl)thiazolium iodide (racemic)(2a). Compound 1a (500 mg) in 12.5 ml of dry acetone was allowed to react for 2 h at room temperature with 0.75 ml of methyliodide. After partial evaporation, the solid was collected and washed with anhydrous diethyl ether (415 mg; yield 53%; m.p. = 131–132°C). ^{1}H NMR (C^2HCl_3): δ (ppm) 0.8–1 (3H,m), 1.4–1.8 (2H,m), 2–2.3 (2H,m), 2.15 (3H,s), 2.33 (3H,s), 7.5–7.6 (4H,m), 8.35 (1H,s). UV (95% ethanol): λ (ε) = 296 nm. (10 900).

3-(2-Propylphenyl)-4-methyl-4-thiazolin-2-one (racemic) (3a). This was synthesized by an adaptation of the procedure for conversion of pyrimidine-2-thione into pyrimidine-2-one[34]. Compound 2a (350 mg) was treated at room temperature for 1 h with a mixture of sodium methoxide (810 mg) in 7.8 ml of methanol. After extraction, washing with water and drying, 211 mg of 3a were obtained as a colourless oil (quantitative yield), which after further purification by liquid chromatography on

MTAC crystallized (m.p. = 58°C). Total yield from 1a = 40%. R_F (silica gel 60, chloroform as eluent) = 0.36. ^{1}H NMR (C^2HCl_3): δ (ppm) 0.9 (3H,t), 1.5 (2H,m), 1.75 (3H,s), 2.40 (2H,m), 5.9 (1H,s), 7–7.5 (4H,m), ^{13}C NMR (C^2HCl_3): δ (ppm) 14.16, 15.63, 22.87, 33.17, 96.31, 127.19, 129.00, 129.59, 130.25, 132.72, 134.37, 141.01, 172.29 (C=O). Mass spectrum (70 eV): *m/z* (%) 233(22), 216(9), 201(16), 160(11), 144(10), 130(9), 91(3), 77(11), 41(8), 39(8). Analysis: calculated for $C_{13}H_{15}NOS$, C 67, H 6.4, N 6, S 13.7; found, C 66.45, H 6.44, N 5.95, S 13.65%.

(+)-3-(2-Propylphenyl)-4-methyl-4-thiazolin-2-one [(+)-3a]. Optically pure (+)-3a was obtained as an oil from (+)-1a by the same procedure as for the preparation of racemic 3a [total isolated yield from (+)-1a 57%]. Optical properties (19.1 mg in 2 ml of 95% ethanol, 25°C): λ (nm), α, [α], Φ 365, +3.0, +315, +734; 436, +1.646, +172.4, +401.7; 546, +0.882, +92.4, +215.2; 578, +0.764, +80., +186.4; 589, +0.727, +76.1, +177.4.

(−)-3-(2-Propylphenyl)-4-methyl-4-thiazolin-2-one [(−)-3a]. Optically pure (−)-3a was obtained as an oil from (−)-1a by the same procedure as for the preparation of racemic 3a [total isolated yield from (−)-1a 64%]. Optical properties (21.1 mg in 2 ml of 95% ethanol, 25°C): λ (nm), α, [α], Φ 365, −3.142, −297.8, −694; 436, −1.718, −162.8, −379.3; 546, −0.920, −87.2, −203.2; 578, −0.796, −75.5, −175.8; 589, −0.759, −71.9, −167.6.

REFERENCES

1 R. W. Souter, *Chromatographic Separations of Stereoisomers*, CRC Press, Boca Raton, FL, 1985, Ch. 3, pp. 87–183.
2 I. W. Wainer, *Trends Anal. Chem.*, 6 (1987) 125.
3 D. Johns, *Int. Lab.*, (1987) 66.
4 R. Däppen, H. Arm and V. R. Meyer, *J. Chromatogr.*, 373 (1986) 1.
5 D. W. Armstrong and W. Demond, *J. Chromatogr. Sci.*, 22 (1984) 411.
6 Y. Okamoto, *Chemtech.*, (1987) 176.
7 S. Allenmark, *J. Liq. Chromatogr.*, 9 (1986) 425.
8 T. J. Ward and D. W. Armstrong, *J. Liq. Chromatogr.*, 9 (1986) 407.
9 G. Wulff, H. G. Poll and M. Minarik, *J. Liq. Chromatogr.*, 9 (1986) 385.
10 V. A. Davankov, A. A. Kurganov and A. S. Bochkov, *Adv. Chromatogr.*, 21 (1984) 1.
11 W. H. Pirkle and J. Finn, in J. D. Morrison (Editor), *Asymmetric Synthesis*, Vol. 1, Academic Press, New York, 1983, pp. 87–124.
12 J. N. Kinkel, W. Fraenkel and G. Blaschke, *Kontakte (Darmstadt)*, 1 (1987) 3.
13 D. W. Armstrong, *Anal. Chem.*, 57 (1987) 84A.
14 M. Lienne, M. Caude, A. Tambute and R. Rosset, *Analusis*, 15 (1987) 431.
15 M. Zief and L. J. Crane (Editors), *Chromatographic Chiral Separations*, Marcel Dekker, New York, 1988.
16 A. Mannschreck, H. Koller and R. Wernicke, *Kontakte (Darmstadt)*, 1 (1985) 40.
17 E. Francotte and D. Lohmann, *Helv. Chim. Acta*, 70 (1987) 1569.
18 G. Blaschke, *Angew. Chem.*, 92 (1980) 14.
19 T. Shibata, I. Okamoto and K. Ishii, *J. Liq. Chromatogr.*, 9 (1986) 313.
20 A. Ichiba and L. Shibata, in M. Zief and L. J. Crane (Editors), *Chromatographic Chiral Separations*, Marcel Dekker, New York, 1988, p. 219.
21 W. H. Pirkle and B. C. Hamper, in B. A. Bidlingmeyer (Editor), *Preparative Liquid Chromatography (Journal of Chromatography Library*, Vol. 38), Elsevier, Amsterdam, 1987, p. 236.
22 C. Roussel, M. Adjimi, A. Chemlal and A. Djafri, *J. Org. Chem.*, 53 (1988) 5076.
23 C. Roussel and A. Djafri, *Nouv. J. Chim.*, 10 (1986) 399.
24 R. Gallo, C. Roussel and U. Berg, *Adv. Heterocycl. Chem.*, 43 (1988) 173.
25 C. Roussel and A. Chemlal, *New J. Chem.*, 12 (1988) 945.
26 H. Koller, K. H. Rimbock and A. Mannschreck, *J. Chromatogr.*, 282 (1983) 89.

27 G. Hesse and R. Hagel, *Justus Liebigs Ann. Chem.*, (1976) 996.
28 G. D. Y. Sogah and D. J. Cram, *J. Am. Chem. Soc.*, 101 (1979) 3035.
29 G. D. Y. Sogah and D. J. Cram, *J. Am. Chem. Soc.*, 98 (1976) 3038.
30 M. J. Gonzalez, A. Jaulmes, P. Valentin and C. Vidal-Madjar, *J. Chromatogr.*, 386 (1987) 333.
31 E. Francotte, R. M. Wolf, D. Lohman and R. Mueller, *J. Chromatogr.*, 347 (1985) 25.
32 G. Hesse and H. Hagel, *Chromatographia*, 9 (1976) 62.
33 C. Roussel and A. Djafri, *Nouv. J. Chim.*, 10 (1986) 399.
34 C. Kashima and A. Katoh, *J. Chem. Soc., Perkin Trans. 1*, (1980) 1599.

Journal of Chromatography, 462 (1989) 105–113
Elsevier Science Publishers B.V., Amsterdam — Printed in The Netherlands

CHROM. 21 029

BESTIMMUNG VON TAURIN: EINFLUSS DER COILTEMPERATUR AUF DIE PEAKREINHEIT DES TAURINS

D. BALSCHUKAT* und H. KUNESCH
Degussa AG, GB Industrie- und Feinchemikalien Anwendungstechnik AV, Postfach 1345, D-6450 Hanau 1 (B.R.D.)

(Eingegangen am 20. Juli 1988; geänderte Fassung eingegangen am 24. August 1988)

SUMMARY

Determination of taurine: influence of the coil temperature on the taurine peak purity

A method is described for the determination of taurine, as well as other supplementary amino acids, using an amino acid analyzer with a coil temperature well above 100°C. The method is reproducible and the recovery is good even though the sample preparation is simple. As higher coil temperatures increase the yield of the ninhydrin reaction product, temperatures above 100°C are nowadays often used. However, this affects the taurine determination in hydrolysates as some compounds that interfere with the taurine determination will also react with ninhydrin at temperatures above 100°C.

The retention behaviour of these substances is similar to that of taurine on a cation-exchange column. The major interfering substance is levulinic acid, which is formed during the acidic treatment of hexoses. The absorption (at 440 and 570 nm) of the products of the reaction between the interfering substances and ninhydrin differs from that of primary and secondary amino acids.

These interfering substances occur mainly in plants, but also (in smaller amounts) in animal products. Therefore, the determination of taurine in hydrolysates is not reliable if a high coil temperature is used.

EINLEITUNG

Taurin (2-Aminoethansulfonsäure) ist ein Endprodukt des Katabolismus von Cystein[1,2]. Katzen sind, im Gegensatz zum Beispiel zu Ratten, nicht in der Lage, Taurin aus Cystein aufzubauen, so dass Katzen für eine optimale Ernährung auf Taurin angewiesen sind[3]. Weiterhin laufen Katzen bei Taurinmangel Gefahr, zu erblinden oder an Herzmuskelschwäche zu erkranken[4]. Deshalb kommt insbesondere dem Taurin-Gehalt von Rohstoffen und Mischfuttern eine nicht unerhebliche Bedeutung zukommt.

Verschiedene Methoden zur quantitativen Bestimmung des Taurins sind beschrieben. Praktisch ausnahmslos handelt es sich um chromatographische Methoden,

0021-9673/89/$03.50

wie z.B. die Gaschromatographie[5], die Ionenaustauschchromatographie[6,7] und die Hochleistung-Flüssigkeitschromatographie (HPLC). Bei der HPLC findet durchgängig die Vorsäulenderivatisierung statt. Verwendet werden insbesondere *o*-Phthaldialdehyd (OPA)[8–12] und 5-Dimethylaminonaphthalinsulfonylchlorid (Dns-Cl)[13], und die Derivate werden anschliessend an Umkehr-Phasen getrennt.

Bestimmt man die Aminosäurenzusammensetzung eines Rohstoffes bzw. die eines Mischfutters mit Hilfe eines Aminosäurenanalysators, so lassen sich ebenfalls Bedingungen einstellen, unter denen man Taurin quantifizieren kann. Eine Methode, die zur quantitativen Bestimmung des Taurins breite Anwendung findet. Schwierigkeiten, den Taurin-Gehalt von Hydrolysaten von Mischfuttern mit Aminosäurenanalysatoren zu bestimmen, die ein Hochtemperaturcoil besitzen, führten zur vorliegenden Arbeit. Darin wird aufgezeigt, worin diese Schwierigkeiten begründet liegen, und es werden Bedingungen entwickelt, die diese Unzulänglichkeiten umgehen.

EXPERIMENTELLES

Materialien

Taurin wurde von Serva (Heidelberg, B.R.D.) und Norleucin von Fluka (Buchs, Schweiz) bezogen. Alle weiteren Substanzen waren von Merck (Darmstadt, B.R.D.).

Reagenzlösungen

(i) Extraktionslösung: 200 mg Norleucin werden in 1000 ml 0,1 *M* Chlorwasserstoffsäure gelöst. (ii) Elutionslösungen: wie in Tabelle I beschrieben. (iii) Ninhydrin-

TABELLE I

PUFFERZUSAMMENSETZUNGEN UND CHROMATOGRAPHISCHE BEDINGUNGEN

Puffer-Bezeichnung	*A*	*B*	*C*	*Verdünnungspuffer*	*Regenerierungslösung*
pH	3,54	3,86	4,31	2,20	–
Na^+ (*M*)	0,1	0,1	0,17	0,1	0,3
Natriumcitrat · $2H_2O$ (g)	9,8	9,8	9,8	9,8	–
Chlorwasserstoffsäure (37% ig) (ml)	1,0	–	–	–	–
Citronensäure · H_2O (g)	14,0	14,0	9,8	14,0	–
Borsäure (g)	–	1,0	1,0	–	–
Natriumchlorid (g)	–	–	4,3	–	–
Methylenglycolmonomethylether (ml)	80,0	–	–	–	–
Thiodiglycol (ml)	–	–	–	20,0	–
Phenol (g)				0,1	–
Natriumhydroxid (g)	–	–	–	–	12,0
Endvolumen (ml)	1000	1000	1000	1000	1000
Pufferdurchflusszeit (min)	19	10	16	–	7

Temperatur 43°C
Harztyp BTC 2710
Trennsäule 400 nm × 3,2 mm I.D.
Pufferdurchfluss 0,27 ml/min
Reagenzdurchfluss 0,153 ml/min

lösung: 20 g Ninhydrin werden in 750 ml Ethylenglycolmonomethylether und 250 ml Natriumacetatpuffer (4 *M*; pH 5,51) gelöst und mit 5 ml Titan(III)chlorid-Lösung versetzt.

Chromatographische Bedingungen

Für die Taurin-Analytik wurde der Aminosäurenanalysator LC5001 von Biotronik (München, B.R.D.) eingesetzt (variabel einstellbare Coiltemperatur). Die Absorptionen bei 440 und 570 nm wurden von einem Spectra-Physics-Integrator SP4270 aufgezeichnet und an die Labordaten-Station Labnet® zur weiteren Verarbeitung weitergesandt.

Probenvorbereitung

Proben von etwa 4 g, genau gewogen, werden in einem 100-ml Becherglas mit 20,0 ml Extraktionslösung und 40 ml 0,1 *M* Chlorwasserstoffsäure versetzt und etwa 30 min bei Raumtemperatur gerührt.

Quantitative Analyse

Zunächst wird der Responsfaktor des Taurins mit einer Eichlösung ermittelt. Hierzu werden 5 ml einer Eichlösung in einem 100-ml Messkolben mit Verdünnungspuffer pH 2,20 zur Marke aufgefüllt und der pH-Wert auf 2,20 eingestellt. Anschliessend wird chromatographiert.

Zur Bestimmung des Taurins in der Probe werden etwa 8 ml der Probesuspension mit 22 ml Verdünnungspuffer versetzt, der pH-Wert gegebenenfalls nachgestellt, und man filtriert über ein Faltenfilter. Nach weiterer Filtration über ein 0,22-μm Membranfilter wird chromatographiert. Der Gehalt an Taurin ergibt sich dann aus dem Responsfaktor, der Einwaage der Probe und der Einwaage an internem Standard.

Isolierung der Interferenzfraktion

Eine Menge von 50 g Mais wurde 24 h in 6 *M* Chlorwasserstoffsäure unter Rückfluss erhitzt. Man saugte über eine Glasfritte ab, verdampfte die Chlorwasserstoffsäure am Rotationsverdampfer und verdünnte den Rückstand mit 100 ml 0,01 *M* Chlorwasserstoffsäure. Man gab diese Lösung auf einen Kationenaustauscher Lewatit S 100 (Säulendimensionen 40 cm × 2 cm) und eluierte mit 500 ml 0,01 *M* Chlorwasserstoffsäure. Das bräunliche Eluat wurde am Rotationsverdampfer auf 100 ml eingeengt und für Vergleichsversuche verwendet. Eine Aminosäurenanalyse zeigte, dass das Eluat frei von Aminosäuren war und nur den Interferenzpeak aufwies. Die HPLC-Analyse ergab, dass das Eluat aus mindestens 50 Komponenten bestand (Detektionswellenlänge 210 nm). Auf eine weitere Reinigung wurde verzichtet, da das Aminosäurenchromatogramm nur die Interferenz als ninhydrinpositive Verbindung aufwies.

ERGEBNISSE UND DISKUSSION

Das Chromatogramm des Maishydrolysates (Fig. 1), das mit einer Coiltemperatur von 125°C aufgenommen worden ist, zeigt, dass die Absorptionen bei 440 nm und 570 nm in Taurin-Bereich ähnlich hohe Werte aufweisen. Misst man jedoch

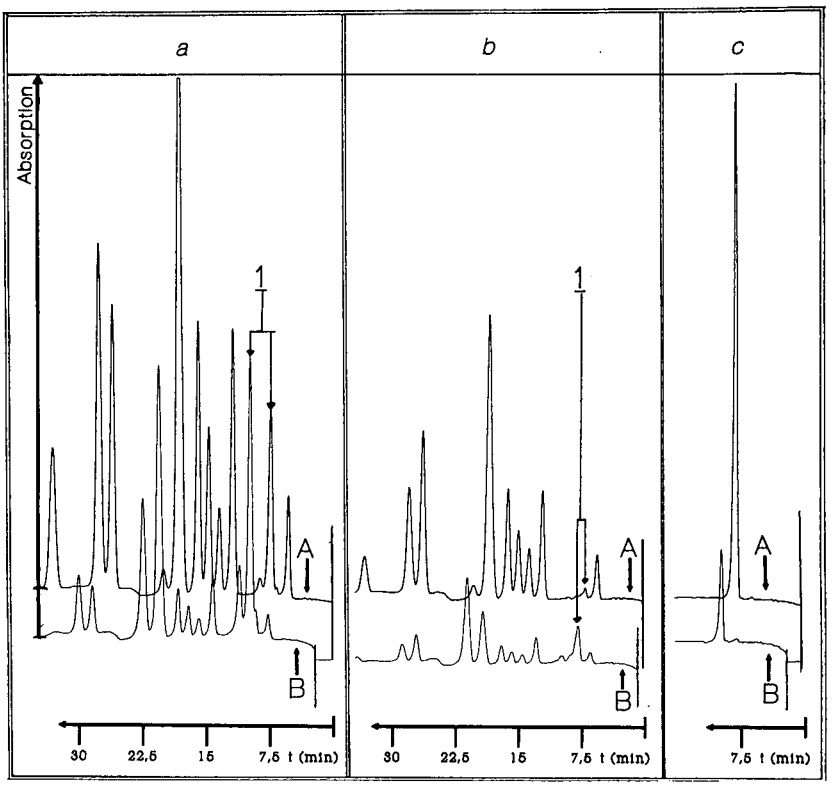

Fig. 1. Ionenchromatogramme eines Maishydrolysates, gemessen bei Coiltemperaturen von 100 (a) und 125°C (b); Vergleich: Taurin bei 125°C (c). Reagens: Ninhydrin; Detektionswellenlängen, A: 570 nm, B: 440 nm. Der interne Standard Norleucin erscheint bei *ca.* 45 min. 1 = Lävulinsäure. Diese Position entspricht auch der Retentionszeit des Taurins.

reines Taurin, so ist das Verhältnis der Absorptionshöhen etwa 1:6 (Fig. 1c). Fig. 1b zeigt das gleiche Maishydrolysat bei einer Coiltemperatur von 100°C.

Fig. 2 zeigt den Einfluss der Coiltemperatur auf die Absorption der Taurin-Interferenz. Man erkennt sehr deutlich, dass insbesondere die Interferenz erheblich sensitiver bei beiden Wellenlängen auf die Reaktionstemperatur reagiert als z.B. das Taurin. Das Absorptionsverhalten des Taurins ist aber charakteristisch für primäre Aminosäuren.

Bereits Krysciak und Nitecka[14] haben darauf hingewiesen, dass im Aminosäurenchromatogramm vor der Asparaginsäure Substanzen eluieren, die eine untypische Farbe bei der Reaktion mit Ninhydrin ergeben. Eine Substanz, die identifiziert wurde, ist die Lävulinsäure, die bei der sauren Behandlung von Hexosen entsteht.

Ältere Modelle von Aminosäurenanalysatoren arbeiten mit einer Coiltemperatur von 100°C. Da hier nie Probleme bei der Bestimmung des Taurins aufgetaucht waren, wurde der Einfluss der Coiltemperatur auf das Absorptionsverhalten der Taurin-Interferenz untersucht.

Lävulinsäure eluiert unter den oben angegebenen Chromatographiebedingun-

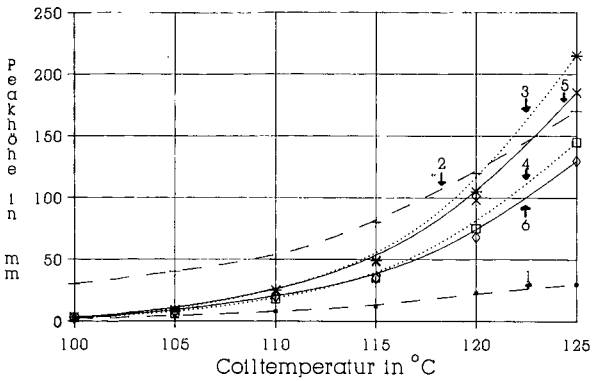

Fig. 2. Abhängigkeit der Absorption bei 440 und 570 nm von der Coiltemperatur für Taurin, Lävulinsäure und Taurin-Interferenz. 1 = Taurin (440 nm); 2 = Taurin (570 nm); 3 = Taurin-Interferenz (440 nm); 4 = Taurin-Interferenz (570 nm); 5 = Lävulinsäure (440 nm); 6 = Lävulinsäure (570 nm). Reagens: Ninhydrin. Nur das relative Absorptionsverhalten ist dargestellt.

gen zur gleichen Zeit wie die Interferenz. Der Fig. 2 kann man entnehmen, dass auch die Kinetik der Anfärbung ähnlich ist. Besonders auffallend ist, dass die Reaktion so sehr stark abhängig ist von der Temperatur des Coils. Dass sich die Interferenz besonders bei pflanzlichen Produkten bemerkbar macht, liegt daran, dass diese bekanntermassen auch über den höchsten Anteil an Hexosen verfügen. Im HPLC lässt sich zeigen, dass die Interferenz auch unter verschiedenen Bedingungen ein identisches Elutionsverhalten aufweist wie Lävulinsäure. Somit ist sicher, dass es die aus Hexosen gebildete Lävulinsäure ist, die die Taurinbestimmung stört.

Fig. 3 zeigt das Absorptions- und Chromatographieverhalten der Taurin-Interferenz und Lävulinsäure in Abhängigkeit von der Coiltemperatur.

Auch Erbersdobler *et al.*[7] haben darauf hingewiesen, dass bei Arbeiten mit Hochtemperaturcoils Schwierigkeiten auftreten. Geht es bei ihnen jedoch insbesondere um Probleme der Abtrennung von Harnstoff und Phosphoethanolamin, so sind die Probleme bei Hydrolysaten gänzlich anders gelagert.

Phosphoethanolamin und Harnstoff verhalten sich bei der Reaktion mit Ninhydrin wie Aminosäuren. Die Interferenz jedoch zeigt das Anfärbeverhalten, wie es in Fig. 2 dargestellt ist. Dies bedeutet, dass man Taurin mit den gängigen Pufferprogrammen *nicht* aus den Hydrolysaten bestimmen darf, wenn man Aminosäurenanalysatoren verwendet, deren Coiltemperatur über 100°C beträgt. Unter diesen Bedingungen stört die bei der Hydrolyse entstehende Lävulinsäure so stark, dass keine exakten Taurin-Werte mehr ermittelt werden können.

Um jedoch weiterhin Taurin mit dem Aminosäurenanalysator quantifizieren zu können, wurde die Probenvorbereitung modifiziert. Diese unterscheidet sich nur unwesentlich von der früher[7] beschriebenen Probenvorbereitung. Grundlage der Änderung ist die Tatsache, dass Taurin als Stoffwechselprodukt nicht gebunden in der Matrix vorliegt, wie dies z.B. auch für supplementierte Aminosäuren gilt. Dies gilt jedoch nicht für Taurin in Darminhalten. Hier kann das Taurin so stark gebunden sein, dass sich diese Verbindungen nicht mit 0,1 *M* Chlorwasserstoffsäure spalten lassen. Demzufolge ist es logisch, die Probenvorbereitung für die Taurin-Bestimmung

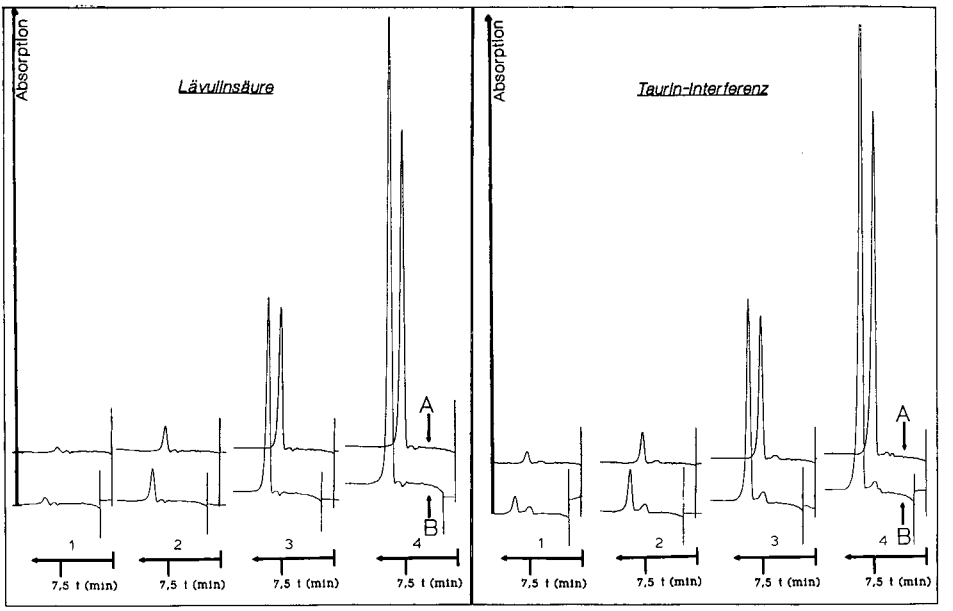

Fig. 3. Ionenchromatogramme des Absorptions- und Chromatographie-Verhaltens der Taurin-Interferenz und Lävulinsäure in Abhängigkeit von der Coiltemperatur. 1 = 100°C; 2 = 110°C; 3 = 120°C; 4 = 125°C. Reagens: Ninhydrin; Detektionswellenlängen, A: 570 nm, B: 440 nm.

der von supplementierten Aminosäuren anzugleichen. Will man jedoch gebundenes Taurin quantifizieren, so muss man drastisch hydrolysieren (6 *M* Chlorwasserstoffsäure, 24 h am Rückfluss). Die Coiltemperatur darf dann aber 100°C nicht überschreiten.

Für die Quantifizierung freien Taurins wird die feingemahlene Probe (0,25 mm)

TABELLE II

VERGLEICH DER TAURIN-WERTE ERMITTELT AUS DER OXIDATION BZW. DER EXTRAKTION AM BEISPIEL VON FISCHMEHL

Probe-Nr.	*Gehalt aus Oxidation (%)*	*Gehalt aus Extraktion mit 0,1 M Chlorwasserstoffsäure (%)*	*Differenz Oxidation/Extraktion (%)*
1	0,721	0,632	+14,3
2	0,689	0,565	+22,0
3	0,266	0,250	+6,4
4	0,700	0,633	+10,6
5	0,167	0,159	+5,0
6	0,318	0,254	+25,2
7	0,886	0,738	+20,1
8	0,916	0,789	+16,1
9	0,591	0,474	+24,7
10	0,411	0,323	+27,2

TABELLE III

WIEDERFINDUNG AN SUPPLEMENTIERTEM TAURIN IM MISCHFUTTER

Supplementierungsrate (%)	*Gehalt aus Extraktion mit 0,1 M Chlorwasserstoffsäure (%)*	*Wiederfindung (%)*
0,005	0,0044	88
0,01	0,009	90
0,02	0,019	95
0,05	0,049	98
0,1	0,099	99
0,2	0,201	100,5

mit 0,1 *M* Chlorwasserstoffsäure 30 Minuten bei Raumtemperatur gerührt und nach Filtration analysiert (Extraktion). Als interner Standard wird Norleucin (bereits in der Chlorwasserstoffsäure gelöst) verwendet. Versuche, Cysteinsäure als internen Standard zu verwenden, um die Analysenzeit drastisch zu senken, scheiterten daran, dass die Region der Cysteinsäure im Chromatogramm nicht interferenzfrei ist.

Der Erfahrung nach sind die grössten Interferenzen bei pflanzlichen Rohstoffen zu erwarten (siehe auch Fig. 1a). Aber auch tierische Produkte sind nicht interferenzfrei, wie Tabelle II zeigt.

Bei der Oxidation wird die zu untersuchende Probe zunächst mit Perameisensäure oxidiert und nach Zersetzung der überschüssigen Perameisensäure mit Bromwasserstoffsäure 24 h in 6 *M* Chlorwasserstoffsäure unter Rückfluss erhitzt. Die Oxidation dient dazu, die hydrolyselabilen Aminosäuren Methionin und Cystin in die stabilen Derivate Methioninsulfon und Cysteinsäure zu überführen.

Wie man jedoch unschwer der Spalte Differenz in Tabelle II entnehmen kann, muss man unter den gewählten Pufferbedingungen auch auf den Taurin-Wert aus den Hydrolysaten tierischer Produkte verzichten. Fischmehl wurde hier als Repräsentant

TABELLE IV

TAURINGEHALTE VERSCHIEDENER ROHSTOFFE

Probe	*Gehalt (%) an Taurin aus Extraktion mit 0,1 M Chlorwasserstoffsäure*
Weizen	n.n.*
Mais	n.n.
Gerste	n.n.
Sojaextraktionsschrot	n.n.
Seidenraupen	n.n.
Blutmehl	n.n.
Fleischknochenmehl	0,061
Federmehl	0,048
Fischmehl	0,555
Geflügelabfallmehl	0,154
Lachsfutter	0,121

* n.n., $\leqslant$ 0.001.

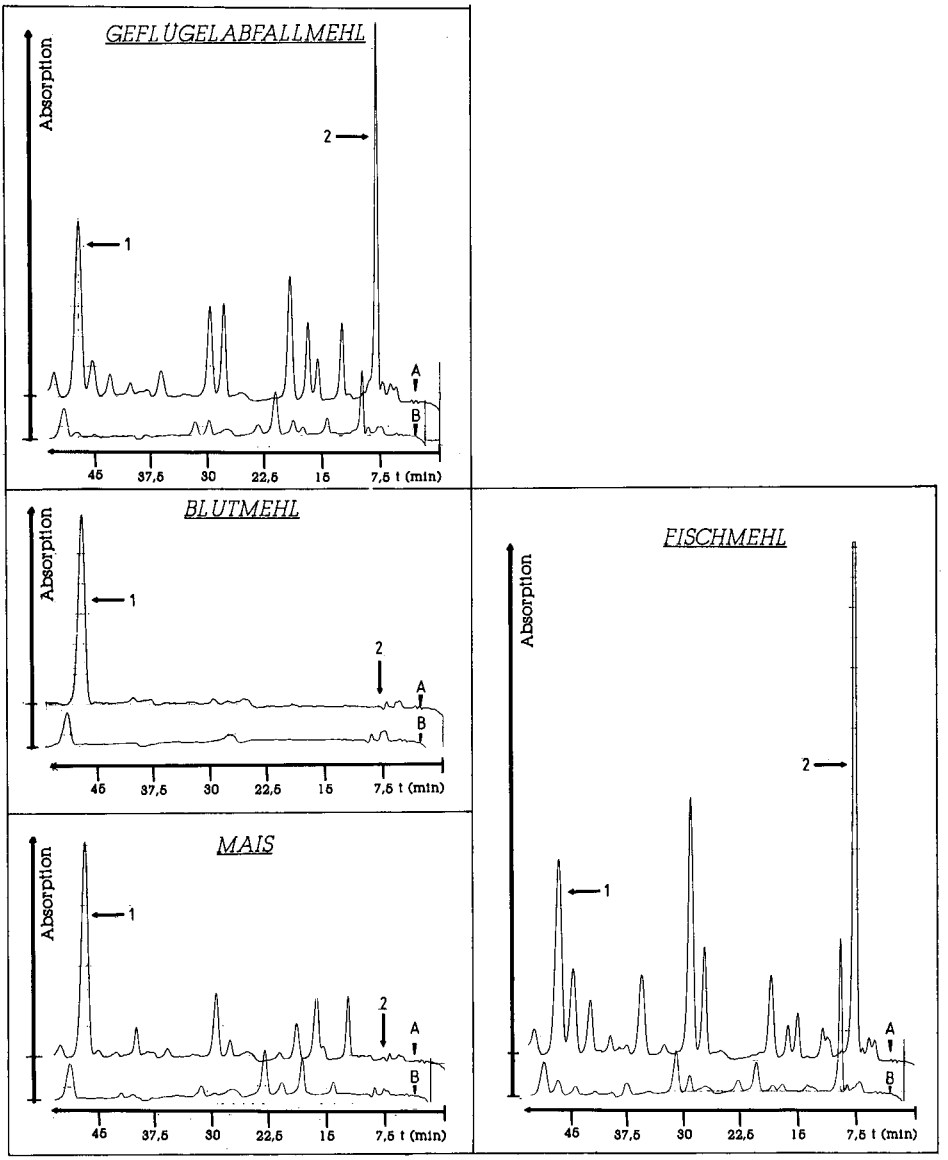

Fig. 4. Ionenchromatogramme der Extraktionen von Rohstoffen: Mais (3,8 g), Blutmehl (3,5 g), Fischmehl (1,56 g), Geflügelabfallmehl (1,86 g) (Einwaage an Rohstoff). 1 = Norleucin; 2 = Taurin. Reagens: Ninhydrin; Detektionswellenlängen, A: 570 nm, B: 440 nm.

tierischer Produkte gewählt, da dieses über recht hohe Gehalte an Taurin verfügt. Die Konsequenz kann an sich nur lauten: Auch tierische Produkte sind bei der Taurin-Bestimmung der Extraktion zu unterwerfen. Die Reproduzierbarkeit der Taurin-Bestimmung nach der Extraktionsmethode wurde an Sojaextraktionsschrot ermittelt, der mit 0,05% Taurin supplementiert war. Die relative Standardabweichung betrug +/–1,65% bei einer Wiederfindung von 98–100% Taurin.

Die nach der vorliegenden Methode ermittelten Wiederfindungsraten verschiedener Supplementierungen sind in Tabelle III zusammengefasst. Weiterhin wurden nach dieser Methode verschiedene Rohstoffe auf ihren Tauringehalt untersucht. Die Ergebnisse sind der Tabelle IV zu entnehmen, und die Chromatogramme sind in Fig. 4 dargestellt.

ZUSAMMENFASSUNG

Es wird eine Methode beschrieben, die es erlaubt, Taurin neben anderen supplementierten Aminosäuren auf einem Aminosäurenanalysator zu analysieren, dessen Coiltemperatur wesentlich über 100°C beträgt. Die Methode zeichnet sich durch eine einfache Probenvorbereitung, sehr gute Reproduzierbarkeit und sehr gute Wiederfindungsraten aus. Die Methode ist insbesondere geeignet für Laboratorien, die die Aminosäurenanalytik mit Aminosäurenanalysatoren betreiben, deren Coiltemperatur über 100°C beträgt. Höhere Coiltemperaturen erhöhen die Farbausbeute, so dass sich dieses Prinzip immer mehr durchsetzt. Die Taurin-Bestimmung aus Hydrolysaten wird jedoch damit fragwürdig.

Es wird weiterhin gezeigt, dass es sich bei den die Taurin-Bestimmung störenden Substanzen um Stoffe handelt, die erst bei Temperaturen ab 100°C mit Ninhydrin reagieren und ein ähnliches Retentionsverhalten am Kationenaustauscher aufweisen wie Taurin. Hauptstörsubstanz ist die Lävulinsäure, die bei der sauren Behandlung von Hexosen entsteht. Das Absorptionsverhalten der Reaktionsprodukte der Störsubstanzen mit Ninhydrin bei 440 und 570 nm ist jedoch gänzlich verschieden von dem Verhalten, wie man es von primären und sekundären Aminosäuren her kennt. Diese Störsubstanzen treten insbesondere bei pflanzlichen, in untergeordnetem Mass jedoch auch bei tierischen Produkten auf, weshalb generell die Taurin-Bestimmung nicht aus den Hydrolysaten erfolgen sollte, wenn mit einem Hochtemperaturcoil gearbeitet wird.

LITERATUR

1 T. P. Singer, in D. M. Greenberg (Herausgeber), *Metabolism of Sulfur Compounds, Metabolic Pathways, Vol. 7*, Academic Press, New York, 1975, S. 535.
2 A. J. L. Cooper, *Ann. Rev. Biochem.*, 52 (1983) 187.
3 K. Knopf, J. A. Sturman, M. Armstrong und K. C. Hayes, *J. Nutr.*, 108 (1978) 773.
4 P. D. Pion, M. D. Kittleson, Q. R. Rogers und J. G. Morris, *Science (Washington, D.C.)*, 237 (1987) 764.
5 H. Kataoka, S. Yamamoto und M. Makita, *J. Chromatogr.*, 306 (1984) 61.
6 H. F. Erbersdobler, H.-G. Greulich, A.-B. Holstein und E. Trautwein, *Landwirtsch. Forsch. Sonderh.*, 38 (1981) 449.
7 H. F. Erbersdobler, H.-G. Greulich und E. Trautwein, *J. Chromatogr.*, 254 (1983) 332.
8 J. D. Stuart, T. D. Wilson, D. W. Hill, F. H. Walters und S. Y. Feng, *J. Liq. Chromatogr.*, 2 (1979) 809.
9 B. R. Larsen, D. S. Grosso und S. Y. Chang, *J. Chromatogr. Sci.*, 18 (1980) 233.
10 G. H. T. Wheler und J. T. Russel, *J. Liq. Chromatogr.*, 4 (1981) 1281.
11 M. Eslami und J. D. Stuart, *J. Liq. Chromatogr.*, 7 (1984) 1117.
12 L. L. Hirschberger, J. De La Rosa und M. H. Stipanuk, *J. Chromatogr.*, 343 (1985) 303.
13 B. A. Biondi, A. Negri und A. Ioppollo, *J. Chromatogr.*, 369 (1986) 431.
14 J. Krysciak und E. Nitecka, *Acta Aliment. Pol.*, 11 (1985) 369.

Journal of Chromatography, 462 (1989) 115–135
Elsevier Science Publishers B.V., Amsterdam — Printed in The Netherlands

CHROM. 20 988

SELECTION OF CONDITIONS FOR THE MOLECULAR SIZE SPECIATION OF VANADIUM AND NICKEL COMPLEXES IN OIL BY SIZE-EXCLUSION CHROMATOGRAPHY COUPLED WITH INDUCTIVELY COUPLED PLASMA-ATOMIC EMISSION SPECTROMETRY

W. A. J. DE WAAL, C. C. H. M. KUIPER, F. J. M. J. MAESSEN and J. C. KRAAK*
Laboratory for Analytical Chemistry, University of Amsterdam, Nieuwe Achtergracht 166, 1018 WV Amsterdam (The Netherlands)
and
R. WIJNANDS and R. J. JONKER
AKZO Chemie, Research Centre Amsterdam, P.O. Box 15, 1000 AA Amsterdam (The Netherlands)
(First received July 6th, 1988; revised manuscript received September 8th, 1988)

SUMMARY

The applicability of size-exclusion chromatography (SEC) with on-line inductively coupled plasma-atomic emission spectrometric (ICP-AES) detection for the determination of nickel and vanadium compounds in oil samples was examined. Four mobile phases, tetrahydrofuran, chloroform, xylene and xylene–methanol, in combination with two stationary phases, a polystyrene–divinylbenzene and a silica-based diol column packing, were characterized with regard to the shapes of the nickel and vanadium elution profiles and overall recoveries. Tetrahydrofuran and chloroform could successfully be introduced into the ICP at conventional flow-rates by the application of an aerosol cooling setup in the SEC-ICP interface. The recoveries on the diol-modified silica gel packing were significantly smaller than those found with the polystyrene–divinylbenzene packing. With tetrahydrofuran and xylene–methanol nearly complete recoveries and similar elution profiles were obtained with the polystyrene–divinylbenzene packing, whereas for chloroform and xylene adsorption of high-molecular-weight components hampered the interpretation.

INTRODUCTION

Heavy oils contain considerable amounts of vanadium and nickel, complexed with porphyrins or porphyrin-like structures[1–6]. The presence of these metals seriously hampers the processing of oils, because they deactivate the catalysts used in hydrotreating and fluid catalytic cracking[1,2]. For this reason, vanadium and nickel are removed from the oil prior to further processing. This is usually done via thermal or catalytic treatment[1,2,6].

In order to optimize the demetallation process, an analytical method is required that not only monitors the vanadium and nickel levels in the original and treated oils,

0021-9673/89/$03.50

but also discriminates the metal complexes on the basis of their molecular size[6–8]. Size-exclusion chromatography (SEC) combined with element-specific detection has been shown to be a promising technique for this purpose[3–6], in particular when on-line inductively coupled plasma-atomic emission spectrometric (ICP-AES) detection is used[9–11].

So far, little attention has been paid to the choice of mobile and stationary phases especially with regard to metal speciation, partly because of the difficulties encountered with element-specific detection techniques. The laboriousness of off-line atomic absorption spectrometric (AAS) techniques makes them impractical for routine applications, whereas the use of volatile solvents in ICP-AES often leads to unstable plasmas. In this paper the results are presented of an investigation aimed at the selection of suitable chromatographic and experimental conditions for the determination of vanadium and nickel in oil fractions by SEC–ICP-AES. The role of the type of column packing and the mobile phase on the elution profiles and recovery of nickel and vanadium from the SEC column is discussed, including the effect of these parameters on the calibration graphs as measured with linear polystyrene standards.

The application of aerosol cooling, previously developed in our laboratory[12,13], to the SEC–ICP interface, eliminates the limitations that were previously experienced in the choice of mobile phases for on-line coupling of SEC and ICP-AES.

EXPERIMENTAL

Equipment

The liquid chromatograph consisted of a high-pressure pump (Model 300C; Gynkotek, Germering, F.R.G.), an injection valve (Model 7120; Rheodyne, Berkeley, CA, U.S.A.) equipped with a 20- or 100-μl sample loop, a variable-wavelength UV–VIS spectrophotometer (Spectroflow 757; Kratos, Ramsey, NJ, U.S.A.) and a recorder (Model BD-7; Kipp & Zonen, Delft, The Netherlands). A refractive index (RI) detector (Model R401, Waters Assoc., Framingham, MA, U.S.A.) was occasionally used.

The spectrometer was an AtomComp Model 975 ICAP multi-channel system, including an additional monochromator (Jarrell-Ash, Waltham, MA, U.S.A.). The specifications of the main characteristics of this system have been given elsewhere[14].

Nebulization was performed with a cross-flow nebulizer (Jarrell-Ash Model 90-790). When chloroform or tetrahydrofuran (THF) was used as the mobile phase, a laboratory-made aerosol cooling coil[12] was inserted between the nebulizer and the torch assembly. The coil was immersed in a thermostated ethanol bath (Haake, Berlin, G.D.R.), which was cooled by an immersion cooler (Model EK 11; Haake).

As the tubing materials for peristaltic pumps are not resistent to THF, a high-performance liquid chromatographic HPLC pump (Eldex, San Carlos, CA, U.S.A.) equipped with PTFE tubing was used to carry the condenser drain to waste. For the same reason the spray chamber was modified with a U-shaped glass syphon (see Fig. 1, component 9).

The multi-channel spectrometer was adapted in-house for continuous readout of the photomultiplier signals. For this purpose the data acquisition system of the spectrometer was replaced with a laboratory interface (Model 1401; Cambridge Electronic Design, Cambridge, U.K.) including 12-bit A/D converters, which was oper-

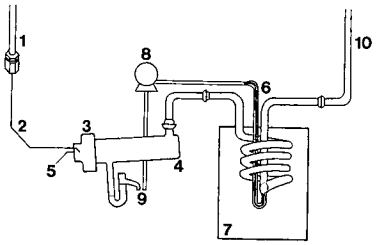

Fig. 1. Experimental setup for the SEC–ICP-AES interface. 1 = SEC column; 2 = PTFE capillary tubing; 3 = nebulizer; 4 = spray chamber; 5 = argon inner-gas inlet; 6 = condenser; 7 = cryostat bath; 8 = drain pump; 9 = drain; 10 = inner tube of ICP torch.

ated under the control of a BBC Master microcomputer (Acorn Computers, Cambridge, U.K.). The 1401 instrument was interfaced to the photomultiplier tubes by means of custom-made current–voltage converters and an eight-channel amplifier–filter system. The data obtained were initially stored on disk on the BBC microcomputer and subsequently sent to a minicomputer (Model HP 1000; Hewlett-Packard, Palo Alto, CA, U.S.A.) for the actual data processing.

Electrothermal atomization AAS (ETA-AAS) measurements were performed with a graphite furnace system (Model HGA 500; Perkin-Elmer, Norwalk, CT, U.S.A.) in combination with an atomic absorption spectrometer (Model 560, Perkin-Elmer).

Materials and chemicals

The solvents were of analytical-reagent grade and were filtered through 0.5-μm Fluoropore filters (Millipore, Bedford, MA, U.S.A.).

Vanadyl mesotetraphenylporphine (VOTPP) was obtained from Strem Chemicals (Newburyport, MA, U.S.A.) and nickel mesotetraphenylporphine (NiTPP), 2,7,12,17-tetraethyl-3,8,13,18-tetramethyl-21*H*, 23*H*-porphine dihydrobromide (Etio), 2,3,7,8,12,13,17,18-octaethylporphine (OEP) and its nickel(II) complex (NiOEP) from Aldrich (Brussels, Belgium). Polystyrene standards were obtained from Merck (Darmstadt, F.R.G.).

The SEC columns used were commercially available prepacked columns: a 300 × 7.5 mm I.D. PL-GEL column (Hewlett-Packard, Waldbronn, F.R.G.), containing a polystyrene–divinylbenzene (PS–DVB) packing with a mean pore diameter of 500 Å and a 250 × 9.5 mm I.D. GF-250 column (DuPont, Wilmington, DE, U.S.A.) containing a 5-μm zirconia-stabilized, diol-modified silica gel with a mean pore diameter of 150 Å.

Chromatography

The SEC experiments were carried out on the two types of column packings described above. Four mobile phases, THF, chloroform, *p*-xylene and a mixture of *p*-xylene and methanol, which are frequently used for the SEC of oils, were applied throughout the study. In all experiments the columns were equilibrated by pumping through at least 100 ml of the mobile phase (about six column volumes) at a flow-rate of 1 ml/min. The injection volume was usually 100 μl and the chromatograms were

TABLE I

ETA-AAS OPERATING CONDITIONS

Parameter	*Nickel*	*Vanadium**
Sample volume	20 µl	20 µl
Drying**	200°C/5s/5s	200°C/5s/5s
Ashing**	800°C/5s/10s	–
Atomization**,***	2700°C/1s/5s	2660°C/1s/5s
Cleaning**	2700°C/1s/2s	2700°C/1s/2s

* For vanadium the entire programme was repeated once between consecutive analyses.

** Values given are temperature (°C)/ramp time (s)/hold time (s).

*** The argon purge flow-rate, 300 ml/min during the complete cycle, was reduced to 30 ml/min during atomization.

recorded by UV measurement at 254 nm, visible-range measurement at 405 nm (Soret absorbance) or by refractive index (RI) or ICP-AES detection.

The molecular weight calibration graphs on the SEC columns were obtained by injecting polystyrene standards of known molecular weights. These standards were dissolved in the mobile phase and their retention volumes were measured using UV or RI detection.

Chromatographic recovery studies

The recovery of V and Ni from the SEC column was determined by analysing both the original sample and a defined collected fraction of the effluent. After injection of 100 µl of sample, the effluent fractions between 1.0 and 2.5 times the exclusion volume of the column were collected and adjusted to a volume of 10 ml. Next, the solvent was evaporated to dryness by means of a stream of nitrogen. The residue was dissolved in 0.4 ml of *p*-xylene and this solution was analysed by ETA-AAS.

In order to analyse the original sample under conditions identically to the SEC fractions, the column was disconnected from the injection valve and the same volume of original sample as used in the SEC procedure was directly injected, via the injection valve, into a measuring bottle and then adjusted to a volume of 10 ml. This solution was similarly treated as described for the SEC fractions. All measurements were carried out in duplicate. After each experiment the columns were eluted with about 100 ml of THF before injecting the next sample.

The experimental conditions for the ETA-AAS measurements are given in Table I.

SEC–ICP coupling

SEC–ICP coupling was accomplished by connecting the outlet of the column to the inlet of the nebulizer by means of PTFE tubing with dimensions of 300 × 0.3 mm I.D. For reasons discussed under Results and Discussion, a setup for aerosol cooling was installed between the nebulizer and the torch assembly, as shown schematically in Fig. 1. By means of a cryostat, cooling temperatures could be adjusted down to −20°C.

TABLE II

ICP-AES OPERATING CONDITIONS

Nebulizer feeding rate corresponds to mobile phase flow-rate.

Parameter	*Solvent*			
	THF	*Chloroform*	*Xylene*	*Xylene–methanol*
Forward power (kW)	1.75	1.75	1.75	1.75
Reflected power (W)	<10	<25	<15	<10
Observation height (mm above load coil)	20/16	20	20	20
Outer gas flow-rate (l/min)	25	25	22	22
Inner gas flow-rate (l/min)	0.7	0.7	0.7	0.7
Intermediate gas flow-rate (l/min)	1.2	1.2	1.4	1.4
Condenser temperature (°C)	−20	−20	20	20

The ICP-AES operating conditions are summarized in Table II. Emission intensities were monitored at 309.311 nm (vanadium/ionic emission) and 341.476 nm (nickel/atomic emission). When both UV and ICP-AES detection were used, the UV detector was placed in series between the column and the nebulizer.

Sample preparation

The oil samples were prepared by dissolving 3% (w/v) of the oil in the applied mobile phase, followed by filtration of this solution through 0.5-μm PTFE filters (Alltech, Deerfield, IL, U.S.A.). Filtered samples were considered to be identical with the original samples as no loss of nickel and vanadium could be detected by ETA-AAS.

RESULTS AND DISCUSSION

Conditions of coupling of SEC with ICP-AES

When using non-aqueous solvents in ICP-AES, special care has to be taken to obtain plasmas that are stable over prolonged periods of time. Compared with water, organic solvents cause a decrease in the plasma excitation temperature and an increase in the background emission intensity[15]. Depending on the type of organic solvent, the deterioration of the excitation conditions may even lead to complete breakdown of the plasma.

It has been found that the plasma becomes unstable when a certain mass flow of organic solvent is exceeded, the so-called maximum tolerable solvent load[12]. This quantity varies with the type of organic solvent and has to be determined experimentally.

The mass flow of organic solvent entering the plasma can either be controlled by application of aerosol introduction rates that have been adapted to the nature of the solvent[16] or by thermal regulation of the plasma loading[12,13]. The latter method

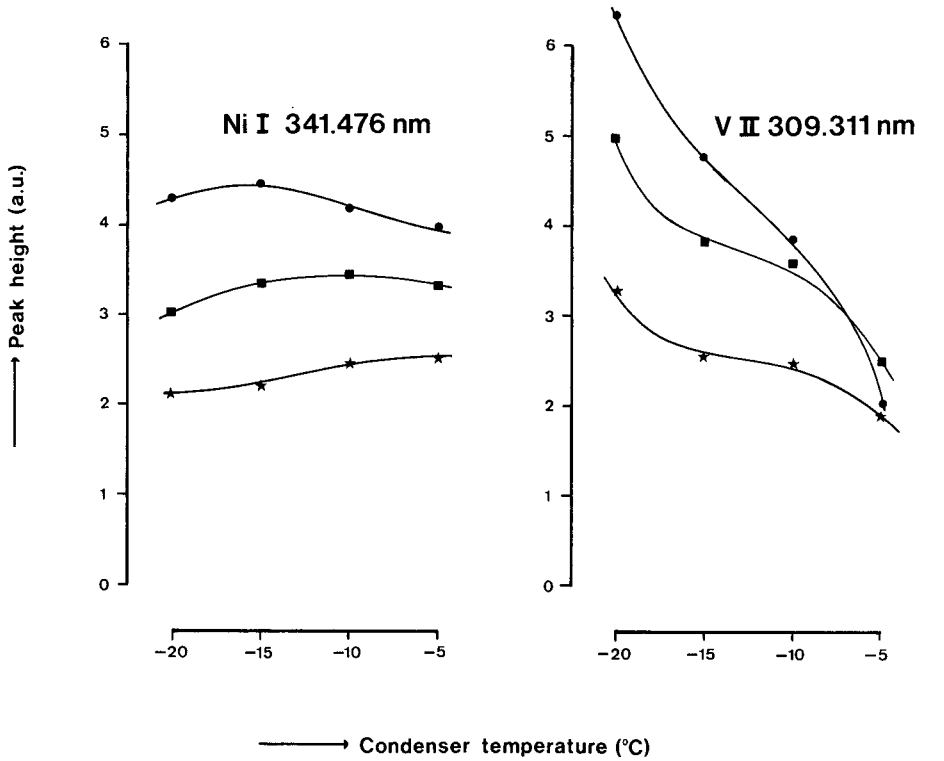

Fig. 2. Peak height of the transient emission intensity signal for a 100-μl injection of nickel and vanadium tetraphenylporphyrin standards in SEC–ICP-AES as a function of condenser temperature for various measuring heights in the plasma: (●) 16 mm, (■) 20 mm and (★) 24 mm above the load coil.

is best suited for liquid chromatography with ICP-AES detection because it does not impose limitations on mobile phase flow-rates. Therefore, a condenser was installed between the nebulizer and the torch assembly (see Fig. 1). The purpose of the cooling unit is to condense a fraction of the organic vapour, via adjustment of the cooling temperature, such that the residual mass flow of organic solvent is kept below the maximum tolerable solvent load of the plasma, while the analyte mass flow is essentially unaffected. The condenser temperature required to accomplish this depends mainly on the volatility of the solvent.

Fig. 2 shows the effect of the condenser temperature on the peak height of the transient emission intensity signals from some standard porphyrins for different observation heights in the plasma and for THF as the solvent. For peak area as a function of the condenser temperature similar results were obtained. It must be noted that the plasma becomes unstable when for THF cooling temperatures above -5°C are applied. As shown in Fig. 2, a decrease in the condenser temperature, and hence of the mass flow of organic vapour, has a favourable effect on the detector response only for vanadium. The reason for the different behaviour of the spectral lines considered on reduction of the solvent loading of the plasma is that the intensity of ionic lines

(V II) is more susceptible to a decrease in the excitation temperature than the intensity of the atomic lines (Ni I)[17].

As the noise levels of the analytical signals do not differ significantly for the various condenser temperatures, the analytical performance of the condenser setup is determined primarily by the net signal intensity. Accordingly, from Fig. 2 it can be concluded that a condenser temperature of −20°C combined with an observation height in the plasma of 16 mm above the load coil makes a good experimental compromise. Optimum ICP-AES experimental conditions for some other solvents, such as chloroform, can be found in refs. 12 and 13.

The use of a condenser introduces additional peak broadening and consequently affects the chromatographic resolution. The magnitude of this peak broadening was determined by measuring the peak widths resulting from 20-μl injections of a standard porphyrin solution directly (column removed) into the ICP with and without the condenser, at a nebulizer feeding rate of 1 ml/min. From these measurements the peak broadening caused by the condenser, expressed as the volume standard deviation, σ_V, was calculated to be 34 μl. The total external peak broadening introduced by the ICP-AES system amounts to 45 μl. This causes about a 35% decrease in column efficiency (*i.e.*, the plate number N) and about a 20% loss in resolution for the two columns under investigation.

Selection of SEC conditions

SEC has been used frequently for the determination of the molecular weight distributions of oils and oil fractions[18–23] and coal-derived liquids[24–27]. The technique has also been shown to be suitable for the molecular speciation of nickel and vanadium complexes in oil, using off-line ETA-AAS or on-line ICP-AES element-specific detection[3–11]. In most instances polystyrene-based SEC packings with pore sizes in the range 50–1000 Å are used. THF, mixtures of benzene and methanol, xylenes, mixtures of xylenes, cresols and pyridine and, to a lesser extent, chloroform usually serve as the mobile phase.

When employing liquid chromatography with ICP-AES detection, xylenes are generally used as the mobile phase, because they can be introduced into the ICP without the need for precautions regarding plasma overloading[16]. However, in addition to the required matching of the organic mobile phase to the ICP, two other requirements have to be fulfilled: (i) the recovery of the metal complexes from the column must be complete and (ii) the chromatographic system has to discriminate the metal complexes solely on the basis of their molecular size. Both requirements may not be met when the metal complexes interact with the column packing material in the presence of the selected mobile phase[18].

Recoveries of V and Ni in the SEC fractionation

For a meaningful interpretation of SEC results in terms of a molecular weight distribution of the oil, forms of retention of the solutes other than sole exclusion, such as adsorption, must be absent and the metal complexes must be stable during the chromatography. If exclusion is the only retention mechanism all metal species will elute from the column within the exclusion limits, *i.e.*, all injected metal compounds are completely recovered in the eluent volume collected between the total exclusion and total permeation volume. Measurement of the recovery of the injected amount of

metal compounds in this collected eluent fraction (defined as the SEC recovery) is therefore an indication of the occurence of retention phenomena other than size exclusion. We therefore determined the V and Ni content in a collected volume between 1 and 2.5 times the total exclusion volume and calculated the SEC recovery from the total metal content in the injection volume. It must be noted that only for a 100% SEC recovery can a reasonably pure exclusion mechanism be assumed; for smaller SEC recoveries this certainly does not hold.

Little is known about the nature and stability of the metal complexes in oil. Ni and V porphyrins appear to be fairly stable under vigorous conditions such as refluxing at increased temperature in trifluorophosphoric or sulphuric acid[28] and it is therefore reasonable to assume that these compounds are stable in the mobile phases applied in this study. However, it has been shown that V and Ni porphyrins form reversible complexes with nucleophiles such as ethanolamine[28,29]. As many nucleophilic compounds are present in oil, the appearance of multi-ligand metal complexes cannot be excluded. However, when dissolving 3% (v/v) of oil in the mobile phase, the sample is so dilute that the possibly formed multi-ligand metal complexes dissociate into the most stable configuration and most probably will remain stable during the chromatography. The same arguments can be assumed to hold for the non-porphyrin-like metal complexes.

The SEC recoveries of Ni and V on the polystyrene and diol-modified silica gel packings as found with THF, chloroform, *p*-xylene and *p*-xylene–methanol (80:20,

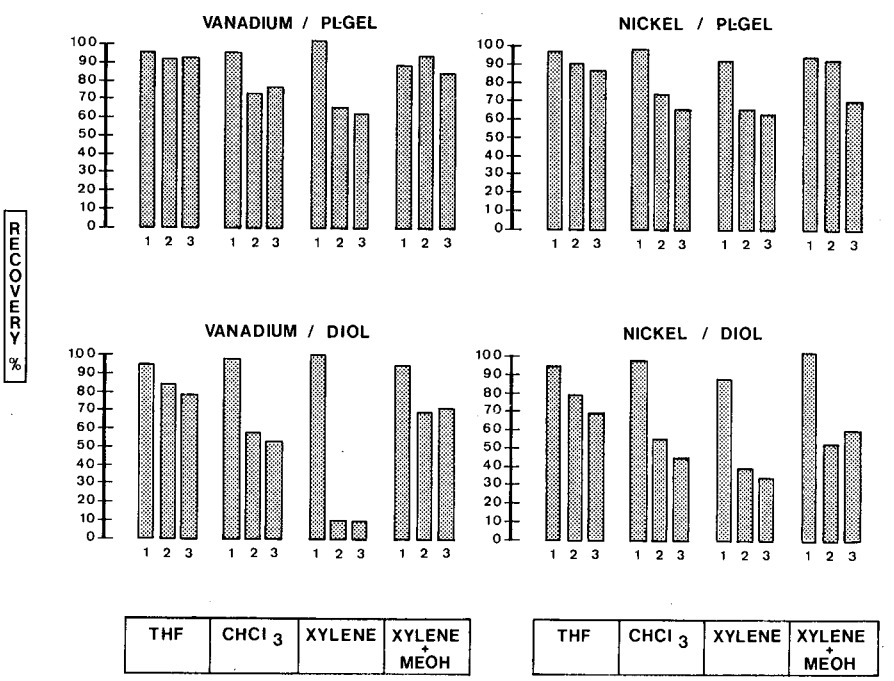

Fig. 3. Recovery of nickel and vanadium in SEC of different samples on PS–DVB and diol-type columns with selected mobile phases. Samples: (1) tetraphenylporphyrin standards; (2) Gach Saran Atmospheric Residue; (3) Arabian Heavy. MeOH = Methanol.

v/v) as mobile phase are shown in Fig. 3. The last mixture was chosen as the addition of methanol to the mobile phase has been reported to result in a better suppression of adsorption effects[3,18]. A methanol concentration of 20% was chosen to obtain the maximum increase in polarity without imposing the need for aerosol cooling. From Fig. 3 it can be seen that, within the experimental error, which is about 5%, in all instances a nearly complete SEC recovery was obtained for the tetraphenylporphyrin standards. With regard to the oil samples, two significant conclusions can be drawn. First, the SEC recoveries of both Ni and V are higher on the polystyrene packing than on the diol-modified silica gel packing. Second, the SEC recoveries decrease substantially with decreasing polarity of the mobile phase according to the sequence THF > chloroform > *p*-xylene. As expected[3,18], the SEC recoveries are significantly increased by the addition of methanol to *p*-xylene. The observed effects can be attributed to the interaction of metal complexes with the packing material. The diol-modified silica gel has a significantly more polar surface than the polystyrene packing and, as a result, the former packing shows greater adsorptive properties for (polar) metal complexes. The greater is the adsorption the weaker is the elution strength (polarity) of the mobile phase. In order to investigate whether the Ni and V compounds irreversibly adsorb on the packings, fractions of the mobile phase eluting after 2.5 times the total exclusion volume were collected and analysed by AAS. From the mass balance it appears that on the polystyrene column with THF all metals could be recovered in a volume fraction between 1 and 3.5 times the total exclusion volume. For *p*-xylene–methanol (80:20), 95% of the metals were found to elute in the volume fraction between 1 and 5 times the total exclusion volume. However, with chloroform and *p*-xylene it appears that a part of the metal compounds absorb strongly on the packing and only about 80% of the metals were recovered in a collected fraction between 1 and 20 times the total exclusion volume. With the diol column and THF as mobile phase all metals could be recovered within an elution volume of 6 times the total exclusion volume. With *p*-xylene–methanol (80:20) as mobile phase the recoveries in the same fraction as with THF were about 85% for V and 70% for Ni. Very strong adsorption of the metals was found with chloroform and in particular of V with *p*-xylene as mobile phase. The recoveries of V and Ni in a fraction of 20 times the exclusion volume ranged between 55 and 65% for chloroform and between 15 and 45% for *p*-xylene.

From the results depicted in Fig. 3 and from the adsorption data, it can be concluded that for the SEC of vanadium and nickel complexes in oil a polystyrene column packing and a medium-polarity solvent have to be used in order to obtain unambiguous results. In particular, the application of weakly eluting solvents, such as chloroform and *p*-xylene, should be avoided because with these solvents a substantial part of the metal complexes adsorbs strongly on the column packing material.

In order to investigate whether the metal compounds adsorb irreversibly on the column packing, in all experiments the mobile phase was changed to THF, after collection of the SEC fraction, and 6 (PS–DVB column) to 10 (diol column) times the total exclusion volume were collected and analysed by AAS. The total recovery from the column was then determined from the mass balance. In all experiments the total recovery of the metal compounds ranged between 95 and 105%, which can be considered as complete within the experimental error of the AAS measurements.

Elution profiles

The effect of the type of mobile phase on the elution profiles as recorded with visible-range and ICP-AES detection is shown in Figs. 4–7. In order to facilitate the comparison of the profiles a bar has been drawn at the maximum of the THF elution curve. The figures show that the profiles differ significantly when different mobile phases are used.

The elution patterns recorded with visible-light detection for tetrahydrofuran and chloroform have similar shapes, although the pattern for chloroform seems to be compressed in comparison with the THF curve. For the xylene-based mobile phases

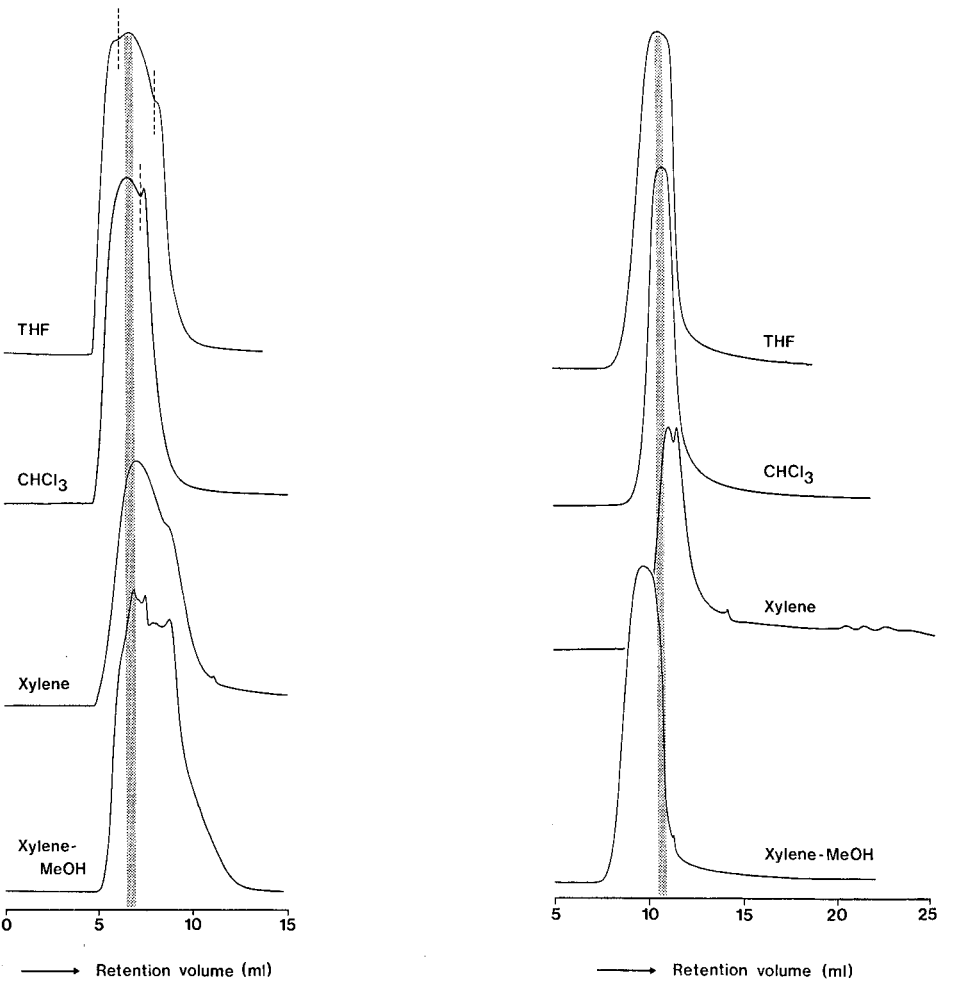

Fig. 4. SEC elution profiles for Gach Saran Atmospheric Residue (3%, w/v) on the PS–DVB column for different mobile phases. Detection, VIS, 405 nm; mobile phase flow-rate, 1 ml/min. The dashed lines refer to fractionation experiments described in the text. MeOH = Methanol.

Fig. 5. SEC elution profiles for Gach Saran Atmospheric Residue (3%, w/v) on the diol-type column for different mobile phases. Detection, VIS, 405 nm; mobile phase flow-rate, 1 ml/min.

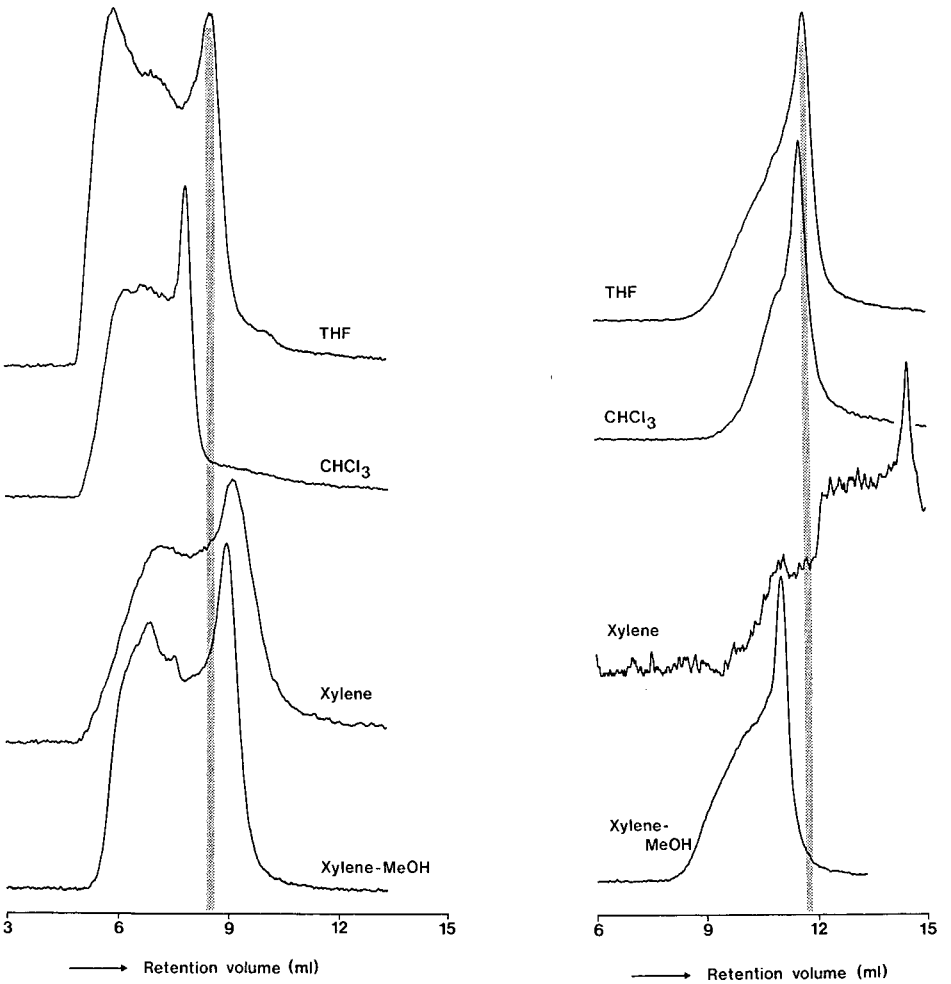

Fig. 6. Elution profiles for vanadium using ICP-AES detection for Gach Saran Atmospheric Residue (3%, w/v) on the PS–DVB column for different mobile phases. Detection wavelength, V, 309.311 nm; mobile phase flow-rate, 1 ml/min. For ICP operating conditions, see Table II.

Fig. 7. Vanadium elution profiles using ICP-AES detection for Gach Saran Atmospheric Residue (3%, w/v) on the diol-type column for different mobile phases. Detection wavelength, Ni, 341.476 nm; mobile phase flow-rate, 1 ml/min. For ICP operating conditions, see Table II.

the chromatogram is broadened and severe tailing is observed, especially for combinations of xylene with the diol-type column and xylene–methanol with the PS–DVB column. The corresponding peak patterns are distinctly different from those obtained using THF or chloroform as the mobile phase.

With respect to the interpretation of the vanadium ICP profiles shown in Figs. 6 and 7, the following comments can be made. Although xylene and xylene–methanol do not require aerosol thermostatting, the experimental setup shown in Fig. 1 was applied so as to make comparison between the profiles more straightforward. Be-

cause of the lower nickel concentration levels in oil samples, in combination with poorer ICP-AES detection limits, the elution patterns for nickel are much more "noisy' than those for vanadium. As the changes in peak profiles were found to be similar for nickel and vanadium, only those for vanadium are shown. As the ICP-AES detector response is dependent on the plasma excitation conditions and therefore on the mobile phase used in the SEC separations, peak heights and areas cannot be compared directly from the diagrams. However, a comparison of signal-to-noise ratios, in combination with the recoveries shown in Fig. 3, leads to the conclusion that the detection capabilities of ICP-AES do not show gross variations with the mobile phases used.

As can be seen from Figs. 6 and 7, the vanadium profiles differ considerably from those recorded with visible-range detection. Compared with the profile obtained with THF on PS–DVB, the chromatogram for chloroform is compressed and that for xylene is broadened. Both profiles lack the maximum at the high-molecular-weight end of the chromatogram. In contrast, the profile for xylene–methanol more closely resembles that for THF, although its visible-range pattern was distinctly different from the profile for THF. The peak positions for the PS–DVB column depend strongly on the mobile phase used.

Except for xylene, the elution profiles on the diol-type column are nearly identical, although the peak positions are different for the different solvents. The large retention and the poor signal-to-noise ratio for xylene suggest strong adsorption on the diol-type column. This is consistent with the 10% recovery shown in Fig. 3. None of the elution patterns for the diol-type column shows a maximum in the high-molecular-weight region.

Molecular weight calibration of the SEC columns

The effect of the type of mobile phase on the calibration of the SEC columns was determined with a standard set of polystyrenes and benzene and is shown in Figs.

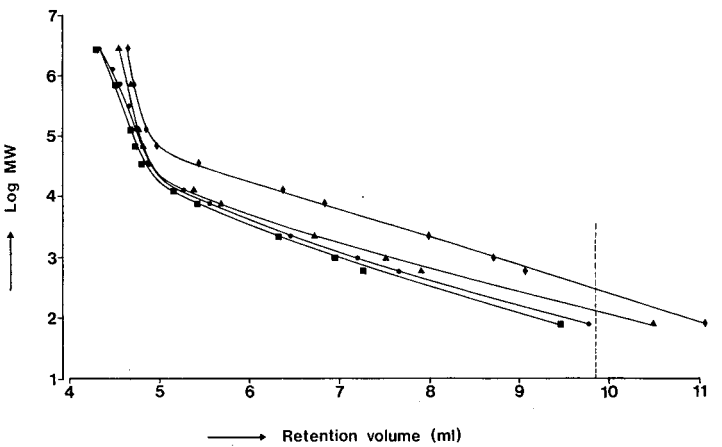

Fig. 8. Molecular weight (MW) calibration graphs for polystyrene standards and benzene on the PL-GEL column using different mobile phases: (●) THF; (■) chloroform; (▲) xylene; (◆) xylene–methanol. Dashed line: total permeation limit.

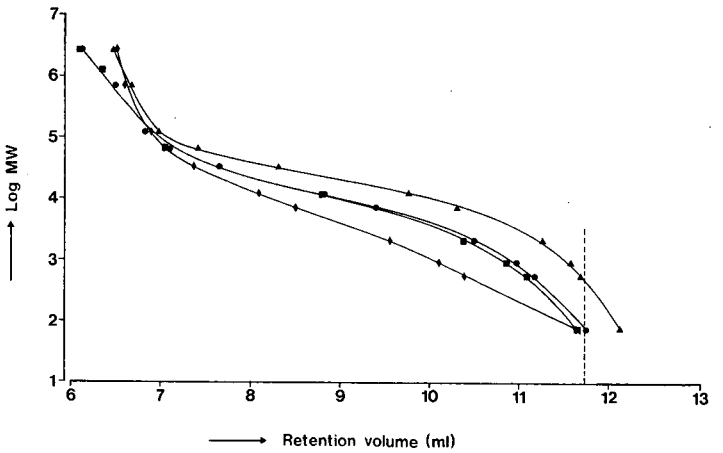

Fig. 9. Molecular weight (MW) calibration graphs for polystyrene standards and benzene on the GF-250 column using different mobile phases: (●) THF; (■) chloroform; (▲) xylene; (◆) xylene–methanol. Dashed line: total permeation limit.

8 and 9. The total permeation limits, as determined by weighing of the column with different solvents, were found to be 9.85 ml for the PL-GEL column and 11.73 ml for the diol column. The elution behaviour of the PS standards on the PL–GEL column with THF and chloroform is nearly identical, except for a constant slight shift in retention volume for the chloroform curve. These small differences in retention can be attributed to the difference in the pore swelling of the gel in chloroform and THF. The lower swelling of the gel in chloroform impairs the resolving power of SEC with this solvent[30]. For xylene there is a small shift towards higher elution volumes, and probably sorption into or on to the packing material will play a part, as is demonstrated by the elution of benzene at a retention volume larger than the total permeation limit.

TABLE III

MOLECULAR WEIGHTS FOR SELECTED MODEL PORPHYRINS DETERMINED EXPERIMENTALLY BY SEC USING THE POLYSTYRENE CALIBRATION GRAPHS

Column	*Solute**	*Real MW*	*MW determined by SEC*			
			THF	*Chloroform*	*Xylene*	*Xylene–methanol*
PS–DVB	VOTPP	679.7	372	440	237	395
	Etio	640.5	337	409	241	472
	OEP	534.8	397	474	397	714
Diol	VOTPP	679.7	240	248	N.D.**	458
	Etio	640.5	330	153	N.D.	355
	OEP	534.8	426	262	N.D.	433

* Model porphyrins: VOTPP = vanadyl mesotetraphenylporphine; Etio = 2,7,12,17-tetraethyl-3,8,13,18-tetramethyl-21*H*, 23*H*-porphine dihydrobromide; OEP = 2,3,7,8,12,13,17,18-octaethylporphine.

** N.D. = Not determined (outside calibration range).

The elution volumes for PS standards in xylene–methanol are larger than those in THF; this difference can be as large as 1.5 ml. Probably a reversed-phase type of distribution towards the packing occurs in the presence of methanol. It can further be noted that the retention of polystyrene standards when using THF as the mobile phase was the same on injecting the standards dissolved in THF or dissolved in the oil samples [3% (w/v) in THF]. This indicates that the sample is sufficiently diluted to avoid the influence of mutual interaction on the retention of the solutes in oil.

For the diol-type column the calibration graphs for THF and chloroform coincide well, but those obtained for the xylene-based mobile phases deviate significantly. With xylene there is an additional retention of the solutes by adsorption on the column packing material. In the presence of methanol the calibration graph is shifted in the opposite direction for unknown reasons.

Molecular weight distributions of oil samples

To examine the suitability of molecular weight calibrations based on PS standards for metal compounds present in oil samples, two different routes were followed. First, the calibration of both columns was checked with a number of model porphyrins. As most of the commercially available metal porphyrins cover only a small molecular weight range, this experiment was performed with both metal-containing and metal-free porphyrins. A selection of results is presented in Table III. For all the solvents used, the molecular weights determined from the PS calibration graphs are much smaller than the real molecular weights. Thus calibration with polystyrenes is insufficient for the determination of the molecular weights of these model porphyrins. However, porphyrins constitute only a minor part of the metal complexes present in oil[1]. Therefore, a second approach involving computerized manipulation of the chromatograms in order to convert the volume axis to a log(molecular weight) axis was adopted. This was done by means of the PS calibration graphs. In the ideal case, this approach would rule out the effects of the mobile phases on the column packing.

The procedure involves a smoothed spline interpolation[31] through the experimental data from the PS calibration graphs. In the present instance the use of the spline interpolation is convenient as it does not require a physical model to fit the data. By means of this interpolation, files were generated that correlate each retention volume data point with a corresponding PS molecular weight value. Subsequent combination of these files with the chromatogram files resulted in profiles of vanadium content *versus* polystyrene-based molecular weights (Fig. 10). It should be noted that the differences in signal height between the converted and the original profiles arise from scaling with the reciprocal slope of the calibration graph, which is necessary for consistency of the distribution[18].

A comparison of Figs. 10 and 6 shows that when the column calibration data are included in the diagrams, there is a better agreement for the elution profiles recorded with THF, chloroform and xylene. The profile for xylene–methanol is "over-compensated". This is probably due to a specific effect of methanol on the polystyrene standards, rather than the result of an overall effect of the mobile phase on the column packing. Except for xylene–methanol, the conversion procedure appears to align the profiles. This could indicate a similar behaviour for solutes present in oil samples and polystyrene standards in three of the mobile phases used.

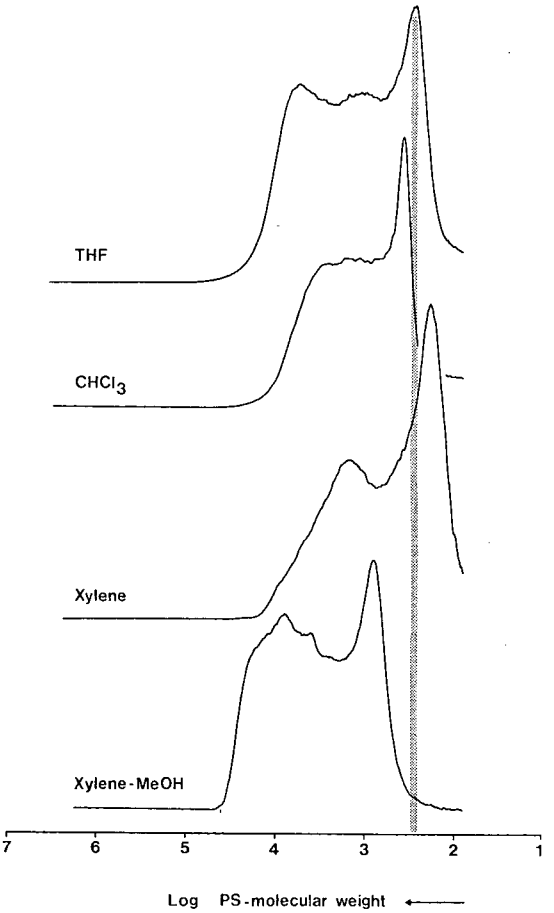

Fig. 10. Vanadium SEC–ICP-AES profiles for Gach Saran Atmospheric Residue on PL-GEL after computerized conversion of the volume axis to a log(PS) molecular weight axis.

Adsorption/association effects

Apart from differences arising from changes in the gel packing, SEC profiles may be affected by solute–solute and solute–solvent associations and by adsorption of solutes on to the gel surface[30]. Although THF and chloroform are reported to be the most compatible solvents for polystyrene stationary phases, with size exclusion being the predominant separation mechanism[20,27,32–34], differences in recoveries (*cf.*, Fig. 3) and the differences in the vanadium profiles for oil samples reveal the occurence of additional interaction mechanisms. The profile in THF, for instance, could indicate that for chloroform and xylene adsorption of high-molecular-weight compounds on to the stationary phase has occurred. This is consistent with the lower recoveries for chloroform and xylene shown in Fig. 3. On the other hand, it is known that in concentrated solutions of asphaltenes in THF self-association can occur[26], which brings about an apparent increase in the molecular weights of these compounds. However, it self-association had occurred, it would be expected to appear

more pronounced in a poorer solvent such as xylene. The lack of a maximum at the high-molecular-weight end of the chromatogram for xylene is not conclusive in this instance because of the simultaneous occurence of adsorption effects.

In order to investigate the role of association effects in more detail, the effluents from the PS-DVB column using THF and chloroform as the mobile phases were collected in three and two fractions, respectively, according to the dashed lines in Fig. 4. After evaporation to dryness, the fractions collected in THF were dissolved and analysed by SEC with chloroform as the mobile phase. The fractions collected in chloroform were treated similarly using THF as the mobile phase. If association had occured in THF, and chloroform were capable of breaking up these associates, the high-molecular-weight fraction collected in THF should reveal the presence of lower molecular weight compounds when analysed in chloroform. In addition, the first fraction collected in chloroform should show a shift towards lower elution volumes (and higher molecular weights) when analysed in THF. However, neither of these effects has been observed. This supports the suggestion that adsorption rather than association is involved. Consequently, the appearance of the high-molecular-weight maximum on the addition of methanol to the xylene mobile phase indicates a significant decrease in the adsorption of the high-molecular-weight compounds.

Detection limits, sample concentrations and matrix effects

The detection limits of nickel and vanadium, based on signals from tetraphenylporphyrin standards equal to three times the standard deviation of the noise and using THF as the mobile phase, were found to be 3.5 and 0.5 ng, respectively. This corresponds to concentration detection limits of 35 and 5 ng/ml for 100-μl injections.

Considering the 30-fold dilution step applied for crudes and derived products, this leads to detection limits in the original sample of 1.2 μg/g for nickel and 0.17 μg/g for vanadium. As the nickel and vanadium levels in crudes range from 4 to 150 and from 8 to 1200 μg/g, respectively[1], and the metal compounds are in general distributed over a large molecular-weight range, the determination of nickel will be limited to samples with a relatively high concentration. The situation is better with vanadium because of the lower detection limits and higher concentration levels in crudes.

As will be clear from the above, relatively high sample concentrations have to be used. This is in agreement with values of 1–10% (w/v) reported by other workers[3,9,10]. As elution anomalies such as association effects tend to increase with increasing sample concentration[20,26], one has to be careful in the interpretation of the SEC patterns and molecular-weight distributions obtained.

SEC–ICP-AES experiments with oil samples spiked with tetraphenylporphyrin standards show that in the presence of an oil matrix the detector response for the tetraphenylporhyrins decreases. The decrease is more pronounced for vanadium (ionic emission) than for nickel (atomic emission), suggesting an effect of the oil matrix on the plasma excitation conditions. Although there is no dramatic decrease in signal intensities (about 10–20% for a 1 ppm NiTPP or VOTPP standard), its occurrence again stresses the potential pitfalls in the interpretation of SEC–ICP-AES results. This holds in particular when the matrix composition differs for different sample types and, moreover, when even in a single chromatogram response factors may vary as a result of changes in the matrix composition due to the separation process.

Recommendations for the SEC–ICP-AES of oil samples

As the number of compounds present in oil samples is enormous, and these compounds have a wide variety of different configurations, it is obvious that no specific combination of column, mobile phase and calibration standards can be recommended for all situations. From this work, it can be concluded that THF and xylene–methanol in combination with a PS–DVB column show the best behaviour in terms of overall recoveries for nickel and vanadium and in revealing the high-molecular-weight part of the SEC profiles. Xylene–methanol would be preferable in SEC–ICP, because no special precautions are required. Nevertheless, preference should be given to THF, because for the polystyrene-type columns its interactions with various types of solutes are well documented [20–23,26,27,30,35–39]. However, the complexity of the separation mechanisms, which are complicated by solute–solvent, solute–gel and solute–solute interactions, requires additional experiments with independent analytical techniques to test the SEC results. Especially with regard to the molecular-weight distributions additional calibrations should be performed, preferably with narrow preparative SEC fractions of materials similar to those under study, with known molecular weights as determined, for example, by vapour-phase osmometry or ultracentrifugation[25,26].

Application of SEC–ICP-AES in catalyst research

An important field of application of the SEC–ICP-AES analysis of oil samples involves monitoring of the hydrodemetallation process. Fig. 11 shows the vanadium and nickel profiles of Gach Saran Resid, a heavy Iranian atmospheric residue, and its products. The properties of the feed are given in Table IV. The resid was treated with two different hydrodemetallation catalysts under the conditions given in Table V. As can be seen from Fig. 11, both nickel and vanadium are removed mainly from the smaller molecules. The selectivity of demetallation for different molecular weights is the same for both catalysts.

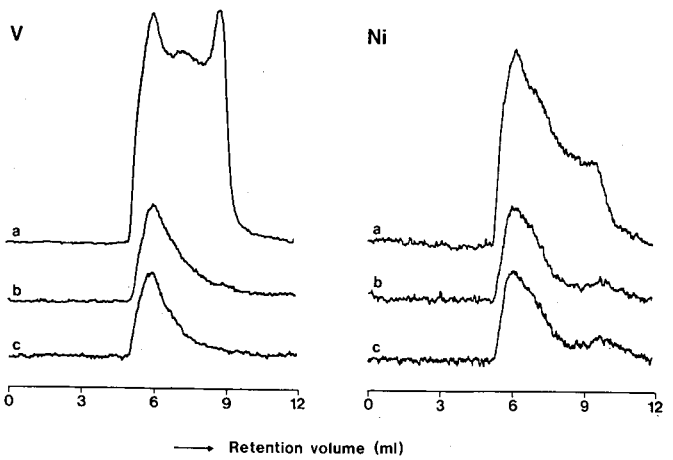

Fig. 11. Vanadium and nickel SEC–ICP-AES profiles for (a) Gach Saran Atmospheric Residue and (b and c) two of its products that followed different hydrotreatment schemes. Sample concentration for nickel analyses: 10% (w/v).

TABLE IV

PROPERTIES OF THE FEEDS USED

Component	*Gach Saran Atmospheric Residue (density 0.9751 g/ml)*	*Kuwait Atmospheric Residue (density 0.9658 g/ml)*
Sulphur (%, w/w)	3.05	3.98
Nitrogen (ppm)	4400	2230
Conradson carbon residue (%, w/w)	11.46	10.18
Nickel (ppm)	70	16
Vanadium (ppm)	229	63

TABLE V

PROCESS CONDITIONS OF CATALYTIC HYDROTREATMENT

Parameter	*Gach Saran Resid*		*Kuwait Atmospheric Resid*		
	Fig. 11b	*Fig. 11c*	*Figs. 12d–14*	*Figs. 12b–14*	*Figs. 12c–14*
LHSV*	0.50	0.50	0.95	0.95	0.95
Temperature (°C)	372	372	370	370	370
H_2 pressure	106	106	136	136	140
Catalyst type	HDM**	HDM	HDM	HDS*** (cat. 1)	HDS (cat. 2)

* LHSV = Liquid hourly space velocity.
** HDM = Hydrodemetallation catalyst.
*** HDS = Hydrodesulphurization catalyst.

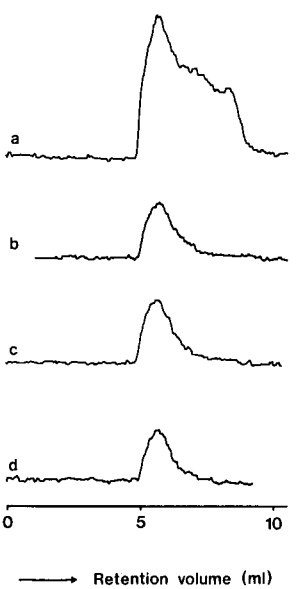

Fig. 12. Vanadium SEC–ICP-AES profiles for (a) Kuwait Atmospheric Residue, (b and c) products formed when the resid is hydrotreated using two different hydrodesulphurization catalysts and (d) a hydrodemetalation catalyst.

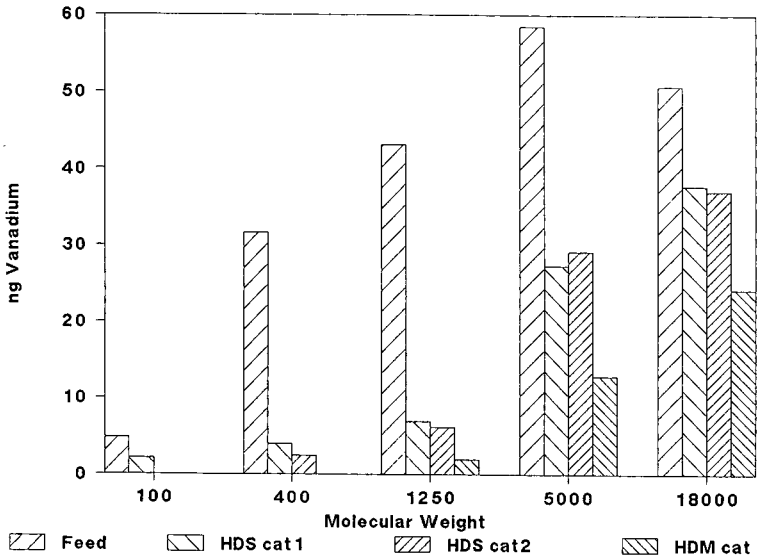

Fig. 13. Vanadium content of five molecular-weight fractions of Kuwait Atmospheric Residue before and after hydrotreatment with different catalysts (cat). The fractions originate from 3 mg of the feed and the products.

Fig. 12 shows the vanadium profiles of Kuwait Atmosperic Resid and different products resulting from treatment with two types of catalysts, *viz.*, two different resid hydrodesulphurization catalysts (Fig. 12b and c) and a hydrodemetallation catalyst

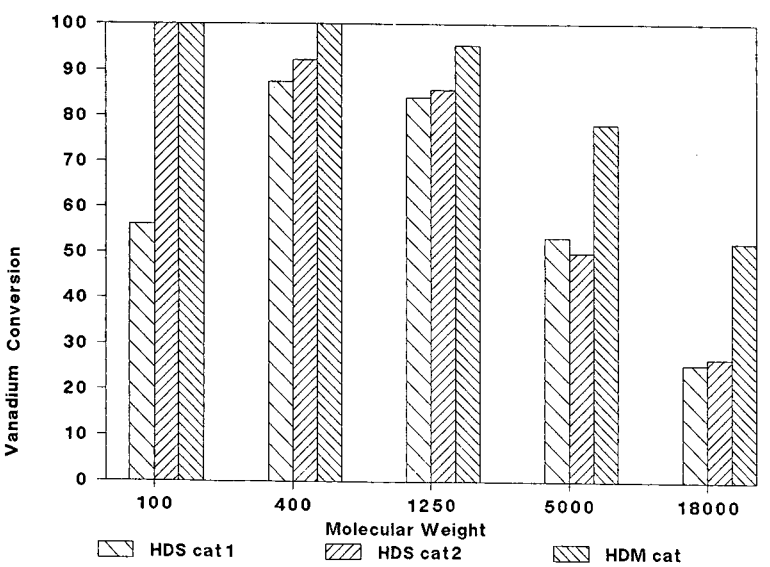

Fig. 14. Conversion of vanadium (in %) of Kuwait Atmospheric Residue as a function of molecular weight for three different hydrotreatment catalysts.

(Fig. 12d). The characteristics of the feed are given in Table IV and the process conditions in Table V. The chromatograms were treated as follows. The area percentages of five fractions of the chromatogram were determined and multiplied by the total amount of vanadium present in the sample (Fig. 13). In doing this, the small changes in signal response that could arise from differences in matrix composition with changing molecular weight are ignored. From Fig. 13 the conversion of vanadium was calculated by dividing the amount of vanadium present in the products and feed in the different fractions.

The difference in performance between the two types of catalysts is clearly shown in Fig. 14. The desulphurization catalysts remove about 20% of the vanadium incorporated in the high-molecular-weight molecules, whereas the conversion of the demetallation catalyst, with larger pores, is about 50%. The difference in performance of the hydrodesulphurization catalysts in the low-molecular-weight region is not considered significant. It can be explained from the less favourable signal-to-noise ratio in this part of the chromatogram. In the other molecular-weight regions the performances of the experimental hydrodesulphurization catalysts are comparable.

This application shows that the SEC–ICP-AES method can indeed be applied to products of low metal level feeds such as Kuwait Atmospheric Resid.

ACKNOWLEDGEMENTS

Thanks are due to S. Heemstra and G. Feenstra for their assistance in the calibration and recovery studies and to H.F.M. Boelens for implementing the spline interpolation program on the HP 1000 system. J. M. Kool is thanked for valuable discussions.

REFERENCES

1 R. Agrawal and J. Wei, *Ind. Eng. Chem., Process Des. Dev.*, 23 (1984) 505.
2 C. Hung and J. Wei, *Ind. Eng. Chem., Process Des. Dev.*, 19 (1980) 250.
3 T. Tsukada, K. Saitoh and N. Suzuki, *Anal. Chim. Acta*, 183 (1986) 97.
4 R. H. Fish and J. J. Komlenic, *Anal. Chem.*, 56 (1984) 510.
5 R. H. Fish, J. J. Komlenic and B. K. Wines, *Anal. Chem.*, 56 (1984) 2452.
6 J. G. Reynolds and W.R. Biggs, Preprints of papers presented at the Chicago meeting of the American Chemical Society, September 1985, *Am. Chem. Soc. Div. Fuel Chem. Prepr.*, 30 (3) (1985) 436.
7 R. Agrawal and J. Wei, *Ind. Eng. Chem., Process Des. Dev.*, 23 (1984) 515.
8 R. A. Ware and J. Wei, *J. Catal.*, 93 (1985) 100.
9 D. W. Hausler, *Spectrochim. Acta*, Part B, 40 (1985) 389.
10 D. W. Hausler and R. S. Carlson, Preprints of papers presented at the Miami Beach meeting of the Division of Petroleum Chemistry of the American Chemical Society, 1985, *Am. Chem. Soc. Div. Pet. Chem. Prepr.*, 30 (1) (1985) 28.
11 W. R. Biggs R. J. Brown and J. C. Fetzer, *ICP Inf. Newsl.*, 11 (1986) 857.
12 F. J. M. J. Maessen, G. Kreuning and J. Balke, *Spectrochim. Acta*, Part B, 41 (1986) 3.
13 F. J. M. J. Maessen, P. J. H. Seeverens and G. Kreuning, *Spectrochim. Acta*, Part B, 39 (1984) 1171.
14 C. H. Gast, J. C. Kraak, H. Poppe and F. J. M. J. Maessen, *J. Chromatogr.*, 185 (1979) 549.
15 T. Brotherton, B. Barnes, N. Vela and J. Caruso, *J. Anal. At. Spectrom.*, 2 (1987) 389.
16 A. W. Boorn and R. F. Browner, *Anal. Chem.*, 54 (1982) 1402.
17 R. K. Winge, V. J. Peterson and V. A. Fassel, *Appl. Spectrosc.*, 33 (1979) 206.
18 K. H. Altgelt and T. H. Gouw (Editors), *Chromatography in Petroleum Analysis*, Marcel Dekker, New York, 1979.
19 H. Reerink and J. Lijzenga, *Anal. Chem.*, 47 (1975) 2160.

20 V. Sanchez, E. Murgia and J. A. Lubkowitz, *Fuel*, 63 (1984) 612.
21 G. A. Haley *Anal. Chem.*, 43 (1971) 371.
22 H. H. Kiet, L. Ph. Blanchard and S. L. Malhotra, *Sep. Sci.*, 12 (1977) 607.
23 J. G. Bergmann, L. J. Duffy and R. B. Stevenson, *Anal. Chem.*, 43 (1971) 131.
24 W. M. Coleman, D. L. Wooton, H. C. Dorn and L. T. Taylor, *Anal. Chem.*, 49 (1977) 533.
25 K. D. Bartle, M. J. Mulligan, N. Taylor, T. G. Martin and C. E. Snape, *Fuel*, 63 (1984) 1556.
26 K. D. Bartle, D. G. Mills, M. J. Mulligan, I. O. Amaechina and N. Taylor, *Anal. Chem.*, 58 (1986) 2403.
27 N. Evans, T. M. Haley, M. J. Mulligan and K. M. Thomas, *Fuel*, 65 (1986) 695.
28 R. Bonnett, P. Brewer, K. Noro and T. Noro, *Tetrahedron* , 34 (1978) 379.
29 J. S. Flynn and D. H. Freeman, *J. Chromatogr.* , 386 (1987) 111.
30 J. G. Hendrickson and J. C. Moore, *J. Polym. Sci. Part A-1*, 4 (1966) 167.
31 R. Sauer and I. Szabo, *Mathematische Hilfsmittel des Ingenieurs*, Part 3, Springer, Berlin, 1970, p. 275.
32 M. K. L. Bicking, *Anal. Chem.*, 56 (1984) 2671.
33 J. R. Adams and M. K. L. Bicking, *Anal. Chem.*, 57 (1985) 2844.
34 M. K.L. Bicking and S. J. Serwon, *J. Liq. Chromatogr.*, 10 (1987) 1369.
35 C. V. Philip and R. G. Anthony, *Fuel*, 61 (1982) 357.
36 A. Lambert, *Anal. Chem.*, 53 (1971) 63.
37 B. K. Friley, J. B. Phelps and J. R. Kincaid, *J. Chromatogr.*, 258 (1983) 310.
38 J. F. McKay and D. R. Latham, *Anal. Chem.*, 45 (1973) 1050.
39 M. Popl, J. Fahnrich and M. Stejskal, *J. Chromatogr. Sci.*, 14 (1976) 537.

Journal of Chromatography, 462 (1989) 137–145
Elsevier Science Publishers B.V., Amsterdam — Printed in The Netherlands

CHROM. 20 993

EFFECTS OF pH ON THE FORMATION OF FLAVOUR COMPOUNDS OF DISRUPTED GARLIC

TUNG-HSI YU* and CHUNG-MAY WU
Food Industry Research and Development Institute (FIRDI), P.O. Box 246, Hsinchu 300 (Taiwan)
(First received May 19th, 1988; revised manuscript received September 12th, 1988)

SUMMARY

The effects of pH adjustment during the blending of garlic cloves on the formation of flavour compounds of garlic were studied by high-performance liquid chromatography (HPLC) and gas chromatography (GC). HPLC analysis showed that maximum allicin formation occurred around pH 6.5. By GC analysis it was also found that the two isomeric cyclic compounds 3-vinyl-(4*H*)-1,2-dithiin and 2-vinyl-(4*H*)-1,3-dithiin, which were artifacts formed from allicin during GC, reached their highest levels around pH 6.5, whereas the formation of diallyl trisulphide, diallyl disulphide, methyl allyl disulphide and diallyl sulphide was favoured around pH 9.0.

INTRODUCTION

Garlic (*Allium sativum* Linn.) has been prized for its flavor and pungency for many centuries. Semmler[1] obtained a steam volatile oil from garlic in low yield (0.1–0.2%) and established the importance of diallyl disulphide and diallyl trisulphide in the flavour of garlic distillate. It was also evident at an early stage that the odorous compounds of interest were not present in the plant as such but were formed enzymically when the cellular tissue was disrupted. Cavallito and Bailey[2] described the isolation of the odoriferous antibacterial substance allicin (diallyl thiosulphinate) by extraction of garlic with ethanol at room temperature. Stoll and Seebeck[3] reported that intact garlic cloves contain 0.24% (w/w) of S-allylcysteine S-oxide (alliin), a colourless, odourless solid, and an enzyme, allinase, which converts alliin into allicin. Subsequent research[4] revealed that the cysteine sulphoxide fraction of garlic consists of 85% of alliin, 2% of S-propylcysteine sulphoxide and 13% of S-methylcysteine sulphoxide. The action of allinase on a mixture of these sulphoxides affords thiosulphinates. In addition to S-substituted cysteine sulphoxides, three (possibly four) γ-L-glutamyl derivatives of S-alk(en)ylcysteine sulphoxides were identified in garlic[5]. These compounds are not cleaved by allinase, they represent only "potentially available" flavor. Consequently, peptidases and transpeptidases which "release" these secondary flavour precursors to primary flavour precursors, that is, thiosulphinates, are important enhancers of the aroma of garlic and its products[5].

The crude cell-free garlic enzyme solution, of unspecified purity, utilized by Stoll

0021-9673/89/$03.50

and Seebeck[3,6] showed a broad pH optimum of 5–8 and a temperature optimum of 37°C under the conditions used. Using protamine and ammonium sulphate as precipitation agents and following precipitation by fractionation on Sephadex G-200, Mazelis and Crews[7] obtained a six-fold purification of the enzyme solution and confirmed the observations of Seebeck and Stoll. The purified enzyme possessed a pH optimum of 6.5 when S-methyl-L-cysteine sulphoxide was used as a substrate.

Using gas chromatographic–mass spectrometric (GC–MS) analysis of garlic extracts. Brodinitz *et al.*[8] revealed the presence of two isomeric cyclic compounds claimed to be 3-vinyl-1,2-dithi-5-ene and 3-vinyl-1,2-dithi-4-ene. These two compounds were postulated to be dehydration products of allicin formed during GC by analogy with the conversion of propyl propanethiosulphinate to 1-propenyl propyl disulphide at 150°C. Brodnitz *et al.* further observed that allicin underwent nearly complete decomposition at 20°C after 20 h. Decomposition of allicin proceeds by several pathways[9], in one of which it decomposes spontaneously to form two isomeric cyclic compounds, 2-vinyl-(4*H*)-1,3-dithiin and 3-vinyl-(4*H*)-1,2-dithiin. We also reported that allicin decomposed into these two compounds during GC[10].

Several methods have been reported for the quantitation of thiosulphinates[11–14]. It might appear that the best method for measuring the flavour and aroma is GC under carefully controlled conditions[15]. The individual components can be separated by GC and identified by MS. However, this method is sometimes unsatisfactory, especially when the compound is unstable to heat. For this reason, high-performance liquid chromatography (HPLC) may be a better method for separating the heat-labile compounds, although it also has the disadvantage of poor resolution. In this study, both GC and HPLC were used to determine the effects of pH adjustment on flavour formation in garlic during the blending of garlic cloves.

EXPERIMENTAL

Materials and chemicals

Garlic cloves, of unknown origin, were purchased locally. 2-Vinyl-[4*H*]-1,3-dithiin and 3-vinyl-[4*H*]-1,2-dithiin were synthesized by the method of Bock *et al.*[16] Allicin was synthesized by the method of Block *et al.*[17] using diallyl disulphide as the starting material.

Sample preparation

Peeled garlic cloves (100 g) were blended with 200 ml of distilled water for 5 min in a Waring blender, the pH during blending being adjusted by adding 0.5 *M* sodium hydroxide or 0.5 *M* hydrochloric acid. The homogenate was filtered through a double layer of cheese-cloth to obtain the garlic extract. For HPLC analysis, dimethyl disulphide stock solution (13 ml, 0.5 g in 500 ml of methanol) was added to 7 ml of garlic extract as an internal standard. After filtration through a filter-paper (Toyo No. 2) and a Minipore (Millipore, FG, 0.22 μm), the sample was applied to the HPLC system. For GC analysis, the garlic extract (20 ml) was extracted three times with one volume of diethyl ether. The ether fractions were combined, dried with anhydrous sodium sulphate and then concentrated to a small volume by blowing nitrogen over the surface of the solution in a hood. Dimethyl disulphide stock solution (2 ml, 0.08 g in 100 ml of diethyl ether) was added to the concentrate as an internal standard and 1 μl of

the sample was then analysed by GC. All the GC and HPLC analyses were carried out immediately after the garlic extract had been prepared.

HPLC analyses

A Shimadzu LC-5A HPLC system was used. An ODS column (200 × 4.6 mm I.D.) (Altex) was used for separation with methanol–water (65:35) (methanol of HPLC grade, Merck) as the mobile phase at a flow-rate of 2 ml/min. Detection was based on UV absorption at 254 nm.

Gas chromatography

GC was conducted on a Shimazu GC-9A instrument equipped with flame ionization detection (FID). A 50 m × 0.22 mm I.D. fused-silica column (Chrompack) coated with CP-Wax 52 CB was used. The oven temperature was programmed from 50 to 200°C at 2°C/min. The injector and detector temperatures were 250°C. The carrier gas was nitrogen at a flow-rate of 0.75 ml/min. The data were recorded on a Shimadzu C-R3A integrator. Values reported are averages of two analyses. The linear retention indices of the volatile components were calculated with C_8–C_{25} *n*-alkanes[18] (Alltech) references.

Gas chromatography–mass spectrometry

GC–MS was conducted with a Hewlett-Packard 5985B system. The gas chromatograph was fitted with a fused-silica capillary column (bonded CP-Wax 52 CB; 50 m × 0.32 mm I.D.). The oven temperature was programmed from 50 to 200°C at 2°C/min, the injector temperature was 250°C, the carrier gas was helium at a flow-rate of 1.8 ml/min, the ionization voltage was 70 eV and the ion source temperature was 200°C.

RESULTS AND DISCUSSION

Fig. 1 shows the HPLC traces of flavour components of garlic formed at (A) pH 2, (B) pH 6 and (C) pH 10. Seven peaks were detected; however, only peak 5, which had an odour reminisent of crushed fresh garlic, was collected and was identified as allicin[10]. Freeman and McBreen[19] described a spectrophotometric method that measures the absorption maximum of the thiosulphinates at 254 nm, and therefore the HPLC detection in this study was based on UV absorption at 254 nm. The significant differences in HPLC profiles among samples A, B and C in Fig. 1 were postulated to be due to the effect of pH on enzyme activities.

Fig. 2 shows the effect of pH (2.0–10.0 at 1.0-unit intervals) on the formation of allicin as analysed by HPLC. The data were relative to dimethyl disulphide as internal standard. Formation of allicin is favoured around pH 6.5; the optimum pH of allinase is also around 6.5, which is consistent with the results found by Mazelis and Crews[7].

Fig. 3 shows the gas chromatograms of the volatile components of garlic formed at (A) pH 2, (B) pH 6 and (C) pH 10. Table I shows a comparison of the concentration of volatile constituents in samples of different pH. Identification of the compounds was reported by us previously[20]. Fig. 4 shows the effect of pH on the formation of 2-vinyl-(4*H*)-1,3-dithiin and 3-vinyl-(4*H*)-1,2-dithiin, which were confirmed as the major artifacts formed from allicin during the GC[9,10]. Formation of these two

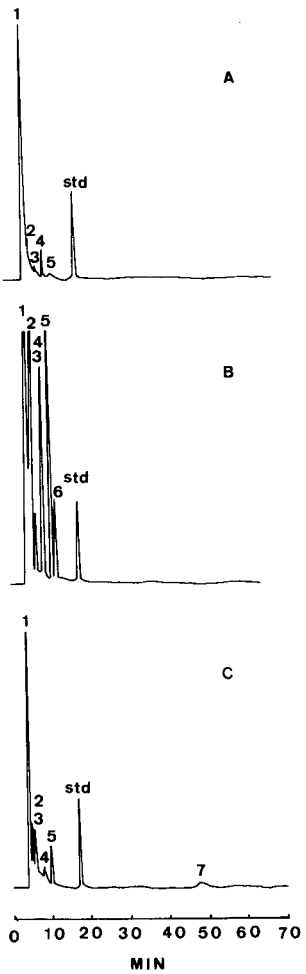

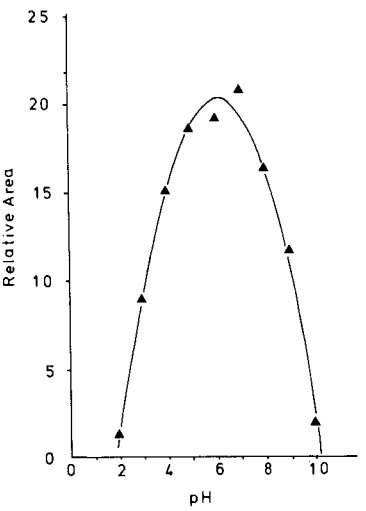

Fig. 1. HPLC separations of flavour compounds of garlic formed at (A) pH 2, (B) pH 6 and (C) pH 10. Peak 5 = allicin.

Fig. 2. Relative amounts of allicin formed at different pHs as determined by HPLC. $Y = -23.4788 + 14.473X - 1.18345X^2$ ($r = 0.99$).

compounds is also favoured around pH 6.5, which is consistent with the peak of allicin shown in HPLC analysis. Cavallito and Bailey[2] found that an aqueous solution of allicin had a pH of approximately 6.5 and, on standing, the acidity slowly increased owing to the formation of small amounts of sulphur dioxide. The antibacterial activity of the solution decreased. Addition of alkalis led to immediate inactivation, with precipitation of allyl disulphide and formation of an alkali sulphite.

Fig. 5 shows the effect of pH on the formation of four additional major compounds, diallyl trisulphide, diallyl disulphide, methyl allyl disulphide and diallyl sulphide. Unlike 2-vinyl-(4*H*)-1,3-dithiin and 3-vinyl-(4*H*)-1,2-dithiin, the formation

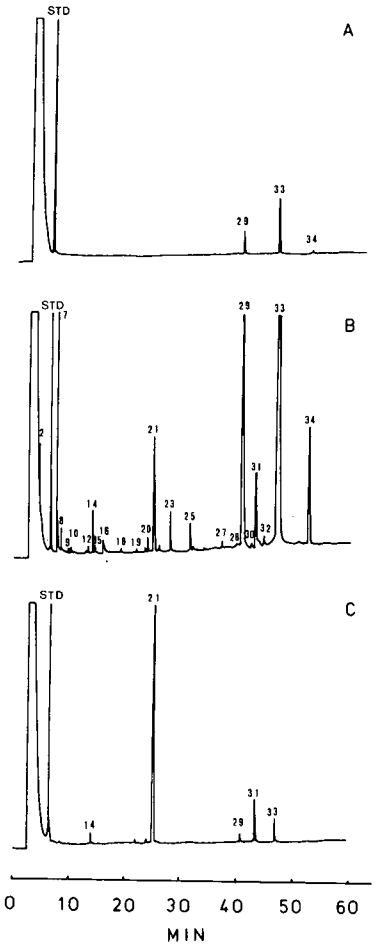

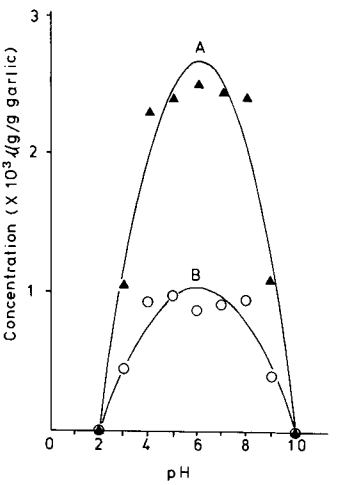

Fig. 3. Capillary gas chromatograms of volatile compounds from garlic formed at (A) pH 2, (B) pH 6 and (C) pH 10.

Fig. 4. Changes in the amount of (A) 2-vinyl-(4*H*)-1,3-dithiin [$Y = -3275.28 + 1984.01X - 165.049X^2$ ($r = 0.98$)] and (B) 3-vinyl-(4*H*)-1,2-dithiin [$Y = -1249.96 + 769.544X - 64.3509X^2$ ($r = 0.97$)] formed at different pH values as determined by GC.

of these compounds is favoured around pH 9.0. Schwimmer and Austin[21] found that γ-glutamyl transpeptidase (GGT) has its optimum activity at pH 9.0. Therefore, it was postulated that these four compounds reach their highest levels around pH 9.0 because allicin readily decomposes into these compounds under alkaline conditions or because the rate of formation of these compounds at pH around 9.0 is greatest as a result of the high activity of GGT. It is possible that GGT in garlic also has an optimum pH at 9.0; at pH around 9.0, GGT readily catalyses the transfer of γ-L-glutamyl-S-allyl sulphoxide to alliin and then alliin is catalysed further by allinase into allicin; under alkaline conditions allicin then readily decomposes into sulphide compounds.

TABLE I

EFFECTS OF pH ON THE FORMATION OF VOLATILE COMPOUNDS OF DISRUPTED GARLIC

*Peak No.**	*Compound***	I_k*** (CP-Wax 52 CB)	*Yield (10^{-6} g/g of garlic bulb)*§								
			pH 2.0	*pH 3.0*	*pH 4.0*	*pH 5.0*	*pH 6.0*	*pH 7.0*	*pH 8.0*	*pH 9.0*	*pH 10.0*
2	Propenylthiol	–	–§§	2.26	13.40	14.39	11.50	8.93	7.55	6.93	–
7	2-Propen-1-ol	1125	–	50.84	237.61	219.01	111.18	129.28	85.65	34.88	–
8	Diallyl sulphide	1148	–	6.86	8.91	10.26	11.53	12.96	13.20	13.31	–
9	Tetrahydro-2,5-dimethylthiophene	1197	–	2.76	3.42	3.98	3.46	–	–	–	–
10	$C_6H_{10}S$ [*m/z*, 45(100), 42(86), 43(86), 29(86), 55(64), 73(48), 71(28), 64(28)]	1233	–	2.64	3.33	3.81	3.33	–	–	–	–
12	3-Methyl-2-cyclopentene-1-thione	1261	–	1.01	3.29	4.39	5.07	16.79	–	–	–
14	Methyl allyl disulphide	1282	–	3.79	27.39	36.05	25.38	23.47	34.09	41.69	6.00
15	1,3-Dithiane	1296	–	1.03	7.65	7.97	6.13	5.06	5.27	–	–
16	Aniline	1328	–	–	4.93	13.75	14.19	19.25	13.32	–	–
18	Dimethyl trisulphide	1380	–	–	3.72	3.97	–	–	–	–	–
19	Propyl allyl disulphide	1432	–	–	1.99	2.53	–	–	–	–	–
20	$C_6H_{10}S_2$ [*m/z*, 73(100), 146(99), 81(79), 41(57), 45(54), 105(45), 39(35), 71(30)]	1471	–	8.37	10.06	11.42	10.33	8.53	7.33	5.74	–
21	Diallyl disulphide	1490	–	35.19	73.97	91.63	81.19	118.05	243.98	1435.89	561.63
23	Unknown [*m/z*, 103(100), 104(64), 45(39), 119(16), 39(15), 69(11), 105(11), 74(8)]	1532	–	15.05	27.15	28.70	25.71	23.14	20.03	10.96	–

25	Methyl allyl trisulphide	1593	–	2.70	21.17	26.81	22.73	22.49	20.00	20.47	–
27	3,5-Diethyl-1,2,4-trithiolane	1682	–	–	5.31	5.31	4.89	3.34	3.70	–	–
28	Isobutyl isothiocyanate	1753	–	–	5.77	1.94	–	–	–	–	–
29	3-Vinyl-(4*H*)-1,2-dithiin	1761	29.35	454.18	946.48	994.78	879.70	927.47	956.56	429.78	6.20
30	Unknown [*m/z*, 146(100), 74(73), 73(64), 117(62), 72(55), 71(32), 138(30), 45(23)]	1772	–	4.44	108.32	121.63	102.26	105.84	94.85	41.41	–
31	Diallyl trisulphide	1806	–	25.14	38.50	48.87	63.07	83.12	126.18	176.08	23.04
32	Unknown [*m/z*, 138(100), 111(92), 109(64), 110(62), 95(60), 123(50), 77(48), 151(36)]	1851	–	2.48	28.44	35.18	35.75	28.64	20.14	10.69	–
33	2-Vinyl(4*H*)-1,3-dithiin	1872	75.28	1058.24	2295.09	2394.87	2501.97	2456.91	2419.54	1097.00	16.27
35	Unknown [*m/z*, 128(100), 45(37), 99(35), 65(26), 113(21), 110(21), 53(16), 85(15)]	1943	5.41	52.25	134.89	194.87	189.20	151.94	136.67	60.48	–
	Total		110.04	1729.23	4010.99	4276.12	4108.57	4145.16	4207.06	3385.31	413.14

* Numbers refer to Fig. 3.
** Numbers in parentheses indicate relative percentage.
*** Calculated Kováts retention indices.
§ Average of two experiments using dimethyl disulphide as internal standard.
§§ Not detected.

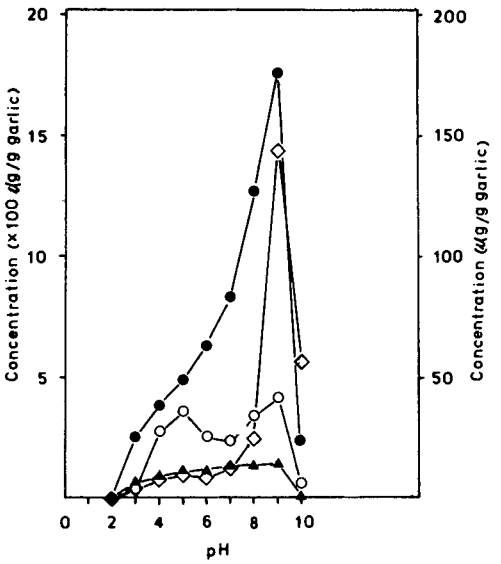

Fig. 5. Volatile compounds of garlic formed at different pH values as determined by GC. ◇, Diallyl trisulphide; ●, diallyl disulphide; ○, methyl allyl disulphide and ▲, diallyl sulphide.

CONCLUSION

The results indicate that HPLC is a good method for analysing allicin in garlic and GC is also a good alternative for analysing allicin with the total amount of 2-vinyl-(4*H*)-1,3-dithiin and 3-vinyl-(4*H*)-1,2-dithiin representing the amount of allicin. Consistent results were obtained when using HPLC and GC to determine the changes in allicin at different pHs. It is also interesting that the formation of diallyl trisulphide, diallyl disulphide, methyl allyl disulphide and diallyl sulphide is favored around pH 9.0.

ACKNOWLEDGEMENT

Grateful acknowledgement is made for financial support from the Council for Agricultural Planning and Development of the Republic of China.

REFERENCES

1 F. W. Semmler, *Arch. Pharm. (Weinheim, Ger.)*, 230 (1892) 434.
2 C. J. Cavallito and J. H. Bailey, *J. Am. Chem. Soc.*, 66 (1944) 1950.
3 V. A. Stoll and E. Seebeck, *Helv. Chim. Acta*, 31 (1948) 189.
4 G. G. Freeman and R. J. Whenham, *J. Sci. Food Agric.*, 26 (1975) 1866.
5 A. I. Virtanen, *Phytochemistry*, 4 (1965) 207.
6 V. A. Stoll and E. Seebeck, *Experientia*, 3 (1947) 114.
7 M. Mazelis and L. Crews, *Biochem. J.*, 108 (1968) 725.
8 M. H. Brodinitz, J. V. Pascale and L. V. Derslice, *J. Agric. Food Chem.*, 19 (1971) 273.
9 E. Block, *Sci. Am.*, March (1985) 94.
10 T.-H. Yu and C.-M. Wu, *J. Food Sci.*, submitted for publication.

11 D. Barnard and E. R. Cole, *Anal. Chim. Acta*, 20 (1959) 540.
12 J. F. Carson and F. F. Wong, *Nature (London)*, 183 (1959) 1673.
13 T. Watanabe and K. Komada, *Agric. Biol. Chem.*, 29 (1966) 418.
14 C. Nakata, T. Nakata and A. Hishikawa, *Anal. Biochem.*, 37 (1970) 92.
15 R. A. Bernhard, *J. Food Sci.*, 33 (1968) 298.
16 H. Bock, S. Mohmand, T. Hirabayashi and A. Semkow, *Chem. Ber.*, 115 (1982) 1339.
17 E. Block, S. Ahmad, J. L. Catalfamo, M. K. Jain and R. Apitz-Castro, *J. Am. Chem. Soc.*, 108 (1986) 7045.
18 P. Majlát, Z. Erdös and J. Takács, *J. Chromatogr.*, 91 (1974) 89.
19 G. G. Freeman and F. McBreen, *Biochem. Soc. Trans.*, 1 (1973) 1150.
20 T.-H. Yu, C.-M. Wu and Y. C. Liou, *J. Agric. Food Chem.*, in press.
21 S. Schwimmer and S. J. Austin, *J. Food Sci.*, 36 (1971) 807.

Journal of Chromatography, 462 (1989) 147–154
Elsevier Science Publishers B.V., Amsterdam — Printed in The Netherlands

CHROM. 21 001

ADJUSTABLE APERTURE-WIDTH DETECTOR CELL FOR ON-COLUMN DETECTION IN CAPILLARY ZONE ELECTROPHORESIS

TIANSONG WANG and RICHARD A. HARTWICK*
Department of Chemistry, Rutgers University, Piscataway, NJ 08854 (U.S.A.)
and
PAUL B. CHAMPLIN
Applied Analytical Technologies, Inc., P.O. Box 668, Narragansett, RI 02882 (U.S.A.)
(First received August 19th, 1988; revised manuscript received September 27th, 1988)

SUMMARY

An on-column UV–VIS detector cell with an adjustable aperture width (coaxial to the capillary) for capillary zone electrophoresis was made and evaluated. The cell increased signal-to-noise ratio almost 6 fold and expanded the linear range of detection about one order of magnitude as compared with a 1.0 mm diameter aperture cell. Capillaries can be readily installed, removed and repositioned with the new design. The relationship between aperture width and observed column efficiency was established by computer simulation and varified by experiment. Both theoretical and experimental results conformed that an aperture width $\leq 1\sigma$ of the peak width will contribute an efficiency loss of no more than 10%. The cell was applied to the separation of monophosphate nucleotides.

INTRODUCTION

Capillary zone electrophoresis (CZE) or high-performance capillary electrophoresis (HPCE) is a very attractive separation technique. Because capillaries with 50–75 μm I.D. allow efficient dissipation of heat, suppress convection and permit faster exchange of molecules between the wall and the center of capillary, CZE can generate 10^5–10^6 theoretical plates within 30 min[1,2]. Although CZE is still in the early stage of development, it has successfully been applied to analysis of varied samples, such as proteins, amino acids, nucleosides, inorganic ions and neutral molecules.

The miniaturization of electrophoresis into capillary format brings numerous advantages, but also creates some difficulties, one of which is detection. For example, the standard deviation of a peak with a retention time 500 s and $2.5 \cdot 10^5$ theoretical plates is 1 s. In a capillary with 50 μm I.D. and a linear velocity of 1 mm/s, one second standard deviation corresponds to only 2 nl in volume. The detector cell volume must be small enough and the detector sensitivity high enough to meet these detection requirements without significant zone dispersion.

In order to cope with the nanoliter volume detection of capillary separations, on-column or in-column[3] detectors have been almost universally used, employing

0021-9673/89/$03.50

fluorescence[4,5], electrochemistry[6,7] and ultraviolet (UV) absorption[8,9] detection methods. UV detectors, though less sensitive than fluorescence detectors, are still the most widely used, because of their relative versatility. Yang[10] constructed an on-column UV detector by stripping the polymer coating of a capillary and placing the capillary into the light path of a detector. Terabe *et al.*[9] used a UV detector with 0.05 × 0.75 mm slit. Walbroehl and Jorgenson[8] used a 100 μm pinhole as the aperture of the detector cell. Spino *et al.*[11] fabricated a detector cell by glueing a capillary and two razor blades onto a cell block, producing an aperture about 6 mm × the capillary inner diameter. Kientz and Verweij[12] made a cell aperture by drilling a 0.4 mm diameter hole into the outer holder of the capillary. Foret *et al.*[13] fabricated an on-column UV detector based on optical fibers. In these designs, the aperture of the detector cell seems to have been selected arbitrarily, even though some authors[4,8,11] have discussed qualitatively the role of aperture width on detector performance.

The design of on-column UV detector cell for CZE should consider three important aspects: (1) Light should pass only through the inner diameter of capillary. When a large amount of light passes through the rim of the capillary, one result is that the signal will be very sensitive to the refractive index changes of solution and the distance between the capillary and photodetector[14]. Another result is that the signal-to-noise ratio (S/N) and the linear range of detection will be reduced[8]. (2) Aperture should have a width (along the axis of capillary) that keeps the efficiency loss within a predefined limit, or ideally the width should be adjustable to meet different requirements. (3) Installation and removal of capillaries should be convenient and accurate.

In this paper, a design of an adjustable aperture-width detector cell for CZE is presented which can meet these requirements. The performance of the new cell were evaluated experimentally. The relationship between the aperture width and apparent column efficiency was established by computer simulation, then verified by experiment.

EXPERIMENTAL

Detector cell construction

Fig. 1 is a schematic diagram of an adjustable aperture-width cell. The aperture body is constructed by sandwiching a shim between two pieces of metal (either stainless steel or brass), then the body is glued on the base. The washer with slits is rotatable. The aperture depends on both the thickness of the shim (25–75 μm) and the dimension of the slit (0.2–2 mm) on the washer. The aperture width along the axis of capillary can be changed by rotation of the washer. On the aperture body, there is a fine groove which retains the capillary in the correct position in the light path. Installation of a capillary is readily accomplished by loosening the capillary retainer, placing the capillary into the groove and tightening the retainer.

Evaluation of the new cell

The new cell aperture (60 μm × 0.95 mm) was examined on a Kratos SF770 UV detector (Applied Biosystems, Ramsey, NJ, U.S.A.) by static method (filling the capillary with test solution with no flow and applied voltage). Fused-silica capillary was 75 μm I.D. × 195 μm O.D. (Polymicro Technology, Phoenix, AZ, U.S.A.).

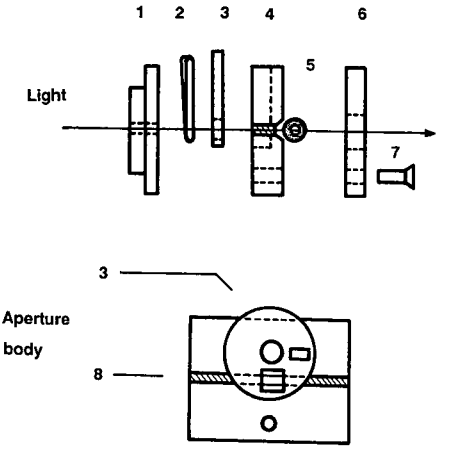

Fig. 1. The schematic diagram of the new cell. (1) Base (Plexiglass); (2) spring; (3) washer with slits; (4) aperture body (stainless steel or brass); (5) capillary; (6) capillary retainer (Plexiglass); (7) screw; (8) shim.

Acetophenone in acetonitrile was used to determine signal-to-noise ratio and linear range of detection. The wavelength of detection was 240 nm ($\varepsilon = 1.3 \cdot 10^4$). "Gradient elution" was performed by alternatively filling the capillary with 100% methanol or methanol–water (60:40), its absorbance being measured at 330 nm.

Since no commercial cells for CZE or capillary HPLC currently are available with which to compare the new cell's performance, an SF770 standard flow cell was used. The capillary was taped on the surface of the SF770 cell and across the aperture (1.0 mm diameter), after which the signal-to-noise ratio and linear range of detection were measured.

In order to demonstrate the performance of the new cell, a mixture of nucleotides (AMP, CMP, GMP and UMP, 1 mg/ml each) was analysed (the instrumentation is described below).

Aperture width and observed column efficiency

Computer simulation of the effect of aperture width on observed column efficiency was performed on an IBM compatible personal computer, using EUREKA software (Borland International, Scotts Valley, CA, U.S.A.).

A CZE apparatus similar to that described by Jorgenson and Lukacs[2] was constructed and used to verify the simulation results. The same detector and cell mentioned above were used. The power supply (0–30 kV) was a model PS/MJ30P0400-11 (Glassman High Voltage, Whitehouse Station, NJ, U.S.A.). Buffer solution was 0.05 *M* sodium dodecyl sulfate (SDS) in borate–phosphate solution (pH = 7.0)[9]. Fused-silica capillary was 50 μm I.D. × 355 μm O.D. The total capillary length was 84 cm, while the length from the injection end to the detector was 60 cm. The capillary was rinsed with 0.1 *M* potassium hydroxide (20 min, about 100 μl), water and the buffer solution respectively, then was conditioned under high voltage for 24 h. The test sample was 0.6 mg/ml thymidine in same buffer solution. Injection: 2.0 kV and 10 s. Analysis: 20 kV and 32 μA. The wavelength of detection was 267 nm, time constant was 0.05 s. All data were collected with MAXIMA™ chromatography software

(Dynamic Solutions, Venture, CA, U.S.A.) at a sampling rate of 20 points/s. The data were then downloaded to Lotus 123™ (rev. 2.01) software (Lotus Development, Cambridge, MA, U.S.A.) where second moments of the peaks were calculated.

RESULTS AND DISCUSSION

Performance of the new cell

Higher signal-to-noise ratio is especially important to the CZE detector, because the amount of sample introduced into the capillary is very limited. In addition to low electronic noise, a well designed cell is critical to enhance the signal-to-noise ratio. Table I presents the data of signal and noise measured with the new cell and with the SF770 cell. From this table, it is seen that although the noise measured with the new cell (60 μm × 0.95 mm aperture) is 2.5 times higher than that with the SF770 cell (1.0 mm diameter aperture), the signal obtained from the new cell is 14.7 times higher than that from the 1.0 mm circular aperture cell, resulting in an overall improvement in signal-to-noise ratio of 5.9-fold.

Measurements of the linear range of detection indicate that the upper limit of concentration is about $3 \cdot 10^{-3}$ *M* for both cells mentioned in Table I. However, the lower limit is different, being $3 \cdot 10^{-5}$ *M* for the new cell (S/N = 2.3, measured), $2 \cdot 10^{-4}$ *M* for the SF770 cell (S/N = 2.5, extrapolated), because the new cell produces a higher signal-to-noise ratio. Therefore, the linear range of detection with the new cell is expanded about one order of magnitude. When using detectors with reduced noise, the linear range and detection limit could be improved further.

As an on-column detector, the capillary as well as the solution in it acts as a lens in the light path. When the photodetector is positioned far from the capillary, the baseline response is sensitive not only to the refractive index of solution, but also to the position of the capillary. Vindevogel *et al.*[14] recommended that gradient elution was a quick method for cell quality determination. The new cell has been examined for refractive index sensitivity by examining baseline shifts using 100% methanol and methanol–water (60:40) solution. The results are summarized in Table II. The data in Table II show that the baseline shift is about 0.02 a.u. This relatively large shift is due largely to the long distance (about 4 cm) between the cell and the photodetector on SF770 detector, which has been shown to cause refractive index sensitivity in the literature[14]. Table II shows that the repeatability of absorbance measurement is good, the maximum difference is $6.2 \cdot 10^{-3}$ a.u. This result indicates that the groove on the new cell can reliably position the capillary.

TABLE I

COMPARISON OF SIGNAL AND NOISE MEASURED WITH TWO CELLS*

Cell	*Aperture dimension*	*Signal (a.u.)*	*Noise (a.u.)*	*S/N*
New cell	60 μm × 0.95 mm	$2.2 \cdot 10^{-2}$	$1 \cdot 10^{-3}$	22
SF770 cell	1.0 mm diameter	$1.5 \cdot 10^{-3}$	$0.4 \cdot 10^{-3}$	3.7

* $3 \cdot 10^{-4}$ *M* acetophenone, 75 μm I.D. × 195 μm O.D. capillary.

TABLE II

BASELINE SHIFT MEASURED WITH NEW CELL (60 μm × 0.95 mm APERTURE)

Solutions	*Absorbance (10^{-3} a.u.)*				
	*1**	*2*	*3*	*4*	$\bar{x} \pm$ *S.D.*
Methanol–water (60:40)	24.4	19.4	22.6	25.6	23.0 ± 2.7
Methanol	1.6	3.1	1.3	1.4	1.9 ± 0.8
Δa.u.	22.8	16.3	21.3	24.2	21.2 ± 3.4

* 1, 2, 3 and 4 means the absorbance values are measured after reinstallation of capillary.

Fig. 2 is an electropherogram obtained using the new cell. The separation is quite good. The column efficiency calculated from the UMP peak is $6.5 \cdot 10^4$ theoretical plates (10% peak height).

Aperture width and observed column efficiency

Required detector cell volumes are often estimated using the model of a mixing chamber[15]. However, this consideration is not applicable for an on-column detector, since the separation is still in progress in an on-column detector cell. In this case, the apparent column efficiency or resolution, as Guthrie and Jorgenson[4] have pointed out, depends on the aperture width along the axis of capillary. However, no quantitative discussion was presented in their paper.

The quantitative relationship can be readily derived as follows. Imagine a gaussian function, g(x), which represents the concentration profile generated by a separated compound, an aperture with a width W is the mathematical equivalent of a rectangle placed over this function, the signal obtained from the aperture at any instant being given by

$$\text{Signal} = \int_{x-W/2}^{x+W/2} g(x)\mathrm{d}x/W \tag{1}$$

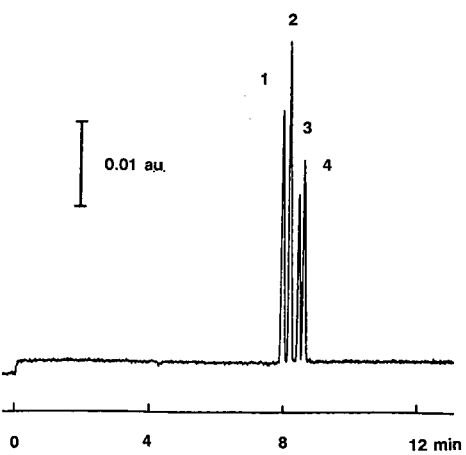

Fig. 2. Separation of nucleotides. 1 = GMP; 2 = AMP; 3 = CMP; 4 = UMP (about 1 mg/ml). 50 μm × 355 μm capillary, 60 cm long to detector. Detector cell aperture, 60 μm × 1.4 mm. 0.05 *M* SDS in borate–phosphate buffer (pH = 7.0). Injection, 2.0 kV and 15 s. Analysis, 25 kV and 50 μA.

The observed function, f(x), will be given by the set of signals calculated from eqn. 1. The loss in efficiency can be expressed as the ratio of second moments:

$$\text{Distortion} = M_{2\text{obs}}/M_{2\text{tru}} = N_{\text{tru}}/N_{\text{obs}} \tag{2}$$

where M_2 is second moment of a peak and N is the theoretical plate number of the peak. The result of a computer simulation according to this consideration is shown in Fig. 3.

From Fig. 3, it can be seen that when the aperture width is larger than 1σ, the distortion becomes significant and increases non-linearly with increasing aperture width. For example, when the aperture width is 3.5 σ, the distortion is about 2, that is, the observed column efficiency is only half of the true efficiency. A regression equation is obtained from the data of Fig. 3:

$$\text{Distortion} = 0.993 + 0.0152W + 0.0771W^2 \tag{3}$$

where W is aperture width in σ units. The regression coefficient is 0.99999.

The theoretical and experimental results relating the effect of aperture width on observed column efficiency are compared in Table III. In general, good agreement is found between experiment and theory. Both experimental and theoretical results indicate that if the aperture width is $\leq 1\sigma$ of the peak width, the loss in column efficiency resulting from aperture width will be no more than 10%. Narrower the aperture width will reduce the loss in column efficiency, but conversely, increase noise. Therefore, it is recommended that when designing an on-column optical detector, aperture width should be about 1σ (in length unit) of the peak interested.

The σ of a peak can be calculated from eqn. 4,

$$\sigma = L/\sqrt{N} \tag{4}$$

where L is the column length from the injection end to the detector. Typically, L is 500 mm and N is $3 \cdot 10^5$, producing a σ value of 0.9 mm.

Another effect of aperture width is decreasing signal intensity. The computer

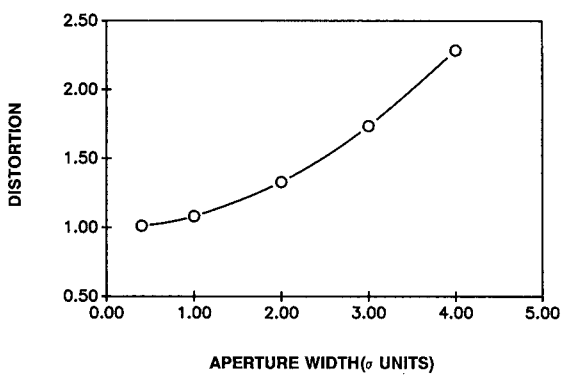

Fig. 3. The computer simulation results of the effect of aperture width on observed column efficiency.

TABLE III

EFFECT OF APERTURE WIDTH ON OBSERVED COLUMN EFFICIENCY

Parameters	*Aperture width*			
	0.22 mm (0.26σ)*	*0.41 mm (0.49σ)*	*0.95 mm (1.13σ)*	*1.4 mm (1.7σ)*
M_{2exp}**	0.33	0.35	0.36	0.39
Distortion (exp)***	1.00	1.06	1.09	1.18
Distortion (eqn. 2)	1.00	1.02	1.11	1.23

* From the peak of thymidine (retention time 6.81 min) $\sigma = M_2^{1/2} \times$ velocity of band $= 0.33^{1/2} \times 600/6.81 \times 60 = 0.84$ mm.

** Second moment (s^2), $n = 3$, S.D. $= 0.01\ s^2$.

*** The M_2 value obtained from 0.22 mm aperture width was assigned to the true M_2 value.

simulation results indicate that observed peak height will decrease with increasing aperture width. For example, as the aperture width increases from 0.1 to 1.0σ, peak height decreases 4%. At present, the precision of peak height measurement in this laboratory is not good enough to verify this theoretical expection.

CONCLUSION

The new cell shown in Fig. 1 was made and evaluated. This cell increases signal-to-noise ratio almost six times and expands the linear range of detection about one order of magnitude over that observed using a simple 1-mm hole for an aperture. The capillaries can be easily installed, removed and repositioned into the new cell.

Computer simulation of the effect of aperture width on apparent column efficiency was performed. The relationship between aperture width and observed column efficiency has been established (eqn. 3) and verified experimentally. Both theoretical and experimental results indicate that when the aperture width $\leq 1\sigma$ of the peak width, the loss in column efficiency resulted from aperture width will be no more than 10%.

ACKNOWLEDGEMENTS

Supports for this research was provided in part by the Center for Advanced Food Technology (CAFT), and by a grant from the PQ Corporation.

REFERENCES

1 J. W. Jorgenson and K. D. Lukacs, *Anal. Chem.*, 53 (1981) 1298.
2 J. W. Jorgenson and K. D. Lukacs, *Science (Washington, D.C.)*, 222 (1983) 266.
3 M. Verzele and C. Dewaele, *J. Chromatogr.*, 395 (1987) 85.
4 E. J. Guthrie and J. W. Jorgenson, *Anal. Chem.*, 56 (1984) 483.
5 D. E. Burton, M. J. Sepaniak and M. P. Maskarinec, *J. Chromatogr. Sci.*, 24 (1986) 347.
6 R. A. Wallingford and A. G. Ewing, *Anal. Chem.*, 59 (1987) 1762.
7 X. Huang, T. J. Pang, M. J. Gordon and R. N. Zare, *Anal. Chem.*, 59 (1987) 2747.
8 Y. Walbroehl and J. W. Jorgenson, *J. Chromatogr.*, 315 (1984) 135.
9 S. Terabe, K. Otsuka, K. Ichikawa, A. Tsuchiya and T. Ando, *Anal Chem.*, 56 (1984) 111.

10 F. J. Yang, *J. High Resolut. Chromatogr. Chromatogr. Commun.*, 4 (1981) 83.
11 L. A. Spino, S. M. Han, D. W. Armstrong and A. R. Parrott, *J. Liq. Chromatogr.*, 10 (1987) 1603.
12 C. Kientz and A. Verweij, *J. High Resolut. Chromatogr. Chromatogr. Commun.*, 11 (1988) 294.
13 F. Foret, M. Deml, V. Kahle and P. Bocek, *Electrophoresis*, 7 (1986) 430.
14 J. Vindevogel, G. Schuddinck, C. Dewaele and M. Verzele, *J. High Resolut. Chromatogr. Chromatogr. Commun.*, 11 (1988) 317.
15 G. Guiochon and H. Colin, in P. Kucera (Editor), *Microcolumn High-performance Liquid Chromatography*, Elsevier, Amsterdam, 1984, p. 1.

Journal of Chromatography, 462 (1989) 155–163
Elsevier Science Publishers B.V., Amsterdam — Printed in The Netherlands

CHROM. 20 997

EFFECT OF PARTICLE TREATMENT OF COMPOSITE FILLER ON ITS INTERACTION COEFFICIENT

MILAN DRESSLER* and MIROSLAV CIGÁNEK
Institute of Analytical Chemistry, Czechoslovak Academy of Sciences, Leninova 82, 611 42 Brno (Czechoslovakia)
(First received June 28th, 1988; revised manuscript received September 19th, 1988)

SUMMARY

The effect of calcium carbonate treatment on its surface activity was studied by inverse gas chromatography, concentrating on the effect of water on the filler surface, the effect of coating the filler surface with stearic acid and the effect of the particle size of the filler. The surface activity was evaluated by determining the interaction coefficient, I_g.

Water on the filler surface decreases the surface activity, especially with untreated calcium carbonate. It also causes a levelling of the difference between the contributions of acid and/or base centres, which can be the cause of incorrect evaluation of their interaction contributions. Consequently, when establishing the filler surface properties, water on the calcium carbonate surface cannot be neglected and thermal conditioning of the filler surface prior to testing is therefore necessary. The dependence of the quality of calcium carbonate surface treatment on the means of adding stearic acid (directly during calcite grinding or from the solution after grinding) was established. The activity of the calcium carbonate surface was found to decrease with increasing particle diameter.

INTRODUCTION

Calcium carbonate is one of the most widely used fillers of polyolefinic composites. Prior to its application as a filler, natural calcium carbonate has to be ground in a ball-mill. The filler obtained has a wide distribution of particle diameters.

The dispersion of fillers in the polymer matrix and the mechanical properties of the filled polymers are influenced by surface interactions. In a non-polar polymer matrix, fillers whose surfaces show neither acid nor base characteristics[1] disperse more quickly (mechanically stronger composites are produced). Calcium carbonate shows very strong surface activity[1–4].

Prior to being added to a non-polar polymer, calcium carbonate is surface treated (the surface is deactivated) to fulfil the above-mentioned requirement of compatibility. The most common reagent in industrial manufacture is stearic acid, which is usually added to calcium carbonate at the grinding stage.

0021-9673/89/$03.50

Different samples of the same filler and samples of different fillers may contain various amounts of water, depending on the sample treatment, its prior storage, the particle size, etc. So far, however, these facts have not been taken into account in the evaluation of the surface activity of fillers.

This paper is concerned with the effect of water present on the calcium carbonate surface on the surface activity of the filler. Also, the activity of the calcium carbonate surface was studied as functions of the method of treatment of the filler with stearic acid and of the particle diameter.

EXPERIMENTAL

The apparatus used was described in detail in a paper on the study of composite fillers by inverse gas chromatography[4]. The measurements were carried out using a Chrom gas chromatograph (Laboratory Instruments, Prague, Czechoslovakia) with a flame ionization detector. The chromatographic column is connected to the detector directly and to the injector with a 30 cm × 0.2 mm I.D. fused-silica capillary. A 0.02-μl volume of the test solute was injected with a 0.5-μl syringe (Scientific Glass Engineering, North Melbourne, Australia). An injector for capillary columns with a stream splitter was used. The splitting ratio of 200:1 permits only *ca.* $1 \cdot 10^{-7}$ g from the originally injected volume of 0.2 μl of the test solute to enter the chromatographic column.

The filler sample (see Table I) was packed into a straight glass chromatographic column (10 cm × 0.3 cm I.D.). During mixing with the polymer (polypropylene), the

TABLE I

CHARACTERISTICS OF THE CALCIUM CARBONATE SAMPLES

Sample No.	*Type and supplier*	*Stearic acid (%)*	*Specific surface area* (m^2/g)	*Particle size distribution*	
				d_{50} (μm)***	d_{97} (μm)***
1	Durcal 2, OMYA, France	0	3.3	3.0	10.0
2	Precipitated, Heating Plant, Brno, Czechoslovakia	0	2.6	–	–
3	Pomezí near Jeseník, ÚNS Kutná Hora, Czechoslovakia	0	4.3	2.3	6.2
4	As 3	0.3	4.3	2.3	6.2
5	As 3	0.5	4.3	2.3	6.2
6	As 3	0.3*	4.3	2.3	6.2
7	As 3	0.5**	4.3	2.3	6.2
8	Pomezí near Jeseník, Chlumčanské Ceramic Works, Poběžovice, Chechoslovakia	0.3	1.6	–	–
9	As 8	0.31	4.6	3.0	10.0

* Sample 3 coated with 0.3% (w/w) of stearic acid from solution in *n*-pentane without thermal surface treatment.

** Sample 3 coated with 0.3% (w/w) of stearic acid from solution in *n*-pentane after thermal surface treatment (3 h at 150°C).

*** The values of d_{50} (d_{97}) mean that 50% (97%) particles in the size distribution have diameters less than this value.

fillers were exposed to temperatures of about 200°C for 2 min. Therefore, the testing of the surface activity was carried out with the sample thermally conditioned at the temperature simulating the conditions of the commercial preparation of the composite. For this purpose the thermostat temperature was increased within 3 min from the laboratory temperature to 200°C, kept at this value for 2 min, then decreased to the test temperature. The testing of fillers was performed after 20 min.

The test temperature was 90°C, unless stated otherwise. The test solutes *n*-pentane, *n*-hexane, *n*-heptane, *n*-octane, dichloromethane, trichloromethane, benzene and furan were of analytical-reagent grade (Lachema, Brno, Czechoslovakia).

The activity of the calcium carbonate surface was evaluated by determining the interaction coefficient, I_g, which expresses the ratio of the specific interaction of the test solute with the filler surface to the non-specific interaction of a hypothetical *n*-alkane with the same vapour tension as the test solute[5]:

$$I_g = \frac{V_g(\text{test solute})}{V_g(\text{hypothetical } n\text{-alkane})} - 1$$

The test solutes were di- and trichloromethane, furan and benzene. The reproducibility of the retention times for one filler packing (sample 4) expressed in terms of the standard deviation of ten measurements was 1% for furan. The reproducibility of I_g for four independent measurements (four columns with the fillers each measured three times) was 5% for furan. Calcium carbonate was used non-sized, except in the study of the grain size effect. Sizing of calcium carbonate into individual fractions according to particle size was carried out with an Alpine 10 MZR apparatus (Alpine, Augsburg, F.R.G.). The surface area of calcium carbonate was measured by the dynamic desorption method[6].

RESULTS AND DISCUSSION

Effect of surface water

Fig. 1 shows the specific retention volumes of the solutes as a function of the temperature of conditioning of calcium carbonate, either untreated or treated with 0.3% stearic acid. The fillers were heated in the column for 10 min at the given temperatures and then tested at a column temperature of 120°C. The retention volumes increases with increasing temperature of conditioning, especially for untreated calcium carbonate (Fig. 1a). At higher temperatures water is desorbed from the surface, the active centres on the sample surface are exposed and, consequently, the surface activity increases (Table II). For the calcium carbonate sample treated with stearic acid (Fig. 1b) the increase in retention is not so evident because the active centres are blocked by stearic acid molecules. The increase in the surface activity with increasing temperature of conditioning is less for the treated filler and above *ca.* 180°C it remains constant (Table II).

The dependence of the specific retention volumes of the tested solutes on the time of sample conditioning is shown in Fig. 2. The retention volumes of the solutes increase with increasing conditioning time, and to a greater extent with the untreated filler (Fig. 2a) than with treated callcium carbonate (Fig. 2b). For the filler treated with stearic acid and conditioned at the temperature used, the retention volume of the solutes is

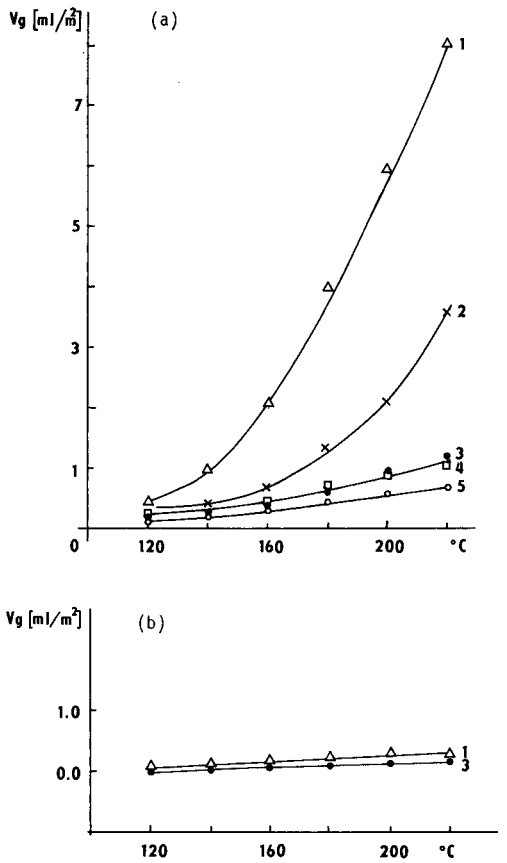

Fig. 1. Dependence of the specific retention volumes of the test solutes (V_g) on the temperature of calcium carbonate conditioning. (a) Sample 3; (b) sample 4 (see Table I). 1 = Furan; 2 = benzene; 3 = *n*-octane; 4 = trichloromethane; 5 = dichloromethane.

constant after *ca.* 3 h. For untreated calcium carbonate, a stable state was not reached even after 5 h of conditioning. The surface activity increases again with the time of conditioning, within 3 h for untreated and within 1 h for treated calcium carbonate (Table III).

It is evident that water has a decisive effect on the surface activity especially of the untreated fillers and it cannot be neglected when establishing the filler surface activity. Fig. 3 shows the values of the interaction coefficient (I_g) for the thermally unconditioned surface of calcium carbonate of different origins at a column temperature of 30°C. Differences in I_g between individual fillers are not very large. Fig. 4 shows the values of I_g after thermal conditioning of the fillers. It is evident that in the latter instance the differences in I_g are substantially higher, the surface activity increasing several fold. For example, I_g of furan for sample 3 is *ca.* 20 times higher for the conditioned fillers even if the testing temperature is 90°C, *i.e.*, 60°C higher than the

TABLE II

DEPENDENCE OF INTERACTION COEFFICIENT (I_g) ON THE TEMPERATURE OF CONDITIONING

Column temperature, 120°C.

Calcium carbonate	*Temperature (°C)*	I_g			
		Dichloromethane	*Trichloromethane*	*Furan*	*Benzene*
Untreated (sample 3)	120	4.9	5.0	36.2	3.2
	140	7.5	5.8	40.7	2.7
	160	5.8	4.9	60.6	4.6
	180	6.9	5.8	90.2	6.6
	200	7.9	6.1	119.2	8.1
	220	8.8	6.4	157.5	12.8
Treated with 0.3% (w/w) of stearic acid (sample 4)	120	0.9	1.0	3.8	0.5
	140	1.1	1.4	5.3	0.5
	160	2.1	1.9	9.9	0.6
	180	2.8	2.4	16.0	0.7
	200	2.2	2.2	14.7	0.6
	220	1.6	1.7	12.2	0.4

TABLE III

DEPENDENCE OF INTERACTION COEFFICIENT (I_g) ON THE TIME OF COLUMN CONDITIONING AT 120°C

Calcium carbonate	*Column temperature (°C)*	*Time (min)*	I_g			
			Dichloro-methane	*Trichloro-methane*	*Furan*	*Benzene*
Untreated (sample 3)	120	20	2.7	2.9	13.8	1.3
		50	2.8	3.1	18.5	2.1
		80	4.4	4.3	27.2	3.3
		130	4.3	4.0	30.3	2.5
		160	4.3	4.1	35.3	2.7
		190	4.5	4.5	37.0	2.9
		230	4.6	4.4	38.8	3.0
		270	4.0	4.0	34.5	2.8
		320	3.4	3.4	28.5	2.4
Treated with 0.3% (w/w) of stearic acid (sample 4)	90	20	1.8	2.0	10.0	0.8
		50	2.4	2.4	15.6	0.9
		80	2.6	2.6	19.0	1.0
		120	2.6	2.6	19.0	1.0
		180	2.2	2.3	17.2	0.8
		240	2.4	2.4	18.0	0.8
		300	2.3	2.3	17.6	0.8

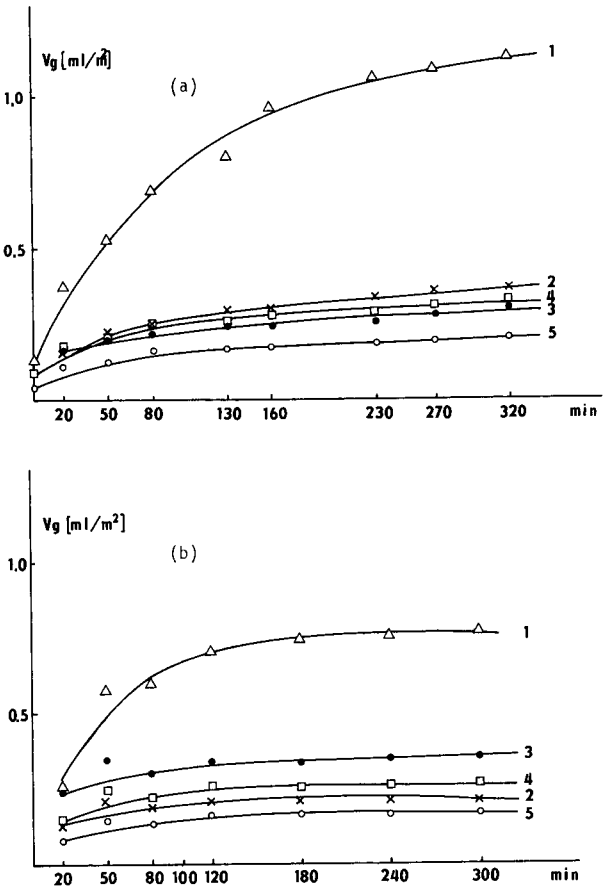

Fig. 2. Dependence of the specific retention volumes of the test solutes (V_g) on the time of calcium carbonate conditioning. (a) Sample 3, column temperature 120°C; (b) sample 4, column temperature 90°C. Lines 1–5 as in Fig. 1.

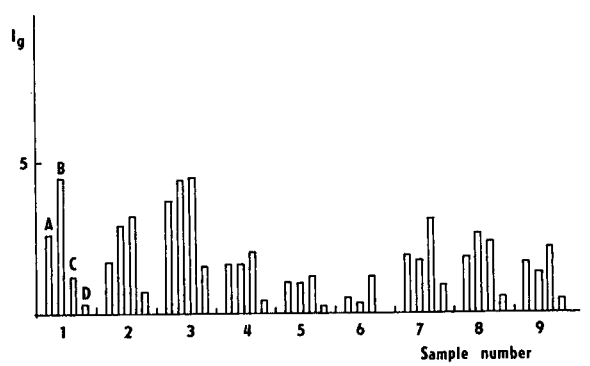

Fig. 3. Values of interaction coefficients (I_g) without prior thermal conditioning of calcium carbonate. A = Dichloromethane; B = trichloromethane; C = furan; D = benzene. For samples 1–9, see Table I. Column temperature, 30°C.

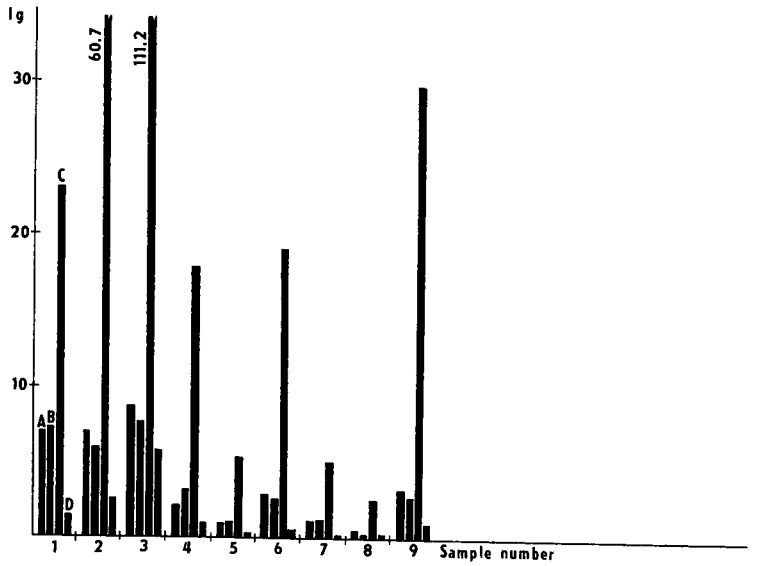

Fig. 4. Values of interaction coefficients (I_g) with calcium carbonate thermally conditioned. A–D as in Fig. 3 and samples 1-9 as in Table I. Column temperature, 90°C.

testing temperature for the same unconditioned fillers. At a testing temperature of 30°C the retention times of the conditioned fillers are very long. Moreover, the molecules of water on the surface of calcium carbonate cause a levelling of the difference between the contributions of acid and/or base centres and, consequently, the I_g for all four test solutes are comparable (see, *e.g.*, sample 3). After conditioning, especially the contribution of acidic centres on the filler surface increases.

The effect of water is also reflected in the fact that the interaction coefficient depends on the testing temperature (Table IV). These changes are so important that they cannot be caused by fortuitous different dependences of the retention volumes of *n*-alkanes and the tested solutes on the temperature of the chromatographic column. At a higher chromatographic temperature the filler sample is, in fact, always conditioned prior to the surface activity measurement.

TABLE IV

EFFECT OF TESTING TEMPERATURE ON INTERACTION COEFFICIENT (I_g)

Sample 3 (see Table I) without thermal conditioning.

Solute	I_g		
	30°C	*90°C*	*120°C*
Dichloromethane	4.0	4.8	6.4
Trichloromethane	4.2	5.0	5.8
Furan	5.2	16.0	35.7
Benzene	1.8	1.8	2.8

Effect of filler surface treatment with stearic acid

As a consequence of the wide distribution of particle diameters of ground calcium carbonate and because stearic acid is added to the filler only mechanically by pouring during grinding, it seems likely that the surface coating of calcium carbonate with stearic acid is not uniform in this instance.

The values of I_g for the calcium carbonate samples both untreated and treated during grinding of the original material with 0.3 and 0.5 wt.-% of stearic acid (Fig. 4, samples 3–5) show that the filler surface activity decreases with increasing amount of stearic acid, which corresponds with the results obtained previously[3].

The original sample of surface-untreated calcium carbonate (sample 3) was treated, before testing, with 0.3 wt.-% of stearic acid from a solution in *n*-pentane in the same manner as used for coating the chromatographic support with a stationary phase, *i.e.*, by gradual evaporation of the solvent (samples 6 and 7). Sample 6 was treated with stearic acid without prior thermal conditioning and sample 7 was conditioned prior to treatment at 150°C for 3 h. This method of filler treatment should make the filler surface coating with stearic acid much more uniform than the treatment directly during grinding. The measured surface activity verified this assumption. The I_g of sample 7 for a 0.3% coating from the solution is close to the values for a 0.5% surface coating during calcium carbonate grinding (sample 5). Again, however, water present on the surface proves to be an important factor. The activity of sample 6 (unconditioned) is comparable to that of sample 4 (0.3% of stearic acid during grinding). This agreement is due to the presence of water on the untreated filler surface prior to its treatment with stearic acid from the solution, which causes imperfect surface coating. Hence, the filler coating with stearic acid by gradual evaporation of the solvent without prior thermal treatment (sample 6) has approximately the same effect on the decrease in surface activity as deactivation with the acid directly during grinding, *i.e.*, when calcium carbonate is treated while the water content on the surface is still low.

Effect of the filler particle size

Untreated calcium carbonate (sample 3) was sized into four fractions: 4.3–6.1, 2.3–3.9, 1.4–2.2 and below 1.4 μm, while the dust (particles below 1 μm) was blown aw y during sizing. The I_g values for all the four fractions (Table V) are evidently lower

TABLE V

VALUES OF INTERACTION COEFFICIENT (I_g) FOR SIZED UNTREATED CALCIUM CARBONATE

Individual fractions were prepared from sample 3 (see Table I).

Particle size distribution (μm)	*Specific surface area (m^2/g)*	I_g			
		Dichloromethane	*Trichloromethane*	*Furan*	*Benzene*
<1.4	6.8	6.4	6.4	73.1	4.3
1.4–2.2	3.5	7.3	7.1	80.0	4.6
2.3–3.9	3.0	5.8	5.4	60.8	2.3
4.3–6.1	2.1	5.1	4.7	49.6	2.1

in comparison with the original non-sized sample (*cf.*, Fig. 4). In spite of the relatively high dispersion of I_g values for different columns with the same filler[4] (the greatest relative error was found for dichloromethane and was 20% for the 2.3–3.9 μm fraction), the trend of decreasing I_g with increasing particle diameter can be seen clearly in Table V. The fact that the I_g values for the non-sized calcium carbonate are higher than those for all the sized fractions can be explained by the blowing away of the dust particles (these particles remain in the filter of the sizing device and so they could not be measured). The changes in I_g values as a function of the particle diameter cannot be explained by the available physico-chemical data. The changes are not related to the content of aluminosilicates.

Sizing of the filler to a fraction with a narrower particle distribution is also important for the chromatographic testing of the surface activity. A chromatographic column packed with the sized material has, at the same flow-rate of the carrier gas, a much lower inlet pressure. This enables carrier gas flow-rates higher than 5 ml/min (the maximum obtainable flow-rate for the column with the non-sized calcium carbonate) to be used, which shortens the time of testing and improves the separation efficiency of the chromatographic column.

CONCLUSIONS

Water present on the filler surface has a great effect on the filler activity. It is therefore necessary to condition the filler thermally prior to testing the activity. To be able to compare the activities of different fillers, it is necessary to condition and measure the fillers at the same temperature.

The method of filler treatment with stearic acid influences the surface activity of the final filler. A more uniform coating of the surface with the acid results in a lower surface activity. Filler treatment in which the surface coating with stearic acid (or other material) is more uniform than is given by simple mixing of the filler and the acid during grinding is, therefore, more suitable for the final composite.

The filler surface activity depends on the particle diameter. Sizing of the original material to a fraction with a narrow particle size distribution with simultaneous removal of the particles having very small diameters (dust) should improve the filler quality. The use of a sized fraction for testing of the filler surface activity is, moreover, more suitable when using inverse gas chromatography.

REFERENCES

1 C. Richard, K. Hing and H. P. Schreiber, *Polym. Composites*, 6 (1985) 201.
2 H. P. Schreiber, M. R. E. Wertheimer and M. Lambla, *J. Appl. Polym. Sci.*, 27 (1982) 2269.
3 E. Papirer, J. Schultz and C. Turchi, *Eur. Polym. J.*, 20 (1984) 1155.
4 M. Cigánek and M. Dressler, *Chem. Prům.*, 38/63 (1988) 315.
5 M. Cigánek and M. Dressler, *Polym. Composites*, in press.
6 F. M. Nelsen, F. T. Eggertsen, *Anal. Chem.*, 30 (1958) 1387.

Journal of Chromatography, 462 (1989) 165–176
Elsevier Science Publishers B.V., Amsterdam — Printed in The Netherlands

CHROM. 21 046

PREPARATION AND USE OF LATEX-COATED RESINS FOR ANION CHROMATOGRAPHY*

LINDA M. WARTH and JAMES S. FRITZ*
Ames Laboratory and Department of Chemistry, Iowa State University, Ames, IA 50011 (U.S.A.)
and
JOHN O. NAPLES
The Rohm and Haas Company, 727 Norristown Road, Spring House, PA 19477 (U.S.A.)
(First received July 26th, 1988; revised manuscript received October 12th, 1988)

SUMMARY

A procedure is described for the preparation of low-capacity anion-exchange resins for use in single-column ion chromatography. The resins are prepared by hydrophobically coating an anion-exchanging latex onto unfunctionalized resins made by Rohm & Haas. The resin exchange capacities are varied by changing the concentration of the sodium chloride or latex in the coating solution. Various resin matrices can be coated and capacities from 5 to over 400 μequiv./g are obtained. The mechanism of latex adsorption is discussed and several highly efficient anion separations are presented.

INTRODUCTION

Since the introduction of suppressed ion chromatography in 1975[1] and single-column ion chromatography (SCIC) in 1979[2], many improvements have been made in stationary phase technology. Agglomerated resins were originally used in suppressed anion chromatography[1]. Polystyrene beads of low cross-linking are lightly sulfonated and made into anion-exchange resins by agglomerating anion-exchanging microparticles onto the surface[3]. The microparticles are held on the resin surface by electrostatic attractions between the fixed ions of opposite charge. Later, more efficient resins were obtained by agglomerating quaternized latexes onto surface-sulfonated resins of small, uniform size[4]. Although further improvements have been made, anion-exchange resins of this general type are still used and sold commercially.

Resins with chemically bonded quaternary ammonium functional groups have been used with considerable success in single-column anion chromatography. Barron and Fritz[5] developed reproducible methods for introducing quaternary ammonium groups to produce resins of almost any desired exchange capacity. However, the

* A U.S.A. Patent Application was been filed covering the subject of this contribution.

0021-9673/89/$03.50

particle size of their resins was larger and less uniform than desired for highly efficient chromatography.

Recently, many researchers have favored using statically or dynamically coated resins for anion separations in SCIC. In most cases, a long-chain quaternary ammonium compound is added to a coating solution or to the eluent. This hydrophobic compound then coats the resin and allows anion exchange to occur. For example, Cassidy and Elchuk[6] used dynamic and permanent coating procedures to coat quaternary ammonium halides on a resin surface and separate inorganic ions. DuVal and Fritz[7] demonstrated the succesful use of dynamically and statically-coated polymeric and reversed-phase columns for anion chromatography using long-chain quaternary compounds as coating agents. All of these studies showed that coated resins could be prepared very quickly and easily using a variety of coating agents and resin matrices. Largely because of the easy preparation of coated anion-exchange resins, several other works have been published[8–10], where these coated resins have been used.

In the present work it is shown that highly efficient resins for anion chromatography can be produced by a simple method of coating quaternized latex particles onto the surface of unsulfonated polymeric resins. A non-porous polystyrene resin of very uniform particle size is described that serves as an excellent substrate for the coated resins. These latex-coated resins are used to obtain highly efficient anion separations.

EXPERIMENTAL

Materials and equipment

All latexes and resins were made by and obtained from Rohm & Haas (Spring House, PA, U.S.A.). All solvents and salts used were reagent grade and were obtained from a number of sources.

The latexes used in this study were strong- or weak-base anion exchangers composed of either polystyrene or acrylic. The latexes vary between 0.08 and 0.60 μm in size and were made by emulsion polymerization followed by chemical functionalization to obtain the appropriate anion-exchange functionality[11].

Four different anion-exchanging latexes were used in this study: strong-base exchanger acrylate latex (AL) with quaternary ammonium groups on 60% of the monomer units and 0.09 μm in size; weak-base exchanger acrylate latex which is 0.08 μm in size (AL-WB); strong-base exchanger polystyrene latex which is 100% functionalized and 0.2 μm in size (PL-100); strong-base exchanger polystyrene latex which is 76% functionalized and 0.6 μm in size (PL-76).

The XAD-1 used chromatographically was 20–26 μm or 30–37 μm in size. Preliminary experiments were carried out using 38–44-μm XAD-1. The polystyrene used in this study was prepared by Rohm & Haas, and is 4.2 μm in size, essentially monodisperse and totally nonporous.

Scanning electron microscopy (SEM) of the uncoated polystyrene was performed by F. Laabs of Ames Laboratory (Ames, IA, U.S.A.) using a JEOL 100CX analytical microscope. The samples were prepared in water, dropped onto a slide and air-dried before SEM examination. SEM of the uncoated polystyrene was performed by Rohm & Haas using an AMRAY 1200C analytical microscope. Samples were prepared by dropping dilute solutions of each onto aluminum SEM support stubs. The samples were allowed to air-dry and were then gold-coated before SEM examination.

All size estimations were performed by a Coulter counter (by Rohm & Haas) except for the sizes of the PL-76 latex and XAD-1 resin, which were determined by estimations from electron micrographs.

Ion chromatography was carried out on a laboratory-built HPLC system previously described[12].

Procedures

The XAD resin was prepared according to a previously published method[12].

To prepare a resin sample for coating, a portion of resin is wetted with acetonitrile, filtered and then rinsed with water to displace the acetonitrile. The resin is then filtered to remove excess water.

To coat the resin, a 25-ml volume of latex/sodium chloride solution is added to the wetted resin. The mixture is stirred and sonicated to remove resin clumps. After allowing time for the latex/resin solution to reach equilibrium conditions (less than 1 h), the samples are filtered and rinsed with deionized, distilled water. The strong-base ion-exchange capacities were determined by a method previously published[12].

All solutions were made up in distilled, deionized water and were prepared from reagent grade salts. Eluents were prepared by dissolving the acid in distilled, deionized water and sodium hydroxide was added, where necessary, to adjust the pH. The eluents were then filtered through a 0.2-μm membrane filter and a vacuum was applied while stirring to remove dissolved gases.

Columns were packed using an upward packed, stirred slurry technique with either a water or an ethylene glycol–sodium chloride–water (40:1:59) packing solvent. The packing pressure was approximately 2000 p.s.i. for the XAD and 3000 to 5000 p.s.i. for the 4.2-μm polystyrene resins. The coated XAD and polystyrene resins were packed in glass-lined stainless steel columns (Scientific Glass Engineering, Austin, TX, U.S.A.). Typical operating pressures for the packed columns using a 0.5 ml/min flow-rate were 100 p.s.i. for the XAD columns and 2000 p.s.i. for the 4.2 μm polystyrene columns.

RESULTS AND DISCUSSION

Resin preparation

A series of experiments were performed in order to determine how well the quaternized latexes coated onto various resins, how to vary the exchange capacity of the coated resins and which coated resins are the most suitable for anion separations by SCIC.

Initial experiments were performed to determine what type of unfunctionalized resins could be coated with the highly charged latexes. Table I shows the exchange capacities obtained after coating several different Rohm & Haas resins with the strong-base anion-exchanging polystyrene and acrylic latexes. All resins were coated using identical coating conditions. After coating, the polystyrene–divinylbenzene, acrylic and amide XAD resins shown in Table I had low capacities which would allow the resins to be used in SCIC. (A typical working capacity range in our laboratories is 5 to 100 μequiv./g.) It is interesting to note that the latex particles are too large to fit into the pores of any of the resins listed in Table I. It is also important to recognize that unlike the electrostatically-coated latex resins[3,4], this procedure does not require

TABLE I

CAPACITY OBTAINED ON VARIOUS LATEX-COATED RESINS

Conditions (except *): 0.25 g of 30–37 μm resin, 1 ml acetonitrile, 1 ml latex solution, diluted to 30 ml with 0.1 *M* sodium chloride; AL = strong-base anion-exchanging acrylic latex (60% functionalized); PL-100 = strong-base anion-exchanging polystyrene latex (100% functionalized); PL-76 = strong-base anion-exchanging polystyrene latex (76% functionalized); DVB = divinylbenzene.

Resin	*Functionality*	*Surface area* (m^2/g)	*Av. pore diameter* (Å)	*Capacity (μequiv./g)*		
				AL	*PL-100*	*PL-76*
XAD-1	Styrene-DVB	100	205	31±2	46±6	–
XAD-2	Styrene-DVB	300	90	29±3	85±7	–
XAD-4	Styrene-DVB	784	50	16±2	26±4	–
XAD-7	Acrylic ester	450	90	25±2	62±9	–
XAD-8	Acrylic ester	140	235	14±2	31±6	–
XAD-11	Amide	69	352	15±2	45±2	–
XAD-1	Styrene-DVB	100	205	–	36±2*	457±2*

* Conditions: 0.15 g of 30–37 μm resin, 0.6 ml acetonitrile, 0.31 ml PL-100 or 0.6 ml PL-76 (to add identical grams of latex), diluted to 10 ml with 0.05 *M* sodium chloride.

the use of a sulfonated resin. Virtually any resin which is sufficiently hydrophobic to allow latex adsorption can be coated and used for SCIC.

Latex-coated resins of varying capacities were prepared by altering the concentration of the inert electrolyte (sodium chloride) or the concentration of the latex slurry used to coat the resin. Fig. 1 shows adsorption isotherms for coating latexes onto XAD-1. An increase in the salt or latex concentration resulted in an increase in exchange capacity. Using various resins and latexes, a capacity range of approximately 5 to 400 μequiv./g was possible. This broad capacity range is ideal for use in SCIC and makes available a wide range of anion separations and sensitivities.

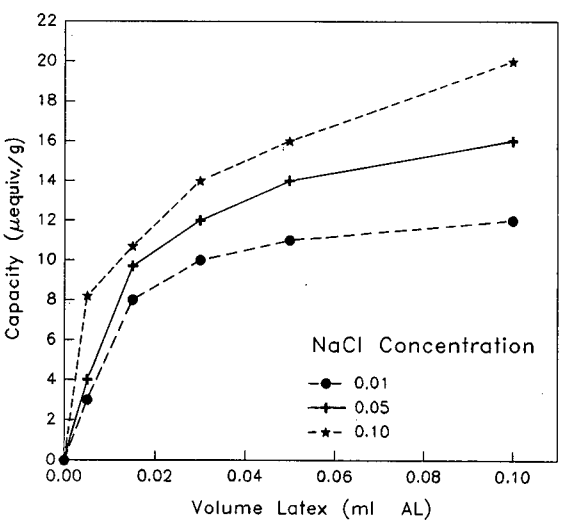

Fig. 1. Adsorption isotherms for AL–XAD-1 (strong-base anion-exchanging latex, AL, coated on 38–44-μm XAD-1).

A new polystyrene resin has been developed[13] that is greatly superior to the XAD resins for preparing latex-coated anion exchangers for use in anion chromatography. This resin is prepared in stages. The first is an emulsion polymerization performed with water-soluble initiators. The resin particles are <1 μm in diameter and are used as seed particles for the subsequent expansion stages. Although conditions can be adjusted to vary the particle size, the materials made available to us had a very uniform particle size of around 4.2 μm (see optical micrograph in Fig. 2a). The particles are approximately spherical but the method of polymerization gives them a somewhat billowy appearance, as show in Fig. 2b. These resins, which will be designated as PS in this paper, have no porosity.

Fig. 2c shows some PS resin beads that have been coated with rather large 0.6-μm polystyrene 76% quaternized particles. The exchange capacity of this coated resin is fairly high (138 μequiv./g) but the sparseness of the coating (Fig. 2c) and the large size of the quaternized latex particles gave very inefficient separations when a column packed with this material was used for ion chromatography.

Polyacrylate latexes (AL) with 60% of the theoretical amount of quaternary ammonium groups were available in smaller particle sizes: 0.09 μm for strong-base acrylate latexes and 0.08 μm for the weak-base acrylate latexes. PS resins coated with these latexes produced columns with very high efficiencies for separating anions (see section on chromatographic separations). Stevens and Langhorst[4] reported that for electrostatically coated latex resins the use of latexes smaller than 0.1 μm gave the most efficient anion separations.

Table II lists the resins which were used chromatographically during the course of this study. The coated polystyrene (PS) gave more efficient separations than the coated XAD resins. Therefore, much of the chromatographic work done in this study was performed using the AL–PS columns. The AL–PS columns had linear pressure *versus* flow behavior up to a least 3500 p.s.i. Flow-rates of 0.5 to 1.0 ml/min were typically used, which gave column pressures of 1000 to 1900 p.s.i.

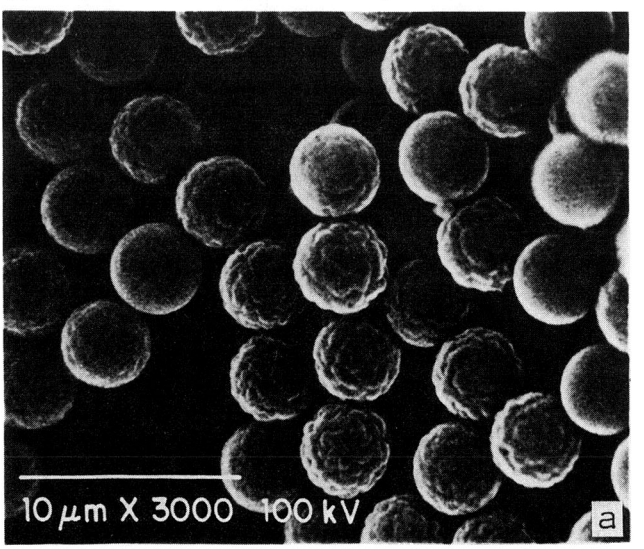

Fig. 2.

(Continued on p. 170)

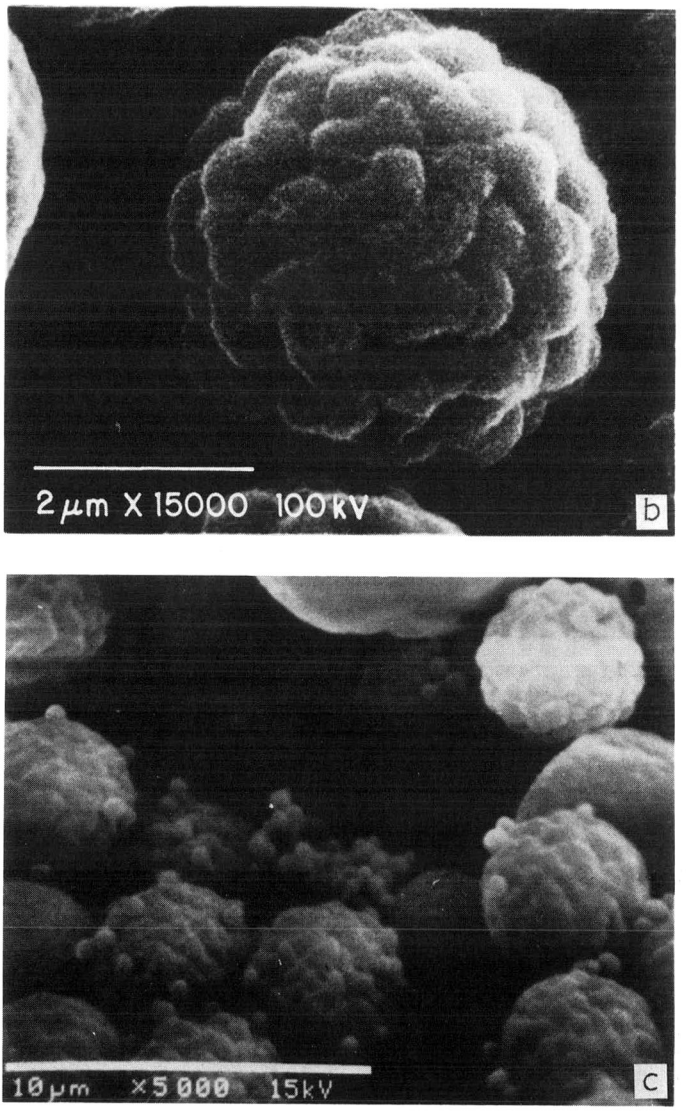

Fig. 2. Electron micrographs of (a) 4.2-μm polystyrene resin particles, (b) a higher magnification showing one polystyrene resin particle and (c) PL-76–PS (strong-base anion-exchanging latex on polystyrene).

Mechanism of latex adsorption

Cantwell and co-workers[14–16] studied the mechanism of organic ion adsorption on a reversed-phase resin, unfunctionalized XAD-2 and sulfonated XAD-2. Using adsorption isotherms, the mechanism was explained by the Stern–Guoy–Chapman (SGC) model of the electrical double layer. According to Cantwell, adsorption of an organic ion onto styrene–divinylbenzene copolymers is due to dispersion forces. As these ions are adsorbed, a resin surface charge is acquired due to the charged

TABLE II

CHARACTERISTICS AND DESIGNATIONS OF COATED RESINS

Designation	*Latex**	*Resin***	*Capacity (μequiv./g)*	*Column size*
AL–XAD-1	AL	XAD-1	Variable	–
AL-WB–XAD-1	AL-WB	XAD-1	18	250 mm × 2.0 mm I.D.
PL-76–PS	PL-76	PS	457	250 mm × 4.0 mm I.D.
AL–PS	AL	PS	27	250 mm × 4.0 mm I.D.
AL–PS	AL	PS	48***	250 mm × 4.0 mm I.D.

* See text for latex descriptions.

** XAD-1 resin is irregularly-shaped and 20 to 26 μm in size. The polystyrene resin (PS) is spherical, non-porous and 4.2 μm in size.

*** The AL–PS column of a higher capacity was prepared by increasing the latex and sodium chloride concentration in the coating solution.

surface groupings on the adsorbed particle. Following the SGC electrical double layer model, addition of an electrolyte to the coating solution increases the number of counterions in the bulk solution. The surface potential remains constant, so more organic ions must adsorb onto the resin surface in order to maintain this potential, thus creating a heavier organic ion coating.

The adsorption isotherms shown in Fig. 1 for latex-coated XAD seem to follow the trends shown in Cantwell's work. Addition of an electrolyte (sodium chloride) to the coating solution causes more latex particles to adsorb onto the support, giving a higher exchange capacity. This leads to the conclusion that a hydrophobic interaction is responsible for the coating of latex particles onto these resin matrices.

Table I also shows the capacities obtained by coating two latexes which differ in their degree of functionalization onto XAD-1. The latexes are 76% and 100% functionalized strong-base exchanger polystyrene (PL-76 and PL-100). The 76% functionalized latex coated 13 times heavier than the 100% functionalized latex (457 and 36 μequiv./g, respectively). With a lower degree of ionic character in the 75.6% functionalized latex, the dispersive forces allow a larger amount of latex to be coated onto the support. This phenomenon also supports the mechanism of hydrophobic interaction between the latexes and the resin supports.

Latex particles held onto the resin surface by a hydrophobic attraction can be washed off by organic solvents. Passing acetonitrile or 2-propanol through a latex-coated column removed part of the latex coating and lowered the column capacity. This observation is similar to results by Iskandarani and Pietrzyk[17] with alkylammonium-coated columns where larger amounts of organic modifiers in the coating solution resulted in a lower degree of resin coating. The latex-coated resins, however, could tolerate low amounts of methanol without significantly affecting the exchange capacity.

The fact that organic solvents alter the column exchange capacity is not a great concern in SCIC. In most cases, aqueous eluents are used and aqueous samples are analyzed. In addition, our work has not found significant advantages from using organic modifiers in the eluents. However, organic solvents can be used to strip the latex off of a fouled or ruined latex-coated column so that the resin can be recoated and used again.

Chromatographic efficiency and selectivity

The best column efficiencies were obtained with the AL–PS (latex-coated 4.2-μm polystyrene) columns. Fig. 3 shows the relationship between the eluent linear velocity (or flow-rate) and the height equivalent to a theoretical plate (HETP) for this column using a 4 m*M* molybdate eluent. The column efficiencies observed during the course of this work varied with different columns, eluents and test analytes. A typical 250 mm × 4.0 mm I.D. column produced plate numbers (N) between 12 000 and 72 000 plates/m between flow rates of 0.23 and 1.05 ml/min. The maximum plate number of 72 000 plates/m for sulfate was obtained at a flow-rate of 0.23 ml/min.

The selectivity of the AL–PS (48 μequiv./g) column for a series of anions using three different eluents is shown in Table III. The selectivity of this column for these anions is very similar to that obtained previously with coated or chemically functionalized resins[7,18], although a few differences were noted. For example, ethyl- and propylsulfonate eluted much earlier than chloride from the AL–PS column. This is unusual because all XAD-based and commercial columns used in our laboratories elute the sulfonates either simultaneously with or later than chloride.

Chromatographic separations

Figs. 4–7 show typical examples of separations that can be achieved with the AL–PS and AL-WB–XAD-1 columns. Fig. 4 shows a good separation of several normally late-eluting anions on a coated XAD column of very low capacity (AL-WB–XAD-1). These latex-coated columns can be prepared very easily with capacities low enough that low eluent concentrations can be used to obtain very sensitive anion determinations. For example, using a AL–XAD-1 column with a capacity of 5 μequiv./g and an eluent concentration of $3.7 \cdot 10^{-5}$ *M* sodium phthalate (pH 6.0), a 0.4-ng detection limit for sulfate was obtained using indirect spectrophotometric detection.

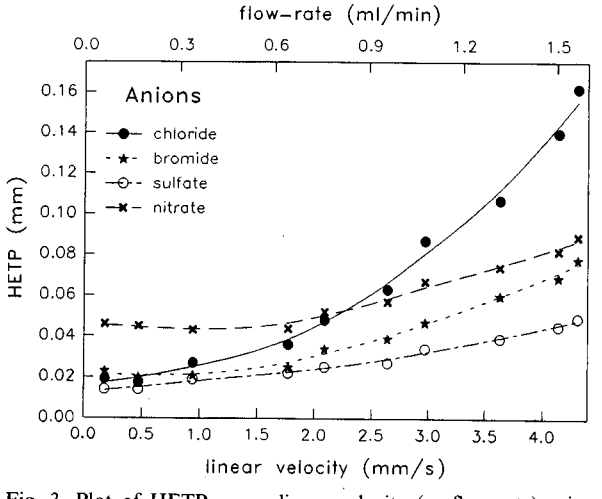

Fig. 3. Plot of HETP *versus* linear velocity (or flow-rate) using the 250 mm × 4.0 mm I.D. AL/PS (48 μequiv./g) column. The eluent was 4 m*M* sodium molybdate.

TABLE III

SELECTIVITY DATA FOR AL–PS COLUMN

Conditions: AL–PS column is 4.2-μm spherical, non-porous polystyrene coated with a strong-base anion-exchanging acrylic latex (48 μequiv./g capacity); 250 mm × 4.0 mm I.D. column; 1.0 ml/min flow-rate; conductivity detection.

Anion	*Capacity factor*		
	90 mM nicotinic acid	*2.4 mM sodium phthalate, pH 6.0*	*4.0 mM sodium molybdate*
Methyl acrylate	1.30	–	–
Lactate	1.85	–	–
Formate	3.45	–	–
Fluoride	3.70	0.36	0.21
Acetate	–	–	0.25
Iodate	6.40	0.36	0.21
Dihydrogen phosphate	8.25	–	–
Monochloroacetate	12.25	–	–
Methylsulfonate	13.50	0.73	0.54
Ethylsulfonate	13.60	0.73	0.54
Sulfamate	15.40	–	–
Propylsulfonate	16.95	0.91	0.75
Bromate	27.20	1.27	0.92
Chloride	28.90	1.45	0.96
Nitrite	31.65	2.04	1.42
Malonate	–	4.27	2.21
Bromide	48.90	5.00	3.13
Nitrate	–	6.73	4.17
Chlorate	–	6.91	4.71
Sulfate	–	7.45	3.17
Thiosulfate	–	32.27	13.58
Retention time for Cl^- (min)	55.00	3.00	2.19

Fig. 5 shows an excellent separation of seven common anions using the AL/PS (27 μequiv./g) column. Baseline resolution was achieved between every peak and the total analysis time was *ca.* 7 min. The molybdate eluent used here serves to elute sulfate immediately after nitrate, and proved to be an excellent eluent for the separation of these anions with these latex-coated columns. Since conductivity detection is not suitable with this eluent, indirect spectrophotometric detection at 250 nm was used.

Fig. 6 shows an excellent separation of 12 anions using the AL–PS (27 μequiv./g) column and a nicotinic acid eluent. Again, baseline resolution was achieved with every peak. The organic acid eluents such as nicotinic acid are very useful for separating large series of weakly-retained monovalent anions with these latex-coated columns.

Fig. 7 shows a separation using a AL–PS resin of a slightly higher capacity than the column used in Figs. 5 and 6 (48 compared to 27 μequiv./g). In this separation, sulfate was eluted before nitrate, an inversion which is rarely seen. Dionex has marketed a proprietary column, HPIC-AS2, which also shows this inversion. This column is useful for determining early-eluting anions in nitric acid digests. Supposedly,

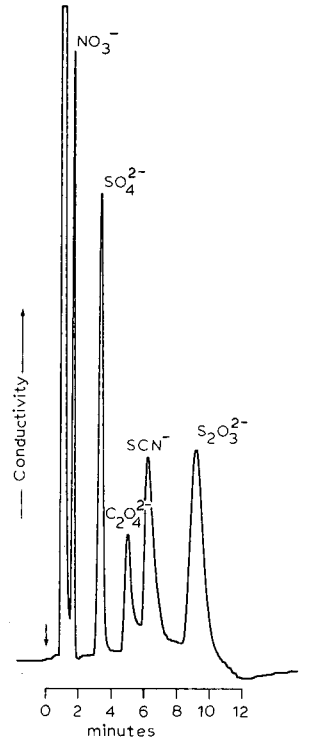

Fig. 4. Separation of late-eluting anions on AL-WB–XAD-1 column using $9 \cdot 10^{-4}$ *M* sodium phthalate at pH 5.10 as the eluent. The flow-rate was 1.3 ml/min and 13 to 17 ppm of each anion was injected.

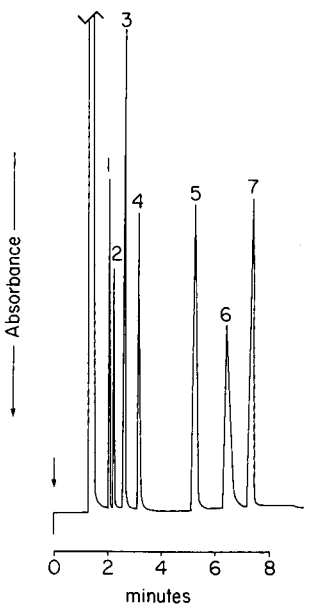

Fig. 5. Separation of 7 common anions on AL–PS (27 μequiv./g) column using a sodium molybdate eluent run at 0.75 ml/min. Indirect spectrophotometric detection was used at 250 nm with 0.05 a.u.f.s. Peaks: 1 = ethylsulfonate; 2 = propylsulfonate; 3 = chloride; 4 = nitrite; 5 = bromide; 6 = nitrate; 7 = sulfate (10–20 ppm each anion).

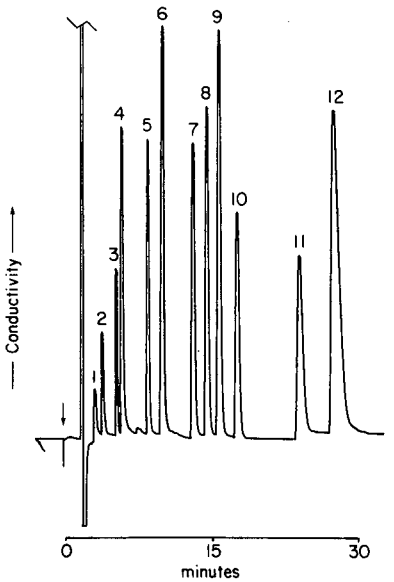

Fig. 6. Separation of 12 monovalent anions on AL–PS (27 μequiv./g) using 70 m*M* nicotinic acid (pH 3.5) as the eluent. The column pressure was 115 bar at a flow-rate of 0.75 ml/min. Conductivity detection was used with 0.1 μS f.s. Peaks: 1 = methyl acrylate; 2 = lactate; 3 = formate; 4 = fluoride; 5 = iodate; 6 = dihydrogen phosphate; 7 = monochloroacetate; 8 = ethylsulfonate; 9 = sulfamate; 10 = *n*-propylsulfonate; 11 = bromate; 12 = chloride (25–100 ppm each).

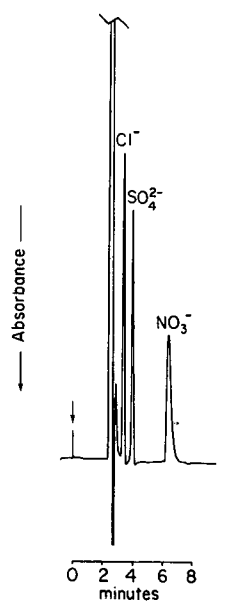

Fig. 7. Separation on AL–PS (48 μequiv./g) showing inversion of nitrate and sulfate. The eluent is 16 m*M* sodium molybdate run at 0.75 ml/min. Indirect spectrophotometric detection is used at 271 nm with 0.01 a.u.f.s.

the nitrate/sulfate inversion on the Dionex resin is brought about because of different resin functional groups. DuVal and Fritz[7] demonstrated this same inversion using tetraoctylammonium chloride coated on XAD-8 as the anion-exchanging resin.

The "nitrate-selective" column utilized in this work is a strong-base anion-exchanging acrylic latex coated on polystyrene. The exchange site is a typical trimethylammonium functional group. The higher capacity of this resin (as compared to the resin used in Fig. 6) along with the molybdate eluent created the nitrate/sulfate inversion. The retention times of chloride, sulfate and nitrate were 3.3, 3.8 and 6.4 min, with a 2.6-min separation between sulfate and nitrate.

ACKNOWLEDGEMENTS

We gratefully acknowledge the supporters of this research, Rohm & Haas of Philadelphia.

We thank Rohm & Haas for supplying the latexes and resins used in this work. We also thank Rohm & Haas and Fran Laabs (Ames Laboratory, Ames, IA, U.S.A.) for supplying the electron micrographs shown in this manuscript.

This work was performed at the Ames Laboratory, which is operated for the U.S. Department of Energy by Iowa State University.

REFERENCES

1 H. Small, T. S. Stevens and W. C. Bauman, *Anal. Chem.*, 47 (1975) 1801.
2 D. T. Gjerde, J. S. Fritz and G. Schmuckler, *J. Chromatogr.*, 186 (1979) 509.
3 H. Small and T. Stevens, *U.S. Pat.*, 4 101 460 (1978).
4 T.S. Stevens and M.A. Langhorst, *Anal. Chem.*, 54 (1982) 950.
5 R. E. Barron and J. S. Fritz, *React. Polymers*, 1 (1983) 215.
6 R. M. Cassidy and S. Elchuk, *J. Chromatogr.*, 262 (1983) 311.
7 D. L. DuVal and J. S. Fritz, *J. Chromatogr.*, 295 (1984) 89.
8 B. B. Wheals, *J. Chromatogr.*, 402 (1987) 115.
9 A. S. Al-Omair and S. J. Lyle, *Talanta*, 43(3) (1987) 361.
10 P. K. Dasgupta, *Anal. Chem.*, 56 (1984) 769.
11 B. P. Chong, *U.S. Pat.*, 4 359 537 (1982).
12 L. M. Warth and J. S. Fritz, *J. Chromatogr. Sci.*, submitted for publication.
13 M. S. Frazza (The Rohm & Haas Company, Philadelphia, PA), U.S. patent to be filed.
14 H. Liu and F. F. Cantwell, *HPLC 86, 10th International Symposium on Column Liquid Chromatography, San Francisco, CA, 1986*, Abstract No. 1101.
15 F. F. Cantwell and S. Puon, *Anal. Chem.*, 51(6) (1979) 623.
16 R. A. Hux and F. F. Cantwell, *Anal. Chem.*, 56 (184) 1258.
17 Z. Iskandarani and D. J. Pietrzyk, *Anal. Chem.*, 54 (1982) 2427.
18 R. E. Barron, *Ph.D. Dissertation*, Iowa State University, Ames, IA, 1983.

Journal of Chromatography, 462 (1989) 177–189
Elsevier Science Publishers B.V., Amsterdam — Printed in The Netherlands

CHROM. 20 983

AFFINITY SEPARATION WITH POLYALDEHYDE MICROSPHERE BEADS

S. MARGEL
Department of Chemistry, Bar-Ilan University, Ramat-Gan 52100 (Israel)
(First received May 27th, 1988; revised manuscript received September 15th, 1988)

SUMMARY

Agarose polyaldehyde microsphere beads were prepared by encapsulating polyaldehyde microspheres of various diameters, *e.g.*, polyacrolein or polyglutaraldehyde microspheres, within agarose beads. Amino ligands such as proteins or drugs can be bound covalently to the beads in a single step at physiological pH. The binding capacity of the beads towards various amino ligands is inversely related to the diameter of the microspheres encapsulated in the agarose matrix. Different reagents, *e.g.*, bovine serum albumin, ethanolamine and hydroxylamine, were studied as blocking reagents of the free aldehyde groups. Blocking the remaining aldehyde groups after coupling the amino ligands to the beads is essential for increasing or retaining the reactivity of the ligands conjugated to the beads. Among the reagent studied, hydroxylamine was found to be the most suitable blocking reagent of the free aldehyde groups of beads conjugated with proteins. The extent of leakage of amino ligands bound to the agarose–polyaldehyde microsphere beads was studied as a function of the pH of aqueous solutions of the beads. At physiological pH the leakage was negligible. At acid pH, leakage of ligands containing several primary amine groups, *e.g.*, proteins, was insignificant. However, significant leakage was detected for ligands containing a single amino group. The leakage of proteins bound to the agarose–polyaldehyde microsphere beads was found to be much less than the leakage of the same proteins bound to agarose beads through the cyanogen bromide activation method.

INTRODUCTION

Affinity chromatograpy is a very useful technique in a variety of analytical and separation procedures. The development and wide use of this technique depends on the support materials and the facile methods for attaching ligands and proteins to them. In order for affinity chromatography to be effective, the ligands coupled to the supports should retain most of their reactivity and the bonds between the ligands and the support materials should be stable under absorbing and eluting conditions. A few recent articles have summarized the support materials and methods of attachment used for purification of biomolecules through the affinity chromatography technique[1–4].

Agarose is the most commonly used support for the affinity purification of

0021-9673/89/$03.50

biomolecules. Agarose contains hydroxy groups through which amino ligands, *e.g.*, proteins, are covalently bound. Few activity methods for coupling proteins to agarose (or other supports with hydroxy groups) have been developped[1]. These activation methods require the use of pure organic solvents and reagents, such as cyanogen bromide, tosyl chloride, tresyl chloride, N-hydroxysuccinimide, imidazoles, chloroformates or activated pyridines. Coupling of proteins to these activated supports usually requires basic conditions. In previous papers we described the synthesis and use of agarose–polyaldehyde microsphere beads (APAMB) for affinity separations[5,6]. These beads were prepared by encapsulating polyacrolein (PA) microspheres or polyglutaraldehyde microspheres of average diameter 0.15 μm in an agarose matrix. The beads formed contained on the surface of the embedded microspheres aldehyde groups through which primary amino ligands, *e.g.*, proteins or drugs, can be bound covalently in a single step at physiological (or other) pH. In further studies of the APAMB we found that their binding capacity towards amino ligands is inversely related to the diameter of the microspheres encapsulated in the agarose matrix. Different reagents, *e.g.*, bovine serum albumin (BSA), ethanolamine and hydroxylamine, were studied as blocking reagents of the free aldehyde groups. Blocking of the remaining aldehyde groups after coupling the amino ligands to the beads is essential for increasing or retaining the reactivity of the ligands conjugated to the APAMB. The extent of leakage of proteins bound to the agarose–polyaldehyde microsphere beads was also examined.

EXPERIMENTAL

Reagents

The following materials were purchased from commercial sources: polyethylene oxide, average mol. wt. 100 000, from Polyscience; human serum albumin (HSA), bovine serum albumin (BSA, fraction V), digoxin, paraquat, chymotrypsin, protein A, biotin and alkaline phosphatase (type VII-NT) from Sigma; goat immunoglobulin (goat Ig), human Ig and concanavalin A from Bioyeda; avidin from Belova; agarose A and Sepharose 4B cross-linked (CL) from Pharmacia; hydroxylamine hydrochloride, ethanolamine, divinyl sulphone and acrolein from Aldrich; and [^{14}C]BSA, [^{14}C]-paraquat and [^{131}I]digoxin from Amersham. Acrolein was distilled at atmospheric pressure before use.

Synthesis of PA microspheres

PA microspheres were obtained as described in previous publications[7,8]. Briefly, microspheres of average diameter 0.15 μm were prepared by irradiation with a cobalt source (0.5 Mrad) of an air-free aqueous solution containing 7.5% (w/v) acrolein and 0.5% (w/v) polyethylene oxide. The microspheres were then washed by repeated centrifugation at 10 000 rpm. The diameter of the microspheres obtained was controlled by changing the surfactant or monomer concentration, *e.g.*, microspheres of 0.08 μm were obtained in a similar procedure using an aqueous solution containing 1% (w/v) of surfactant and 5% (w/v) of monomer.

Synthesis of the APAMB

The APAMB were synthesized as previously described[5]. Briefly, an aqueous

solution at 80°C containing 3% PA microspheres with the desired diameter and 4% agarose was poured into stirred peanut oil at 70°C, then the solution was cooled with ice. The APAMB obtained were purified from the oil by several extractions with diethyl ether, which was then removed by evaporation. APAMB with diameters ranging from 100 to 200 μm were obtained by sieving the APAMB. The APAMB were cross-linked with divinyl sulphone according to a previously described procedure[9]. The APAMB were stored at 4°C with 0.05% (w/w) merthiolate.

Antiserum

Rabbit antiserum was obtained by immunizing rabbits with an emulsion containing the appropriate antigen in Freund's complete adjuvant[5,9–11].

Determination of proteins

The amounts of proteins bound to the APAMB were determined by measuring the unbound proteins with Folin–Ciocalteau reagent using Lowry *et al.*'s method[12]. The amounts of proteins bound to the immuno-APAMB were determined by measuring the unbound proteins by the quantitative precipitin reaction[13]. The amounts of eluted proteins were also determined by the method of Lowry *et al.*[12]. Avidin was determined by a sensitive enzyme assay as described by Bayer *et al.*[11]. Digoxin, Paraquat, rabbit antidigoxin and rabbit antiparaquat were determined by radioimmunoassay (RIA)[9,10].

Preparation of the immuno-APAMB

APAMB (1 g) in PBS (5 ml) were shaken for 12 h at room temperature with an appropriate amount of the desired protein and unbound protein was removed by repeated decantation with PBS. The remaining free aldehyde groups were then blocked by shaking 1 ml of the immuno-APAMB in 5 ml of PBS for 12 h at room temperature with one of the following reagents: BSA (10 mg), aqueous ethanolamine solution at pH 7.2 (1 ml) or aqueous hydroxylamine solution (100 mg/g) at pH 7.2 (1 ml). The blocked immuno-APAMB were washed free of unbound hydroxylamine by repeated decantation with PBS. Non-covalently adsorbed proteins or blocking reagents were removed by washing the beads with buffers at pH 4 (0.1 *M* acetate buffer containing 1 *M* sodium chloride) followed by a buffer solution at pH 8 (0.1 *M* hydrogencarbonate buffer containing 1 *M* sodium chloride). Then the beads were resuspended in PBS.

Affinity separations

The separation of proteins by affinity chromatography with the immuno-APAMB was performed as previously described[5]. Briefly, the immune serum was passed at a rate of 1 ml/min through a column containing the appropriate immunoabsorbent (5–10 ml of serum for each gram of the immunobeads). The immunobeads were washed several times with PBS. Absorbed antibodies were then eluted with 0.2 *M* glycine–hydrochloric acid buffer solution at pH 2.4, neutralized with sodium hydroxide, dialysed aganst PBS and then analysed by polyacrylamide gel electrophoresis[14]. The immunobeads, after the treatment with glycine–hydrochloric acid buffer, were washed several times with PBS and stored at 4°C in the presence of sodium azide (0.05%) until reused.

Binding capacity of PA towards amino ligands

PA microspheres of average diameter 0.15 μm (100 mg) in water (5 ml) were shaken at room temperature for 48 h with various amino ligands (500 mg of each ligand in 5 ml of aqueous solution at pH 7.0). Proteins, *e.g.*, BSA, were determined by measuring the unbound protein by Lowry *et al.*'s method[12]. Other amino ligands, *e.g.*, hydroxylamine or ethanolamine, were determined by removal of the ligand solution by at least six repeated centrifugation cycles through water at 12 000 rpm. The conjugated product was then vacuum dried at 60°C and submitted to nitrogen analysis.

Kinetic studies

APAMB (1 g) bound to rabbit antidigoxin or protein A were shaken at room temperature with PBS (50 ml) containing digoxin or human Ig, respectively. Samples were taken at intervals and checked for digoxin by RIA[9] or protein A by measuring the absorption at 280 nm.

Stability and safety

The release of microspheres or beads fragments into saline during perfusion was studied as previously described[10]. Briefly, saline was circulated through cross-linked APAMB (25 g, containing microspheres of size 0.15, 0.08 and .03 μm) for 2 days at a flow-rate of 150 ml/min. Samples of saline were taken periodically and measured for their turbidity (Hach 2100A turbidimeter). The limit of detection of the instrument was found to be 30 ng/ml. Release of monomeric acrolein was studied by measuring the absorbance of the samples at 210 nm. The limit of detection of acrolein by this method is 1 μg/ml

Stability of the covalent APAMB–amino ligand bond

Leakage of proteins bound to APAMB was studied by sampling the supernatant APAMB solution at intervals and determining the protein content. In some instances the leakage of proteins was also studied under perfusion conditions. Leakage of BSA and human Ig was determined by coupling to the APAMB 2 μCi [^{14}C]BSA and cold BSA, or 3 μCi [^{14}C]human Ig and cold human Ig, respectively. The conjugated APAMB (1 g) were stored in PBS (2 ml) at 4°C and sampled at intervals to measure the radioactivity in the supernatant. At each sampling period the supernatant was replaced with the same volume of PBS. Under similar conditions leakage of avidin was determined by an enzyme assay[11]. Leakage of avidin, rabbit antidigoxin and rabbit antiparaquat in plasma and PBS was also studied under the following perfusion conditions: plasma or saline (35 ml of each) was circulated (35–50 ml/min) at room temperature or 37°C through columns containing 10 g of the conjugated APAMB. Samples were taken after 4 h of perfusion and analysed. Antibodies were quantified by RIA, using ^{131}I for antidigoxin and ^{14}C for antiparaquat[9,10]. Avidin was determined as mentioned above by an enzyme assay[11].

Leakage of the blocking reagents, *e.g.*, hydroxlamine, was studied under physiological and acidic conditions. PA microspheres of average diameter 0.15 μm or APAMB coupled with hydroxylamine (100-mg microspheres or 1 g of APAMB) were added to PBS solution (20 ml) or to 0.2 *M* glycine–hydrochloric acid solution at pH 2.4 (20 ml). The supernatant of the beads was replaced each day after repeated centrifugation at 12 000 rpm or by decantation. After a week, all samples of the water-washed beads were vacuum dried at 60°C and submitted to nitrogen analysis.

RESULTS AND DISCUSSION

Photomicrographs

Fig. 1A shows a light microscopy photomicrograph of the APAMB. Fig. 1B is a transmission electron microscopy photomicrograph of the APAMB, showing the PA microspheres of average diameter 0.15 μm encapsulated within the agarose.

Effect of the diameter of the encapsulated microspheres on the binding capacity

Table I illustrates the inverse relationship between the binding capacity of the APAMB towards amino ligands and the diameter of the PA microspheres encapsulated in the agarose. For example, under the conditions described in Table I, APAMB containing PA microspheres of diameter 0.15 μm bind only 5 mg from an initial amount of 15 mg of goat Ig, whereas APAMB containing microspheres of 0.03 μm diameter completely bind the entire 15 mg of goat Ig. When the initial amount of goat Ig is 100 mg, 18 mg of the protein are bound to beads containing microspheres of diameter 0.15 μm, whereas 70 mg of the protein are bound to beads containing microspheres of diameter 0.03 μm. Similar differences were obtained with other proteins, *e.g.*, avidin, HSA and chymotrypsin.

The performance of the conjugated APAMB containing microspheres of smaller

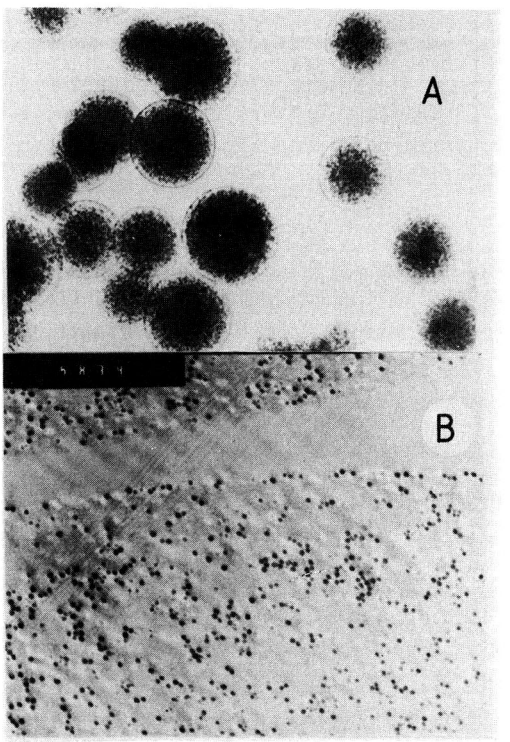

Fig. 1. (A) A light microscopy photomicrograph of the APAMB. (B) A transmission electron microscopy photomicrograph of a thin section of the APAMB showing PA microspheres of average diameter 0.15 μm within the agarose matrix. Peripheries of two beads are depicted.

TABLE I

EFFECT OF THE DIAMETER OF THE ENCAPSULATED MICROSPHERES ON THE BINDING CAPACITY OF THE APAMB

APAMB (1 g) in 5 ml of saline were shaken at room temperature with various amounts of proteins for 12 h.

Ligand	*Amount (mg)*	*Bound ligand (mg/g beads)*		
		0.15-μm microspheres	*0.08-μm microspheres*	*0.03-μm microspheres*
Goat Ig	15	6	13	15
	30	–	20	30
	100	18	30	70
HSA	15	3	4	6
	30	–	–	20
	100	14	–	40
Concanavalin A	100	54	–	72
Chymotrypsin	100	8	–	52
Avidin	15	13	–	15
Protein A	15	5	8	13

diameter in the affinity purification of proteins is also significantly improved, as shown in Table II. After three affinity separation cycles the amount of antiavidin eluted through avidin–APAMB containing microspheres of diameter 0.08 μm is 2.5 times higher than that of antiavidin eluted through conjugated beads containing microspheres of diameter 0.15 μm. Antiavidin antibodies eluted from the various kinds of avidin–APAMB shown in Table II were submitted to analysis by polyacrylamide gel electrophoresis and were found to contain only IgG.

Reagents for blocking remaining unreacted aldehyde groups

Table III illustrates the extent of reaction between PA microspheres and various amino ligands. The degree of reaction between the microspheres and the ligands did not change significantly on washing the microspheres with distilled water to remove

TABLE II

EFFECT OF THE DIAMETER OF THE ENCAPSULATED MICROSPHERES ON THE ISOLATION OF RABBIT ANTIAVIDIN

APAMB (1 g) in 5 ml of saline were shaken at room temperature with 20 mg of avidin for 12 h. Unbound avidin was then washed by repeated decantation. Immune serum was passed at a rate of 1 ml/min through a column containing the APAMB–avidin conjugate. Adsorbed antibodies were eluted with 0.2 *M* glycine–hydrochloric acid buffer solution (pH 2.4).

Encapsulated microspheres diameter (μm)	*First run*		*Second run*		*Third run*	
	Amount of bound antiavidin (mg)	*Amount of antiavidin eluted (mg)*	*Amount of bound antiavidin (mg)*	*Amount of antiavidin eluted (mg)*	*Amount of bound antiavidin (mg)*	*Amount of antiavidin eluted (mg)*
0.08	19	18	18	16	16	16
0.15	12	9	9	6.5	6.5	6.5

TABLE III

BINDING CAPACITIES FOR THE REACTION OF PA MICROSPHERES AND AMINO LIGANDS

Microspheres (diameter 0.15 μm) (100 mg) in 5 ml of water were shaken at room temperature for 48 h with 500 mg of the appropriate amino ligands in 5 ml of aqueous solution at pH 7.0. The microspheres were thoroughly washed with distilled water by repeated centrifugation to remove free ligands.

Ligand	*N (%)*	*Bound ligand (mmol/g microspheres)*
Hydroxylamine	14	10
Hexanediamine	1.8	1.3
Ethanolamine	2.0	1.4
Glycine	0.6	0.4
Phenylalanine	0.6	0.4
BSA	—	$4.2 \cdot 10^{-2}$

free ligands. On the other hand, a gradual decrease in the extent of reaction of the microspheres with the primary amino ligands was observed when washing of the microspheres was accomplished at acidic pH [*e.g.*, glycine–hydrochloric acid buffer, 0.2 *M* (pH 2.4)].

Hydroxylamine is a common reagent for the determination of aldehyde groups in insoluble polymers[15–17]. As expected, this reagent interacted completely with the aldehyde groups of the PA microspheres. On the other hand, other amino ligands reacted to a much smaller extent with the aldehyde groups of the PA. For example, ethanolamine reacted with 14% of the total aldehyde functionality, whereas glycine blocked only 4% of the aldehyde groups. Further evidence for the complete reaction of PA with hydroxylamine is illustrated in Fig 2. The aldehyde absorption of PA at 1720 cm^{-1} (Fig. 2A) decreased slightly after the interaction with ethanolamine (Fig. 2B) and almost disappeared on reaction with hydroxylamine (Fig. 2C).

The effect of blocking the remaining aldehyde groups after coupling proteins to the APAMB is illustrated in Fig. 3. The reactivity of antidigoxin–APAMB for the removal of digoxin is increased by approximately 40% by blocking the remaining aldehyde groups with hydroxylamine after coupling the rabbit antidigoxin. The reactivity of the blocked antidigoxin–APAMB was retained with time, *e.g.*, 3 months. On the other hand, the reactivity of the non-blocked antidigoxin–APAMB decreased by 20% after 3 months. However, by blocking these non-conjugated beads the reactivity towards digoxin increased to the original value obtained with the blocked conjugated APAMB. A similar effect was obtained when protein A was coupled to the APAMB. The reactivity of the bound protein A to human Ig was 30–50% higher when the remaining aldehyde groups were blocked with ethanolamine or hydroxylamine.

Stability and safety

The nephelometric experiments showed no detectable release of microspheres or agarose fragments, indicating that strong physical forces (*e.g.*, hydrogen bonds and Van der Waals forces) hold the microspheres within the agarose matrix. Spectrophotometric measurement showed no detectable release of acrolein from the APAMB.

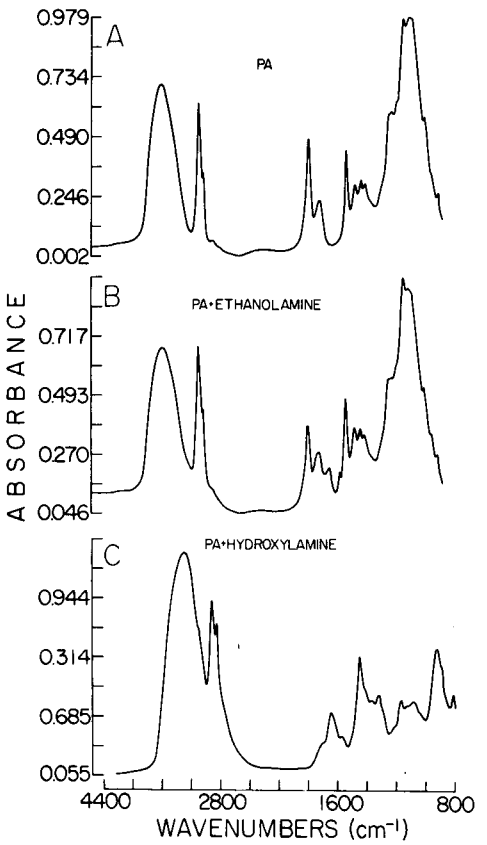

Fig. 2. (A) Infrared spectra of PA microspheres, (B) after reaction with ethanolamine and (C) after reaction with hydroxylamine. PA microspheres (average diameter 0.15 μm) (100 mg) in 5 ml of saline were shaken at room temperature for 48 h with 500 mg of ethanolamine or hydroxylamine in 5 ml of aqueous solution at pH 7.0.

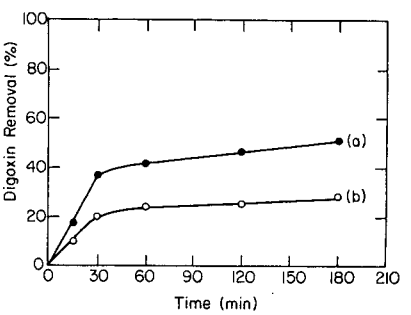

Fig. 3. Kinetics of removal of digoxin from PBS with antidigoxin–APAMB: (a) with hydroylamine as a blocking reagent; (b) without a blocking reagent. Antidigoxin–APAMB (4 mg of antidigoxin were bound to 1 g of APAMB containing PA microspheres of average diameter 0.15 μm) were shaken at room temperature in 50 ml of PBS containing 0.4 μg/ml of digoxin.

TABLE IV

LEAKAGE OF PROTEINS BOUND TO APAMB AND TO SEPHAROSE 4B CL

APAMB (1 g) (containing PA microspheres of average diameter 0.15 μm) and Sepharose 4B CL conjugated with proteins (BSA, 3 mg; human Ig and avidin, 10 mg each) were held in 2 ml of PBS at 4°C. For each period of time the supernatant was applied and reconstituted with the same volume of PBS.

Time (days)	*Amount released (%)*			
	*BSA–APAMB**	*Human IG–APAMB**	*Avidin–APAMB*	*Avidin–Sepharose 4B CL*
1	$1.5 \cdot 10^{-3}$	$4 \cdot 10^{-3}$	0**	0.1
7	$7 \cdot 10^{-3}$	$8.5 \cdot 10^{-3}$	0**	0.4
90	$7.5 \cdot 10^{-3}$	$38 \cdot 10^{-3}$	0**	0.4

* These experiments were carried out both under physiological conditions (PBS) and under aqueous acidic conditions [0.2 *M* glycine–hydrochloric acid buffer (pH 2.4)]. Similar results for the leakage were obtained.

** The detection limit for avidin using an enzyme assay[11] is 0.15 μg/ml or $3 \cdot 10^{-3}$% of released avidin.

Stability of the APAMB–amino ligands bond

Leakage of proteins bound to APAMB is low, as illustrated in Tables IV and V. BSA, human Ig and rabbit antidigoxin were detected in trace amounts in the supernatant of the conjugated APAMB. Avidin was detected in low levels in plasma and saline at 37°C. On the other hand, avidin in saline at room temperature and antiparaquat in plasma were not detected at all. The detection limit for avidin determination using the enzyme assay[11] is 0.15 μg/ml, or 0.3 μg/g of beads. Hence leakage of avidin bound to APAMB is at least 30 times lower than the leakage of avidin bound to Sepharose 4B via the cyanogenbromide activation method (Table V).

The leakage of ligands containing single primary amine group, *e.g.*, hydroxylamine, is illustrated in Table VI. Under physiological conditions the leakage, if any, is insignificant. However, under acidic conditions [0.2 *M* glycine–hydrochloric acid (pH 2.4)] which mimic the eluting conditions used to break the bond between antigen and antibody, a significant leakage of hydroxylamine was noted.

TABLE V

LEAKAGE OF PROTEINS BOUND TO APAMG DURING PERFUSION WITH PLASMA OR SALINE

Plasma or saline (35 ml) was circulated (at 30–50 ml/min) at room temperature and at 37°C through columns containing 10 g of APAMB (containing PA microspheres of average diameter 0.15 μm) conjugated with proteins (antidigoxin, 5 mg/g; antiparaquat, 18 mg/g; avidin, 10 mg/g). Samples were assayed after perfusion for 4 h.

Ligand	*Temperature (°C)*	*Medium*	*Ligand released (%)*
Antidigoxin	37	Plasma	$0.3 \cdot 10^{-3}$
Antiparaquat	37	Plasma	0
Avidin	37	Plasma	$9 \cdot 10^{-3}$
Avidin	Room	Plasma	$9 \cdot 10^{-3}$
Avidin	37	Saline	$2 \cdot 10^{-3}$
Avidin	Room	Saline	0

DISCUSSION

In previous papers we described the synthesis and use of APAMB for affinity chromatography[5,6,18]. During extensive studies carried out with the APAMB, several difficulties became apparent and were resolved.

Binding capacity

The binding capacity of APAMB containing microspheres of average diameter 0.15 μm toward amino ligands were described previously[1], *e.g.*, 1 g of APAMB bound 6 mg of goat Ig from a solution containing 15 mg of goat Ig. In order to increase the binding capacity of the APAMB, PA microspheres of smaller diameter were encapsulated in the agarose matrix. Microspheres with a smaller diameter have a much higher surface area and thereby their binding capacity is increased significantly (Table I). APAMB containing PA microspheres with diameters smaller than 0.1 μm possess additional useful characteristics and advantages compared with beads containing PA microspheres with diameters larger than 0.15 μm. They are more transparent, they have higher porosity and their performance in affinity separation is significantly improved (Table II).

Blocking the remaining aldehyde groups

In previous papers describing the use of polymeric beads containing aldehyde groups for affinity purification, the reagents examined and used for blocking remaining aldehyde groups, after coupling of the proteins, were glycine, BSA or ethanolamine[5,18–21]. However, glycine and BSA bind only 4% of the remaining aldehyde groups whereas ethanolamine blocks 14% of the remaining aldehyde groups (Table III). Therefore, it is expected that the reactivity of proteins bound to polyaldehyde beads blocked with the above reagents would not be optimal and may decrease with time because of the continued interaction of the lysine residue of the proteins bound to the APAMB with the free aldehyde groups on the beads. The hydroxylamine reagent interacts completely with all of the remaining aldehyde functionality of PA (Table III and Fig. 2). Therefore, this reagent seems to be a better choice for blocking the unreacted aldehyde groups.

Stability of the bond between APAMB and amino ligands

PA interacts reversibly with water to form various hydrated products[22,23]. Several of these hydrated forms are shown in Fig. 4. Primary amino ligands could bind to the aldehyde groups of PA through the free aldehyde form to give reversible Schiff base bonds and through the hydrated forms to give the irreversible cyclic products based on aminotetrahydropyran (Fig. 5). The lack of leakage obtained on reaction of proteins and PA may be explained by the resultant polyvalent bond, which is

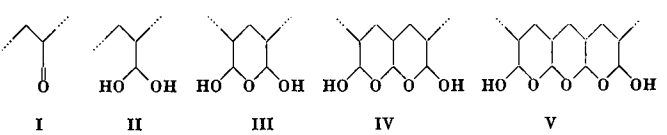

Fig. 4. Illustration of some products obtained by the reversible reaction of PA with water.

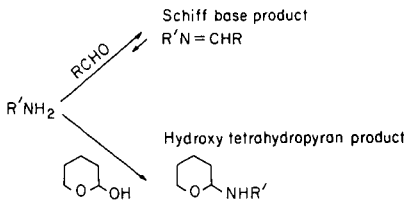

Fig. 5. Scheme of the reaction of primary amino ligands with the aldehyde groups of PA via the free aldehyde form and through the 2-hydroxytetrapyran form.

composed partially of Schiff base bonds and partially of the derivatized amino-tetrahydropyran forms. Amino ligands containing a single primary amino group, *e.g.*, hydroxylamine, may form two main types of products by their reaction with PA. The first is composed of a single Schiff base bond, which may lead eventually to leakage of the bound ligand from the APAMB into the solution. The second type of product may be based on the formation of a single derivatized aminotetrahydropyran form and should be stable.

Tables III and VI show that under physiological conditions the leakage of hydroxylamine bound to APAMB is insignificant. However, at acidic pH (2.4), which mimics the conditions employed to break the bond between antigen and antibody, a significant leakage of hydroxylamine bound to APAMB was obtained (Table VI). Therefore, it is suggested that when a low pH is used to break the antigen–antibody bond one should again block the remaining aldehyde groups after each five to eight affinity chromatography cycles. Another possibility for obviating the need for the reblocking step is to use conditions of high ionic strength at neutral pH, *e.g.*, 3.5 *M* aqueous sodium thiocyanate, to break the antigen–antibody bond.

Other possible reagents that can sometimes be used to stabilize the bond between the APAMB and ligands containing a single amino group are borohydride reducing reagents, *e.g.*, sodium borohydride or sodium cyanoborohydride[24]. Further, sodium borohydride may sometimes also be an efficient blocking reagent of the remaining

TABLE VI

LEAKAGE OF HYDROXYLAMINE BOUND TO PA MICROSPHERES AND TO APAMB

PA microspheres of average diameter 0.15 μm (100 mg) and 1 g of APAMB (containing PA microspheres of average diameter 0.15 μm) blocked with hydroxylamine were added to 20 ml of PBS solution or to 20 ml of 0.2 *M* glycine–hydrochloric acid solution at pH 2.4. The supernatant of the beads was replaced by the same volume each day. After 1 week, samples of washed beads were vacuum dried and submitted to nitrogen analysis.

Conditions	*PA microsperes*		*APAMB*	
	N (%)	*Hydroxylamine bound per 100 mg of PA (mmol)*	*N (%)*	*Hydroxylamide bound per gram of APAMB (mmol)*
Before treatment	14	1	7	0.5
pH 7.2	13.7	0.98	6.8	0.49
pH 2.4 once and then pH 7.2	11	0.78	6	0.43
pH 2.4	8.8	0.63	5	0.36

aldehyde groups (experiments in our laboratory at a variety of pHs, *e.g.*, pH 3, 4 and 5, showed that sodium cyanoborohydride in aqueous solution did not reduce the aldehyde groups of PA microspheres). However, our and other studies[24,25] indicated that in many instances the immunological activity of proteins, *e.g.*, antibodies, bound to various supports decreased significantly because of the use of the borohydride reducing reagents.

The search for new, effective immunoadsorbents is still continuing[26,27]. Most of the current advanced studies are carried out with polymeric beads containing hydroxy groups, *e.g.*, silica beads or Sepharose beads. The standard cyanogen bromide activation method that is used to bind amino ligands, to polymeric beads containing hydroxy groups suffers from several major disadvantages, *e.g.*, high toxicity of the cyanogen bromide reagent, a low yield of the reaction and instability of the isourea bond formed by the cyanogen bromide activation method towards hydrolysis and nucleophilic substitution reactions[26]. Recently, Wilchek and co-workers[28,29] elucidated the mechanism of the cyanogen bromide activation method. On the basis of their studies, they were able to increase the yield of the reaction between amino ligands and polysaccharide resins and thereby the amount of cyanogen bromide required for the activation could be decreased significantly. However, the instablity of the isourea bond still create a major difficulty in some systems. In order to eliminate the unstable bonds created by the cyanogen bromide activation method, Kohn *et al.*[30] developed alternative methods for the activation and immobilization of proteins to polymeric beads containing hydroxy groups based on reagents such as *p*-nitrophenyl chloroform at, N-hydroxysuccinimide chloroformate and trichlorophenyl chloroformate.

Several publications on the synthesis of beads derivatized with aldehyde groups suggest their use in affinity chromatography. An aldehyde-activated polyacrylamide support was prepared by Fiddler and Gray[31] from a commercially available aminoethyl polyacrylamide gel. Guesdon and Avrameas[20] prepared aldehyde-activated polyacrylamide agarose beads. Miron *et al.*[19] synthesized aldehyde-activated beads by reacting cyanogen bromide-activated agarose with varous bishydrazides to give hydrazidoagarose. Here, we have described the synthesis and studies performed with the improved APAMB. These beads are stable[10,18], they covalently bind amino ligands in a single step at physiological (or other) pH, they have a high binding capacity to amino ligands, the leakage of proteins bound to the APAMB is insignificant and they are highly biocompatible and blood compatible[18]. Very recent studies showed that the porosity of the APAMB (containing PA microspheres of average diameter 0.15 μm) is slightly lower than that of Sepharose 4B, and that the reactivity of a few proteins (*e.g.*, protein A) bound to similar APAMB, quenched with hydroxylamine, is similar to the reactivity of the same proteins bound to Sepharose 4B via the cyanogen bromide activation method. Further studies are in progress in our laboratory.

REFERENCES

1 E. V. Groman and M. Wilchek, *TIBTECH*, 5 (1987) 220–224.
2 P. Mohr and K. Pommerening, in *Affinity Chromatography*, Marcel Dekker, New York, 1985, pp. 7–15.
3 J. Turkova, in Z. Deyl (Editor), *Separation Methods*, Elsevier, Amsterdam, 1984, 321–357.
4 E. A. Hill and M. D. Hirtenstein, *Adv. Biotechnol. Processes*, 1 (1983) 31–63.
5 S. Margel and M. Offarim, *Anal. Biochem.*, 128 (1983) 342–350.
6 S. Margel, *Appl. Biochem. Biotechnol.*, 8 (1983) 523–539.

7 S. Margel and E. Wiesel, *J. Polym. Sci., Chem. Ed.*, 22 (1984) 145–158.
8 S. Margel, *Methods Enzymol.*, 112 (1985) 164–175.
9 L. Marcus, S. Margel, H. Savin and M. Ravid, *Am. Heart J.*, 110 (1985) 30–39.
10 R. Azhari, A Labes and Y. Haviv, *J. Biomed. Mater. Res.*, 21 (1987) 25–41.
11 E. A. Bayer, H. Ben-Hur and M. Wilchek, *Anal. Biochem.*, 154 (1986) 367–370.
12 O. H. Lowry, N. J. Rosebrough, A. L. Farr and R. J. Randall, *J. Biol. Chem.*, 193 (1951) 265–275.
13 M. Heidelberger and F. E. Kendall, *J. Exp. Med.*, 50 (1929) 809–819.
14 D. Rodbard, G. Kapadia and A. Chrambad, *Anal. Biochem.*, 40 (1971) 135–157.
15 J. W. Sloan, B. T. Hofreiter, R. L. Mellies and I. A. Walff, *Ind. Eng. Chem.*, 48 (1956) 1165–1168.
16 P. J. Borchert, *Kunststoffe*, 51 (1961) 137–139.
17 A. Rembaum, S. Margel and J. Levy, *J. Immunol. Methods*, 24 (1978) 239–250.
18 S. Margel and L. Marcus, *Appl. Biochem. Biotechnol.*, 12 (1986) 37–66.
19 T. Miron, W. G. Carter and M. Wilchek, *J. Solid-Phase Biochem.*, 1(1976) 225–236.
20 J. L. Guesdon and S. Avrameas, *J. Immunol. Methods*, 11 (1976) 129–133.
21 S. Margel, S. Zisblatt and A. Rembaum, *J. Immunol. Methods*, 28 (1979) 341–353.
22 R. C. Schultz, K. Meyersen and W. Kern, *Makromol. Chem.*, 59 (1962) 123–136.
23 M. Chang, G. Richards and A. Rembaum, *Methods Enzymol.*, 112A (1985) 150–154.
24 L. Peng, G. J. Calton and J. W. Burnett, *Appl. Biochem. Biotechnol.*, 14 (1987) 91–99.
25 S. K. Roy, D. F. Weber and W. C. McGregor, *J. Chromatogr.*, 303 (1984) 225–229.
26 G. R. Gray, *Anal. Chem.*, 52 (1980) 9R–15R.
27 W. Brummer, *J. Solid-Phase Biochem.*, 4 (1979) 171–187.
28 F. Pittner, T. Miron, G. Pittner and M. Wilchek, *J. Solid-Phase Biochem.*, 5 (1980) 147–150.
29 J. Kohn and M. Wilchek, *Enzyme Microb. Technol.*, 4 (1982) 161–163.
30 J. Kohn, R. Langer and M. Wilchek, *Appl. Biochem. Biotechnol.*, 8 (1983) 227–235.
31 M. B. Fiddler and G. R. Gray, *Anal. Biochem.*, 86 (1978) 716–724.

Journal of Chromatography, 462 (1989) 191–204
Elsevier Science Publishers B.V., Amsterdam — Printed in The Netherlands

CHROM. 20 991

CHROMATOGRAPHIC SEPARATION AND PURIFICATION OF XENON-133

YUN JAO, WU-LONG CHENG and GANN TING*
Institute of Nuclear Energy Research, Atomic Energy Council, P.O. Box 3-6, Lung-Tan 32500 (Taiwan)
(First received May 16th, 1988; revised manuscript received September 13th, 1988)

SUMMARY

A process has been developed for the separation of Xe-133 from a fission product gas mixture, consisting in collection of fission noble gases with a charcoal cold trap and purification and dispensation of xenon by chromatographic separation using activated charcoal as adsorbent. Impurities such as hydrogen, oxygen, oxides of nitrogen and krypton are almost completely removed from the xenon product. Analyses of the fission gas components were performed by gas chromatography using Porapak Q, Spherocarb and molecular sieves as adsorbents. The purity and yield of the product are satisfactory for domestic requirements in nuclear medical applications.

INTRODUCTION

Radioactive krypton and xenon are normally emitted with the off-gas during the dissolution of irradiated uranium. Rare gases can be separated from gas mixtures by physical means[1], *e.g.*, preferential adsorption on solids, absorption in liquids, low-temperature distillation and several differential diffusion processes[2,3]. Usually, krypton and xenon are recovered together in most processes and they are separated by distillation, selective adsorption or gas chromatography.

The rare gas isotopes most useful in nuclear medicine and industry are ^{133}Xe and ^{85}Kr. The fission yields for thermal neutron bombardment of ^{235}U are 6.8% for ^{133}Xe and 0.29% for ^{85}Kr[4]. As ^{85}Kr decays primarily by beta-emission associated with gamma rays only to the extent of 0.4% of its decay, this isotope is of limited use for *in vivo* measurements[5]. ^{133}Xe decays with a half-life of 5.25 days by emitting a beta-particle accompanied by 81 keV gamma radiation[6]. Currently, ^{133}Xe is the most commonly used radioactive gas isotope in nuclear medicine for imaging in lung ventilation studies[7–9], in organ blood flow measurements[5,10,11] and in the determination of tissue lipid and lipid-free fractions[12,13].

A method for the collection and concentration of rare gases has been established in this study. Activated carbon has previously been demonstrated to be successful for the chromatographic separation of rare gases at various temperatures[14–17]. In this work, a procedure for the pre-treatment and chromatographic separation of krypton and xenon at room temperature and atmospheric pressure was established[18]. The dispensation of the xenon product can be performed by using a gas diffusion device.

0021-9673/89/$03.50

EXPERIMENTAL

Collection of rare gases

The system design for the collection of rare gases from the fission product gas mixture source is shown in Fig. 1. The charcoal trap is connected to the fission product gas system by using a bypass loop and a four-way ball-valve.

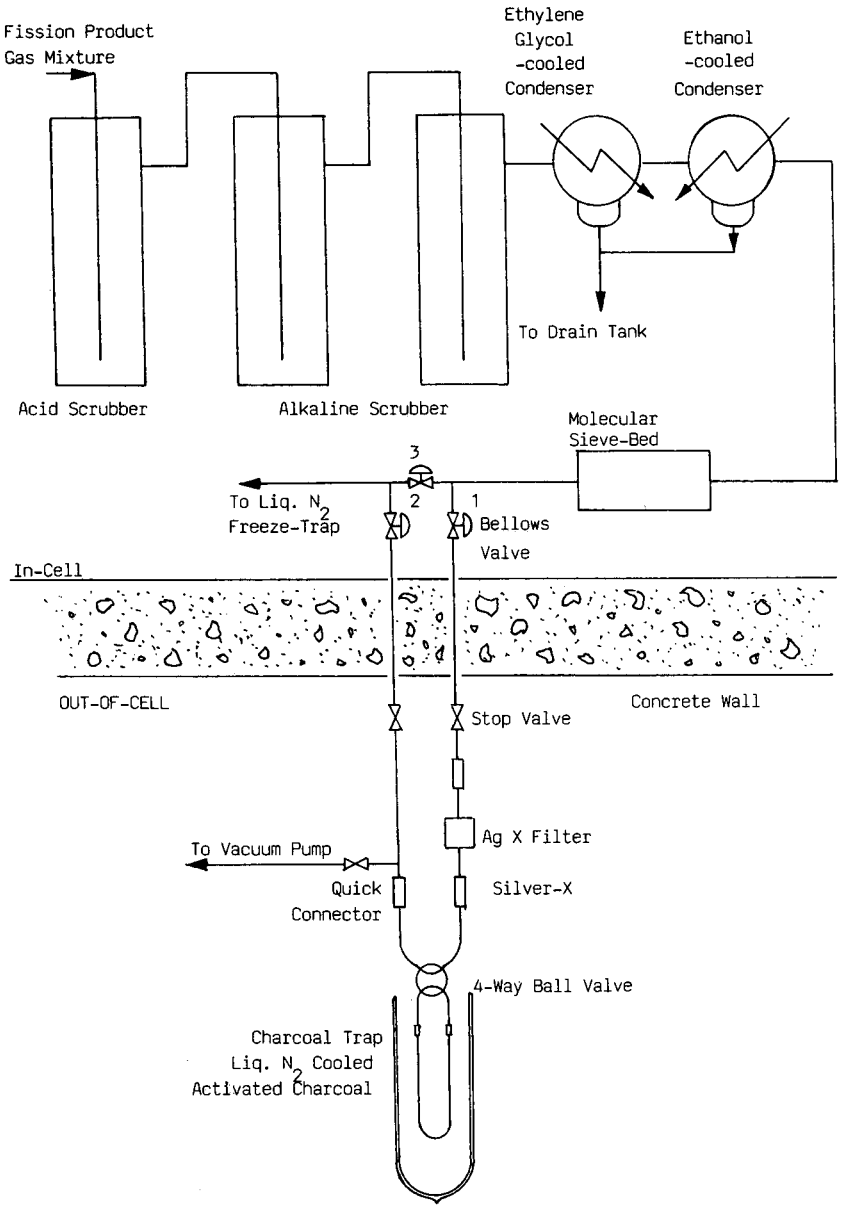

Fig. 1. Rare gas collection from fission product gas mixtures using a charcoal trap.

Off-gas pre-treatment. The in-cell off-gas system provides pre-treatment of the incoming gas stream. Prior trapping of water vapour and other gases such as the oxides of nitrogen and carbon is essential in order to prevent saturation of the adsorber or to avoid plugging of the cold trap. Radioactive iodine is separated by passing off-gases to acid and alkaline scrubbers in sequence. Nitrogen dioxide and carbon dioxide are also trapped in the alkaline scrubbers. Water vapour can be removed by condensation of the off-gas stream and by adsorption on a molecular sieve bed. It was found that the pre-treated inlet gas stream had a dew point below $-78°C$, and trace amounts of radioactive organic iodine had to be separated.

Rare gas collection. The rare gas collection system located out of the cell consists of an inlet–outlet gas line, a silver halide filter and a charcoal trap. Residual organic iodine compounds can be separated by chemisorption using silver zeolite.

The charcoal trap was made from a U-shaped piece of copper tubing; activated charcoal was held in the trap with glass-wool and stainless-steel screens. The copper tube filled with charcoal was accommodated in a Dewar flask. During operation, the liquid nitrogen level was maintained at about 2 in. below the top of the flask, which was covered with two pieces of half-moon Polylon plate. The collection efficiency of the trap was found to be essentially 100% for both xenon and krypton at gas flow-rates below 3 l/min. This trap was also used for the recovery of chromatographically purified xenon.

Principle of chromatographic separation of krypton and xenon

Because the activity of ^{85}Kr (39.5 mCi) is low, application of the chromatographic process with activated charcoal is limited to the purification of ^{133}Xe only. The process sequence is illustrated in Fig. 2, and consists of the following steps.

(1) Adsorption of He–Kr–Xe mixture at room temperature and atmospheric pressure up to the first breakthrough. During this step, the outflowing gas is free of krypton and xenon and is vented to waste.

(2) The adsorption phase is continued. The outflowing gas contains krypton at the same concentration as that in feed gas ($C = C_F$) and is vented to waste.

(3) After the adsorption phase, the adsorber is flushed with helium at room temperature and atmospheric pressure until the krypton concentration in outflowing gas has fallen to $0.001 C_F$. During this flushing step, no significant xenon breakthrough takes place.

(4) Xenon is then desorbed by flushing the adsorber with heated (60°C) helium under atmospheric pressure. The released xenon is collected and concentrated in a liquid nitrogen-cooled charcoal trap.

(5) When xenon desorption is completed, the inlet and outlet valves of the adsorber are closed to keep the adsorbent dry.

The process is based on the concept that the co-adsorbed krypton is more easily desorbed than xenon during the flushing step. This makes it possible to carry out the adsorption–desorption process at normal pressures and temperatures (preferably at room temperature). Sufficient separation of krypton from xenon can be achieved by appropriate control of the adsorption and desorption operation.

Equipment and procedure

A simplified scheme of the experimental equipment is shown in Fig. 3. The

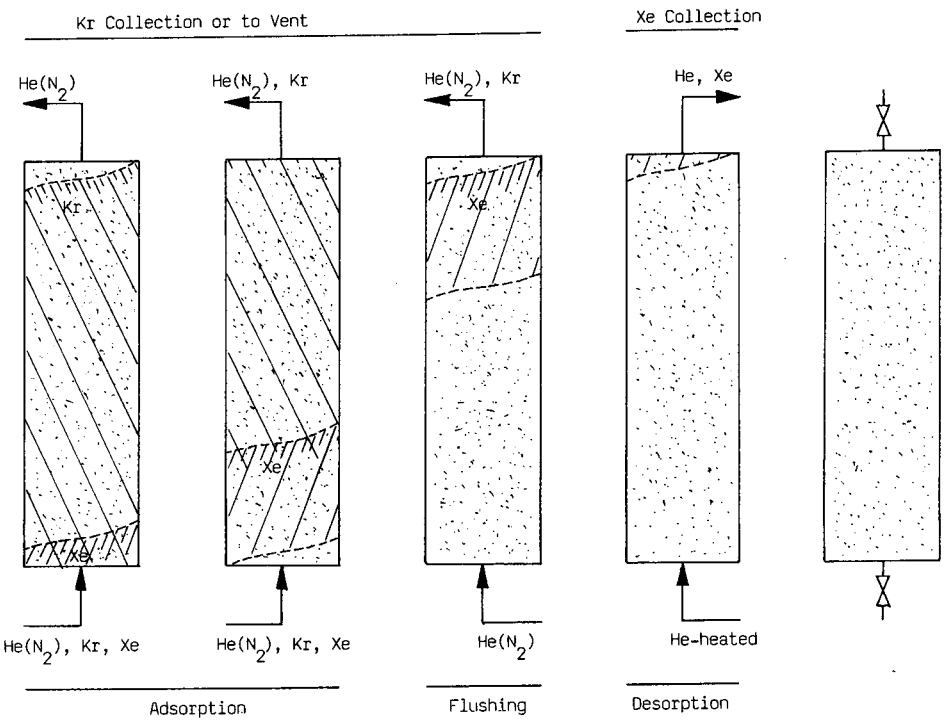

Fig. 2. Basic principle of separation of krypton and xenon by adsorption and desorption.

apparatus makes it possible to adjust various operating parameters such as the gas flow-rate, pressure, carrier gas, temperature, adsorber length, particle size of adsorbent and rare gas concentrations. The flow-rate was controlled by needle valves. Temperature was measured by means of thermocouples and indication controllers. The adsorbers used, 50–100 cm in length and 2 cm I.D., were filled with activated charcoal and preheated with heating tape for 2 h at 60°C under a nitrogen sweep and a negative pressure of 100 Torr.

The operating procedure for a typical run consists of three steps: (1) adsorption, (2) flushing and (3) desorption. For the adsorption step, a flow of dry helium or nitrogen containing a known concentration of admixed krypton or xenon was passed through a charcoal bed at room temperature and under atmospheric pressure. The outlet gas samples were taken with small vacuum bulbs at sufficient intervals to give effluent concentration–time curves. Gas sampling was carried out at constant flow-rates and samples were analysed by gas chromatography[19]. An HP Model 5840 A gas chromatograph (Hewlett-Packard) equipped with a thermal conductivity detector was used. Porapak-Q, Spherocarb and molecular sieve columns were examined for the analysis of the different components involved such as krypton, xenon, hydrogen, nitrogen, oxygen, methane, carbon dioxide, nitrogen dioxide and dinitrogen oxide. The rare gas concentration at the outlet was compared with that at the inlet.

For the flushing step, a flow of helium or nitrogen was passed through the

charcoal bed and the procedure followed was the same as for adsorption. For the desorption step, the charcoal bed was flushed with heated helium or nitrogen under atmospheric pressure and the desorbed gas was sampled in order to measure the xenon concentrations with the gas chromatograph. The chromatographically purified xenon was recovered by using the same charcoal trap as for rare gas collection.

RESULTS AND DISCUSSION

Information on the penetration of rare gases through the charcoal bed is needed in order to specify appropriate desorption conditions for the separation and recovery of the krypton and xenon fractions. In a series of experiments, the effects of flow-rate, carrier gas, temperature, length of charcoal bed, particle size of adsorbent and concentration on rare gas penetration were examined by measuring the shapes and positions of the krypton and xenon breakthrough curves.

Adsorption of krypton and xenon

The effect of nitrogen carrier gas at flow-rates in the range 250–750 ml/min on the breakthrough of krypton and xenon was studied, as shown in Table I. The results indicate that krypton and xenon are separated under the experimental conditions. Decreasing the flow-rate increases the separation efficiency, but consequently also lengthens the separation time. When helium was used as the carrier gas, the same krypton breakthrough curve was observed, but the residence time of xenon was 5.3 min longer. It was also found that krypton and xenon did not affect each other's separation behaviour in the studied concentration range. This is consistent with the results reported by Eshaya and Kalinowski[20].

The effect of temperature on the breakthrough of krypton and xenon was studied at 17 and 28°C with a helium flow-rate of 250 ml/min. The results (Table II) indicate that an increase in temperature reduces the residence time by 32 min for xenon. The Antoine equation[21] for gas adsorption is

$$K_d = \exp[A + B/(C + T)] \quad (1)$$

TABLE I

EFFECT OF CARRIER GAS FLOW-RATE ON THE BREAKTHROUGH OF KRYPTON AND XENON

Charcoal bed, 100 cm × 2 cm I.D.; activated charcoal, 8–14 mesh, 125 g; temperature, 16 ± 1°C; krypton flow-rate, 5 ml/min; xenon flow-rate, 5 ml/min.

Carrier gas	*Flow-rate (ml/min)*	*Column head pressure (kg)*	*Breakthrough time at C/C_F = 0.5 (min)**	
			Krypton	*Xenon*
Nitrogen	750	0.7 ± 0.03	6.8	85.8
Nitrogen	500	0.32 ± 0.02	9.1	92.9
Nitrogen	250	0.13 ± 0.01	15.3	133.8
Helium	250	0.05 ± 0.01	15.3	139.1

* C = concentration; C_F = inlet concentration.

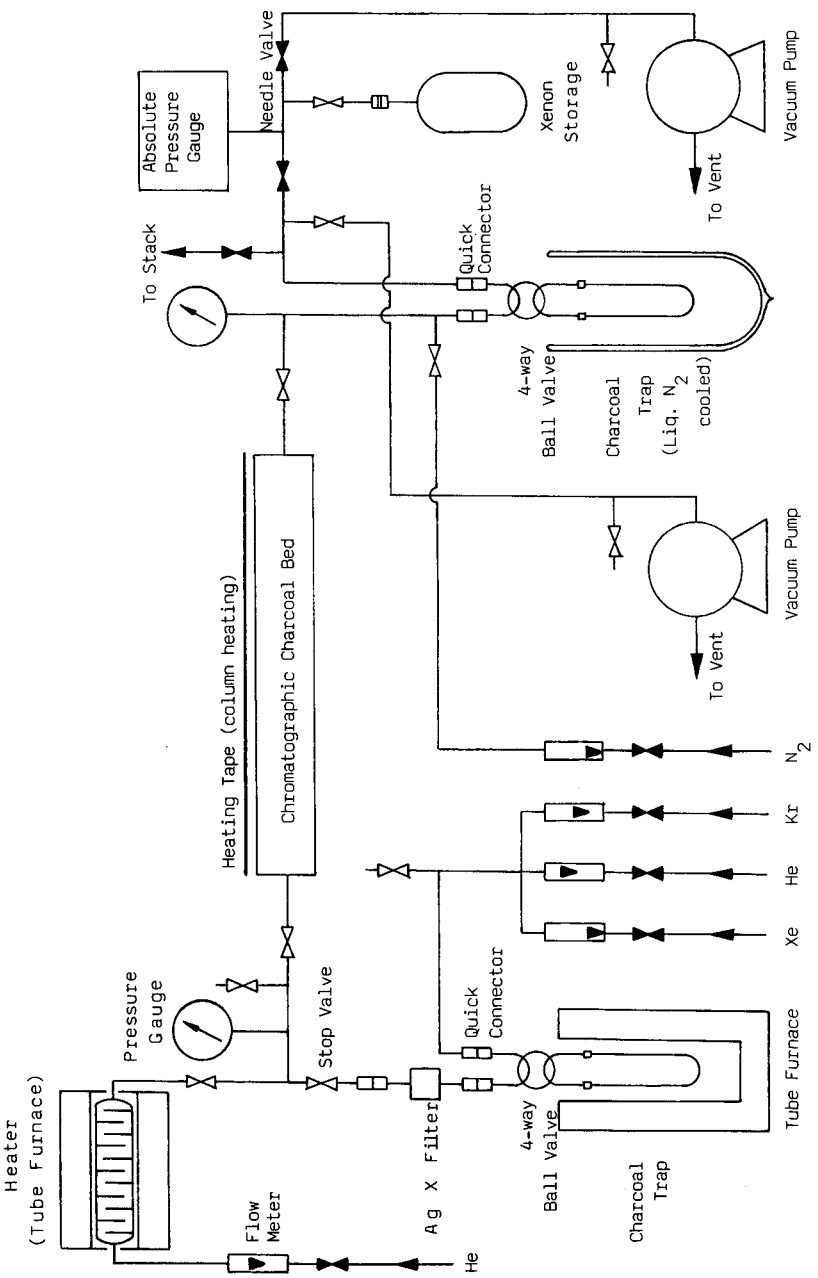

Fig. 3. Experimental equipment for the study of the chromatographic separation of krypton and xenon.

where K_d is the dynamic adsorption coefficient (cm^3/g), A, B and C are constants and T is temperature (°C). The adsorption behaviour of rare gases on activated charcoal can be described in terms of the number of theoretical plates[22], which leads to the conclusion that the predicted breakthrough curves converge to an integral Gaussian distribution equation. The theoretical results show that the mean residence time of the adsorbate gas in an adsorbent bed is given by

$$t_m = \left(\frac{N-1}{N}\right) \cdot \frac{K_d M}{F} \tag{2}$$

where t_m is the mean residence time (min), N the number of theoretical plates, M the mass of the adsorbent (g) and F the flow-rate of the gas containing the adsorbate (cm^3/min). When the number of theoretical plates is large, eqn. 2 reduces to

$$t_m = \frac{K_d M}{F} \tag{3}$$

Substituting eqn. 1 into eqn. 3, we obtain

$$\frac{t_m}{t'_m} = \frac{\exp[A + B/(C+T)]}{\exp[A + B/(C+T')]} \tag{4}$$

which is the working equation used for calculating the breakthrough times for rare gases on activated charcoal. Using eqn. 4, the calculated breakthrough times (at $C/C_F = 0.5$) for krypton and xenon are as shown in Table II. The deviations of the calculated data from the experimental results are possibly due to the different charcoal adsorbents and experimental equipment used[21].

The effect of the bed length on the adsorption of krypton and xenon was investigated. The results show that a 50% reduction in the bed length causes a 50% decrease in the residence times of krypton and xenon. Activated charcoal was used as the adsorbent in this study because it has substantially better adsorption properties than molecular sieves and silica gel. The ratio of the bed diameter to mean particle

TABLE II

EFFECT OF TEMPERATURE ON THE BREAKTHROUGH OF KRYPTON AND XENON

Charcoal bed, 100 cm × 2 cm I.D.; activated charcoal, 8–14 mesh, 125 g; helium flow-rate, 250 ml/min; krypton flow-rate, 5 ml/min; xenon flow-rate, 5 ml/min; column head pressure, 0.05 ± 0.01 kg.

Parameter	*Breakthrough time at $C/C_F = 0.5$**			
	Krypton		*Xenon*	
Ambient temperature (°C)	17	28	17	28
Experimental result (min)	15	12	139	107
Calculated result (min)	16	11	160	93

* C = concentration; C_F = inlet concentration.

diameter, 20/1.5 = 13, was sufficient to reduce wall effects to a negligible level. Wall effects might become important if larger charcoal granules were used in the bed. The effect of the particle size of the charcoal on the breakthrough curves was examined at room temperature (*ca.* 29°C) with 8–14, 14–18, 18–25 and 25–50 mesh charcoal. No significant effect was observed in the four experimental runs. The xenon breakthrough time at $C/C_F = 0.5$ was nearly constant. Nevertheless, it was found that the use of higher than 50 mesh charcoal granules would increase the column head pressure.

As the adsorption capacity of a rare gas is reduced in the presence of water vapour on the charcoal bed[2], the use of untreated activated charcoal containing about 10% (w/w) of adsorbed water led to a decrease in the residence time from 59 to 35 min for xenon. Therefore, it is necessary to remove moisture, carbon dioxide and other condensable materials from the activated charcoal before it is used as an adsorbent. The charcoal bed was heated at 60°C and swept with nitrogen gas at 1 l/min under a negative pressure of 100 Torr to remove the undesirable materials.

Fig. 4 shows the effect of the inlet xenon concentration on the breakthrough curves of xenon. Increasing the xenon concentration from 0.64 to 4.00 vol.% causes a decrease in the residence time from 90 to 50 min. Fig. 4 also indicates that the higher the xenon concentration, the sharper is the breakthrough curve. Broadening effects might be expected to dominate the adsorption at very low concentrations of xenon. Certain concentrations of krypton and xenon were used in these experiments to eliminate the possibility of distortion of the breakthrough curves by a non-linear isotherm.

Removal of krypton by flushing

After the adsorption step, the charcoal bed was flushed with carrier gas at the same flow-rate of 250 ml/min until the krypton concentration in the effluent was reduced to less than 0.1 vol.-% of the initial concentration. Fig. 5 indicates that complete removal of krypton is achieved in 40 min with either nitrogen or helium flushing, while xenon at this point is still maintained in the charcoal bed.

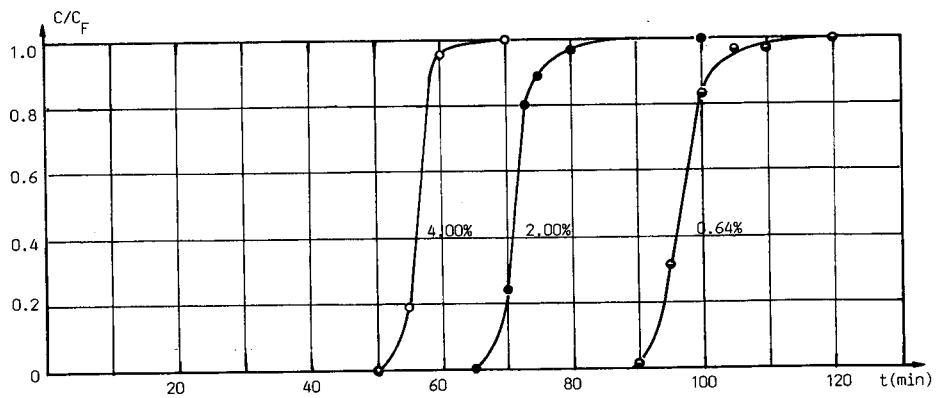

Fig. 4. Effect of xenon concentration on the breakthrough curve at 19 ± 1°C, a helium flow-rate of 250 ml/min and a column bead pressure of 0.05 ± 0.01 kg. C = concentration; C_F = inlet concentration. Charcoal bed, 50 cm × 2 cm I.D.; activated charcoal, 8–14 mesh, 62 g. Xenon flow-rate, ○, 10; ●, 5; and ◒, 1.6 ml/min.

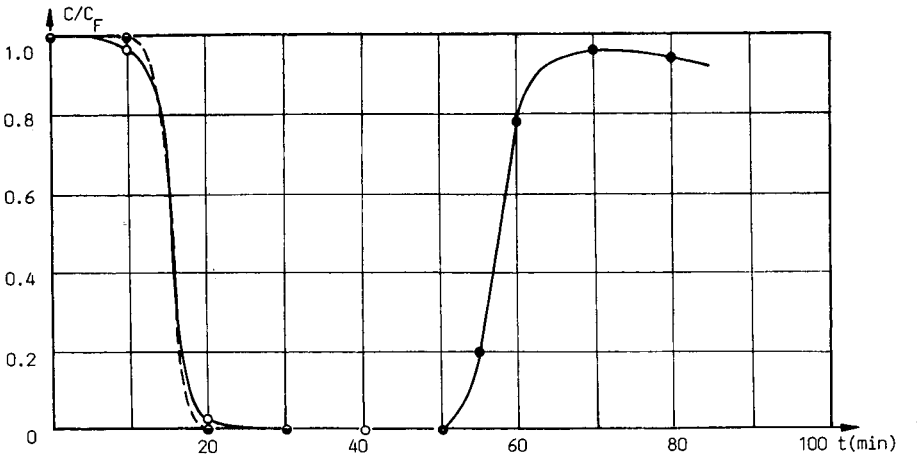

Fig. 5. Variation of krypton and xenon concentrations with time during the flushing step. C = concentration; C_F = inlet concentration. Charcoal bed, 100 cm × 2 cm I.D.; activated charcoal, 8–14 mesh, 125 g; feed gas, helium (250 ml/min) + 2.00% (v/v) krypton + 2.00% (v/v) xenon; adsorption time, 80 min. Temperature, 17°C; helium (nitrogen) flow-rate, 250 ml/min; column head pressure, 0.05 kg (helium) or 0.13 kg (nitrogen). ○, Krypton in helium; ◒, krypton in nitrogen; ●, xenon in helium.

In order to verify the feasibility of the chromatographic separation process, the efficiency of removal of rare gas by flushing in a 50 cm × 2 cm I.D. charcoal bed was examined. Aliquots of xenon and krypton were injected into the liquid nitrogen-cooled charcoal trap, which was then heated at 220°C for 30 min. The released rare gases were then removed with helium carrier gas and fed into the charcoal bed, and the krypton and xenon breakthrough curves were measured. The results in Fig. 6 indicate that a successful separation of krypton and xenon was achieved.

Desorption of xenon

For the study of xenon desorption, a 100 cm × 2 cm I.D. charcoal bed was previously fed with nitrogen (250 ml/min) + xenon (5 ml/min) for 80 min and flushed with nitrogen (250 ml/min) for 40 min at room temperature. The effect of temperature on xenon desorption was examined at a nitrogen flow-rate of 500 ml/min. The results show that the desorption rate increases with the increasing carrier gas temperature. However, desorption at temperatures higher than 250°C is unsafe owing to the fire hazard with activated charcoal beds[23].

The effect of carrier gas flow-rate on desorption at constant temperature (60°C) is shown in Fig. 7. Increasing the nitrogen flow-rate can cause the rapid desorption of xenon and a considerable increase in the column head pressure. With helium flushing for desorption, complete desorption of xenon from the charcoal bed is achieved in 40 min with heated helium at 60°C at a flow-rate of 1000 ml/min. Desorption experiments were also made at various sub-atmospheric pressures with prior evacuation of the adsorber. The experiments showed that xenon was desorbed completely within a relatively short time of 1 h at pressures down to about 100 Torr with nitrogen or helium flushing at 60°C at a flow-rate of 1000 ml/min. However, quantitative collection of the desorbed xenon with a liquid nitrogen-cooled charcoal trap was difficult at this low pressure.

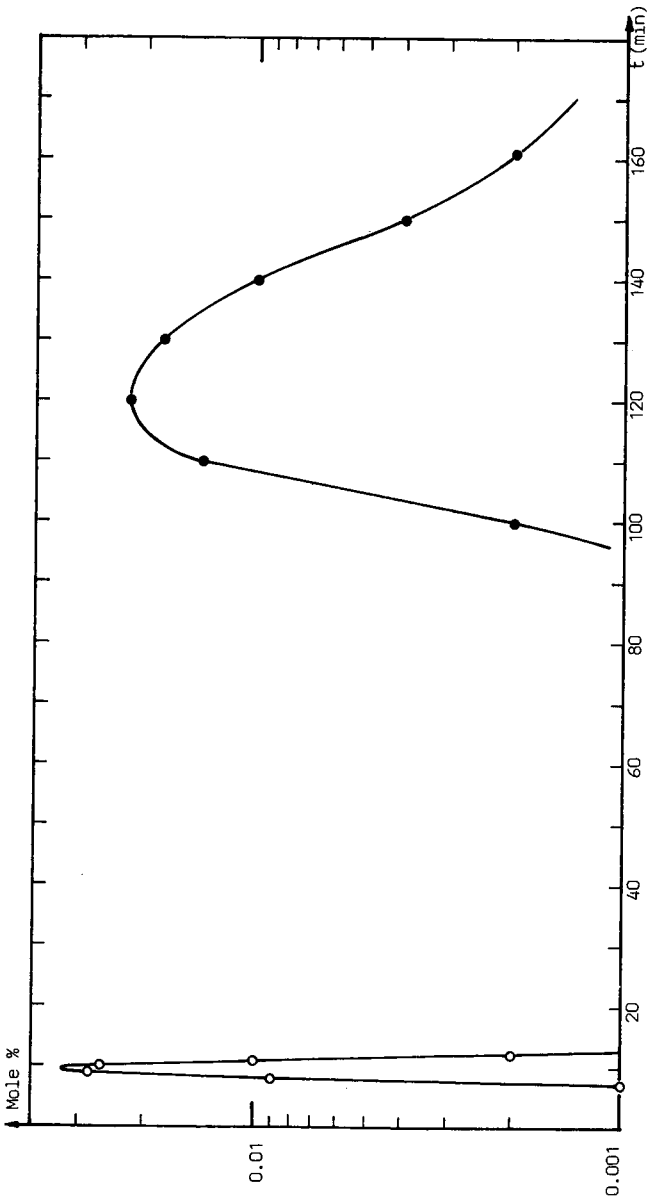

Fig. 6. Variation of krypton and xenon concentrations with flushing time. Feed gas, krypton–xenon–helium mixture from heated charcoal trap. Temperature, 20°C; helium flow-rate, 250 ml/min; column, 50 cm × 2 cm I.D. activated charcoal, 8–14 mesh, 62 g; column head pressure, 0.05 kg. ○, Krypton, 1.2 mg; ●, xenon, 14 mg.

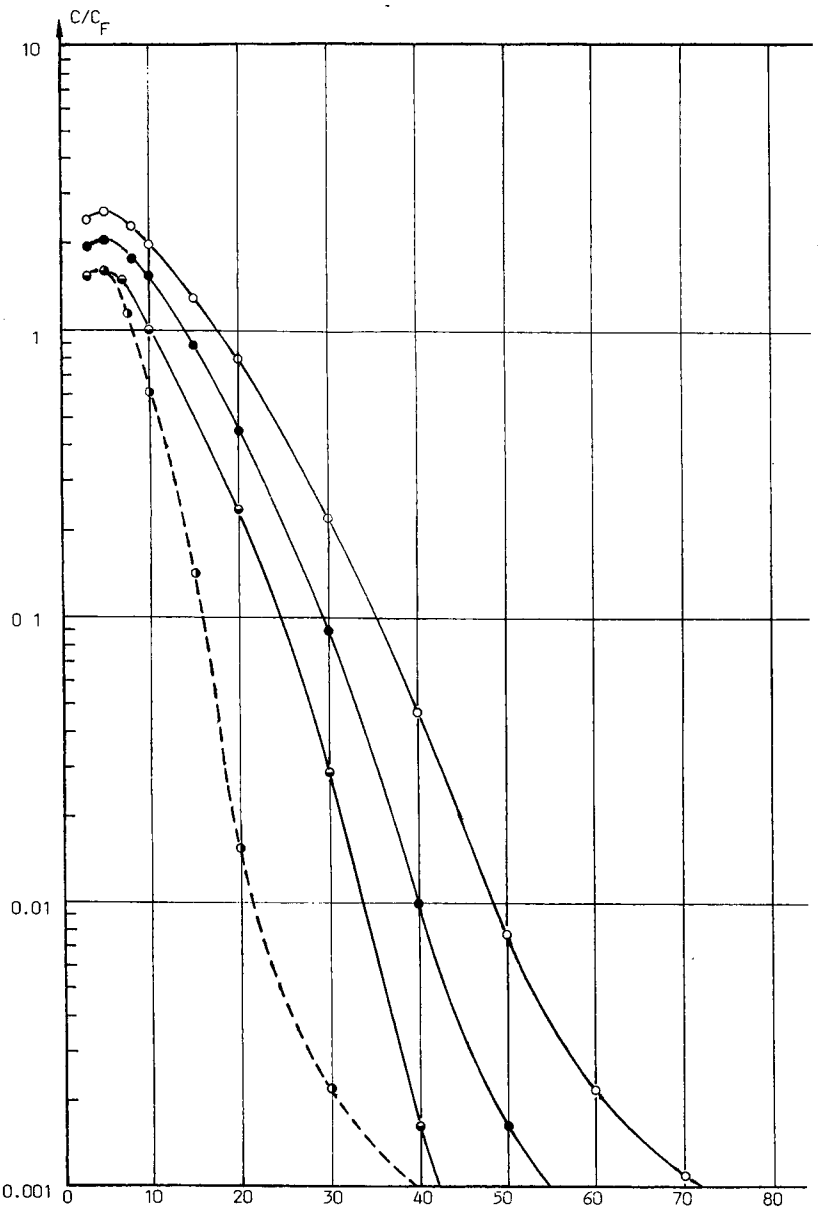

Fig. 7. Xenon concentration *versus* desorption time at different flow-rates. Charcoal bed, 100 cm × 2 cm I.D., activated charcoal, 8–14 mesh, 125 g; adsorption, nitrogen (250 ml/min) + xenon (5 ml/min) for 80 min at room temperature; flushing, nitrogen (250 ml/min) for 40 min at room temperature. Desorption conditions: nitrogen (helium) temperature, 60 ± 1°C; flow-rate and column head pressure, ○, 500 ml/min (nitrogen) and 0.34 ± 0.02 kg; ●, 750 ml/min (nitrogen) and 0.75 ± 0.03 kg; ◒, 940 ml/min (nitrogen) and 1.5 ± 0.05 kg; ◑, 1000 ml/min (helium) and 0.5 ± 0.02 kg.

The results of the above laboratory studies make it possible to suggest a process for the separation of krypton and xenon from fission product gases with activated charcoal. Fig. 8 summarizes the overall procedure for the separation and purification of ^{133}Xe from fission product gas mixtures by charcoal adsorption–desorption.

Dispensation of xenon-133 product

Xenon-133 is administered by either inhalation or injection in saline for medical diagnostic applications. In both instances the activity must be apportioned into unit doses (20–30 mCi) which are suitable for patient use[5]. The most practical method of dispensation of ^{133}Xe is to inject it as a gas in sealed glass ampoules. The dispensing system used is shown in Fig. 9. Basically, it consists of storage facilities of known volume (1000 ml, 100 ml), an absolute pressure gauge, a dispenser and a vacuum

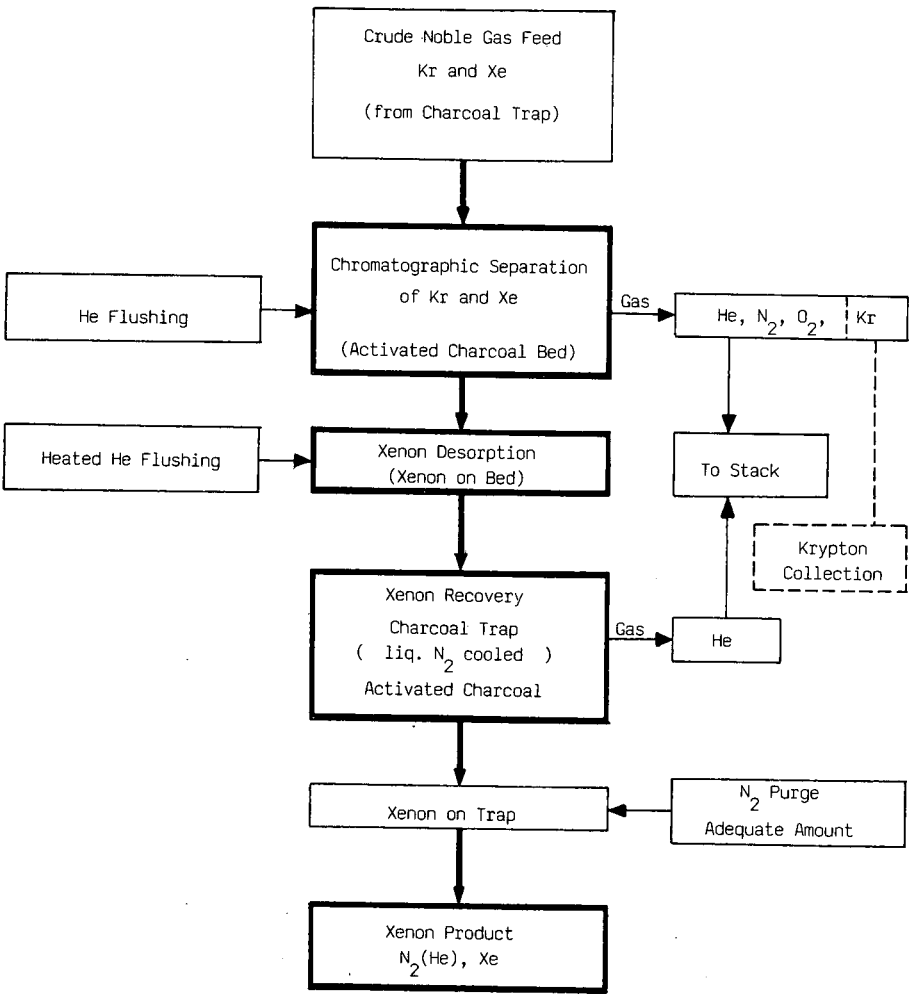

Fig. 8. Chromatographic separation process for recovery of xenon-133 from trapped rare gases.

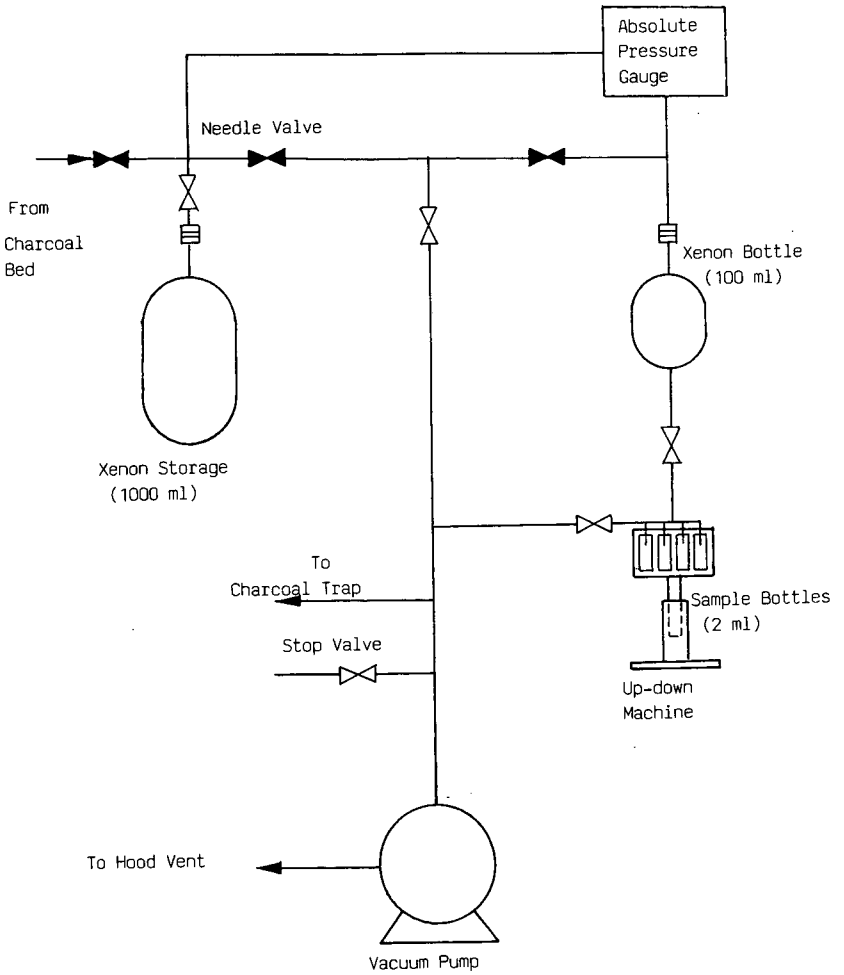

Fig. 9. Xenon-133 dispensing system.

pump. The volume of the sections of the system line is determined from the gas equation $P_1V_1 = P_2V_2$. Dispensation of the ^{133}Xe product is carried out simply by transferring ^{133}Xe quantitatively from the storage bottle to the vacuum bottle upstream to the dispenser. Losses of ^{133}Xe from the dispensing system are inevitable, hence the system should be stored in a well ventilated hood.

CONCLUSION

The charcoal trap of a U-shaped copper tube, filled with activated carbon and cooled in liquid nitrogen, proved very effective for the collection of rare gases. The efficiency of the collection of krypton and xenon is essentially 100% at a flow-rate of helium carrier gas of 3 l/min.

The breakthrough curves (C/C_F *vs.* t) indicate that the adsorption behaviour of

krypton–xenon–helium mixtures is the same as that of xenon–helium and krypton–helium mixtures in the gas concentration range investigated. From the previous investigation, it is concluded that a 50-cm activated charcoal adsorption column is sufficient for the separation and purification of ^{133}Xe from fission product gases at temperatures below 35°C. This established chromatographic separation process is suitable for the production of ^{133}Xe for medical diagnostic applications in local hospitals.

The advantages of the developed chromatographic separation process are (1) operation at ambient temperature and pressure, (2) cost effective in operation and (3) separation of small amounts of ^{85}Kr and ^{133}Xe to provide a high-purity ^{133}Xe product.

REFERENCES

1 H. Schnez, *United States–German High Temperature Reactor Research Exchange Program*, ERDA Technical Information Center, GERHTR-158, Oak Ridge, TN, 1975, p. 35.
2 C. M. Slansky, *At. Energy Rev.*, 9 (1971) 423.
3 Y. Jao, W. L. Cheng and G. Ting, *Separation and Treatment of Radioactive Noble Gases Krypton and Xenon*, CAEC Rep. INER-T0975, Taiwan, 1984.
4 M. E. Meek and B. F. Rider, *Compilation of Fission Product Yields*, Vallecitos Nuclear Center, Report NEDO-12154, Pleasanton, CA, 1972.
5 M. R. Zalutsky, *Radiotracers for Medical Applications*, Vol. II, CRC Press, Boca Raton, FL, 1983, p. 95.
6 M. J. Martin, *Nuclear Decay Data for Selected Radionuclides*, USAEC Rep. ORNL-5114, Oak Ridge, TN, 1976.
7 J. Milic-Emili, *Semin. Nucl. Med.*, 1 (1971) 246.
8 R. A. Schot, D. M. Shames, P. M. Weber and L. V. Dos Remedios, *J. Nucl. Med.*, 19 (1978) 348.
9 C. Fallais, F. Smal and M. Guillaume, *Rev. IRE*, 8 (1984) 44.
10 W. D. Heiss, *Radionuclide Imaging*, Pergamon Press, Oxford, 1982, p. 131.
11 N. A. Lassen, *J. Nucl. Med.*, 24 (1983) 17.
12 L. E. Preuss, F. P. Bolin, D. G. Piper and C. K. Bugenis, *Int. J. Appl. Radiat. Isot.*, 26 (1976) 329.
13 J. C. Harbert and H. J. Dipiazza, *J. Nucl. Med.*, 25 (1984) 1051.
14 R. Aubeau, L. Champeix and J. Reiss, *J. Chromatogr.*, 6 (1961) 209.
15 H. Jüntgen, H. J. Schröter, R. V. Ammon and C. H. Leichsenring, *Kerntechnik*, 20 (1978) 450.
16 E. J. Wilson and K. J. Taylor, *The Separation and Purification of Krypton-85 at the Multicurie Level*, UKAEA Rep. AERE I/R-2693, Windscale, 1958.
17 C. B. Amphlett, *Treatment and Disposal of Radioactive Wastes*, Pergamon Press, New York, 1961, p. 246.
18 Y. Jao, W. L. Cheng and G. Ting, *The Process for Separation of Xenon-133 from Dissolver Off Gas of Irradiated Natural UO_2*, Chinese Patent, No. 28281, 1987.
19 Y. Jao, W. L. Cheng and C. Ting, *Nucl. Sci.*, 21 (1984) 5.
20 A. M. Eshaya and W. L. Kalinowski, *Adsorption of Krypton and of Mixed Xenon and Krypton on Activated Charcoal*, USAEC Rep. BNL-724 (T-258), Upton, NY, 1961.
21 D. W. Underhill and D. W. Moeller, in *Proceedings of the 16th DOE Nucl. Air Clean. Conf.*, CONF-801038, 1980, p. 141.
22 D. P. Siegwarth, C. K. Neulander, R. T. Pao and M. Siegler, in *Proceedings of the 12th AEC Air Clean. Conf.*, CONF-720823, 1972, p. 28.
23 J. L. Kovack and J. E. Green, *Nucl. Saf.*, 8 (1966) 41.

Journal of Chromatography, 462 (1989) 205–217
Elsevier Science Publishers B.V., Amsterdam — Printed in The Netherlands

CHROM. 20 972

COMPARISON OF REVERSED-PHASE THIN-LAYER AND HIGH-PERFORMANCE LIQUID CHROMATOGRAPHY OF FLAVONOID COMPOUNDS

F. DONDI*
Analytical Chemistry Laboratory, Department of Chemistry, Via L. Borsari 46, I-44100 Ferrara (Italy)
G. GRASSINI-STRAZZA
Institute of Chromatography, Monterotondo Stazione, I-00016 Rome (Italy)
Y.D. KAHIE
Analytical Chemistry, Somali National University, P.O. Box 1081, Mogadishu (Somalia)
and
G. LODI, C. PIETROGRANDE, P. RESCHIGLIAN and C. BIGHI
Analytical Chemistry Laboratory, Department of Chemistry, Via L. Borsari 46, I-44100 Ferrara (Italy)
(Received September 5th, 1988)

SUMMARY

The reversed-phase high-performance liquid (HPLC) and thin-layer chromatographic (TLC) behaviour of flavonoids with methanol, tetrahydrofuran and acetonitrile as organic modifiers was compared. Twenty-six different correlation cases, together with their statistical parameters, are presented and discussed. Both TLC and HPTLC plates were considered. The dependence of TLC incremental R_m values from different group substitutions on solvent type, solvent composition and type of plate is considered. A method for establishing HPLC gradient elution conditions by using TLC data is discussed.

INTRODUCTION

Reversed-phase high-performance liquid (HPLC) and thin-layer chromatography (TLC) are well established separation methods in flavonoid analysis[1–12]. In previous papers the behaviour of flavonoid compounds in several reversed-phase HPLC partition systems differing in (1) column type, (2) acid modifier, (3) organic modifier [methanol, tetrahydrofuran (THF) and acetonitrile] was considered and the selectivity properties with reference to isocratic and gradient elution separations were discussed[13–16].

Despite the many publications on TLC flavonoid analysis[6–12], no general and systematic study of the influence of experimental variables such as the solvent, composition and type of plate could be found. In this work these aspects were examined with reference to reversed-phase systems and the relationship between HPLC and TLC was studied. The last approach, because of its many useful practical implica-

0021-9673/89/$03.50

tions[17–23], appears to be promising for solving many complex problems of flavonoid analysis.

EXPERIMENTAL

The TLC measurements were carried out on three different reversed-phase C_{18} pre-coated layers: (a) TLC KC18F (Cat. No. 4803-800) (Whatman, Clifton, NJ, U.S.A.), (b) TLC pre-coated plate RP-18F_{254}S (Cat. No. 15423) (Merck, Darmstadt, F.R.G.) and (c) HPTLC pre-coated plate RP-18WF_{254}S (Cat. No. 13124) (Merck); these are referred to as TLC (W), TLC (M) and HPTLC (M), respectively.

The following parameters were kept constant: size of the plates (10 cm × 10 cm), solvent volume (20 ml) in the developing tank (10 cm high × 20 cm × 5 cm), distance of the starting line from the bottom (1 cm) and distance of development (5 cm). After the application of the spots (0.1–0.2 μl) of standard solutions, ascending development was carried out at room temperature. The spots were located under UV light by quenching of the fluorescence at 254 nm. R_F measurements were repeated four times on the same plate washed with methanol after each development. No drift in the retention data was observed and the standard error over the mean R_m value was always between 0.07 and 0.03.

The solvents were of HPLC grade from Rudi-Pont (Parsippany, NJ, U.S.A.). Methanol, acetonitrile and THF were utilized as organic modifiers in binary mixtures with water. The aqueous phase was buffered at pH 2–3 in 80 m*M* citric or acetic acid – 8 m*M* disodium hydrogenphosphate (Carlo Erba, Milan, Italy). The selected flavonoid standards were Extrasyntese (Genay, France), used as received and dissolved in ethanol (HPLC grade) to give 1000 ppm solutions. The selected standards represent flavones, flavonols, flavanones and glycosides and are listed in Table I.

TABLE I

LIST OF FLAVONOID COMPOUNDS STUDIED

No.	*Compound*	*No.*	*Compound*
1	Acacetin	10	Luteolin 7-O-glucoside
2	Apigenin	11	Morin
3	Apigenin 7-O-glucoside	12	Naringenin
4	Apiin	13	Quercetagetin
5	Chrysin	14	Quercetin
6	Chrysoeriol	15	Quercitrin
7	Eriodictyol	16	Rutin
8	Galangin	17	Myricetin
9	Luteolin	18	Vitexin

All the HPLC data were obtained on a μBondapak C_{18} column (Waters, Milford, MA, U.S.A.) (W1 and W3 data from refs. 15 and 16). Retention data with a given organic modifier were obtained on the same column. HPLC data for vitexin and myricetin were obtained on column W3 by following the experimental procedure in refs. 15 and 16.

THEORETICAL

The comparison between TLC and HPLC is based on the study of the relationship

$$\log k' = f(R_M) \tag{1}$$

where k' is the capacity factor and R_M is defined as

$$R_M = \log(1/R_F - 1) \tag{2}$$

The most commonly used form of eqn. 1 is the linear relationship

$$\log k' = A + BR_M \tag{3}$$

and using different test compounds it has proved to be followed by different HPLC and TLC systems[22]. When $A=0$ and $B=1$ both the partition processes are the same and

$$\log k' = R_M \tag{4}$$

Any departure from this ideal behaviour may have a simple thermodynamic explanation. In fact, remembering that

$$k' = KV_s/V_m \tag{5}$$

where V_s and V_m are the stationary phase and mobile phase volumes, respectively, and K is the distribution constant, an A value other than zero can mean either a different phase ratio value or a multiplying factor acting on K. As

$$\Delta\mu^0 = -RT \ln K \tag{6}$$

where $\Delta\mu^0$ is the standard Gibbs free energy change for a solute in the mobile phase passing into the stationary phase, a multiplying factor on K means a constant shift $\Delta(\Delta\mu^0)$ for all the solute samples. A non-unit value of B in eqn. 3 appears as a constant multiplying factor over the whole scale of the free energy of transfer, implying more complex differences in the thermodynamic partition properties of the two systems being compared. In order to understand better the underlying changes in solute–stationary phase interactions, the comparison of TLC and HPLC can be further analysed by studying the following relationship:

$$\Delta \log k' = f(\Delta R_M) \tag{7}$$

where $\Delta \log k'$ and ΔR_M are calculated over solute pairs differing in some characteristic substituent groups. Such a study can highlight specific polarity, lipophilicity, hydrogen bonding and dipolar interaction changes of the two chromatographic systems being compared.

In addition to these purely thermodynamic effects, other phenomena pertaining to the chromatographic process itself may be responsible for the departure from the theoretical relationship with unit slope and zero intercept, which is observed even when the same material is used for the HPLC column packing and the TLC layer. In fact, it is well known that there is no perfect equivalence between TLC development and HPLC elution and many physical peculiarities have been described and discussed, *e.g.*, the roles of the interphases, capillary forces and demixing processes[24,25]. As these effects are dependent on the mobile phase volume composition (Φ), some insight into them can be attained by studying the log k'–R_M and $\Delta\log k'$–ΔR_M relationships with changing Φ. For example, if $\Delta\log k'$ group contributions in an HPLC system are independent of Φ and the TLC and HPLC systems are identical, the ΔR_M values will be not affected by effects due to changes in the mobile phase composition and their values will be equal to $\Delta\log k'$. Obviously many other cases could be described implying a complex integral effect of R_M with changing Φ. For the above arguments, an exhaustive description of the TLC *vs.* HPLC relationship must take into account a broad range of different independent variables if the aim is to achieve precision and accuracy and also to check different theoretical hypotheses.

RESULTS AND DISCUSSION

All the HPLC reference data taken into consideration in this work were obtained on a μBondapak C_{18} column. In a previous study[15] it was shown that no substantial difference in the relative retentions of flavonoid compounds is observed when using C_8 or C_{18} bonded phases from different manufacturers, so the results of this study can be easily extended to these different systems. The only parameter affected will be A in eqn. 3, which reflects the phase volume ratio.

In Table II the results of 26 linear HPLC–TLC correlations are reported. In this study six different factors were considered: (a) different TLC layers (TLC, HPTLC); (b) different manufacturers (W,M); (c) different solvent volume fraction (Φ); (d) different solvents (methanol, acetonitrile, THF); (e) different acid modifier with the same solvent (citric and acetic acid in methanol); and (f) repeatibility (systems 16, 17 and 18, 19 in Table II).

A number of compounds generally between ten and twenty were employed in establishing HPLC–TLC correlations. R_M values in the range -0.2 to 1.2 were considered. This range is different from that recommended for physico-chemical studies (-0.6 to 0.6), but it is commonly accepted for correlation studies[26]. In addition, both the log k' and R_M ranges were homogeneously covered. As a general remark, it was observed that M layers exhibit lower retentions than W layers. Good correlation coefficients (greater than 0.95) were observed. Minor exceptions were observed at water concentrations higher than 50% in the eluent phase and with methanol as organic modifier both on TLC and HPTLC plates (systems 1,2 and 15 in Table II). These last cases are probably due to demixing phenomena in the mobile phase, which was indeed observed experimentally.

Disregarding the above-mentioned demixing effects, systematic differences are observed between TLC and HPTLC plates in methanol. For the first system a unit slope with a low and nearly constant intercept (-0.20) is observed in most instances whether on plates from different manufacturers or with different acid modifiers in the

TABLE II

HPLC–TLC CORRELATION RESULTS ACCORDING TO EQUATION LOG $k' = A + BR_M$
Acid modifier: acetic acid except where specified otherwise.

System No.	*Plate*	*Source*	*Solvent*	*Φ (%)*	*A*	*B*	*R**	$\sigma_{y.x}$**
1	TLC	W	Methanol	40	−0.20±0.21	1.03±0.24	0.89	0.12
2	TLC	W	Methanol	45	−0.16±0.22	0.80±0.28	0.76	0.14
3	TLC	W	Methanol	50	−0.19±0.04	0.97±0.06	0.98	0.06
4	TLC	W	Methanol***	50	−0.43±0.05	1.00±0.08	0.97	0.09
5	TLC	W	Methanol	55	−0.19±0.03	0.99±0.06	0.99	0.05
6	TLC	W	Methanol	60	−0.13±0.02	0.92±0.05	0.99	0.07
7	TLC	W	Methanol***	60	−0.23±0.02	0.96±0.05	0.99	0.05
8	TLC	M	Methanol	50	−0.22±0.02	1.03±0.03	0.99	0.02
9	TLC	M	Methanol	55	−0.24±0.03	1.02±0.07	0.98	0.05
10	TLC	M	Methanol	60	−0.42±0.02	1.16±0.05	0.99	0.06
11	TLC	W	THF	45	−0.36±0.03	1.56±0.07	0.99	0.07
12	TLC	W	Acetonitrile	40	−0.04±0.02	1.06±0.04	0.99	0.06
13	TLC	M	THF	45	−0.41±0.01	1.55±0.02	0.99	0.02
14	TLC	M	Acetonitrile	40	−0.14±0.01	1.03±0.03	0.99	0.04
15	HPTLC	M	Methanol	45	−0.16±0.30	0.85±0.41	0.64	0.16
16	HPTLC	M	Methanol	50	−0.27±0.07	1.19±0.10	0.97	0.08
17	HPTLC	M	Methanol	50	−0.31±0.05	1.17±0.08	0.98	0.07
18	HPTLC	M	Methanol	55	−0.27±0.04	1.36±0.07	0.98	0.08
19	HPTLC	M	Methanol	55	−0.21±0.04	1.37±0.08	0.98	0.09
20	HPTLC	M	Methanol	60	−0.38±0.03	1.43±0.11	0.97	0.09
21	HPTLC	M	THF	40	−0.61±0.04	1.05±0.04	0.99	0.05
22	HPTLC	M	THF	45	−0.66±0.03	1.19±0.04	0.99	0.05
23	HPTLC	M	THF	50	−0.35±0.02	0.98±0.05	0.98	0.05
24	HPTLC	M	Acetonitrile	40	−0.39±0.03	1.49±0.05	0.99	0.03
25	HPTLC	M	Acetonitrile	45	−0.25±0.05	1.52±0.09	0.98	0.06
26	HPTLC	M	Acetonitrile	50	−0.14±0.02	1.46±0.98	0.99	0.05

* R = Correlation coefficient.
** $\sigma_{y.x}$ = Standard error of regression.
*** Citric acid as acid modifier.

mobile phase. The only exception is the lower intercept (−0.43) with citric acid modifier at 50% methanol (system 4 in Table II). This last finding, if related to the abrupt change in the HPLC solvent strength observed at this particular organic modifier composition[13,14], may not be particularly remarkable.

In the HPTLC system, slopes always greater than unity with a significantly lower intercept are observed (systems 16 and 17 in Table II). The former analysis suggests that in contrast to HPLC, TLC plates in methanol behave as a nearly ideal system, whereas departures from ideality are apparently exhibited by HPTLC plates. If, on the other hand, different organic modifiers are also considered, one can see that this sharp differentiation does not reappear. In fact, with 40% acetonitrile a unit slope is observed on TLC plates (systems 12 and 14) but with 45% THF (systems 11 and 13) on the same type of plates the slope is 1.6. The reverse is observed for HPTLC plates, but with the THF intercept being very negative (systems 24–26 for acetonitrile and 21–23 for THF). Hence one can conclude that the nearly ideal behaviour (unit slope and low intercept value) observed with TLC plates is the combined result of the use of

TABLE III

SUBSTITUENT GROUP CONTRIBUTIONS (ΔR_M OR Δ LOG k') TO RETENTION WITH DIFFERENT C_{18} REVERSED-PHASE CHROMATOGRAPHIC SYSTEMS

Methanol as organic modifier with different acid modifiers. Data reported as mean ΔR_M or $\Delta \log k'$ values with their standard errors. Three or four different mobile phase compositions in the reported composition range were considered.

Group contribution	*Compounds*	*TLC (W) (citric acid), 0.40–0.60**	*TLC (W) (acetic acid), 0.40–0.60**	*TLC (M) (acetic acid), 0.45–0.65**	*HPTLC (M) (acetic acid), 0.45–0.65**	*HPLC** (citric acid), 0.40–0.70**	*HPLC*** (acetic acid), 0.40–0.70**
3-OH	14–9	−0.18±0.07	−0.12±0.03	−0.14±0.04	−0.08±0.02	−0.15±0.05	−0.13±0.06
6-OH	13–14	−0.87±0.07	−0.75±0.13	–	–	−0.94±0.09	−0.80±0.11
3′-OH	9–2	−0.25±0.04	−0.29±0.03	−0.25±0.03	−0.19±0.06	−0.20±0.04	−0.22±0.04
3′-OH	10–3	−0.17±0.05	–	−0.13±0.03	−0.11±0.04	−0.21±0.14	−0.18±0.01
3′-OH	7–12	−0.26±0.02	−0.26±0.02	−0.25±0.04	−0.14±0.04	−0.24±0.02	−0.24±0.03
4′-OH	2–5	−0.40±0.09	−0.37±0.08	−0.31±0.03	−0.14±0.01	−0.30±0.08	−0.29±0.03
5′-OH	17–14	−0.30±0.04	−0.30±0.05	–	–	–	−0.27±0.01
3′-OCH_3(-HO)	6–2	0.06±0.02	0.03±0.03	0.03±0.02	0.04±0.02	0.06±0.01	0.06±0.01
4′-OCH_3	1–5	0.14±0.03	0.11±0.06	0.16±0.03	0.16±0.03	0.13±0.03	0.14±0.01
2,3-Unsaturation	12–2	−0.42±0.03	−0.43±0.05	−0.43±0.07	−0.34±0.06	−0.47±0.13	−0.39±0.02
2,3-Unsaturation	7–9	−0.48±0.06	−0.41±0.06	−0.45±0.09	−0.38±0.03	−0.51±0.12	−0.33±0.11
3-Glycoside (rhamnose)	15–14	−0.30±0.02	−0.33±0.03	−0.28±0.04	−0.18±0.02	−0.22±0.07	−0.35±0.07
3-Glycoside (rutinose)	16–14	−0.52±0.04	−0.52±0.04	−0.48±0.04	−0.31±0.04	−0.47±0.03	−0.42±0.04
7-Glycoside (glucose)	3–2	−0.73±0.01	−0.72±0.06	−0.69±0.07	−0.49±0.07	−0.77±0.18	−0.68±0.03
7-Glycoside (glucose)	10–9	−0.70±0.09	–	−0.60±0.10	−0.41±0.05	−0.71±0.04	−0.71±0.04
7-Glycoside (apiosylglucose)	4–2	−0.85±0.07	−0.77±0.04	−0.75±0.06	−0.53±0.06	−0.77±0.06	−0.77±0.03
8-C-Glycoside (glucose)	18–1	−1.14±0.06	−1.09±0.08	–	–	–	−1.06±0.04

* Mobile phase composition range.

** All the reported data except for 5′-OH and 8-C-glycoside are taken from ref. 15.

TLC plates and methanol as organic modifier in the Φ range 50–60%, as no other plate–solvent combination gives this effect. In Fig. 1a and b the above-described main types of behaviour are shown; Fig. 1a is an example of an "ideal' correlation with TLC–methanol systems and Fig. 1b is an example of the correlation on HPTLC plates with a slope significantly greater than unity.

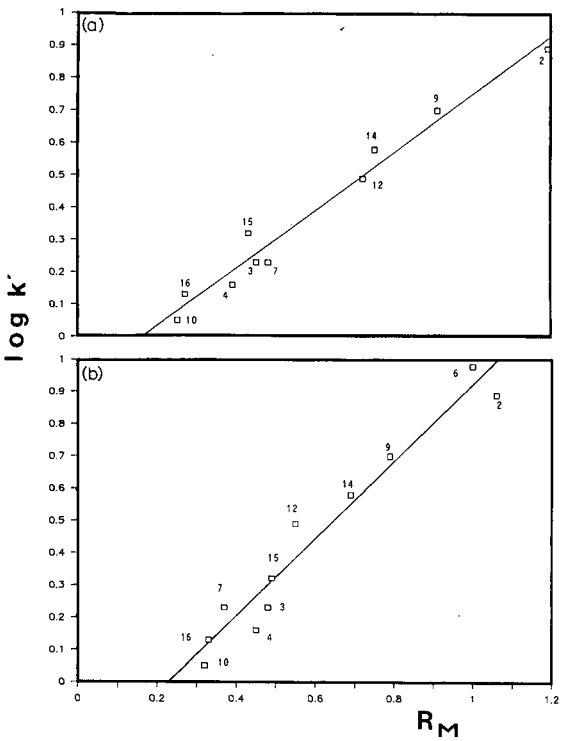

Fig. 1. HPLC–TLC correlation; 50% methanol as organic modifier and acetic acid as acid modifier. The numbers refer to the compounds listed in Table I. (a) TLC (W); (b) HPTLC (M). HPLC data from ref. 15.

The correlation between the $\Delta\log k'$ and ΔR_M values responsible for a particular substituent group within the molecule can help to explain the observed behaviour (see Table III). The group contributions in the methanol systems, in HPLC found to be independent of the volume fraction Φ, column type and acid modifier (citric or acetic)[15], are analysed first (Table III). One can see that the agreement between $\Delta\log k'$ and ΔR_M values is very satisfactory for TLC plates and only small systematic differences are observed with HPTLC. In addition, the insensitivity towards Φ is exhibited by all the TLC systems, as revealed by the low standard errors reported in Table III.

Fig. 2a shows the strict correlation between HPLC $\Delta\log k'$ and TLC ΔR_M data, with a slope equal to unity and an intercept nearly equal to zero. Fig. 2b shows the correlation with HPTLC data. In the latter instance the intercept is again nearly equal to zero but the slope is greater than unity. These last findings can give some insight

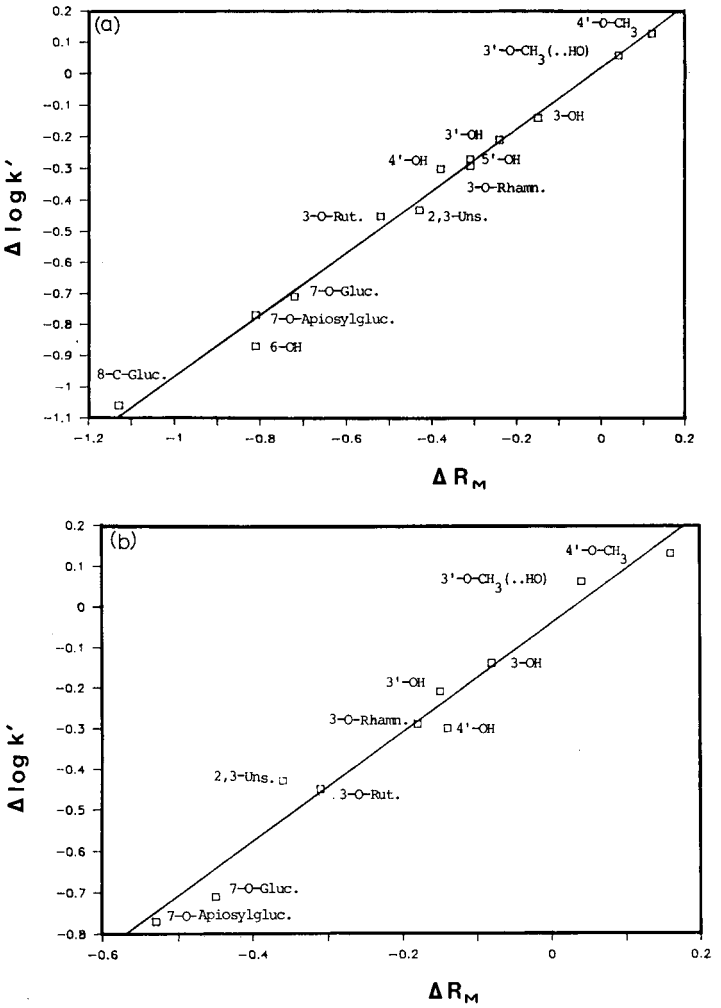

Fig. 2. ΔLog k' (HPLC) *vs.* ΔR_M (TLC) for (a) TLC (W) and (b) HPTLC (M). See Table III. Abbreviations: Gluc. = glucose; Rhamn. = rhamnose; Rut. = rutinose; Uns. = unsaturation.

into the different, previously mentioned behaviour of TLC and HPTLC plates. The constancy of the group retention contributions in the first instance means an equivalence of the partition properties of TLC and HPLC systems. The HPTLC plates appear instead to be about 1.5 times more polar than the two previous systems. At this point one might ask whether this polarity increase is a pure thermodynamic effect or rather an apparent effect due to the composition changes during the chromatographic development. As mentioned in the Theoretical section, we believe that methanol as organic modifier is probably unable to cause such an effect because in it the group contributions are largely insensitive towards composition with all the partition systems examined (HPLC, TLC, HPTLC). Hence it can be assumed that there is an effective polarity difference between TLC and HPTLC plates without ruling out

TABLE IV

SUBSTITUENT GROUP CONTRIBUTIONS [ΔR_M (TLC) OR ΔLOG k' (HPLC) WITH 45% TETRAHYDROFURAN IN THE MOBILE PHASE
Acetic acid as acid modifier. HPLC data taken from ref. 16.

Group contribution	*Compounds*	*TLC (W)*	*TLC (M)*	*HPTLC (M)*	*HPLC*
3-OH	8–5	0.15	0.12	0.13	0.20
3-OH	14–9	0.08	0.09	0.10	0.12
6-OH	13–14	−0.47	−0.48	–	−0.70
3′-OH	9–2	−0.05	−0.04	−0.12	−0.07
3′-OH	10–3	−0.04	−0.04	−0.06	−0.04
3′-OH	7–12	−0.06	−0.06	–	−0.11
4′-OH	2–5	−0.11	−0.14	−0.11	−0.20
3′-OCH_3(-HO)	6–2	−0.03	−0.04	−0.08	−0.05
4′-OCH_3	1–5	−0.01	−0.03	−0.06	−0.02
2,3-Unsaturation	12–2	0.07	0.05	–	0.13
2,3-Unsaturation	7–9	0.06	0.03	0.04	0.09
3-Glycoside (rhamnose)	15–14	−0.28	−0.37	−0.43	−0.55
3-Glycoside (rutinose)	16–14	−0.54	−0.57	−0.70	−0.72
7-Glycoside (glucose)	3–2	−0.35	−0.38	−0.54	−0.62
7-Glycoside (glucose)	10–9	−0.34	−0.38	−0.48	−0.59
7-Glycoside (apiosylglucose)	4–2	−0.40	−0.45	−0.64	−0.72

gradient composition effects during development. A full explanation of such a hypothesis would require a systematic investigation by means of an extended polarity scale of both the eluent and test sample compounds. This aspect is outside the scope of this paper.

In Tables IV and V the dependence of the group contributions on the partition

TABLE V

SUBSTITUENT GROUP CONTRIBUTIONS [ΔR_M (TLC) OR ΔLOG k' (HPLC) WITH 40% ACETONITRILE IN THE MOBILE PHASE
Acetic acid as acid modifier. HPLC data taken from ref. 16.

Group contribution	*Compounds*	*TLC (W)*	*TLC (M)*	*HPTLC (M)*	*HPLC*
3-OH	8–5	0.00	0.11	0.05	0.08
3-OH	14–9	0.02	0.04	0.13	0.03
6-OH	13–14	−0.37	−0.38	–	−0.37
3′-OH	9–2	−0.20	−0.21	−0.15	−0.22
3′-OH	10–3	−0.04	−0.04	−0.05	−0.01
3′-OH	7–12	−0.16	−0.19	–	−0.22
4′-OH	2–5	−0.42	−0.43	−0.29	−0.45
3′-OCH_3(-HO)	6–2	0.00	0.02	0.02	0.03
4′-OCH_3	1–5	0.00	0.04	0.03	0.05
2,3-Unsaturation	12–2	−0.08	−0.05	–	0.01
2,3-Unsaturation	7–9	−0.04	−0.03	−0.05	0.01
3-Glycoside (rhamnose)	15–14	−0.28	−0.29	−0.23	−0.38
3-Glycoside (rutinose)	16–14	−0.38	−0.39	−0.39	−0.38
7-Glycoside (glucose)	3–2	−0.48	−0.53	−0.41	−0.58
7-Glycoside (glucose)	10–9	−0.32	−0.36	−0.31	−0.37
7-Glycoside (apiosylglucose)	4–2	−0.52	−0.57	−0.41	−0.56

system with THF and acetonitrile, respectively, are presented. If these data are compared with those for methanol (Table III), it can be seen that there is general agreement between the HPLC and TLC group contribution patterns on changing organic modifier. Hence the solvent selectivity properties and their usefulness in flavonoid identification, previously considered for HPLC[16], are conserved in TLC systems. If these data are analysed more closely, it can be seen that no distinct behaviour is followed by a particular type of plate or a particular organic modifier, the only major finding being the constant behaviour of both types of TLC (W, M) plates. In addition, the differences between ΔR_M and $\Delta \log k'$ data are always more detectable than those found in methanol. This finding, common to all types of plates, is probably due to the marked dependence of the group contributions on Φ with these solvents, resulting from the effects of composition changes on the plate, although polarity differences of the HPTLC layer cannot be ruled out. In support of this hypothesis, one can see the dependence of ΔR_M and $\Delta \log k'$ on Φ, compared in Fig. 3 for the HPTLC plate. For certain group contributions a parallel behaviour is observed but for others (see, *e.g.*, 3-O-Rut.) more complex behaviours with intercrossing occur, which admittedly may result from both polarity and composition gradient effects.

Let us now consider the practical relevance of the useful effects. A slope greater than unity means substantial compression of the useful HPLC chromatographic space (*i.e.*, $1 < k' < 10$) when it is projected over the corresponding TLC or HPTLC space. Hence a slope of unity would be preferable because this adverse effect would be avoided. If in addition the intercept is near to zero, retention data can be easily transferred from HPLC to TLC and *vice versa*. Another interesting property of TLC plates is their use in compound identification: as the ΔR_M values are equal to $\Delta \log k'$ to within ± 0.03 unit in the $\Delta \log k'$ range 0–0.40, relative retention in HPLC can be

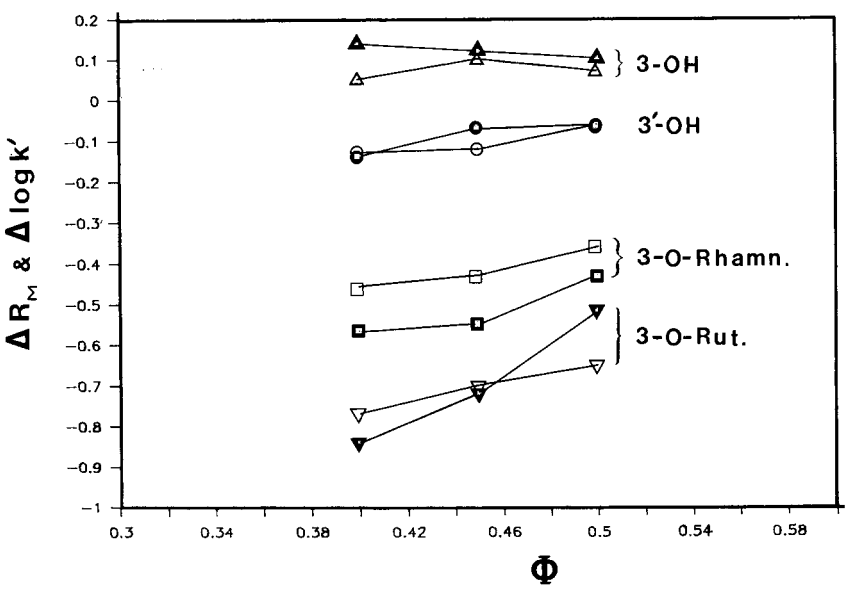

Fig. 3. ΔR_M (TLC) and $\Delta \log k'$ (HPLC) dependence with THF. TLC data were obtained on HPTLC plates. HPLC data were obtained from ref. 16. Closed symbols, HPTLC; open symbols, HPLC.

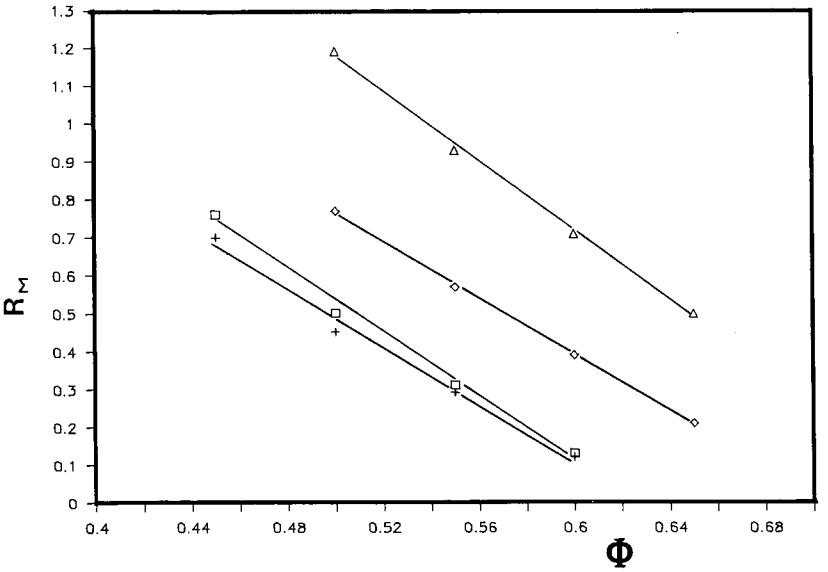

Fig. 4. R_M *vs.* methanol concentration (Φ) in the mobile phase. TLC (M). Compounds: △ = apigenin; ◇ = quercetin; □ = quercitrin; + = eriodictyol.

predicted with an accuracy of ±5%. On both TLC and HPTLC plates retention requires a calibration graph and, in the most favourable instance with log k' = 0.5 (k' = 3), the standard error of the fitting (Table II) implies an accuracy of 12% in the absence of demixing effects.

Another useful application of the TLC system with methanol would be its usefulness in establishing HPLC gradient elution conditions. It is well known that this procedure consists in determining the useful Φ range of the gradient, which is where log k' is in the range 1–0 (k' = 10–1), and then calculating the solvent strength values ($S = \Delta \log k'/\Delta\Phi$), determining the gradient steepness according to the Snyder linear solvent strength theory[27,28]. In order to do this by using only TLC R_M data, a method is proposed which consists in constructing R_M *vs.* Φ plots such as those reported in Fig. 4. From these plots gradient elution conditions were determined and compared with data obtained by HPLC (see Table VI). It can be seen that the agreement is generally satisfactory for the useful $\Delta\Phi$ range, whereas more significant differences were found in solvent strength evaluation. The latter failure is not critical, however, because gradient steepness must be often optimized in order to achieve optimum separations[13,14].

CONCLUSIONS

The correlation between HPLC and TLC is a very important experimental factor which can be of great value for the rapid and economical development of chromatographic methods for flavonoid analysis. However, the significant differences observed here suggest that care is necessary when using unvalidated data. The fact

TABLE VI

USEFUL Φ RANGES FOR GRADIENT ELUTION AND MEAN SOLVENT STRENGTH VALUES CALCULATED FROM LOG k' OR R_M DATA
Methanol as organic modifier. Acetic acid as acid modifier. HPLC data taken from ref. 16.

Compound	*HPLC*			*HPTLC (M)*			*TLC (M)*			*TLC (W)*		
	Φ $(k'=10)$	Φ $(k'=1)$	S	Φ $(k'=10)$	Φ $(k'=1)$	S	Φ $(k'=10)$	Φ $(k'=1)$	S	Φ $(k'=10)$	Φ $(k'=1)$	S
Eriodictyol	39	55	6.2	30	62	3.1	37	63	3.8	38	60	4.5
Naringenin	34	61	3.7	36	67	3.2	45	61	6.2	46	64	5.5
Acacetin	49	82	3.0	51	72	4.8	53	75	4.5	53	70	5.9
Apigenin	46	74	3.6	51	72	4.8	53	75	4.5	53	70	5.9
Apigenin 7G	36	54	5.5	35	64	3.4	38	61	4.3	40	59	5.3
Apiin	37	53	6.3	35	62	3.7	36	60	4.2	39	58	5.3
Chrysin	56	80	4.2	–	–	–	–	–	–	–	–	–
Chrysoeriol	45	72	3.7	51	72	4.8	54	78	4.2	54	73	5.3
Luteolin	43	65	4.5	45	71	3.8	49	69	5.0	48	66	5.5
Luteolin 7G	33	52	5.3	31	66	3.4	32	59	3.7	–	–	–
Galangin	54	80	3.8	54	75	4.8	60	81	4.8	60	81	4.8
Morin	36	58	4.5	–	–	–	–	–	–	–	–	–
Quercetagetin	28	45	5.9	–	–	–	–	–	–	–	–	–
Quercetin	42	59	5.9	41	70	3.4	46	69	4.3	45	65	5.0
Quercitrin	38	56	5.5	34	65	3.2	39	62	4.3	39	59	5.0
Rutin	34	52	5.5	29	60	3.2	33	58	4.0	35	56	4.8

that solvent selectivity effects previously described in HPLC are conserved in TLC makes the latter superior to HPLC owing to the possibility of enhancing the peak capacity through two-dimensional development[29]. This last point and its applications deserve a separate investigation.

ACKNOWLEDGEMENTS

This work was supported by the Italian Ministry of Public Education (MPI), the Italian Ministry of Foreign Affairs (MAE) and the Somali National University.

REFERENCES

1 J. B. Harborne, in E. Heftmann (Editor), *Chromatography, Part B, Applications (Journal of Chromatography Library*, Vol. 22B), Elsevier, Amsterdam, 1986, p. B407.
2 K. Hostettmann and M. Hostettmann, in J. B. Harborne and T. J. Mabry (Editors), *The Flavonoids: Advances in Research*, Chapman and Hall, London, 1982, pp. 1–18.
3 J. B. Harborne and M. Boardley, *J. Chromatogr.*, 299 (1984) 377.
4 L. W. Wulf and C.W. Nagel, *J. Chromatogr.*, 116 (1976) 271.
5 K. Vande Casteele, H. Geiger and C. F. van Sumere, *J. Chromatogr.*, 240 (1982) 81.
6 H. Wagner, S. Bladt and E. M. Zgainski, *Plant Drug Analysis*, Springer, Berlin, 1984.
7 J. B. Harborne, *Phytochemical Methods*, Chapman and Hall, London, 1984.
8 K. R. Markham, *Techniques of Flavonoid Identification*, Academic Press, New York, 1982.
9 M. Vanhaelen and R. Vanhaelen-Fastré, *J. Chromatogr.*, 187 (1980) 255.
10 A. Hierman, *J. Chromatogr.*, 174 (1979) 478.
11 H. Becker, J. Exner and T. Bingler, *J. Chromatogr.*, 172 (1979) 420.
12 D. Heimler, *J. Chromatogr.*, 366 (1986) 407.
13 F. Dondi, Y.D. Kahie, G. Lodi, M. Remelli, P. Reschiglian and C. Bighi, *Anal. Chim. Acta*, 191 (1986) 261.
14 F. Dondi, Y.D. Kahie, G. Lodi, P. Reschiglian, C. Pietrogrande, C. Bighi and G.P. Cartoni, *Chromatographia*, 23 (1987) 844.
15 F. Dondi, G. Blo, Y.D. Kahie, G. Lodi, C. Pietrogrande and P. Reschiglian, *Chromatographia*, 25 (1988) 423.
16 F. Dondi, Y.D. Kahie, G. Lodi, G. Blo, C. Pietrogrande and P. Reschiglian, *J. Chromatogr.*, 461 (1989) 281.
17 H. Schlitt and F. Geiss, *J. Chromatogr.*, 67 (1972) 261.
18 W. Golkiewicz, *Chromatographia*, 14 (1981) 411.
19 W. Golkiewicz, *Chromatographia*, 14 (1981) 629.
20 J. K. Rozylo, J. Gross, M. Poniewaz, R. Lodkowski and B. Buszewski, *J. Liq. Chromatogr.*, 7 (1984) 1301.
21 T. Dzido and E. Soczewinski, *J. High Resolut. Chromatogr. Chromatogr. Commun.*, 1 (1978) 254.
22 W. Jost, H.E. Hauck and F. Eisenbeiss, *Kontakte*, 3 (1984) 45.
23 C. Gonnet and M. Marichy, *Analusis*, 4 (1979) 204.
24 L. R. Snyder, *Principles of Adsorption Chromatography*, Marcel Dekker, New York, 1968.
25 F. Geiss, *Parameter der Dunnschicht-Chromatographie*, Vieweg, Braunschweig, 1972.
26 E. Tomlinson, *J. Chromatogr.*, 113 (1975) 1.
27 L. R. Snyder, J. W. Dolan and J. R. Gant, *J. Chromatogr.*, 165 (1979) 3.
28 J. W. Dolan, J. R. Gant and L. R. Snyder, *J. Chromatogr.*, 165 (1979) 31.
29 G. Guiochon, M. F. Gonnord, A. Siouffi and M. Zakaria, *J. Chromatogr.*, 250 (1982) 1.

Journal of Chromatography, 462 (1989) 219–232
Elsevier Science Publishers B.V., Amsterdam — Printed in The Netherlands

CHROM. 21 020

EVALUATION OF THE LIQUID CHROMATOGRAPHIC SEPARATION OF MONOSACCHARIDES, DISACCHARIDES, TRISACCHARIDES, TETRASACCHARIDES, DEOXYSACCHARIDES AND SUGAR ALCOHOLS WITH STABLE CYCLODEXTRIN BONDED PHASE COLUMNS

DANIEL W. ARMSTRONG* and HENG L. JIN
Department of Chemistry, University of Missouri-Rolla, Rolla, MO 65401-0249 (U.S.A.)
(First received September 2nd, 1988; revised manuscript received September 30th, 1988)

SUMMARY

Both α- and β-cyclodextrin (CD) bonded phase columns were evaluated for their ability to separate carbohydrates and related molecules. Chromatographic data on approximately 50 solutes are reported. Mobile phases consisting of acetonitrile–water or acetone–water produce the best separations. Separations could be run in isocratic or gradient modes. The α-CD column produced slightly more efficient separations than the β-CD column. Both cyclodextrin columns seemed to be more efficient and selective than alkylamine and ion-exchange columns. The stability and reproducibility of the CD columns were excellent and showed little deterioration after several thousand injections. The retention of saccharides on CD bonded phases seems to be related to the number of available hydroxy groups per solute and to the size of the solute. Analysis times and detection sensitivity are discussed.

INTRODUCTION

The separation, identification and quantitation of carbohydrates by liquid chromatography (LC) have received an increasing amount of attention in recent years. Earlier paper and thin-layer chromatographic methods tended to be relatively time consuming and often afforded less resolution than needed for complex mixtures[1–6]. Gas chromatographic methods gave sample resolution and sensitivity but the analytes required prior derivatization to make them volatile[7–10]. Many of the earlier LC methods also used carbohydrate derivatives rather than native compounds[11–16]. The most recent reports involve the direct LC analysis of underivatized carbohydrates[17–19]. Often these separations require specific types of columns such as alkylamine bonded phases, polyol derivatized phases or various ion-exchange media in which specific counter ions are added to affect the separation. Each of these stationary phases have characteristics that are useful for carbohydrate separations. However, there can also be shortcomings, particularly in terms of column stability, lifetimes and reproducibility. An alternative approach is to use an underivatized stationary phase and add a diamine modifier to the mobile phase[20]. Both comprehensive[21,22] and critical[23,24] reviews on the LC separation of carbohydrates have been published.

0021-9673/89/$03.50

Cyclodextrin (CD) bonded phase LC columns developed in our laboratory are used extensively for the separation of optical, geometric and structural isomers[25–31]. Also, they are used increasingly in routine reversed-phase and normal-phase LC separations[32]. CD bonded phase media is relatively stable, particularly in eluents such as those used to separate carbohydrates on alkylamine, diol and polyol stationary phases (i.e., water–organic mixtures containing high percentages of the organic modifier). As the CD bonded phase contains no amine functionality, Schiff base formation is avoided, which should make quantitative results more reliable. In this work, two different CD bonded phase columns (α- and β-CD) were evaluated for the separation of a large variety of saccharides. The effect of different organic modifiers was examined and column efficiency, stability and reproducibility were evaluated. Also considered were the effect of isocratic *versus* gradient separation, detection methods and anomer formation.

EXPERIMENTAL

All the carbohydrates were obtained from Sigma (St. Louis, MO, U.S.A.) except heptose, which was obtained from Aldrich (Milwaukee, WI, (U.S.A.) and α-, β- and γ-CD, which were obtained from Ensuiko Sugar Refining (Japan). All high-performance liquid chromatographic (HPLC) grade solvents were obtained from Fisher Scientific (St. Louis, MO, U.S.A.). All chemicals were used without further purification.

CD bonded phase columns (α-CD or Cyclobond III and β-CD or Cyclobond I) were obtained from Advanced Separation Technologies (Whippany, NJ, U.S.A.). The 250 × 4.6 mm I.D. stainless-steel columns were packed with 5 μm diameter stationary phase support.

A Shimadzu LC-6A liquid chromatograph was used for all separations. A C-R3A or C-R2AX Chromatopac was used to record the chromatograms and for data reduction. Either a Simadzu variable-wavelength detector or a Waters R401 differential refractometer was used to detect the eluted species. Molar absorptivities were measured by use of a Hitachi U-2000 spectrophotometer. All separations were done at room temperature (22°C).

RESULTS AND DISCUSSION

General behavior

The effect of three different organic modifiers (methanol, acetonitrile and acetone) on the separation of a variety of saccharides and related solutes on CD bonded phases was examined. In general the best separations occurred with water–organic solvents containing a high percentage of organic modifier (65–90%). Methanol consistently produced the poorest separations and was not considered to be a viable modifier for most carbohydrate separations on these columns. When methanol was used, the retention times often were too short and similar for many of the solutes. However, excellent chromatochrams could be obtained when using acetonitrile or acetone as modifier. Fig. 1 shows a typical isocratic separation of seventeen mono-, di- and trisaccharides on an α-CD column with an acetonitrile modifier. Fig. 2 shows a gradient separation of nineteen saccharides on a β-CD column, also with an

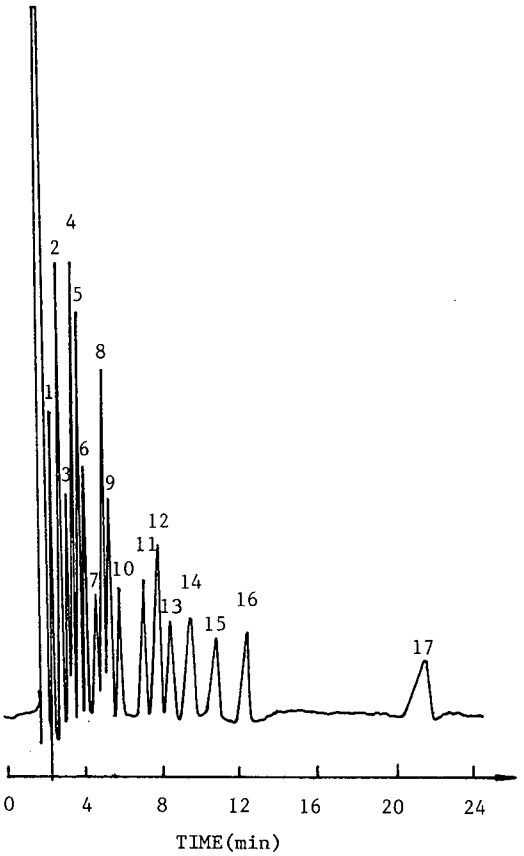

Fig. 1. Isocratic separation of mono-, di- and trisaccharides on a 25-cm α-CD bonded phase column. Mobile phase, acetonitrile–water (78:22, v/v); flow-rate, 1.5 ml/min; refractive index detection. Approximately 40 μg of each sample were injected. Peaks: 1 = phenyl-β-D-glucopyranoside; 2 = 1-deoxy-1-nitro-D-sorbitol; 3 = D-erythrose; 4 = 2-deoxy-D-ribose; 5 = ribose; 6 = lyxose; 7 = tagatose; 8 = xylose; 9 = glucose; 10 = galactitol; 11 = sucrose; 12 = cellobiose; 13 = lactose; 14 = melibiose; 15 = melezitose; 16 = raffinose; 17 = stachyose.

acetonitrile modifier. Gradient separations were very straightforward on CD bonded phases. Column re-equilibration was rapid (2–3 column volumes of mobile phase) and it offered traditional advantages of peak sharpening and reduction of retention for late-eluting solutes. The addition of salts or buffers to the mobile phase seemed to offer no particular advantage with respect to separation efficiency or selectivity. This is very different from what was observed for the separation of ionizable enantiomers on these columns[30]. Consequently, no additional mobile phase additives were used for any of the carbohydrate separations reported here.

Table I gives retention data for a variety of different saccharides and related compounds on the β-CD column and Table II for the α-CD column. Results for both acetonitrile and acetone modifiers are shown. The relative retention order of the saccharides is similar for both α- and β-CD columns, although there are a few

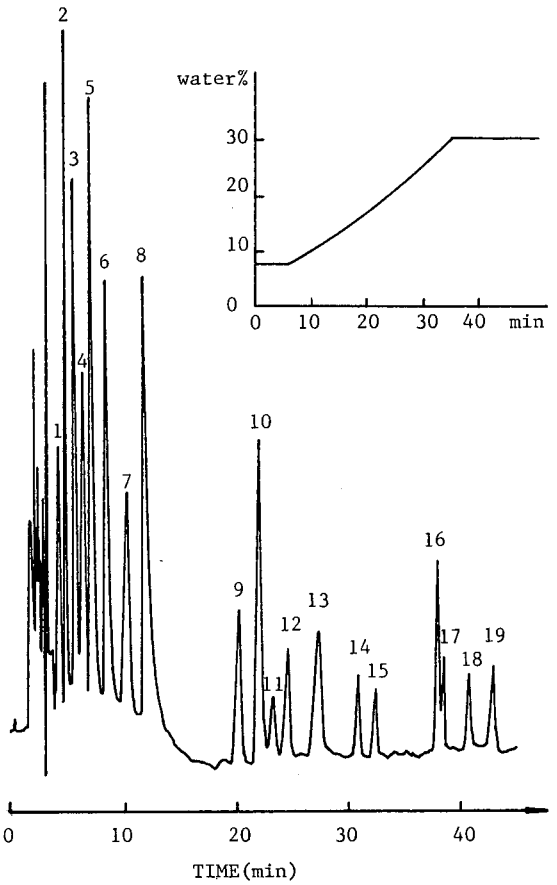

Fig. 2. Gradient separation of nineteen carbohydrates on a 25-cm β-CD bonded phase column. An acetonitrile–water mobile phase was used and the change in composition is shown in the insert. The flow-rate was 1.0 ml/min and UV detection (195 nm) was used. Peaks: 1 = phenyl-β-D-glucopyranoside; 2 = 2-deoxy-D-ribose (8 μg); 3 = ribose (8 μg); 4 = xylose (24 μg); 5 = talose (24 μg); 6 = sorbose (24 μg); 7 = glucose (24 μg); 8 = sorbitol (24 μg); 9 = sucrose (31 μg);10 = turanose (31 μg); 11 = maltose (31 μg); 12 = lactose (31 μg); 13 = melibiose (31 μg); 14 = melezitose (31 μg); 15 = maltotriose (31 μg); 16 = stachyose (31 μg); 17 = α-cyclodextrin (58 μg); 18 = β-cyclodextrin (68 μg); 19 = γ-cyclodextrin (78 μg).

differences. In general, the monosaccharides elute before diaccharides, which elute before trisaccharides. By controlling the mobile phase composition one can separate a wide range of different carbohydrates (as in Fig. 1 and 2) or one can alter the conditions to obtain maximum separation of related compounds of similar size (Fig. 3). Another interesting fact that is apparent from the data in Tables I and II is that there is a consistant elution order for families of deoxy-sugars, sugars and sugar alcohols. The deoxy-sugar tends to elute before the related sugar and they both elute before the analogous sugar alcohol. In general, the greater the number of available hydroxy groups in a compound, the greater is the retention. Also, some disaccharide pairs that are reportedly difficult to separate (*e.g.*, maltose and lactose) are easily resolved on both α- and β-CD columns.

TABLE I

CHROMATOGRAPHIC RETENTION DATA FOR SACCHARIDES SEPARATED ON A β-CYCLODEXTRIN COLUMN WITH TWO DIFFERENT MOBILE PHASES

Compound	*Mobile phase acetonitrile–water (85:15, v/v)*		*Mobile phase acetone–water (90:10, v/v)*	
	t_r *(min)*	k'	t_r *(min)*	k'
Erythrose	3.12	0.48	4.23	0.41
2-Deoxy-D-ribose	3.45	0.64	–	–
Glycerine	3.47	0.65	–	–
Glyceraldehyde	3.57	0.71	4.56	0.53
Rhamnose	3.63	0.73	–	–
Ribose	3.74	0.78	4.60	0.53
6-Deoxy-D-glucose	3.83	0.82	–	–
Lyxose	4.04	0.93	4.84	0.61
2-Deoxy-D-glucose	4.05	0.93	–	–
Erythritol	4.07	0.94	–	–
Threitol	4.10	0.95	–	–
Xylose	4.12	0.96	4.97	0.66
6-Deoxy-D-galactose	4.13	0.97	–	–
2-Deoxy-D-galactose	4.17	0.99	–	–
Talose	4.23	1.02	4.82	0.61
Arabinose	4.30	1.05	5.15	0.72
Tagatose	4.54	1.16	5.18	0.73
Fructose	4.73	1.25	5.43	0.81
Ribitol	4.73	1.25	–	–
Arabitol	4.80	1.29	–	–
Sorbose	4.81	1.29	5.44	0.81
Xylitol	4.88	1.33	–	–
Allose	4.91	1.34	–	–
Mannose	4.91	1.34	–	–
Glucose	5.36	1.55	5.87	0.96
Galactose	5.57	1.65	6.17	1.06
Sorbitol	5.77	1.75	–	–
Mannitol	5.80	1.76	–	–
Galactitol	5.87	1.80	–	–
D-*gluco*-D-*gulo*-Heptose	6.17	1.94	6.13	1.04
Sucrose	7.79	2.71	6.99	1.33
Turanose	8.51	3.05	7.38	1.46
myo-Inositol	8.62	3.10	–	–
Cellobiose	9.02	3.30	8.23	1.60
Maltose	9.09	3.33	7.87	1.62
Maltitol	10.00	3.76	–	–
Lactulose	–	–	8.66	1.74
Lactose	10.16	3.84	8.85	1.95
Gentiobiose	10.75	4.12	9.50	2.00
Melibiose	11.56	4.51	9.67	2.23
Melezitose	14.18	5.76	10.13	2.38
Maltotriose	16.44	6.83	11.61	2.67
Raffinose	17.20	7.19	12.29	2.88
Stachyose	39.0	17.57	26.0	7.23

TABLE II

CHROMATOGRAPHIC RETENTION DATA FOR SACCHARIDES SEPARATED ON AN α-CYCLODEXTRIN COLUMN WITH TWO DIFFERENT MOBILE PHASES

Compound	*Mobile phase acetonitrile–water (80:20, v/v)*		*Mobile phase acetone–water (85:15, v/v)*	
	t_r *(min)*	k'	t_r *(min)*	k'
Erythrose	5.82	0.74	4.53	0.24
Rhamnose	–	–	4.81	0.32
Glyceraldehyde	–	–	4.83	0.33
2-Deoxy-D-ribose	6.23	0.86	4.86	0.34
Glycerine	6.47	0.94	5.09	0.40
Ribose	6.74	1.01	4.98	0.37
6-Deoxy-D-glucose	6.79	1.04	5.08	0.40
3-O-Methyl-D-glucose	7.05	1.11	–	–
2-Deoxy-D-glucose	7.19	1.15	5.19	0.43
Lyxose	7.24	1.17	5.21	0.43
Xylose	7.32	1.20	5.33	0.46
2-Deoxy-D-galactose	–	–	5.40	0.48
Erythritol	7.47	1.23	5.54	0.50
Talose	7.51	1.27	5.13	0.41
6-Deoxy-D-galactose	–	–	5.71	0.57
Arabinose	7.87	1.35	5.73	0.57
Tagatose	8.01	1.40	5.51	0.51
Ribitol	8.30	1.48	5.72	0.57
Fructose	8.32	1.50	5.84	0.60
Sorbose	8.38	1.52	5.62	0.53
Arabitol	8.43	1.53	5.91	0.62
Mannose	8.47	1.54	5.79	0.59
Allose	–	–	6.00	0.65
Xylitol	8.48	1.54	6.01	0.65
Glucose	9.04	1.74	6.20	0.70
Galactose	9.45	1.83	–	–
D-*gluco*-D-*gulo*-Heptose	–	–	6.38	0.75
Sorbitol	9.56	1.86	6.43	0.77
Mannitol	9.62	1.88	–	–
Galactinol	9.74	2.01	6.56	0.80
Sucrose	11.31	2.40	6.63	0.82
Turanose	11.61	2.48	6.98	0.92
Cellobiose	12.27	2.64	7.85	1.16
Maltose	12.33	2.70	7.30	1.01
myo-Inositol	13.04	2.91	9.70	1.67
Maltitol	13.23	2.97	7.03	0.93
Lactose	13.23	2.97	8.22	1.26
Melibiose	14.40	3.30	8.83	1.43
Melezitose	15.62	3.68	8.53	1.34
Maltotriose	–	–	8.80	1.42
Raffinose	17.58	4.26	9.25	1.54
α-Cyclodextrin	–	–	12.97	2.56
Stachyose	27.87	7.34	13.88	2.81
β-Cyclodextrin	–	–	15.6	3.29
γ-Cyclodextrin	–	–	18.93	4.20

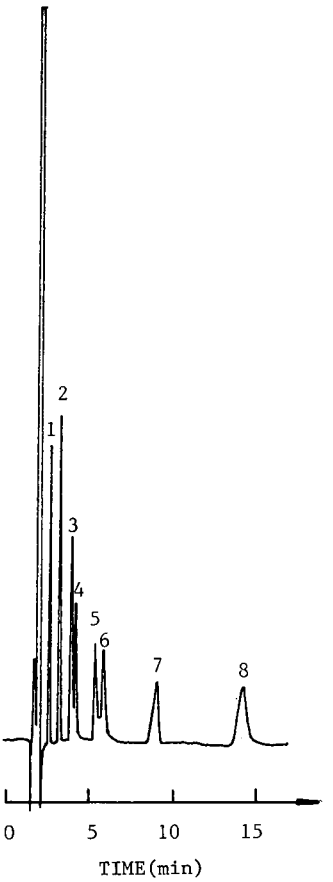

Fig. 3. Chromatogram showing the isocratic separation of eight sugar alcohols on a 25-cm β-CD column. Mobile phase, acetonitrile–methanol–water (95:5:5, v/v); flow-rate, 2.0 ml/min; refractive index detection. Approximately 80 μg of each solute were injected. Peaks: 1 = glycerine; 2 = erythritol; 3 = ribitol; 4 = arabitol; 5 = sorbitol; 6 = galactitol; 7 = *myo*-inosytol; 8 = maltitol.

The concentration of organic modifier in the mobile phase controls the retention and selectivity of the saccharide on cyclodextrin columns. The retention tends to increase with increasing modifier concentration (see Fig. 4 and 5). This retention behavior is analogous to that reported for sugars on alkylamine, polyol and diol columns[24]. At equivalent mobile phase compositions, α-CD columns generally show a greater retention than β-CD columns (Figs. 4 and 5).

Efficiency

Van Deemter plots for several saccharides are shown in Figs. 6 and 7 for the α- and β-CD column, respectively. The optimum efficiency (*i.e.*, the smallest height equivalent to a theoretical plate, *H*) varied from solute to solute. The α-CD column seemed to produce more efficient separations than the β-CD column. Both columns contained an identical 5-μm spherical silica support. The efficiencies at optimum

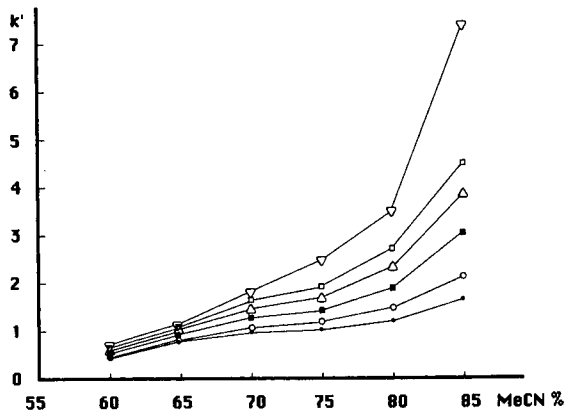

Fig. 4. Plot showing the effect of acetonitrile (MeCN) concentration (%, v/v) in the mobile phase on the capacity factors of several carbohydrates eluted from a 25-cm α-CD column. Solutes: ● = ribose; ○ = lyxose; ■ = fructose; △ = glucose; □ = sorbitol; ▽ = sucrose.

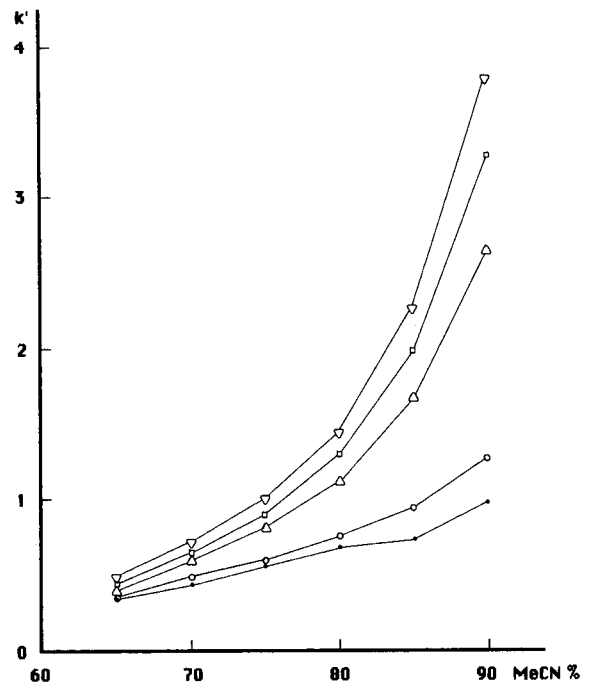

Fig. 5. Plot showing the effect of acetonitrile (MeCN) concentration (%, v/v) in the mobile phase on the capacity factors of several carbohydrates eluted from a 25-cm β-CD column. Solutes: ● = fructose; ○ = glucose; △ = sucrose; □ = maltose; △ = lactose.

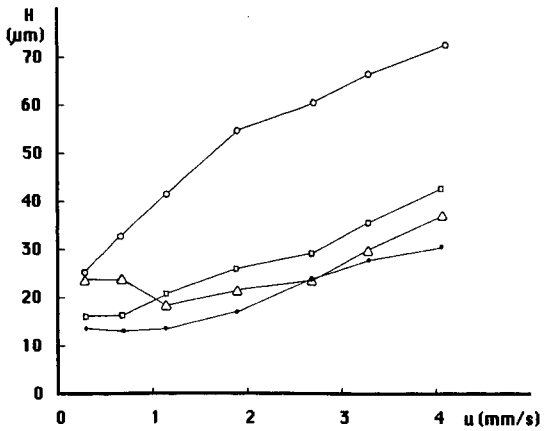

Fig. 6. Van Deemter plots of flow-rate *versus* height equivalent to a theoretical plate (H) for ● = ribose; △ = sorbitol; □ = sucrose and ○ = glucose. A 25-cm α-CD column was used with acetonitrile–water (78:22, v/v) as mobile phase.

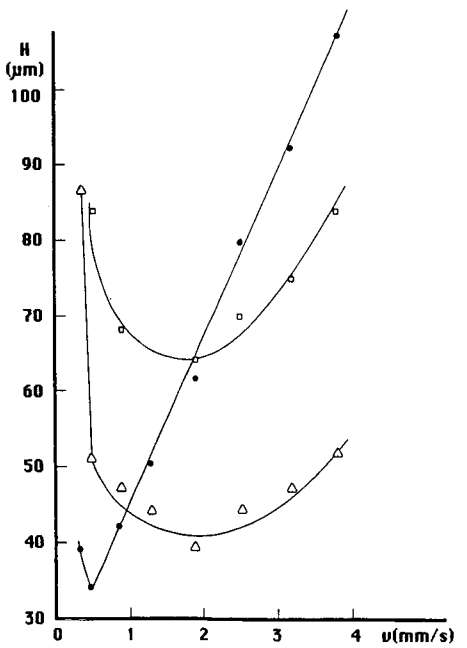

Fig. 7. Van Deemter plots of flow-rate *versus* height equivalent to a theoretical plate (H) for ● = fructose; △ = sucrose and □ = lactose. A 25-cm β-CD column was used with acetonitrile–water (85:15, v/v) as mobile phase.

flow-rates ranged from *ca.* 4000 to 8000 plates per 25 cm column for β-CD and from *ca.* 6000 to 19000 plates per column for α-CD. These efficiencies are higher than those reported for other columns used to separate carbohydrates[24]. There are a number of possible reasons for the higher efficiency. First, the mobile phase can be adjusted easily to suppress or enhance the separation of most anomers. This, coupled with small temperature modifications, can eliminate most band broadening due to the partial separations of anomers. Anomeric separations are very sensitive to mobile phase composition. In general, mobile phases containing higher percentages of organic modifiers tend to enhance the separation of anomers and *vice versa*. An extensive study of the separation of sugar anomers has been completed recently[33]. Retention of saccharides on cyclodextrin bonded phases is probably due to adsorption via hydrogen bonding and dipolar interactions but not to inclusion complex formation. The CD cavity is probably occupied by the organic modifier, which is present in very high concentrations. Further, the large, bulky CDs tend sterically to prohibit solute molecules from reaching the silica gel surface where other retention mechanisms may be important (*e.g.*, binding to free silanols). Thus the exchange kinetics of saccharides between stationary and mobile phases may be more rapid for CD bonded phases under the conditions outlined above. Another possible factor that could contribute to efficiency is that the base packing material (silica gel) and packing method for the CD bonded phases might be better than that of other columns used for carbohydrate analysis. As CD columns are used extensively for difficult enantiomeric separations, both the silica gel and packing technology had to be optimized and continuously checked. However, the manufacturing and packing procedures used by the companies that produce different LC columns are often unknown and it is therefore difficult to know the significance of these factors or compare them.

Stability and reproducibility of CD columns

One of the advantages of α- and β-CD columns for the analysis of carbohydrates is their high stability and reproducibility. As no amine functionality exists on these bonded phases, the formation of Schiff bases is avoided. Consequently, quantitative results may be more accurate[24]. Also, self-hydrolysis is not a significant problem as it is for alkylamine bonded phases. As an example, a β-CD column approximately 1 year old that had received over 3000 standard injections was compared with a new column. The chromatograms are shown in Fig. 8. It is apparent that the older β-CD column is nearly as selective and efficient as the new column. Two aspects of these results should be emphasized. First, the separations were done with pure sales. If samples are injected that contain impurities which are irreversibly adsorbed on the column, then the retention behavior must change with time. This is true for any column. Second, CD bonded phases are particularly stable in water–organic solvents containing $>50\%$ modifier. Many times when separating compounds other than carbohydrates predominantly aqueous mobile phases are used. In these instances, it remains advisable to place a presaturator containing silica gel prior to the injection loop. Again, this is advisable for any silica gel-based column.

Analysis time

The time of analysis can be controlled by adjusting the mobile phase composition, the flow-rate and, to a lesser extent, the temperature. As indicated in

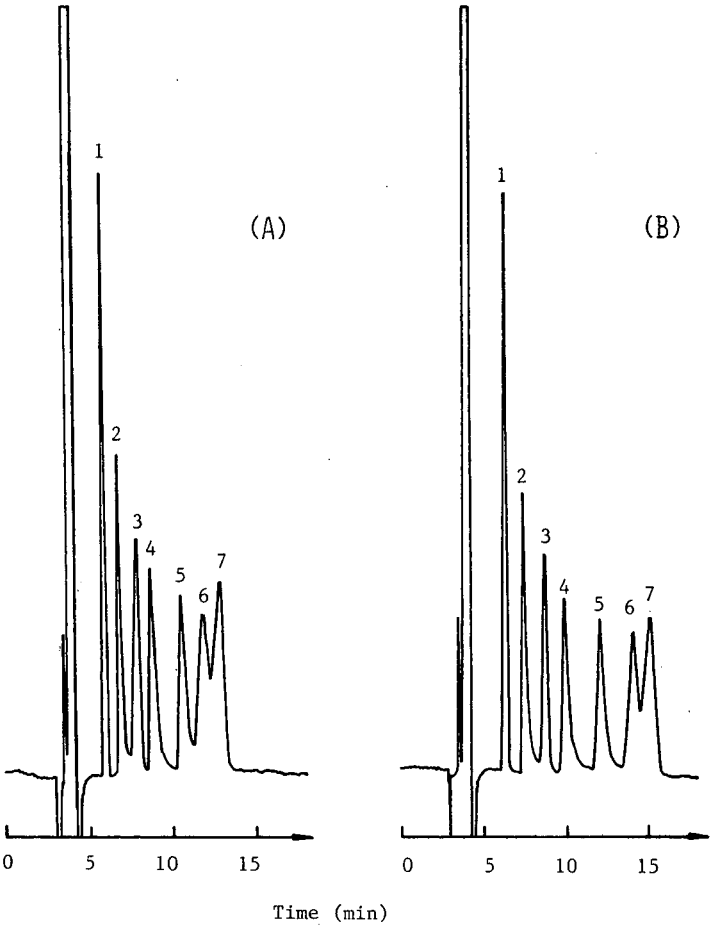

Fig. 8. Comparison of the separations obtained on (A) an old β-CD column (25 cm × 4.6 mm I.D., *ca.* 1 year old and with > 3000 injections) and (B) an analogous new β-CD column. In both instances the mobile phase was acetonitrile–water (95:5, v/v) and the flow-rate was 1.0 ml/min. Peaks: 1 = 2-deoxy-D-ribose; 2 = ribose; 3 = xylose; 4 = talose; 5 = sorbose; 6 = mannose; 7 = glucose.

Figs. 4 and 5, the retention of saccharides decrease as the water content of the mobile phase increases (*i.e.*, the opposite of traditional reversed-phase LC). This allows one to decrease the analysis time, often at the expense of resolution. The optimum efficiency occurs at normal LC flow-rates between 0.5 and 2.0 ml/min (Fig. 6 and 7). Most of the chromatograms shown in this work were generated using a flow-rate of 1.5 ml/min; however, flow-rates of 3.0 and 4.0 ml/min have been used for many saccharide separations. In general, the analysis times on CD bonded phase columns under conditions of optimum efficiency are comparable to those reported for octadecylated silica gel and are less than those reported for amino phases and ion-exchange phases[24].

Detection

It was noted previously that when using an acetonitrile–water mobile phase,

TABLE III

MOLAR ABSORPTIVITIES OF SACCHARIDES AT WAVELENGTHS BETWEEN 190 AND 215 nm

Aqueous solutions were used in all determinations.

Compound	*Wavelength (nm)*					
	190	*195*	*200*	*205*	*210*	*215*
Ribose	149	53	16	6	4	3
Lyxose	114	39	12	4	2	2
Glucose	45	11	3	1	1	1
Fructose	144	57	20	9	4	3
Sorbitol	95	31	9	2	1	1
Sucrose	139	45	13	5	2	1
Lactose	73	17	3	1	0	0
Raffinose	173	42	8	2	0	1
α-Cyclodextrin	64	15	7	4	3	3
β-Cyclodextrin	82	30	14	12	11	11
γ-Cyclodextrin	121	34	17	12	10	9

many saccharides can be detected via absorption (of wavelengths $\leqslant 200$ nm)[34]. The molar absorptivities of several saccharides (at wavelengths between 190 and 215 nm) are given in Table III. At lower wavelengths, UV detection of saccharides is sometimes (but not always) more sensitive than refractive index detection. The relative sensitivity

TABLE IV

COMPARISON OF THE SENSITIVITIES OF ULTRAVIOLET AND REFRACTIVE INDEX DETECTION OF SACCHARIDES

Data were calculated from chromatograms generated with a β-CD column. The flow-rate was 1.5 ml/min and the mobile phase composition was acetonitrile–water (85:15, v/v), except where indicated otherwise.

Compound	*Minimum detectable amount (μg)*	
	UV (195 nm) (0.01)	*RI (8×)*
2-Deoxy-D-ribose	0.084	0.88
Ribose	0.094	1.2
Xylose	0.43	2.2
Fructose	0.13	2.2
Glucose	0.47	2.0
Sorbitol	0.23	1.7
Sucrose	0.91	3.1
Turanose	0.50	2.3
Maltose	2.6	4.7
Lactose	2.1	4.0
Melibiose	1.9	5.2
Melezitose	3.0	5.2
Maltotriose	5.3	8.7
α-Cyclodextrin*	16.2	2.0
β-Cyclodextrin*	18.9	2.6
γ-Cyclodextrin*	23.6	2.9

* Mobile phase: acetonitrile–water (70:30, v/v).

depends on the nature of the saccharide (*i.e.*, molar absorptivity) and its size. The minimum detectable amounts of sixteen saccharides for the variable-wavelength UV and refractive index (RI) detectors used in this study are given in Table IV. In general, UV detection can be up to ten times more sensitive for the smaller monosaccharides on a weight basis. UV and RI detection are of approximately equal sensitivity for trisaccharides but RI detection is more sensitive for larger carbohydrates such as CDs (Table IV).

CONCLUSIONS

Both α- and β-CD bonded phase columns appear to separate a variety of carbohydrates. The smaller saccharides usually elute before the larger polysaccharides. It appears that retention is closely related to the number of available hydroxy group per molecule. This may explain why deoxy-sugars are retained less than the analogous sugars and that neither are retained as much as the corresponding sugar alcohols. The efficiency and stability of CD columns appear to be superior to those of alkylamine bonded phases. The analysis times on CD bonded phases are comparable to those on reversed-phase columns and often shorter than those on amino and ion-exchange stationary phases. The choice of UV *versus* RI detection is dependent on the mobile phase used and the molecular weight of the carbohydrates.

ACKNOWLEDGEMENT

Support of this work by the National Institute of General Medical Sciences (BMT 1R01 GM36292) is gratefully acknowledged.

REFERENCES

1 D. M. Carlson, *J. Biol. Chem.*, 243 (1968) 616.
2 M. D. G. Oates, A. C. Rosbottom and J. Schrager, *Carbohydr. Res.*, 34 (1974) 115.
3 W. E. Trevelyan, D. P. Proctor and J. S. Harrison, *Nature (London)*, 166 (1980) 444.
4 K. R. Anunula and R. G. Spiro, *J. Biol. Chem.*, 258 (1983) 15274.
5 B. L. Slomiany, A. Slomiany and A. Zdebska, *J. Biol. Chem.*, 257 (1984) 2863.
6 A. Slomiany, E. Zdebska and B. L. Slomiany, *J. Biol. Chem.*, 259 (1984) 14743.
7 S. Hakomori, *J. Biochem. (Tokyo)*, 55 (1964) 205.
8 G. Peterson, *Tetrahedron*, 25 (1969) 4437.
9 T. Bhatti, R. E. Chambers and J. R. Clamps, *Biochim. Biophys. Acta*, 222 (1970) 339.
10 K. Stellner, H. Saito and S. Hakomori, *Arch. Biochem. Biophys.*, 155 (1973) 464.
11 J. Lehrfeld, *J. Chromatogr.*, 120 (1976) 141.
12 G. D. McGinnis and P. Fang, *J. Chromatogr.*, 130 (1977) 181.
13 G. D. McGinnis and P. Fang, *J. Chromatogr.*, 130 (1978) 107.
14 G. B. Wells and R. L. Lester, *Anal. Biochem.*, 97 (1979) 184.
15 N. W. H. Cheetham and P. Sirimanne, *J. Chromatogr.*, 196 (1980) 171.
16 N. W. H. Cheetham and P. Sirimanne, *J. Chromatogr.*, 208 (1981) 100.
17 V. Kahle and Tesařik, *J. Chromatogr.*, 190 (1980) 121.
18 M. Verzele and F. Van Damme, *J. Chromatogr.*, 362 (1986) 23.
19 J. D. Olechno, S. R. Carter, W. T. Edwards and D. G. Gillen, *Am. Biotechnol. Lab.*, Sept.–Oct. (1987) 38.
20 M. Boumahraz, V. Ya. Davydov and A. V. Kiselev, *Chromatographia*, 15 (1982) 751.
21 A. Heyraud and M. Rinaudo, *J. Liq. Chromatogr.*, 4, Supl. 2 (1981) 175.
22 K. Robards and M. Whitelaw, *J. Chromatogr.*, 373 (1986) 81.
23 L. A. Th. Verhaar and B. F. M. Kuster, *J. Chromatogr.*, 220 (1981) 313.

24 M. Verzele, G. Simoens and F. Van Damme, *Chromatographia*, 23 (1987) 292.
25 D. W. Armstrong and W. DeMond, *J. Chromatogr. Sci.*, 22 (1984) 411.
26 D. W. Armstrong, W. DeMond and B. P. Czech, *Anal. Chem.*, 57 (1985) 481.
27 D. W. Armstrong, T. J. Ward, A. Czech, B. P. Czech and R. A. Bartsch, *J. Org. Chem.*, 50 (1985) 5556.
28 T. J. Ward and D. W. Armstrong, *J. Liq. Chromatogr.*, 9 (1986) 407.
29 D. W. Armstrong, T. J. Ward, R. D. Armstrong and T. E. Beesley, *Science (Washington, D.C.)*, 232 (1986) 1132.
30 D. W. Armstrong and W. Li, *Chromatography*, 2 (1987) 43.
31 D. W. Armstrong, S. F. Yang, S. M. Han and R. Menges, *Anal. Chem.*, 59 (1987) 2594.
32 D. W. Armstrong, A. Alak, W. DeMond, W. L. Hinze and T. E. Riehl, *J. Liq. Chromatogr.*, 8 (1985) 261.
33 D. W. Armstrong and H. L. Jin, *Chirality*, 1 (1989) in press.
34 H. Binder, *J. Chromatogr.*, 189 (1980) 414.

Journal of Chromatography, 462 (1989) 233–241
Elsevier Science Publishers B.V., Amsterdam — Printed in The Netherlands

CHROM. 20 978

HIGH-PERFORMANCE LIQUID AND GAS CHROMATOGRAPHY OF DIALKYLPHOSPHATES, DIALKYLTHIOPHOSPHATES AND DIALKYLDITHIOPHOSPHATES AS THEIR PENTAFLUOROBENZYL DERIVATIVES

V. BARDAROV
Institute of Hygiene and Occupational Health, 1431 Sofia (Bulgaria)
and
M. MITEWA*
Department of Chemistry, University of Sofia, 1126 Sofia (Bulgaria)
(First received December 29th, 1987; revised manuscript received August 26th, 1988)

SUMMARY

High-performance liquid and gas chromatographic (GC) procedures for the separation and determination of dialkylphosphates, dialkylthiophosphates and dialkyldithiophosphates (alkyl = methyl or ethyl), the main hydrolytic metabolites of organophosphate pesticides, are described. The application of different procedures and their limits of detection are discussed. The GC proposed procedures were applied to the analysis of urine samples from humans exposed and not exposed to organophosphates.

INTRODUCTION

Dialkylphosphates (DAP), dialkylthiophosphates (DATP) and dialkyldithiophosphates (DADTP) (Fig. 1), being hydrolytic metabolites of organophosphorus (OP) pesticides, are excreted in urine[1–3]. Their level of excretion is a convenient indicator of human exposure to OP pesticides[3,4]. The application of such an indicator, however, requires the development of a suitable method for the routine simultaneous determination of all DAP, DATP and DADTP and in some instances also alkylphosphates, alkylthiophosphates, alkyldithiophosphates, thiophosphoric acid and dithiophosphoric acid.

A number of procedures have been developed, based on different derivatization procedures followed by gas chromatographic (GC) determination of the derivatives using a phosphorus-specific detector. The procedures involving alkylation with diazomethane[3,5], diazoethane[3] or diazopentane[6–8] proved to be inconvenient for routine analysis, however, owing to the high toxicity and thermal instability of the chemicals used, the strong interference from the inorganic phosphates present in the urine and the formation of more than one derivative of DATP. Alternative procedures, based on the methylation with phenyltrimethylammonium hydroxide in methanol[9,10], are applicable only to thio- and dithiophosphates. The third possibility, involving the

0021-9673/89/$03.50

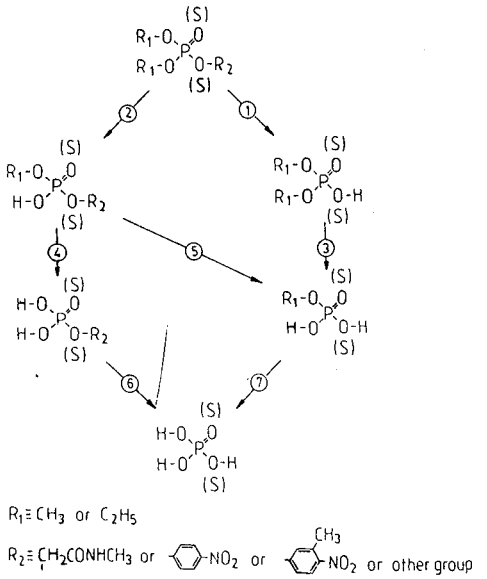

Fig. 1. Hydrolytic metabolism of organophosphates.

determination of the *p*-nitrobenzyl ester derivatives[11], excludes the use of nitrogen–phosphorus detection (NPD).

The determination of alkylphosphates following their conversion into their pentafluorobenzyl esters[12,13] seems to be the most convenient method, as these esters exhibit suitable GC properties and suffer no obvious interference from inorganic phosphates. In addition, the use of both NPD and flame-photometric detection (FPD) is possible. Nevertheless, some problems concerning the sample preparation, GC separation and the use of NPD hinder their application in routine analysis. The investigation of some of these problems and the application of high-performance liquid chromatography (HPLC) to dialkylphosphates are reported in this paper.

EXPERIMENTAL

Standards and reagents

Dimethyl phosphate (DMP), diethyl phosphate (DEP), the sodium salt of DMP and the potassium salts of dimethyl thiophosphate (DMTP), diethyl thiophosphate (DETP), dimethyl dithiophosphate (DMDTP) and diethyl dithiophosphate (DEDTP) were supplied by EPA (Research Triangle Park, NC, U.S.A.). Standard solutions were prepared weekly in acetonitrile [acetonitrile–water (99:1) for DAP and its sodium salt] and stored at 0–5°C.

2,3,4,5,6-Pentafluorobenzyl bromide (PFB-Br) (99+%) was obtained from Janssen (Nettetal, F.R.G.).

HPLC-grade pentane, methanol, ethanol and water and spectroscopic-grade cyclohexane and potassium bromide were used.

Acetonitrile, dichloromethane, acetone, heptane, anhydrous potassium carbonate, sodium perchlorate, sodium dihydrogenphosphate, dipotassium hydrogen-

phosphate and sodium hydroxide were of analytical-reagent grade. Tetraalkylammonium salts, tetraphenylarsonium chloride and dicyclohexyl-18-crown-6 were obtained from Fluka (Buchs, Switzerland) and Merck (Darmstadt, F.R.G.).

Liquid chromatography

Apparatus. The HPLC experiments were performed on a Perkin-Elmer LC system consisting of a series 4 pump, a 550 SE UV–VIS spectrometer with an 8-μl flow cell, a Rheodyne 7125 injection valve with a 300-μl loop for preparative work and a 20-μl loop for analytical work and an R-100 recorder. For electrochemical detection (ED) a Model 4B detector from Bioanalytical systems was used equipped with a glass carbon working electrode.

Chromatographic conditions. An anion-exchange column (250 × 4.6 mm I.D.) of SAX, 10 μm (Whatman, Clifton, NJ, U.S.A.) was used. The mobile phase was 0.05 *M* sodium perchlorate in 0.05 *M* phosphate buffer (pH 7.2) at a flow-rate of 1 ml/min and ED with a glassy carbon working electrode at a potential of 1.05 V *vs.* silver–silver chloride with 1 *M* potassium chloride reference electrode was used for the determination of DATP and DADTP.

The normal-phase (NP) preparative separation of PFB derivatives was performed with a 250 × 10 mm I.D. silica-50 (7 μm) column (Macherey, Nagel & Co., Düren, F.R.G.) with different mobile phases: 2% methanol and 2% ethanol in pentane for DAP-PFB separation, 1% methanol and 1% ethanol in pentane for DATP-PFB separation and 0.5% methanol and 0.5% ethanol in pentane for DADTP-PFB separation, with UV detection at 260 nm. In order to avoid fluctuation of the flow-rate an overpressure (helium, 30 p.s.i.) was applied in the mobile phase containers.

Gas chromatography

Apparatus. GC was performed on a Perkin-Elmer series 8300 instrument equipped with a heated injector for packed columns, a split–splitless injector for capillary columns, a nitrogen–phosphorus detector and a GP-100 printer.

Chromatographic conditions. The stationary phases used for packed columns were SE-30, DC-200, OV-17, OV-25, OV-225, QF-1, and Carbowax 20M and their binary mixtures coated on Chromosorb G HP (100–120 mesh) or Chromosorb W HP (100–120 mesh). The column temperature was held at 185°C for 8 min, then increased linearly to 240°C at 20°C/min. The carrier gas was nitrogen at a flow-rate of 35 ml/min. The temperature increase ensures both the elution of di- and tri(pentafluorobenzyl) phosphates and purification of the column when urine samples are analysed.

The capillary columns used were as follows: 25 m × 0.25 mm I.D. fused silica with Carbowax 20M, SP-1000 or OV-101 as the stationary phase and 50 m × 0.23 mm I.D. fused silica with polyvinylmethylsilicone (PVMS) as the stationary phase. The carrier gas was helium at a flow-rate of 3 ml/min. In all instances temperature programming was performed. In order to achieve high sensitivity, splitless injection was applied with the split flow valve in the "on" position 0.6 min after injection and with the column temperature programmed from 75 to 270°C (heptane was used as the solvent).

Detection. NPD in the phosphorus mode was applied at hydrogen flow-rate of 44 ml/min and, in order to achieve higher sensitivity, oxygen was used instead of air at a flow-rate of 32 ml/min when packed columns were used. NPD in the nitrogen–

phosphorus (NP) mode was applied with hydrogen and air flow-rates as recommended in the manual when capillary columns were used.

Additional apparatus

UV and IR spectra were recorded on Perkin-Elmer Lambda-5 UV–VIS and Perkin-Elmer 883 IR spectrometers (potassium bromide disks), respectively.

A rotary vacuum evaporator together with a thermostated water-bath, dry thermostat and Supelco Microware G/G kit (Part No. 6-4692) were used.

PFB derivatization of standards

Standard solutions of DAP, DATP and DADTP (treated in the same manner as the samples) and their PFB derivatives, methyldi(pentafluorobenzyl) phosphate [$MP(PFB)_2$] and tri(pentafluorobenzyl) phosphate [$P(PFB)_3$] solutions were used for calibration of the retention times and response factors.

Derivatization was performed in a reaction mixture consisting of DAP (or DATP or DADTP), PFB-Br and potassium carbonate (as catalyst) in acetonitrile or acetone after incubation at an appropriate temperature. The PFB derivatives were isolated by extraction with heptane. A typical preparative procedure was incubation of 1–5 mg of the appropriate phosphate, 40–60 μl of PFB-Br and 30–60 mg of potassium carbonate in 0.5 ml of acetonitrile (for DAP derivatization) or 1 ml of acetone (mainly for DATP and DADTP derivatization) for 0.5–3 h at 40–90°C, followed by extraction with heptane (wnen acetone was used as the solvent it was purged before extraction).

Sample preparation

(1) Extractive alkylation according to Bradway et al.[12]. Sealed stoppered tubes containing 1.0 ml of urine, 2 ml of dichloromethane, 1 ml of a 0.1 *M* aqueous solution of the ion-pair reagent and 30 μl of PFB-Br were shaken at ambient temperature for 1 h. After centrifugation, the organic phase was dried with 0.5 g of anhydrous sodium sulphate, 1 ml of it was evaporated under nitrogen to a residue of *ca.* 30 μl and then 0.50 μl of heptane and 5 μl of 10% sulphuric acid were added. Aliquots of the organic phase were analysed by GC.

(2) Procedure of Reid and Watts[13]. A 1.0-ml sample of urine and 7.0 ml of acetonitrile were mixed and centrifuged, 4.0 ml of the supernatant were transferred into a 10-ml reaction vessel and the solvent was removed using a rotary vacuum evaporator at 30–40°C or by means of a nitrogen flow at 60°C. The derivatization was performed by adding 0.5 ml of acetone and 20 μl of PFB-Br and incubation at ambient temperature for 30–60 min in a sealed reaction vessel. Then the acetone was removed with a nitrogen flow and the PFB derivatives of DATP and DADTP were extracted with 0.50 ml of heptane. The supernatant was separated after centrifugation and an aliquot (0.30 ml) was transferred into a sample vessel. The derivatization procedure was repeated for the residue (kept in the reaction vessel) at higher temperature: 0.5 ml of an acetonitrile solution of dicyclohexyl-18-crown-6 (0.2%), 30 mg of potassium carbonate and 20 μl of PFB-Br were added and the vessel was sealed and incubated for 1–2 h at 90°C. Then 0.50 ml of heptane and 5 ml of 10% sulphuric acid were added and 0.30 ml of the organic phase was taken and added to the first aliquot in the sample vessel.

RESULTS AND DISCUSSION

The absorption spectra and molar absorptivities of DMP, DMTP and DMDTP are shown in Fig. 2A and B. The molar absorptivities are moderate for DMTP and DMDTP and negligible for DMP in the non-specific region of the UV spectrum (200–220 nm), thus limiting significantly both the sensitivity and selectivity of their HPLC determination with spectrophotometric detection. On the other hand, the electrochemical activity of DMTP, DETP, DMDTP and DEDTP (Fig. 2C) makes HPLC determination with ED possible. The separation achieved for DMTP, DETP, DMDTP and DEDTP by means of ion-exchange HPLC with ED at a glass carbon working electrode potential of 1.05 V is demonstrated in Fig. 2D. It is evident that at potentials higher than 1.15 V for DMTP and DETP and higher than 1.00 V for DMDTP and DEDTP their direct determination is possible at concentrations less than 2 nmol/l. The existence of many other electrochemically active components (at the potentials mentioned above), however, hampers their direct determination in urine unless a complicated sample purification is carried out. On the other hand, HPLC with ED is a suitable variant for the determination of DATP and DADTP in aqueous sample, whereas DAP proved to be electrochemically inactive.

The data obtained showed that HPLC with spectrophotometric detection might be successfully applied to the determination and preparative isolation of PFB derivatives of DMP, DEP, DMTP, DETP, DMDTP and DEDTP, exhibiting absorption bands at 260 nm (Fig. 3B). Fig. 3A shows a typical chromatogram of a heptane extract containing PFB derivatives of DMP (after derivatization). Applying preparative normal-phase HPLC (UV detection at 260 nm) with manual collection of

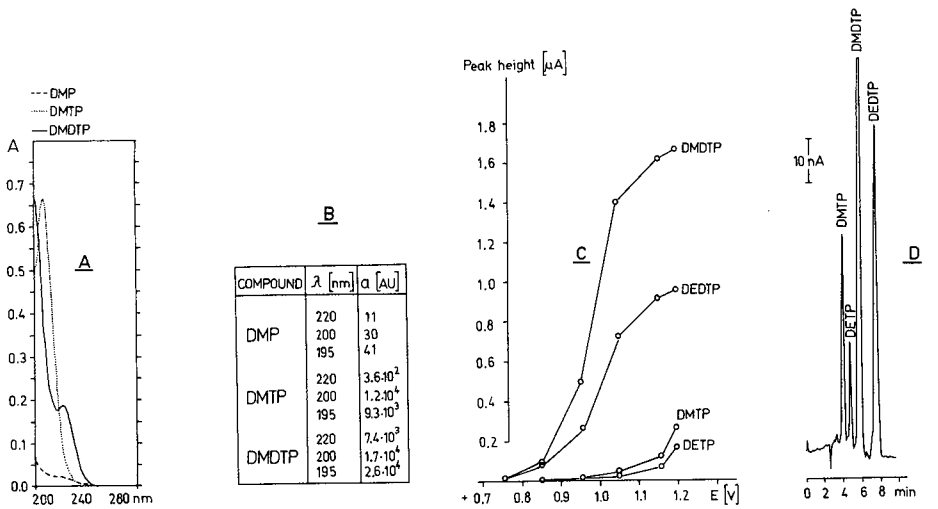

Fig. 2. Spectral, electrochemical and chromatographic characteristics of DMP, DMTP and DMDTP. (A) UV spectra (aqueous solutions), 1-cm cells; (B) molar absorbtivity data; (C) hydrodynamic voltammogram for DMTP, DETP, DMDTP and DEDTP [eluent, 0.05 *M* sodium perchlorate in 0.05 *M* phosphate buffer (pH 7.2), flow-rate 1 ml/min, glassy carbon working electrode, silver–silver chloride with 1 *M* potassium chloride reference electrode]; (D) HPLC with ED of DMTP (450 ng), DETP (450 ng), DMDTP (25 ng) and DEDTP (25 ng) using a 250 × 4.6 mm I.D. SAX (10 μm) column and mobile phase and flow-rate as in C.

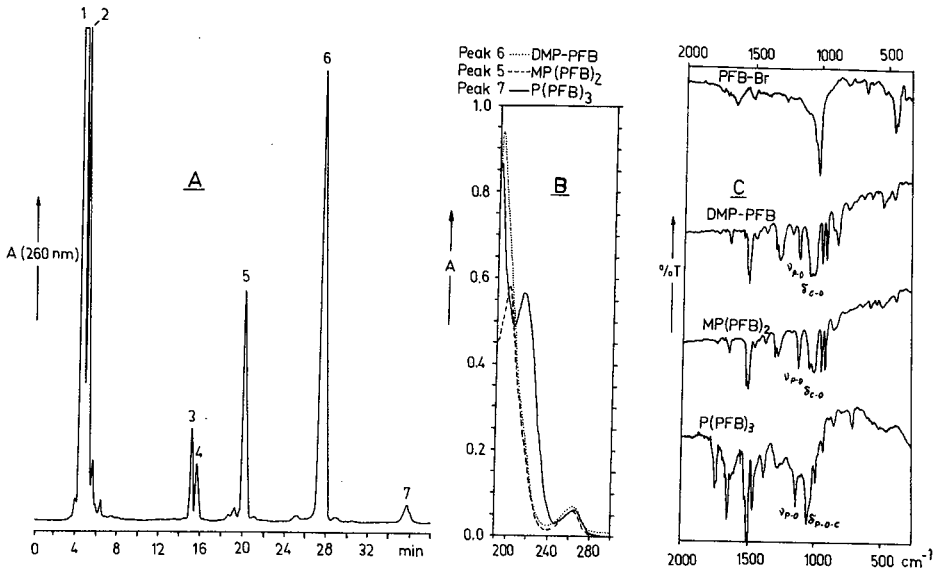

Fig. 3. (A) Preparative HPLC of heptane extract from reaction mixture (5 mg of sodium DMP + 60 μl of PFB-Br + 60 mg of potassium carbonate in 0.5 ml of acetonitrile, incubated for 3 h at 90°C); 250 × 10 mm I.D. Si-50 (7 μm) column, 2% methanol + 2% ethanol in pentane as the mobile phase at a flow-rate of 6 ml/min, UV detection at 260 n. (B) UV spectra and (C) IR spectra of the corresponding fractions.

the fractions, the compounds corresponding to peaks 1–7 were isolated. Using GC with NPD it was proved that compounds 5–7 contain phosphorous. In Figs. 3B, 3C and 4 the corresponding GC peaks and the UV and IR spectra are shown. It is evident that in the IR spectra bands due to ν_{P-O} are observed, confirming that they contain phosphorus. Similarly, the PFB derivatives of DATP and DADTP were isolated by means of preparative HPLC.

These data show that a satisfactory separation of the hydrolytic metabolites of OP pesticides is achieved using ion-exchange HPLC (or ion-pair HPLC) without preliminary derivatization. However, the absence of a specific detector highly sensitive to OP compounds hinders their direct quantitation by HPLC when present in low concentrations. This problem can only be partially solved using HPLC with ED for the determination of thio- and dithiophosphates in aqueous solution, and even in urine and other samples after purification. For this reason GC after derivatization was applied using both packed and capillary columns.

A systematic investigation of the GC separation of DMP-PFB, DEP-PFB, DMTP-PFB, DETP-PFB, DMDTP-PFB, DEDTP-PFB, $MP(PFB)_2$ and $P(PFB)_3$ (the last two are formed as side-products in the course of derivatization) using packed columns with different stationary phases was performed. SE-30, DC-200, OV-17, OV-25, OV-225, QF-1, Carbowax 20M and their binary mixtures were tested. The results showed that satisfactory separation was obtained using OV-17 (better when coated on Chromosorb G than on Chromosorb W) and much better when a column packed with a mixture of 2% OV-225 coated on Chromosorb W HP (100–120 mesh) and 3% OV-17 coated on the same support in a ratio of 1:2 was used. Fig. 4A shows a typical chromatogram obtained on this stationary phase mixture packed in

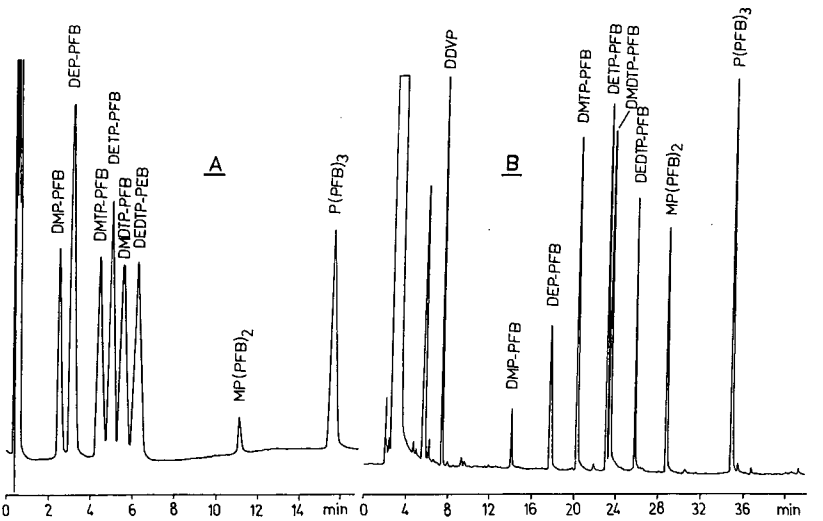

Fig. 4. GC of a heptane solution of PFB derivatives. (A) 2 m × 1.75 mm I.D. glass column packed with mixture of 2% OV-225 on Chromosorb W HP (100–120 mesh) and 3% OV-17 on the same support in the ratio 1:2; injector temperature, 240°C; column temperature, 185°C for 8 min then increased to 240°C at 20°C/min; NPD in P-mode at 280°C, hydrogen flow-rate 44 ml/min and oxygen flow-rate 32 ml/min; carrier gas, nitrogen at a flow-rate of 35 ml/min. (B) 50 m × 0.23 mm I.D. fused-silica capillary column, PVMS stationary phase; injector temperature, 240°C; column temperature programmed from 75 to 270°C in three ramps; NPD in NP mode at 250°C; carrier gas, helium at a flow-rate of 3 ml/min.

a 2 m × 1.75 mm I.D. glass column with the column temperature programmed from 185°C (8 min) to 240°C at 20°C/min. The chromatogram also indicates that under these conditions the presence of nitrogen in the stationary phase (OV-225) does not interfere and NPD can be used at column temperatures up to 240°C. It was also shown that silylation of both the column and injector (with pentafluorophenyldimethylchlorosilane as the silylating agent at 150°C) influences the efficiency (in this procedure the column should be disconnected from the detector).

Several different types of capillary columns were also checked for the separation of PFB derivatives. It was found that columns with Carbowax 20M and SP-1000 are not convenient (low temperature limit), but the column with PVMS as stationary phase proved to be suitable for the separation of the all PFB derivatives of OP compounds and also DDVP, which can be used as an internal standard (added after derivatization). The separation of DMP-PFB, DEP-PFB, DMTP-PFB, DETP-PFB, DMDTP-PFB, DEDTP-PFB, $MP(PFB)_2$, $P(PFB)_3$ and DDVP on a 50 m × 0.23 mm I.D. fused-silica capillary column is illustrated in Figs. 4B and 5. The high temperature limit of the column permits the determination of di- and tri-PFB derivatives and also the purging of higher boiling compounds (column purification) when urine samples are analysed. In the chromatograms of urine samples from persons exposed to OP pesticides, peaks with retention times in the range 25–40 min are observed (Fig. 5), but not in those of urine from non-exposed persons. Their intensities increase with increasing storage time of the samples up to 100 days after collection. They are probably due to other derivatives of OP pesticides, such as di- and/or tri-PFB thio- and dithiophosphates. Unfortunately, these peaks could not be identified as no standard substances were available.

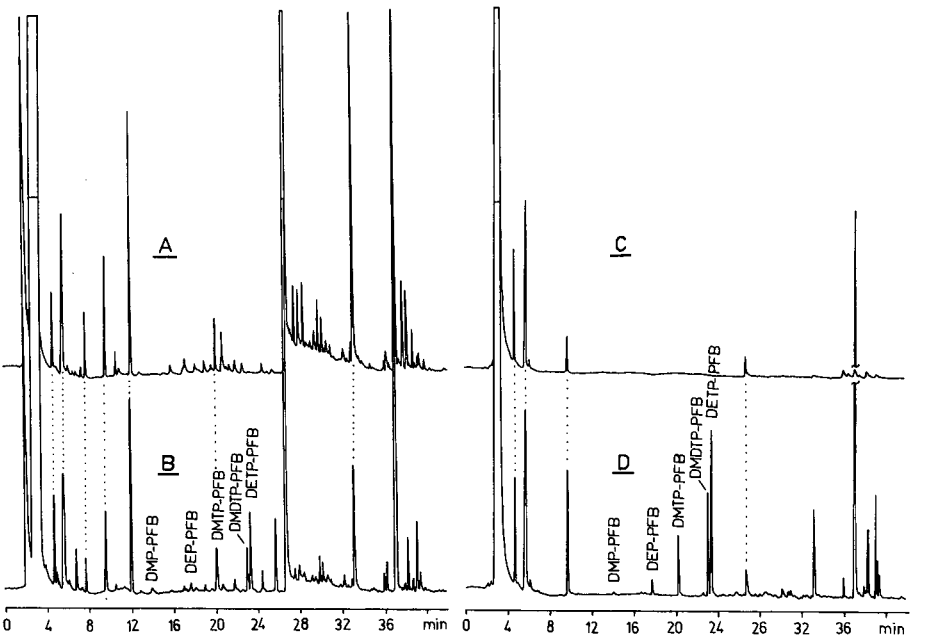

Fig. 5. GC of urine samples from non-exposed persons (A, C) and persons exposed to Supracide, Fenitrothion and Dursban (B, D). GC conditions as in Fig. 4B. (A, B) Chromatograms of heptane extracts after derivatization without acid washing; (C, D) chromatograms of the same extracts after acid washing.

TABLE I

RECOVERY DATA FOR EXTRACTIVE ALKYLATION

Ion-pair reagent	*Recovery (%)*					
	DMP	*DEP*	*DMTP*	*DETP*	*DMDTP*	*DEDTP*
Benzyltetrabutylammonium chloride (276)*, 0.1 *M* solution in 0.1 *M* NaOH	1	1	10	65	40	70
Benzyldimethylhexadecyl-ammonium chloride (360)* 0.1 *M* solution in 0.1 *M* NaOH	1	1	20	80	70	80
N-Benzyl-N,N-dimethyl-4-(1,1,3,5-tetramethylbutyl)-phenoxyethoxyethyl-ammonium chloride (412)*, 0.1 *M* aqueous solution	5	10	50	80	70	80
Tetraphenylarsonium chloride (383)*, 0.1 *M* solution in 0.1 *M* NaOH	5	5	50	80	70	80
Dicyclohexyl-18-crown-6 (411)**, 0.1 *M* solution in 0.05 *M* K_2CO_3	1	1	60	80	90	80

* Ionic mass of the corresponding cations.
** Ionic mass of the K^+ complex.

In order to optimize the conditions for the extractive alkylation according to Bradway *et al.*[12], the type of ion-pair reagent and the acidity of the aqueous phase were varied. The results obtained are given in Table I. It is evident that the procedure is not applicable to DMP and DEP as the analytical yields are low.

Using the procedure of Reid and Watts[13], derivatization of all phosphates soluble in water–acetonitrile was achieved. In this instance, however, other problems were encountered, namely different rates of esterification of different phosphates and the occurrence of side-reactions. For this reason we examined the applicability of the derivatization using other experimental conditions: (a) when the derivatization was performed in acetone and in the presence of potassium carbonate at 45°C for 4 h no side-reactions were found, but the analytical yield was still low (less than 40% for DEP and less than 30% for DMP); (b) application of a K^+–crown ether complex as a catalyst for he derivatization[14] (1 mg of crown ether and 20 mg of potassium carbonate per millilitre of reaction mixture) proved to be effective in acetonitrile medium (no catalytic effect was observed in acetone medium), the rate of derivatization for DMP and DEP increasing more than 3-fold at 90°C.

The standardization of the derivatization provides an opportunity to exclude the derivatization of the reference substances and the use of their PFB derivatives for calibration of the retention times and R_F values in the course of their quantitation. The acid washing of the extract obtained from the reaction mixture proposed before the GC determination (Fig. 4) leads to a significant improvement in the selectivity.

REFERENCES

1 L. E. John, Jr. and D. J. Lisk, *J. Agric. Food Chem.*, 16 (1968) 48.
2 T. Popov, Z. Zaprjanov, I. Bentchev and G. Georgiev, *Atlas po Toxicokinetika*, Medizina i Fizkultura, Sofia, 1985, p. 192.
3 M. T. Shafic and H. F. Enos, *J. Agric. Food Chem.*, 17 (1969) 1186.
4 V. Bardarov, *Khig. Zdraveopaz*, 31, No. 2 (1988) 81.
5 V. Drevenkar, M. Stipcevic, B. Stengl and Z. Stefanac, *Mikrochim. Acta*, I (1979) 385.
6 *Analysis of Pesticide Residue in Human and Environmental Samples*, U.S. Environmental Protection Agency, Research Triangle Park, NC, 1980, Section 6, A(2).
7 E. M. Lores and D. E. Bradway, *J. Agric. Food Chem.*, 25 (1977) 75.
8 T. Shafik, D. E. Bradway, H. F. Enos and A. R. Yobs, *J. Agric. Food Chem.*, 21 (1973) 625.
9 F. C. Churchill, D. N. Ku and J. W. Miles, *J. Agric. Food Chem.*, 26 (1978) 1108.
10 R. P. Moody, C. A. Franklin, D. R. Riedel, N. I. Muir, R. Greenhalgh and A. Hiedke, *J. Agric. Food Chem.*, 33 (1985) 464.
11 D. Y. Takade, J. M. Reynolds and J. H. Nelson, *J. Agric. Food Chem.*, 27 (1979) 746.
12 D. E. Bradway, R. Moseman and R. May, *Bull. Environ. Contam. Toxicol.*, 26 (1981) 520.
13 S. J. Reid and R. R. Watts, *J. Anal. Toxicol.*, 5 (1981) 126.
14 D. Durst, M. Milano, E. J. Mikta, Jr., S. A. Connelly and E. Grushka, *Anal. Chem.*, 47 (1975) 1797.

Journal of Chromatography, 462 (1989) 243–254
Elsevier Science Publishers B.V., Amsterdam — Printed in The Netherlands

CHROM. 20 980

REVERSED-PHASE HIGH-PERFORMANCE LIQUID CHROMATOGRAPHIC ANALYSES OF INSULIN BIOSYNTHESIS IN ISOLATED RAT AND MOUSE ISLETS*

S. LINDE*, J. H. NIELSEN, B. HANSEN and B. S. WELINDER
Hagedorn Research Laboratory, Niels Steensensvej 6, DK-2820 Gentofte (Denmark)
(Received June 28th, 1988)

SUMMARY

Two RP-HPLC systems were developed for the separation of the products of the conversion of proinsulin into insulin in rat and mouse islets, including proinsulin I and II. Peaks were identified by microsequencing and radiosequencing. It was confirmed that mouse C-peptide I has a two amino acid deletion compared to rat C-peptide I. A marked species difference in the ratio between insulin I and II was observed, *i.e.*, 2:1 in the rat and 1:2 in the mouse. Pulse-chase experiments in rat islets have demonstrated that the ratio between insulin I and II in newly synthesized insulin is higher than that of the stored insulin, indicating a slower conversion rate of proinsulin II compared to proinsulin I.

INTRODUCTION

Several reports have described the use of reversed-phase high-performance liquid chromatography (RP-HPLC) for the separation of insulin, insulin-related and non-insulin-related polypeptides from species producing a single insulin (see ref. 1 for a review). The rat and mouse endocrine pancreas secrete two insulins (I,II)[2,3] coded for by two non-allelic genes[4,5]. Their biosynthesis involves rapid removal of a signal peptide from the precursor preproinsulin, and under normal conditions only the two proinsulins can be detected as precursors in the islets.

The two rat proinsulins differ in 4 of the 86 amino acid residues, 2 in the B-chain and 2 in the C-peptide[2]. Mouse insulin I and II have amino acid sequences identical to those of the rat insulins[6]. Recently, Wentworth *et al.*[7] cloned and sequenced the two mouse preproinsulin genes confirming the sequence for the two mouse insulins, but the nucleotide sequence indicated that the mouse C-peptide I has a deletion of two amino acids compared to the mouse C-peptide II.

Investigation of the rat and mouse insulin biosynthesis requires a method sep-

* Presented in part at the *12th International Symposium on Column Liquid Chromatography, Washington, DC, June 19–24, 1988*. The majority of the papers presented at this symposium have been published in *J. Chromatogr.*, Vols. 458 (1988), 459 (1988) and 461 (1989).

0021-9673/89/$03.50

arating both the two proinsulins and the conversion products, insulin I and II and C-peptide I and II. The separation of proinsulins and insulins was previously attempted using polyacrylamide gel electrophoresis (PAGE) at pH 4.4[3], 8.9[8] and HPLC[9–11]. Only acid PAGE can separate the two proinsulins, but none of the systems is capable of resolving all conversion products.

The aim of the present study was to develop an RP-HPLC system which allows separation of all six main products of the insulin biosynthesis in rat and mouse islets in order to study the regulation of the biosynthesis of the two non-allelic insulin gene products which occurs in these species. The identification of the individual peaks after RP-HPLC fractionation of extracts from 4700–9500 islets was based upon amino acid sequencing using microsequencing and radiosequencing. The conversion of the two rat proinsulins into insulin I and II and C-peptide I and II was elucidated in pulse-chase experiments.

MATERIALS AND METHODS

RP-HPLC

The HPLC system consisted of Waters M6000A pumps, a WISP 710A, a 660 solvent programmer, a 730 data module and a Pye Unicam LC-UV detector. The columns were LiChrosorb RP-18, 5 μm, 250 mm × 4.0 mm I.D. (Merck) and Ultrasphere ODS, 5 μm, 250 mm × 4.6 mm I.D. (Beckman). Acetonitrile was used as the organic modifier in 0.125 *M* triethylammonium phosphate (TEAP), pH 4.0 or 0.1% trifluoroacetic acid (TFA). The columns were eluted at 1 ml/min using linear acetonitrile gradients from 25 to 30% and 30 to 36%, respectively. The column eluate was monitored at 210 nm and collected in 0.5- or 0.3-min fractions (FRAC 300 fraction collector, Pharmacia). All separations were performed at room temperature.

Reagents

Phosphoric acid (p.a.) was from Merck, trifluoroacetic acid (Peptide Synthesis Grade) from Applied Biosystems, triethylamine (99%) from Janssen Chimica and acetonitrile (HPLC grade S) from Rathburn Chemicals. All other chemicals were of analytical reagent grade. Distilled water was drawn from a Millipore Milli Q plant and all buffers were filtered (0.45 μm, Millipore) and vacuum/ultrasound degassed before use.

Standards

Medium from cultured newborn rat islet cells containing 44 μg/ml insulin I + II as well as equimolar amounts of C-peptide I and II, rat pancreatic polypeptide (Penninsula) and porcine glucagon (NOVO) were used.

Islet isolation and culture

Islets from newborn (3–5 days) Wistar rats and 3-weeks-old NMRI mice fed with 5% glucose overnight were isolated by the collagenase method [12] and cultured at 37°C in RPMI 1640 supplemented with 10% newborn calf serum.

Pulse-chase labelling

One hundred newborn rat islets were precultured for 2 weeks and pulse-labelled

with 50 μCi [^{3}H]leucine (130 Ci/mmol) and 50 μCi [^{35}S]methionine (> 1000 Ci/mmol) from Amersham for 20 min followed by chase periods with non-radioactive amino acids from 0 to 40 min. For preparative purposes, 5000–9500 rat islets were precultured for 2–7 days and labelled for 60 min with 250 μCi [^{3}H]leucine and 250 μCi [^{35}S]methionine. All pulse-chase experiments were performed at 37°C.

Sample preparation

Harvested islets were homogenized by sonication or extracted in 3 *M* acetic acid containing 0.1% human serum albumin, and centrifuged at 10 000 *g* to remove any particulate content.

Radioactivity measurement

A 4-ml volume of Optiphase "HiSafe" (LKB) was added to each fraction followed by counting in a Packard Tri-Carb liquid scintillation counter (Model 460 C).

Radioimmunoassay

Collected fractions containing TFA–acetonitrile were dried in a Speed-Vac Concentrator (Savant). Radioimmunological determination of insulin was performed using rat insulin (NOVO) as a standard and anti-mouse insulin antibodies (developed in this laboratory) as described[13]. Radioimmunological determination of glucagon was performed using a kit from NOVO[14].

Amino acid analysis

Amino acid analysis was performed using the PICO-TAG method (Waters) as described by the manufacturer.

Amino acid sequencing

Amino acid sequencing was performed using a gas-phase protein sequencer (Applied Biosystems, model 475A) equipped with on-line HPLC analysis (120A Analyser). In radiosequencing an aliquot (60%) from each step was collected and the radioactivity counted as described above.

RESULTS

Separation of polypeptides from rat islets

The separation of rat insulins (I and II) and C-peptides (I and II) secreted to the culture medium from rat islets using two different RP-HPLC columns and buffer systems is shown in Fig. 1. The peaks shown with dashed lines are due to standards of rat pancreatic polypeptides (peak 5) and porcine glucagon (peak 6) (same amino acid sequence as rat glucagon[15]). The identities of the C-peptide I (peak 2), C-peptide II (peak 1), insulin I (peak 3) and insulin II (peak 4) were verified by amino acid analysis and amino acid sequencing. The three chromatograms all show baseline separation of the analyzed polypeptides.

Preparative RP-HPLC fractionation of 1400 rat islets is shown in Fig. 2. The positions of the insulin and glucagon peaks were confirmed using radioimmunological analyses of the individual fractions. The later peaks F, G, H and I were insulin immunoreactive, and preliminary amino acid analysis and sequencing indicates a

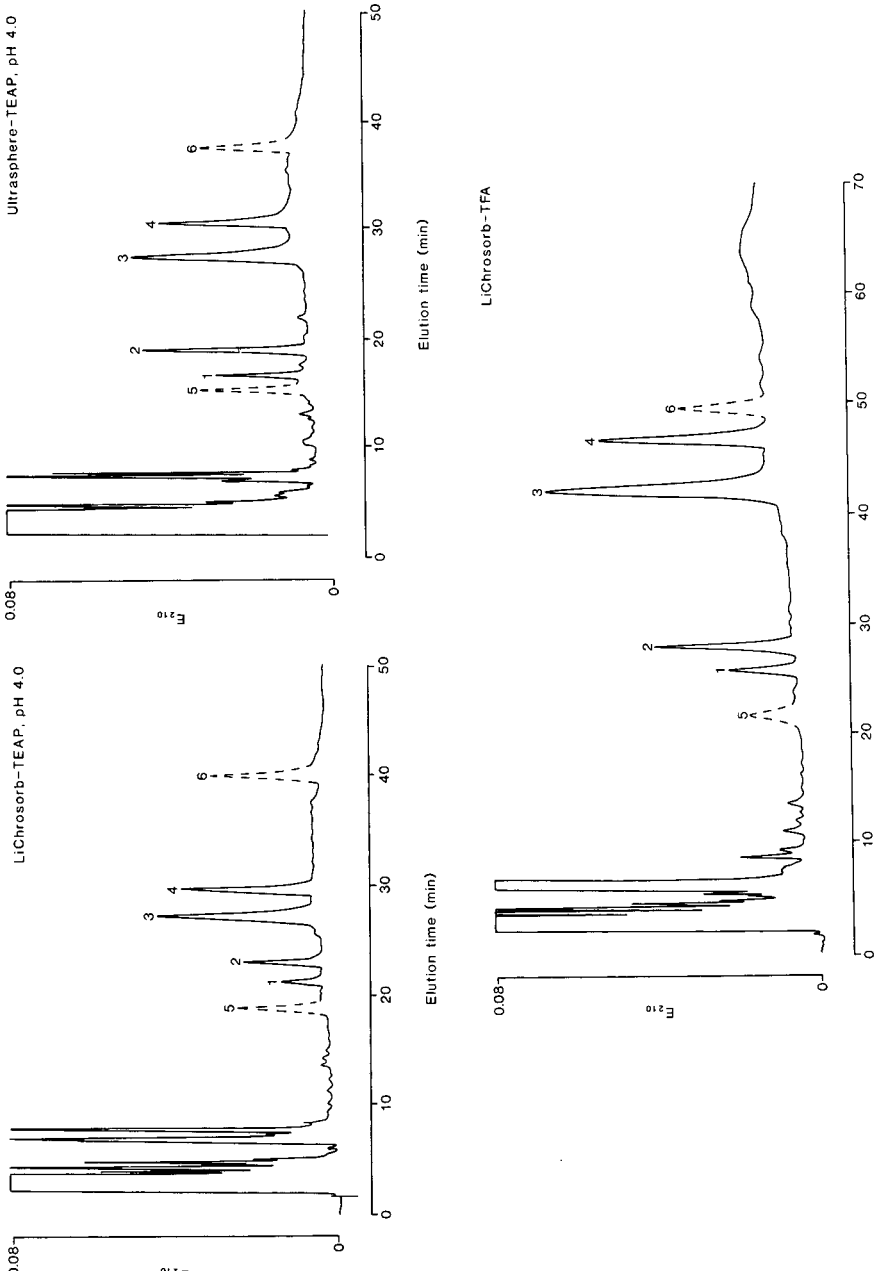

Fig. 1. RP-HPLC separation of rat islet cell culture medium containing insulin I (peak 3), insulin II (peak 4), C-peptide I (peak 2) and C-peptide II (peak 1) plus added rat pancreatic polypeptide (peak 5) and porcine glucagon (peak 6). Upper left and lower panel: LiChrosorb RP-18, 5 μm, 250 mm × 4.0 mm I.D. Upper panel right: Ultrasphere ODS, C_{18}, 5 μm, 250 mm × 4.6 mm I.D. The columns were eluted with a linear acetonitrile gradient (25 to 30%) in 0.125 *M* TEAP, pH 4.0 during 30 min (upper panels) or 30 to 36% in 0.1% TFA during 60 min (lower panel). Flow-rate 1.0 ml/min.

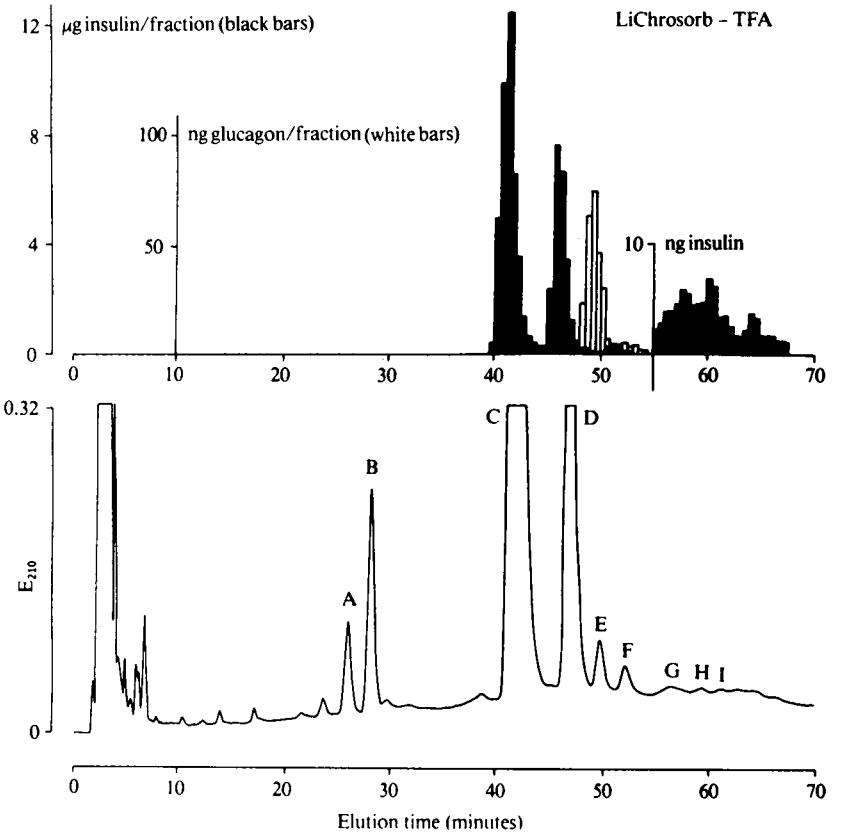

Fig. 2. RP-HPLC separation of 1400 rat islets extracted in 3 *M* acetic acid using a LiChrosorb RP-18, 5 μm, 250 mm × 4.0 mm I.D. column eluted at 1.0 ml/min with a linear acetonitrile gradient (30 to 36%) in 0.1% TFA during 60 min. Black bars represent insulin immunoreactivity, white bars represent glucagon immunoreactivity measured in the 0.5-min fractions collected. Peaks: A = C-peptide II; B = C-peptide I; C = insulin I; D = insulin II; E = glucagon; F and G = proinsulin-like; H = proinsulin I; I = proinsulin II.

proinsulin-like amino acid composition. Peaks.H and I show B-chain sequences corresponding to 18 and 20 steps of proinsulin I and II, respectively. The amino acid differences between rat proinsulin I and II are shown in Fig. 3.

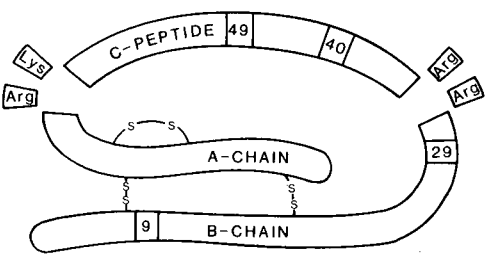

Fig. 3. Products of the conversion of proinsulin into insulin in rat islets. Amino acid differences in rat proinsulin I and II are in position 9 = Pro/Ser, position 29 = Lys/Met, position 40 = Pro/Ala and position 49 = Glu/Gly, respectively.

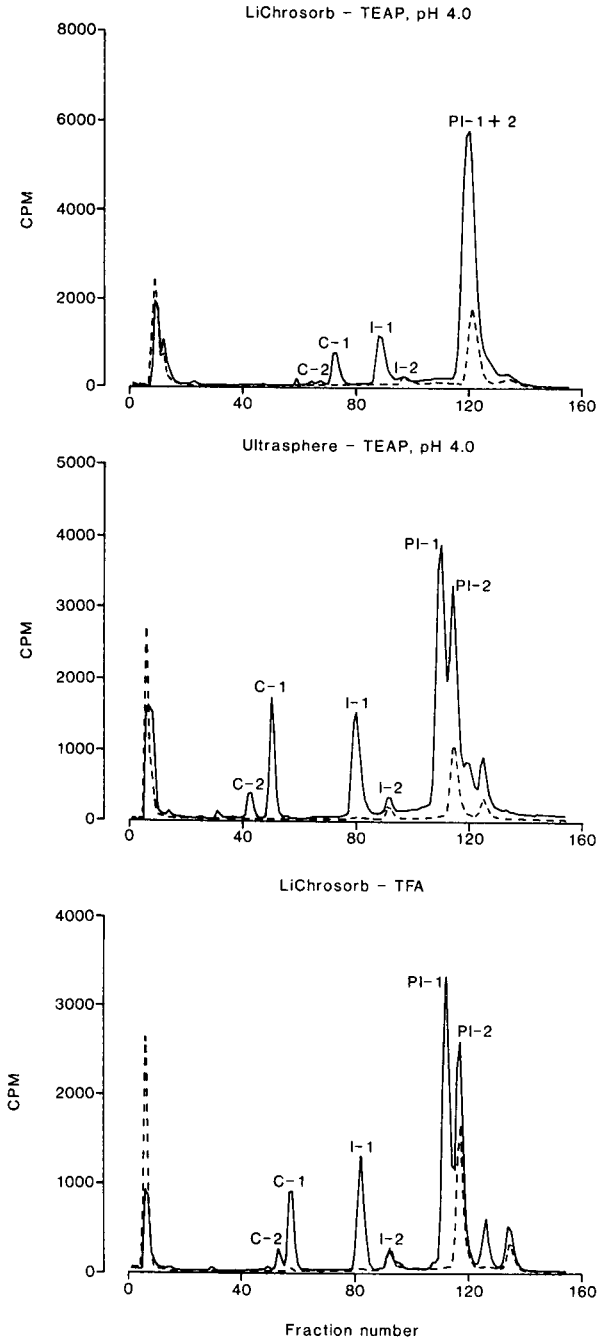

Fig. 4. RP-HPLC separation of rat islets pulse-labelled for 60 min with [^{3}H]leucine and [^{35}S]methionine as described in the legend to Fig. 1. The solid line represents ^{3}H-radioactivity, the dashed line ^{35}S-radioactivity. The peaks are C-1 and C-2 (C-peptides I and II), I-1 and I-2 (insulins I and II), PI-I and PI-2 (proinsulins I and II).

Radioactive labelling of rat islets

Rat islets, 5000 and 9500 were pulse-labelled for 60 min with [^{3}H]leucine (present in both proinsulin and insulin I and II) and [^{35}S]methionine (present only in proinsulin and insulin II). Aliquots of acetic acid extracts of the labelled islets were fractionated using the same HPLC columns and buffers as in Fig. 1. The resulting radioactivity patterns are shown in Fig. 4. The radioactivity in the first fractions is due to remaining free amino acids. The next four peaks correspond to the C-peptides and insulin peaks identified in Fig. 1. The expected proinsulin peaks eluted around fractions 110–120 were separated in two of the systems.

The labelled islets were fractionated preparatively in the LiChrosorb–TFA system (lower panel in Fig. 4) and pooled fractions from the two "proinsulin" peaks were subjected to microsequencing. The correct amino acids were identified in 39 and

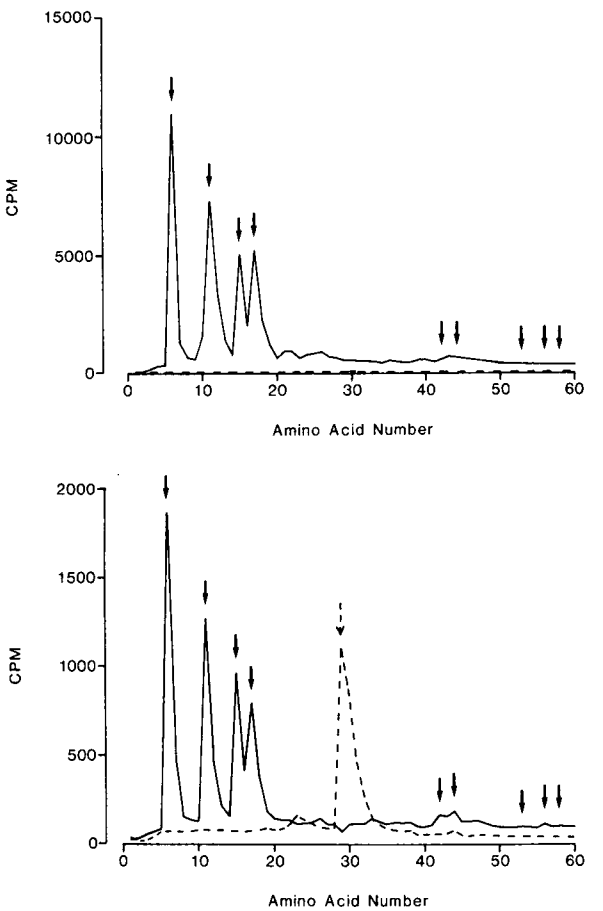

Fig. 5. Radiosequencing of pooled proinsulin fractions from preparative RP-HPLC fractionation of 5000 or 9500 rat islets pulse-labelled for 60 min with [^{3}H]leucine and [^{35}S]methionine. The solid line represents ^{3}H radioactivity, the dashed line ^{35}S-radioactivity. The solid arrows indicate the known positions of leucines, the dashed arrow the position of methionine. Upper panel shows the sequencing of proinsulin I, lower panel that of proinsulin II.

36 steps for proinsulin I and II, respectively, corresponding to 9 and 6 steps in the C-peptide regions of proinsulin I and II, respectively.

Taking advantage of the [^{3}H]leucine and [^{35}S]methionine labelling, it was possible to demonstrate the correct position of Leu-6, -11, -15, -17, and even Leu-42 and -44 can be detected, see Fig. 5. The presence of [^{35}S]methionine in position 29 in proinsulin II was also clearly demonstrated.

Separation of polypeptides present in mouse islets

Fig. 6 shows the RP-HPLC fractionation of acetic acid extracts of isolated mouse islets compared to extracted rat islets. It is seen that the retention times for the

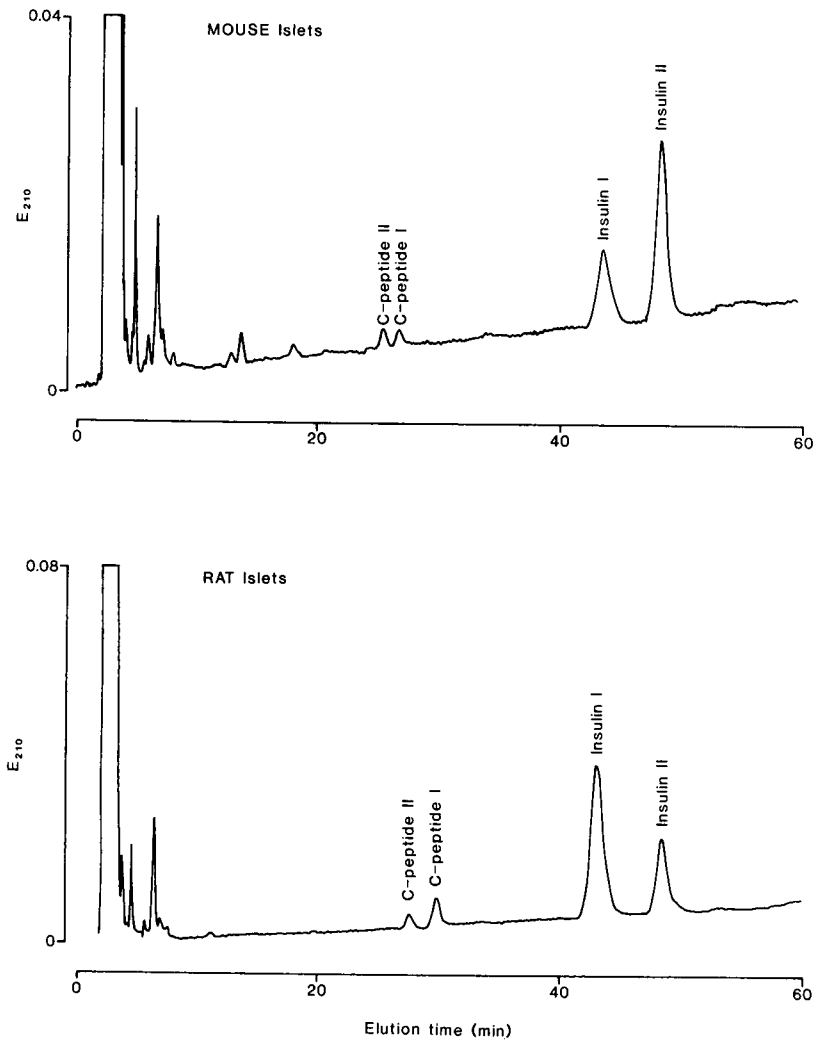

Fig. 6. RP-HPLC separation of acetic acid extracts of isolated mouse and rat islets using a LiChrosorb RP-18, 5-μm column, 250 × 4.0 mm I.D. eluted at 1.0 ml/min with a linear acetonitrile gradient (30 to 36%) in 0.1% TFA during 60 min.

presumed mouse C-peptides are somewhat lower than those for the rat C-peptides. Mouse islets (4700) were extracted with 3 *M* actic acid and the extract separated using the LiChrosorb–TFA system, analogously with the separation in Fig. 6. The expected C-peptide fractions were pooled and subjected to microsequencing. The resultant sequences are shown in Table I in comparison with the rat C-peptide sequences.

Biosynthesis of insulin in rat islets

Pulse-chase labelling was performed at 37°C with [^{3}H]leucine and [^{35}S]methionine in samples containing 100 rat islets. The pulse period was 20 min, ensuring that only proinsulins were labelled. The chase periods were 0, 10, 20 and 40 min. RP-HPLC fractionation of the media showed that no radioactive insulin and C-peptide were secreted during the pulse-chase experiment. RP-HPLC fractionation of the islet extracts separated proinsulin I and II, insulin I and II as well as C-peptide I and II

TABLE I

AMINO ACID SEQUENCES OF RAT AND MOUSE C-PEPTIDES

Amino acid number	*Rat C-I*	*Mouse C-I*	*Rat C-II*	*Mouse C-II*
1	Glu	Glu	Glu	Glu
2	Val	Val	Val	Val
3	Glu	Glu	Glu	Glu
4	Asp	Asp	Asp	Asp
5	Pro	Pro	Pro	Pro
6	Gln	Gln	Gln	Gln
7	Val	Val	Val	Val
8	Pro	Glu*	Ala	Ala
9	Gln	Gln	Gln	Gln
10	Leu	Leu	Leu	Leu
11	Glu	Glu	Glu	Glu
12	Leu	Leu	Leu	Leu
13	Gly	Gly	Gly	Gly
14	Gly	Gly	Gly	Gly
15	Gly	Ser*	Gly	Gly
16	Pro	Pro	Pro	Pro
17	Glu	*	Gly	Gly
18	Ala	*	Ala	Ala
19	Gly	Gly	Gly	Gly
20	Asp	Asp	Asp	Asp
21	Leu	Leu	Leu	Leu
22	Gln	Gln	Gln	Gln
23	Thr	Thr	Thr	Thr
24	Leu	Leu	Leu	Leu
25	Ala	Ala	Ala	Ala
26	Leu	Leu	Leu	Leu
27	Glu	Glu	Glu	Glu
28	Val	Val	Val	Val
29	Ala	Ala	Ala	Ala
30	Arg	Arg	Arg	Gln*
31	Gln	Gln	Gln	Gln

* Difference in amino acid sequence of the mouse C-peptides compared to the rat C-peptides.

TABLE II

INSULIN BIOSYNTHESIS IN RAT ISLETS

Conversion of proinsulin I and II into insulin I and II in pulse-chase experiments with [^{3}H]leucine and [^{35}S]methionine.

Pulse (min)	*Chase (min)*	*Proinsulin I to insulin I (%)*	*Proinsulin II to insulin II (%)*	*Insulin I/insulin II*	
				UV	*cpm*
20	0	0	0	2.1	–
20	10	4.8	0	2.1	–
20	20	11.6	3.4	2.2	5.4
20	40	47.4	16.1	1.9	6.0

(same separation pattern as in Fig. 4, lower panel). The ^{3}H- and ^{35}S-radioactivities in the fractions corresponding to proinsulin I and II and insulin I and II were added and the molar amounts of proinsulin and insulin were calculated taking account of the difference in leucine content (11 leucine and 6 leucine, respectively). The calculated conversions of proinsulins into insulins are shown in Table II.

DISCUSSION

The presence of two non-allelic insulin genes in mouse and rat has raised the question how the expression of the two genes is regulated. A prerequisite for a detailed analysis of the latter is a separation system which allows identification of the individual biosynthesis and processing prodcuts, *i.e.*, the two proinsulins, insulins and C-peptides.

Two HPLC methods were recently described for the study of insulin biosynthesis in rat islets[10,11]. Neither of these systems separated the two proinsulins and the C-peptides were not identified.

By comparing different RP-HPLC systems which have been applied for the separation of insulin and related peptides, we have developed two systems which permit separation of these six major peptides (Figs. 1 and 2). Compared with the Ultrasphere–TEAP system we found that the LiChrosorb–TFA system gave a better separation of the two rat proinsulins and as the TFA buffer can be lyophilized the fractions can be subjected to amino acid analysis and sequencing without buffer exchange.

By a combination of microsequencing and radiosequencing we have identified the individual peaks by comparison with published sequence data: rat C-peptide I and II, rat insulin I and II and rat proinsulin I and II (partial sequences).

The elution order of insulin I and II was reversed in the HPLC system used by Gishizky and Grodsky[11] compared to out findings in spite of the similarity in buffers, but was perhaps caused by the use of another HPLC column (Dupont PEP-R C_8 instead of LiChrosorb). We also noticed a reversal of the elution order of mouse C-peptide I and II on the LiChrosorb column when changing from TFA to TEAP, pH 4.0[16], demonstrating the versatility of he HPLC systems.

Both after preparative fractionation and after labelling with radioactive amino

acids, two peaks with higher retention times than those of the proinsulins were observed. Since they showed insulin-like immunoreactivity and proinsulin-like amino acid composition, appeared after the initial proinsulin synthesis and could be converted into the two insulins by trypsin and carboxypeptidase B (ref. 17), they probably represent intermediary split products of the proinsulins, although human split proinsulins appear earlier than human proinsulin in this system (data not shown). The final identity of these peaks must await isolation of more material.

During this study we noted that the molar ratio between insulin and C-peptide was 1 in the culture medium and the newly synthesized products of the islets, but always much higher in the stored insulin (compare Fig. 1, lower panel and Fig. 4, lower panel with Fig. 6, lower panel). Whether this is due to a more rapid intracellular degradation of the C-peptides or to insufficient extraction is not known at present.

The sequences of the two mouse insulins have long been known to be identical to those of the rat insulins[6], but it was only recently that the sequences of the C-peptides were found to differ as predicted by the nucleotide sequences of the c-DNA[7]. These differences give a change in retention time of the mouse C-peptides from those of the rat (Fig. 6). By amino acid sequencing of the isolated peaks we confirmed the two amino acid deletion in the mouse C-peptide I, and two and one amino acid differences from rat C-peptide I and II, respectively (Table I).

The RP-HPLC separation was used to study the conversion of the two rat proinsulins into the corresponding insulins (Table II). It was observed that the ratio between insulin I and II was about 2 in the stored insulin (UV absorption at 210 nm) and as high as 5–6 in the newly synthesized insulins (^{3}H-radioactivity) as also reported by Gishizky and Grodsky[11]. The calculated conversion rates showed an higher conversion rate of proinsulin I than of proinsulin II (Table II) as already suggested by Clark and Steiner[3]. This is also supported by our previous finding that inhibition of the insulin biosynthesis with interleukin-1 resulted in an increased ratio between newly synthesized insulin I and II which can be explained by a more pronounced attenuation of the conversion of proinsulin II[18].

We also observed that the usual ratio between insulin I and II in the rat, about 2:1, was reversed in the mouse, about 1:2 (Fig. 6). A similar ratio was reported by Markussen[6] in crystalline mouse insulin, but was assumed to be due to a selection by the separation procedure. By immunoelectrophoresis, Kakita *et al.*[19] always found more insulin I than II in the pancreas of both rats and mice. Variations in the ratio with age and metabolic state have been reported[19–21] but the effect of glucose was not confirmed by HPLC[22]. In rat insulinomas a ratio of 10:1 has been found although the two genes were equally transcribed[23]. Recently, neither age, glucose nor growth hormone were found to change the ratio between transcription of the two genes in rats *in vitro*[24], indicating that if a change in the ratio between the two insulins occurs, it is probably due to a variation in translation, conversion or degradation. Further studies on the insulin biosynthesis in mouse islets may reveal by which mechanism the odd ratio occurs.

ACKNOWLEDGEMENTS

Dr. Steinunn Bækkeskov is thanked for providing mouse and rat islet cell material used in parts of this study and Dr. Stephen Bayne for performing the amino acid

analysis. We thank Linda Larsø, Ragna Jørgensen, Erna Engholm Pedersen, Lene Møller-Petersen, Ingelise Fabrin, Tina Nielsen and Hanne Richter-Olesen for skilful technical assistance.

REFERENCES

1 B. S. Welinder, H. H. Sørensen and B. Hansen, *J. Chromatogr.*, 361 (1986) 357–367.
2 L. F. Smith, *Am. J. Med.*, 40 (1966) 449–455.
3 J. L. Clark and D. F. Steiner, *Proc. Natl. Acad. Sci., U.S.A.*, 62 (1969) 278–285.
4 B. Cordell, G. Bell, E. Tischer, F. M. De Noto, A. Ulrich, R. Pictet, W. J. Rutter and H. M. Goodman, *Cell*, 18 (1979) 533–543.
5 P. Lomedico, N. Rosenthal, A. Efstratiadis, N. Gilbert, R. Kofodner and R. Tizard, *Cell*, 18 (1979) 545–558.
6 J. Markussen, *Int. J. Pept. Protein Res.*, 3 (1971) 149–155.
7 B. M. Wentworth, I. M. Schaefer, L. Villa-Komaroff and J. M. Chirgwin, *J. Mol. Evol.*, 23 (1986) 305–312.
8 L. B. Rall, R. L. Pictet and W. J. Rutter, *Endocrinology*, 105 (1979) 835–841.
9 B. D. Noe, G. Debo and J. Spiess, *J. Cell Biol.*, 99 (1984) 578–587.
10 P. A. Halban, C. J. Rhodes and S. E. Shoelson, *Diabetologia* 29 (1986) 893–896.
11 M. L. Gishizky and G. M. Grodsky, *FEBS Lett.*, 2 (1987) 227–231.
12 J. Brunstedt, J. H. Nielsen and Å. Lernmark, in J. Larner and S. Pohl (Editors), *Methods in Diabetes Research*, Vol. 1, Wiley, New York, Toronto, 1984, Part C, pp. 254–258.
13 L. G. Heding, *Diabetologia*, 8 (1972) 260–266.
14 L. G. Heding, *Diabetologia*, 7 (1971) 10–19.
15 F. Sundby and J. Markussen, *Horm. Metab. Res.*, 3 (1971) 184–187.
16 S. Efrat, S. Baekkeskov, S. Linde, H. Kofod, D. Spector, M. Delannoy, S. Grant and D. Hanahan, *Proc. Natl. Acad. Sci., U.S.A.*, in press.
17 S. Linde, unpublished results.
18 B. S. Hansen, J. H. Nielsen, S. Linde, G. A. Spinas, B. S. Welinder, T. Mandrup-Poulsen and J. Nerup, *Biomed. Biochim. Acta*, 47 (1988) 305–309.
19 K. Kakita, K. O'Connell and M. A. Permutt, *Diabetes*, 31 (1982) 841–845.
20 K. Kakita, S. Giddings and M. A. Permutt, *Proc. Natl. Acad. Sci. U.S.A.*, 79 (1982) 2803–2807.
21 M. De Gasparo and M. Faupel, *J. Chromatogr.*, 357 (1986) 139–146.
22 C. J. Rhodes, C. A. Lucas and P. A. Halban, *FEBS Lett.*, 215 (1987) 179–182.
23 B. Cordell, D. Diamond, S. Smith, J. Pünter, H. H. Schöne and H. M. Goodman, *Cell*, 31 (1982) 531–542.
24 S. J. Giddings and L. R. Carnaghi, *J. Biol. Chem.*, 263 (1988) 3845–3849.

Journal of Chromatography, 462 (1989) 255–268
Elsevier Science Publishers B.V., Amsterdam — Printed in The Netherlands

CHROM. 20 999

HIGH-PERFORMANCE LIQUID CHROMATOGRAPHIC SEPARATION OF MEMBRANE PROTEINS ISOLATED FROM ERYTHROCYTE GHOSTS

BENNY S. WELINDER*
Hagedorn Research Laboratory, Niels Steensensvej 6, DK-2820 Gentofte (Denmark)
HANS H. SØRENSEN
Nordisk Gentofte A/S, DK-2820 Gentofte (Denmark)
and
BRUNO HANSEN
Hagedorn Research Laboratory, Niels Steensensvej 6, DK-2820 Gentofte (Denmark)
(First received June 28th, 1988; revised manuscript received September 22nd, 1988)

SUMMARY

Membrane proteins extracted from erythrocyte ghosts with sodium dodecyl sulphate (SDS), 3-(3-cholamidopropyl)-dimethylamminopropane sulfonate (CHAPS) or octylglucoside have been analyzed in various reversed-phase high-performance liquid chromatographic systems. Only SDS was able to solubilize considerable amounts of membrane proteins with mol.wt. $>15\,000$ daltons, but these membrane proteins were recovered in poor yield from a silica-based C_4 column eluted with an acetonitrile gradient in trifluoroacetic acid (TFA). A resin-based phenyl column eluted with a similar TFA–acetonitrile gradient was found to be a better choice with respect to the recovery of membrane proteins with mol.wt. $>15\,000$ daltons, and when this column was eluted with an acetic acid gradient with increasing amounts of acetonitrile, erythrocyte ghost membrane proteins solubilized in SDS (mol.wt. 10 000–200 000 daltons) were separated in six major and several minor components with satisfactory recovery.

INTRODUCTION

Due to their lipophilic character, the solubilization and separation of membrane proteins normally require the use of detergents and classical protein purification strategies —designed for water-soluble proteins— are of limited value. Consequently the number of reports dealing with high-performance liquid chromatographic (HPLC) separation of membrane proteins is limited. The development of stationary phases for protein separation has been directed towards the

* Presented in part at the *12th International Symposium on Column Liquid Chromatography, Washington, DC, June 19–24, 1988*. The majority of the papers presented at this symposium have been published in *J. Chromatogr.*, Vols. 458 (1988), 459 (1988) and 461 (1989).

0021-9673/89/$03.50

water-soluble proteins with molecular weight (MW) <25 000 daltons, and reversed-phase separation has been the most popular separation principle. Only a few new stationary phases for high-performance ion-exchange chromatography (HPIEC), hydrophobic interaction chromatography (HIC) or size-exclusion chromatography (SEC) have been commercially available in the last few years.

The separation principle in reversed-phase (RP)-HPLC is hydrophobic interaction between the stationary phase and hydrophobic areas in the sample molecules, but due to the extremely high hydrophobicity of most membrane proteins, the binding forces between membrane proteins and most RP stationary phases are too strong. In order to elute the membrane proteins, extremely rigorous mobile phases have to be used, and even then many membrane proteins are recovered in very poor yield.

Moreover, the detergents normally used for solubilizing many membrane proteins are not compatible with RP stationary phases for protein separation. Consequently the most common HPLC techniques used for the purification of membrane proteins have been HPSEC (which may be used in the presence of ionic as well as non-ionic detergents) and —to a lesser extent— HPIEC and HIC (compatible with non-ionic detergents).

We have recently evaluated a number of commercially available HIC stationary phases for their potential use for the separation of membrane proteins from erythrocyte ghosts using mobile phases containing 3-(3-cholamidopropyl)-dimethylamminopropane sulfonate (CHAPS), octylglucoside or sulfobetaine[1]. In this report we present the separation of erythrocyte membrane proteins extracted with sodium dodecyl sulphate (SDS), CHAPS or octylglucoside using a silica-based as well as a resin-based reversed-phase column eluted with trifluoroacetic acid (TFA)–acetonitrile. A novel mobile phase additive (acetic acid) was evaluated in the resin-based RP column, and the resulting separations of the extracted membrane proteins have been evaluated with SDS polyacrylamide gel electrophoresis (PAGE) followed by silver staining.

MATERIALS AND METHODS

HPLC equipment

Pumps: Waters M6000A or M510, Gynkotek 300C or Spectra Physics SP 8700. Sample injectors: U6K, WISP 710B or 712 (Waters), Rheodyne 7125. Gradient controllers: Waters 760, 721 or 840 chromatography control station, Gynkotek 250 B. UV-Photometers: Linear UVIS 200, Waters M440 and M481 or Hitachi L4200. Columns: TSK Phenyl 5 PW RP (75 mm × 4.6 mm I.D.) (Toyo Soda), Nucleosil C_4 (300 Å) (250 mm × 4.0 mm I.D.) (Macherey Nagel).

The mobile phases are given in the figure legends.

Chemicals

TFA was sequential grade (Applied Biosystems). All other chemicals were of HPLC quality or similar purity. Water was drawn from a Milli-Q plant, and the buffers were Millipore-filtered (0.45 μm) and degassed (ultrasound/vacuum) before use.

The columns were operated at room temperature (*ca.* 22°C) at 1.0 or 0.5 ml/min. The UV absorption of the column eluate was measured continuously (210 or 280 nm) and fractions were collected manually.

Samples

Erythrocyte ghosts were prepared as described[2] with the exception that trasylol was added to the washing buffer (0.15 mg/ml) in order to reduce the enzymatic digestion during the washing procedure. The erythrocyte ghosts were extracted with 1% SDS, CHAPS or octylglucoside in 10 m*M* Tris · HCl–5 m*M* EDTA pH 8.0 and remaining solid material was removed by centrifugation before analysis.

The protein concentration in the SDS extract was 2.2–5.1 mg/ml (Bio-Rad Coomassie Blue protein assay, serum albumin as a standard).

SDS-PAGE was performed in a Pharmacia Phast-Gel apparatus (8–25% gradient gels with separation range 8000–300 000 daltons). The electrophoresis and the silver staining were performed as described by the manufacturer[3].

RESULTS

TSK Phenyl 5 PW RP

The separation of SDS-solubilized membrane proteins from erythrocyte ghosts using the TSK Phenyl 5 PW RP column eluted with 0.1% TFA–acetonitrile is shown in Fig. 1. Although the acetonitrile gradient was extended up to 90%, virtually no material was eluted from the column in the first half of the chromatogram. Injection of 25 μl membrane protein solution resulted in a separation of 10–15 components with fairly good peak shape (Fig. 1, upper panel) and when the extraction buffer was injected the column had virtually no "memory" from the previous injection of membrane proteins. Injections of 100 and 200 μl membrane protein solution resulted in a gradually reduced separation efficiency (Fig. 1, middle and lower panels).

The fractions marked A–D were diluted in one volume of distilled water and lyophilized. The residue was dissolved in Tris–SDS–mercaptoethanol, placed in a bath of boiling water for 5 min and analyzed by SDS–PAGE (Fig. 2). The membrane proteins are separated into fractions primarily according to their molecular weight: in the first part of the chromatogram two major components with MW slightly lower and higher than the lowest molecular weight marker (14 400 daltons) are seen, and one of them probably represents the globin chains from residual haemoglobin (MW 15 000 daltons). In the last fraction (D), membrane proteins with MW > 80 000 daltons are found, clearly separated from components with lower MW.

Membrane proteins extracted with 1% CHAPS or 1% octylglucoside were analyzed under similar conditions, and the column separations are shown in Fig. 3. When 200 μl membrane protein solution were injected the resulting chromatograms showed that the amount of material eluted from the TSK Phenyl 5 PW RP column was much less for CHAPS and octylglucoside-solubilized membrane proteins than for SDS-solubilized membrane proteins (judged by the area under the UV curves in Fig. 1, lower panel and Fig. 3, upper and lower panels). SDS-PAGE of collected fractions corresponding to the major peaks obtained after fractionation of CHAPS and octylglucoside-solubilized membrane proteins showed no material with MW higher than *ca.* 15 000 daltons (data not shown) in accordance with SDS-PAGE of the three extracts of erythrocyte ghosts (Fig. 4): none or extremely small amounts of material with MW > 15 000 daltons was found in the octylglucoside and the CHAPS extracts, whereas several components with MW from 15 000 to 200 000 daltons were present in the SDS extract.

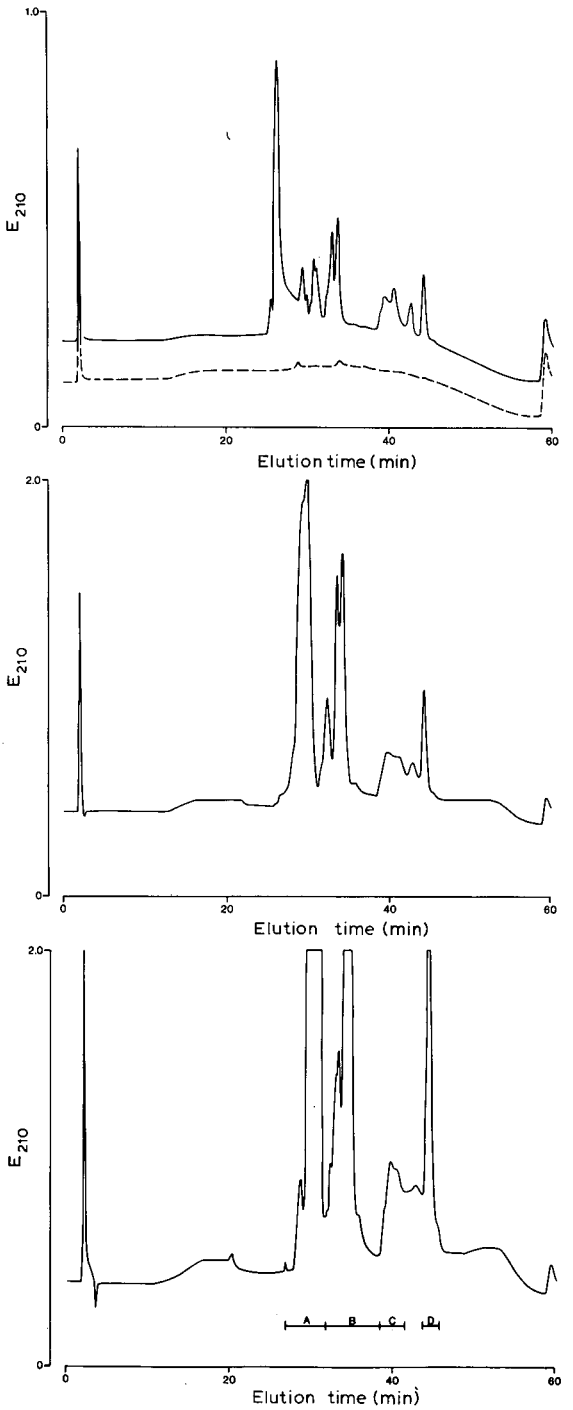

Fig. 1. Separation of 25 (upper panel), 100 (middle panel) and 200 μl (lower panel) SDS-solubilized erythrocyte membrane proteins using a TSK Phenyl 5 PW RP column (75 mm × 4.6 mm I.D.) eluted at 0.5 ml/min with an acetonitrile gradient (0–90%) in 0.1% TFA during 45 min. In the upper panel the broken line indicates the injection of 25 μl of the SDS extraction buffer. E_{210} = Absorbance at 210 nm.

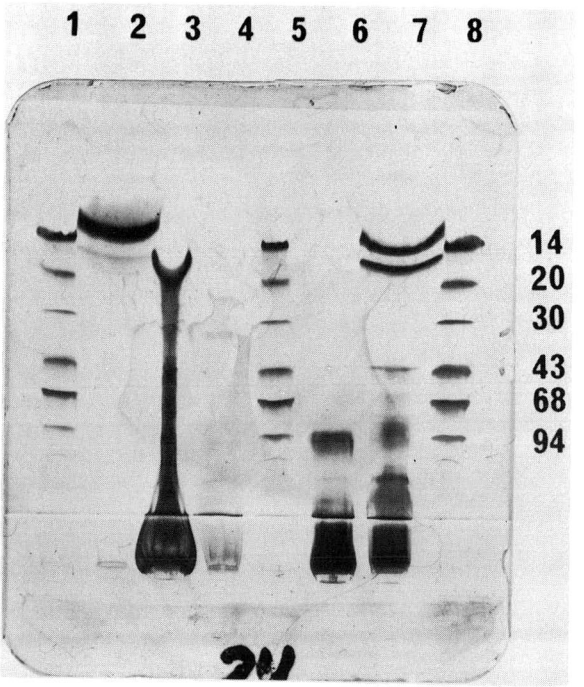

Fig. 2. SDS-PAGE of fractions A–D in Fig. 1 (lower panel). Lanes 1–8 show the separation in 8–25% gradient. SDS-PAGE gels (separation range 8000–200 000 daltons) of molecular weight markers (lanes 1, 5 and 8), fractions A (lane 2), B (lane 3), C (lane 4), D (lane 6) and the total eluate collected from 0 to 60 min (lane 7).

In order to obtain a better distribution between the peptide-like material (with MW $\leqslant$ 15 000 daltons) and membrane proteins with MW 25 000–200 000 daltons the TSK Phenyl 5 PW RP column was eluted with an acetic acid gradient in combination with increasing amounts of acetonitrile, and the resulting separation of SDS-solubilized erythrocyte ghost membrane proteins is shown in Fig. 5. Four major fractions as well as several minor components were separated when 100 μl membrane protein solution were applied to the column. Injection of 250 and 500 μl membrane protein solution resulted in a compressed chromatogram with reduced resolution of the first fractions.

The fractions indicated in Fig. 5, right panel, were analyzed by SDS-PAGE (Fig. 6), and it was demonstrated, that the elution order was correlated to MW in SDS, *i.e.*, the components eluted in the last part of the gradient were those with the highest MW. The last half of the chromatogram corresponded to membrane proteins with MW $>$ 60 000 daltons, and components with MW higher than the upper fractionation range for the SDS-PAGE gel (200 000 daltons) were demonstrated in the last fraction.

It was further demonstrated that the amount of membrane protein which could be extracted with CHAPS was considerably smaller than that obtained using SDS for the extraction, and that the CHAPS-solubilized membrane components were eluted

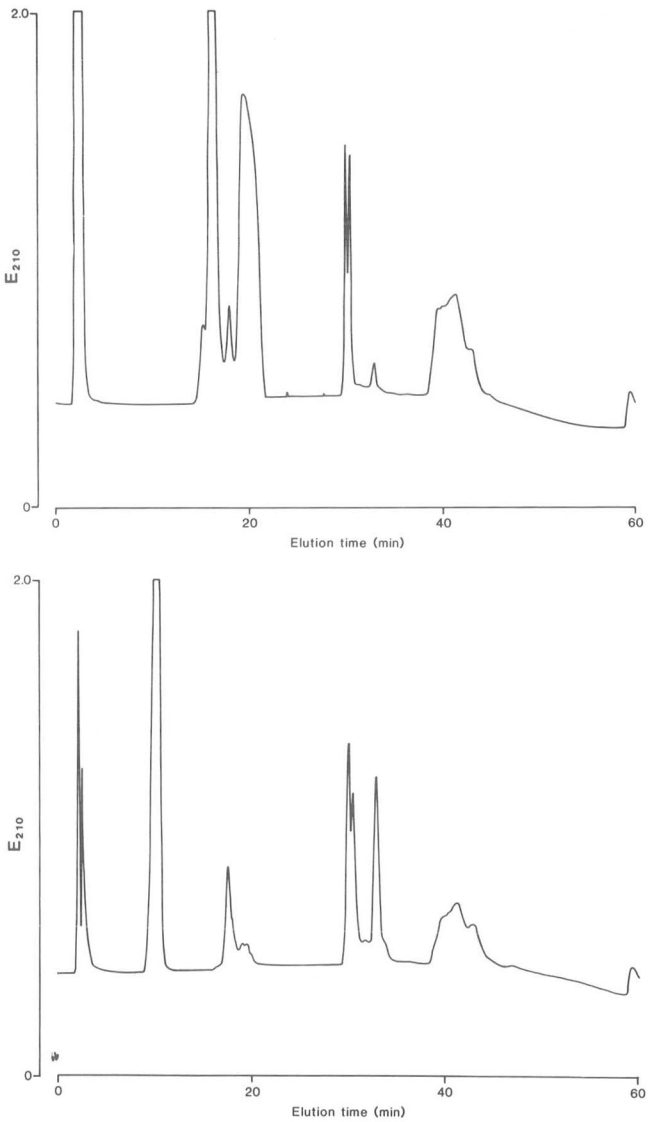

Fig. 3. Separation of 200 μl erythrocyte membrane proteins extracted in 1% CHAPS (upper panel) or in 1% octylglycoside (lower panel). Chromatographic conditions as in Fig. 1.

in the part of the chromatogram which corresponds to membrane components with MW $<$ 15 000 daltons (Fig. 5, lower panel left). The recovery of the membrane proteins in this acetic acid–acetonitrile mobile phase was estimated by comparing the area under the UV curve after gradient elution of membrane protein solution to that obtained after sample injection directly in the UV-photometer. A recovery of 95–100% was measured for the SDS-solubilized membrane proteins.

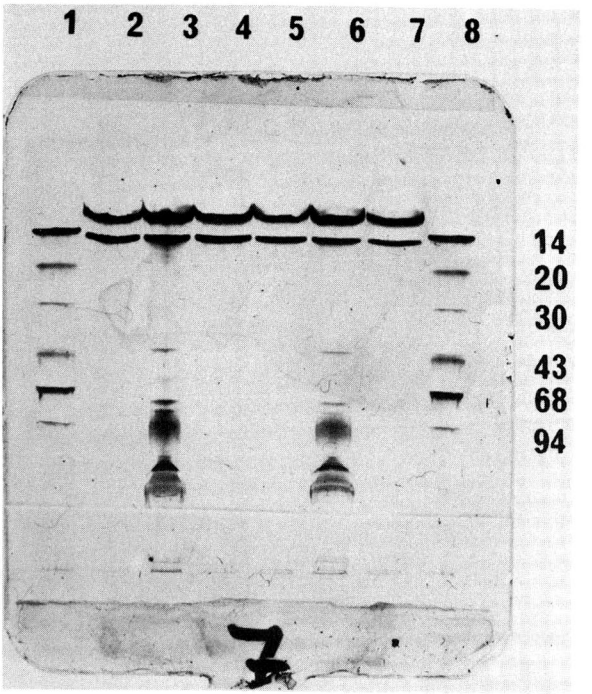

Fig. 4. SDS-PAGE of erythrocyte membrane proteins extracted in 1% SDS (lane 3 and 6), CHAPS (lanes 2 and 5) or octylglucoside (lanes 4 and 7). Molecular weight markers (are in lanes 1 and 8).

If the gradient was changed from the "simple" linear 0–100% to a gradient composed of two linear segments in order to obtain an higher resolution especially in the first part of the chromatogram, an improved separation of erythrocyte membrane proteins was obtained (Fig. 7, upper panel). SDS-PAGE of the individual fractions clearly demonstrated that the resolution was the best obtained so far (Fig. 8) and that isolation of individual membrane proteins may be possible with this technique.

The mobile phases used for eluting the TSK Phenyl 5 PW RP column are slightly more acidic than recommended by the manufacturer, and during continuous use for several months an increase in back pressure and reduced column performance were noticed. Whether this was caused by statioary phase degradation or was the result of several injections of rather crude, unfiltered biological samples is not clear at present, but the column performance as well as the back pressure could be normalized after eluting the column with 0.2 *M* sodium hydroxide and cleaning the dismounted inlet and outlet filters in 50% nitric acid in an ultrasonic bath for 30 min.

Nucleosil C_4

In order to compare a silica-based reversed-phase column to the resin-based TSK Phenyl column, a Nucleosil C_4 (300 Å) column was eluted with an acetonitrile gradient in 0.1% TFA. The membrane proteins extracted in SDS were separated into a major and several minor components (Fig. 7, lower panel), but only the minor

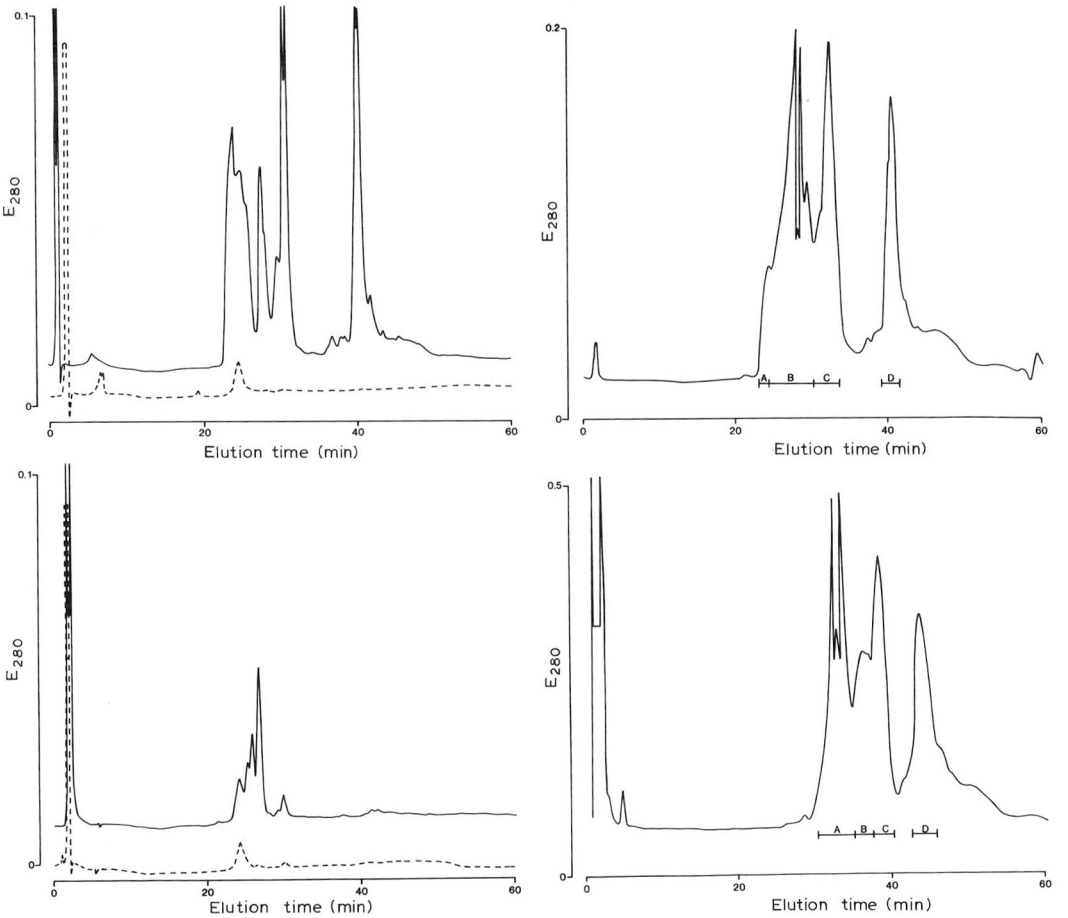

Fig. 5. Separation of 100 (upper panel left), 250 (upper panel right) or 500 μl (lower panel right) SDS-solubilized erythrocyte membrane proteins and 100 μl CHAPS-solubilized erythrocyte membrane proteins (lower panel left). Column: TSK Phenyl 5 PW RP (75 mm × 4.6 mm I.D.). Buffers: A, 20% acetic acid; B, acetic acid–acetonitrile (40:60). A linear gradient from 100% A to 100% B during 45 min was used at 0.5 ml/min. The dashed lines indicate the injection of 100 μl of the buffer used for extraction of the membrane proteins.

peaks in the last part of the chromatogram were found to contain membrane proteins with MW > 15 000 daltons, and a considerably lower amount than was found after elution of the TSK Phenyl column with the similar mobile phase (Fig. 9).

DISCUSSION

The erythrocyte membrane contains *ca.* 52% protein, 40% lipid and 8% carbohydrate[4] and the membrane proteins extracted with detergents have been analyzed primarily using SDS-PAGE[2,4]. It has been demonstrated that SDS-PAGE will separate six major and several minor components with MW from 15 000 (globin chains

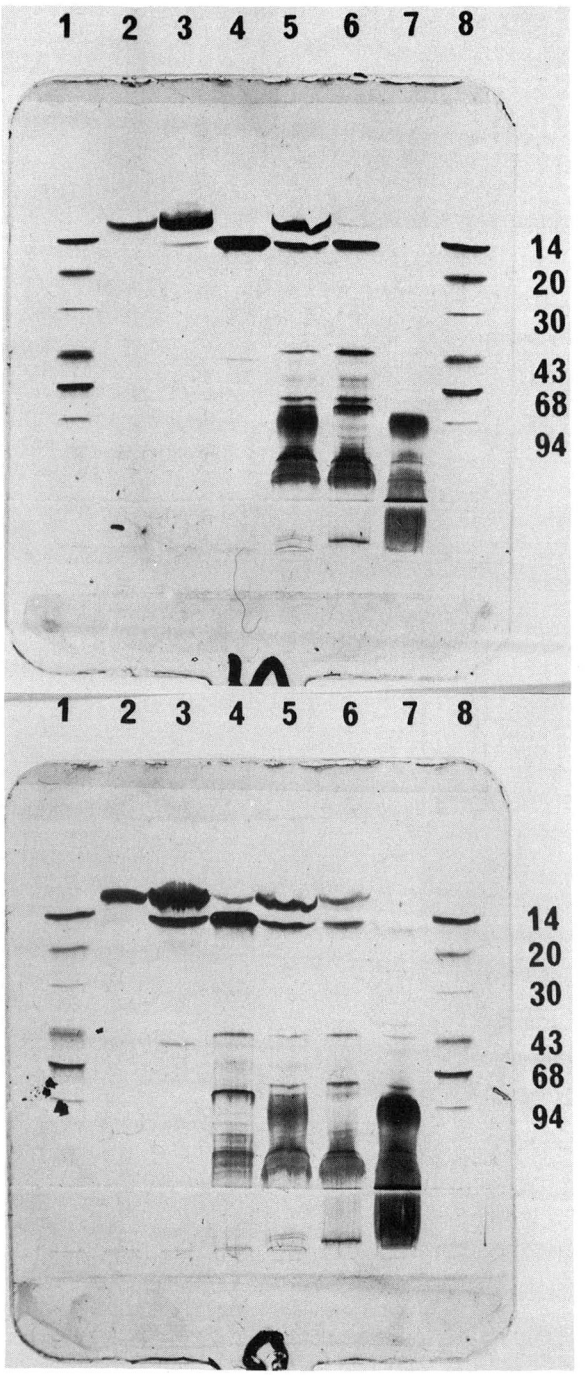

Fig. 6. Upper gel: SDS-PAGE of the fractions indicated in Fig. 5, upper panel right; fraction A (lane 2), the major peak in fraction B (lane 3), the minor peak in fraction B (lane 4), total membrane extract in SDS (lane 5), fraction C (lane 6), fraction D (lane 7) and molecular weight markers (lanes 1 and 8). Lower gel: SDS-PAGE of the fractions indicated in Fig. 5, lower panel right; fraction A (lane 2), fraction B, initial half (lane 3), fraction B, terminal half (lane 4), total membrane extract in SDS (lane 5), fraction C (lane 6), fraction D (lane 7) and molecular weight markers (lane 1 and 8).

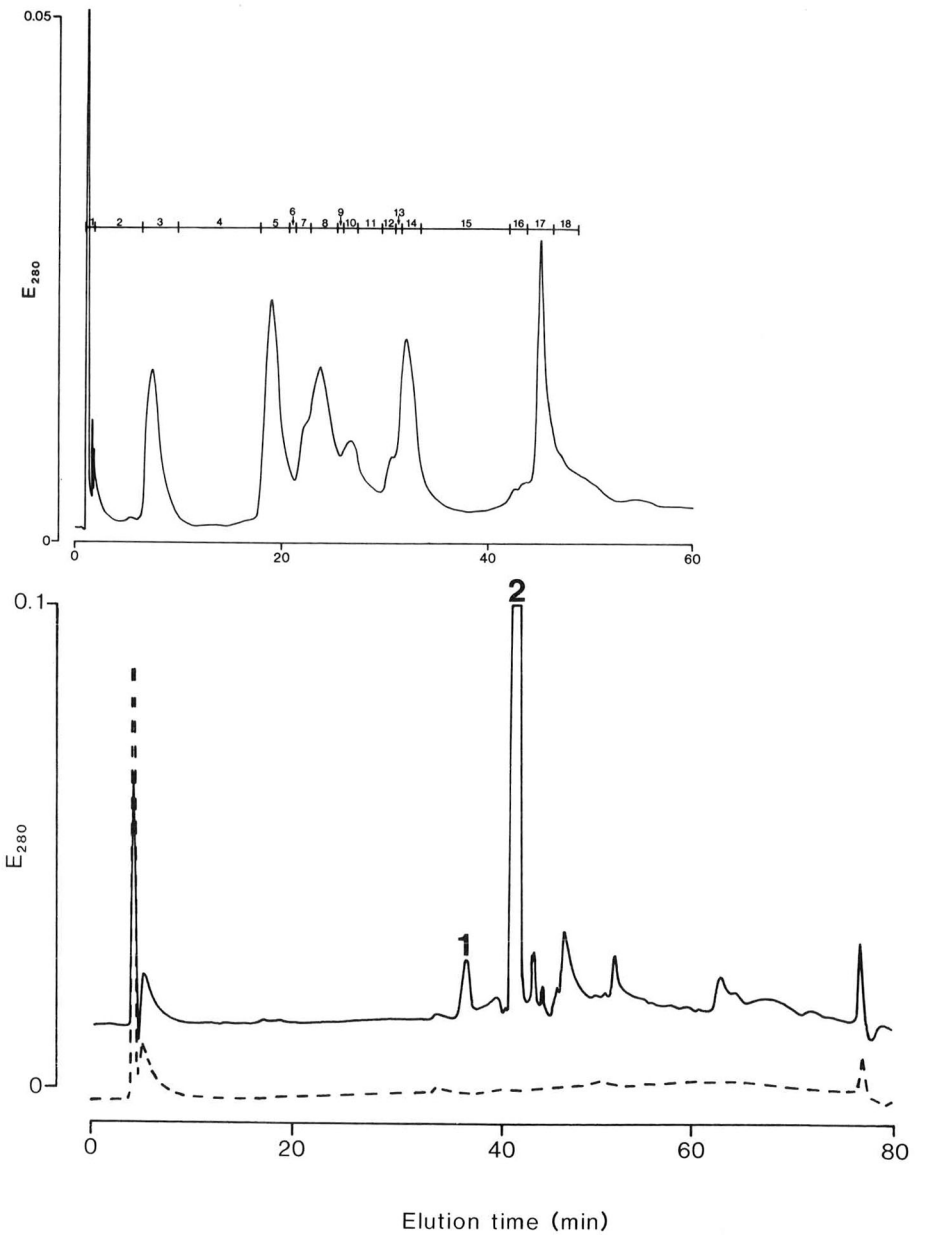

Fig. 7. Upper panel: separation of 100 μl SDS-solubilized erythrocyte membrane proteins using the stationary and mobile phase decribed in Fig. 5. Gradient 80% A (10 min), 80 to 50% A (35 min), 50 to 0% A (15 min), 0% A (15 min). Flow-rate: 0.5 ml/min. Lower panel: separation of 200 μl SDS-solubilized erythrocyte membrane proteins using a 250 mm × 4.0 mm I.D. Nucleosil C_4 (300 Å) column eluted at 1.0 ml/min with an acetonitrile gradient (0 to 90%) in 0.1% TFA over 60 min. The dashed line indicates injection of 100 μl SDS extraction buffer.

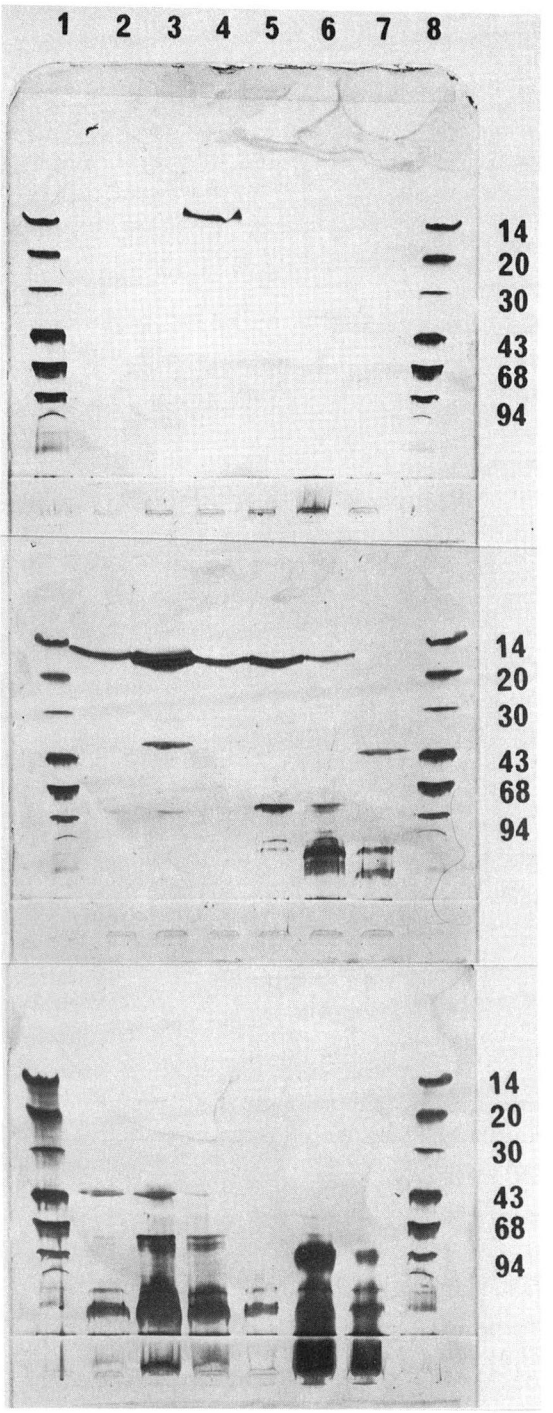

Fig. 8. SDS-PAGE of fractions 1–18 indicated in Fig. 7. Upper gel: lanes 2–7 correspond to fractions 1–6 respectively. Middle gel: lanes 2–7 c orrespond to fractions 7–12 respectively. Lower gel: lanes 2–7 correspond to fractions 13–18 respectively. In all three gels the molecular weight markers are shown in lanes 1 and 8.

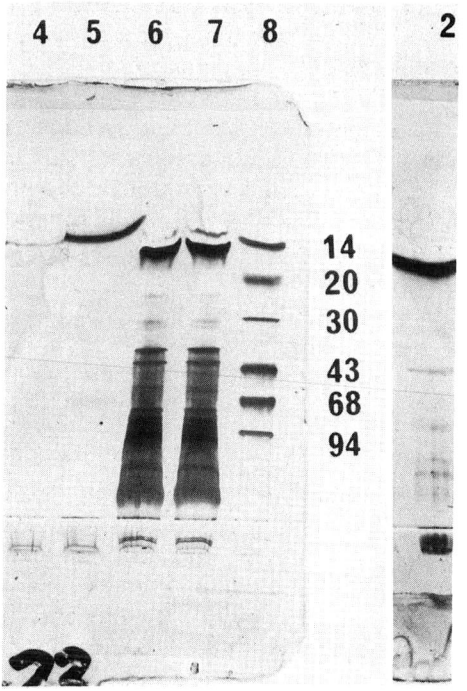

Fig. 9. SDS-PAGE of the peaks indicated in Fig. 7: peak 1 (lane 4), 2 (lane 5), total membrane proteins extracted in SDS (lane 6 and 7), molecular weight markers (lane 8) and the pooled column eluate collected from immediately after peak 2 to the end of the chromatogram (lane 2).

from haemoglobin) to >150 000 daltons. Due to easy accessibility and a variety of proteins with well known MW, this source of membrane protein seems attractive for initial investigations concerning the potential use of HPLC for the separation and isolation of membrane proteins.

Erythrocyte ghost membrane proteins extracted with polyoxyethylene glycol alkyl ether ($C_{12}E_8$) have been analyzed using HPIEC with the same detergent in the mobile phase. The separation was reasonably good judged by SDS-PAGE, but only the non-ionic detergent was used for membrane protein extraction. No recovery figures were given[5]. The influence of the type of detergent used for solubilizing the erythrocyte ghost has been examined using HPSEC with the proper detergent in the mobile phase. The elution strength was found to be SDS > CHAPS > Triton X-100, and it was concluded that HPSEC is a useful technique for monitoring the solubilizing process[6].

TSK Phenyl 5 PW RP as well as TSK Phenyl 5 PW columns have been evaluated for the potential separation of SDS-solubilized erythrocyte ghost membrane protein or whole ghosts injected directly. An acetonitrile gradient (0 to 95%) in 0.05% TFA was used. Compared to other RP columns with smaller pore sizes, the resolution of the large-pore TSK Phenyl columns was found to be advantageous. The column eluate was not characterized in any respect (except for the UV absorption)[7].

The recovery of erythrocyte membrane proteins from the two TSK Phenyl

columns has been estimated using the TFA–acetonitrile gradient described above. It was concluded that it was advantageous to solubilize the membrane proteins in SDS before analysis, but even then recoveries of up to 40–50% are predictable[8].

In the present study we have eluted a TSK Phenyl 5 PW RP column with TFA–acetonitrile and with a new mobile phase containing increasing amounts of acetic acid (20–40%) in an acetonitrile gradient (0–60%). In both cases it could be demonstrated, that CHAPS and octylglucoside primarily solubilized membrane components with MW < 15 000 daltons, whereas the SDS-solubilized membrane proteins in addition to the 15 000 daltons material included several proteins with MW 25 000–200 000 daltons. Although such membrane proteins can be eluted from the TSK Phenyl column with TFA–acetonitrile, the chromatogram in Fig. 1 clearly shows that the column eluted under these conditions favours the separation of lower MW polypeptides, *i.e.*, from 3000 to 15 000 daltons. These components may be separated completely, whereas the membrane proteins with higher MW are eluted in one or two groups virtually without separation.

However, the elution of hydrophobic proteins with MW around 100 000 daltons from a RP column is quite remarkable. In order to expand the high-molecular-weight separation range, the TSK Phenyl column was eluted with an acetic acid gradient in acetonitrile. It was clearly demonstrated that the column now operated in another fashion to that obtained with TFA–acetonitrile, since the CHAPS membrane extracts (which contained only membrane components with MW < 15 000 daltons) were eluted in the initial quarter of the chromatogram (Fig. 5), whereas the membrane proteins solubilized with SDS and containing components with MW 15 000–200 000 daltons were resolved in several fractions in the major part of the chromatogram (Fig. 7, upper panel). Isolation of membrane proteins with MW > 50 000 daltons, sufficiently pure for sequencing, should be possible with minor developmental work.

HPLC separation of a membrane protein mixture is an enormous challenge due to the complexity of the sample and (partly) the inapplicability of several HPLC principles which have produced brilliant results in the separation and characterization of water-soluble proteins. Due to the well known principle for estimating the molecular weight of polypeptides in SDS, HPSEC with mobile phases containing SDS has traditionally been the initial step in an HPLC characterization of membrane proteins, but HPSEC offers probably the least satisfactory separation capacity of the most common HPLC methods, and for several reasons, primarily economic, preparative HPSEC of polypeptides has been reported in very few cases.

RP-HPLC of water-soluble polypeptides is normally optimized by varying the stationary as well as the mobile phase, and as indicated in the present report, successful RP-based separation of membrane proteins depends upon similar developmental work: a silica-based C_4 column eluted with TFA–acetonitrile (a perfect combination for several polypeptide separations) was considerably less suited for membrane protein separation than was the resin-based phenyl column (with a different chemistry) eluted with the same mobile phase.

Further, a considerable expansion of the separation range for the resin-based RP column resulted from exchanging TFA with acetic acid as the mobile phase additive. The use of high amounts of acetic acid seems a promising alternative to the classical RP mobile phase additives. Good resolution and high recovery of erythrocyte membrane proteins was obtained, and the degree of solubilization using various detergents can be rapidly estimated.

Similar separations to those reported here were obtained if the TSK Phenyl column was eluted with an acetic acid gradient, *i.e.*, 20–90% acetic acid without addition of any organic modifier[9], indicating the possibility to perform RP-HPLC analyses of proteins without incorporation of acetonitrile, propanol or other organic solvents.

However, only few commercially available RP columns will tolerate continuous use of high concentrations of acetic acid, and this mobile phase is far from any physiological level. A successful separation of many membrane proteins will therefore require new concepts in column design as well as a critical revision of the choice of mobile phases. Investigations concerning the last point are in progress in this laboratory.

ACKNOWLEDGEMENTS

We thank Ingelise Fabrin and Helle Boysen Kofoed for excellent technical assistance.

REFERENCES

1 B. S. Welinder, S. Linde, H. H. Sørensen, K. R. Hejnæs and B. Hansen, in M. T. W. Hearn (Editor), *HPLC of Proteins, Polypeptides and Polynucleotides*, VCH, New York, in press.
2 G. Fairbanks, T. L. Steck and D. F. H. Wallach, *Biochemistry*, 10 (1971) 2606–2617.
3 *Bulletins Nos. 110* and *210*, Pharmacia, Uppsala, 19—.
4 T. L. Steck, *J. Cell. Biol.*, 62 (1974) 1–19.
5 H. Ikigai, T. Nakae and Y. Kato, *J. Chromatogr.*, 322 (1985) 212–219.
6 R. S. Matson and S. C. Goheen, *J. Chromatogr.*, 359 (1986) 285–295.
7 S. C. Goheen and T. M. Chow, *J. Chromatogr.*, 359 (1986) 297–305.
8 S. C. Goheen, in *Proc. Membr. Protein. Symp.*, Bio-Rad Labs., Richmond, CA, 1986, pp. 259–265.
9 B. S. Welinder, unpublished results.

Journal of Chromatography, 462 (1989) 269–279
Elsevier Science Publishers B.V., Amsterdam — Printed in The Netherlands

CHROM. 21 040

CHROMATOGRAPHIC AND SPECTROSCOPIC PROPERTIES OF HEMIACETALS OF AFLATOXIN AND STERIGMATOCYSTIN METABOLITES

DONNA L. ORTI*, JAMES GRAINGER, DAVID L. ASHLEY and ROBERT H. HILL, Jr.
Division of Environmental Health Laboratory Sciences, Center for Environmental Health and Injury Control, Centers for Disease Control, Public Health Service, U.S. Department of Health and Human Services, Atlanta, GA 30333 (U.S.A.)
(First received August 8th, 1988; revised manuscript received October 11th, 1988)

SUMMARY

Improved fluorescence detection of aflatoxin B_1 by chromatographic analysis is accomplished by conversion to the corresponding hemiacetal, aflatoxin B_{2a}. Because the metabolites aflatoxin M_1, aflatoxin P_1, aflatoxin Q_1, sterigmatocystin, and O-methylsterigmatocystin have the same molecular conversion site, we investigated the chromatographic and spectroscopic properties of hemiacetals of these compounds to assist in confirming aflatoxins and sterigmatocystins in human urine. Nuclear magnetic resonance and infrared absorbance were used to confirm the hemiacetal structure for aflatoxin B_1 and sterigmatocystin. The ultraviolet absorbance, fluorescence, and chromatographic properties of the metabolites were investigated. Using these data, we optimized the detection and solvent conditions for high-performance liquid chromatography. We determined that, of the conditions studied, maximum sensitivity and resolution for the native aflatoxins were achieved with a mobile phase of methanol, tetrahydrofuran, and water, a C_8 column in series with a C_{18} column, and fluorescence detection with 365 nm excitation and 430 nm emission wavelengths for aflatoxins B_1 and M_1 and with 500 nm emission wavelength for aflatoxins P_1 and Q_1. For the analysis of the hemiacetals, a mobile phase of methanol, acetonitrile, and water provided better chromatography and fluorescence detection. Sterigmatocystin and O-methylsterigmatocystin were readily converted to the hemiacetal forms, which, like the aflatoxins, were more polar and, therefore, earlier eluting by reversed-phase HPLC (methanol, acetonitrile, and water, 236 nm absorbance). These data are important to maximize the sensitivity and confidence for detecting the mycotoxin metabolites in biological specimens.

INTRODUCTION

In 1966, the hemiacetals of aflaloxins B_1 and G_1 were first reported[1]. These hemiacetals could be synthesized by the acid-catalyzed addition of water across the vinyl ether (C2,3) double bond (Fig. 1)[2] and were found to be more intensely fluorescent than the corresponding naturally occurring mycotoxins[3]. The ease of produc-

tion and the enhanced fluorescence of the hemiacetals have encouraged investigations of the hydrated form rather than the native compound by high-performance liquid chromatography (HPLC)[4–7]. When aflatoxin B_1 is acted on by the liver enzymes (rat, mouse, monkey, and human), it is hydroxylated to the metabolites aflatoxins M_1, P_1 and Q_1 (refs. [8–12]) (Fig. 1), which are conjugated with glucuronic acid when excreted in the urine[9].

Sterigmatocystin (STR) is similar to aflatoxin: it is produced by species of *Aspergillus* that contaminate stored nuts and grain, it has the 7,8-dihydrofurano-[2,3-*b*]furan moiety where a vinyl ether double bond is located, and it is conjugated with glucuronic acid when excreted in the urine[13]. Unlike aflatoxin, however, unless it is dissolved in a strong acid such as sulfuric acid, STR in not intensely fluorescent[14]. Typically, HPLC of STR uses ultraviolet (UV) absorbance for detection[15–17].

We have been interested in analyzing for the mycotoxins in human specimens[18,19]. We present chromatographic and spectroscopic properties of the hemiacetals of aflatoxin B_1 (AFB), aflatoxin M_1 (AFM), aflatoxin P_1 (AFP), aflatoxin Q_1 (AFQ), sterigmatocystin (STR), and O-methylsterigmatocystin (OMS). The results of this study were used to enhance sensitivity and confidence in the HPLC determination for these mycotoxin metabolites in human urine[19].

EXPERIMENTAL

Equipment and reagents

Standards of AFB, AFM, AFP, AFQ, STR and OMS (Sigma, St. Louis, MO U.S.A.), were prepared in acetonitrile. Because these mycotoxins are highly toxic and carcinogenic, standards were prepared in a glove box. Trifluoroacetic acid (TFA) (Aldrich, Milwaukee, WI, U.S.A.) and orthophosphoric acid (Fisher Scientific, Fair

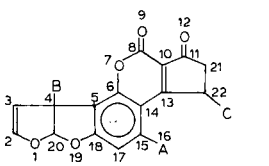

aflatoxin	A	B	C
B1	-OMe	-H	-H
M1	-OMe	-OH	-H
P1	-OH	-H	-H
Q1	-OMe	-H	-OH

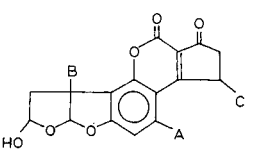

aflatoxin	A	B	C
B2a	-OMe	-H	-H
M2a	-OMe	-OH	-H
P2a	-OH	-H	-H
Q2a	-OMe	-H	-OH

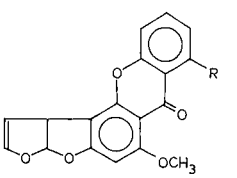

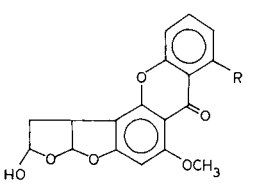

	R
sterigmatocystin	-OH
O-methylsterigmatocystin	-OMe
sterigmatocystin-hemiacetal	
O-methylsterigmatocystin-hemiacetal	

Fig. 1. Chemical structures of the native and hemiacetal forms of the mycotoxins studied. Me = Methyl.

Lawn, NJ, U.S.A.) were reagent grade. All solvents were HPLC-grade (Burdick & Jackson, Muskegon, MI, U.S.A.).

HPLC was performed with a Waters system, incorporating an M6000A pump, an M721 data module, an M720 system controller, and an M710B WISP injector (Millipore, Milford, MA, U.S.A.). Detectors were a Perkin-Elmer LS-4 and a Perkin-Elmer 650-10S fluorescence spectrophotometers (Norwalk, CT, U.S.A.) and a Waters 480 spectrophotometer. Either a Sepralyte C_8 (25 cm × 2.1 mm I.D., 10-μm) column (Analytichem, Harbor City, CA, U.S.A.) or a Spherisorb C_8 (15 cm × 4.0 mm I.D., 5 μm) (Chromanetics, Sci-Con, Winter Park, FL, U.S.A.) in series with a Spherisorb C_{18} (15 cm × 4.0 mm I.D., 5 μm) column were used as the stationary phases. A Waters 990 photodiode array detector was used for determining the UV absorbance spectra of the mycotoxins. A Nicolet 170SX Fourier transform infrared (FT-IR) spectrometer (Nicolet, Madison, WI, U.S.A.) was used for the IR analyses. Samples were analyzed as KBr pellets. The instrumentation and conditions for the nuclear magnetic resonance (NMR) analyses are described elsewhere[20].

Preparation of the mycotoxin hemiacetals

Hexane (200 μl) and TFA (50 μl) were added to 2 μg of the mycotoxin. After 15 min at 60°C, 950 μl of water–acetonitrile (9:1) was added, the solution was vortexed, and the lower aqueous layer was transferred to a vial for HPLC analysis[18,21]. By convention, the hemiacetal of aflatoxin B_1 is called aflatoxin B_{2a} (AFB_{2a})[1]; following this convention the hemiacetals of AFM, AFP, and AFQ have been designated AFM_{2a}, AFP_{2a} and AFQ_{2a}.

RESULTS AND DISCUSSION

The purity of the standards was evaluated by HPLC. When only one fluorescent (365 nm excitation, 430 nm emission) peak was present in the HPLC chromatogram, the standard was regarded as pure. We evaluated the standards in this fashion because very small amounts of aflatoxins P_1 and Q_1 were available. When the standards were dissolved in methanol, they deteriorated in a few weeks, this has also been observed by other investigators[22]. Aflatoxin Q_1 deteriorated most quickly and began to show multiple HPLC peaks after two weeks. Greater stability was obtained when the aflatoxins were dissolved in acetonitrile. Aflatoxin Q_1 produced one HPLC peak for more than a month.

Hemiacetal synthesis

The conversion of the native mycotoxin to the hemiacetal was evaluated by the disappearance of the native peak and the appearance of a fluorescent HPLC peak for the hydrated structure. As shown in Table I, using reversed-phase isocratic HPLC, the hemiacetals eluted faster than their corresponding native mycotoxins. Table II shows minimum detectable amounts of each aflatoxin and its hemiacetal under various conditions. The aflatoxins were generally more fluorescent in the hemiacetal form. The reduction in the retention time and the increased fluorescence of the hemiacetals serve to confirm the parent mycotoxin. Three variations of the TFA-catalyzed addition of water to aflatoxin were evaluated: in method 1[21], 200 μl of dry hexane and 50 μl of TFA were mixed with the mycotoxin. The reaction proceeded for 15 min at

TABLE I

RELATIVE RETENTION TIMES OF THE HEMIACETAL STRUCTURES OF AFLATOXIN AND STERIGMATOCYSTIN METABOLITES

Mobile phase: acetonitrile–methanol–water (3:2:5), 0.3 ml/min. Column: Sepralyte C_8, 250 mm × 2 mm I.D., 10 μm. Relative retention times calculated as retention time (hemiacetal)/retention time (native mycotoxin).

	Relative retention time
Aflatoxins	
B	0.56
M	0.65
P	0.63
Q	0.84
Sterigmatocystins	
STR	0.43
OMS	0.48

room temperature, and then 950 μl of water–acetonitrile (9:1) was added and the solution vortexed. The lower, aqueous layer was transferred to another vial for analysis. In method 2[23], hexane and TFA were added as in method 1, but the solution was incubated at 40°C for 15 min. After incubation, the reaction mixture was evaporated to dryness with a gentle stream of nitrogen and 40°C heat, then dissolved in 1 ml of

TABLE II

INFLUENCE OF MOBILE PHASE AND EMISSION WAVELENGTH ON THE RELATIVE FLUORESCENCE OF AFLATOXINS*

(a) Methanol–THF–0.3% H_3PO_4 (35:5:60), 0.5 ml/min. (b) Methanol–THF–water (35:5:60), 0.5 ml/min. (c) Methanol–acetonitrile–water (35:5:60), 0.5 ml/min.

Aflatoxin	*Mobile phase*	*Emission wavelength (nm)***			
		430		*500*	
		Native (ng)	*Hemiacetal (ng)*	*Native (ng)*	*Hemiacetal (ng)*
B	a	0.43	0.03	2.8	0.07
	b	0.34	0.05	2.0	0.11
	c	1.7	0.03	5.6	0.06
M	a	0.15	0.07	0.27	0.19
	b	0.15	0.08	0.24	0.19
	c	0.08	0.06	0.27	0.19
P	a	16	12	1.4	1.7
	b	8.0	3.0	0.59	0.77
	c	25	2.8	1.0	1.1
Q	a	17	0.16	7.5	0.05
	b	12	0.17	3.0	0.06
	c	12	0.05	5.6	0.02

* Shown as the minimum detectable amount in ng, signal-to-noise ratio is 3:1.

** 365 nm was used as the excitation wavelength.

acetonitrile. In method 3[7], 1 ml of TFA–water (9:1) was added to the dried standard material and the mixture reacted for 15 min at room temperature. Each sample was then analyzed by HPLC. HPLC determined that AFB was easily and completely converted to its hemiacetal by all three methods, but the other metabolites (AFM, AFP, AFQ, STR and OMS) were not as reactive and, therefore, not completely hydrated. Other investigators have noted the incomplete reaction by AFM with TFA[24]. Similarly, substituting 50% aqueous trichloroacetic acid for TFA readily converted AFB but not the other metabolites. Moderate heat (60°C) was necessary to ensure complete reaction of all of the metabolites. The method described in *Preparation of the mycotoxin hemiacetals* completely converted each of the six mycotoxins to their hemiacetal structure.

The hemiacetal of sterigmatocystin

IR and NMR analyses confirmed the hemiacetal structure of sterigmatocystin (Fig. 1). After determining the IR and NMR spectra for aflatoxin B_{2a}, we compared the spectra for sterigmatocystin. The IR spectrum of AFB_{2a} demonstrated the addition of water to the C2,3 double bond by the appearance of a broad O–H stretching band at 2458 cm^{-1} and by the disappearance of the double bond 1620 cm^{-1} band. Additionally, a new band at 1086 cm^{-1} was observed for the hemiacetal C–O stretching, while the band from 1199 cm^{-1} vinyl ether C–O–C stretching in five membered ring disappeared. This spectrum closely agreed with published results[3,25]. In the IR spectra for STR hemiacetal, the presence of 3220 cm^{-1} band (aliphatic O–H stretch) and the 1442 cm^{-1} and 1420 cm^{-1} bands (O–H bend), and the absence of the 1620 cm^{-1} band, supported addition of water across the vinyl ether double bond. The NMR spectra of AFB, STR and their hemiacetals, and selective homodecoupling experiments used to make assignments, are described elsewhere[20]. These spectra verify that (a) water was added across the double bond of the vinyl ether, (b) the hydroxyl group was attached to the alpha carbon, and (c) two hemiacetal configurations were produced by the hydroxyl group occurring in an up (beta structure) or a down (alpha structure) orientation. These data confirm that the hemiacetal of sterigmatocystin can be easily synthesized.

The UV, fluorescent, and chromatographic properties of the hemiacetals of sterigmatocystin and O-methylsterigmatocystin were investigated. Fig. 2 shows that the UV spectra of STR and OMS hemiacetals were not different from the spectra for the native mycotoxins. STR is reported to be fluorescent under strong acidic conditions[13]; however, because strong acids cannot be used as a mobile phase for HPLC, UV absorbance is used as the method of detection. Converting the parent structure of STR or OMS to the hemiacetal, likewise, did not produce a structure that was suitably fluorescent when using HPLC. Table I gives the relative retention times of hemiacetals of STR and OMS. The hydrated structures clearly are more polar than the native forms and, therefore, earlier eluting by reversed-phase liquid chromatography (RPLC). These results parallel the observed chromatography of the aflatoxin hemiacetals.

The hemiacetal of aflatoxin B_1 (AFB_{2a})

The UV spectrum of aflatoxin B_1 was not significantly affected by the conversion to the hemiacetal (Fig. 2), although, the fluorescence intensity was. As shown

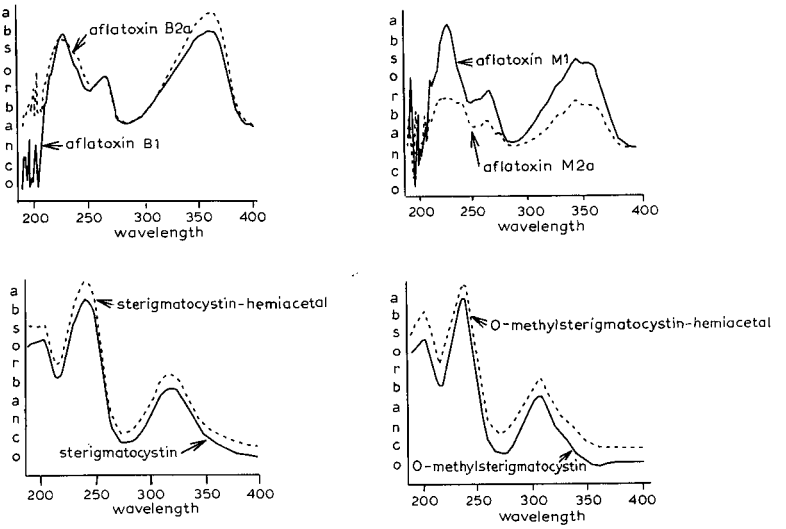

Fig. 2. UV spectra of native and hemiacetal structures of aflatoxin B_1, aflatoxin M_1, sterigmatocystin, and O-methylsterigmatocystin. See text for details. Wavelength in nm.

in Table II, depending on the mobile phase and the emission wavelength used, AFB_{2a} was nearly seven times more fluorescent than AFB. Maggon and Gopal[26] reported that the excitation maximum for AFB_{2a} dissolved in methanol shifted to 405 nm. When we tried to use 405 nm as the excitation wavelength with 430 nm as the emission wavelength, however, the signal-to-noise ratio increased significantly, reducing the overall detection limit. Because of the better signal-to-noise ratio with 365 nm excitation wavelength, this setting was used. By using the excitation wavelength of 365 nm and emission wavelength of 430 nm, 340 pg of AFB could be detected in 35% methanol mobile phase modified with THF; its hemiacetal could be detected at 50 pg in acetonitrile-modified mobile phase. The synthesis of the hemiacetal by the method we used was confirmed by NMR and IR. The hemiacetal was more polar and, therefore, earlier eluting by RPLC. In fact, relative to the parent molecule, AFB_{2a} was the most polar of the aflatoxin hemiacetals. The combination of increased fluorescence and reduced retention time can be used to confirm the presence of the native mycotoxins in a sample.

The hemiacetal of aflatoxin M_1 (AFM_{2a})

As with AFB, the shape of the UV spectra curves of AFM and its hemiacetal, as shown in Fig. 2, was not significantly different. Unlike AFB, the fluorescence of AFM was less affected by the mobile phase or the conversion to the hemiacetal. The greatest sensitivity for AFM (see Table II) was in an acetonitrile-modified methanol mobile phase where 80 pg could be detected when an emission wavelength of 430 nm was used. Under these same conditions, the greatest sensitivity for the hemiacetal could be obtained (60 pg). Fig. 3 shows the detector response to 10 ng of AFM and AFM_{2a} under these conditions. The conversion to the hemiacetal did not improve the detection limit for this mycotoxin by more than two times under any of the conditions tested. The native toxin, however, is detectable at lower levels (80 pg) than any of the

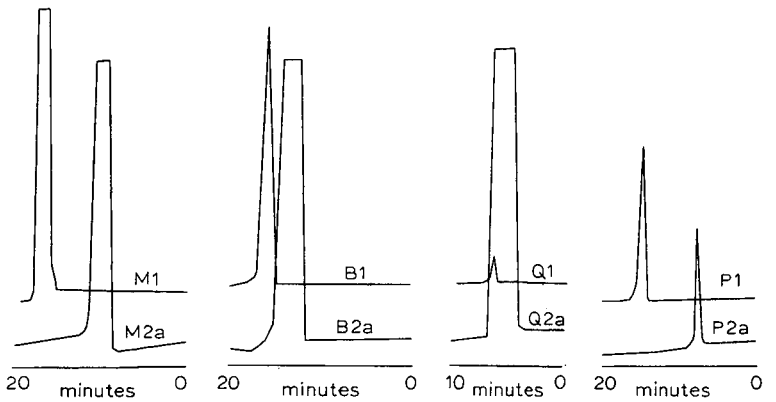

Fig. 3. Detector responses to 10 ng of analyte. With the fluorescence wavelength set at 365 nm, the conditions for optimal detection of aflatoxin metabolites are shown. See text for details.

other aflatoxin metabolites. The lower detection limit for the hemiacetal could be simply due to the fact that it is more polar and, therefore, earlier eluting than the native structure. Table III shows that of the aflatoxin metabolites, the conversion to the hemiacetal had the least effect on the retention time for AFM (relative retention times of the hemiacetal to the native compound ranged from 0.58 to 0.63). Investigators using RPLC for AFM analysis have been converting the native toxin to the hemiacetal to enhance fluorescence[23,24,27–29]. Using an excitation wavelength of 365 nm and emission wavelengths greater than 400 nm with mobile phases of methanol and/or acetonitrile, researchers were able to achieve between a two-fold and six-fold increase in fluorescence of AFM_{2a} over AFM[27–29]. Although we did not see such a marked improvement in fluorescence of the hemiacetal, it is not clear if this was because of improved detection for AFM by us or diminished detection for AFM_{2a}. Differences in detectors, filters, diffraction gradings, and chemical interaction greatly influence the fluorescence production and detection.

TABLE III

EFFECT OF THE MOBILE PHASE MODIFIER ON RETENTION TIMES

Column: Spherisorb C_8, 150 mm × 4 mm I.D. plus Spherisorb C_{18}, 150 mm × 4 mm I.D. Mobile phase: water–methanol–modifier (60:35:5). Modifiers: (a) THF + 0.3% H_3PO_4; (b) THF; (c) acetonitrile. Flow-rate: 0.5 ml/min.

Alfatoxin	*Mobile phase*					
	a		*b*		*c*	
	Native (min)	*Hemiacetal (min)*	*Native (min)*	*Hemiacetal (min)*	*Native (min)*	*Hemiacetal (min)*
B	23.0	10.0	16.4	8.2	38.0	13.6
M	12.0	7.6	9.8	6.2	16.8	9.8
P	17.4	8.4	13.4	6.8	19.0	9.0
Q	10.2	5.8	8.4	5.2	13.6	6.2

The hemiacetal of aflatoxin Q_1 (AFP_{2a})

As the native structure, the detection limit of aflatoxin Q_1 was nearly 100 times less sensitive than that of aflatoxin M_1. When 430 nm excitation was used, the detection limit was 12 ng. An emission wavelength of 500 nm, however, gave more sensitivity for this analyte with THF-modified methanol mobile phase providing the best sensitivity (detection limit 3 ng). As shown in Table II, synthesis of the hemiacetal improved the sensitivity 150 times (detection limit 20 pg; acetonitrile modifier, 500 nm wavelength). Of the four aflatoxins, AFQ demonstrated the greatest enhancement in fluorescence by the hydration reaction and was changed from one of the least fluorescent of the native toxins to the most fluorescent of the hemiacetals (see Fig. 3). Thus, we believe that the key to detecting AFQ by HPLC is to analyze for the hemiacetal.

The hemiacetal of aflatoxin P_1 (AFP_{2a})

Under similar conditions, the hemiacetals of AFB, AFM, and AFQ were always more fluorescent than the native toxin; however, this was not true for AFP. Table II shows that while AFP_{2a} was more fluorescent than the native toxin at the 430 nm emission wavelength, at the 500 nm wavelength the fluorescent signal for the native toxin was stronger. Because the fluorescence signal at 500 nm emission (0.6–1.4 ng) was more than ten times more intense than at 430 nm (8–25 ng), the longer wavelength should be used to analyze for the native toxin. By using 500 nm as the emission wavelength, however, conversion to the hemiacetal would not improve the detection limit for AFP (0.8–1.7 ng), but the shift in retention time would confirm its presence. Of the four aflatoxin metabolites, we found the hemiacetal of AFP to be the least fluorescent under the conditions tested (see Fig. 3).

Many HPLC methods use gradient elution to resolve the very similar structures of these mycotoxins. We were able to improve peak resolution by using two types of reversed-phase columns in series; when a C_{18} was coupled with a C_8 column, all of the peaks (four native aflatoxins and four hemiacetals) were resolved (Fig. 4 and 5). To optimize resolution, we evalutated three ternary mobile phases. Methanol modified with acetonitrile has been used by several investigators for RPLC[4–6], and others have added acid to the mobile phase[7]. THF was investigated as a modifier because it is less polar than either methanol or acetonitrile. Although the hemiacetals for AFB, AFM, and AFQ were more intensely fluorescent in the mobile phase modified with acetonitrile, the native toxins for AFB, AFP, and AFQ were more fluorescent when THF was used as the modifier. Acidification of the mobile phase with orthophosphoric acid modified with THF did not significantly enhance the fluorescence. More intense fluoresence signals were obtained for AFB, AFM, and their hemiacetals (AFB_{2a} and AFM_{2a}) by using 430 nm as the emission wavelength, whereas an emission wavelength of 500 nm allowed more intense signals for AFQ, AFP, and their hemiacetals (AFQ_{2a} and AFP_{2a}) (Fig. 4 and 5). Of those tested, a mobile phase of methanol–THF–water (35:5:60) provided the best resolution of the mycotoxins on the double-column system (Table III). In routine laboratory analysis for aflatoxins, the native structures are analyzed separately from the hemiacetals. We found that the conditions to best analyze for the native aflatoxins are a mobile phase of methanol, THF, and water, a C_{18} plus a C_8 column, an excitation wavelength of 365 nm, and an emission wavelength of 430 nm for detection of AFB and AFM and an emission

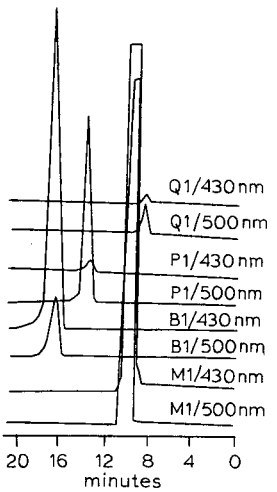

Fig. 4. Composite of chromatograms of 10 ng samples of native aflatoxins. A Spherisorb C_8 column was used in series with a Spherisorb C_{18} column. The mobile phase was a 35% aqueous methanol solution modified with 5% THF. The flow-rate was 0.5 ml/min. Fluorescence detection used 365 nm as the excitation wavelength; the emission wavelength was as indicated.

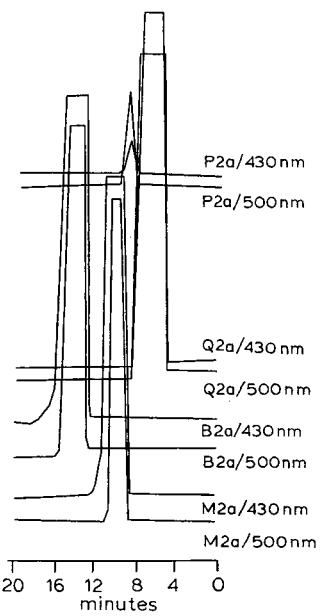

Fig. 5. Composite of chromatograms of 10-ng samples of the hemiacetal forms of aflatoxins. Column, flow-rate and detector conditions are as described in Fig. 4. The mobile phase was 35% aqueous methanol solution modified with 5% acetonitrile.

wavelength of 500 nm for detection of AFP and AFQ (Fig. 4). For detection of the hemiacetals, a mobile phase of methanol, acetonitrile, and water with the same detector settings provided maximum sensitivity, resolution, and confirmation (Fig. 5). Although these conditions may not be optimal for each of the mycotoxins, they are the good compromise of those tested.

CONCLUSION

In this study we showed that the hemiacetals for the metabolites of aflatoxin and sterigmatocystin can be easily prepared, and we confirmed this with NMR and IR for AFB and STR. The hemiacetals for AFP, AFQ and OMS have not been reported before. These hemiacetals have distinctive chromatographic and fluorescence properties (in the case of the aflatoxins) that can be used to confirm the identification and improve the detection of the mycotoxins. The native mycotoxins and the more polar hemiacetals can be resolved by HPLC. Many investigators use emission wavelengths of 435 nm, but for the fluorescence of AFP and AFQ, a wavelength of 500 nm results in greater sensitivity. The fluorescence is also influenced by the composition of the mobile phase. Maximum sensitivity for detection of these mycotoxins is obtained by optimizing the emission wavelength and the mobile phase composition. The ease in preparing the hemiacetal of these mycotoxins, the improved sensitivity for three aflatoxin metabolites, and the reduced retention time make this a good confirmatory test for the HPLC analysis.

REFERENCES

1 M. F. Dutton and J. G. Heathcote, *Biochem. J.*, 101 (1966) 21P.
2 A. E. Pohland, M. E. Cushmac and P. J. Andrellos, *J. Assoc. Off. Anal. Chem.*, 51 (1968) 907.
3 K. K. Maggon, S. Gopal, L. Viswanathan, T. A. Venkitasubramanian and S. S. Rathi, *Indian J. Biochem. Biophys.*, 9 (1972) 195.
4 D. M. Takahashi, *J. Chromatogr.*, 131 (1977) 147.
5 D. M. Takahashi, *J. Assoc. Off. Anal. Chem.*, 60 (1977) 799.
6 H. H. L. Chang, J. W. DeVries and W. E. Hobbs, *J. Assoc. Off. Anal. Chem.*, 62 (1979) 1281.
7 J. E. Hutchins and W. M. Hagler, Jr., *J. Assoc. Off. Anal. Chem.*, 66 (1983) 1458.
8 R. Dahms and H. L. Gurtoo, *Res. Commun, Chem. Pathol. Pharmacol.*, 15 (1976) 11.
9 C. I. Wei and M. R. Marshall, *Food Cosmet. Toxicol.*, 23 (1985) 809.
10 R. I. Krieger, A. S. Salhab, J. I. Dalezois and D. P. H. Hsieh, *Food Cosmet. Toxicol.*, 13 (1975) 211.
11 J. I. Dalezois and G. N. Wogan, *Cancer Res.*, 32 (1972) 2297.
12 G. H. Buchi, P. M. Muller, B. D. Roebuck and G. N. Wogan, *Res. Commun. Clin. Pathol. Pharmacol.*, 8 (1974) 585.
13 P. G. Thiel and M. Steyn, *Biochem. Pharmacol.*, 22 (1973) 3267.
14 D. D. Maness, L. W. Schneider, G. Sullivan, G. J. Yakatan and J. Scholler, *J. Agric. Food Chem.*, 24 (1976) 961.
15 R. Schmidt, J. Mondani, E. Ziegenhagen and K. Dose, *J. Chromatogr.*, 207 (1981) 435.
16 D. G. I. Kingston, P. N. Chen and J. R. Vercellotti, *J. Chromatogr.*, 118 (1976) 414.
17 P. Lepom, *J. Chromatogr.*, 354 (1986) 518.
18 D. L. Orti, R. H. Hill, Jr., J. A. Liddle, L. L. Needham and L. Vickers, *J. Anal. Toxicol.*, 10 (1986) 41.
19 D. L. Orti and R. H. Hill, Jr., *194th American Chemical Society National Meeting, New Orleans, LA, 1987*, Abstract Envr. No. 69.
20 D. L. Ashley, D. L. Orti and R. H. Hill, Jr., *J. Agric. Food Chem.*, 35 (1987) 782.
21 E. J. Tarter, J.-P. Hanchay and P. M. Scott, *J. Assoc. Off. Anal. Chem.*, 67 (1984) 597.
22 I. Chang-Yen, V. A. Stoute and J. B. Felmine, *J. Assoc. Off. Anal. Chem.*, 67 (1984) 306.
23 K. Hisada, H. Terada, K. Yamamoto, H. Tsubouchi and Y. Sakabe, *J. Assoc. Off. Anal. Chem.*, 67 (1984) 601.

24 R. D. Stubblefield, *J. Assoc. Off. Anal. Chem.*, 70 (1987) 1047.
25 R. Cole and R. Cox, *Handbook of Toxic Fungal Metabolites*, Academic Press, New York, 1981.
26 K. K. Maggon and S. Gopal, *Agric. Biol. Chem.*, 38 (1974) 681.
27 H. L. Chang and J. W. DeVries, *J. Assoc. Off. Anal. Chem.*, 66 (1983) 913.
28 R. M. Bebe and D. M. Takahashi, *J. Agric. Food Chem.*, 28 (1980) 481.
29 A. Carisano and G. Della Torre, *J. Chromatogr.*, 355 (1986) 340.

Journal of Chromatography, 462 (1989) 281–292
Elsevier Science Publishers B.V., Amsterdam — Printed in The Netherlands

CHROM. 21 024

DETERMINATION OF GALLAMINE AND ITS IMPURITIES BY REVERSED-PHASE ION-PAIR HIGH-PERFORMANCE LIQUID CHROMATOGRAPHY AND COMPARISON WITH THIN-LAYER CHROMATOGRAPHY

P. A. MOURIER
Rhône-Poulenc Santé, Centre de Recherches de Vitry, 13 Quai Jules Guesde, 94403 Vitry-sur-Seine (France)
(First received June 10th, 1988; revised manuscript received October 4th, 1988)

SUMMARY

A reversed-phase, ion-pair high-performance liquid chromatographic (HPLC) method for the determination of gallamine and its impurities is described. The separation is achieved on a Nucleosil C_{18} column with acetonitrile–aqueous phosphate buffer (pH 3.0) (31:69, v/v) containing 0.1 *M* sodium perchlorate as eluent and on-line UV detection at 200 nm. The method is sensitive (the detection limit is 0.7 ng injected) and reproducible, with a peak area coefficient of variation of 0.19% ($n = 15$; 3 μg injected) and 1.65% ($n = 15$; 10 ng injected) for a gallamine assay; the detector response is linear over the concentration range 0.5–250 μg/ml of gallamine triethiodide with a correlation coefficient of 0.9997. The method has been used to isolate the two main impurities contained in gallamine triethiodide batches; their structures have been determined by NMR and fast atom bombardment mass spectrometry. Various gallamine triethiodide batches have been analysed and the HPLC results compared with those obtained by thin-layer chromatography.

INTRODUCTION

Gallamine triethiodide (Fig. 1a), a substitute for curare, was first synthesized in France by Rhône-Poulenc in 1947. Since then, it has been used mainly as a non-depolarizing neuromuscular blocking agent in anaesthetic practice.

Several methods for gallamine triethiodide assay have been proposed. Some workers used dye-binding fluorescence methods[1–4] but these were not suitable for the assay of both gallamine and its impurities. Recently, two chromatographic methods[5,6] have been proposed for these determinations but the results were not very convincing.

This paper describes a method for the determination of gallamine triethiodide and its main impurities by high-performance liquid chromatography (HPLC). Two impurities were isolated by preparative chromatography and their structures were determined. The results obtained by HPLC and thin-layer chromatography (TLC)[7] were compared.

0021-9673/89/$03.50

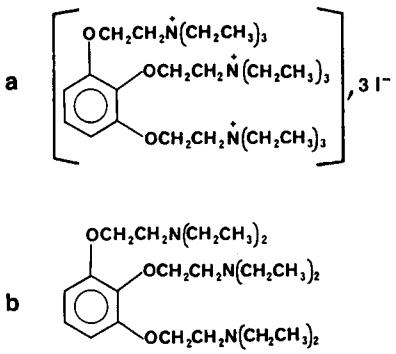

Fig. 1. Structures of (a) gallamine triethiodide and (b) gallamine base.

EXPERIMENTAL

Chemicals

Gallamine triethiodide samples were from different sources. HPLC-grade acetonitrile was purchased from Prolabo (Paris, France). Deionized water was further purified on a Milli-Q system (Millipore, Bedford, MA, U.S.A.). All other chemicals were of analytical-reagent grade from Prolabo.

Apparatus

The HPLC system consisted of a Gilson (Villiers-le-Bel, France) gradient chromatograph equipped with a Rheodyne 20-μl sample loop injector, a Gilson Model 231 autosampler, a Kratos (Ramsey, NJ, U.S.A.) Spectroflow 757 UV detector and a Perkin-Elmer (Wilton, CT, U.S.A.) LCI100 integrator recorder coupled with a Perkin-Elmer Model 7700 datastation. Detection was also carried out with a Hewlett-Packard (Palo Alto, CA, U.S.A.) Model 1040 A diode array detector.

The impurities were isolated with a semi-preparative chromatograph consisting of a Gilson Model 303 HPLC pump coupled with a Model 803C manometric module. Rheodyne 6-ml sample loop injector was used. The UV detector was an LDC Spectromonitor III (Laboratory Data Control, Riviera Beach, FL, U.S.A.) equipped with a 35-μl semi-preparative cell.

HPLC conditions

Chromatographic columns (25 cm × 0.46 cm I.D.) were packed with either 5-μm Nucleosil octadecyl-bonded silica, 5-μm Nucleosil cyanopropylsilica or 5-μm Nucleosil bare silica (mean pore diameters 100 Å) (SFCC, Gagny, France). Sodium perchlorate was added to the buffer–acetonitrile mobile phase. The aqueous part of the mobile phase was adjusted to pH 3 by adding sodium hydroxide to 0.05 *M* phosphoric acid solution. Mobile phases containing 0–0.5 *M* sodium perchlorate were prepared.

On the octadecyl bonded silica, either isocratic or gradient elution was used. For isocratic elution the mobile phase consisted of acetonitrile–20.3 g/l sodium perchlorate solution buffered at pH 3 (31:69, v/v). This mobile phase also gave good results on cyanopropyl-bonded silica. In some instances, gradient elution was neces-

sary. Two solvent mixtures were prepared: solvent A [acetonitrile–15.5 g/l sodium perchlorate solution buffered at pH 3 (10:90, v/v)] and solvent B [acetonitrile–40 g/l sodium perchlorate solution buffered at pH 3 (65:35, v/v)]. At time zero, the mobile phase was a mixture of 25% B in A, increased linearly to 50% in 20 min and to 65% after 25 min. This level was maintained until the end of the elution.

On bare silica, the best mobile phase was acetonitrile–17.5 g/l sodium perchlorate solution buffered at pH 3 (20:80, v/v). However, the octadecyl-bonded silica gave the best results.

Volumes of 20 μl of gallamine solutions were injected. The solutions were prepared by adding 0.05–40 mg of a gallamine triethiodide sample to 100 ml of mobile phase. The flow-rate was 1 ml/min. The analysis was performed at room temperature and the UV wavelength was 200 nm.

Preparative liquid chromatographic conditions

We used a 25 cm × 2.1 cm I.D. column packed with 5-μm Nucleosil octadecyl-bonded silica. The mobile phase composition was as specified above for isocratic elution and the flow-rate was 12 ml/min. A 100-mg amount of a gallamine triethiodide batch, added to 100 mg of sodium perchlorate and dissolved in 6 ml of mobile phase, was injected (a counter ion has to be added to prevent peak broadening). The UV wavelength was set at 230 nm instead of 200 nm to avoid UV saturation.

After collection, the fractions containing the impurities were immediately neutralized to avoid acidic degradation. Acetonitrile and part of the water were evaporated under vacuum at 30°C. The concentrated impurities were nearly insoluble in the aqueous phase overloaded with phosphate and perchlorate. Hence they were excluded from the aqueous phase and it was possible to collect them in the supernatant without contamination by sodium perchlorate of sodium dihydrogenphosphate.

TLC conditions[7]

Silica gel pre-coated flexible TLC sheets (20 cm × 20 cm) were purchased from Prolabo (F 1500, Schleicher et Schüll). The plates were activated at 110°C for 30 min and 5 μl of a 20 mg/ml methanolic solution of gallamine triethiodide were applied.

Development was achieved with acetone–11 *M* hydrochloric acid–water (50:25:25, v/v). After migration, the plates were dried and sprayed with a solution of 1 g of hexachloroplatinic acid dissolved in 4 ml of hydriodic acid (sp. gr. 1.7).

Structure determination

The mass spectra of the two unknown impurities were recorded by fast atom bombardment mass spectrometry (FAB-MS) using a Kratos AEI MS 50 mass spectrometer.

^{1}H NMR spectra were recorded at 250 MHz on a Bruker (Wissembourg, France) WM 250 instrument in DMSO-d_6 solution, using dimethyl sulphoxide (DMSO) as a reference (δ DMSO = 2.5 ppm). Coupling constants (J) were measured in hertz.

^{13}C NMR spectra were recorded at 50.3 MHz on a Bruker WP 200 SY instrument in DMSO-d_6 solutions, using DMSO as a reference (δ DMSO = 39.5 ppm). The carbon multiplicity was determined by a spin–echo J modulation experiment.

RESULTS AND DISCUSSION

Separation principles

Many drug substances contain nitrogen with basic properties. As these substances are often soluble in water and acetonitrile, reversed-phase HPLC seems to be a suitable technique for their determination. In water–acetonitrile mixtures, they cannot be chromatographed in their non-ionized from because the mobile phase is alkaline and damages the silica-based stationary phase. Consequently, a counter ion has to be added to an acidic mobile phase to allow ion pairing with the solute[8,9]. Often, however, tailing effects or even irreversible adsorption on the stationary phase are observed, probably owing to the presence of residual silanol groups in the stationary phase[10–13]. End-capped stationary phases[14,15] can reduce this tailing effect. Another remedy is to add anti-tailing agents such as long-chain quaternary ammonium[10,16–20] to the eluent. Even though the change may be impressive, the resulting mobile phase is complex; further, these agents are usually paired to anions (*e.g.*, bromide) absorbing at 220 nm, which is a major drawback for the detection of many compounds.

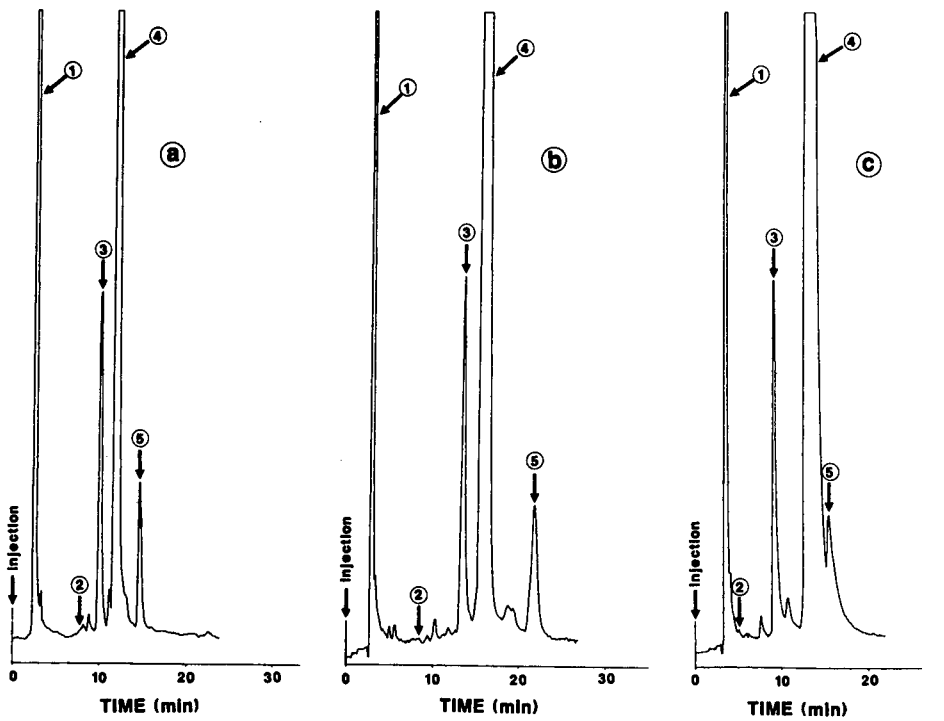

Fig. 2. Influence of the nature of the support on the separation of the main components of a gallamine triethiodide sample. Columns, 25 × 0.46 cm I.D.; stationary phase, (a) 5-μm Nucleosil octadecyl-bonded silica, (b) 5-μm Nucleosil cyanopropyl-bonded silica and (c) 5-μm Nucleosil silica. HPLC conditions: all mobile phases contained 0.1 *M* sodium perchlorate (pH 3); (a) and (b) acetonitrile–water (69:31, v/v); (c) acetonitrile–water (80:20, v/v). Flow-rate, 1 ml/min; detection, UV at 200 nm. Solutes: peaks 1 and 4, gallamine triethiodide; 2 represents the retention time of gallamine base; 3 and 5 are impurities. The appearance of two peaks for gallamine triethiodide is explained in the text.

On the other hand, a small lipophilic counter ion, such as perchlorate, can be used with the highly positively charged ammonium salts such as gallamine triethiodide in order to avoid peak broadening due to slow complex formation kinetics. There are many examples in the literature[13,21–23] in which perchlorates were used as counter ions to quaternary ammonium compounds without any peak tailing.

Retention mechanisms

Using acetonitrile as organic modifier and a perchlorate concentration of 0.1 *M*, the nature of the stationary phase has a minor effect on the retention of gallamine. The elution order is the same on octadecyl-bonded silica, cyanopropyl-bonded silica and bare silica (Fig. 2). Moreover, with these three supports, a decrease in the acetonitrile content of the mobile phase (at a constant perchlorate concentration) increases solute retention. The same phenomenon was observed by Abidi[21] on octadecyl-, cyanopropyl- and phenylpropyl-bonded silica with similar mobile phases.

We studied the dependence of retention on mobile phase perchlorate concentration (Fig. 3). The most important differences were observed between the silica and the two other bonded phases; they were significant at low sodium perchlorate concentration (below 0.1 *M*). Variations of the capacity factors with salt concentration were less pronounced over the concentration range 0.1–0.5 *M*.

The influence of sodium perchlorate on the retention on the cyanopropyl–bonded phase is similar to that on the octadecyl-bonded phase. The affinity of acetonitrile for the cyanopropyl bonds may be greater than that of water because of their chemical similarity. Consequently, the bonded groups could be surrounded by acetonitrile in the same way as octadecyl bonds, which could explain the similarities in chromatographic behaviour (Fig. 3a and b). The shape of the curve of k' *versus* sodium perchlorate concentration obtained is well known and has been thoroughly studied by many workers[24–26].

In reversed-phase ion-pair chromatography, two retention mechanisms are distinguished: the first stipulates the formation of ion pairs in the mobile phase prior to retention on the bonded support; the second predicts ion exchange between the cationic solute and the counter ion already adsorbed on the stationary phase[24–28].

Even though both mechanisms may occur together, the second probably predominates[25,26,28,29], at least with alkylsulphate or alkylsulphonate counter ions. With perchlorate, a much more hydrophilic counter ion, the first mechanism cannot be eliminated. If this mechanism were to predominate, however, the three different stationary phases, assumed to be free of adsorbed counter ions, would show great differences in selectivity and the mobile phase polarity would have opposite effects on retention on these supports. Consequently, the second mechanism based on ion exchange must also play a role. At high concentration, perchlorates are likely to cover the stationary phase pores entirely, whatever the support may be, and there would be ionic interactions between perchlorates and the quaternary ammonium of gallamine.

A decrease in solute retention on silica on increasing the counter ion concentration such as shown in Fig. 3c has already been observed[23,30–32]. Moreover, we observe that the influences of mobile phase polarity and of counter ion concentration were similar to those noted in a previous study[30–32]. Perchlorates are partly adsorbed on silica. The retention mechanism is probably based on ion exchange either directly on silanol (SiO^-H^+) groups (at low sodium perchlorate concentration) or on per-

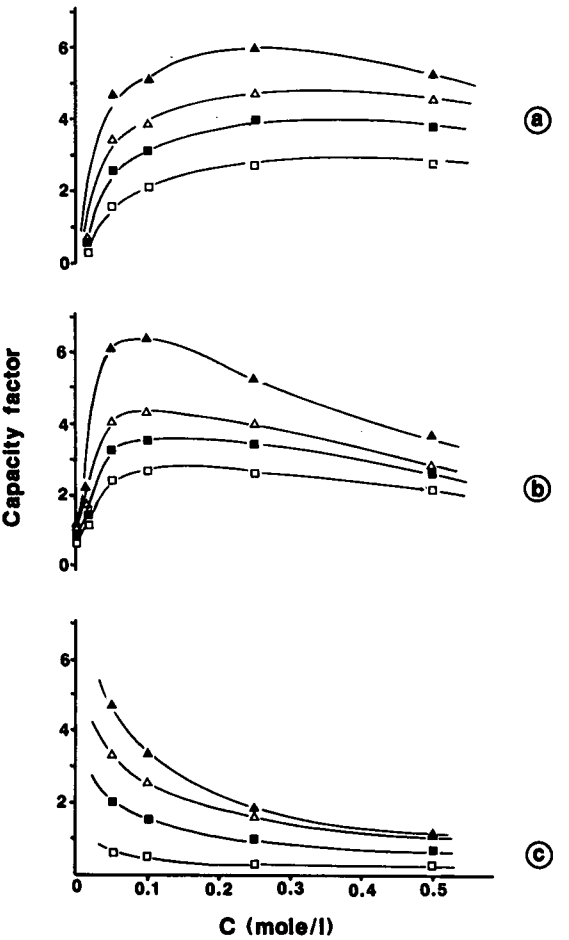

Fig. 3. Influence of the sodium perchlorate concentration in the mobile phase on the capacity factors of the gallamine derivatives. (a) 5-μm Nucleosil octadecyl-bonded silica; (b) 5-μm Nucleosil cyanopropyl-bonded silica; (c) 5-μm Nucleosil silica. HPLC conditions: aqueous phases buffered at pH 3; (a) and (b) acetonitrile–water (69:31, v/v); (c) acetonitrile–water (80:20, v/v). (□) Gallamine base; (■) impurity 3; (△) gallamine triethiodide (peak 4); (▲) impurity 5.

chlorate. The solute retention decrease with increase in sodium perchlorate concentration could be due to the substitution of perchlorate for silanols as interacting points and to the increase in solvent strength. The retention increase with decrease in acetonitrile content in the mobile phase is a consequence of the decreased perchlorate concentration in the stationary phase.

Nucleosil octadecyl-bonded silica was used in the remainder of this study; cyanopropyl-bonded silica also gave good separations but the results were less reproducible.

Identification of chromatographic peaks and optimization of detection parameters

Peak 1 identification was achieved using iodide; the chromatographic peaks ob-

tained after injection of sodium or potassium iodide solution (Fig. 2a) have the same retention times as peak 1. Moreover, the UV spectra [measured by diode array detection (Fig. 4a)] were similar. Hence we conclude that there is an immediate substitution of perchlorate for iodide on gallamine after injection. The iodides, paired with sodium ions, elute in peak 1. Gallamine base is at pH 3.0 triprotonated and coupled to three perchlorate ions; it is eluted in peak 2. Peak 4 detected in gallamine triethiodide batches is due to gallamine triethylperchlorate. We observe that the injected gallamine triethiodide batch contains two impurities (called impurities 3 and 5) corresponding to peaks 3 and 5.

Their structures, determined by NMR and mass spectrometry, are presented in Fig. 5. After their isolation by preparative chromatography, the impurities were paired to perchlorate, which confirms the ion exchange between iodide and perchlorate. Thus, in the gallamine batches, impurities 3 and 5 are gallamine diethiodide and 1,2,3-tris(2-triethylammonioethoxy)-4- (2-triethylammonioethyl)benzene tetraiodide, respectively.

Optimization of the detection wavelength was achieved with a diode array detector. Maximum absorbance of gallamine triethiodide is at 225 nm (Fig. 4b). Gallamine triethiodide, however, contains two chromophores: the aromatic ring and the iodide ions (Fig. 4a). Maximum UV absorbance at 225 nm is due to iodide instead of gallamine. The gallamine UV spectrum, obtained by diode array detection on peak

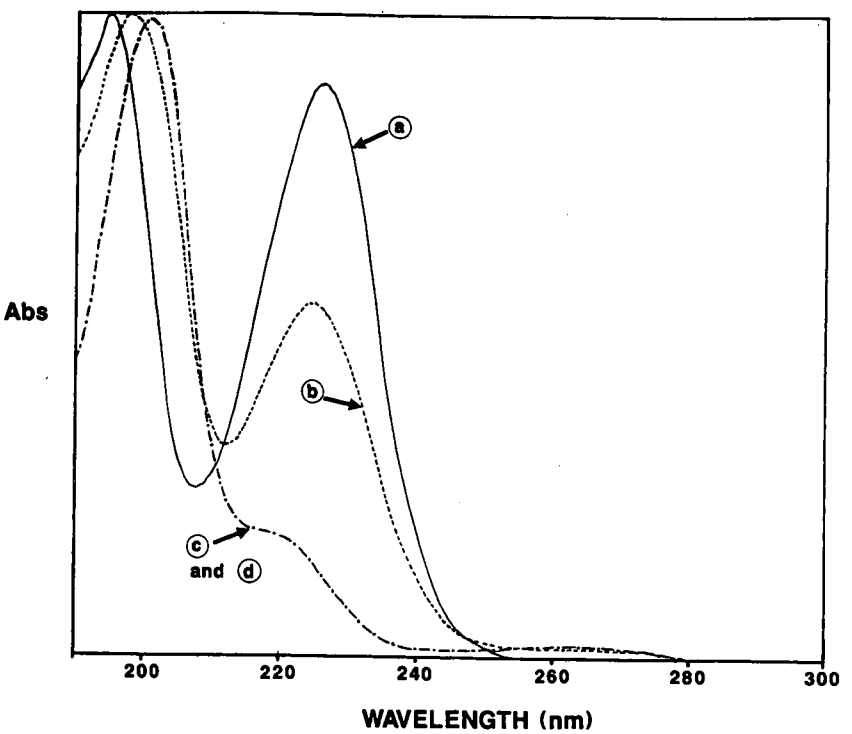

Fig. 4. UV spectra of (a) sodium iodide, (b) gallamine triethiodide, (c) gallamine base and (d) gallamine triethylperchlorate (measured on peak 4 by diode array detection).

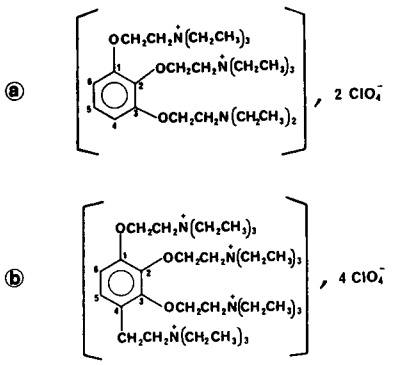

Fig. 5. Structures of (a) impurity 3 and (b) impurity 5.

4 when perchlorate replaces iodide on gallamine (Fig. 4d), is identical with that of gallamine base (Fig. 4c). Its maximum at 200 nm is the optimum detection wavelength (note that we observe a blue shift of about 3 nm for that maximum in the case of gallamine triethiodide. This is due to the merging of iodide and gallamine absorption bands).

In the chromatogram obtained, the iodide to gallamine peak-area ratio depends strongly on detection wavelength (Table I).

When the detection wavelength is set at 230 nm, the peak of gallamine is seven times smaller than that of iodide and this may induce chromatographic errors.

The difficulties in recent studies[5,6] in determining gallamine triethiodide by HPLC and in explaining the retention mechanisms can be understood if we assume that the compound determined was iodide instead of gallamine. In fact, in both instances, the detection wavelength was 230 and 229 nm and gallamine could not be detected.

Quantitative study

Calibration and reproducibility. Based on an acceptable signal-to-noise ratio of 3:1, the detection limit of gallamine at 200 nm is 35 ng/ml of gallamine triethiodide in the injection solution, which corresponds to 0.7 ng injected.

HPLC calibration has been performed on gallamine itself (peak 4) and on iodide. The concentrations of the injected gallamine triethiodide varied from 0.5 to

TABLE I

INFLUENCE OF THE DETECTION WAVELENGTH ON THE AREAS OF IODIDE AND GALLAMINE PEAKS

Parameter	*Wavelength (nm)*			
	200	*210*	*220*	*230*
Iodide peak area	825	339	644	817
Gallamine peak area	1114	609	236	117
Iodide to gallamine peaks-area ratio	0.74	0.56	2.73	6.98

TABLE II

ANALYSIS OF DATA FOR THE REPRODUCIBILITY OF THE ASSAY OF GALLAMINE AND IODIDE

Concentration (μg/ml)	*n*	*Iodide*		*Gallamine*	
		Mean peak area	*C.V.* (%)*	*Mean peak area*	*C.V. (%)*
151.9	15	6487	0.36	8748	0.19
0.50	15	29.6	5.14	29.18	1.65

* Coefficient of variation.

500 μg/ml. The correlation coefficient for gallamine of 0.9997 ($n = 58$) indicates excellent linearity for gallamine triethiodide concentrations between 0.5 and 250 μg/ml.

The same calculations were also done with iodide. The linearity is not as good as with gallamine and the correlation coefficient of 0.9995 ($n = 30$) indicates good linearity but in a more restricted concentration range (7–75 μg/ml). This is mainly caused by the low retention of iodide; peak broadening is weak and UV saturation appears at lower concentrations. On the other hand, at low iodide concentrations, a peak due to the solvent front disturbs the iodide quantification. Consequently, even though this method allows a good evaluation of iodide concentration, it is less precise than a volumetric method of quantification.

The accuracy of the method is shown in Table II. Excellent reproducibility is obtained, even at low concentrations, except for iodide which is difficult to measure for concentrations lower than 15 μg/ml.

We checked the stability of the gallamine triethiodide solution: after 1 week at room temperature, the variations in the iodide and gallamine peak area were not significant (Table III).

Quantification of impurities. The precise measurement of the response coefficients of the impurities, *i.e.*, gallamine base and impurities 3 and 5, requires large amounts of product. However, owing to substitution of perchlorate for iodide in the mobile phase, these impurities contain the same chromophore; all their UV spectra

TABLE III

ANALYSIS OF DATA FOR THE STABILITY OF GALLAMINE TRIETHIODIDE IN THE INJECTION SOLUTION (CONCENTRATION 151.9 μg/ml)

Time (days)	*n*	*Iodide*		*Gallamine*	
		Mean peak area	*C.V. (%)*	*Mean peak area*	*C.V. (%)*
0	15	6487	0.36	8748	0.19
1	4	6508	0.49	8735	0.04
2	4	6483	0.30	8760	0.21
5	4	6474	1.08	8729	0.14
7	4	6542	0.38	8747	0.12

are therefore nearly identical (similar to that of 1,2,3-trimethoxybenzene). Consequently, to a first approximation, their molar absorptivities are identical and the response coefficients to apply to the chromatographic results are roughly proportional to the molecular weight of the impurity.

We tested this hypothesis and found that the gallamine base response coefficient is 0.475 times that of gallamine triethiodide. This agrees well with the gallamine base to gallamine triethiodide molecular weight ratio (0.47).

TLC: Results and comparison with HPLC

Using TLC, the chloride ions, which are very concentrated in the mobile phase, immediately form ion pairs with gallamine, and iodide is eluted in the solvent front. This type of TLC system, in which counter ions such as Cl^-, Br^-, I^- or ClO_4^- are used with quaternary ammonium- or protonated amine-containing solutes has been described[30–32]. The retention mechanism is identical with that described above for silica.

Fig. 6 shows a thin-layer chromatogram of some gallamine batches. Five gallamine triethiodide batches of three different origins were applied to the plate (spots a–e) in addition to gallamine base (spot f) and a mixture of gallamine base, gallamine triethiodide and the two identified impurities (spot g). The R_F valves of gallamine base, impurity 3, gallamine triethiodide and impurity 5 are 0.79, 0.63, 0.53 and 0.39, respectively. For the two gallamine triethiodide batches spotted at a and b (Fig. 6) we observe another unknown impurity with $R_F = 0.18$.

To compare the HPLC results with those obtained by TLC, we injected the same gallamine batches into the HPLC system (Fig. 7). It was necessary to use a

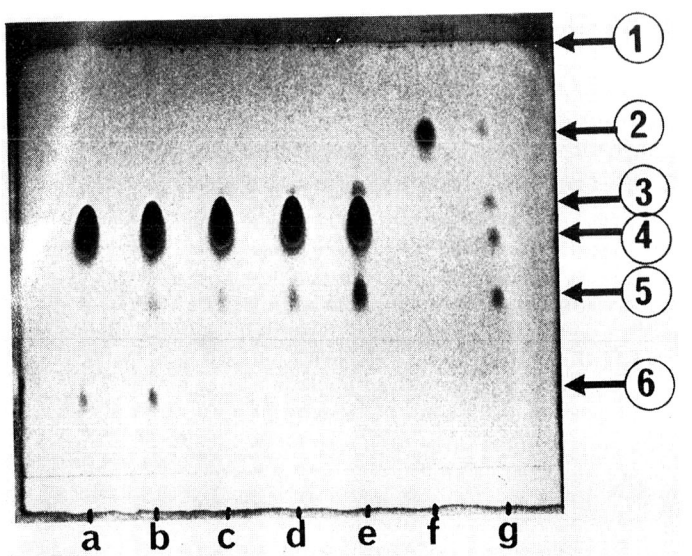

Fig. 6. Thin-layer chromatogram of some gallamine batches. Chromatographic conditions as described under Experimental. Solutes injected: (a–e) gallamine triethiodide batches; (f) gallamine base batch; (g) mixture of gallamine base, gallamine triethiodide and impurities 3 and 5. Spot identification: (1) chloride; (2) gallamine base; (3) impurity 3; (4) gallamine triethylchloride; (5) impurity 5; (6) unidentified.

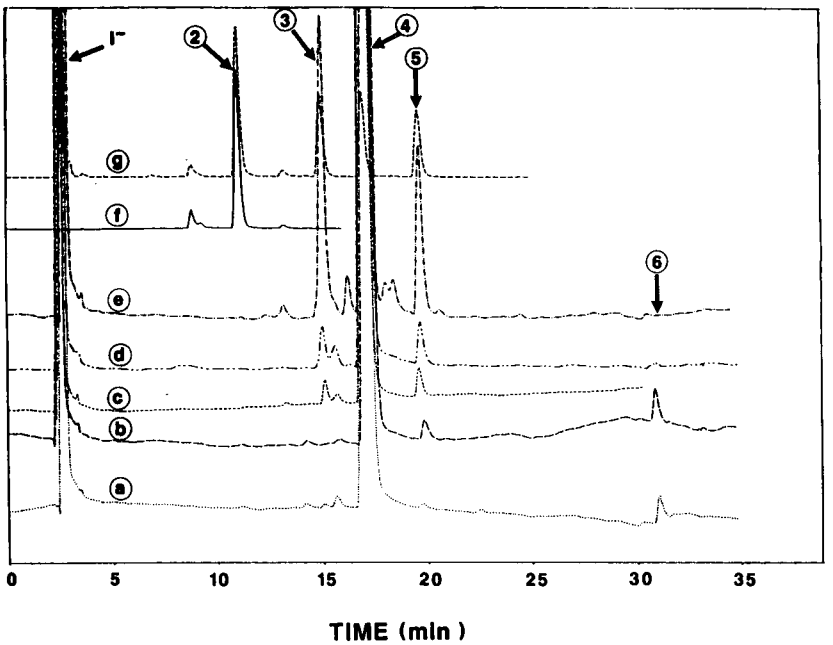

Fig. 7. Chromatograms of gallamine batches obtained with an elution gradient. Column and detection as in Fig. 2a; flow-rate, 1 ml/min. Mobile phase: the sodium perchlorate concentration was kept at 0.1 *M* and the water solution was buffered at pH 3; at time zero the composition was water–acetonitrile (76:24, v/v), changed linearly to (62:38, v/v) at 20 min and (54:24, v/v) at 25 min. (a–e) Gallamine triethiodide batches; (f) gallamine base; (g) synthetic mixture of gallamine basé, gallamine triethiodide and impurities 3 and 5. Solutes: (2) gallamine base; (3) impurity 3; (4) gallamine triethylperchlorate; (5) impurity 5; (6) unknown impurity.

gradient to elute the impurity which may correspond to that revealed in TLC (R_F = 0.18). We observed perfect agreement between the impurities detected in HPLC and in TLC. Even though the new impurity has not yet been identified, and the detection methods used for HPLC and TLC are different (the spray reagent reveals the nitrogen-containing compounds), the new HPLC impurity (peak 6) probably corresponds to that marked 6 (R_F = 0.18) in TLC.

The elution order of all the gallamine impurities was the same in all the TLC and HPLC systems. This similarity between the elution order on octadecyl-bonded silica and on bare silica with an acidic water–organic solvent mobile phase and a counter ion such as perchlorate has already been observed at the beginning of the study.

CONCLUSION

An HPLC method for the determination of gallamine that gives precise and reproducible results has been developed. It was used on a semi-preparative scale to isolate and determine the structure of the two main impurities present in batches of gallamine. They can be quantified by this method as good estimates of their response coefficients compared with that of gallamine are given. The results obtained using a

TLC method for the examination of gallamine triethiodide are consistent with those obtained by HPLC.

ACKNOWLEDGEMENTS

We are very grateful to Mrs. Danzer, Mr. Vuilhorgne and Mr. Monegier du Sorbier for their contributions to the structure determinations.

REFERENCES

1 S. Agonston, G. A. Vermeer, U. W. Kersten and A. H. Scaf, *Br. J. Anaesth.*, 50 (1978) 345.
2 M. I. Ramzan, E. J. Triggs and C. A. Shanks, *Eur. J. Clin. Pharmacol.*, 17 (1980) 135.
3 M. I. Ramzan, E. J. Triggs and C. A. Shanks, *Eur. J. Clin. Pharmacol.*, 17 (1980) 145.
4 M. I. Ramzan, E. J. Triggs and C. A. Shanks, *Eur. J. Clin. Pharmacol.*, 17 (1981) 141.
5 M. J. Shao, K. D. Fallon, S. N. Khalil and E. Abouleish, *J. Chromatogr.*, 345 (1985) 184.
6 I. M. Ramzan, *J. Chromatogr.*, 417 (1987) 428.
7 M. Beaumont, unpublished results.
8 G. Schill, *Nat. Bur. Stand. (U.S.) Spec. Publ.*, No. 519 (1979) 509.
9 G. Schill, *Acta Pharm. Fenn.*, 90 (1981) 43.
10 S. H. Hansen, P. Helboe and M. Thomsen, *J. Chromatogr.*, 409 (1987) 71.
11 W. E. Rudzinski, D. Benett and V. Garica, *J. Liq. Chromatogr.*, 5 (1982) 1295.
12 K.-G. Wahlund and S. Sokolowski, *J. Chromatogr.*, 151 (1978) 299.
13 F. P. Schmiidtchen and H. Oswald, *J. Liq. Chromatogr.*, 9 (1986) 993.
14 *Supelco HPLC Reporter,* Vol. 3, No. 2, Supelco, Bellefonte, PA, 1981.
15 J. A. de Schutter and P. de Moerloose, *J. Chromatogr.*, 437 (1988) 83.
16 M. G. M. de Ruyter, R. Cronnelly and N. Castagnoli, Jr., *J. Chromatogr.*, 183 (1980) 193.
17 M. Wolff, E. M. Winkler, D. Kersten and B. Goeber, *Pharmazie*, 40 (1985) 624.
18 B. A. Persson, S. O. Jansson, M. L. Johansson and P. O. Lagerstrom, *J. Chromatogr.*, 316 (1984) 291.
19 M. J. M. Wells, *J. Liq. Chromatogr.*, 5 (1982) 2293.
20 J. S. Kiel, S. L. Morgan and R. K. Abramson, *J. Chromatogr.*, 320 (1985) 313.
21 S. L. Abidi, *J. Chromatogr.*, 324 (1985) 209.
22 P. A. Mourier, *Analusis,* 17 (1989) 67.
23 J. E. Greving, H. Bouman, J. H. G. Jonkman, H. G. M. Westenberg and R. A. de Zeeuw, *J. Chromatogr.*, 186 (1979) 683.
24 J. H. Knox and R. A. Hartwick, *J. Chromatogr.*, 204 (1981) 3.
25 R. B. Taylor, R. Reid and C. T. Hung, *J. Chromatogr.*, 316 (1984) 279.
26 R. H. A. Sorrel and A. Hulshoff, *Adv. Chromatogr.*, 21 (1983) 87.
27 W. R. Melander and S. Horváth, in M. T. W. Hearn (Editor), *Ion-Pair Chromatography*, Marcel Dekker, New York, 1985, pp. 27–75.
28 A. Bartha, H. A. H. Billiet, L. de Galan and G. Vigh, *J. Chromatogr.*, 291 (1984) 91.
29 A. Bartha, G. Vigh, H. A. H. Billiet and L. de Galan, *J. Chromatogr.*, 303 (1984) 29.
30 R. Giebelmann, *Pharmazie*, 40 (1985) 299.
31 R. Giebelmann, *Pharmazie*, 36 (1981) 857.
32 R. Giebelmann, *Pharmazie*, 40 (1985) 108.

Journal of Chromatography, 462 (1989) 293–301
Elsevier Science Publishers B.V., Amsterdam — Printed in The Netherlands

CHROM. 21 003

ION CHROMATOGRAPHY METHOD FOR IMINODIACETIC ACID DETERMINATION IN BIOLOGICAL MATRICES IN THE PRESENCE OF NITRILOTRIACETIC ACID

RENÉ P. SCHNEIDER, FRITZ ZÜRCHER, THOMAS EGLI* and GEOFFREY HAMER
Institute of Aquatic Sciences, Swiss Federal Institute of Technology (ETH) Zürich and Swiss Federal Institute for Water Resources and Water Pollution Control, Überlandstrasse 133, CH-8600 Dübendorf (Switzerland)

(First received July 29th, 1988; revised manuscript received September 27th, 1988)

SUMMARY

A sensitive ion chromatographic method for the determination of iminodiacetic acid in the presence of nitrilotriacetic acid in cell-free extracts is described using a mixture of carbonate, sodium hydroxide and 4-cyanophenol as the eluent. The eluent conductivity was chemically suppressed with a membrane suppressor and a conductivity detector was used for subsequent detection. The membrane was continuously regenerated with a sulphuric acid solution. Using a 20-μl injection loop, the detection limit for iminodiacetic acid was 230 μg/l. The influence of the eluent composition on the chromatography of iminodiacetic acid and interference by compounds present in biological matrices are discussed.

INTRODUCTION

The widespread eutrophication of lakes and rivers can be related to phosphate-containing discharges and run-off. A significant part of the phosphates in discharges from municipal sewage treatment works, which frequently are not equipped for effective phosphate elimination, is derived from household washing powders. In order to reduce phosphate loads in municipal sewage there is a trend towards replacement of the polyphosphates in washing powders by other chelating agents, *e.g.*, nitrilotriacetate (NTA). Hence, it has become essential to determine the fate of NTA in aqueous environments.

NTA has been shown to be biodegraded under both oxic and anoxic conditions[1–5]. The first enzyme involved in the metabolic pathway of NTA degradation in obligately aerobic bacteria was shown to be a monooxygenase which cleaves NTA into glyoxylate and iminodiacetic acid (IDA)[5–7]. However, the correct stoichiometry of this reaction has not yet been established and the metabolic fate of IDA still has to be elucidated[8].

Methods for the determination of NTA and glyoxylate in cell-free extracts are available[9,10]. Existing techniques for the determination of IDA have been evaluated

0021-9673/89/$03.50

and found to be ineffective for the problem cited above. The spectrophotometric method proposed by Bhattacharyya and Saha[11] was subject to interference by NTA, whilst gas chromatographic procedures[12,13] are both tedious and of poor reproducibility in cell-free extracts. Therefore, it became necessary to develop the new method described herein.

EXPERIMENTAL

Chemicals

All chemicals used were either of reagent grade or better and were obtained from either Fluka (Buchs/SG, Switzerland) or Merck (Darmstadt, F.R.G.).

Apparatus

The chromatographic system consisted of a Dionex DQP-1 pump, a Rheodyne 7125 injection valve fitted with an actuator position sensing switch (Rheodyne, Cotati, CA, U.S.A.), a 50-mm precolumn (Omnifit, Cambridge, U.K.) packed with a mixture of three parts of neutral precolumn material and two parts of macroporous cation-exchange resin (both from Sykam, Gauting, F.R.G.), an HPIC-AS3 ion chromatography column and an AMMS-1 anion micromembrane suppressor from Dionex (Sunnyvale, CA, U.S.A.). The eluent and regenerant were degassed under vacuum in collapsible containers (Cole-Palmer Instrument Company, Chicago, IL, U.S.A.). The regenerant was delivered to the suppressor with a minimicro 2/6 peristaltic pump (Ismatec, Zürich, Switzerland). With the exception of manufacturer fitted steel capillaries associated with the pump and the injection system and for Tygon tubing employed in the peristaltic pump, all connections were made of PTFE. The conductivity of the eluent was measured with a Sykam S3110 conductivity detector. The chromatogram was recorded on a W + W 600 recorder (W + W, Basle, Switzerland).

Reagents

Pure water was obtained from a NANOpure system (Barnstead, Boston, MA, U.S.A.). Eluent was delivered at 1 ml/min with a pressure of 4.4 MPa. A 0.05 *M* sulphuric acid solution was used as the regenerant at a flow-rate of 3.3 ml/min.

Solutions used for calibration

Pure water + IDA. Samples were prepared from a stock solution containing 30 mg/l IDA.

Tris–HCl + IDA. A 30 m*M* Tris solution containing 30 mg/l IDA was prepared and pH was adjusted to 7.5 with hydrochloric acid. Samples were obtained by appropriate dilution in 30 m*M* Tris–HCl pH 7.5.

Determination of IDA in cell-free extracts

The culture, harvest and disruption of cells from *Pseudomonas* sp. ATCC 29600 were performed as described by Schneider *et al.*[9]. Samples for calibration were prepared by diluting a cell-free extract stock solution containing 30 mg/l IDA in cell-free extract. Protein was precipitated by boiling of samples for 5 min. The precipitate was removed by centrifugation at 18 000 *g* for 5 min and the supernatant was used for IDA determination. Protein was determined by the method of Bradford[14].

Ion-exclusion chromatography (IEC)

IEC was performed as described by Schneider *et al.*[9].

RESULTS AND DISCUSSION

A primary problem in ion chromatographic analysis of IDA is its diprotic nature, *i.e.*, it changes its speciation with pH. This requires definition of the most appropriate of the three IDA species, $IDAH_2$, $IDAH^-$, IDA^{2-} (Fig. 1) for effective analysis.

Chromatography of $IDAH_2$

Under the acidic conditions (pH 2.8) prevalent in IEC, which was successfully employed for analysis of the structurally similar NTA[9], $IDAH_2$ is the predominant species. However,injection of this compound into the IEC system resulted in no peak, indicating a very strong affinity of $IDAH_2$ for the matrix material (IDA would have been detected as $IDAH^-$, as the pH of the eluent after passage through the suppressor was 7.0). Therefore, for analysis of IDA to be successful the pH of the eluent has to be increased to values where $IDAH^-$ or IDA^{2-} exist. This is the ideal operating range of standard ion chromatography, where IDA is detected as $IDAH^-$.

Chromatography of $IDAH^-$

First chromatography of the $IDAH^-$ species was evaluated using 0.5 m*M* bicarbonate, pH 8.3. Under these conditions no IDA peak was detected (Fig. 2, curve A). As only one carboxylic group is deprotonated at this pH, a large part of the $IDAH^-$ molecule containing the nitrogen-atom and the neutral carboxylic group might interact non-ionically with the resin matrix. This non-ionically adsorbed $IDAH^-$ might not be efficiently displaced by HCO_3^- and therefore no IDA peak was observed. Addition of 0.8 m*M* 4-cyanophenol to this eluent (pH maintained at 8.3) resulted in a broad, near symmetrical IDA peak (Fig. 2, curve B). This clearly demonstrates the ability of 4-cyanophenol to act as a modifier by reducing the column's capacity for non-ionic interaction. Even so, this column modification failed to give satisfactory chromatographic elution, suggesting that $IDAH^-$ is unsuitable for analysis.

Chromatography of IDA^{2-}

The alternative was to promote formation of the IDA^{2-} species by operation at even higher pH values. This was achieved by using different carbonate solutions as eluents. For an eluent containing 0.20 m*M* carbonate and 0.84 m*M* 4-cyanophenol (pH 9.5) a sharp peak with extensive tailing resulted (Fig. 2, curve C). In order to reduce the tailing, which was caused by the remaining $IDAH^-$, the carbonate concen-

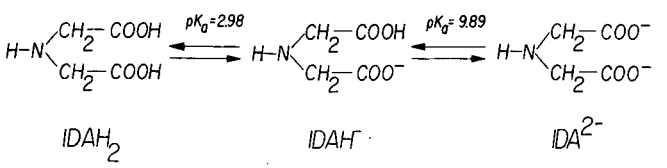

Fig. 1. Structures of the three possible IDA species and the respective pK_a values.

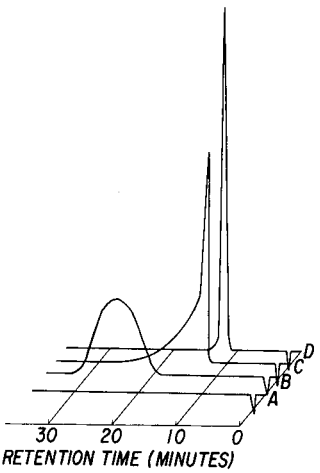

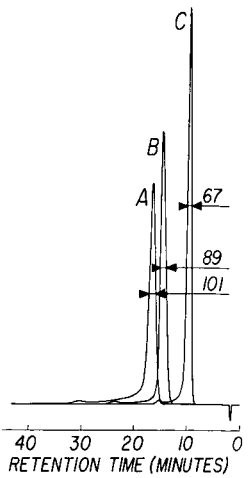

Fig. 2. Effect of different eluent compositions on chromatography of IDA: (A) 0.5 m*M* bicarbonate, pH 8.3; (B) 0.5 m*M* bicarbonate + 0.84 m*M* 4-cyanophenol, pH 8.3; (C) 0.2 m*M* carbonate + 0.84 m*M* 4-cyanophenol, pH 9.5; (D) 1.15 m*M* carbonate + 0.84 m*M* 4-cyanophenol, pH 10.2. A 20-μl volume of IDA standard solution (120 mg/l) was injected.

Fig. 3. Effect of different eluent compositions on chromatography of IDA^{2-}. Peak widths (in seconds) are given. (A) 0.98 m*M* carbonate, pH 10.7; (B) 1.16 m*M* carbonate + 2 m*M* sodium hydroxide, pH 10.90; (C) 1.11 m*M* carbonate + 2 m*M* sodium hydroxide + 0.84 m*M* 4-cyanophenol, pH 10.84. A 20-μl volume of IDA standard solution (120 mg/l) was injected.

tration in the above mentioned eluent was increased to 1.15 m*M* (resulting in pH 10.2). With this eluent, tailing was almost eliminated (Fig. 2, curve D), clearly indicating that for effective chromatography it is essential to convert most of the IDA into IDA^{2-}.

In order to comprehensively investigate the chromatographic behaviour of IDA^{2-}, further experiments were conducted with carbonate eluents (Fig. 3). With an eluent containing only carbonate (0.98 m*M*, pH 10.71) a broad peak (width 100.8 s) and slight tailing resulted (Fig. 3, curve A). The tailing was virtually eliminated by addition of 2.0 m*M* sodium hydroxide which increased the pH to 10.90 and also gave increased sensitivity (peak width 88.8 s; Fig. 3, curve B). Addition of 0.84 m*M* 4-cyanophenol to the carbonate–sodium hydroxide eluent resulted in a further improvement in sensitivity, the resulting peak width being 67.2 s with an eluent of pH 10.84 (Fig. 3, curve C).

From Figs. 2 and 3 it is clear that the eluent composition not only determines the peak shape but also affects the retention time. As there are four ionic species, *i.e.*, HCO_3^-, OH^-, CO_3^{2-} and deprotonated 4-cyanophenol (cnp^-) present in the eluent, experiments were conducted with controlled eluent compositions to investigate the impact of each ionic species on the residence time of IDA^{2-}. As the pH must be kept above 10.8 for efficient IDA chromatography (Fig. 3), changes in the species distribution in the HCO_3^-/CO_3^{2-} (pK_a 10.25) system have to be considered, whereas the speciation of cnp^- (pK_a 7.98) and OH^- are not affected at pH values above 10.8. In Fig. 4 the relationship between the retention time and the actual carbonate concentra-

tion is shown for a range of 4-cyanophenol concentrations in the eluent. The upper line represents pure carbonate, achieved either with carbonate alone or with added OH^-. The pH increase due to addition of OH^- will cause the HCO_3^-/CO_3^{2-} equilibrium to shift towards CO_3^{2-}. The points representing carbonate–sodium hydroxide eluents fit on the same line as points representing pure carbonate eluents (Fig. 4). Thus the carbonate concentration is the determining factor with respect to the retention time, whereas OH^- and HCO_3^- *per se* do not affect the elution strengths of the eluents. The remaining lines in Fig. 4 represent increasing 4-cyanophenol concentrations, 0.25, 0.50 and 0.84 m*M*, respectively, showing that 4-cyanophenol is, in addition to CO_3^{2-}, a retention time determinant.

It has already been shown that 4-cyanophenol functions as a modifier in the case of $IDAH^-$ (Fig. 2), but it is important to determine whether its effect is the same in the case of IDA^{2-}. In experiments where 4-cyanophenol–sodium hydroxide eluents (pH 10.8) were used, retention times for IDA^{2-} were inordinately long even at the highest 4-cyanophenol concentration tested, *i.e.*, > 50 min for 1.25 m*M* 4-cyanophenol, showing these combinations to be extremely weak eluents. The marked effect of 4-cyanophenol in carbonate eluents, as shown in Fig. 4, strongly suggests that 4-cyanophenol interaction with the column material also plays a rôle in the case of IDA^{2-}. As shown in Fig. 3, 4-cyanophenol addition to an eluent where most of the IDA is converted into IDA^{2-} does not dramatically affect the peak shape. This means that the mechanism of 4-cyanophenol action in chromatography of IDA^{2-} differs from its effect on analysis of $IDAH^-$. In the former case, 4-cyanophenol acts essentially as an accelerating agent, probably by blocking positively charged ion-exchange groups inside the resin, thereby leaving only the easily accessible cationic exchange groups on the resin surface to interact with IDA^{2-} and CO_3^{2-}, thus shortening diffusion pathways. Therefore, this mechanism should not be restricted to IDA^{2-}, as it is not based on a specific property of the IDA^{2-} molecule, but should

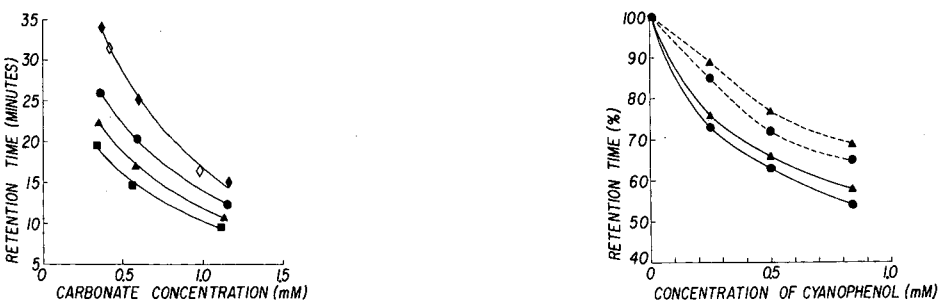

Fig. 4. Influence of carbonate and 4-cyanophenol on the retention time of IDA. The following eluent compositions are shown: ◇ = carbonate; ◆ = carbonate + 2 m*M* sodium hydroxide; ● = carbonate + 2 m*M* sodium hydroxide + 0.25 m*M* 4-cyanophenol; ▲ = carbonate + 2 m*M* sodium hydroxide + 0.50 m*M* 4-cyanophenol; ■ = carbonate + 2 m*M* sodium hydroxide + 0.84 m*M* 4-cyanophenol. Carbonate concentrations given in the figure are actual concentrations in the eluent. Lines connect eluents with constant 4-cyanophenol concentrations.

Fig. 5. Effect of 4-cyanophenol on the retention of IDA^{2-} (▲) and SO_4^{2-} (●). Dashed lines represent an eluent containing 0.37 m*M* carbonate + 2 m*M* sodium hydroxide; continuous lines represent an eluent containing 1.16 m*M* carbonate + 2 m*M* sodium hydroxide. Retention times are given relative to eluents containing no 4-cyanophenol.

also apply to other typical anions such as SO_4^{2-}. In Fig. 5 the effects of the 4-cyanophenol concentration on the retention time for both IDA^{2-} and SO_4^{2-} are shown for two carbonate eluents (0.37 m*M* carbonate + 2 m*M* sodium hydroxide; 1.16 m*M* carbonate + 2 m*M* sodium hydroxide). The similar behaviour of IDA^{2-} and SO_4^{2-} strongly supports the postulate that the mechanism of 4-cyanophenol action generally applies for anions and that IDA^{2-} behaves as a typical doubly charged anion.

Precipitation of proteins

For the analysis of IDA in cell-free extracts, the protein must be precipitated from the samples prior to chromatography. Protein precipitation with trichloroacetic acid (TCA) was successfully employed in the determination of NTA[9], but in the case of IDA this simple procedure was impossible because interference occurred between TCA and IDA during chromatography.

One possible solution to this problem is removal of TCA from samples prior to analysis. If the pH of the sample is adjusted to 1.8, most of the IDA present will be fully protonated ($IDAH_2$), whereas TCA will remain predominantly in the anionic state. As mentioned above, $IDAH_2$ is effectively adsorbed on resin material. Therefore, the use of a cationic exchange resin should allow efficient adsorption of $IDAH_2$, whereas negatively charged TCA anions should be excluded by the negatively charged resin. Acidified samples (pH 1.8 with hydrochloric acid) were applied to a 50-mm column (Omnifit) packed with Dowex 50W-X4 (20–50 mesh) (Fluka) which had been previously conditioned with hydrochloric acid, pH 1.8. The column was washed with five volumes of hydrochloric acid, pH 1.8. IDA was totally retained on the column and most of the TCA was removed in the waste. Elution of retained substances with an eluent containing 0.56 m*M* carbonate + 0.84 m*M* 4-cyanophenol + 2 m*M* sodium hydroxide was retarded due to initially complete protonation of the eluent ions by the excess of protons (H^+) which were loaded on the column during the conditioning and washing procedure. This caused the temporary build up of a pH gradient along the column. Desorption of IDA started only when most of the H^+ were neutralized such that the inlet composition of the eluent was progressively re-established. The pH gradient caused IDA to elute as a very broad peak, similar to that shown in Fig. 2 (curve B) but the residual TCA, which remained adsorbed on the resin after the washing procedure, still caused strong interference with IDA. The retardation effect and the pH gradient were almost eliminated by diluting the cationic exchange resin in neutral material, 98% styrene + 2% divinylbenzene copolymer (Fluka), but interference from TCA still remained prohibitive.

Another possibility for effective TCA removal is acidification to pH 0 with hydrochloric acid followed by extraction of the sample with diethyl ether[15]. IDA remains in the aqueous phase probably because of its positive charge due to protonation at the nitrogen atom. As diethyl ether is soluble in water at this low pH and as it decomposes the resin material, it had to be removed by extraction with tetrachloroethylene. The resulting solution could then be injected into the system without affecting its integrity. Although TCA had been quantitatively removed, no analysis of IDA was possible due to the high concentrations of inorganic anions introduced into the sample by acidification with hydrochloric acid.

Therefore, alternative methods for removing protein from the samples to be

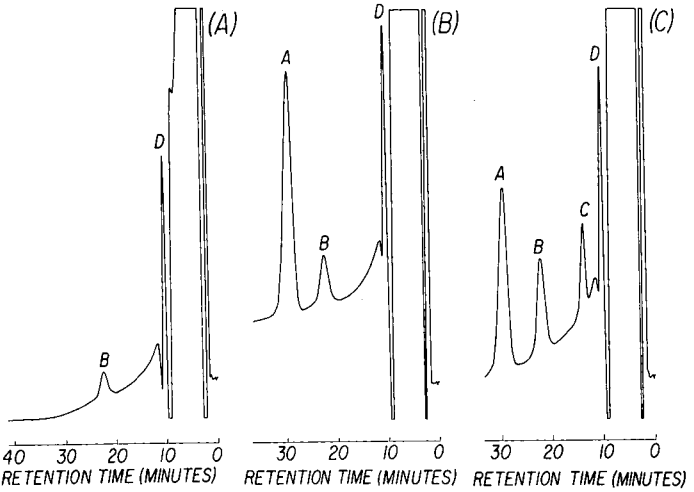

Fig. 6. Influence of matrix components on chromatography of IDA. (A) Tris–HCl buffer, 30 m*M*; (B) Tris–HCl buffer, 30 m*M*, containing cell-free extract; (C) same as (B) but containing 1 mg/l IDA. Protein concentration 3.0 mg/ml. Peaks: A = PO_4^{3-}; B = SO_4^{2-}; C = IDA^{2-}; D = unidentified compound. A 20-μl volume of sample was injected.

analysed were investigated. Filtration through protein-impermeable membranes (MPS-1; Amicon, Danvers, MA, U.S.A.) proved unsuccessful because of poor recovery of IDA in the filtrate. However, by boiling samples, protein could be denatured and precipitated such that it could be effectively removed by subsequent centrifugation with good recovery of IDA.

Analysis of cell-free extract

Final optimization of the eluent for use in the chromatographic analysis of IDA in cell-free extracts resulted in the following eluent composition: 0.56 m*M* carbonate + 0.84 m*M* 4-cyanophenol + 2 m*M* sodium hydroxide. In Fig. 6 three chromatograms are illustrated: (A) 30 m*M* Tris–HCl buffer; (B) cell-free extract in Tris–HCl buffer and (C) cell-free extract with IDA in Tris–HCl buffer. Several predominant peaks were associated with the Tris–HCl buffer employed, especially SO_4^{2-} (peak B) and an unidentified substance (peak D). The presence of 4-cyanophenol in the eluent was essential to move IDA (peak C) away from peak D. In the absence of 4-cyanophenol, peak D and IDA (peak C) overlapped irrespective of the carbonate concentrations employed.

Interferences

In the analysis of specific compounds in complex biological matrices, numerous materials that are generally present in variable concentrations frequently interfere with analytical procedures developed with artificial systems. To evaluate the extent of such potential interference, retention times for a wide range of possible interfering substances were determined in the system proposed (Table I). In general, interference was minimal, provided relatively low concentrations of the various compounds evaluated were present in the samples to be analysed.

TABLE I

RETENTION TIMES OF SOME POTENTIALLY INTERFERING COMPOUNDS COMMONLY FOUND IN BIOLOGICAL MATRICES

The concentrations tested were 200 mg/l and the injection volume was 20 μl. The eluent was 0.5 m*M* carbonate + 2.0 m*M* sodium hydroxide + 0.84 m*M* 4-cyanophenol.

Compound	*Retention time (min)*	*Compound*	*Retention time (min)*
Water	2.4	IDA	14.7
Propionate	2.4	Succinate	16.5
Acetate	2.4	Malonate	17.7
Butyrate	2.7	Maleate	18.9
Glycolate	3.0	NTA	22.0
Pyruvate	3.3	SO_4^{2-}	22.2
Cl^-	5.7	Oxalate	25.8
EDTA	8.4	PO_4^{3-}	28
NO_3^-	8.4	Fumarate	39
N-Methyl-IDA	12.3	Glycine	–*
TCA	12.3	Sarcosine	–*
Malate	14.4		

* Compound not detected.

Calibration curves and sensitivity

In order to evaluate the efficacy of the proposed chromatographic method, analyses were performed for known concentrations of IDA in three different matrices: distilled water, 30 m*M* Tris–HCl buffer and cell-free extract. The results obtained are shown in Fig. 7. The calibration plots are parallel indicating no influence of the

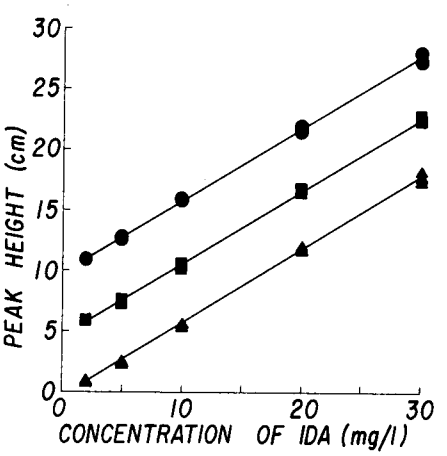

Fig. 7. Calibration plots obtained for IDA in different matrices. ● = IDA in pure water; ■ = IDA in Tris–HCl buffer, 30 m*M*; ▲ = IDA in cell-free extract (protein concentration in 300 m*M* Tris–HCl buffer, pH 7.5, was 30 mg/ml). To clearly distinguish between the different calibration plots shown in the figure, 5 cm and 10 cm were added to peak height values obtained from IDA in 30 m*M* Tris–HCl, pH 7.5 and for IDA in pure water, respectively. Three experiments were performed for each concentration tested. Calibration plots were obtained from linear regression analysis. A 20-μl volume of sample was injected.

matrix on the peak response. Replicate analyses were reproducible to within 2.8%. The calculated limit of determination[16] using a 20-μl injection loop was 230 μg IDA per litre for samples containing cell-free extract; it was considerably below 50 μg/l in distilled water, but no attempts were made to extensively characterize the system performance in this range. As the eluent pH has to be kept above 10.8 and interferences by other compounds in chromatography of IDA have to be avoided, very little flexibility with respect to modification in eluent composition exists. Such minor possible modification will not affect the sensitivity because a very small change in the ionic composition of the eluent will cause only a slight shift in eluent pH after suppressor passage such that neither background conductivity nor IDA protonation will change considerably. The sensitivity for determination of IDA in cell-free extract can be improved by utilizing off-line concentration columns of the type used for removal of TCA. If samples with low concentrations of IDA are to be analysed it is indispensable to use detectors equipped with well designed thermostated conductivity cells. In our experience, electronic temperature compensation of poorly (thermally) insulated detector cells produced unacceptable noise levels when high sensitivity measurements were needed.

ACKNOWLEDGEMENTS

R. P. S. thanks the Research Commission of ETH Zürich for financial support. Our thanks are due to Walter Suter, Hans-Ulrich Weilenmann and Mario Snozzi for technical and scientific support and to Mr. P. Schlup for photographic work.

REFERENCES

1 L. Anderson, E. Bishop and L. Campbell, *CRC Crit. Rev. Toxicol.*, 15 (1985) 1.
2 T. Egli, H. U. Weilenmann, T. El-Banna and G. Auling, *System. Appl. Microbiol.*, 10 (1988) 297.
3 S. O. Enfors and N. Molin, *Water Res.*, 7 (1973) 881.
4 T. Egli and H. U. Weilenmann, *Experientia*, 42 (1986) 1061.
5 M. K. Firestone and J. M. Tiedje, *Appl. Environ. Microbiol.*, 35 (1978) 955.
6 R. E. Cripps and A. S. Noble, *Biochem. J.*, 136 (1973) 1059.
7 M. K. Firestone, S. D. Aust and M. Tiedje, *Arch. Biochem. Biophys.*, 190 (1978) 617.
8 T. Egli, *Microbiol. Sci.*, 5 (1988) 36.
9 R. P. Schneider, F. Zürcher, T. Egli and G. Hamer, *Anal. Biochem.*, 173 (1988) 278.
10 F. Trijbels and G. D. Vogels, *Biochim. Biophys. Acta*, 113 (1966) 292.
11 S. N. Bhattacharyya and N. C. Saha, *Talanta*, 23 (1976) 331.
12 C. B. Warren and E. J. Malec, *J. Chromatogr.*, 64 (1972) 219.
13 R. A. Larson, J. C. Weston and S. M. Howell, *J. Chromatogr.*, 111 (1975) 43.
14 M. Bradford, *Anal. Biochem.*, 72 (1976) 248.
15 R. M. C. Dawson, D. C. Elliott, W. H. Elliott and K. M. Jones, *Biochemical Databook*, Clarendon Press, Oxford, 3rd ed., 1986.
16 W. Funk, V. Dammann, C. Vonderheid and G. Oehlmann, *Statistische Methoden in der Wasseranalytik*, VCH, Weinheim, 1st ed., 1985.

Journal of Chromatography, 462 (1989) 303–313
Elsevier Science Publishers B.V., Amsterdam — Printed in The Netherlands

CHROM. 21 042

MISE AU POINT D'UNE MÉTHODE PAR CHROMATOGRAPHIE LIQUIDE HAUTE PERFORMANCE ÉCHANGEUSE D'IONS EN DÉTECTION ULTRAVIOLETTE, POUR LE DOSAGE DES CATIONS DANS LES SÈVES XYLÉMIQUES

BRUNO SARROBERT, PHILIPPE BRUNET et NICOLE PARIS-PIREYRE*
Laboratoire de Physiologie Végétale, Université des Sciences et Techniques du Languedoc, Place E. Bataillon, 34060 Montpellier Cedex (France)
(Reçu le 3 octobre 1988)

SUMMARY

Determination of cations in xylem sap by ion-exchange high-performance liquid chromatography with ultraviolet detection

An high-performance liquid chromatographic method is described for the simultaneous determination of cations in xylem sap without pretreatment. In order to reduce analysis time and to improve peak separation we calculated the mobile phase velocity and the Ce^{3+} concentration in the mobile phase using the capacity factor, the separation factor and the peak width at half height. Xylem sap was analyzed under optimal conditions. The reproductibility of this method was determined and compared with that of flame spectrophotometric methods. No significant differences were found between the two methods described. Advantages of the new method and its application to a wide range of biological samples are discussed.

INTRODUCTION

Durant ces dix dernières années, de nombreuses recherches ont été effectuées sur l'utilisation de l'analyse par chromatographie liquide haute performance (HPLC) pour la séparation et la quantification d'ions inorganiques. Les premiers travaux dans ce domaine furent réalisés par Small *et al.*[1] qui utilisaient un système de séparation à double colonne couplé à un conductimètre. Depuis, ce dispositif a été amélioré. En effet, la mise au point de nouvelles phases stationnaires avec des polymères échangeurs d'ions à faible capacité greffés sur des résines de faible granulométrie, ainsi que de nouvelles méthodes de détection, a permis une réduction du temps d'analyse et un gain de sensibilité[2–6].

Si la détection par conductimétrie reste encore la plus employée, la détection par chromatographie par détection photométrique indirecte (IPC) devient de plus en plus populaire[7]. Son principe est basé sur la mesure en UV, à une longueur d'onde

0021-9673/89/$03.50

appropriée, de la diminution de l'absorbance initiale de l'éluant due au passage d'ions dans la cellule de détection[8,9]. Ainsi, il est possible de doser selon le type de colonnes et d'éluants, soit les anions[10,11] soit les cations[12].

Si, dans le domaine de l'analyse cationique de l'eau, cette méthode a été immédiatement pressentie[13] et employée[14], seuls quelques rares travaux portent sur l'analyse d'extraits biologiques, tel le sérum humain[15] ou différents jus de légumes[16]. Pour les sèves xylémiques, l'emploi des méthodes classiques de dosages par spectrophotométrie de flamme reste prépondérant[17–20]. Dans notre laboratoire, la méthode de dosage au microanalyseur à sonde électronique selon la technique de Roinel[21], a été adaptée avec succès par Gartner *et al.*[22,23]. Mais à notre connaissance aucune approche utilisant les technique d'analyses par HPLC n'a été réalisée.

En conditions de cultures normales, les cations présents et analysés dans les sèves xylémiques sont le sodium, le potassium, le magnésium, le calcium, et selon l'apport d'azote dans le milieu de culture, l'ammonium. Les méthodes classiques d'analyses cationiques nécessitent souvent un volume de prise d'essai trop important par rapport aux volumes exsudés limitant très souvent les dosages, particulièrement pour des plantes mises en conditions de stress (salin, froid ...).

Conscients des avantages que procure l'emploi de l'HPLC pour l'analyse des sèves xylémiques[24], nous nous sommes inspirés des travaux de Sherman et Danielson[14] pour mettre au point une méthode adaptée à notre matériel en vue de dosages répétitifs et rapides.

MATÉRIEL ET MÉTHODES

Instrumentation

L'appareil d'HPLC utilisé est un Varian LC 5000, équipé d'une boucle d'injection de 10 μl, et couplé à un détecteur Varian UV 100. Un intégrateur Varian 4270 est utilisé pour le tracé des chromatogrammes et le calcul des concentrations. Les séparations sont réalisées sur une colonne ION 210 (Interaction Chemicals, Mountain View, CA, U.S.A.), de dimension 100 × 3,2 mm I.D., à température ambiante. La phase est constituée de particules de 5 μm de résine de polystyrène–divinylbenzène greffée de ponts sulfoniques.

Notre dispositif étant prévu pour des analyses de sèves par injection directe sans purification préalable, une pré-colonne (Interaction GC-200) est montée afin de préserver la colonne.

Pour la vérification de la méthode par HPLC, nous avons dosé en parallèle les cations des différents types de sèves sur un spectrophotomètre de flamme IL 4000, en émission pour K^+ et Na^+ et en absorption pour Ca^{2+} et Mg^{2+}.

L'ion NH_4^+ est dosé selon la méthode de Solarzano[25] par colorimétrie sur un spectrophotomètre Lambda 3 (Perkin-Elmer, Norwalk, CO, U.S.A.). Les spectres d'absorption sont réalisés sur le même appareil couplé à un intégrateur Shimadzu C-R4A (Shimadzu, Kyoto, Japan).

Réactifs

Les solutions étalons sont préparées à partir de produits Merck pour analyse (Darmstadt, F.R.G.). L'éluant est une solution de Ce^{3+} [$Ce_2(SO_4)_3 \cdot 8H_2O$, Aldrich, Gold Label]. Nous utilisons de l'eau bidistillée et dé-ionisée sur un appareil Waters.

Les solutions sont filtrées sur filtres Millipore (Millipore, Bedford, MA, U.S.A.) HATF (hydrosol analysis triton free) de 0,45 μm.

Prélèvements des sèves xylémiques

Les conditions de culture et de prélèvements des sèves xylémiques sont celles décrites par Lakhdari[26]. Le matériel végétal choisi est la tomate (*Lycopersicon esculentum* Mill.). Les analyses sont effectuées à partir d'un mélange prélevé sur huit plantes poussant dans les mêmes conditions de culture. Les stress appliqués sont le froid (10°C) ou un apport de chlorure de sodium (50 m*M*) dans la solution de culture durant 14 jours avant la récolte.

RÉSULTATS

Partant des travaux de Sherman et Danielson[14], nous avons défini les conditions chromatographiques pour l'analyse simultanée des cations majeurs présents dans les sèves xylémiques de tomate.

Détermination des conditions chromatographiques

Choix des paramètres de détection

Détermination de la longueur d'onde optimale. L'origine et la qualité du solvant d'élution pouvant intervenir sur le profil du spectre d'absorption en UV, et de ce fait nuire à la qualité de la détection par IPC, nous avons jugé nécessaire de fixer la longueur d'onde où la différence d'absorption entre l'éluant pur et en présence d'une solution de chlorure de sodium est maximale. La Fig. 1 nous montre que, dans notre dispositif, c'est à 254 nm que cette différence est la plus grande.

Sensibilité du détecteur. La détection en UV, par rapport à d'autres détections telle la fluorimétrie, entraîne des fluctuations et parfois des dérives de lignes de bases importantes malgré l'emploi d'un solvant en condition isocratique. Ces fluctuations peuvent être autant de sources d'erreurs pour le calcul des surfaces des pics détectés. Les travaux de Sherman et Danielson[14] ont montré que l'emploi du $Ce_2(SO_4)_3$ comme solvant d'élution en IPC par rapport au $CuSO_4$ permet d'abaisser les limites de détection pour un grand nombre de cations. De plus, les différentes analyses de sèves xylémiques que nous avons effectuées (Tableau I), montrent que les teneurs des différents cations sont bien au-delà du seuil de sensibilité défini par ces auteurs. Cela nous permet de diluer par dix les exsudats et de constituer pour la suite des travaux la solution étalon suivante: NaCl, 1 m*M*; KNO_3, 1 m*M*; $MgSO_4$, 0,25 m*M*; $CaSO_4$, 0,5 m*M*.

En faisant varier la sensibilité du détecteur (0,002, 0,005, 0,01, 0,02 et 0,05 A.U. mV^{-1}), nous avons constaté qu'au fur et à mesure que la sensibilité augmente, la ligne de base devient de plus en plus instable. Afin d'obtenir une ligne de base qui fluctue peu, tout en conservant une bonne intégration, nous avons retenu une sensibilité de 0,01 A.U. mV^{-1} pour la suite des experiences.

Choix des paramètres sur l'HPLC

Afin de pouvoir analyser un grand nombre d'échantillons, il était important pour nous de reduire le plus possible la durée de l'analyse sans nuire à sa qualité. Pour

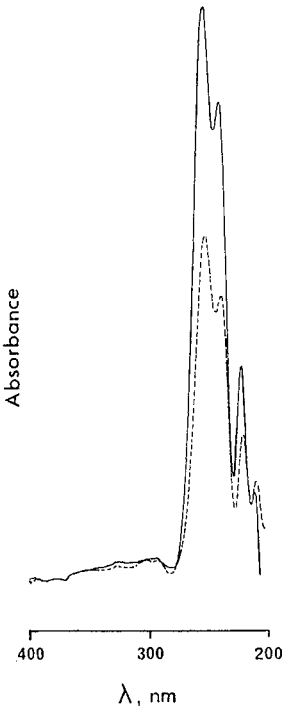

Fig. 1. Spectres d'absorption d'une solution $Ce_2(SO_4)_3 \cdot 8H_2O$ (0,2 m*M*) sans (——) et avec (– – –) NaCl (1 m*M*).

cela, nous avons étudié d'une part le flux du solvant, d'autre part la concentration en Ce^{3+} dans le solvant. L'influence de ces paramètres a été mesurée par le calcul des facteurs suivants: (i) le facteur de capacité du soluté, $k' = (t_R - t_0)/t_0$ (t_R = temps de rétention du soluté; t_0 = temps de rétention du pic négatif); (ii) le facteur de séparation entre deux pics consécutifs, $\alpha = k'_2/k'_1$; (iii) la largeur du pic à mi-hauteur: $PW_{1/2}$, mesurée en secondes.

Détermination du flux. Nous avons testé différents flux pour une concentration en Ce^{3+} de 0,05 m*M*. Pour évaluer le temps maximum d'analyse, nous considérons le

TABLEAU I

COMPOSITION CATIONIQUE (m*M*) DES SÈVES XYLÉMIQUES DE TOMATE SELON DIFFÉRENTES CONDITIONS CULTURALES.

Analyses par spectrophotométrie de flamme. Les valeurs entre parenthèses donnent les limites de détection (m*M*) selon Sherman et Danielson[14].

	Na^+ $(0{,}175 \cdot 10^{-3})$	K^+ $(0{,}5 \cdot 10^{-3})$	Mg^{2+} $(0{,}25 \cdot 10^{-3})$	Ca^{2+} $(0{,}2 \cdot 10^{-3})$
Témoin	Traces	17	1,66	2,05
Froid (10°C)	Traces	8,75	1,25	3,87
NaCl (50 m*M*)	25,80	21,03	4,42	10,52

TABLEAU II

ÉVOLUTION DES FACTEURS k' ET α EN FONCTION DU FLUX

$[Ce^{3+}] = 0{,}05$ mM. $\alpha = k'_2/k'_1$.

Flux (*ml min*$^{-1}$)	k'_1 (Na^+)	k'_2 (K^+)	k'_3 (Mg^{2+})	k'_4 (Ca^{2+})	α
0,5	0,70	2,31	6,19	16,23	3,30
0,6	0,71	2,27	5,80	15,21	3,20
0,7	0,73	2,29	5,20	12,83	3,13
0,8	0,69	1,79	4,80	12,70	2,60
0,9	0,58	1,37	4,30	11,30	2,35
1	0,49	1,10	3,81	10,80	2,25

k' du calcium qui est le dernier cation élué. Le Tableau II montre qu'on peut réduire le temps d'analyse d'environ 40% en passant de 0,5 ml min^{-1} à 1 ml min^{-1}. Cependant ce gain de temps se fait au détriment de la qualité de la séparation entre K^+ et Na^+. En effet, le calcul des α donné par le Tableau II, montre qu'à partir de 0,8 ml min^{-1}, les valeurs α passent de 2,60 à 2,35 ce qui indique une baisse sensible du pouvoir de séparation de la colonne. De plus, dans le cas de plantes poussant sur des solutions salines, les fortes concentrations en sodium attendues (*cf.* Tableau I) ne peuvent que nuire à la séparation Na^+/K^+. Nous choisissons donc de nous placer à un flux de 0,7 ml min^{-1} qui, tout en réduisant la durée de l'analyse (env. 20%), permet de conserver une distance entre les pics Na^+ et K^+ garantissant une bonne séparation ainsi qu'une pression raisonnable (72 atm) au niveau de la colonne.

Détermination de la concentration en Ce^{3+}. En chromatographie échangeuse d'ions, l'élution des cations divalents nécessite, par rapport aux monovalents, un solvant de force ionique supérieure. La Fig. 2 montre que le profil d'élution des pics de Mg^{2+} et de Ca^{2+} est peu satisfaisant (base trop large donnant un aspect de pic trainant) à une concentration en Ce^{3+} de 0.05 mM. Nous avons augmenté la concentration en Ce^{3+} dans la phase mobile. Pour en estimer l'influence, nous mesurons $PW_{1/2}$.

Le Tableau III montre qu'au fur et à mesure que la concentration en Ce^{3+} augmente, le facteur $PW_{1/2}$ diminue, signe d'une meilleure élution. Mais le calcul des k' (*cf.* Tableau IV) d'après les chromatogrammes obtenus, dénote, pour les concentrations élevées (0,3 et 0,4 mM), une mauvaise séparation entre les monovalents. Par contre, la durée de l'analyse est fortement réduite. Devant cette alternative, nous retenons comme concentration en Ce^{3+} dans la phase mobile, 0,2 mM, qui représente un bon compromis (*cf.* Fig. 2).

La solution consistant à faire varier les conditions chromatographiques (flux et $[Ce^{3+}]$) entre le pic de K^+ et celui de Mg^{2+}, a été examinée. Mais, dans notre dispositif, le temps de stabilisation de la colonne s'est avéré trop important pour que l'élution du pic de Mg^{2+} ne soit pas perturbée.

Choix des paramètres d'intégration

L'experience acquise avec notre matériel, nous a permis de fixer la plupart des paramètres d'intégration sans avoir recours à une mise au point. Ainsi nous avons

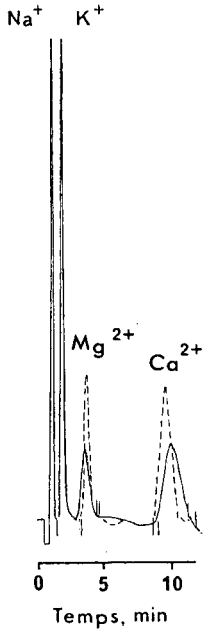

Fig. 2. Chromatogrammes d'une solution étalon pour une concentration en Ce^{3+} de 0,05 m*M* (—) et de 0,2 m*M* (– – –).

TABLEAU III

ÉVOLUTION DU $PW_{1/2}$ POUR Ca^{2+} ET Mg^{2+} EN FONCTION DE LA CONCENTRATION EN CÉRIUM

Flux = 0,7 ml min^{-1}.

$[Ce^{3+}]$ (*mM*)	Mg^{2+}	Ca^{2+}
0,05	36	96
0,10	30	84
0,20	24	60
0,30	24	54
0,40	23	53

TABLEAU IV

ÉVOLUTION DES FACTEURS *k'* ET α SELON LA CONCENTRATION EN CÉRIUM

Flux = 0,7 ml min^{-1}. $\alpha = k'_2/k'_1$

$[Ce^{3+}]$ (*mM*)	k'_1 (Na^+)	k'_2 (K^+)	k'_3 (Mg^{2+})	k'_4 (Ca^{2+})	α
0,05	0,73	2,29	5,20	12,83	3,13
0,10	0,74	2,31	4,60	11,60	3,12
0,20	0,76	2,52	4,08	10,00	3,31
0,30	0,73	2,04	3,90	9,70	2,79
0,40	0,73	1,84	3,60	9,50	2,52

programmé: atténuation, AT = 0,5; vitesse de déroulement du papier, CS = 0.5 cm min^{-1}; pics marqueurs, PM = 1; rapport hauteur/largeur pics, PW = 1; auto-zéro, AZ = 1; méthode de calcul, MN = 0.

Cependant, la présence d'un pic négatif due à l'élution des anions d'accompagnement, nous a conduit à examiner l'influence du paramétre NP (negative peak) sur le calcul des aires. En effet, la programmation de ce paramétre (NP = 1) ne fait débuter le calcul de l'aire qu'une fois la ligne de base franchie. Par contre, en NP = 0 (valeur par défaut), l'intégration commence au départ du pic, même si celui-ci n'est pas visible sur le tracé.

Afin d'évaluer l'importance de ce facteur, pour chacun des cations, nous avons effectué une régression linéaire du type: aire du pic = f (concentration). Les coefficients de corrélation obtenus (cf. Tableau V) nous montrent que la progammation NP = 1 ne peut pas être utilisée dans le cas du sodium.

Application au dosage des sèves

Etude qualitative

Nous avons examiné trois types d'exsudats xylémiques, récoltés à partir: de plantes témoins, de plantes soumises au froid (T = 10°C) et de plantes soumises à un stress salin ([NaCl] = 50 mM). Les exsudats sont dilués par dix avec de l'eau bidistillée, et injectés directement. La Fig. 3 montre que les tracés obtenus à partir des sèves sont de qualité comparable à celui de la solution étalon. De plus dans le cas des plantes stressées (Fig. 3 c et d), il apparait un pic nouveau que nous avons identifié comme étant de l'ammonium, preuve d'une modification du métabolisme azoté en relation avec le stress. Nous avons donc modifié la solution étalon en incorporant 1 mM de NH_4NO_3 et vérifié que les réglages définis précédemment sont valables. Le chromatogramme de la solution étalon définitive est donné par la Fig. 4. Nous remarquons également (*cf.* Fig. 3b) la présence d'une pic de Na^+ dans des sèves de plantes cultivées en absence de NaCl, due en partie à l'ajustement du pH des solutions nutritives avec de la soude. D'autre part des contaminations semblent inévitables au cours des différentes étapes de la culture.

Validité de la méthode

Pour vérifier la reproductibilité d'une analyse sur l'autre, nous avons procédé à trois injections consécutives de la solution étalon définitive. Les pourcentages de déviation standart relative pour chacun des cations sont: Na^+, 2,85%; NH_4^+, 0,95%,

TABLEAU V

COEFFICIENTS DE CORRÉLATION ENTRE DIFFÉRENTES CONCENTRATIONS EN CATIONS ET LEURS AIRES AVEC OU SANS LE FACTEUR NP

	NP = 0	*NP = 1*
Na^+	0,997	0,754
K^+	0,999	0,996
Mg^{2+}	0,993	0,994
Ca^{2+}	0,998	0,997

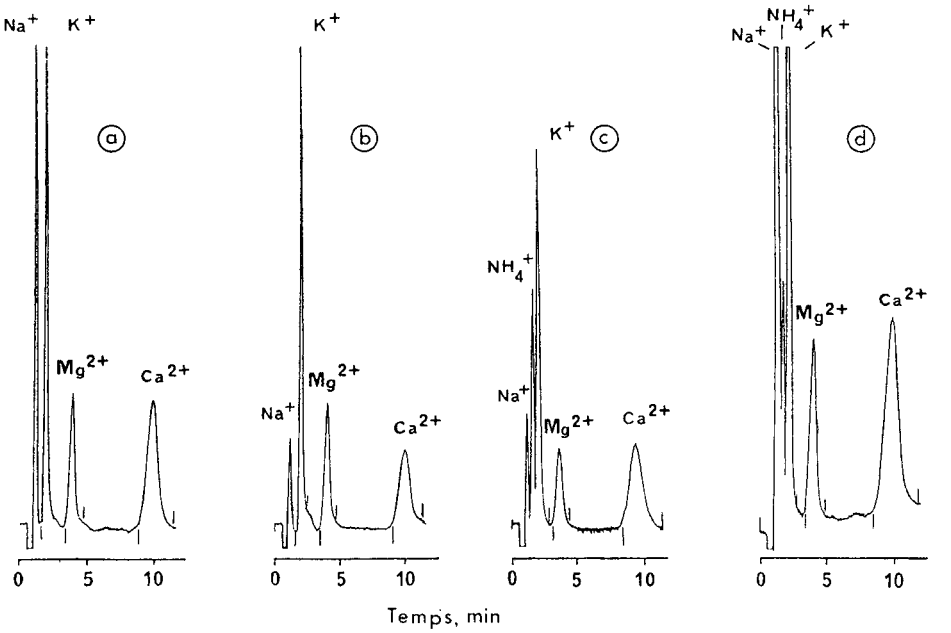

Fig. 3. Chromatogrammes d'une solution étalon et de différents échantillons de sèves. (a) Étalon; (b) témoin; (c) froid, 10°C; (d) NaCl, 50 m*M*.

K^+, 2,42%; Mg^{2+}, 1,25%; Ca^{2+}, 2,56%. Ces valeurs, toutes inferieures à 3%, nous assurent d'une bonne reproductibilité des analyses, ce qui nous permet de comparer, sur nos différents échantillons de sèves, des dosages effectués par cette nouvelle méthode avec ceux réalisés par les méthodes classiques. Celles-ci nécessitant des volumes de prise d'essai importants, nous avons mélangé les sèves de plantes d'un même milieu de culture. Chaque échantillon ainsi obtenu est dosé à la fois sur HPLC et par spectrophotométrie avec trois répétitions.

Nous avons comparé les deux méthodes en utilisant le Test de Moyenne de Student[27]. Les résultats consignés dans le Tableau VI montrent que les deux méthodes sont comparables au seuil de 5%.

DISCUSSION

Nous venons de démontrer que l'utilisation de l'HPLC pour le dosage des cations dans les sèves xylémiques donne des résultats équivalents en qualité à ceux obtenus par les méthodes spectrophotométriques. De plus, la méthode que nous venons de décrire possède certains avantages qui, dans le cas de l'analyse des sèves, nous semblent prépondérants. Ce sont: (i) une injection directe de l'échantillon sans préparation; (ii) un volume d'injection faible (10 μl); (iii) le dosage simultané des cinq principaux cations au cours d'une même analyse. Grâce à cela, des bilans cationiques, plante par plante et sur un grand nombre d'individus, sont réalisables, ce qui est d'un grand intérêt pour des études physiologiques.

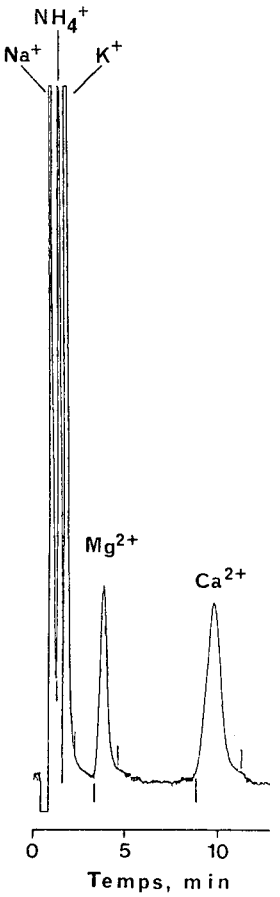

Fig. 4. Chromatogramme de la solution étalon définitive.

TABLEAU VI

COMPARAISON STATISTIQUE SELON UN TEST "t" DE STUDENT ENTRE LES DEUX TECHNIQUES DE DOSAGES CATIONIQUES UTILISÉES

Les valeurs entre parenthèses représentent les écarts types.

	HPLC (IPC)			*Spectrophotométrie*		
	Témoin	*Froid (10°C)*	*NaCl (50 mM)*	*Témoin*	*Froid (10°C)*	*NaCl (50 mM)*
Na^+	Traces	Traces	29,06 (0,33)	Traces	Traces	25,80 (2,07)
NH_4^+	Traces	1,53 (0,07)	4,89 (0,35)	Traces	1,40 (0,10)	4,54 (0,37)
K^+	16,98 (0,60)	8,72 (0,13)	20,53 (1,00)	17,00 (0,75)	8,75 (0,31)	21,03 (1,67)
Mg^{2+}	1,70 (0,05)	1,30 (0,05)	4,48 (0,07)	1,66 (0,05)	1,25 (0,08)	4,42 (0,19)
Ca^{2+}	2,13 (0,08)	3,82 (0,11)	10,95 (0,24)	2,05 (0,08)	3,87 (0,30)	10,52 (0,55)

Cependant la détection par IPC en UV, même si elle est plus sensible que la conductimétrie, est plus délicate à maîtriser et plus onéreuse[3]. En effet, le système est parfois long à se stabiliser. Aussi, plutôt que des utilisations ponctuelles, nous recommandons de travailler par grandes séries. Ceci est d'autant plus concevable que le dispositif d'analyse peut être aisément automatisé. Nous avons également remarqué que la phase employée, résine avec des ponts sulfoniques, est plus fragile que les phases classiques à base de silice greffée, d'où une durée de vie de la colonne plus courte, malgré de nombreuses précautions.

CONCLUSION

La méthode que nous venons de décrire, possède les avantages requis pour se substituer aux méthodes classiques d'analyses cationiques, notamment dans le cas des échantillons de faible volume. Bien que l'analyse des sèves xylémiques au microanalyseur à sonde électronique nécessite des volumes d'échantillons trés faibles (de l'ordre du nl) et se prête également à des analyses en série, la préparation est trop complexe et trop longue pour envisager son application dans le cas d'analyses de routine. De plus, les récents travaux que nous avons effectués dans notre laboratoire sur l'analyse par HPLC des anions et des acides organiques des sèves xylémiques (résultats non publiés), ainsi que nos précédents travaux sur l'analyse des acides aminés[24], nous permettent maintenant de réaliser des bilans ioniques complets avec une prise d'essai minimale. D'autre part, ces techniques ne se limitent pas aux sèves, mais leur emploi peut-être envisagé dans d'autres domaines (analyse des eaux, de liquides biologiques entre autres).

RÉSUMÉ

Nous décrivons une méthode pour l'analyse simultanée par chromatographie liquide haute performance des cations majeurs des sèves xylémiques. Pour réduire le temps d'analyse et améliorer la séparation entre les pics, nous avons déterminé le flux et la concentration en Ce^{3+} dans la phase mobile en utilisant les grandeurs fondamentales: k', α et $PW_{1/2}$. Nous avons testé ces nouvelles conditions dans le cas de l'analyse des sèves xylémiques. La reproductibilité de cette méthode a été vérifiée. La comparaison avec les méthodes classiques de spectrophotométrie de flamme ne donne aucune différence significative. Les avantages et les applications possibles de cette technique sont discutés.

BIBLIOGRAPHIE

1 H. Small, T. S. Stevens et W. C. Bauman, *Anal. Chem.*, 47 (1975) 1801.
2 D. T. Gjerde et J. S. Fritz, *J. Chromatogr.*, 176 (1979) 199.
3 P. R. Haddad et A. L. Heckenberg, *J. Chromatogr.*, 252 (1982) 177.
4 H. Hershcovitz, C. Yarnitzky et G. Schmuckler, *J. Chromatogr.*, 252 (1982) 113.
5 S. H. Lee et L. R. Field, *Anal. Chem.*, 56 (1984) 2647.
6 I. S. Krull, dans M. Bernhard, F. E. Brinckman et P. J. Sadler (Editors), *The importance of Chemical "Speciation" in Environmental Processes*, Springer-Verlag, Berlin, 1986, p. 579.
7 K. Harrison, W. C. Beckham Jr., T. Yates et C. D. Carr, *Am. Lab. (Fairfield, Conn.)*, 17 (5) (1985) 114–121.
8 H. Small et T. E. Miller Jr., *Anal. Chem.*, 54 (1982) 462.

9 R. C. L. Foley et P. R. Haddad, *J. Chromatogr.*, 366 (1986) 13.
10 D. R. Jenke, *Anal. Chem.*, 56 (1984) 2468.
11 D. R. Jenke, *Anal. Chem.*, 56 (1984) 2674.
12 Z. Iskandarani et T. E. Miller, Jr., *Anal. Chem.*, 57 (1985) 1591.
13 A. Laurent et R. Bourdon, *Ann. Pharm. Fr.*, 36 (1978) 453.
14 J. H. Sherman et N. D. Danielson, *Anal. Chem.*, 59 (1987) 490.
15 H. Shintani, *J. Chromatogr.*, 341 (1985) 53.
16 K. Hayakawa, R. Ebina, M. Matsumoto et M. Miyazaki, *Bunseki Kagaku*, 33 (1984) 390.
17 G. E. Wilcox, C. A. Mitchell et J. E. Hoff, *J. Am. Soc. Hort. Sci.*, 102 (1977) 192.
18 M. J. Armstrong et E. A. Kirkby, *Plant Physiol.*, 63 (1979) 1143.
19 A. E. S. Macklon et A. Sim, *Physiol. Plant.*, 49 (1980) 449.
20 M. C. White, A. M. Decker et R. L. Chaney, *Plant Physiol.*, 67 (1981) 292.
21 N. Roinel, *J. Microsc.*, 123 (1981) 311.
22 S. Gartner, L. Lefaucheur, N. Roinel et N. Paris-Pireyre, *Scanning Electron Microscopy*, IV (1984) 1739.
23 S. Gartner, *Diplôme de Doctorat*, Université des Sciences et Techniques du Languedoc, Montpellier, 1985.
24 P. Brunet, B. Sarrobert et N. Paris-Pireyre, *J. Chromatogr.*, 455 (1988) 173.
25 L. Solarzano, *Limnol. Oceanogr.*, 15 (1969) 799.
26 F. Lakhdari, *Diplôme de Doctorat*, Université des Sciences et Techniques du Languedoc, Montpellier, 1986.
27 P. Dagnelie, *Théorie et Méthodes Statistiques: Applications Agronomiques*, Les Presses Agronomiques de Gembloux, Gembloux, 1986.

Journal of Chromatography, 462 (1989) 315–322
Elsevier Science Publishers B.V., Amsterdam — Printed in The Netherlands

CHROM. 20 966

IMPROVEMENT OF CHEMICAL ANALYSIS OF ANTIBIOTICS

XV*. ISOCRATIC HIGH-PERFORMANCE LIQUID CHROMATOGRAPHIC METHODS FOR THE ANALYSIS AND PREPARATIVE SEPARATION OF THE COMPONENTS OF BACITRACIN

HISAO OKA*, YOSHITOMO IKAI, NORIHISA KAWAMURA and MASUO YAMADA
Aichi Prefectural Institute of Public Health, Tsuji-machi, Kita-ku, Nagoya 462 (Japan)
and
KEN-ICHI HARADA, YUMIKO YAMAZAKI and MAKOTO SUZUKI
Faculty of Pharmacy, Meijo University, Tempaku, Nagoya 468 (Japan)
(First received April 21st, 1988; revised manuscript received July 18th, 1988)

SUMMARY

Isocratic high-performance liquid chromatographic (HPLC) systems were established for analytical and preparative separation of the components of the antibiotic preparation bacitracin (BC). The best analytical results were obtained using a C_{18} modified silica gel column (Capcell Pak C_{18}) with a solvent system of 0.04 *M* disodium hydrogenphosphate buffer and methanol (4:6), pH 9–10. The calibration graphs showed good linear relationships between 50 and 1000 ng for BC-A and between 65 and 1000 ng for BC-F. With respect to the preparative HPLC, a Capcell Pak C_{18} column with methanol–0.05 *M* aqueous sodium sulphate solution (6:4) as a mobile phase gave satisfactory results. The isolation of BC-A and -F was readily achieved without decomposition of the components by using the present preparative HPLC followed by desalting on a prepacked C_{18} cartridge.

INTRODUCTION

Bacitracin (BC) is one of the most commonly used antibiotics in the world as an animal feed additive[1,2]. A large consumption of BC may increase the risk of residues of BC in food, so a simple, rapid and reliable method for the analysis of BC is required to monitor BC in food and feed. Although conventional microbiological assay procedures have good sensitivity, they are time consuming and cannot identify the individual components of BC. Therefore, a number of chemical analysis methods have been reported using high-performance liquid chromatography (HPLC)[3–5] and thin-layer chromatography (TLC)[6–15].

BC consists of more than twenty components with different antimicrobial activ-

* For Part XIV, see ref. 17.

0021-9673/89/$03.50

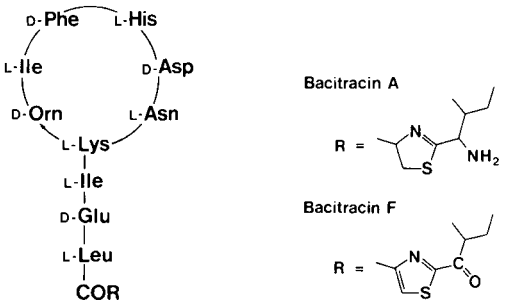

Fig. 1. Structures of bacitracin A and F.

ities. The main antimicrobial components are BCs A and B; the main degradation product is BC-F, which is devoid of antimicrobial activity and has nephrotoxicity[16]. The structures of the components have been determined only for BC-A and -F (Fig. 1). Therefore it is important to separate BC-A and -F from other components.

In the previous report[17], we established a combinational technique using normal-phase and reversed-phase (RP) high-performance thin-layer chromatography (HPTLC) for the identification of the components of BC. Although TLC can identify the various BC components, the advantages of HPLC are that it is useful in both the quantitation as well as the preparation of the individual components. All of the previously reported RP-HPLC methods used complicated gradient elution systems having long analysis times[3–5]. We could not obtain reproducible results under these chromatographic conditions. Additionally, ion-exchange HPLC gave low resolution of the BC components[6]. Therefore, we would like to establish a simple and reliable HPLC method for the analysis and preparative separation of the components of BC using isocratic elution.

According to preliminary studies, BC appears as tailing peaks on a conventional octadecylsilyl (C_{18}) silica gel column, probably due to interaction between the amino group of BC and residual silanol groups on the column. Use of a silanol-free stationary phase would prevent tailing of solute peaks. Capsule[18] and polymer[19] type RP-HPLC columns are made from silica gel coated with a silicone polymer and a porous polymer gel modified with hydrophobic materials such as C_{18}, respectively, so they are free from silanol groups. Accordingly, we decided to investigate the separation of the components of BC on capsule and polymer type RP-HPLC columns. In this paper, we report techniques for the analytical and preparative HPLC of the components using an isocratic system.

EXPERIMENTAL

Materials

Methanol, sodium hydroxide, phosphoric acid, disodium hydrogenphosphate, potassium phosphate, sodium sulphate, potassium sulphate, sodium chloride and potassium chloride were analytical grade reagents. Bacitracin was obtained from P-L Biochemicals (Milwaukee, WI, U.S.A.).

A Baker 10 C_{18} cartridge (7020-3) was obtained from J. T. Baker (Phillips-

burgh, NJ, U.S.A.). Capcell Pak C_8 (5 μm, 150 mm × 4.6 mm I.D., Lot No. 30006) and C_{18} (5 μm, 150 mm × 4.6 mm I.D., Lot No. 20138) columns were obtained from Shiseido (Tokyo, Japan). TSK gel Octadecyl-4PW (7 μm, 150 mm × 4.6 mm I.D., Lot No. OPWD0061) and Asahipak ODP-50 (5 μm, 150 mm × 6.0 mm I.D., Lot No. 8706439) columns were obtained from Tosoh (Tokyo, Japan) and Asahi Chemical Industry (Kawasaki, Japan), respectively.

High-performance liquid chromatography

A chromatograph equipped with a constant-flow pump (LC-5A; Shimadzu, Kyoto, Japan) was used with a variable wavelength UV detector (Shimadzu SPD-2AM) operated at 234 nm. The separations were performed on Capcell Pak C_{18} with methanol–0.04 *M* aqueous disodium hydrogenphosphate solution (6:4) and with methanol–0.05 *M* aqueous sodium sulphate solution (6:4) as the mobile phases for analytical HPLC and for preparative HPLC, respectively, at a flow-rate of 1.3 ml/min.

RESULTS AND DISCUSSION

Analytical HPLC conditions for the components of BC

The best result was obtained by elution with methanol–0.04 *M* aqueous disodium hydrogenphosphate solution (6:4) on a Capcell Pak C_{18} column. This is the first time that the components of BC have been completely separated into 22 peaks using an isocratic solvent system. A typical separation under the optimum conditions is illustrated in Fig. 2.

Various experimental results are discussed below using chromatographic behaviour of ten main components (peaks 11–18, 20 and 22 in Fig. 2).

Comparison of HPLC columns. We expected that capsule type and polymer type columns would give satisfactory results because their residual silanol groups are either covered with silicone polymer or essentially absent. The suitability of Capcell

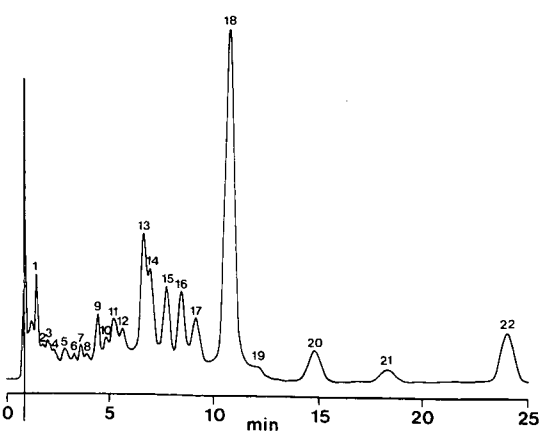

Fig. 2. Separation of the components of bacitracin using analytical HPLC conditions. Column: Capcell Pak C_{18} (5 μm, 150 mm × 4.6 mm I.D.). Mobile phase: methanol–0.04 *M* aqueous disodium hydrogenphosphate solution (6:4). Flow-rate: 1.3 ml/min. Detection: 234 nm. Peak identity: 18, BC-A; 22, BC-F.

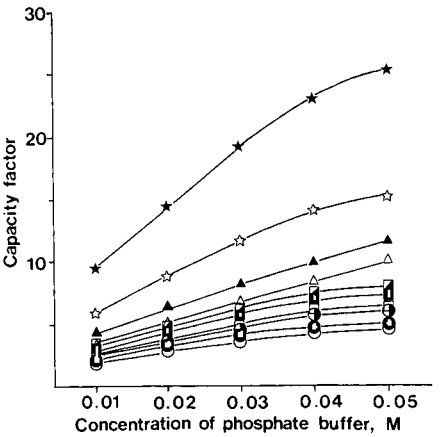

Fig. 3. Influence of disodium hydrogenphosphate concentration on the capacity factor. Column as in Fig. 2. Mobile phase: methanol–aqueous disodium hydrogenphosphate solution (pH 9.4) (6:4). Flow-rate and detection as in Fig. 2. Symbols: ○ = peak 11; ● = peak 12; ◐ = peak 13; □ = peak 14; ■ = peak 15; ◪ = peak 16; △ = peak 17; ▲ = peak 18 (BC-A); ☆ = peak 20; ★ = peak 22 (BC-F).

Pak C_8 and C_{18} as capsule type columns, and Asahipak ODP-50 and TSK gel Octadecyl-4PW as polymer type columns, for the analysis of the components was examined using methanol–0.04 *M* aqueous disodium hydrogenphosphate solution (6:4) as the mobile phase. Among these four columns, Capcell Pak C_{18} yielded 22 peaks with excellent resolution, whereas Capcell Pak C_8 and Asahipak ODP-50 columns produced 20 peaks, and TSK gel Octadecyl-4PW produced one broad peak. On the basis of these findings, we considered Capcell Pak C_{18} as the best choice in subsequent experiments.

Addition of disodium hydrogenphosphate. Because use of a mobile phase containing inorganic salt sometimes improves peak resolution in RP chromatography[20], we added disodium hydrogenphosphate to various mobile phases. Using methanol–*x M* aqueous disodium hydrogenphosphate solution (pH 9.4) (6:4) the influence of the concentration of the salt on the separation and resolution was investigated. Low resolution peaks of the components appeared on the chromatogram using disodium hydrogenphosphate-free mobile phase; however, the components were clearly resolved above 0.01 *M*. The capacity factors (k'), of the components show (Fig. 3) that the separation, especially among peaks 11–17, is improved with increasing salt concentration. Optimum separation is obtained above 0.04 *M*, but when 0.05 *M* is used the retention time of BC-F is too long. Accordingly, we chose 0.04 *M* aqueous disodium hydrogenphosphate solution in this study.

Influence of pH of aqueous disodium hydrogenphosphate solution. The influence of the pH of the aqueous disodium hydrogenphosphate solution on k' and the peak resolution of the components of BC were investigated using methanol–0.04 *M* aqueous disodium hydrogenphosphate solution (6:4). In general, conventional C_{18} silica gel is used under acidic conditions, because it is unstable under basic conditions. However, since the Capcell Pak C_{18} column can be used under basic conditions[18], the pH was varied between 2.0 and 10.0. The pH of the aqueous solutions was adjusted

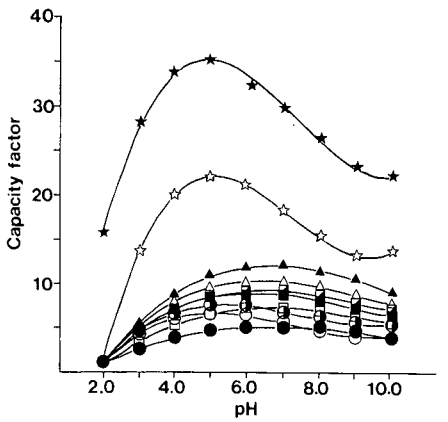

Fig. 4. Influence of pH of aqueous disodium hydrogenphosphate solution on the capacity factor. Column: as in Fig. 2. Mobile phase: methanol–0.04 *M* aqueous disodium hydrogenphosphate solution (6:4). Flow-rate and detection as in Fig. 2. Symbols as in Fig. 3.

with 0.04 *M* aqueous phosphoric acid and 0.04 *M* aqueous sodium hydroxide solutions. The k' of the components show that peak separation is improved with increasing pH of the mobile phase (Fig. 4). Satisfactory separation and resolution occur between pH values of 8.0 and 10.0. Peak 22 has too long a retention time below pH 9.0. Because the pH of 0.04 *M* aqueous disodium hydrogenphosphate solution is 9.4, we did not adjust the pH value in our subsequent work.

Proportion of methanol and aqueous disodium hydrogenphosphate solution. The ratio of the organic solvent and aqueous solution is one of the most important parameters in RP chromatography[21]. As the organic solvent we used methanol which produced better separations than acetonitrile. Various ratios of methanol and 0.04 *M* aqueous disodium hydrogenphosphate solution as mobile phases were examined to

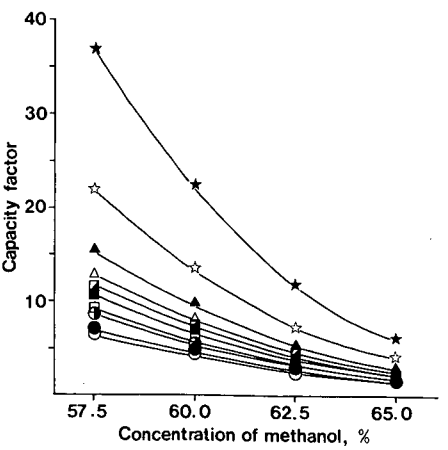

Fig. 5. Effect of the ratio of methanol and aqueous disodium hydrogenphosphate solution on the capacity factor. Column as in Fig. 2. Mobile phase: mixtures of methanol and 0.04 *M* aqueous disodium hydrogenphosphate solution. Flow-rate and detection as in Fig. 2. Symbols as in Fig. 3.

obtain the optimum proportion. Concentrations of methanol higher than 60% in the mobile phase result in unsatisfactory separation of BC components. The best separation was obtained below 60% (Fig. 5). Because a long analytical time was needed to elute all components using 57.5% methanol in the mobile phase, we recommend methanol–0.04 *M* aqueous disodium hydrogenphosphate solution (6:4) as the mobile phase.

Determination of BC-A and -F. It was reported that BC-A is unstable in solution[16], so we investigated the stability of components of BC during chromatography under the present HPLC conditions. After standing of BC in the mobile phase at 25°C for 30, 60, 90, 120, 150, 180 and 210 min, these samples were injected into the HPLC system and the peak heights of the components of BC were compared. No change in peak heights was observed within 90 min. Therefore, we used the present HPLC system for the quantitative analysis of BC-A and -F obtained as described in the next section. With purified samples, linear relationships were found between 50 and 1000 ng ($y = 0.055x + 2.76$) for BC-A and between 65 and 1000 ng ($y = 0.015x + 4.02$) BC-F.

Preparative HPLC conditions for the components of BC

In order to isolate the components, preparative HPLC was attempted using the above analytical HPLC conditions. However, it was impossible to concentrate the chromatographic fractions, because BC-A was decomposed by disodium hydrogenphosphate during evaporation. Therefore, we tried to develop preparative HPLC conditions using a suitable mobile phase which can preserve all components of BC during evaporation as judged by the changes in peak height. As mentioned above, if disodium hydrogenphosphate is eliminated from the mobile phase, the chromatography produced low resolution peaks, probably due to dissociation of amino groups in BC. Addition of neutral and inert inorganic salt to the solvent system is sometimes effective for control of the dissociation of analyte[22], so mobile phases containing several neutral and inert salts (potassium and sodium chloride or sulphate) instead of disodium hydrogenphosphate were tried on a Capcell Pak C_{18} column using methanol–0.05 *M* aqueous salt solution (6:4). With sodium and potassium chloride there were no clearly resolved peaks. We could not make a mixture of methanol and 0.05 *M* potassium sulphate (6:4) because of precipitation of the latter. However, addition of sodium sulphate to the mobile phase resulted in good separation. As shown in Fig. 6, although it shows lower resolution in comparison with that with the mobile phase containing disodium hydrogenphosphate, we consider that a mobile phase containing sodium sulphate is the most suitable for the preparative HPLC of the components, because the components were not decomposed in the mobile phase during evaporation.

Finally, we isolated the major peak (peak 18) and one of minor peaks (peak 22) using the present preparative HPLC conditions followed by chromatography on a prepacked C_{18} cartridge. Peaks 18 and 22 were fractionated, and after concentration below 30°C, the desalting was carried out using a prepacked C_{18} cartridge. The solution was applied to a Baker 10 C_{18} cartridge activated with methanol and water, and the cartridge was washed with 10 ml of water. The components were eluted with 10 ml of methanol and were evaporated under vacuum below 30°C. Purified peaks 18 and 22 were analysed using the analytical HPLC described above, which showed that

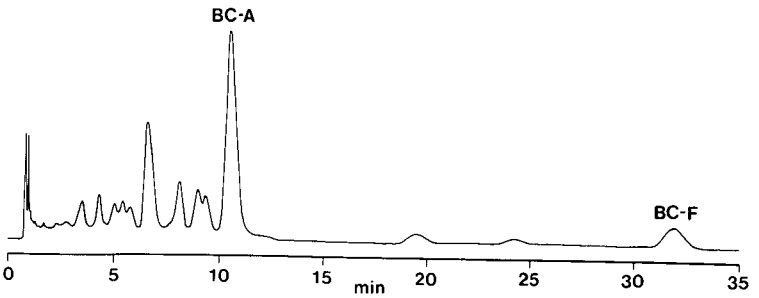

Fig. 6. Separation of the components of bacitracin using preparative HPLC conditions. Column as in Fig. 2. Mobile phase: methanol–0.05 *M* aqueous sodium sulphate solution (6:4). Flow-rate and detection as in Fig. 2.

both components were isolated without any decomposition. Peaks 18 and 22 were finally identified as BC-A and -F, respectively[16], by secondary ion mass spectrometry which produced a strong protonated molecule, $(M+H)^+$ (*m/z* 1422 for BC-A and *m/z* 1419 for BC-F) indicating that minor decomposition products are not coeluted with intact BC-A or -F in this HPLC system. Therefore, we recommend a combination of a Capcell Pak C_{18} column and methanol–0.05 *M* aqueous sodium sulphate solution (6:4) for the preparative HPLC of the components of BC.

CONCLUSIONS

The analytical and preparative HPLC methods for the identification and isolation of BC components were first established using an isocratic mobile phase on a capsule type C_{18} modified silica gel column (Capcell Pak C_{18}). These HPLC methods have the following characteristics. The best separation was obtained by the combination of a Capcell Pak C_{18} column and a methanol–0.04 *M* aqueous disodium phosphate solution (6:4) as a mobile phase. By this system the components of BC were successfully separated within 25 min and the calibration graphs showed good linear relationships between 50 and 1000 ng for BC-A and between 65 and 1000 ng for BC-F. With respect to the preparative HPLC, optimum conditions were found on a Capcell Pak C_{18} column using methanol–0.05 *M* aqueous sodium sulphate solution (6:4) as the mobile phase. The isolation of BC-A and -F was readily achieved without any decomposition of the components by the preparative HPLC conditions. Therefore, we recommend these HPLC methods for analytical and preparative separation of BC. At present we are attempting to characterize the structures of the components of BC and to develop a sample preparation system using a prepacked cartridge for detection of BC in feed and biological samples. These results will be reported elsewhere in the near future.

ACKNOWLEDGEMENTS

We are grateful to Dr. Shin Isomura, Director of Aichi Prefectural Institute of Public Health, for his encouragement, and to Dr. Y. Ohtsu, Shiseido Research Center, for helpful discussions.

REFERENCES

1 D. J. Hanson, *Chem. Eng. News*, 63 (1985) 7.
2 T. Yagasaki, *J. Food Hyg. Soc. Jpn.*, 27 (1986) 451.
3 K. Tsuji and J. H. Robertson, *J. Chromatogr.*, 112 (1975) 663.
4 K. Tsuji, J. H. Robertson and J. A. Bach, *J. Chromatogr.*, 99 (1975) 597.
5 J. B. Gallagher, P. W. Love and L. L. Knotts, *J. Assoc. Off. Anal. Chem.*, 65 (1982) 1178.
6 S. Gupa, E. Pfannkoch and F. E. Regnier, *Anal. Biochem.*, 128 (1983) 196.
7 R. J. Stretton, J. P. Carr and J. Watson-Walker, *J. Chromatogr.*, 45 (1969) 155.
8 T. Ikekawa, F. Iwami, E. Akita and H. Umezawa, *J. Antibiot. Ser. A*, 16 (1963) 56.
9 I. J. McGilveray and R. D. Strickland, *J. Pharm. Sci.*, 56 (1976) 77.
10 A. Aszàlos, S. Davis and D. Frost, *J. Chromatogr.*, 37 (1968) 487.
11 R. Bossuyt, R. Van Renterghem and G. Waes, *J. Chromatogr.*, 124 (1976) 37.
12 F. J. Van De Vaart, A. Hulshoff and A. W. M. Indemans, *Pharm. Weekbl. Sci. Ed.*, 5(1983) 113.
13 H. J. Langner, U. Teufel, M. Siegert and M. Frommhold, *Chem. Mikrobiol. Technol. Lebensm.*, 2 (1973) 71.
14 K. Pauncz, *J. Antibiot.*, 25 (1972) 677.
15 A. Aszalos and A. Aquilar, *J. Chromatogr.*, 290 (1984) 83.
16 G. A. Brewer, *Anal. Profiles Drug Subst.*, 9 (1980) 1.
17 H. Oka, Y. Ikai, N. Kawamura, M. Yamada, K.-I. Harada, Y. Yamazaki and M. Suzuki, *J. Chromatogr.*, 449 (1988) 448.
18 Y. Ohtsu, H. Fukui, T. Kanda, K. Nakamura, M. Nakano, O. Nakano and Y. Fujiyama, *Chromatographia*, 24 (1987) 380.
19 K. Yasukawa, Y. Tamura, T. Uchida, Y. Yanagihara and K. Noguchi, *J. Chromatogr.*, 410 (1987) 129.
20 B. A. Bidlingmeyer, *J. Chromatogr. Sci.*, 18 (1980) 525.
21 J. C. Touchstone and M. F. Dobbins, *Practice of Thin Layer Chromatography*, Wiley, New York, 2nd ed., 1983, p. 336.
22 H. Oka, Y. Ikai, N. Kawamura, M. Yamada, H. Inoue, T. Ohno, K. Inagaki, A. Kuno and N. Yamamoto, *J. Chromatogr.*, 411 (1987) 437.

Journal of Chromatography, 462 (1989) 323–332
Elsevier Science Publishers B.V., Amsterdam — Printed in The Netherlands

CHROM. 21 016

USE OF A POST-COLUMN REACTION AND A SPECTROPHOTOMETRIC DETECTOR FOR THE LIQUID CHROMATOGRAPHIC DETERMINATION OF WATER*

NANCY E. FORTIER and JAMES S. FRITZ*
Ames Laboratory and Department of Chemistry, Iowa State University, Ames, IA 50011 (U.S.A.)
(First received June 28th, 1988; revised manuscript received September 19th, 1988)

SUMMARY

A sensitive method for the determination of water in the presence of common interferents is presented. An ion-exchange column in the Li^+ form and acetonitrile–methanol (60:40) as eluent are used to separate water from other sample components. The detection system is based on the effect of water on the equilibrium which results from the reaction of cinnamaldehyde (added to the eluent) and methanol in the eluent to form cinnamaldehyde dimethylacetal plus water. This equilibrium is shifted in the catalytic atmosphere of an H^+-form post-column reactor. The extent of the shift and the resulting change in absorbance at 310 nm are proportional to the amount of water present. The method is rapid, sensitive, relatively free from interferences and gives a linear calibration graph over approximately three orders of magnitude difference in water concentration.

INTRODUCTION

The determination of water in organic and inorganic materials is one of the most important and frequently encountered analytical problems. The Karl Fischer method has long been the most widely used method for the determination of water. However, it requires some skill to carry out and cannot be used for samples that contain oxidizing or reducing substances, or certain other chemicals. A number of gas chromatographic (GC) methods have been proposed for the determination of water[1]. The actual method chosen is dependent on the sample matrix. GC method are slow for samples containing late-eluting compounds. Decomposition of samples leading to contamination of the column can also be a problem. GC methods often cannot be used at all for samples containing non-volatile constituents.

The determination of water can be based on the reaction of phenyl isocyanate with water to produce N,N′-diphenylurea, which can then be determined by liquid chromatography[2]. However, the total reaction time prior to the chromatography is 45 min.

* A U.S.A. Patent Application has been filed covering the work presented in this study.

0021-9673/89/$03.50

Ion-exclusion chromatography is a fast and efficient way to separate and determine compounds such as carboxylic acids, carbon dioxide (as carbonic acid)[3] and neutral substances such as alcohols and sugars[4]. The determination of water by ion-exclusion chromatography should also be possible provided a suitable detection method is available. Stevens *et al.*[5] recently published a chromatographic method for water using a hydrogen-form cation-exchange column in conjunction with a methanol eluent containing a low concentration of sulfuric acid. A conductivity detector was employed, giving a decreased conductivity for the water peak. Their data indicated a response factor that varied widely with changing water concentration.The average response factor (μs per 1% water) was 240 in the 0.02–0.12% water range, 105 in the 0.22–0.42% range, 50 in the 0.42–0.80% range and 6.7 in the 1.6–3.1% range.

A method for the chromatographic determination of water is presented here that combines separation by ion-exclusion chromatography with a novel and sensitive method of detection. The eluent is a low concentration of cinnamaldehyde in methanol or in a mixture of methanol and acetonitrile. In one mode of operation, the separation column contains a cation-exchange resin in the H^+ form which causes the cinnamaldehyde and methanol to react to produce water plus an acetal that has a much lower absorbance at an appropriate wavelength than the free cinnamadehyde. In another mode of operation the chromatograpic separation of water takes place on a cation-exchange column in the Li^+ form. An H^+-form catalytic column placed just after the separation column then catalyses the reaction of cinnamaldehyde with methanol. In both modes, water in the sample partially reverses this reaction, giving an increase in absorbance for detection of the water peak. The method is fast and sensitive; it is highly selective for water and has a large, linear dynamic range.

EXPERIMENTAL

Apparatus

The instrument consisted of a Gilson Model 302 single-piston pump, a Rheodyne Model 7125 injector quipped with either a 20-μl or a 100-μl sample loop, a Scientific Systems Model LP-21 Lo-Pulse pulse damper, either a glass 10 cm × 8 mm I.D. or a stainless-steel 5 cm × 4.6 mm I.D. column packed with Bio-Rad Aminex Q-150S in the Li^+ form (separation column), a 10 cm × 2 mm I.D. stainless-steel column packed with Bio-Rad Aminex Q-150S in the H^+ form (catalyst column), a Kratos Spectroflow 783 absorbance detector and a Curken strip-chart recorder. The one-column method used either a stainless-steel 10 cm × 4.6 m I.D. or a glass 10 cm × 8 mm I.D. column packed with Aminex Q-150S in the H^+ form. The columns were packed using upward slurry packing. However, a balanced density method was not used. Owing to the large degree of shrinking and swelling that occurs in polystyrene–divinylbenzene resins when a change in solvent occurs, it was necessary to pack the column in the solvent used in the mobile phase.

Eluent and sample solution

trans-Cinnamaldehyde, 99% (Aldrich Chemical), was used without purification. Analytical-reagent grade methanol (Mallinckrodt) and HPLC-grade acetonitrile (Fisher Scientific) were dried by storing over activated 3 Å molecular sieves (Aldrich) for at least 1 week. 3-Mercaptopropionic acid (Aldrich) was 99+% pure. All other samples were of analytical-reagent grade and used without purification.

For maximum sensitivity and reproducibility, the eluent and all samples were prepared in a nitrogen-filled glove-bag. Once prepared, the eluent was protected from atmospheric moisture by bubbling nitrogen through the solution using a drying tube filled with anhydrous calcium sulfate (Drierite). All sample solutions were placed in vials equipped with Mininert valves (Supelco) prior to removal from the glove-bag. The valve and septum of the Mininert caps allowed the removal of an aliquot without exposing the remainder of the sample to atmospheric moisture.

Titrations

Karl Fischer reagent (titer 2.8 mg/ml) was purchased from Aldrican and standardized. The buret was flushed with nitrogen prior to being filled and then blanketed with nitrogen during the titration. A large (50-ml) buret was used so that a standard and three samples could be titrated without refilling the buret. Samples were titrated in volumetric flasks blanketed with nitrogen to minimize exposure to atmospheric moisture. A visual end-point was used.

Chromatographic conditions

For the two-column method, chromatography was performed at flow-rate of either 1 ml/min (with the long separation column) or 0.8 ml/min (with the short separation column). A detection wavelength of 310 nm was used. The eluent was 0.79 m*M* *trans*-cinnamaldehyde in acetonitrile–methanol (60:40). This concentration of *trans*-cinnamaldehyde gave the best signal-to-noise ratio for water determination.

When only one column in the H^+ form was used, the eluent was 0.32 m*M* *trans*-cinnamaldehyde in methanol. With the 4.6 mm I.D. column a flow rate of 1 ml/min was used and with the 8 mm I.D. column a flow-rate of 1.2 ml/min was used. Detection was at 310 nm.

RESULTS AND DISCUSSION

Detection system

A column packed with a cation-exchange resin in the H^+ form has been shown to separate water chromatographically using dilute sulfuric acid in methanol as the eluent[5]. The separation is probably based on an ion-exclusion mechanism in which ions and most organic sample components pass rapidly through the column, but water can enter the resin beads and therefore is eluted later as a well resolved peak.

A stable and sensitive detection system is critical to the success of any chromatographic method for the separation and determination of water. Our method is based on the shift in chemical equilibrium caused by low concentrations of water. This shift in equilibrium causes an increase in absorbance that is proportional to the amount of water.

A detection system is set up by adding a low concentration (0.8 m*M*) of *trans*-cinnamaldehyde to the eluent. Cinnamaldehyde can react with methanol in the eluent to form an acetal plus water. However, spectral evidence indicates that reaction only occurs when a catalyst is present, such as when the eluent passes through a cation-exchange column in the H^+ form:

$$C_6H_5CH{=}CHCHO + 2\,CH_3OH \xrightarrow{H+} C_6H_5CH{=}CHCH(OCH_3)_2 + H_2O \quad (1)$$

The cinnamaldehyde absorbs strongly at the detection wavelength of 310 nm, while the acetal of cinnamaldehyde shows little absorbance at this wavelength (see Fig 1). When a solution of cinnamaldehyde in methanol (with no catalyst present) was allowed to stand for 2 days, the absorbance at 310 nm remained unchanged. Although the spectrophotometric data presented in Fig. 1 indicate that a wavelength lower than 310 nm should be used for maximum sensitivity, the optimal signal-to-noise ratio was obtained at 310 nm, where the background absorbance is low.

Water in a sample injected into the chromatographic column forces the equilibrium in the reverse direction when an acid catalyst is present:

$$H_2O + C_6H_5CH{=}CHCH(OCH_3)_2 \xrightarrow{H+} C_6H_5CH{=}CHCHO + 2\,CH_3OH \quad (2)$$

Usually the amount of water from the sample will be substantially greater than the background water. The shift in equilibrium is measured by the increased absorbance at 310 nm, which is proportional to the amount of water in the sample.

Separation–detection systems

One-column method. In this method a single column is used that contains Aminex Q-150S in the H^+ form. In the presence of the H^+-form resin in the column, water in the sample reacts with the cinnamaldehyde dimetylacetal, pushing the equilibrium in eqn. 2 further to the right. As cinnamaldehyde absorbs more strongly than the acetal at the detection wavelength used, the chromatogram shows a positive peak that is proportional to the amount of water in the sample. This peak appears a short time after the initial injection peak on the chromatogram and is well resolved from the injection peak.

The reason why the water peak has a longer retention time than the injection peak is not entirely clear. Perhaps the reaction of water with cinnamaldehyde dimethylacetal is not instantaneous in the column and water therefore moves at

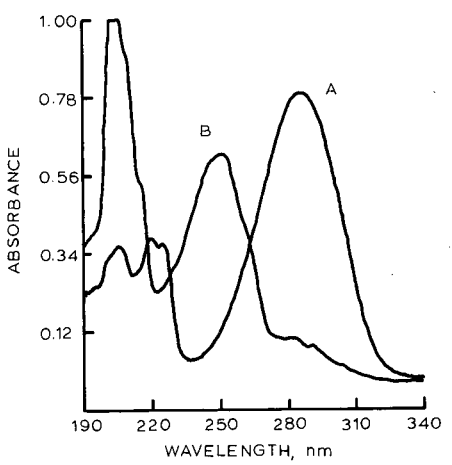

Fig. 1. Spectra of 0.0318 m*M* *trans*-cinnamaldehyde in methanol. (A) Spectrum immediately after the solution was prepared; (B) spectrum after the solution had been shaken with Aminex Q-150S in the H^+ form.

a slower rate through the column until reaction 2 is complete. Also, other retention experiments indicate that cinnamaldehyde moves at a slightly slower rate through the column than the acetal.

Water can be determined with excellent sensitivity using the one-column method of separation with spectrophotometric detection at 310 nm. An injection of a 20-μl sample of methanol containing only 10 ppm of water yielded an easily measured peak. A calibration graph of standard solutions of water in methanol was linear from 0.0051 to 2.40% water (correlation coefficient for linear regression 0.9995).

Many types of organic sample components either do not absorb at the detection wavelength (310 nm) or else are sufficiently well separated from water not to interfere. However, aldehydes and ketones are likely to interfere by virtue of their retention on the column (see Table I) or by reacting with methanol to produce additional water.

Two-column method. Interference from aldehydes and ketones, and possibly from other types of sample components, can be avoided by using a cation-exchange column in the Li^+form for the chromatograhic separation of water, followed by a short cation-exchange column in the H^+ form to catalyze the reaction needed for detection. No reaction occurs in the first column (Li^+ form); the water itself is separated from organic and inorganic components in the sample. When the eluent enters the second, catalytic column, the reaction in eqn. 1 takes place and gives a low background absorbance. However, when the water peak enters the catalytic column, the equilibrium is shifted to the formation of more aldehyde in proportion to the amount of water injected.

The system described here is an example of a post-column reaction system which uses a solid-phase reactor. The set-up is simple and works very well. The reactants are already present in the mobile phase. The reaction simply does not occur until the catalyst column is reached. No additional reagents are mixed with the effluent stream. There is no need for the additional hardware (second pump, mixing tee or reaction chamber) commonly used in post-column reaction systems. Consequently, the problems inherent in a typical post-column reaction system are avoided. These include mixing problems, excess dead volume in the tee and reaction coil and baseline noise due to the reagent pump.

This method for the determination of water is so powerful because it combines a selective detection method with the selectivity of chromatography. Because the reaction occurs after the separation, water can be determined in the presence of substances which would interfere if the separation column were not employed, *i.e.*, aldehydes and ketone, which react with methanol in the presence of an acid catalyst to form water. This was tested by determining water in acetone (Fig. 2). Acetone would be expected to react with methanol to form water (plus a ketal) when it entered a catalytic column. However, it is already separated chromatographically from the water in the sample before it reaches the second, catalytic column and no interference is encountered.

The same reasoning holds for sample components that absorb at the detection wavelength. They do not interfere with the determination of water provided they are separated chromatographically before entering the catalytic detection system. Cinnamaldehyde works better than many aldehydes in the detection system because the wavelength of 310 nm is above the UV cut-off for many organic solvents.

Although good results were obtained with the one-column method for water

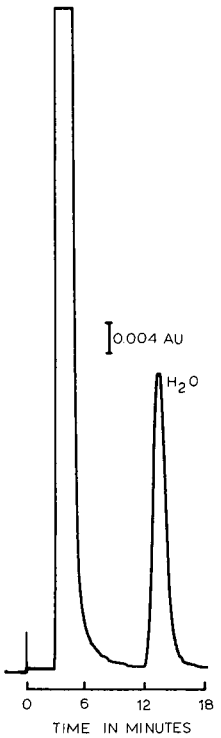

Fig. 2. Spectrum of 0.321% water in acetone. Sample loop, 20 μl; separation column, 10 cm × 8 mm I.D.; flow-rate, 1 ml/min. Other conditions are given in the text.

determination, fewer interferences were encountered with the two-column method. The remaining discussion therefore focuses on the latter method for water determination.

Column length

Many of the separations were performed on a fairly long column (10 cm × 8 mm I.D. with a 10 cm × 2 mm I.D. catalyst column) in order to obtain good resolution of the water peak in some difficult samples. The separation of water from acetone shown in Fig. 2 and the separation of water from a sample of 3-mercaptopropionic acid in Fig. 3 are examples.

In many instances a shorter column can be used and the chromatographic separation of water greatly speeded up. Using a short column (5 cm × 4.6 mm I.D. with a 10 cm × 2 mm I.D. catalyst column), good separations were obtained for 367 ppm of water in isopropyl alcohol (Fig. 4) and for 184 ppm of water in toluene (Fig. 5).

Calibration graphs

Calibration graphs were obtained with both the long and short columns using methanol containing varying amounts of water as standards. For the long column a plot of points ranging from 0.00128 to 3.40% of water had a linear regression correlation coefficient of 0.9998. Slight curvature was observed at the higher

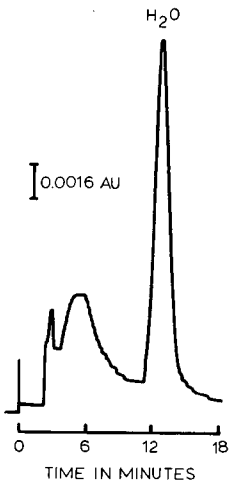

Fig. 3. Spectrum of 0.138% water in a methanolic solution of 1.15 *M* 3-mercaptopropionic acid. Sample loop, 20 μl; separation column, 10 cm × 8 mm I.D.; flow-rate, 1 ml/min. Other conditions are given in the text.

concentration end of the plot (above 3.0%). The lower end of the plot appeared to be strictly linear with a correlation coefficient of 0.999996 for 0.00128–0.0800% water. For the short column, similar results were obtained for calibration graphs ranging from 0.0064 to 0.50% of water.

The respons factor (*RF*) of the chromatographic detection system for water was measured in the following units:

$$RF = \frac{\text{signal (absorbance) at 310 nm}}{\text{0.1\% water in sample}} \tag{3}$$

Response factors of 0.012 and 0.071 were obtained for the long column with a 20-μl sample loop and the short column with a 100-μl sample loop, respectively. These are

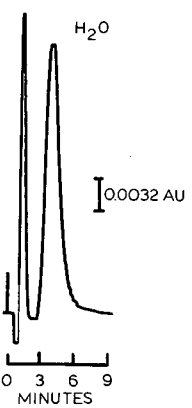

Fig. 4. Spectrum of 367 ppm water in isopropanol. Sample loop, 100 μl; separation column, 5 cm × 4.6 mm I.D.; flow-rate, 0.8 ml/min. Other conditions are given in the text.

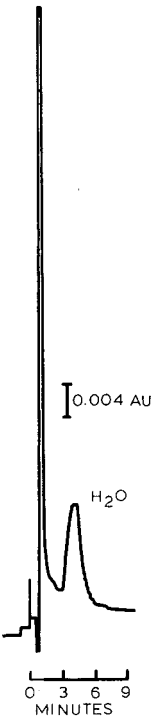

Fig. 5. Spectrum of 184 ppm water in toluene. Sample loop, 100 μl; separation column, 5 cm × 4.6 mm I.D.; flow-rate, 0.8 ml/min. Other conditions are given in the text.

fairly good, considering that the baseline noise with this system was approximately $2 \cdot 10^{-5}$ absorbance.

The limit of detection for water will depend on the response factor, the size of sample loop use and the amount of water in the eluent. The water content of the eluent can be determined by extrapolating a linear plot of peak height *vs.* water concentration in standards to zero peak height. Such an extrapolation of data from the short column gave approximately 30 ppm as the water content of the eluent. Injections of samples containing less water than the eluent give negative peaks at the retention time for water. This effect was previously noted with a different chromatographic system for water[5]. In principle, these negative peaks could be used to determine lower sample concentrations of water than those in the eluent, but we did not obtain a reasonable calibration graph for the negative peaks.

The most critical factor in obtaining extremely low detection limits for water is to prepare and use an eluent of exceptionally low water content. Because of the possibility of obtaining negative peaks when the sample contains less water than the eluent, it is not legitimate to take a positive water peak of substantial height and calculate the limits of detection by dividing the peak height (and concentration) by 2.5 times the noise[5]. By injecting 20-μl samples of decreasing water concentration on to the long column, we were able to obtain a detection limit of approximately 12.5 ppm of water (260 ng absolute) at a signal-to-noise of 3 (see Fig. 6).

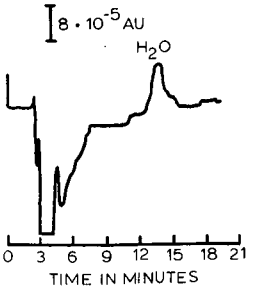

Fig. 6. Spectrum showing the limit of detection obtained with the long separation column (10 cm × 8 mm I.D.) to be 260 ng of water. Sample injected, 12.8 ppm of water in methanol; sample loop, 20 μl; flow-rate, 1 ml/min. Other conditions are given in the text.

Scope and quantitative results

The utility of this method was demonstrated by separating and determining water on the long column in each of the following samples: toluene, ethyl acetate, acetone, 3-mercaptopropionic acid, ascorbic acid (dissolved in methanol) and copper(II) chloride dihydrate (dissolved in methanol). Samples analyzed for water on the short column included isopropyl alcohol, toluene, ethyl acetate and absolute ethanol. Analysis of the mercaptan, ascorbic acid and copper(II) chloride samples by the Karl Fischer method would not be possible. Likewise, aldehydes and ketones interfere in a liquid chromatographic method that uses a different detection system[5].

Results are shown in Tables I and II. The results in Table I, for toluene, ethyl acetate and acetene, were compared with those obtained by the Karl Fischer method. Water was also determined in an ethyl acetate sample which was spiked with 0.100% water. The recovery was excellent. Table II shows results for samples for which a Karl Fischer titration would have yielded erroneous results[6]. The water content of these samples was determined by analyzing a blank, then spiking the sample and re-analyzing. With 3-mercaptopropionic acid, owing to the small amount of mercaptan available, a 10.00% solution of the mercaptan in methanol was spiked. The recoveries were again very good.

Another application of this method is the determination of water of hydration in inorganic salts. A sample of copper(II) chloride dihydrate was analyzed and found to contain 1.99 mol of water per mole of copper(II) chloride. This determination could not be effected with a Karl Fischer titration as the copper(II) would be reduced to copper(I) by the reagent[6].

TABLE I

LIQUID CHROMATOGRAPHIC DETERMINATION OF WATER IN ORGANIC SOLVENTS

Sample	*Water added (%)*	*Water found (%)*	
		This method	*Karl Fischer method*
Toluene	0	0.0253	0.0251
Acetone	0	0.321	0.325
Ethyl acetate	0	0.0950	–
Ethyl acetate	0.100	0.196	0.198

TABLE II
LIQUID CHROMATOGRAPHIC DETERMINATION OF WATER IN THE PRESENCE OF COMMON INTERFERENTS

Sample	*Water added (%)*	*Water calculated (spike plus blank) (%)*	*Water found (%)*
3-Mercaptopropionic acid	0	N.A.*	0.494
Methanolic solution of 10.00% 3-mercaptopropionic acid	0.200	0.249	0.246
Methanolic solution of 0.057 *M* ascorbic acid	0	N.A.	0.0080
Methanolic solution of 0.057 *M* ascorbic acid	0.100	0.108	0.104

* N.A. = Not available.

Interferences

Of the organic samples tested, only dimethyl sulfoxide (DMSO) was found to interfere. DMSO produced a very large peak that obscured the water peak. Inorganic metal hydroxides were also found to interfere, possibly by reaction with H^+ to produce additional water.

Samples containing large amounts of ionic materials can pose a problem by displacing more and more Li^+ from the separation column. The Li^+ removed from the separator column will exchange with the H^+ of the catalyst column, decreasing its ability to catalyze the reaction. Likewise, a large number of acidic samples will convert much of the separation column to the H^+ form and thereby cause a change in the retention time of the water peak. Periodic regeneration or the use of a replaceable Li^+-form precolumn should alleviate these difficulties.

ACKNOWLEDGEMENTS

One of the authors (N.E.F.) thanks N. K. Kildahl of Worcester Polytechnic Institute, Worcester, MA, U.S.A., for instructon in the handling of air-sensitive materials. Ames Laboratory is operated for the U.S. Department of Energy under Contract No. W-7405-ENG-85. This work was supported by the Director of Energy Research, Office of Basic Energy Sciences.

REFERENCES

1 J. Mitchell, Jr. and D. M. Smith, *Aquametry*, Part I, Wiley-Interscience, New York, 1977.
2 B. Bjorkqvist and H. Toivonen, *J. Chromatogr.*, 178 (1979) 271.
3 K. Tanaka and J. S. Fritz, *J. Chromatogr.*, 361 (1986) 151.
4 K. Tanaka and J. S. Fritz, *J. Chromatogr.*, 409 (1987) 271.
5 T. S. Stevens, K. M. Chritz and H. Small, *Anal. Chem.*, 59 (1987) 1716.
6 J. Mitchell, Jr. and D. M. Smith, *Aquametry*, Part III, Wiley-Interscience, New York, 1980.

Journal of Chromatography, 462 (1989) 333–340
Elsevier Science Publishers B.V., Amsterdam — Printed in The Netherlands

CHROM. 20 982

ANALYSIS OF LUPINE ALKALOIDS IN PLANTS BY HIGH-PERFORMANCE LIQUID CHROMATOGRAPHY*

KAZUKI SAITO* and KUMIKO KOBAYASHI
Faculty of Pharmaceutical Sciences, Chiba University, Yayoi-cho, Chiba 260 (Japan)
SHIGERU OHMIYA and HIROTAKA OTOMASU
Faculty of Pharmaceutical Sciences, Hoshi University, Shinagawa-ku, Tokyo 142 (Japan)
and
ISAMU MURAKOSHI
Faculty of Pharmaceutical Sciences, Chiba University, Yayoi-cho, Chiba 260 (Japan)
(First received October 7th, 1986; revised manuscript received September 13th, 1988)

SUMMARY

A high-performance liquid chromatographic method was devised for the qualitative and quantitative analysis of lupine alkaloids in plants. The separation of 22 naturally occurring lupine alkaloids was performed by adsorption chromatography (silica gel) with three solvent systems consisting of diethyl ether, methanol and ammonia solution and reversed-phase chromatography (octadecylsilica) with a buffered aqueous solution containing acetonitrile. The elution of alkaloids was monitored by UV absorption at 220 and 310 nm. Lupine alkaloids containing a 2-pyridone ring were detected by UV absorption at both wavelengths, while the alkaloids that do not possess this unsaturared heterocyclic ring lack UV absorption at 310 nm. The determination of lupine alkaloids was carried out by an external standard method using (−)-cytisine as the standard. The peak area for 1 μg of each alkaloid detected at 220 nm was measured and normalized for that of (−)-cytisine, and these relative factors were used for the determination of the alkaloids. The qualitative and quantitative analysis of lupine alkaloids in plants of the genus *Thermopsis* was performed by this method.

INTRODUCTION

Lupine alkaloids occur particularly in several Leguminosae genera and are also found sporadically in other plant families[1,2]. All contain one or two quinolizidine ring systems and are therefore called quinolizidine alkaloids. Their carbon skeleton is built up from two or three C_5 units of cadaverine derived from lysine[3,4]. Lupine

* Presented at the *23rd International Symposium on Advances in Chromatography, Chiba, October 7–9, 1986*. The majority of the papers presented at this symposium have been published in *J. Chromatogr.*, Vols. 399 and 400 (1987).

0021-9673/89/$03.50

A. Lupinine-type

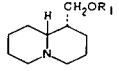

1 (-)-lupinine: R_1=H

2 (-)-(4'-hydroxycinnamoyl)lupinine: R_1=4'-hydroxycinnamoyl

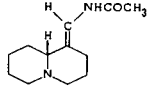

3 (-)-lusitanine

B. Matrine-type

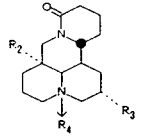

4 (+)-matrine: R_2=H, R_3=H, R_4=lone pair

5 (+)-sophoranol: R_2=OH, R_3=H, R_4=lone pair

6 (+)-5α,9α-dihydroxymatrine: R_2=OH, R_3=OH, R_4=lone pair

7 (+)-matrine N-oxide: R_2=H, R_3=H, R_4=O

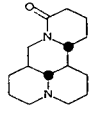

8 (+)-allomatrine

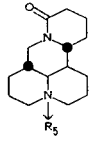

9 (-)-sophoridine: R_5=lone pair

10 (-)-sophoridine N-oxide: R_5=O

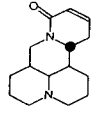

11 (-)-sophocarpine

C. Sparteine-type

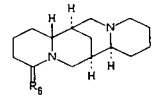

12 (-)-sparteine: R_6=H_2

13 (+)-lupanine: R_6=O

D. Anagyrine-type

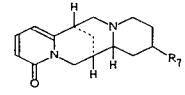

14 (-)-anagyrine: R_7=H

15 (-)-baptifoline: R_7=OH

E. Cytisine-type

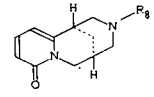

16 (-)-cytisine: R_8=H

17 (-)-N-methylcytisine: R_8=CH_3

18 (-)-12-cytisineacetic acid: R_8=CH_2COOH

19 (-)-methyl 12-cytisineacetate: R_8=CH_2COOCH_3

F. Mamanine-type

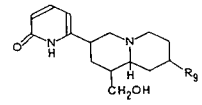

20 (+)-mamanine: R_9=H

21 (+)-13β-hydroxymamanine: R_9=OH

G. Tsukushinamine-type

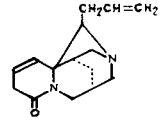

22 (-)-tsukushinamine A

Fig. 1. Structures of lupine alkaloids. The absolute configurations (+)-mamanine (20) and (+)-13β-hydroxymamanine (21) have not been determined.

alkaloids are well known as constituents of poisonous plants because of their toxicity towards mammals. Some of them exhibit potentially useful pharmacological activities[5].

The most important methods for the determination of lupine alkaloids in biochemical and chemotaxonomic studies have hitherto been gas chromatography (GC), gas chromatography–mass spectrometry (GC–MS) and thin-layer chromatography (TLC)[5]. These methods, however, have some disadvantages with regard to resolution and involatile samples. High-performance liquid chromatography (HPLC) is expected to be superior for the determination of lupine alkaloids in plant extracts, but no systematic investigation of its application has been reported so far.

In this study, we devised a qualitative and quantitative HPLC method for lupine alkaloids.

EXPERIMENTAL

Chemicals

The 22 natural lupine alkaloids used as standard samples were isolated and identified in the course of our recent studies[6–14]. Their structures are shown in Fig. 1. Diethyl ether, methanol and water were used immediately after all-glass distillation. Ammonia solution and acetonitrile of the highest grade available were used without further purification.

HPLC

LiChrosorb Si 60 (5 μm) was purchased from Kanto Chemicals (Tokyo, Japan) and Inertsil ODS (5 μm) from Gaschro-Kogyo (Tokyo, Japan). HPLC was carried out with a Senshu HPLC system constiting of an SSC-3100 pump, an SSC-3110 pump controller and SSC-E1E005 manual injector, equipped with a 4- or 20-μ sample loop, an SASC-3510 column oven, an SSC Y-1000 variable UV detector and a Sekonic SS-250F recorder. As highly volatile diethyl ether is used as a component of the eluent, the temperature of the column oven was maintained at 20°C. The eluents were sonicated for 1 min before use. The sample was dissolved in methanol and filtered through a Shodex DT filter (ED-03, 0.45 μm) prior to injection.

Plant extracts

The aerial parts of *Thermopsis lupinoides* Link and *T. chinensis* were collected in the Medicinal Plant Gardens of Chiba University in May 1986. Fresh plant tissues were homogenized and extracted with 75% ethanol. The neutral and acidic materials were removed by extraction with dichloromethane (twice) after acidification (pH 1) with hydrochloric acid. The basic fraction was extracted with dichloromethane (twice) from the saturated solution made alkaline with potassium carbonate. The basic fraction were analysed by HPLC after filtration.

RESULTS AND DISCUSSION

The HPLC conditions for the separation of lupine alkaloids are summarized in Table I. The separation of the alkaloids was performed satisfactorily in both the normal-phase (silica gel) and reversed-phase (octadecylsilica) modes.

TABLE I

HPLC CONDITIONS FOR THE ANALYSIS OF LUPINE ALKALOIDS

Mode	*Column*	*Solvent*	*Flow-rate (ml/min)*	*Detection (nm)*
Normal phase	LiChrosorb Si 60 (5 μm), 250 × 4.6 mm I.D.	(A) 15% Methanol in diethyl ether–5% ammonia solution (25:1, v/v) (B) 25% Methanol in diethyl ether–5% ammonia solution (25:1, v/v) (C) 50% Methanol in diethyl ether–5% ammonia solution (25:2, v/v)	1.5	220 and 310
Reversed phase	Inertsil ODS (5 μm), 150 × 4.6 mm I.D.	(D) Acetonitrile–5 m*M* potassium phosphate buffer (pH 5.5) (1:9, v/v)	1.0	220 and 310

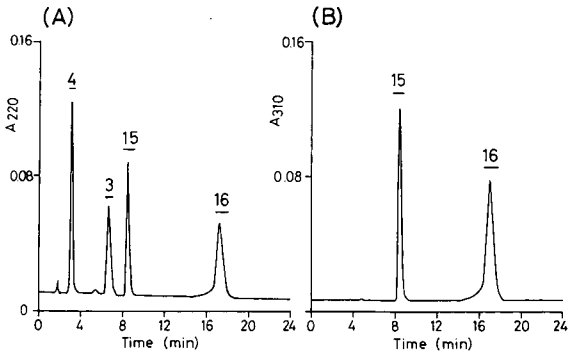

Fig. 2. HPLC profile of standard alkaloids with solvent system B. HPLC was carried out according to Table I. The sample consisted of (−)-lusitanine (3) (0.4 μg), (+)-matrine (4) (2.0 μg), (−)-baptifoline (15) (2.0 μg), (−)-cytisine (16) (2.0 μg) and (+)-matrine N-oxide (2.0 μg). UV detection: (A) 220 nm; (B) 310 nm.

The chromatographic patterns of standard alkaloids are shown in Figs. 2 and 3 (normal-phase mode) and in Fig. 4 (reversed-phase mode). Table II summarizes the retention times of lupine alkaloids in four chromatographic systems and the cytisine constants (see below). The N-oxides of lupine alkaloids, such as matrine N-oxide (7) and sophoridine N-oxide (10), were not eluted from the LiChrosorb Si 60 column by solvents A and B, but they were eluted by solvent C. The N-oxides were also chromatographed on the ODS column with slight tailing.

For the qualitative analysis of lupine alkaloids, their elution was monitored by

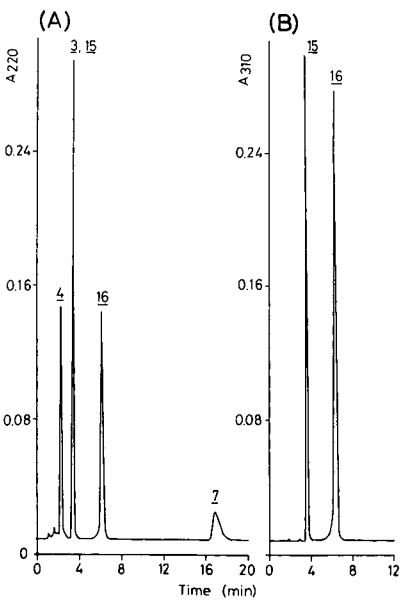

Fig. 3. HPLC profile of standard alkaloids with solvent system C. Conditions and samples as in Table I and Fig. 2.

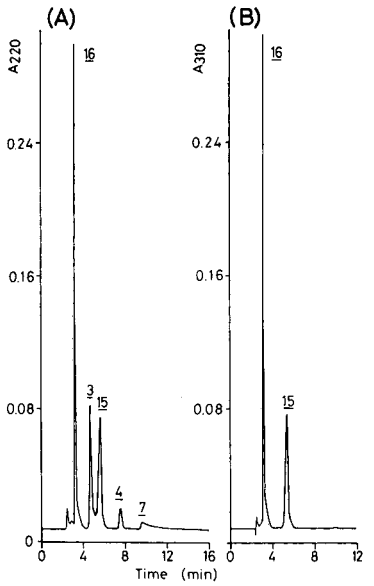

Fig. 4. HPLC profile of standard alkaloids solvent with system D. Conditions and samples as in Table I and Fig. 2.

UV absorption at 220 and 310 nm. The alkaloids that contain a 2-pyridone ring, such as (−)-cytisine, (−)-baptifoline and (+)-mamanine, were detected by their UV absorption at both wavelengths[15]. On the other hand, the alkaloids that do not possess this unsaturated heterocyclic ring, such as (+)-matrine and its N-oxide (+)-lupanine, (−)-lusitanine and (−)-sparteine, lack UV absorption at 310 nm. From these characteristic UV properties and the retention times in four chromatographic systems, we were able to identify the alkaloids in plant extracts with the known lupine alkaloids.

In order to determine the amount of each alkaloid in the plant extracts, the alkaloids were analysed by adsorption chromatography with the solvent systems B and C. The lupine alkaloids were determined by the external standard method, using (−)-cytisine as the standard. The peak area of 1 μg of each alkaloid at 220 nm was measured and normalized to that of (−)-cytisine as 1.00. Hence the "cytisine constant" is the relative absorbance at 220 nm of 1 μg of each alkaloid with respect to cytisine. The area of the cytisine peak varies linearly with its concentration. The cytisine constants of lupine alkaloids are summarized in Table II. From these data, the 22 lupine alkaloids can be determined. The limit of detection was 0.01–0.2 μg for each alkaloid.

We applied this HPLC method to the qualitative and quantitative analysis of lupine alkaloids in the aerial parts of plants of the genus *Thermopsis* growing in Japan. We were able to identify the five major alkaloids in the basic fraction prepared as described under Experimental. As shown in Table III, these plants accumulated alkaloids of the sparteine, anagyrine and cytisine types and not those of the lupinine and matrine types. The main base in *T. chinensis* is N-methylcytisine, as reported previously[16]. It is assumed to be biosynthesized from cytisine by a cytisine-specific N-methyltransferase[17,18]. The main alkaloid in *T. lupinoides*, in contrast, is lupanine,

TABLE II

RETENTION TIMES AND CYTISINE CONSTANTS OF LUPINE ALKALOIDS

The retention times were determined in four chromatographic systems. Cytisine constants were obtained by normalizing the peak area of 1 μg of each alkaloid to that of (−)-cytisine as 1.00. Determinations were carried out by adsorption chromatography.

*Alkaloid No.**	*Absorption at 310 nm*	*Retention time in four solvent systems*** *(min)*				*Cytisine constant*
		A	*B*	*C*	*D*	
1	−	8.03	7.90	5.83	9.50	0.10
2	−	2.56	2.70	1.93	−***	0.65
3	−	6.72	6.90	3.52	4.30	2.84
4	−	3.42	3.12	2.10	7.01	0.64
5	−	5.20	4.03	2.61	8.51	0.59
6	−	13.0	6.15	2.73	4.28	0.36
7	−	−	−	16.9	8.80	0.53
8	−	6.31	6.45	3.58	5.90	0.48
9	−	9.72	10.7	5.42	4.95	0.47
10	−	−	−	21.4	9.32	0.31
11	−	3.26	3.20	2.43	8.30	0.14
12	−	21.3	35.0	−	−	0.39
13	−	5.17	5.40	3.20	4.90	0.33
14	+	3.83	3.75	2.46	7.02	0.44
15	+	13.2	8.40	3.52	4.71	0.55
16	+	23.8	17.1	5.86	2.73	1.00
17	+	5.97	4.62	2.86	5.90	0.80
18	+	−	18.4	1.88	2.68	1.21
19	+	4.25	3.38	2.43	8.30	0.86
20	+	11.7	7.73	3.34	4.20	0.74
21	+	−	26.7	5.47	2.62	0.60
22	−	9.30	8.16	4.14	5.14	0.40

* See Fig. 1.
** See Table I.
*** The sample was not eluted from the column.

TABLE III

LUPINE ALKALOIDS IN PLANTS OF THE GENUS *THERMOPSIS*

The fresh aerial parts of *T. chinensis* and *T. lupinoides* were extracted and the basic fractions were analysed by HPLC as described under Experimental.

Alkaloid	*Concentration (mg/g fresh weight)*	
	T. chinensis	*T. lupinoides*
Anagyrine (14)	0.017	0.141
N-Methylcytisine (17)	0.212	0.164
Lupanine (13)	0.004	1.273
Baptifoline (15)	0.010	0.082
Cytisine (16)	0.048	0.003

which is regarded as the precursor of alkaloids of the anagyrine and cytisine types[19]. Hence it is suggested that the ability to oxidize lupanine to anagyrine and cytisine is low in the aerial parts of *T. lupinoides* compared with that in *T. chinensis*. Biosynthetic and stereochemical relationships of these alkaloids are further problems to be solved.

Tsukushinamine-type alkaloids are new cage-type lupine alkaloids isolated from *Sophora franchetina* Dunn, which is a native and very rare shrub in Japan[9]. As far as we know, alkaloids of this type have not so far been found in other plant species. Our HPLC method should be useful not only for screening lupine alkaloids in plants but also for biochemical, physiological, and chemotaxonomic studies of these alkaloids.

REFERENCES

1 J. A. Mears and T. J. Mabry, in J. B. Harborne, D. Boulter and B. L. Turner (Editors), *Chemotaxonomy of the Leguminosae*, Academic Press, London, 1971, Ch. 3, p. 73.
2 A. D. Kinghorn and S. J. Smolenski, in P. M. Polhill and P. H. Raven (Editors), *Advances in Legume Systematics, Part 2*, Royal Botanic Gardens, Kew, 1981, p. 585.
3 T. Robinson, *The Biochemistry of Alkaloids*, Springer, New York, 2nd ed., 1981, p. 67.
4 H. W. Liebisch and H. R. Schutte, in K. Mothes, H. R. Schutte and M. Luckner (Editors), *Biochemistry of Alkaloids*, VCH, Weinheim, 1985, Ch. 12, p. 128.
5 A. D. Kinghorn and M. F. Balandrin, in S. W. Pelletier (Editor), *Alkaloids: Chemical and Biological Perspectives*, Vol. 2, Wiley, New York, 1984, Ch. 3, p. 105.
6 I. Murakoshi, K. Sugimoto, J. Haginiwa, S. Ohmiya and H. Otomasu, *Phytochemistry*, 14 (1975) 2714.
7 S. Ohmiya, K. Higashiyama, H. Otomasu, I. Murakoshi and J. Haginiwa, *Phytochemistry*, 18 (1979) 645.
8 S. Ohmiya, H. Otomasu, J. Haginiwa and I. Murakoshi, *Phytochemistry*, 18 (1979) 649.
9 J. Bordner, S. Ohmiya, H. Otomasu, J. Haginiwa and I. Murakoshi, *Chem. Pharm. Bull.*, 28 (1980) 1965.
10 I. Murakoshi, E. Kidoguchi, M. Nakamura, J. Haginiwa, S. Ohmiya, K. Higashiyama and H. Otomasu, *Phytochemistry*, 20 (1981) 1725.
11 I. Murakoshi, M. Ito, J. Haginiwa, S. Ohmiya, H. Otomasu and R. T. Hirano, *Phytochemistry*, 23 (1984) 887.
12 I. Murakoshi, M. Watanabe, T. Okuda, E. Kidoguchi, J. Haginiwa, S. Ohmiya and H. Otomasu, *Phytochemistry*, 24 (1985) 2707.
13 K. Saito, T. Shi, S. Ohmiya, H. Otomasu and I. Murakoshi, *Chem. Pharm. Bull.*, 34 (1986) 3982.
14 K. Saito, T. Yoshino, T. Shi, S. Ohmiya, H. Kubo, H. Otomasu and I. Murakoshi, *Chem. Pharm. Bull.*, 35 (1987) 1308.
15 A. W. Sangster and K. L. Stuart, *Chem. Rev.*, 65 (1965) 69.
16 S. Ohmiya, H. Otomasu, I. Murakoshi and J. Haginiwa, *Phytochemistry*, 13 (1974) 643.
17 I. Murakoshi, A. Sanda, J. Haginiwa, N. Suzuki, S. Ohmiya and H. Otomasu, *Chem. Pharm. Bull.*, 25 (1977) 1970.
18 M. Wink, *Planta*, 161 (1984) 339.
19 M. Wink and T. Hartmann, in R. I. Zalewski and J. J. Skolik (Editors), *Natural Products Chemistry*, Elsevier, Amsterdam, 1985, p. 511.

Journal of Chromatography, 462 (1989) 341–347
Elsevier Science Publishers B.V., Amsterdam — Printed in The Netherlands

CHROM. 20 992

IMPROVED METHOD FOR AMINO ACID ANALYSIS OF STAINED COLLAGEN BANDS FROM POLYACRYLAMIDE GELS USING HIGH-PERFORMANCE LIQUID CHROMATOGRAPHY

YOKO HASHIMOTO

Department of Biochemistry, School of Dentistry, Aichi-Gakuin University, 1-100 Kusumoto-cho, Chikusa-ku, Nagoya 464 (Japan)

(Received September 7th, 1988)

SUMMARY

A procedure is described for the determination of the amino acid composition of stained collagen bands separated by sodium dodecyl sulphate polyacrylamide gel electrophoresis using high-performance liquid chromatography and post-labelling with *o*-phthalaldehyde. Six α-chain bands from collagens I, III and V were analysed directly after gel electrophoresis, Coomassie blue staining and destaining. It was shown that good accuracy and reproduciblity can be attained using this method, which makes it possible to determine simultaneously nineteen amino acids: Asx, Thr, Ser, Glx, Pro, Cys, Gly, Ala, Val, Met, Ile, Leu, Tyr, Phe, His, Lys and Arg together with 4-Hyp and Hyl, specific amino acids found in collagen.

INTRODUCTION

The procedure described previously[1] for amino acid analysis with *o*-phthalaldehyde (OPA) of stained protein bands, in which the stained gel slices were directly hydrolysed with hydrochloric acid, was suitable for the determinaton of the amino acids aspartic acid, threonine, serine, glutamic acid, proline, cysteine, glycine, alanine, valine, methionine, isoleucine, leucine, tyrosine, phenylalanine, histidine, lysine and arginine. However, there was a "buffer-change" peak having the same retention time as histidine, so subtraction of its peak value in the determination of histidine was necessary. Also, one could not determine the amino acid compositions of collagen samples by this method because (1) the hydroxylysine content might be slightly above its true value, (2) the arginine peak was eluted as a shoulder on the ammonia peak and (3) the resolution of 4-hydroxyproline from aspartic acid was not always satisfactory. The method described here served for the analysis of nineteen amino acids, including 4-hydroxyproline and hydroxylysine, by a single-step procedure without any correction, using six α-chain bands derived from collagens I, III and V.

0021-9673/89/$03.50

EXPERIMENTAL

Chemicals

Amino acid standard CH was purchased from Pierce (Rockford, IL, U.S.A.) and acrylamide and N,N′-methylenediacrylamide were from Merck (Darmstadt, F.R.G.). Coomassie Brilliant Blue R (CBB) and sodium dodecyl sulphate (SDS) were obtained from Sigma (St. Louis, MO, U.S.A.), thioglycolic acid, super special grade constant-boiling hydrochloric acid, OPA and sodium citrate buffer solution (pH 2.2) for sample preparation from Wako (Osaka, Japan), 10% sodium hypochlorite solution from Yoneyama Yakuhin Kogyo (Osaka, Japan) and distilled water for injection from Otsuka Pharmaceutical (Tokyo, Japan).

Sample preparation

Human collagens I, III and V were obtained from post-burn granulation tissues by pepsinization and salt fractionation[2]. The surgically obtained tissues were provided by Dr. H. Aoyama of Aichi Medical College. Sodium dodecyl sulphate polyacrylamide gel electrophoresis (SDS-PAGE) was carried out by the method reported by Laemmli[3]. About 40 μg of each type of collagen sample were subjected to slab gel (1 mm thick) electrophoresis to separate α-chains. The gel was visualized by staining with CBB. The Coomassie blue-stained gel slices, washed with destaining solution and acetone and then dried by flushing with nitrogen gas were directly hydrolysed under reduced pressure at 110 $\pm$ 1°C for 20 h with 5 μl of thioglycolic acid and 0.5 ml of 6 *M* constant-boiling hydrochloric acid. The hydrolysate was evaporated and dissolved in 50 μl of 0.067 *M* sodium citrate buffer (pH 2.2) (stock sample solution); after centrifugation to remove the insoluble material, an aliquot of the stock sample solution was subsequently diluted with the same buffer to give a concentration of 20–40 μg/ml of protein (diluted sample solution). Then, 25 μl of the sample were injected into the column.

Apparatus

The chromatographic equipment was obtained from Shimadzu (Kyoto, Japan). An LC-4A high-performance liquid chromatography (HPLC) apparatus was connected to an RF-540 spectrofluorimeter and a Model C-R3A recording integrator. Detection was accomplished by post-column reaction with OPA at 55°C using a Model PRR-2A minipump post-column reactor.

Chromatography

A sulphonated polystyrene cation-exchange resin column (150 × 4 mm I.D.) (Shimadzu gel ISC-07/S1504, particle size 7 μm), together with a Dowex 50W-16 resin column (250 × 4 mm I.D.) (Shimadzu gel ISC-50) as the precolumn, were used for the separation of amino acids. Amino acids were separated using a gradient programme of the mobile phase (Fig. 1) in a Shimadzu Model LC-4A HPLC apparatus using solutions A, B and C, where solution A was 7% (v/v) ethanol in 0.067 *M* sodium citrate (pH 3.15), solution B was 0.2 *M* sodium citrate (pH 10.0) and the solution C was 0.2 *M* sodium hydroxide. The flow-rate was 0.3 ml/min at 55°C. The post-column labeling method was essentially the same as that reported by Ishida *et al.*[4], except that the OPA concentration was raised from 0.08 to 0.4%[1]. Sodium hypochlorite reagent was

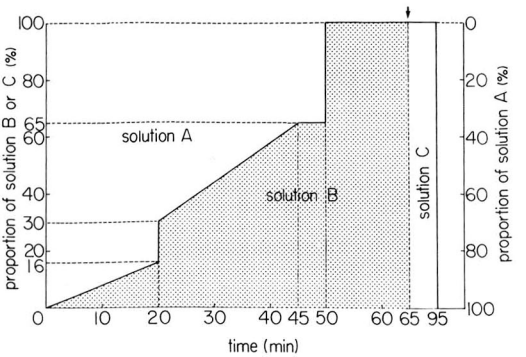

Fig. 1. Gradient profile of the mobile phase. The arrow indicates the switching point from solution B to solution C.

prepared by adding 0.2 ml of 10% sodium hypochlorite to 500 ml of buffer solution (pH 10.0) containing sodium carbonate (0.384 *M*), boric acid (0.216 *M*) and potassium sulphate (0.108 *M*). A fluorescence reagent was prepared by mixing 2.0 g of OPA in 15 ml of ethanol and 1 ml of 2-mercaptoethanol and 2 ml of 10% Brij 35 in 500 ml of the above alkaline buffer. The flow-rates of the sodium hypochlorite and OPA solutions were set at 0.2 ml/min. The fluorescence intensity of the effluent was measured at excitation and emission maxima of 348 and 450 nm, respectively.

RESULTS AND DISCUSSION

Fig. 2 (lanes a, b and c) shows the SDS-PAGE patterns of collagens I, III and V, respectively, obtained by the Laemmli method[3], which uses Tris–glycine buffer as the electrode buffer. These six α-chains were analysed. Typical chromatograms of each α1-chain collagen hydrolysate, which was derived from collages I, III and V, are shown in Fig. 3b, c and d, respectively. One sample analysis took about 80 min.

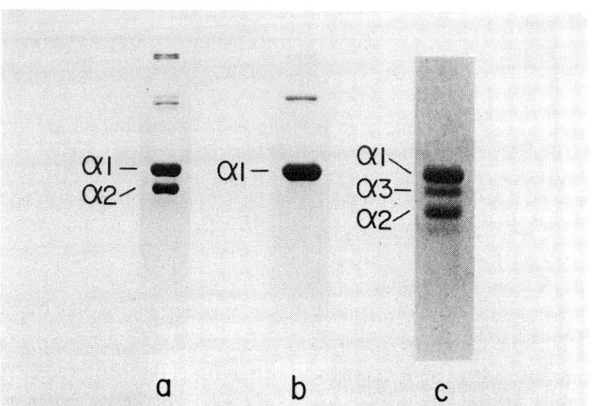

Fig. 2. SDS-PAGE of about 40 μg each of type I (lane a), type III (lane b) and type V (lane c) collagens by the Laemmli method[3]. Acrylamide concentrations were 8% for lanes a and b and 5% for lane c.

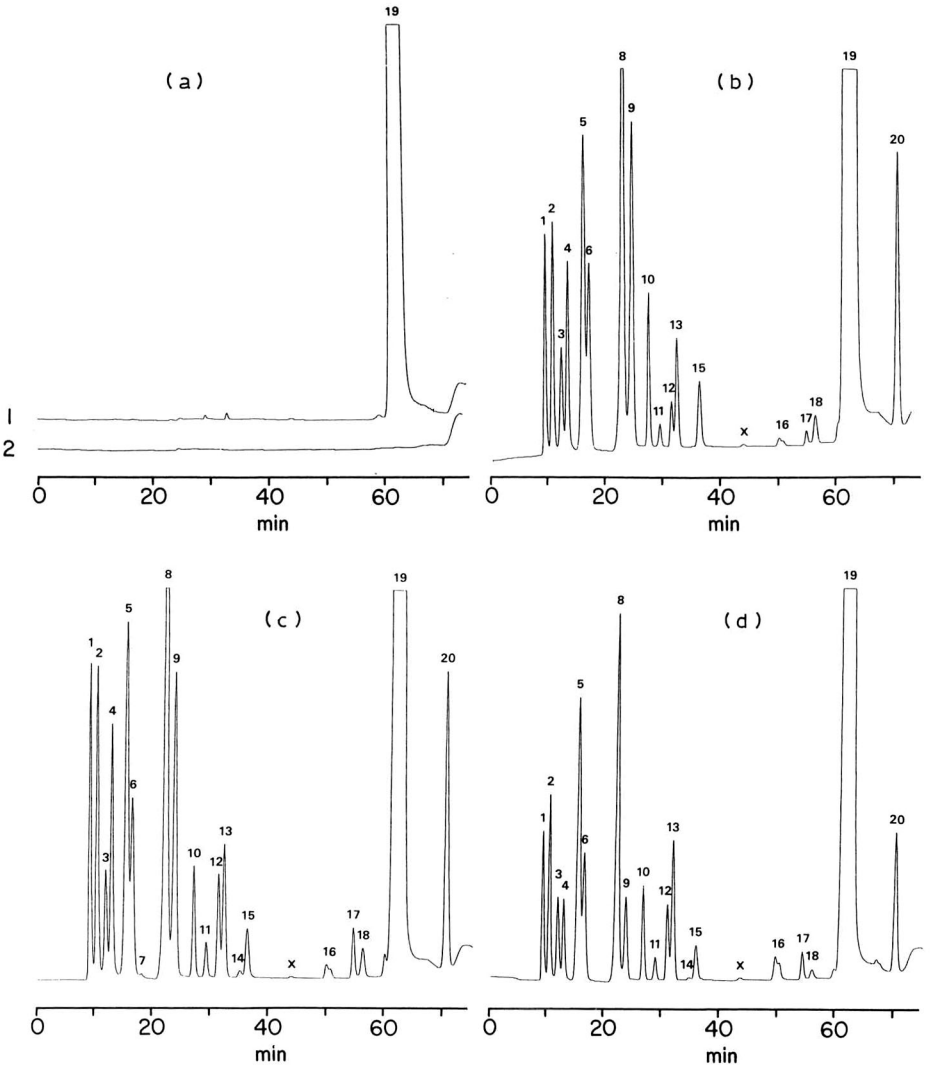

Fig. 3. Elution chromatograms showing relative fluorescence of each amino acid of the empty gel and those of α1-chains derived from collagens I, III and V. a-1, empty gel + CBB (2 μg); a-2, buffer alone; b, α1 (I) chain; c, α1 (III) chain; d, α1 (V) chain. Peaks: (1) 4-Hyp; (2) Asx; (3) Thr; (4) Ser; (5) Glx; (6) Pro; (7) Cys; (8) Gly; (9) Ala; (10) Val; (11) Met; (12) Ile; (13) Leu; (14) Tyr; (15) Phe; (16) Hyl; (17) His; (18) Lys; (19) NH_3; (20) Arg.

One could not determine the amino acid compositions of collagen samples by the method reported previously[1], for the following reasons: (1) the hydroxylysine content might be slightly above its true value, because methionine sometimes decomposes into an unidentified compound which elutes just after histidine and overlaps with the hydroxylysine peak[5]; (2) as the ratio of gel to each α-chain of collagen was high, the arginine peak was eluted as a shoulder on the ammonia peak, so another run was

needed in order to obtain better resolution of arginine by switching the buffer system from the pH gradient type to one at pH 5.28[5]; and (3) the resolution of 4-hydroxyproline from aspartic acid was not always satisfactory. The method described here was able to overcome these disadvantages by changing the gradient programme of mobile phase.

Fig. 1 shows the gradient programme used for the mobile phase. When the concentration of solution B gradually rose from 30% to 65%, the peak of hydroxylysine separated from that of the breakdown product derived from methionine decomposition (16 and X in Fig. 3b, c and d), and the "buffer-change" peak disappeared (Fig. 3a-2). When solution B was maintained at 65% for 5 min (Fig. 1), the arginine peak was separated well from the ammonia peak without eluting as a shoulder on the ammonia peak (19 and 20 in Fig. 3b, c and d). After washing in solution C for 30 min and equilibrating in solution A for another 30 min, analysis was performed in accordance with the gradient. In this way the 4-hydroxyproline and aspartic acid could be separated consistently (1 and 2 in Fig. 3b, cand d). Under these conditions, the hydroxylysine, both in the hydrochloric acid-hydrolysed sample and the L-hydroxylysine standard, showed two neighbouring peaks, for unknown reasons (16 in Fig. 3b, c and d).

The electrode buffer components, Tris and glycine, were reportedly removed by simply washing the gel slices several times with destaining solution and then five times with 3 ml of acetone following the destaining procedure[1]. As shown in Fig. 3a-1, the empty gel and CBB (2 μg) used showed negligible contamination, if any, by amino acids, and they were free from glycine in particular.

The amino acid compositions of the six α-chain samples are summarized in Table I. Fairly satisfactory results were obtained for the amino acid compositions of the six α-chains derived from collagens I, III and V. Every collagen sample has high glycine, proline and hydroxyproline contents, and collagen III has the highest levels of glycine and hydroxyproline and contains cysteine. Table I indicates that the mean values of the glycine, proline and hydroxyproline contents in the six α-chain collagens were about 34%, 11% and 10%, respectively. These concentrations are virtually the same as the reported values, indicating that they are all collagenous. The data are reasonably consistent with the previously reported values. Thioglycolic acid provided effective protection against the decomposition of tyrosine, cysteine and methionine; however, the recovery of methionine was inconsistent[1].

Amino acid analysis with the OPA reagent is fairly sensitive, and one must be very careful to minimize background contaminants through all the steps of the preparative procedure. Contamination by serine and glycine has been traced to fingerprints and micron-size particles of skin[9], and glass tubes sometimes contain glycine and other amino acids (>10 pmol per tube)[10]. Most of the above problems can be solved by protecting the gels from fingerprints by wearing rubber gloves and pyrolysing the glassware, especially the hydrolysing and evaporating tubes, in a flame before use[1].

CONCLUSIONS

A method has been developed for amino acid analysis with a single-stained collagen band directly hydrolysed with a polyacrylamide gel slice using HPLC and

TABLE I

AMINO ACID COMPOSITIONS DETERMINED FROM STAINED GEL BANDS OF THE SIX α-CHAINS OF COLLAGENS I, III AND V

Results are expressed as the number of residues per 1000 total residues.

Amino acid	*α1 (I)*		*α2 (I)*		*α1 (III)*		*α1 (V)*		*α2 (V)*		*α3 (V)*	
	Mean (n=3)	*Reported*[6]	*Mean (n=3)*	*Reported*[6]	*Mean (n=4)*	*Reported*[7]	*Mean (n=3)*	*Reported*[8]	*Mean (n=3)*	*Reported*[8]	*Mean (n=3)*	*Reported*[8]
3-Hyp	ND*	1	ND	1	ND	0	ND	0.9	ND	1.1	ND	0.9
4-Hyp	97	108	84	93	121	125	107	99	106	107	96	91
Asx	40	42	43	44	47	42	48	50	49	50	47	42
Thr	17	16	19	19	16	13	20	22	30	26	23	19
Ser	31	34	28	30	36	39	20	23	32	34	30	34
Glx	75	73	67	68	72	71	100	100	86	88	104	98
Pro	125	124	106	113	100	107	126	125	105	105	103	99
Cys	0	0	0	0	2	2	0	1.2	0	ND	0	1.3
Gly	343	333	344	338	359	350	336	325	343	325	334	332
Ala	114	115	108	102	89	96	40	41	54	57	45	49
Val	21	21	37	35	13	14	20	21	30	31	27	29
Met	3	7	4	5	4	8	6	6.8	11	10	7	8.1
Ile	7	6	17	14	13	13	18	20	14	18	17	20
Leu	21	19	34	30	23	22	42	44	36	39	53	56
Tyr	Trace	1	2	4	2	3	2	2.5	Trace	2.1	2	2.4
Phe	13	12	11	12	8	8	11	12	11	11	11	9.2
Hyl	8	9	12	12	12	5	41	46	19	23	35	43
His	3	3	12	12	7	6	7	6.3	10	9.9	14	14
Lys	28	26	18	18	23	30	14	15	12	13	13	15
Arg	55	50	56	50	53	46	43	42	55	52	42	42

* ND = Not detected.

a post-labelling method with OPA. By this method, it is possible to determine nineteen amino acids, including 4-hydroxyproline and hydroxylysine, by a single-step procedure. This method will be very useful for the amino acid analysis of collagens composed of heterogeneous α-chains, especially those which can be resolved only by PAGE.

ACKNOWLEDGEMENTS

Thanks are due to Drs. Sadako Yamagata, Michihiko Fujiwara and Taro Hayakawa for their many valuable suggestions and to Ms. Tomoko Kataka for assistance with the manuscript.

REFERENCES

1 Y. Hashimoto, S. Yamagata and T. Hayakawa, *Anal. Biochem.*, 160 (1987) 362.
2 Y. Hashimoto, T.-Y. Shieh, H. Aoyama, Y. Izawa and T. Hayakawa, *J. Invest. Dermatol.*, 87 (1986) 540.
3 U. K. Laemmli, *Nature (London)*, 227 (1970) 680.
4 Y. Ishida, T. Fujita and K. Asai, *J. Chromatogr.*, 204 (1981) 143.
5 Y. Hashimoto, K. Kobayashi, T. Hoshino, H. Aoyama and T. Hayakawa, *J. Invest. Dermatol.*, 91 (1988) 238.
6 E. J. Miller and S. Gay, *Methods Enzymol.*, 82 (1982) 3.
7 E. Chung and E. J. Miller, *Science (Washington, D.C.)*, 183 (1974) 1200.
8 H. Sage and P. Bornstein, *Biochemistry*, 18 (1979) 3815.
9 K. S. Lee and D. G. Drescher, *Int. J. Biochem.*, 9 (1978) 457.
10 H. Yoshida and H. Imai, *Kagakuzoukan*, 102 (1984) 13.

Journal of Chromatography, 462 (1989) 349–356
Elsevier Science Publishers B.V., Amsterdam — Printed in The Netherlands

CHROM. 21 048

LIQUID CHROMATOGRAPHIC DETERMINATION OF DOMOIC ACID IN SHELLFISH PRODUCTS USING THE PARALYTIC SHELLFISH POISON EXTRACTION PROCEDURE OF THE ASSOCIATION OF OFFICIAL ANALYTICAL CHEMISTS

JAMES F. LAWRENCE*, CLAUDETTE F. CHARBONNEAU and CATHIE MÉNARD
Food Research Division, Bureau of Chemical Safety, Food Directorate, Health Protection Branch, Ottawa, Ontario K1A 0L2 (Canada)
and
MICHAEL A. QUILLIAM and P. GREIG SIM
Marine Analytical Chemistry Standards Program, National Research Council of Canada, Atlantic Research Laboratory, Halifax, Nova Scotia B3H 3Z1 (Canada)
(First received July 29th, 1988; revised manuscript received October 13th, 1988)

SUMMARY

Domoic acid, the recently discovered toxic substance found in contaminated mussels from an area in eastern Prince Edward Island (Canada) was extracted from mussel tissue using the procedure of the Association of Official Analytical Chemists for paralytic shellfish poisons. This involved a 5-min boiling of the sample with 0.1 *M* hydrochloric acid then cooling and centrifuging. An aliquot of the supernatant was diluted ten to one-hundred times with water, filtered and analysed by reversed-phase liquid chromatography with a mobile phase consisting of acetonitrile–water (12:88) at pH 2.5 and an absorption wavelength of 242 nm. The detection limit was about 0.5 mg/kg domoic acid in seafood samples. The technique was successfully applied to a variety of commercially purchased shellfish and shellfish products.

INTRODUCTION

Domoic acid (Fig. 1) was recently isolated and identified as the toxic substance found in contaminated blue mussels (*Mytilus edulis*) from eastern Prince Edward

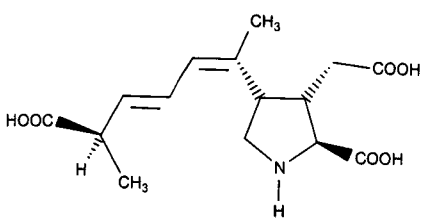

Fig. 1. Structure of domoic acid.

0021-9673/89/$03.50

Island (Canada)[1]. This neurotoxic amino acid is a naturally-occurring metabolite first isolated from the red alga, *Chondria armata*, by Japanese workers[2,3]. The substance has been synthesized[4] and evaluated for its insecticidal properties[5,6]. The source of the domoic acid found in the mussels is still under investigation, but results to date indicate that the marine pennate diatom *Nitzschia pungens*, is the most likely candidate[7].

The Association of Official Analytical Chemists (AOAC) mouse bioassay method for paralytic shellfish poisons (PSP) was found to be applicable to the detection of domoic acid[8]. About 40 mg/kg in wet mussel tissue may induce some characteristic symptoms of domoic acid intoxication while levels near 150 mg/kg produce repeatable time-to-death values. The method proved to be very useful since both types of shellfish toxins could be monitored by a single bioassay method, rather than by specific methods for each. However, domoic acid positive samples must be confirmed by an independent technique capable of accurately quantitating the substance. Trace analytical methodology for domoic acid in mussels was first developed employing a boiling water extraction followed by liquid chromatography (LC) with ultraviolet absorption detection as the determinative step[9]. This approach was simple and could detect less than 1 mg/kg domoic acid in mussel samples. The purpose of the work described in this report is to evaluate the application of LC to the detection and quantitation of domoic acid in shellfish using the AOAC PSP extraction procedure employed for the mouse bioassay. In this way both analytical and biological tests can be performed on the same extract.

EXPERIMENTAL

Reagents

Domoic acid was isolated from contaminated mussel tissue, purified (>95% purity) and characterized as described elsewhere[1]. Water was twice deionized (Milli-Q, Millipore, Bedford, U.S.A.), acetonitrile was HPLC-grade. All other solvents and chemicals were analytical-reagent grade materials. Standard solutions of domoic acid were prepared in water and diluted as required. All domoic acid standard and sample solutions were refrigerated when not in use.

Liquid chromatography

The system consisted of a Model 110B pump (Beckman), a 20-μl loop injector (Beckman), a Supelcosil LC-18 column (15 cm × 4.6 mm I.D., 5 μm), a variable-wavelength UV detector (Micromeritics) set to 242 nm (wavelength maximum for domoic acid) and 0.02 absorbance units full scale (a.u.f.s.), and a Varian 4270 integrating recorder. The mobile phase was acetonitrile–water (12:88, v/v) adjusted to pH 2.5 with 2% (v/v) orthophosphoric acid, degassed and filtered before use. The flow-rate was 1.0 ml/min.

Sample extraction

The sample preparation and extraction were carried out exactly as described earlier[10]. Briefly, 100 g of homogenized shellfish tissue was mixed thoroughly with 100 ml of 0.1 *M* hydrocloric acid in a 500-m beaker. The contents were heated with stirring on a hot plate and allowed to boil gently for a period of 5 min. The mixture was then removed and permitted to cool in a refrigerator (4°C) for 30 min. The contents were

then quantitatively transferred to a graduated cylinder and diluted to exactly 200 ml. The contents were returned to the beaker, stirred and an aliquot of about 50 ml was removed and centrifuged for 5min at *ca.* 3000 rpm (700 *g*). A 0.5-ml portion of the clear supernatant was diluted to 25 ml with water in a volumetric flask and mixed thoroughly. About 2 ml of the solution were filtered (Millex HV, 0.45 μm, Millipore) for analyis by LC.

For comparison purposes, the above procedure was repeated using water instead of 0.1 *M* hydrochloric acid for the extraction.

RESULTS AND DISCUSSION

Chromatography

Fig. 2 shows typical chromatograms obtained for domoic acid in a mussel sample. A number of C_{18} reversed-phase columns (including, Ultrasphere 5-μm, Spherisorb 5-μm, μBondapak 10-μm, Vydac 5-μm, Lichrosorb 5-μm) were evaluated and all functioned well for the determinations. The only change necessary was an adjustment of the acetonitrile concentration (usually 12–18%) in the mobile phase to produce an acceptable retention time for domoic acid We have found that 6–10 min was optimal with the columns studied. At acetonitrile concentrations greater than 18% in the mobile phase, domoic acid was not completely resolved from other co-extractives in the samples. This was particularly a problem at low concentrations (<20 mg/kg) of domoic acid in the tissue where more concentrated sample extracts had to be injected. Ion-exchange chromatography employing a Vydac 302 IC column with

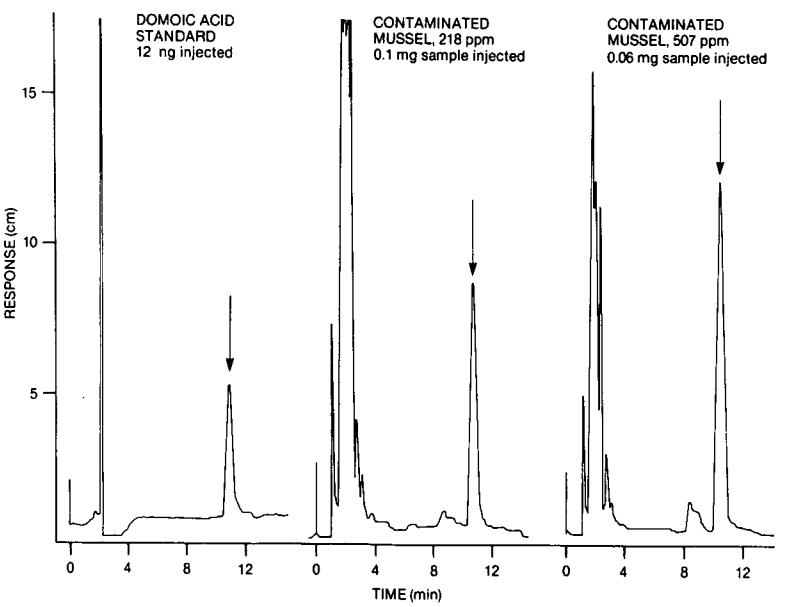

Fig. 2. Typical chromatograms of standard domoic acid and contaminated mussel samples. Mobile phase, acetonitrile–water (12:88) (pH 2.5). Supelcosil LC-18 (15 cm × 4.6 mm I.D.) column. UV detection at 242 nm and 0.02 a.u.f.s. Arrow indicates domoic acid retention time. Quantity of sample injected is equivalent to 0.1 and 0.06 mg, as indicated (ppm = mg/kg).

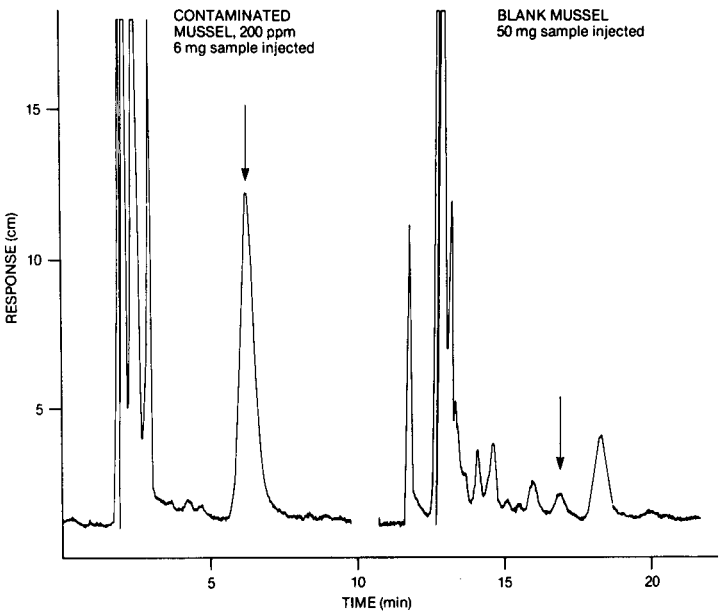

Fig. 3. Chromatograms of contaminated and blank mussel samples. Vydac 302 IC column. Mobile phase, 5% (v/v) acetonitrile in 0.008 *M* KH_2PO_4 (pH 6.9) at 2.0 ml/min. UV detection at 242 nm and 0.02 a.u.f.s. Arrow indicates domoic acid retention time. Quantity of sample injected is equivalent to 6 and 50 mg, as indicated (ppm = mg/kg).

a mobile phase of 5% acetonitrile in 0.008 *M* potassium dihydrogenphosphate (pH 6.9) at 2.0 ml/min was also successful in quantitating domoic acid in mussel extracts. Fig. 3 shows typical chromatograms obtained with the system. The peak corresponding to about 1 mg/kg in the blank sample was an interfering substance and not domoic acid since no peak was observed for domoic acid in this sample when reversed-phase chromatography was used. The ion-exchange system is useful for confirmation of reversed-phase results for domoic acid at high levels (*e.g.* > 10 mg/kg) in shellfish.

From earlier work[9] it was observed that a mobile phase pH of 2.5 gave a symmetrical peak for domoic acid. We found that changing the pH to 2.0 or 3.0 caused a slight shift in retention time (more acidic, shorter retention) but peak symmetry and efficiencty remained essentially the same. A pH of 2.5 was selected for routine work.

Sample analysis

The AOAC PSP extraction procedure[10] was compared to the water extraction method reported earlier[9]. It was found that the PSP procedure consistently yielded lower domoic acid values for both spiked and naturally contaminated mussel tissue. In order to study this in more detail, boiling time studies were carried out with both acid and water extraction procedures. It was found that at 200 mg/kg in mussel tissue, domoic acid steadily decreased with increased boiling time resulting in a 7% decrease after 10 min and a 16% decrease after 20 min compared to the 5-min value.

TABLE I

COMPARISON OF PSP AND WATER EXTRACTION PROCEDURES FOR DOMOIC ACID IN MUSSELS

*Sample**	*Domoic acid found (mg/kg)*		*Ratio PSP:water (%)*
	PSP extraction	*Water extraction*	
Blank mussel	<1	<1	–
Blank mussel +19 mg/kg	14.3	16.3	88
Contaminated mussel 1	103	112	92
Contaminated mussel 2	202	231	87
Contaminated mussel 3	417	576	72
Contaminated mussel 4	156**	198**	79
Contaminated mussel 4 (refrigerated after heating and before centrifugation)	171**	193**	89

* Samples cooled at room temperature for 30 min after heating and before centrifugation; boiling time, 5 min.

** Average of duplicates.

For the water extraction no change was observed up to 10 min while at 20 min a 12% decrease was observed. Although the actual fate of domoic acid during the heating is not known, the boiling time was kept at exactly 5 min, in accordance with the AOAC collaboratively studied PSP procedure.

Table I shows results obtained comparing acid and water extractions with boiling times of 5 min for samples containing different levels of domoic acid. It can be seen that acid extraction produced 72–92% of the water extraction values when extracts were permitted to cool on the bench at room temperature. This is not attributed to a poorer extraction efficiency but to a degradation of domoic acid during the extraction and subsequent cooling. If the extracts were refrigerated for 30 min immediately after heating to cool them to room temperature before centrifugation, the amount of domoic acid recovered increased from 79 to 89% relative to the water extraction (see Table I, contaminated mussel 4). Refrigeration of the acid extracts was found to markedly improve the long term stablity of domoic acid. Mussel extracts that were permitted to sit at room temperature for five days showed a 30–50% decrease in domoic acid content, whereas when refrigerated (4°C), there was no significant change after three weeks. As a result of these studies, all sample extracts were refrigerated immediately after heating as well as during storage. Stability can also be improved by passing the extracts trough a reversed-phase C_{18} solid phase extraction cartridge as demonstrated earlier[9].

The repeatability of the method using the above conditions was quite acceptable. Coefficients of variation for replicate determinations ranged from 2.9 to 6.8% for mussel samples containing 4.0–500 mg/kg domoic acid. The detection limit was estimated to be about 0.5 mg/kg (signal-to-noise ratio of 3:1) depending upon quantity and type of sample injected. Fig. 4 shows a typical result for an extract of a blank

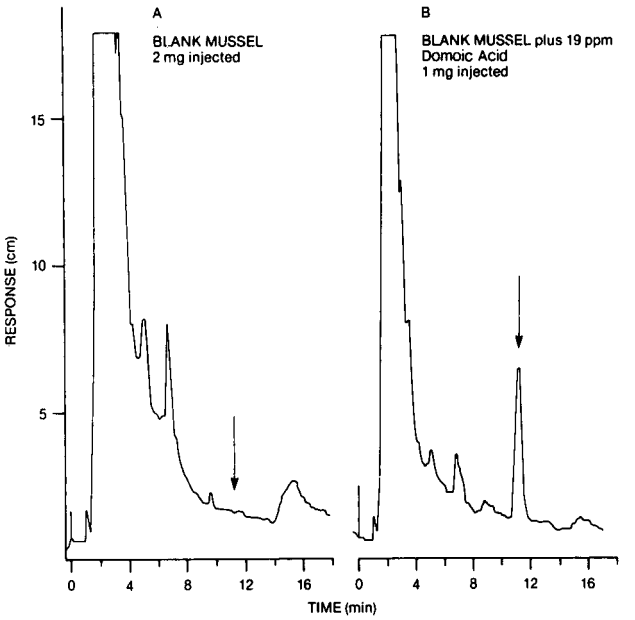

Fig. 4. Chromatograms of (A) blank mussel and (B) blank mussel plus 19 mg/kg domoic acid. Conditions as in Fig. 1. Arrow indicates domoic acid retention time. Quantity of sample injected is equivalent to 2 and 1 mg, as indicated (ppm = mg/kg).

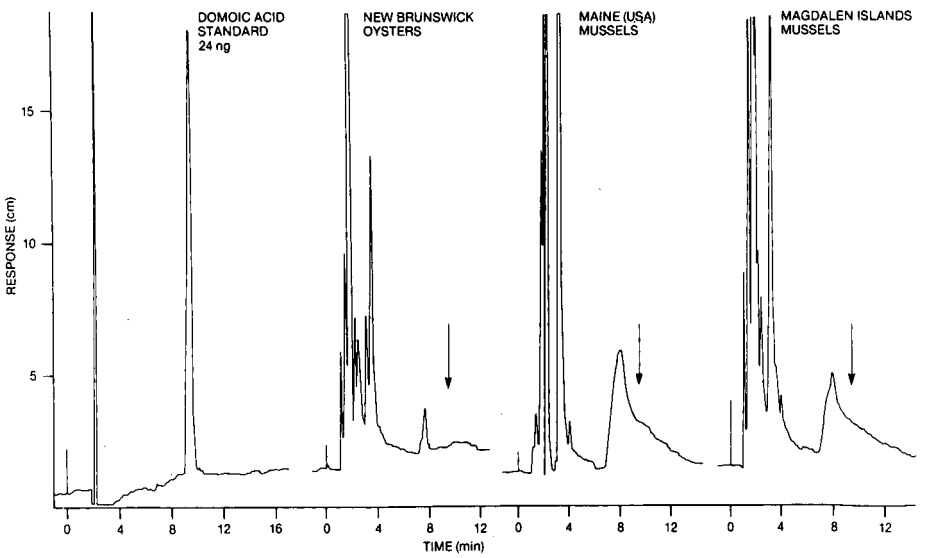

Fig 5. Chromatograms of oyster and mussel samples from the Atlantic region of Canada and a mussel sample from Maine, U.S.A.; 0.2 mg of equivalent sample injected. Conditions as in Fig. 1 except that the mobile phase contained 12.5% acetonitrile. Arrow indicates domoic acid retention time.

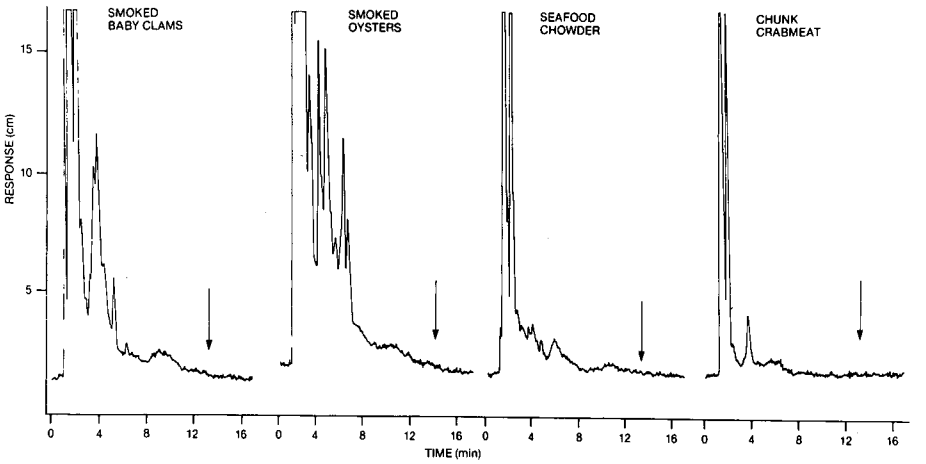

Fig. 6. Chromatograms of different seafood products; 0.5 mg of equivalent sample injected. Conditions as in Fig. 1 except that a Spherisorb ODS 15 cm × 4.6 mm I.D. column was employed. Arrow indicates domoic acid retention time.

mussel which was obtained from the Atlantic coast of Nova Scotia. When spiked with 19 mg/kg domoic acid before acid extraction, good recovery was observed (Table I).

Fig. 5 shows results obtained with oysters and mussels from the Atlantic coast outside the area of eastern Prince Edward Island. No domoic acid was found in any of the samples. The broad tailing peak in the mussels from Maine, U.S.A., and the Magdalen Islands in the Gulf of St. Lawrence was not observed in mussels from Prince Edward Island nor Nova Scotia (blank, Fig. 3).

Fig. 6 shows chromatograms of various seafood products obtained using the acid extraction procedure. The method worked well for all shellfish products tested including oysters, mussels and clams (canned, pickled and smoked), as well as shrimp, crab, lobser and seafood chowders. Recoveries were verified by regularly including spike samples in the analysis scheme. No domoic acid was found in any of 44 different retail products analysed.

CONCLUSION

The PSP extraction procedure employing 0.1 *M* hydrochloric acid was found to provide reproducible results with sufficient sensitivity to detect domoic acid in shellfish down to less than 1 mg/kg. This level is far more than adequate to confirm positive results employing the mouse bioassay procedure. Although the recoveries and stability of the acid extracts are not as good as extracts obtained using boiling water extraction, reliable results may be obtained with certain precautions such as keeping the boiling time to exactly 5 min and refrigerating the samples immediately after extraction and during long term storage. The advantage of the acid extraction is that both PSP toxins and domoic acid can be screened using the mouse bioassay on the same sample extract and confirmation of domoic acid by LC can also be done using the same extract.

REFERENCES

1 J. L. C. Wright *et al.*, *Can. J. Chem.*, in press.
2 T. Takemoto, K. Daigo, Y. Kondo and K. Kondo, *Yakugaku Zasahi*, 86 (1966) 874.
3 M. Maeda, T. Kodama, T. Tanaka, H. Yoshizumi, T. Takemoto, K. Nomoto and T. Fujita, *Chem. Pharm. Bull.*, 34 (1986) 4892.
4 Y. Ohfune and M. Tomita, *J. Am. Chem. Soc.*, 104 (1982) 3511.
5 M. Maeda, T. Kodama, M. Saito, T. Tanaka, H. Yoshizumi, K. Nomoto and T. Fujita, *Pestic. Biochem. Physiol.*, 28 (1987) 85.
6 M. Maeda, T. Kodama, T. Tanaka, Y. Ohfune, K. Nomoto, K. Nishimura and T. Fujita, *J. Pestic. Sci.*, 9 (1984) 27.
7 D. V. Subba Rao, M. A. Quilliam and R. Pocklington, *Nature (London)*, in press.
8 Bureau of Chemical Safety, Healt Protection Branch, Ottawa, unpublished results.
9 M. A. Quilliam, P. G. Sim, A. W. McCulloch and A. G. McInnes, *Int. J. Environ. Anal. Chem.*, in press.
10 *Official Methods of Analysis*, Association of Official Analytical Chemists, Arlington, VA, 14th ed., 1984, 18.086–18.092.

Journal of Chromatography, 462 (1989) 357–364
Elsevier Science Publishers B.V., Amsterdam — Printed in The Netherlands

CHROM. 20 979

HIGH-PERFORMANCE LIQUID CHROMATOGRAPHIC METHOD FOR THE SIMULTANEOUS ANALYSIS OF α-SOLANINE AND α-CHACONINE IN POTATO PLANTS CULTURED *IN VITRO*

K. KOBAYASHI*, A. D. POWELL, M. TOYODA and Y. SAITO
Division of Foods, National Institute of Hygienic Sciences, 1-18-1, Kamiyoga, Setagaya-ku, Tokyo 158 (Japan)

(First received June 10th, 1988; revised manuscript received September 9th, 1988)

SUMMARY

An high-performance liquid chromatography (HPLC) method utilizing a μBondapak NH_2 column was developed for the simultaneous measurement of the *cis*-glycoalkaloids α-solanine and α-chaconine present in 1 g of potato tissue. Shoot tissue was extracted twice with methanol and the extract purified on an acetic pretreated silica gel column and a Sep-Pak C_{18} cartridge. Alkaloids were separated by HPLC with a μBondapak NH_2 column and a mobile phase of ethanol–acetonitrile–potassium dihydrogenphosphate (3:2:1). The recoveries of α-solanine and α-chaconine were 91.4 ± 6.5 ($n=3$) and 98.8 ± 12.2% ($n=3$) respectively when spiked to potato shoot material (100 mg/100 g) prior to extraction. The contents of α-solanine and α-chaconine in *in vitro* plantlet material of *Solanum tuberosum* (Danshyaku) were 13.1 ± 1.2 mg/100 g ($n=3$) and 5.2 ± 0.5 mg/100 g ($n=3$) respectively.

INTRODUCTION

Many analytical methods have been reported for glycoalkaloid quantification in potato tissues[1]. These include titrimetry, dye binding colorimetry[2], gas chromatography[3], high-performance liquid chromatography (HPLC)[4–7], radioimmunoassay and enzyme-linked immunosorbent assay[8,9]. These have, however, often required large amounts of material or do not discriminate between α-solanine and α-chaconine.

The *cis*-glycoalkaloids, α-solanine and α-chaconine, account for 95% of the total glycoalkaloids in potato, but differ in structure only in two of their three sugar moieties. This, coupled with the fact that their absorption maxima are 205 nm, which limits the choice of HPLC mobile phase to those with low UV absorptions, makes it difficult to separate them.

Some success in separating these two compounds has been reported. A μBondapak NH_2 column and a tetrahydrofuran–potassium dihydrogenphosphate (1.7 g/100 ml)–acetonitrile (50:25:25) mobile phase were able to separate α-solanine and α-chaconine in standard solutions[4]. However, when potato tuber tissue was analysed, contamination of the α-solanine peak with unknown substances was

0021-9673/89/$03.50

observed. A C_8 or C_{18} column and a solvent system of acetonitrile–water–ethanolamine (55:45:0.1 or 45:55:0.1 respectively) were able to resolve the two *cis*-glycoalkaloids[10] but UV absorption by ethanolamine could sometimes be a problem.

There is an increasing need for a rapid determination method for the above glycoalkaloids. New biotechnological approaches to plant breeding and selection can produce many plantlets through a variety of procedures. Although selections may be for a variety of beneficial traits, *e.g.*, disease resistance, temperature stress resistance, secondary product production, it is necessary to determine alkaloid levels to ensure that the synthetic apparatus has not been perturbed during the selection process. Rapid and accurate measurements are paramount in those projects, *e.g.*, ref. 11, where alkaloid levels are specifically being selected for. Greatest efficiency will be achieved when plant material can be analyzed at the earliest stage possible, so analytical procedures using small tissue samples are also essential.

This paper outlines the development of a new HPLC method to determine α-solanine and α-chaconine in as little as 1 g of potato shoot material.

EXPERIMENTAL

Apparatus

A 880 PU pump, 7125 injector, 870-UV detector (Japan Spectroscopic, Tokyo, Japan) and a Chromatopac C-R3A integrator (Shimadzu, Kyoto, Japan) were used. Two columns, an Hypersil ODS (10 cm × 2.1 mm I.D.) and a μBondapak NH_2 (30 cm × 3.9 mm I.D.) (Waters Assoc., Milford, MA, U.S.A.), were employed.

Mobile phase

Methanol–water–phosphoric acid (95:30:0.1) was used with the Hypersil ODS column, while ethanol–acetonitrile–0.005 *M* potassium dihydrogenphosphate (3:2:1) was used with the μBondapak NH_2 column.

Reagents

All chemicals were of special grade with the exception of acetonitrile which was of HPLC grade, and were obtained from Wako (Osaka, Japan). α-Solanine and α-chaconine were supplied by Sigma (St. Louis, MO, U.S.A.).

Plant material

In vitro Solanum tuberosum (Danshyaku) plantlets were obtained from the National Center for Seeds and Seedlings and propagated by single node cutting in MS (Murashige and Skoog) salts[12] and vitamins, 3% sucrose and 0.15% gellan gum at 20°C under a 4000-Lux fluorescence light source.

Extraction of α-solanine and α-chaconine

A 1-g amount of shoot tissue was chopped into small pieces and 5 ml methanol were added prior to homogenation. The homogenized sample was filtered under suction using Toyo No. 5C filter-paper and the residue reextracted as above. The filtrates were pooled and made up to 10 ml with methanol.

Purification of the extract and alkaloid content determination

A 2-ml volume of extract solution was concentrated to dryness by rotary evaporation at 50°C, redissolved in 2 ml methanol and purified on a silica gel column. The silica gel was washed twice with methanol–water–acetic acid (70:30:0.15), three times with methanol and, after drying, activated at 140°C for 24 h. A 3.5-g amount of the treated silica gel was suspended in 20 ml methanol, and packed into a glass column to a height of 8 cm. The packed column was washed with methanol–water–acetic acid (10 ml:0.3 ml:5 μl) and then 15 ml methanol. The 2-ml sample was loaded and allowed to drain until the surface of the gel was just covered. A 1-ml methanol rinse of the sample flask was also applied in this way. The column was left for 15 min and then washed with 12 ml methanol at a flow-rate of *ca.* 0.5 ml/min. Alkaloids were eluted with 20 ml methanol–water–acetic acid (80:20:0.1). The eluate was concentrated almost to dryness, dissolved in 10 ml water and purified on a Sep-Pak C_{18} cartridge column, which was washed first with 10 ml methanol, then 10 ml 1% acetic acid and finally 20 ml water. The 10-ml sample was loaded and the column washed with 2 ml water and then 5 ml 30% methanol. Alkaloids were eluted with 5 ml methanol. The eluate was concentrated to dryness and dissolved in 1 ml ethanol–acetonitrile–0.005 *M* potassium dihydrogenphosphate (3:2:1). An aliquot was then applied to the HPLC column.

RESULTS AND DISCUSSION

Extraction of α-solanine and α-chaconine from young potato plantlets

The poor solubility of α-solanine and α-chaconine limits the choice of extraction solvent, however aqueous acetic acid solutions and aqueous ethanol or methanol mixtures with, or without, the addition of 5% acetic acid are most commonly used[8]. The methanol extraction procedure of Kajiwara *et al.*[13] was used in this study.

Purification by silica gel column chromatography

When α-solanine and α-chaconine (in standard solution) were loaded onto a silica gel column they were bound tightly and elution was poor. If the column was pretreated with a mixture of 10 ml methanol, 0–0.3 ml water and 0–5.0 μl acetic acid prior to elution with 20 ml of methanol–water–acetic acid (80:20:0.1), recovery was

TABLE I

EFFECT OF PRETREATMENT ON RECOVERY OF α-SOLANINE FROM A SILICA GEL COLUMN

Solvent systems for pre-treatment of silica gel column			*Recovery of α-solanine (%)*
Methanol (ml)	*Water (ml)*	*Acetic acid (μl)*	
10	0.0	0.0	41
10	0.3	0.0	70
10	0.3	1.0	85
10	0.3	2.5	92
10	0.3	5.0	100

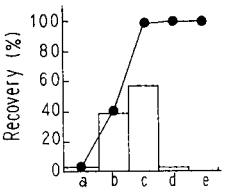

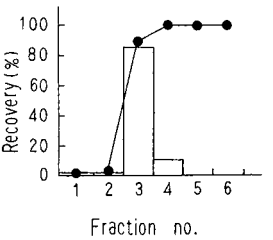

Fig. 1. Stepwise elution of α-solanine from a silica gel column. An 150-μg amount of α-solanine was loaded onto a pre-treated silica gel column. Eluents were used in the following order: a, 12 ml methanol; b, 10 ml methanol–water–acetic acid (99:1:0.005); c, 10 ml (95:5:0.025); d, 10 ml (80:20:0.1); e, 10 ml (70:30:0.15). Each column in the figure represents recovery of α-solanine from a fraction, and the closed circles represent total recovery.

Fig. 2. Isocratic elution of α-solanine from a silica gel column with methanol–water–acetic acid (80:20:0.1). The loaded column was washed with methanol (fraction 1) and eluted (fractions 2–6). Each fraction was 5 ml. Other conditions as in Fig. 1.

improved. Recovery percentages for α-solanine are shown in Table I. Maximum elution efficiency was achieved when a pretreatment with 10 ml methanol, 0.3 ml water and 5 μl acetic acid was included.

The most effective elution solvent was then investigated. An 150-μg amount of α-solanine in 1 ml methanol was loaded onto a pretreated column. The column was washed with 12 ml methanol and eluted with mixtures of methanol, water and acetic acid in the ratios and order 99:1:0.005; 95:5:0.25; 80:20:0.1 and 70:30:0.15. The elution profile is shown in Fig. 1. The second and third solutions eluted most α-solanine but total recovery was achieved only after addition of the fourth (80:20:0.1) mixture.

An isocratic elution with the 80:20:0.1 mixture was carried out to try to simplify the elution procedure. Fig. 2 shows that three 5-ml elution fractions were effective in the elution of 100% of the α-solanine. A total volume of 20 ml was utilized for elution in later experiments to allow for variability in column conditions.

Purification on a Sep-Pak C_{18} cartridge

Further purification was carried out on a Sep-Pak C_{18} cartridge. Elution of a standard amount of α-solanine was performed in steps using the water–methanol

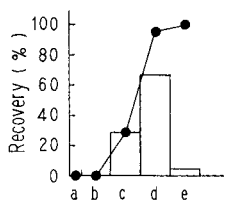

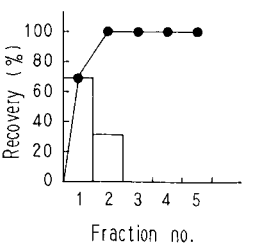

Fig. 3. Stepwise elution of α-solanine from Sep-Pak C_{18}. An 150-μg amount of α-solanine was loaded onto a pre-washed Sep-Pak C_{18} cartridge column. Eluents were used in the following order: a, 2 ml water; b, 10 ml 30% methanol; c, 10 ml 50% methanol; d, 10 ml 75% methanol; e, 10 ml methanol.

Fig. 4. Isocratic elution of α-solanine from Sep-Pak C_{18}. The loaded column was washed with water and 30% methanol, then eluted with methanol. Each methanol fraction was 1 ml. Other conditions as in Fig. 3.

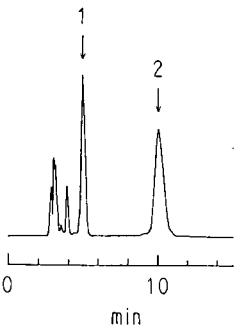

Fig. 5. Chromatogram of α-chaconine and α-solanine standard solution. HPLC conditions: column: μBondapak NH_2 (30 cm × 3.9 mm); mobile phase, ethanol–acetonitrile–0.005 *M* potassium dihydrogenphosphate (3:2:1); detector sensitivity, 64 mV a.u.f.s. Peaks: 1 = α-chaconine; 2 = α-solanine.

mixtures outlined in Fig. 3. α-Solanine was eluted with solutions c, d and e (50, 75 and 100% methanol respectively). It was decided to use a 30% methanol wash of the Sep-Pak cartridge followed by 100% methanol to elute the α-solanine. A 2-ml volume of 100% methanol was effective in totally removing the α-solanine from the Sep-Pak cartridge (Fig. 4).

Similar investigations were carried out with α-chaconine standard solutions, and the silica gel column and Sep-Pak C_{18} procedures were found to be equally effective in purification and recovery.

HPLC conditions

Resolution of α-solanine and α-chaconine was first attempted using an ODS column and mobile phase which included tetrahydrofuran or ethanolamine. It was not possible to separate the glycoalkaloids however, because of the instability of the baseline. A methanol–water–phosphoric acid mobile phase was also unable to resolve the two glycoalkaloids, with retention times of 4.4 and 4.9 min for α-chaconine and α-solanine respectively (data not presented). A modification of Bushway's method[4] utilizing μBondapak NH_2 was then used. Ethanol was substituted for tetrahydrofuran in the mobile phase because of its low UV absorption. This column and a mobile phase of ethanol–acetonitrile–0.005 *M* potassium dihydrogenphosphate (3:2:1) was able to separate α-solanine and α-chaconine (Fig. 5). Retention times of

TABLE II

EFFECT OF COMPOSITION OF MOBILE PHASE ON THE RETENTION OF α-SOLANINE AND α-CHACONINE

HPLC conditions: column μBondapak NH_2 (30 cm × 3.9 mm I.D.); flow-rate, 1.5 ml/min; wavelength, 205 nm.

Ethanol–acetonitrile–0.005 M KH_2PO_4	*Retention time (min)*	
	α-Solanine	*α-Chaconine*
1:2:1	3.6	2.4
2:2:1	5.1	2.8
3:2:1	7.3	3.2

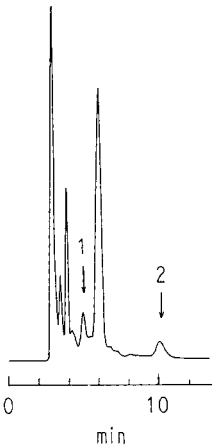

Fig. 6. Chromatogram of the eluate from Sep Pak C_{18} of an extract from young *S. tuberosum* plantlets first separated on a silica gel column. This figure represents sample 2 in Table IV.

α-solanine and α-chaconine could be increased by increasing the proportion of ethanol in the mobile phase (Table II).

The contents of α-solanine and α-chaconine in potato plantlet material could also be determined using this column and mobile phase provided the silica gel and Sep-Pak C_{18} chromatography purification procedures outlined earlier were followed (Fig. 6). Previous methods of extracting from large amounts of plant material precipitated alkaloids from methanol extracts by ammonium hydroxide addition[4,6]. This, however, could not be used in the present studies as only 1 g of material was used and insufficient precipitation occurred. The two clean-up procedures of the extracts eliminated the need for such a precipitation. Sensitivity was also increased because the substitution of tetrahydrofuran by ethanol in the HPLC mobile phase allowed the use of a detection wavelength of 205 nm rather than the 215 nm utilized with a tetrahydrofuran-containing mobile phase[7]. The former wavelength corresponds to the maximum absorption of these alkaloids.

TABLE III

RECOVERIES OF α-SOLANINE (100 mg/100 g) AND α-CHACONINE (100 mg/100 g), SPIKED TO YOUNG *S. TUBEROSUM* PLANTLETS

Sample No.	*Recovery (%)*	
	α-Solanine	*α-Chaconine*
1	97.3	90.7
2	84.5	112.8
3	92.4	93.0
Av. ± S.D.	91.4 ± 6.5	98.8 ± 12.2

TABLE IV

α-SOLANINE AND α-CHACONINE OF YOUNG *S. TUBEROSUM* PLANTLETS

Sample No.	*α-Solanine (mg/100 g)*	*α-Chaconine (mg/100 g)*
1	14.3	5.4
2	13.1	5.6
3	11.9	4.6
Av. ± S.D.	13.1 ± 1.2	5.2 ± 0.5

Analysis of α-solanine and α-chaconine in in vitro potato plantlets

Table III shows recoveries of α-solanine and α-chaconine from *Solanum tuberosum* (Danshyaku) plantlets cultured *in vitro*, each spiked at 100 mg/100 g. Recovery was 91.4 ± 6.5 ($n=3$) and 98.8 ±12.2% ($n=3$) for α-solanine and α-chaconine respectively. No binding of glycoalkaloids to plant components appears to occur. The detection limits were 2 mg/100 g for α-solanine and 1 mg/100 g for α-chaconine.

Table IV shows the glycoalkaloid content in young *in vitro* plantlets. The α-solanine content was 13.1 ± 1.2 mg/100 g and that of α-chaconine was 5.2 ± 0.5 mg/100 g. Previous reports have noted glycoalkaloids contents in the range of 10–100 mg/100 g but comparison with the data presented here is difficult. As culture conditions play an important role in the accumulation of glycoalkaloids, it is appropriate only to make comparisons when more data are collected from material cultured *in vitro*. Nonetheless, this work is an important step towards the rapid screening of *in vitro* material since these compounds can be determined in tissue samples as small as 1 g.

ACKNOWLEDGEMENTS

We thank Dr. Y. Tashiro in the National Center of Seeds and Seedlings for his gift of young plantlets of *S. tuberosum* (Danshyaku), and Dr. Y. Irikura in the National Institute of Agrobiological Resources for his advice on tissue culture procedures. This work was conducted while Dr. A. D. Powell held a Japan Health Sciences Foundation Visiting Scientist Fellowship. The research was supported by a grant from Japan Health Sciences Foundation.

REFERENCES

1 D. T. Coxon, *Am. Potato J.*, 61 (1984) 169.
2 D. T. Coxon, K. R. Price and R. G. Jones, *J. Sci. Food Agric.*, 30 (1979) 1043.
3 R. J. Bushway, D. F. McGram and A. A. Bushway, *J. Agric. Food Chem.*, 32 (1984) 548.
4 R. J. Bushway, E. S. Barden, A. W. Bushway and A. A. Bushway, *J. Chromatogr.*, 178 (1979) 533.
5 R. J. Bushway, E. S. Barden, A. M. Wilson and A. A. Bushway, *J. Food Sci.*, 45 (1980) 1088.
6 R. J. Bushway and R. Ponnampalam, *J. Agric. Food Chem.*, 29 (1981) 814.
7 R. J. Bushway, *J. Chromatogr.*, 247 (1982) 180.
8 M. R. A. Morgan, R. McNerney, J. A. Matthew, D. T. Coxon and H. W.-S. Chan, *J. Sci. Food Agric.*, 34 (1983) 593.

9 M. R. A. Morgan, D. T. Coxon, S. Bramham, H. W.-S. Chan, W. M. J. van Gelder and M. J. Allison, *J. Sci. Food Agric.*, 36 (1985) 282.
10 S. C. Morris, T. H. Lee, *J. Chromatogr.*, 219 (1981) 403.
11 S. L. Sinden, L. L. Sanford and K. L. Deahl, *J. Agric. Food Chem.*, 50 (1986) 372.
12 T. Murashige and F. Skoog, *Physiol. Plant*, 15 (1962) 473.
13 N. Kajiwara, T. Ninomiya, H. Kawai and Y. Hosogai, *J. Food Hyg. Soc. Jpn.*, 25 (1984) 256.

Journal of Chromatography, 462 (1989) 365–375
Elsevier Science Publishers B.V., Amsterdam — Printed in The Netherlands

CHROM. 21 050

Note

Characterization of the direct-probe open-tubular liquid chromatography–mass spectrometry interface parameters

JOS S. M. DE WIT* and KENNETH B. TOMER*
Laboratory of Molecular Biophysics, National Institute of Environmental Health Sciences, P.O. Box 12233, Research Triangle Park, NC 27709 (U.S.A.)
and
JAMES W. JORGENSON
Department of Chemistry, University of North Carolina at Chapel Hill, Chapel Hill, NC 27514 (U.S.A.)
(First received July 19th, 1988; revised manuscript received September 19th, 1988)

We recently reported the design of an interface coupling open-tubular liquid chromatography (OTLC) (using columns of 2–10 μm I.D.) and mass spectrometry (MS)[1]. Coupling of OTLC and MS presents several advantages over other methods of LC–MS coupling. The low flow-rates utilized in OTLC (<0.1 μl/min) permit introduction of the entire effluent into the mass spectrometer. The resultant source pressures are low enough for the production of electron impact (EI) spectra.

The direct-probe OTLC–MS interface that we developed[1] has several advantages over previous OTLC–MS interface designs[2–4]. The direct liquid introduction (DLI)-OTLC–MS interface requires additional liquid flow for proper operation which prohibits operation of the mass spectrometer in the EI mode[2,3]. In the capillary vapor jet inlet interface, complete vaporization of the solvent takes place inside the capillary tubes[5,6]. This can lead to precipitation of less volatile analytes in the capillary tube[4]. Our direct-probe OTLC–MS interface (a capillary vapor-jet variation) uses a tapered column tip which decreases the evaporation surface and increases the effluent's linear velocity. This causes the vaporization to take place very near the orifice which eliminates the deposition of less volatile analytes in the capillary column[1].

A variety of parameters such as the orifice diameter, mobile phase velocity and temperature can influence the performance of the interface. The orifice diameter can be viewed as a non-variable interface parameter, while the mobile phase velocity and temperature can be varied during operation. We have recently reported several applications of OTLC–MS to the separation and analysis of pesticides[1], PNAs[1], pesticide metabolites[7] and herbicide metabolites[8]. Here we report the results of our study of the optimization of these parameters for the direct probe OTLC–MS interface and the results of our study of the range of compounds for which this interface is applicable. For this study we have used flow injection analysis in order to remove any effects of the chromatographic process on the behaviour of the interface.

* Also at the Department of Chemistry, University of North Carolina at Chapel Hill, Chapel Hill, NC 27514, U.S.A.

0021-9673/89/$03.50

EXPERIMENTAL

OTLC

The OTLC system used in this work has been described previously[1]. A brief description follows. The mobile phase is kept under helium pressure in a 70-ml reservoir. Flow-rates are varied by varying the head pressure and linear velocities are determined from the column volume and measurement of the dead time of the column. The reservoir is connected to a stainless-steel tee with $\frac{1}{16}$-in. stainless-steel tubing through a 4-port injection valve and an in-line filter. This tee holds the OTLC column with a Vespel ferrule. Since no mechanical pumps are used, the flow-rate is pulse free. Injection are made by introducing a plug of sample solution onto the column[1,7]. The amount injected is controlled by the injection time; at a typical flow-rate of 1 nl/s, a 1-s injection results in a 1-nl injection volume. For this work only untreated fused-silica columns (1 m × 10 μm I.D.) (Polymicro Technologies, Phoenix, AZ, U.S.A.) containing no stationary phase are employed.

MS

Two Finnigan 3300 quadrupole mass spectrometers were used for this work: a chemical ionization mass spectrometer, previously modified for negative ion detection, and an electron ionization mass spectrometer. A Finnigan/Incos 2300 data system is interfaced to both mass spectrometers.

OTLC–MS interface

The interfacce probe has been described previously[1]. A description follows. The probe is constructed from an 8 in. long hollow stainless-steel shaft, on which a copper tip is silver soldered. The temperature of this tip is controlled and monitored by a cartridge heater and a thermocouple connected to an Omega 4001 temperature controller (Omega Engineering, Stamford, CT, U.S.A.). A 12-in. long piece of $\frac{1}{16}$-in. stainless-steel tubing goes through the entire probe and protrudes 2 mm beyond the copper probe tip. The OTLC column goes through this $\frac{1}{16}$-in. stainless-steel tubing and it protrudes beyond the stainless-steel tube an additional 2 mm.

Tapering

Tapering of the fused-silica tubing was achieved by quickly drawing the tubing out in a hot methane–air flame. This was done with 800 p.s.i. air flowing through the column. In case of coated columns the heat and air served to pyrolyze the stationary phase and to remove it from the column end to avoid plugging. The air flow also allowed one to determine whether or not the column was still open by immersing the column tip in water, and observing the formation of bubbles. Examination by electron microscopy (Model DS-130 electron microscope, International Scientific Instruments, Milpitas, CA, U.S.A.) of twelve tapered column ends with outer diameters varying from 150 to 20 μm and inner diameters varying from 10 to 1.5 μm showed that the ratio of the I.D. to the O.D. of the capillary did not change, even at the smallest diameters. It is therefore possible to calculate the taper orifice by measuring the outer diameter using a 100× optical microscope. A comparison of the twelve orifice diameters calculated from the O.D. and directly measured with an electron microscope resulted in a maximum of 5% difference between these two methods. To obtain accurate I.D. to

O.D. ratios, the O.D. and I.D. of the capillary need to be measured (with the optical 100 × microscope) prior to tapering, but with the polyimide coating removed. This is more reliable than using the manufacturer's data on I.D., O.D. and thickness of the polyimide coating.

Sample injection

To evaluate the performance of the interface, 10-s long injections were made, which ideally should result in the formation of broad flat-topped peaks. This allows study of the vaporization process over an extended period of time.

Reagents

The mobile phases used were water, methanol, acetonitrile (HPLC-grade, Fischer) and mixtures thereof. Cholesterol, isoleucine, adenine and adenosine were obtained from Sigma (St. Louis, MO, U.S.A.). Epinephrine, naphthalene, acridine, nitropyrene, pyrene, and perylene were obtained from Aldrich (Milwaukee, WI, U.S.A.). The pesticides were obtained from the U.S. Environmental Protection Agency (EPA Pesticides & Industrial Chemicals Repository, Research Triangle Park, NC, U.S.A.).

RESULTS AND DISCUSSION

The purpose of this study was to investigate the effect of the three main parameters (orifice diameter, mobile phase velocity and temperature) on the performance of the capillary interface. The acquired knowledge can be used to optimize operating conditions and expand the limits of application to compounds of lower volatility.

Selection of test compounds

To avoid effects due to other influences, such as chemical ionization (CI) reagent gas, the experiments were done under EI conditions. To further eliminate effects due to molecular ion fragmentation, we selected naphthalene as a relatively volatile standard compound (mol.wt. = 128, b.p. = 218°C) and perylene as a standard compound of lower volatility (mol. wt. = 252, b.p. = 400°C) since these compounds do not fragment appreciably. Preliminary tests have indicated that perylene could be detected with acceptable peak shape only under optimum interface conditions[1]. Toluene was used as the internal standard since, under all testing conditions, it was easily vaporized and detected, resulting in ideal peak shapes.

Goodness of fit

For a variety of compounds the long injections resulted in badly spiking and tailing peaks. We devised a quantitative means to evaluate such peak shapes by comparing the peak shape of an easily vaporized compound with that of a compound of lower volatility. The compounds were coinjected. The degree of overlap gives an indication of the effectiveness of vaporization of that compound. The goodness of fit (GOF)[9] is direct measure of this degree of overlap. For the interface evaluation experiments, the GOF between the square topped peak from the internal standard (toluene) and the peak of the test compound (perylene or naphthalene) was calculated.

As the interface performance degrades, the amount of overlap decreases, which results in a larger number for the goodness of fit. A perfect peak will overlap entirely with the internal standard and have a GOF value equal to 1. The GOF is calculated as follows:

$$\text{GOF} = \sum_{S} \left| \frac{I_C}{A_C} - \frac{I_S}{A_S} \right|$$

Where S is the scan number, I_C is the intensity for the compound at that scan, A_C is the total area of the square topped peak, I_S is the intensity of the internal standard, and A_S is the area of the internal standard. The values of the GOF for several different peak shapes are shown in Fig. 1.

Absolute area and relative area

The absolute peak areas are calcuated for all three compounds. These peak areas indicate a high transfer efficiency for the interface. The relative areas are calculated for perylene and naphthalene with respect to toluene in order to closely examine the results due to differences in vaporization. All values are the average of five replicates.

Effect of orifice diameter

In this experiment seven different taper orifice diameters were evaluated: 1.5, 2.0, 3.0, 4.1, 4.9, 6.0 and 10 μm (no taper). Taper diameters smaller than 1.5 μm required mobile phase head pressures in excess of that which can safely be used with this OTLC

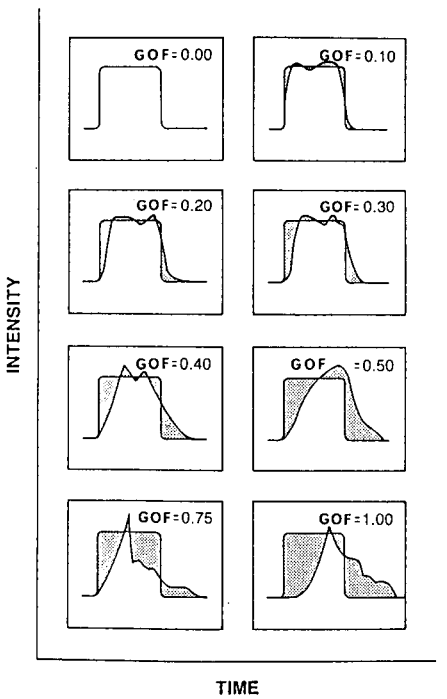

Fig. 1. Values for the GOF values calculated for increasingly degraded peak shapes.

system. The probe tip temperature for these experiments was 300°C, at which temperature a stable vapor-jet is formed resulting in constant source pressure, and the mobile phase linear velocity was held at 1 cm/s (a normal OTLC linear flow-rate for these diameters).

The effect of the orifice diameter on peak shape is shown in Fig. 2A. For the volatile compound, naphthalene, the effect is small, and little variation in the GOF as a function of diameter is observed. This is not the case for perylene for which peak shapes become unacceptable for taper diameters above 2 μm. At taper diameters of 4 μm and larger, perylene could not be detected.

The transfer efficiency as a function of orifice diameter and expressed by the absolute peak areas (Fig. 2B) is the highest at smaller diameters for both test compounds and the internal standard. It decreases and then becomes constant for naphthalene and toluene above 3 μm. For perylene no signal can be obtained at the larger diameters.

The difference in volatality between the two test compounds and the resulting effect of interface parameters is shown in Fig. 2C. The relative peak area for naphthalene does not change with orifice diameter, while the relative peak area for perylene drops rapidly to zero for orifice diameters of 3 μm or greater.

Effect of mobile phase velocity

The effects of mobile phase velocities from 0.25 to 3.4 cm/s have been evaluated at a probe tip temperature of 300°C and at a taper diameter of 1.5 μm (Fig. 3).

The effect of the mobile phase velocity on peak shape is shown in Fig. 3A. Even at low velocities the GOF indicates acceptable peak shapes, and the GOF remains relatively constant throughout the range of velocities evaluated.

Above a linear mobile phase velocity of 0.5 cm/s there is a significant increase in peak area as a function of mobile phase velocity (Fig. 3B), as would be expected due to the increase in the mass flux of the analyte. At lower velocities, however, there is very little increase in area as a function of eluent velocity. Apparently there is a critical minimum linear velocity required for the formation of a vapor jet which allows efficient introduction and detection of the analytes. The relative areas (Fig. 3C) show a decrease as a function of mobile phase velocity. This effect is more pronounced for perylene than for naphthalene.

Effect of temperature

Two processes can take place as a function of temperature: vaporization and thermal degradation. High probe tip temperatures are needed to vaporize compounds of lower volatility, but excessive temperatures can lead to thermal degradation of analytes. Ideally, the minimum probe tip temperature which satisfactory vaporizes analytes is the optimum probe tip temperature. This temperature, however, is compound dependent.

Naphthalene, for example, gives a peak shape that is chromatographically acceptable above 200°C, and the GOF remains constant at the good value of approximately 0.15 (Fig. 4A). Perylene, in constrast, requires temperatures above 275°C.

The effect of temperature on efficiency of vaporization (*i.e.* the absolute peak area) has also been examine (Fig. 4B). The absolute area for the volatile toluene and

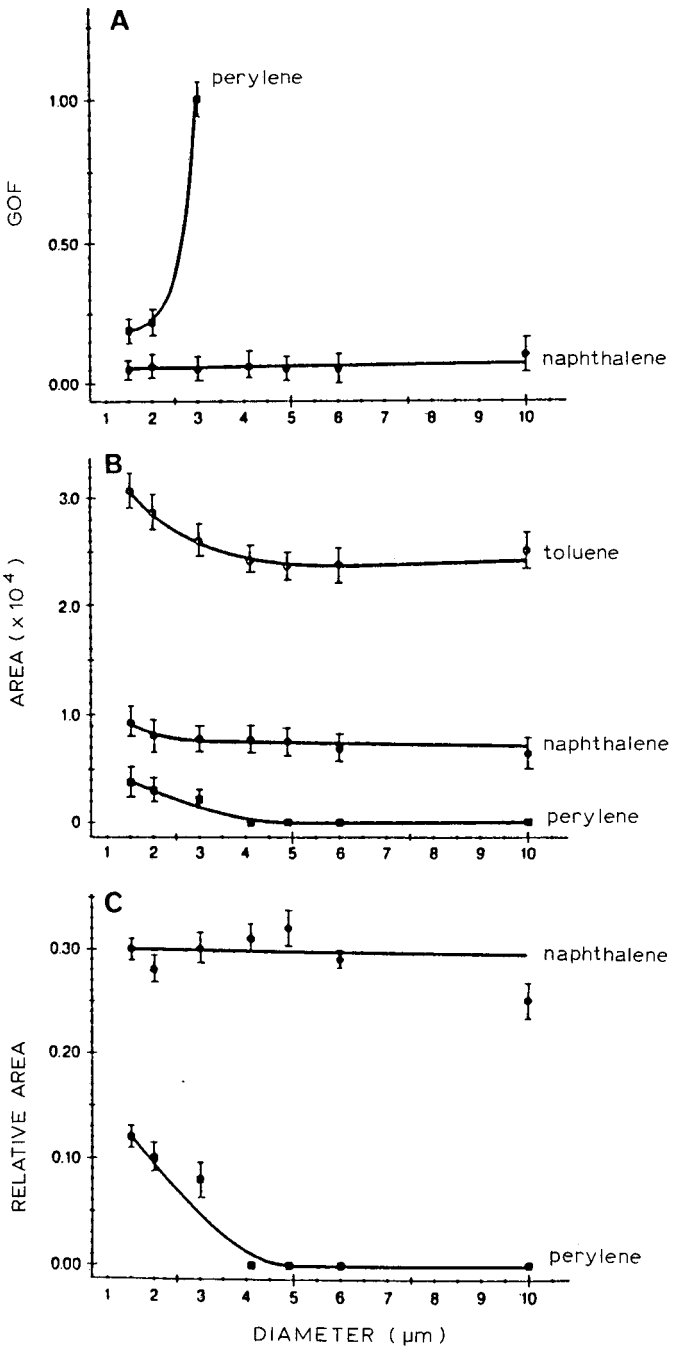

Fig. 2. Effect of the orifice diameter on interface performance.(A) Effect on GOF; (B) effect on absolute area; (C) effect on relative peak area.

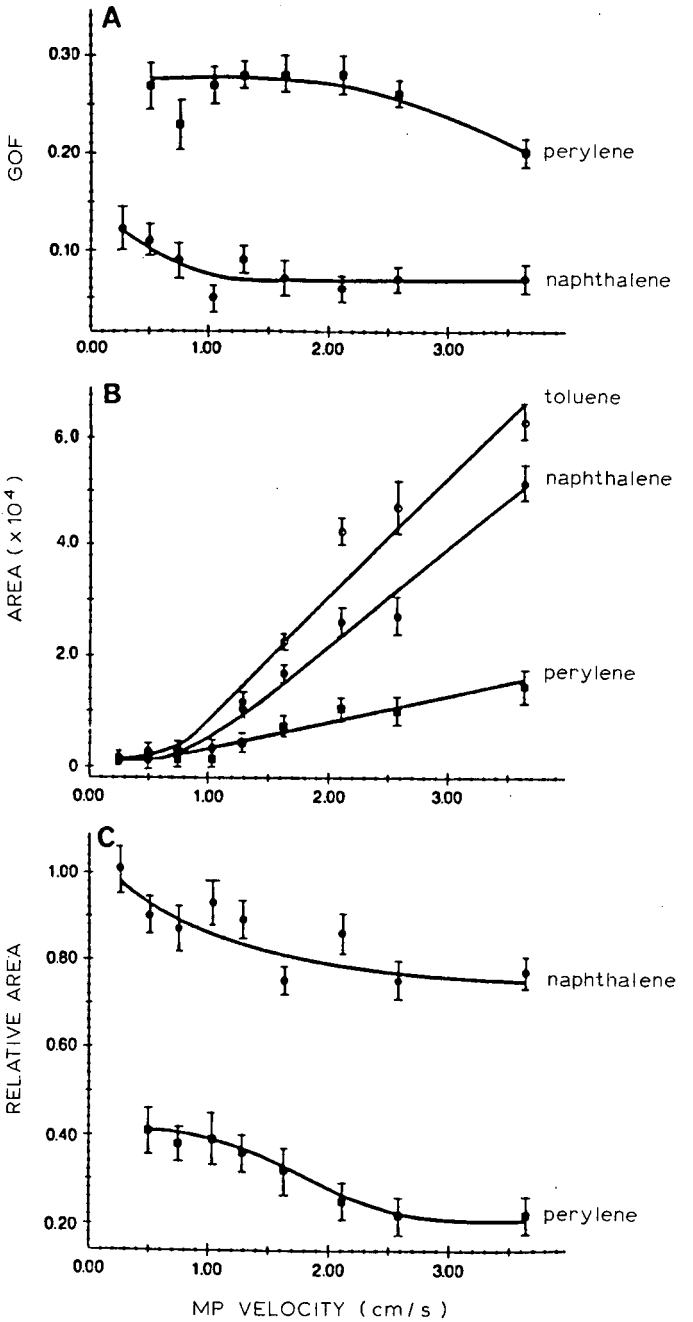

Fig. 3. Effect of mobile phase velocity on interface performance. (A) Effect on GOF; (B) effect on absolute area; (C) effect on relative peak area.

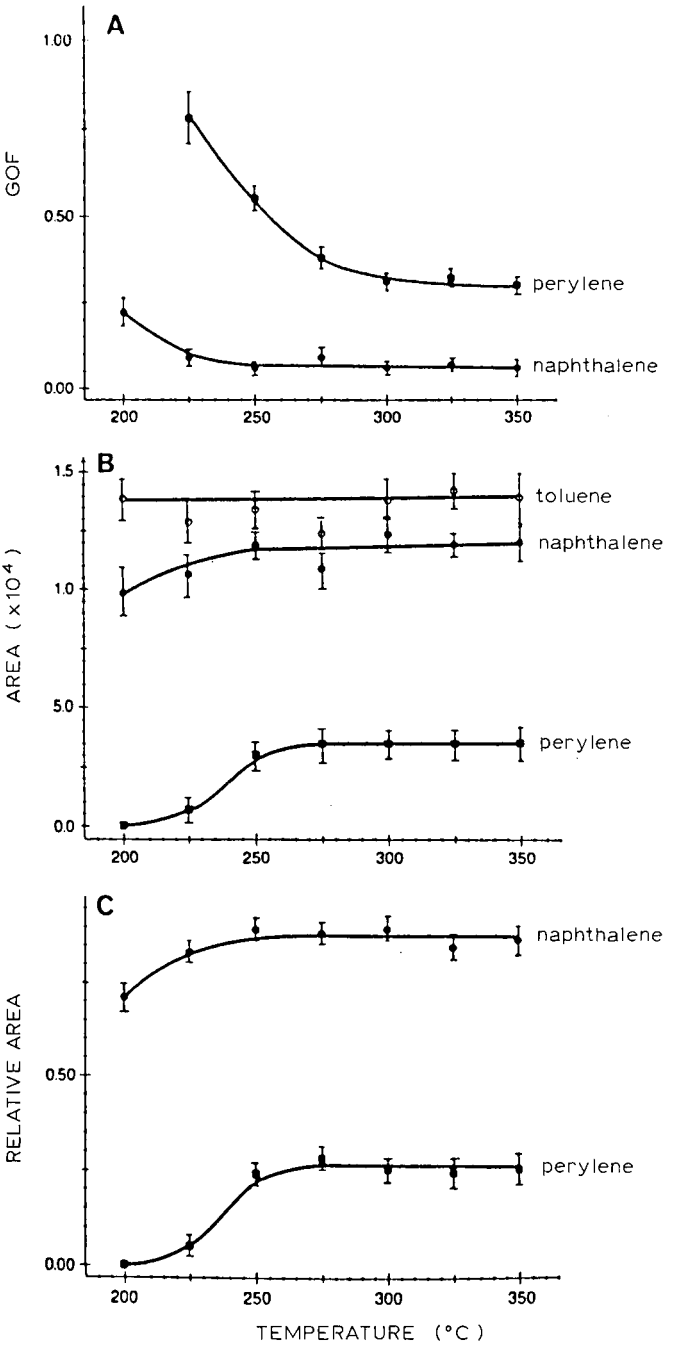

Fig. 4. Effect of probe tip temperature on interface performance. (A) Effect on GOF; (B) effect on absolute peak areas; (C) effect on relative peak areas.

naphthalene remain constant from 200 to 300°C. Perylene can not even be detected at 200°C, but the perylene peak area is constant from 250 to 350°C. The relative areas for both test compounds also remains constant above 250°C (Fig. 4C).

Thermal degradation

Cholesterol was used to examine the effect of probe tip temperature on thermal degradation. It is well known that cholesterol readily undergoes dehydration as a result of thermal degradation. A comparison was made between a mass spectrum obtained with a solid probe (Fig. 5A), under which conditions little thermal degradation takes place, a mass spectrum obtained from 100 ng by direct probe (Fig. 5B) (the lowest amount of analyte which gave a useful spectrum by direct probe on this system) and a mass spectrum obtained with the OTLC system from a 50-ng injection at a probe tip temperature of 325°C (Fig. 5C). More water loss (m/z 368) is observed under OTLC conditions. The remainder of the spectra compare well. The degree of thermal degradation was further studied by examining the relative intensities of $M^{+\cdot}$ ($m/z = 386$) and $[M-H_2O]^{+\cdot}$ ($m/z = 368$) as a function of probe tip temperature (Fig. 6). It is clear that the thermal degradation reached a maximum at 225°C and that the amount of degradation is limited. We can conclude that, although some thermal degradation of labile compounds can occur, it does not preclude their analysis.

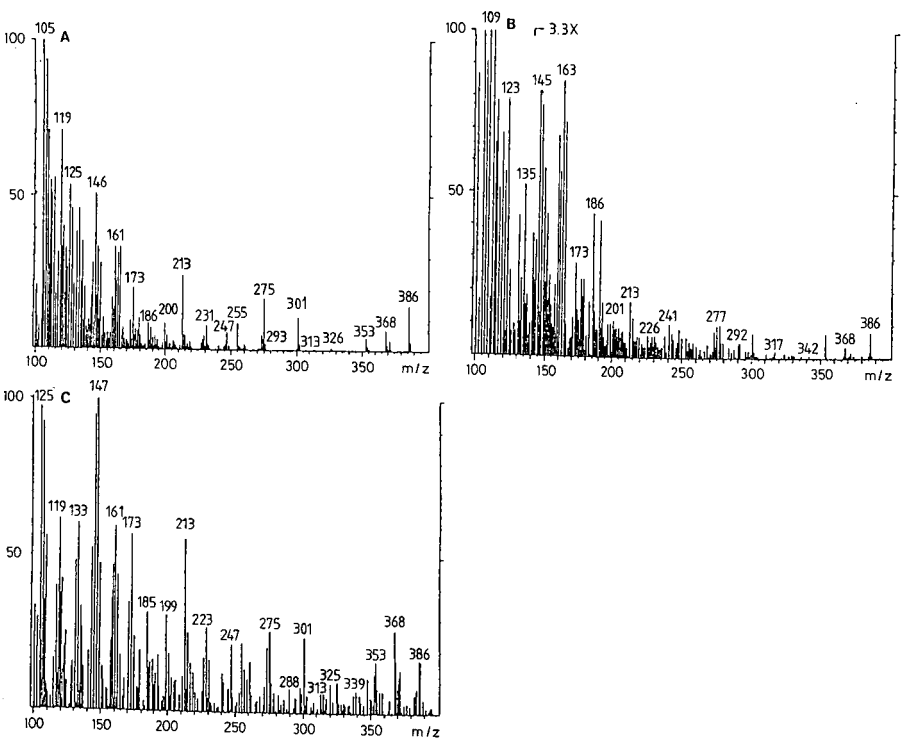

Fig. 5. (A) EI mass spectrum of cholesterol obtained on 100 μg with solid insertion probe. (B) EI mass spectrum of 100 ng of cholesterol obtained with solid insertion probe. (C) EI mass spectrum of cholesterol obtained on 50 ng by OTLC. Probe tip temperature was 325°C, solvent was methanol.

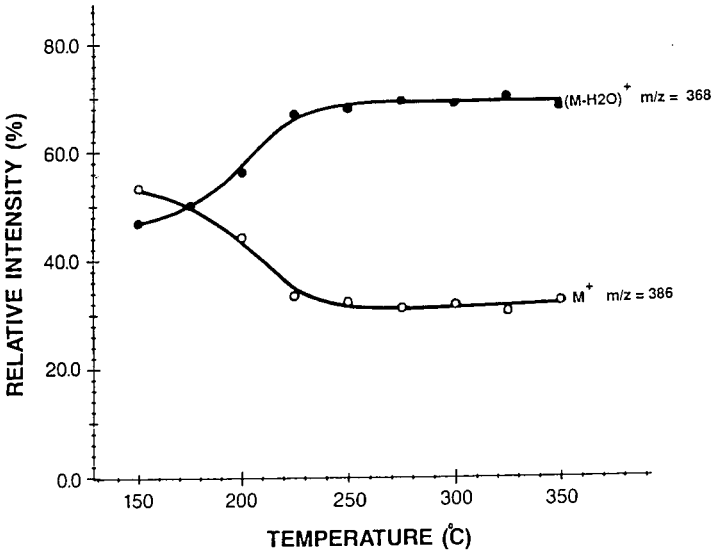

Fig. 6. Effect of probe tip temperature on loss of water in cholesterol. Relative intensity of parent ion ($m/z = 386$) (open circles) and $[M-18]^{+\cdot}$ ($m/z = 368$) (closed circles) as a function of probe tip temperature.

TABLE I

RANGE OF APPLICABILITY

Experimental conditions: probe tip temperature was 300°C; orifice diameter was 1.5 μm; mobile phase velocity was 1 cm/s. All data obtained with selected ion monitoring and EI ionization (except trifluralin, which was done under methane negative CI conditions).

Compounds	*Molecular weight*	*b.p. (°C)*	*MDQ**	*GOF*
Isoleucine	131	–	–**	–
Adenine	135	–	–	–
Adenosine	267	–	–	–
Epinephrine	183	–	1 ng	0.6
Benzene	78	80	10 pg	0.05
Naphthalene	128	218	10 pg	0.10
Anthracene	178	342	10 pg	0.10
Pyrene	202	404	10 pg	0.15
Perylene	252	400	20 pg	0.25
Nitropyrene	247	–	50 pg	0.10
Catechol	110	245	50 pg	0.15
Acridine	179	346	20 pg	0.10
Propazine	229	–	10 pg	0.15
Trifluralin	335	–	1 pg	0.15
Cholesterol	384	360	5 ng	0.4

* MDQ = minimum detectable quantity defined as a signal-to-noise ratio of 3:1 under selected ion monitoring.

** No mass spectral peaks observed.

A comparison of Fig. 5B and C indicates that the OTLC system provides approximately a ten-fold increase in sensitivity over the direct probe since the capillary injection can deliver a higher sample flow into the source than does the direct probe.

CONCLUSION

The parameters controlling the performance of this capillary interface for OTLC–MS have been systematically investigated. The importance of tapering and temperature had previously been demonstrated[1]. Without a tapered tip most compounds used with this interface could not be detected. For the OTLC system used in our laboratory, and orifice diameter of approximately 1.5 μm, mobile phase velocities above 0.25 cm/s, and temperatures around 300°C will give optimal operating conditions.

For the OTLC system we used, a 1.5-μm I.D. orifice diameter is a practical lower limit allowing safe helium head pressures, but the experiments show that smaller orifice diameters might give better results. With high pressure pumps these smaller diameters should not present a problem.

As is illustrated with the EI spectra of cholesterol, the thermal degradation introduced by the interface is limited. This is probably due to the short residence time of the compound at the hot column tip.

Since the interface requires vaporization of the analytes, its applicability is limited to non-polar to moderately polar compounds, with molecular weight below approximately 400 g/mol. This is demonstrated in Table I. The compounds examined were selected to cover a wide range of boiling points and polarities. While this limitation poses somewhat of a restriction on its utility, it should prove useful for the analysis of compounds such as pesticides[7].

A similar probe is being developed in our laboratory for use with a magnetic sector mass spectrometer. From results published by Alborn and Stenhagen[10] the high electrostatic fields may improve the performance of the interface ad increase its range of applicability.

REFERENCES

1 J. S. M. de Wit, C. E. Parker, K. B. Tomer and J. W. Jorgenson, *Anal. Chem.*, 59 (1987) 2400.
2 R. Tijssen, J. P. A. Bleumer, A. L. C. Smit, M. E. J. van Kreveld, *J. Chromatogr.*, 218 (1981) 137.
3 W. M. A. Niessen and H. Poppe, *J. Chromatogr.*, 323 (1985) 37.
4 W. M. A. Niessen and H. Poppe, *J. Chromatogr.*, 385 (1987) 1.
5 A. P. Bruins and B. F. H. Drenth, *J. Chromatogr.*, 271 (1983) 71.
6 J. P. Arpino, P. Krien, S. Vajta and G. Devant, *J. Chromatogr.*, 203 (1981) 117.
7 J. S. M. de Wit, C. E. Parker, J. W. Jorgenson and K. B. Tomer, *Biomed. Environ. Mass Spectrom.*, 17 (1988) 47.
8 B. H. Escoffier, C. E. Parker, J. S. M. de Wit, T. C. Mester and K. B. Tomer, *Proceedings of the 36th ASMS Conference on Mass Spectrometry and Allied Topics, San Francisco, CA, June 5–10, 1988*, p. 906.
9 H. Cramer, *Mathematical Methods of Statistics*, Princeton University Press, Princeton, NJ, 1971, Ch. 30.
10 H. Alborn and G. Stenhagen, *J. Chromatogr.*, 394 (1987) 35.

Journal of Chromatography, 462 (1989) 376–381
Elsevier Science Publishers B.V., Amsterdam — Printed in The Netherlands

CHROM. 21 002

Note

Modified column system for pyrolysis capillary gas chromatography

HUWEI LIU, RUONONG FU*, ZHENXI GUAN and LINXIANG TIAN
Department of Chemical Engineering, Beijing Institute of Technology, P.O. Box 327, Beijing (China)
(First received June 21st, 1988; revised manuscript received September 20th, 1988)

Pyrolysis–gas chromatography (PGC) is now universally accepted as a powerful method in organic and polymer analysis. In recent years, pyrolysis–capillary gas chromatography (PCGC), known as high-resolution PGC[1], has been used in a variety of applications[2,3] and was demonstrated to be more efficient than packed column PGC, and even IR and NMR spectroscopy in special cases. Nevertheless, when a pyrolyser is attached directly to a gas chromatograph, the vaporizer of the chromatograph forms a dead volume, which results in a loss of resolution. On the other hand, column contamination is a serious problem affecting the separating capacity in PCGC, because tarry components, which are produced to various extents by the pyrolysis of high polymers, and residues of the sample may enter the capillary column.

To overcome these problems, several modified interfaces and techniques have been studied[3–6]. Sugimura and Tsuge[4] used a glass tube with a splitter and precolumn, which protected the capillary column from contamination. However, the chromatographic vaporizer constituted a dead volume and, morever, an additional module was needed to control the precolumn temperature. In the pyrolysis system employed by Raynor *et al.*[5], the injection port, fitted with a precolumn glass frit insert, was still empty although it was loosely packed with silanized glass-wool to prevent non-volatile material from entering the capillary column. Whiton and Morgan[6] utilized a modified capillary inlet with small dead volume, but the column contamination was not eliminated and the vertical positioning of the probe precluded the use of a coil filament probe with a quartz sample tube. Another technique, reported by Liebman *et al.*[3], cannot be used with a glass capillary column, in addition to the column contamination problem.

In this work, a modified column system was designed and constructed for PCGC, involving a precolumn placed in the injection port of the gas chromatograph. The system was applied to different polymers.

EXPERIMENTAL

Materials

Polystyrene (PS), poly(vinyl chloride), (PVC), isotactic polypropylene (Iso-PP), poly(methyl methacrylate) (PMMA), methyl methacrylate–styrene copolymer (MS), acrylonitrile–styrene copolymer (AS), butadiene–styrene copolymer (BS), acrylo-

0021-9673/89/$03.50

nitrile–butadiene–styrene terpolymer (ABS) and methyl methacrylate–butadiene–styrene terpolymer (MBS) were used in the PCGC experiments. A mixture of isomers of mononitrotoluene (MNT), dinitrotoluene (DNT) and trinitrotoluene (TNT) was separated in conventional capillary GC experiments. The mixture was dissolved in toluene.

Instruments

A 150 Pyroprobe solid pyrolyser (Chemical Data Systems) was used consisting of a heated interface, a platinum coil probe and an electronic control module. The interface was connected to the chromatographic injection port via a thin stainless-steel tube. One end of this tube pierced the silicone-rubber septum and the other end was attached to the interface outlet by a tightly fitting septum and a nut. Fig. 1 is a schematic diagram of the pyrolysis system. All polymer samples were pyrolysed at 750°C for 20 s with the heating rate "off" and the interface temperature set at 250°C.

A GC-5A gas chromatograph (Shimadzu) with a flame ionization detector was employed. The instrument was equipped with a modified column system as indicated in Fig. 1. Its injection port was fitted with a stainless-steel precolumn, which was packed with 8.3% OV-101 on Celite (60–80 mesh). The temperature of the precolumn was controlled by use of the original controller of the gas chromatograph. Separations were performed on a 50 m × 0.28 mm I.D. glass capillary column coated with OV-101 by the static method[7]. In order to compare PCGC with packed column PGC, a 3 m × 4 mm I.D. stainless-steel column packed with 8.3% OV-101 on Celite (60–80 mesh) was also used in polymer pyrolysis. Nitrogen was used as the carrier gas; the GC conditions are given in the figure captions.

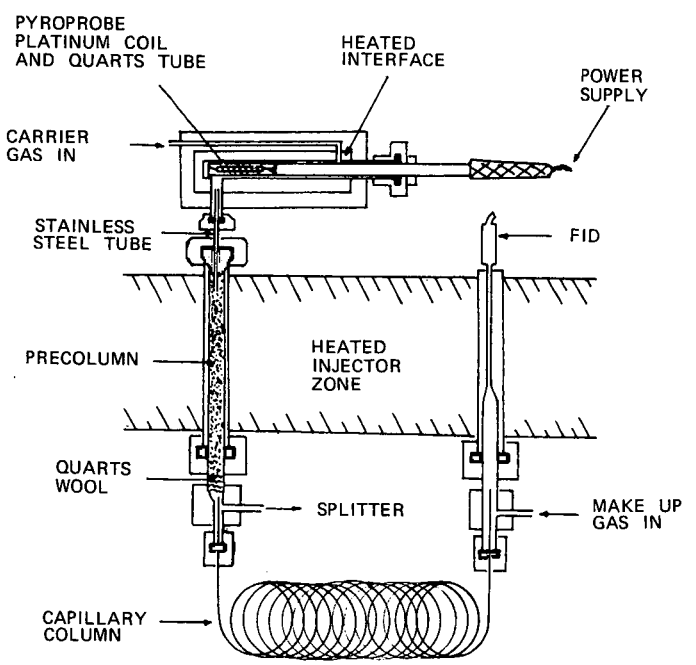

Fig. 1. Schematic diagram of the pyrolysis system.

When the precolumn was not packed and the pyrolyser was removed, the modified system was used for conventional capillary GC analysis, which was performed on a 16 m × 0.31 mm I.D. glass capillary column coated with cross-linked SE-54[8]. The experiments were performed under the following conditions: carrier gas, nitrogen at 25 ml/min; column temperature, programmed from 100°C (4 min) to 250°C at 4°C/min; splitting ratio, 40:1.

RESULTS AND DISCUSSION

Precolumn

It was reported[4] that a packed precolumn can prevent column contamination and improve the separation efficiency of the pyrolysis system. This was also demonstrated in these experiments. Some tarry substances were found in the precolumn after a period of operation and the separation efficiency of the system decreased. When the precolumn was repacked with fresh packing, the separation capacity increased again. If the precolumn temperature was properly set, the maximum molecular weight of pyrolysates eluted from the capillary column was controlled. The packing material should be renewed regularly, with the result that the precolumn can help to improve the separation power because the precolumn was packed with the same stationary phase as that in the glass capillary column.

Compared with the other techniques mentioned above, this modified system has additional advantages. First, it has a minimum dead volume because the precolumn is placed in the chromatographic vaporizer and it is commensurate with a short packed column. Second, it is simple and economic to construct because an additional module

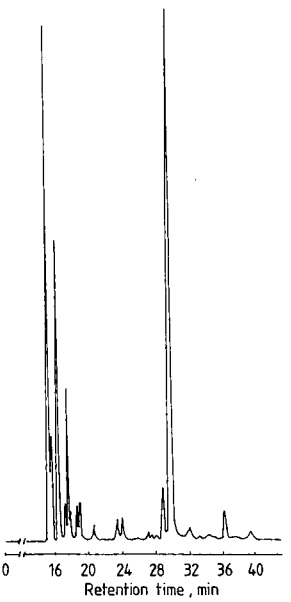

Fig. 2. Pyrogram of Iso-PP separated on a 50 m × 0.28 mm I.D. glass capillary column coated with OV-101. Experimental conditions: pyrolysis temperature, 750°C; pyrolysis interval, 20 s; heating rate, "off"; column temperature, 90°C; detection temperature, 250°C; carrier gas, nitrogen at 25 ml/min.

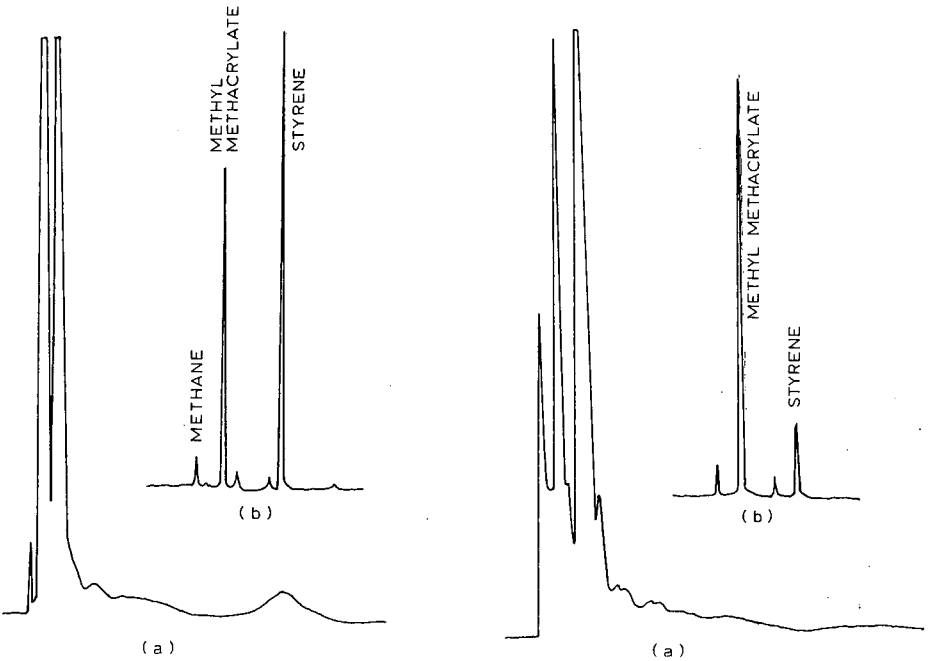

Fig. 3. Pyrograms of MS: separation on (a) the packed column and (b) the capillary column. Column temperature, 110°C; other conditions as in Fig. 2.

Fig. 4. Pyrograms of MBS: separation on a (a) the packed column and (b) the capillary column. Experimental conditions as in Fig. 3.

is not needed to control the precolumn temperature, this being controlled by the original controller of the injection port temperature. Finally, this system can also be used in ordinary capillary GC if the precolumn is not packed.

Separation capacity

The high efficiency of the PCGC system can be seen in Figs. 2–4, which show typical pyrograms of Iso-PP, MS and BMS, obtained under the conditions mentioned

TABLE I

REPRODUCIBILITY OF RETENTION TIMES OF PYROLYSATES OF MS

Experimental conditions as in Fig. 3; α = relative retention. The results were obtained by five repeated experiments.

Parameter	*Methane*		*Methyl methacrylate*		*Styrene*	
	t_R *(min)*	α	t_R *(min)*	α	t_R *(min)*	α
Mean retention	13.27	1.00	15.41	1.16	20.42	1.54
Standard deviation	0.0586	0.0000	0.0593	0.0045	0.0747	0.0084
Coefficient of variation (%)	0.4414	0.0000	0.3850	0.3855	0.3658	0.5413

TABLE II

QUANTITATIVE REPRODUCIBILITY OF PYROLYSIS OF PS

Experimental conditions as in Fig. 3; A = area percentage of chromatographic peak (normalization). The results were obtained by six repeated experiments.

Parameter	*Toluene*		*Styrene*		*Methylstyrene*	
	α	*A (%)*	α	*A (%)*	α	*A (%)*
Mean	0.82	1.7303	1.00	96.3060	1.24	0.8384
Standard deviation	0.0041	0.0567	0.0000	0.2695	0.0000	0.0573
Coefficient of variation (%)	0.5000	3.2769	0.0000	0.2798	0.0000	6.8380

above. It is obvious that the separation capacity of PCGC is much higher than that of packed column PGC at the same column temperature. These results show that the modified column system is applicable to the PCGC analysis of high polymers.

Reproducibility

The reproducibility of the modified system was measured. Table I shows the reproducibility of the retention times of the pyrolysates of MS. The standard deviation of relative retention is not greater than 1%. Table II illustrates the reproducibility of the quantitative analysis of PS.

From these results, it can be concluded that the quantitative reproducibility of the main pyrolysates can meet the needs of PCGC analysis. The yield of monomeric styrene was greater than 95%, and the coefficient of variation was very small although the standard deviation was slightly greater. Similar results were obtained for the other

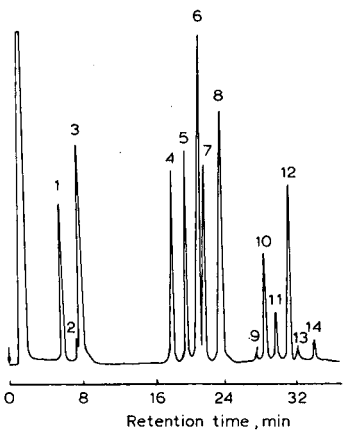

Fig. 5. Chromatogram of a mixture of the isomers of MNT, DNT and TNT separated on a 16 m × 0.31 mm I.D. glass capillary column coated with cross-linked SE-54. The column temperature was programmed from 100°C (4 min) to 250°C at 4°C/min. Detection temperature, 250°C; carrier gas, nitrogen at 25 ml/min; splitting ratio, 40:1. Peaks: 1 = *o*-MNT; 2 = *m*-MNT; 3 = *p*-MNT; 4 = 2,6-DNT; 5 = 2,5-DNT; 6 = 2,3-DNT + 2,4-DNT; 7 = 3,5-DNT; 8 = 3,4-DNT; 9 = 2,4,6-TNT; 10 = 2,3,6-TNT; 11 = 2,4,5-TNT; 12 = 2,3,5-TNT; 13 = 3,4,5-TNT; 14 = 2,3,4-TNT.

polymer samples. The reproducibility of the determination of the pyrolysates which were produced in low concentrations was not very good because of variations in the sample amounts and the power source. As for the modified system itself, the experimental reproducibility was satisfactory.

Applications

The modified system was successfully applied to the PCGC analysis of various polymers. It can also be used in conventional capillary GC analysis when the precolumn is not packed. In the previous capillary column system of the GC-5A chromatograph, there was a stainless-steel tube about 20 cm long between the injector and the capillary column and therefore the dead volume was high. However, in the modified system, the capillary column was directly linked with the vaporizer, and the empty precolumn corresponded to a lining in the injection port. As a result, the dead volume was greatly reduced and the separation efficiency was improved. Fig. 5 shows the chromatogram of a mixture of isomers of MNT, DNT and TNT, from which the high performance and thermal stability can be seen. Using a cross-linked glass capillary column, the baseline drift was only $1.8 \cdot 10^{-12}$ A when the column temperature was as high as 320°C. In this experiment, the splitting ratio was maintained essentially constant.

CONCLUSION

The modified column system can be used for both PCGC and conventional capillary GC analysis. The packed precolumn not only eliminates column contamination, but also reduces the dead volume and improves the separation efficiency of the pyrolysis system. The separation capacity and the experimental reproducibility are satisfactory. This system is simple to construct and easy to operate.

ACKNOWLEDGEMENT

The authors thank Mr. Zengyi Pang for help with the preparation of the modified system.

REFERENCES

1 S. Tsuge, *Bunseki Kagaku*, 35 (1986) 417–438.
2 S. A. Liebman and E. J. Levy, *Pyrolysis and GC in Polymer Analysis*, Marcel Dekker, New York and Basle, 1985.
3 S. A. Liebman, T. P. Wampier and E. J. Levy, *J. High Resolut. Chromatogr. Chromatogr. Commun.*, 7 (1984) 172–184.
4 Y. Sugimura and S. Tsuge, *Anal. Chem.*, 50 (1978) 1968–1972.
5 M. W. Raynor, R. M. Waring and L. L. Davies, *J. Chromatogr. Sci.*, 25 (1987) 104–111.
6 R. S. Whiton and S. L. Morgan, *Anal. Chem.*, 57 (1985) 778–780.
7 Z.-X. Guan, F.-M. Xia and R.-N. Fu, in *Proceedings of the 6th National Conference on Chromatography, October 5–9, 1987*, Chinese Chemical Society, Shanghai, 1987, pp. 130–131.
8 R.-N. Fu, L.-X. Tian, Z.-X. Guan and H.-W. Liu, *Chin. J. Chromatogr.*, 5 (1987) 203–207.

Journal of Chromatography, 462 (1989) 382–386
Elsevier Science Publishers B.V., Amsterdam — Printed in The Netherlands

CHROM. 21 000

Note

(*R*)-N-(3,5-Dinitrobenzoyl)-1-naphthylglycine as a chiral stationary phase for the separation of enantiomers by high-performance liquid chromatography

NAOBUMI ÔI*, HAJIMU KITAHARA, YONEZO MATSUMOTO, HISAKO NAKAJIMA and YASUHIKO HORIKAWA

Sumika Chemical Analysis Service, Ltd., 3-1-135 Kasugade-naka, Konohana-ku, Osaka 554 (Japan)

(First received July 18th, 1988; revised manuscript received September 20th, 1988)

In 1981 Pirkle and Finn[1] developed the chiral stationary phase I, consisting of (*R*)-N-(3,5-dinitrobenzoyl)phenylglycine ionically bonded to γ-aminopropyl silanized silica, which offers superior performance for the separation of arylalkylcarbinols by high-performance liquid chromatography (HPLC). Soon it was clear that this phase can also separate enantiomers of various compounds[2]. This phase contains a dinitrobenzoyl group, which acts as a π-acceptor, and it was found that the combination of the π–π donor–acceptor interaction with diastereomeric hydrogen bonding is very effective for chiral recognition.

On the other hand, we have developed some π-donor type chiral phases consisting of (*S*)- or (*R*)-1-(α-naphthyl)ethylamine and showed that the naphthyl group attached to the asymmetric carbon atom plays effective role in chiral recognition[3–5].

In this work, we prepared a chiral stationary phase II consisting of (*R*)-N-(3,5-dinitrobenzoyl)-1-naphthylglycine ionically bonded to γ-aminopropyl silanized silica, which contains both a dinitrobenzoyl group and a naphthyl group attached to an asymmetric carbon atom, and its chromatographic properties were investigated.

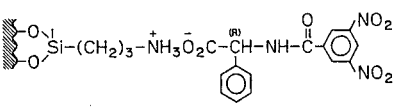

[I]

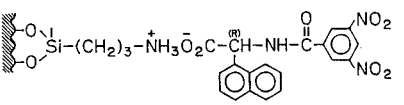

[II]

EXPERIMENTAL

Preparation of stationary phase II

(*R,S*)-1-Naphthylglycine methyl ester was synthesized from 1-naphthylaceto-

0021-9673/89/$03.50

nitrile (Wako, Osaka, Japan) according to the procedure described by Baumgarten *et al.*[6]. (*R,S*)-N-(3,5-Dinitrobenzoyl)-1-naphthylglycine methyl ester was prepared from (*R,S*)-1-naphthylglycine methyl ester by reaction with 3,5-dinitrobenzoyl chloride in dry tetrahydrofuran at room temperature. (*R,S*)-N-(3,5-Dinitrobenzoyl)-1-naphthylglycine was isolated by the subsequent acid hydrolysis of (*R,S*)-N-(3,5-dinitrobenzoyl)-1-naphthylglycine methyl ester. (*R*)-N-(3,5-Dinitrobenzoyl)-1-naphthylglycine (m.p. 138.3°C) was obtained from the racemic compound by HPLC separation with a SUMIPAX OA-4000 chiral column (250 × 8 mm I.D.) (Sumitomo Chemical, Osaka, Japan). Elemental analysis: calculated for $C_{19}H_{13}N_3O_7$, C 57.73, H 3.31, N 10.63; found, C 56.81, H 3.71, N 10.18%. NMR (acetone-d_6): δ 6.58 (d, 1H), 7.40–8.30 (m, 8H), 9.00–9.14 (m, 3H). IR (potassium bromide): 3400–3080, 1725 (vs), 1650 (vs), 1530 (vs), 1340 (vs), 1180, 1075, 915, 780, 720 cm^{-1}. High-resolution mass spectrum: calculated for $C_{19}H_{13}N_3O_7$, 395.0752; found, 395.0728. Treatment of γ-aminopropyl silanized silica (LiChrosorb NH_2, 5 μm; E. Merck, Darmstadt, F.R.G.) with (*R*)-N-(3,5-dinitrobenzoyl)-1-naphthylglycine affords ionically bonded chiral stationary phase II.

Liquid chromatography

The experiments were carried out using a Shimadzu LC-5A high-performance liquid chromatograph equipped with a UVD-2 ultraviolet detector (254 nm). A stainless-steel column (250 × 4 mm I.D.) was slurry packed with stationary phase II using a conventional technique. The column packed with stationary phase I was represented by SUMIPAX OA-2000I (250 × 4 mm I.D.) (Sumitomo Chemical). The chromatographic conditions are given in Table I. The solutes and solvents were of analytical-reagent grade. Some compounds were provided by Sumitomo Chemical. The structures of the components used are shown in Fig. 1.

S-3308

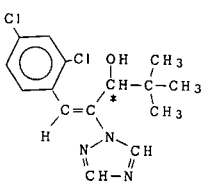

S-3307

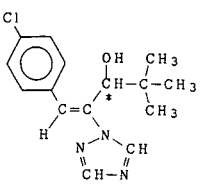

Fenpropathrin

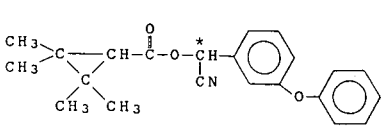

Terallethrin

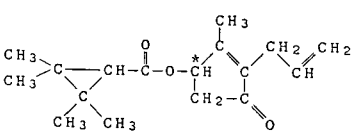

Fig. 1. Structures of compounds used (see Table I).

TABLE I

HPLC SEPARATION OF ENANTIOMERS ON CHIRAL STATIONARY PHASES

The separation factor of the enantiomers, α, is the ratio of the capacity factors; k'_1 is the capacity factor for the initially eluted enantiomer. Mobile phase: (A) hexane–ethanol (300:1); (B) hexane–1,2-dichloroethane–ethanol (400:40:1); (C) hexane–1,2-dichloroethane–ethanol (100:20:1); (D) hexane–1,2-dichloroethane–ethanol (500:20:0.1); (E) hexane–1,2-dichloroethane–ethanol (500:30:0.15); (F) hexane–1,2-dichloroethane–ethanol (500:15:1); (G) hexane–ethanol (100:1). A flow-rate of 1.0 ml/min was used for the 250 × 4 mm I.D. column at room temperature.

Compound	*Phase I*				*Phase II*			
	α	k'_1	*First eluted enantiomer*	*Mobile phase*	α	k'_1	*First eluted enantiomer*	*Mobile phase*
1-Phenylethanol	1.03	6.59	(−)-	A	1.06	6.10	(−)-	A
1-(α-Naphthyl)ethanol	1.03	8.28	(−)-	B	1.10	8.80	(−)-	B
Benzoin	1.04	3.10	(+)-	C	1.12	3.01	(+)-	C
S-3308*	1.00	4.56		C	1.14	3.87	(*R*)-	C
S-3307*	1.00	5.57		C	1.09	5.75	(*R*)-	C
Fenpropathrin*	1.04	5.66	(*R*)-	D	1.09	5.98	(*R*)-	D
Terallethrin*	1.00	7.39		E	1.13	9.68	(+)-	E
1-Phenylethylamine**	1.13	4.26	(+)-	F	1.41	3.81	(+)-	F
2-(4-Chlorophenyl)isovaleric acid***	1.04	4.50	(+)	G	1.30	3.88	(+)-	G

* Structures as in Fig. 1.
** Resolved as N-acetyl derivative.
*** Resolved as isopropylamide derivative.

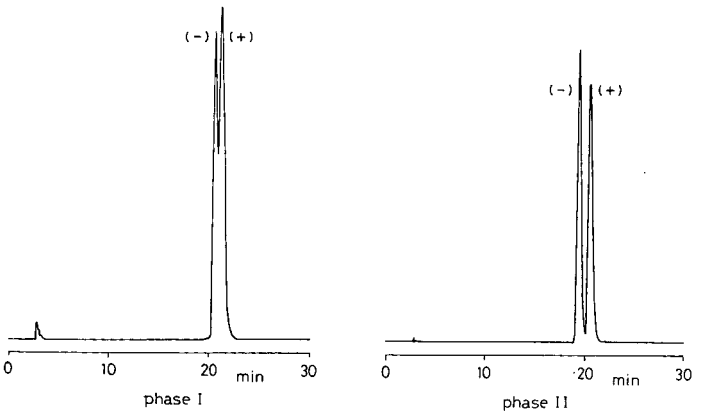

Fig. 2. Separation of the enantiomers of racemic 1-phenylethanol on chiral stationary phases I and II. Chromatographic conditions as in Table I.

RESULTS AND DISCUSSION

The chiral stationary phase II is a modification of phase I. In order to investigate the effect of the replacement of the phenyl group in phase I by a 1-naphthyl group, the retention and enantioselectivity of several racemates were measured under identical conditions on both chiral phases. The results of these measurements are given in Table I.

The capacity factors for these solutes do not differ greatly, but the enantioselectivity differs significantly on the two phases. All of the racemates in Table I show larger α values on phase II than on phase I. It is emphasized that phase II can resolve well some alcohol and ester racemates that can hardly be resolved in phase I. Typical chromatograms are shown in Figs. 2 and 3. These results clearly show that the

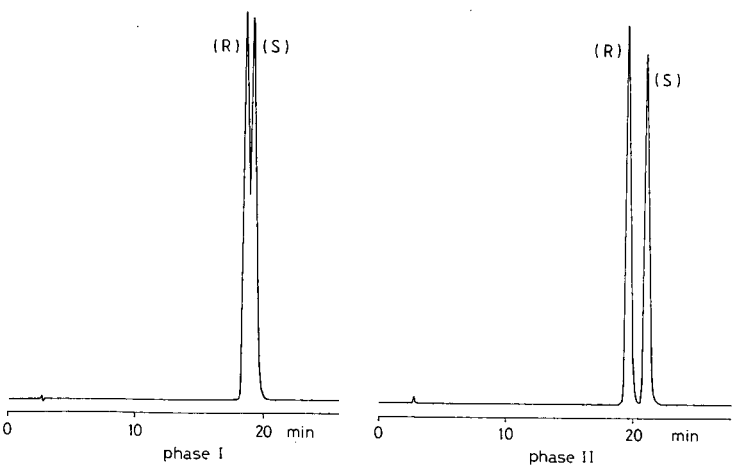

Fig. 3. Separation of the enantiomers of racemic fenpropathrin on chiral stationary phases I and II. Chromatographic conditions as in Table I.

naphthyl group in phase II plays a much more effective role in chiral recognition than the phenyl group in phase I.

The enantiomeric solution orders of these solutes, including aromatic alcohols, esters and amides, are identical on phase I and II. This result suggests but does not prove that a similar chiral recognition mechanism is operating on both phases. Various interactions, such as hydrogen bonding, π–π donor–acceptor interactions, dipole–dipole stacking and Van der Waals interactions seem to contribute for to the enantiomer separation, as demonstrated by many workers[7].

Prikle's original stationary phase I is very well known and widely used, and the modified chiral stationary phase II, which has excellent enantioselectivity, is very promising for the separation of enantiomers of a wide range of classes of compounds.

REFERENCES

1 W. H. Pirkle and J. M. Finn, *J. Org. Chem.*, 46 (1981) 2935.
2 W. H. Pirkle, J. M. Finn, J. L. Schreiner and B. C. Hamper, *J. Am. Chem. Soc.*, 103 (1981) 3964.
3 N. Ôi, M. Nagase and T. Doi, *J. Chromatogr.*, 257 (1983) 111.
4 N. Ôi and H. Kitahara, *J. Liq. Chromatogr.*, 9 (1986) 511.
5 N. Ôi, H. Kitahara and R. Ôsumi, *Nippon Kagaku Kaishi*, (1986) 999.
6 H. E. Baumgarten, J. E. Dirks, J. M. Petersen and R. L. Zey, *J. Org. Chem.*, 31 (1966) 3708.
7 R. R. Brügger, A. R. Marti, V. R. Meyer and H. Arm, *J. Chromatogr.*, 440 (1988) 197.

Journal of Chromatography, 462 (1989) 387–391
Elsevier Science Publishers B.V., Amsterdam — Printed in The Netherlands

CHROM. 21 009

Note

Comparison of capillary gas chromatography with ^{1}H and ^{13}C nuclear magnetic resonance spectroscopy for the quantitation of pyrrolizidine alkaloids from *Senecio vernalis*

L. A. PIETERS*

Department of Pharmaceutical Sciences, University of Antwerp (UIA), Universiteitsplein 1, B-2610 Antwerp (Belgium)

T. HARTMANN

Institut für Pharmazeutische Biologie der Technischen Universität Braunschweig, Mendelssohnstrasse 1, D-3300 Braunschweig (F.R.G.)

and

J. JANSSENS and A. J. VLIETINCK

Department of Pharmaceutical Sciences, University of Antwerp (UIA), Universiteitsplein 1, B-2610 Antwerp (Belgium)

(First received May 11th, 1988; revised manuscript received September 27th, 1988)

Plants that contain hepatotoxic pyrrolizidine alkaloids occur all over the world. The pyrrolizidines may be of greater importance as a cause of human disease than the presently known outbreaks of poisoning would indicate. Poisoning in man can occur by the use of pyrrolizidine-containing plants as medicinal herbs, or by accidental contamination of food by such plants[1–3]. Therefore reliable and accurate methods for the quantitation of pyrrolizidine alkaloids are necessary. A titrimetric procedure[4] and a spectrophotometric method based on a colour reaction[5,6] have been described for the estimation of the total pyrrolizidine alkaloid level in biological samples. In recent years these methods have been replaced in many cases by quantitative ^{1}H nuclear magnetic resonance (NMR) spectroscopy[7–10]. Several analytical techniques have been described for the determination of individual pyrrolizidines in mixtures, including relative densitometric estimations, which are not generally applicable because the differences in R_F values may be quite small[4,11], high-performance liquid chromatography (HPLC)[12] and, more recently, quantitative ^{13}C NMR spectroscopy[9,10,13]. In this work, ^{1}H NMR was compared with gas chromatography (GC) for the determination of the total pyrrolizidine alkaloid level, and for the quantitative analysis of the individual pyrrolizidines ^{13}C NMR was compared with GC. *Senecio vernalis* Waldst. & Kit. (Asteraceae) was chosen as the pyrrolizidine-containing plant. The pyrrolizidine alkaloids seneciphylline, senecionine, integerrimine, retrorsine, senecivernine and senkirkine have been reported as constituents of *Senecio vernalis*[14–16]. With the exception of senkirkine, they are synthesized and accumulated as N-oxides[16,17]. In this study the alkaloid N-oxides were reduced during sample preparation to give the respective tertiary alkaloids.

0021-9673/89/$03.50

EXPERIMENTAL

A voucher specimen of *Senecio vernalis* Waldst. & Kit. is kept at the Institut für Pharmazeutische Biologie, Braunschweig. Samples were prepared from freeze-dried flower heads of *Senecio vernalis* according to a known procedure[8].

^1H and ^{13}C NMR

A Jeol FX 200 Fourier transform (FT) NMR system, exhibiting standard resonance frequencies of 199.50 MHz for ^1H and 50.10 MHz for ^{13}C, was used. Samples were dissolved in [^2H] chloroform (99.8%). Chemical shift values are reported on the δ scale, relative to tetramethylsilane. ^1H and ^{13}C NMR recording conditions for quantitative measurements were selected[8,10,13]. To perform quantitative ^1H NMR experiments, a precisely weighed amount of *p*-dinitrobenzene was added to the sample as an internal standard.

Gas chromatography–mass spectroscopy (GC–MS)

All GC–MS analyses were performed on an Hewlett-Packard 5890 A GC-5970 B quadrupole mass spectrometer, equipped with an Hewlett-Packard 12 m × 0.203 mm cross-linked methyl silicone fused-silica capillary column and a split/splitless injection system, used in the split mode (20:1). The initial oven temperature was 150°C, and programmed to 275°C at 10°C/min (2-min solvent wait, isothermal). Helium was used as the carrier gas at a flow-rate of 1 ml/min. The column was inserted directly into the mass spectrometer. Data acquisition and reprocessing were carried out on an Hewlett-Packard 9816 Workstation with a 15 MB Winchester disc. Electron impact (EI) (70 eV) mass spectra were recorded, scanning continuously from *m/z* 50 to 500. Retention times: senecivernine, 12.3 min (*m/z* 335, $[M]^+$); senecionine, 12.4 min (*m/z* 335, $[M]^+$); seneciphylline, 12.6 min (*m/z* 333, $[M]^+$); integerrimine, 12.9 min (*m/z* 365, $[M]^+$); retrorsine, 14.3 min (*m/z* 351, $[M]^+$).

Quantitative analysis by capillary GC

The mixture of tertiary alkaloids prepared according to ref. 8 was dissolved in methanol and was separated and evalutated quantitatively on wall-coated open tubular fused-silica columns (15 m × 0.25 mm; DB-1, J & W Scientific). Conditions: injector, 250°C; temperature programme, 120–290°C, 6°C/min; splitting ratio 1:50; injection volume 1–2 μl; carrier gas, helium 0.7 bar; detectors, flame ionization detector, nitrogen selective detector. Senecionine or monocrotaline, obtained from Aldrich, was used as the external standard. The retention indices of the individual alkaloids are given in ref. 17.

RESULTS AND DISCUSSION

The ^1H NMR spectrum of a mixture of pyrrolizidine alkaloids from *Senecio vernalis* is very complex, and contains many overlappling signals. The vinylic C-2 hydrogen of macrocyclic diester pyrrolizidines, such as the alkaloids from *Senecio vernalis*, always resonates at 6.2 ppm. A known amount of *p*-dinitrobenzene is added to the sample as an internal standard, and the total pyrrolizidine alkaloid level is calculated by comparing the integration value of this signal, occurring at 8.43 ppm,

with the integration value of the signal at 6.2 ppm. The pyrrolizidine alkaloid content was calculated as senecionine (molecular weight 335), which appeared to be the principal alkaloid in our samples. The molecular weight of senecivernine and integerrimine are also 335. Because of the complexity of the ^{1}H NMR spectrum, it is not possible to estimate the individual alkaloids[7,8].

^{13}C NMR spectroscopy was used for the quantitation of the individual pyrrolizidine alkaloids. ^{13}C NMR spectral data for all the pyrrolizidines from *Senecio vernalis* have already been published[10,14]. The ^{13}C NMR signals of pyrrolizidine alkaloids are very sensitive to structural variation in both the diester moiety and the heterocyclic ring system. The usefulness of ^{13}C Fourier transform NMR as an analytical technique stems from the potentially direct relationship between the area under a NMR peak and the number of nuclei that give rise to the signal. Unfortunately, extracting the desired quantitative information from a ^{13}C NMR spectrum is hampered by several experimental and instrumental limitations, which have been discussed[10,13]. In addition, only carbon atoms having a relatively short spin–latice relaxation time, T_1, can be used. A list of ^{13}C resonance signals that are well resolved, that are specific for one individual alkaloid or for the total alkaloid content and that have a $T_1 < 1.5$ s is given in Table I. Because the minimal pulse delay for quantitative measurements using ^{13}C NMR is 6.5 T_1, a T_1 of 1.5 s corresponds to a pulse delay of 10 s, which is still an acceptable value for long accumulations.

Some specific and well resolved resonance signals, *e.g.*, the C-8 carbonyl signal of senkirkine, cannot be used for quantitative ^{13}C NMR measurements because their relaxation is very slow. More information about these relaxation times and related problems can be found in refs. 9, 10 and 13. By integrating the resonance signals listed in Table I, it is possible to obtain an integration value for each individual alkaloid and for the total alkaloid content.

TABLE I

SOME CHARACTERISTIC ^{13}C NMR SIGNALS USEFUL FOR THE QUANTITATIVE ANALYSIS OF MIXTURES OF PYRROLIZIDINE ALKALOIDS FROM *SENECIO VERNALIS*

*Carbon No.**	*Signal (ppm)*	*Alkaloid*
20	120.3	Senecivernine
19	113.9	Seneciphylline
9	63.7	Senkirkine
3	58.3	Senkirkine
5	52.7–52.9	Total
13	39.3	Integerrimine
14	37.4	Senkirkine
6	36.0	Senkirkine
6	33.5	Integerrimine
14	29.4	Integerrimine
18	25.9	Senecivernine
18	25.0	Integerrimine
9	11.6	Integerrimine
19	10.8	Senecionine
19	5.4	Senecivernine

* Numbering of the carbon atoms of the pyrrolizidine alkaloids (senecane structure) according to ref. 18.

TABLE II

QUANTITATIVE EVALUATION OF THE ALKALOID CONTENT AND PATTERN OF *S. VERNALIS* BY ^{1}H AND ^{13}C NMR IN COMPARISON TO CAPILLARY GC

Total alkaloid level (%, dry weight)			*Individual alkaloids (%)*	
^{1}H NMR	*GC*		*^{13}C NMR*	*GC*
0.54	0.54	Senecionine	38.0	44.0
		Integerrimine	6.2	5.9
		Senecivernine	33.3	28.2
		Senkirkine	10.6	11.3
		Seneciphylline	9.6	10.6
		Retrorsine	2.3	Traces

In order to obtain quantitative results, the same procedure as for *Senecio vulgaris* and *Senecio jacobaea*[9,10,13], was used. The results of the quantitative ^{1}H and ^{13}C NMR analyses were compared with those obtained with GC (Table II). The results for the total alkaloid level are in good agreement with each other. Both methods produce reliable results, but the sensitivity of GC is higher. As far as the individual alkaloids are concerned, there is a difference for senecionine and senecivernine. This may be due to the fact that their retention times hardly differ, and that the signals may not be completely resolved. There is a good agreement for the sum of the results for senecionine and senecivernine. The results for the other alkaloids are in good agreement with each other.

It appears that the two methods are equivalent for the quantitative analysis of mixtures of pyrrolizidine alkaloids. Some characteristics of GC and quantitative ^{13}C NMR are summarized in Table III. The main disadvantage of ^{13}C NMR when compared with GC is that the sensitivity is rather low. The minimum sample size for ^{13}C NMR is about 10 mg, and a long accumulation time is necessary. A quantitative GC analysis is less time-consuming, but care must be taken that no overlapping of

TABLE III

COMPARISON OF GC AND ^{13}C NMR FOR THE QUANTITATION OF PYRROLIZIDINE ALKALOIDS

Characteristic	*GC*	*^{13}C NMR*
Reliability	Good	Good
Precision	Good	Good
Sensitivity	High	Low
Interferences (impurities)	Good	Good
Manipulation time	Short	Short
Blocking of apparatus	Slight	Important
Adaption to other assays	Easy	Easy
Apparatus cost price	High	High
Reagent cost price	Low	High
Personnel qualifications	Normal	High

peaks occurs. In order to perform a quantitative ^{13}C NMR experiment, it is essential that the ^{13}C NMR spectral data and the most important relaxation times of all the components of the mixture are known.

The detection and identification of an unexpected or new alkaloid in a mixture by ^{1}H and ^{13}C NMR may be rather difficult, in particular if it is only a minor component. If all the signals are completely resolved, a GC–MS experiment would show a new peak providing additional information (retention time, mass spectral data) for identification purposes. The same techniques can also be applied for other plants containing pyrrolizidine alkaloids.

ACKNOWLEDGEMENT

L.A.P. is a senior research assistent of the National Fund for Scientific Research (Belgium).

REFERENCES

1 L. W. Smith, C. C. J. Culvenor, *J. Natl. Prod.*, 44 (1981) 129.
2 R. J. Huxtable, *Trends Pharmacol. Sci.*, 1 (1980) 299.
3 R. J. Huxtable, *Perspect. Biol. Med.*, 24 (1980) 1.
4 L. B. Bull, C. C. J. Culvenor and A. T. Dick, *The Pyrrolizidine Alkaloids*, North-Holland, Amsterdam, 1968.
5 A. R. Mattocks, *Anal. Chem.*, 39 (1967) 443.
6 A. R. Mattocks, *Anal. Chem.*, 40 (1968) 1749.
7 R. J. Molyneux, A. E. Johnson, J. N. Roitman and M. E. Benson, *J. Agric. Food Chem.*, 27 (1979) 494.
8 L. A. Pieters and A. J. Vlietinck, *Fresenius' Z. Anal. Chem.*, 321 (1985) 355.
9 L. A. Pieters, A. Van Zoelen, K. Vrieling and A. J. Vlietinck, *J. Natl. Prod.*, (1988) submitted for publication.
10 L. A. Pieters, *Ph. D. Thesis*, University of Antwerp (UIA), Antwerp, 1988.
11 H. J. Huizing, *Ph. D. Thesis*, State University of Groningen, Groningen, 1985.
12 L. A. Pieters and A. J. Vlietinck, *J. Liq. Chromatogr.*, 9 (1986) 745.
13 L. A. Pieters and A. J. Vlietinck, *Magn. Reson. Chem.*, 25 (1987) 8.
14 T. Hartmann and M. Zimmer, *J. Plant Physiol.*, 122 (1986) 67.
15 H. Wiedenfeld, U. Pastewka, P. Stengl and E. Röder, *Planta Med.*, 41 (1981) 124.
16 E. Röder, H. Wiedenfeld and U. Pastewka, *Planta Med.*, 37 (1979) 131.
17 G. Toppel, L. Witte, B. Riebesehl, K. v. Borstel and T. Hartmann, *Plant Cell Rep.*, 6 (1987) 466.
18 A. J. Jones, C. C. J. Culvenor and L. W. Smith, *Aust. J. Chem.*, 35 (1982) 1173.

Journal of Chromatography, 462 (1989) 392–397
Elsevier Science Publishers B.V., Amsterdam — Printed in The Netherlands

CHROM. 21 043

Note

Gas chromatographic determination of phenols in waste water–oil emulsions

M. M. KOPEČNI*, M.V. TARANA, S. D. ČUPIĆ and J. J. ČOMOR
Chemical Dynamics Laboratory, Boris Kidrič Institute of Nuclear Sciences, P.O. Box 522, 11001 Belgrade (Yugoslavia)
(First received May 16th, 1988; revised manuscript received August 27th, 1988)

Phenols are common pollutants in wastes arising from the petrochemical industry or any other industry involving large amounts of kerosene[1], oil, naphtha or coal. Based on many years' experience in this Laboratory, it has been observed that the concentration of phenols in some of the samples coming from such industries exceeds by several orders of magnitude the permitted level for liquid wastes.

A standard procedure[2] for the determination of phenols involves steam distillation, extraction of the distillate with chloroform and spectrophotometric determination. The method is suitable for volatile phenols, *i.e.*, phenol, cresols, xylenes, guaiacol, thymol and some chloro derivatives. Some of the phenols, however, particularly nitro-substituted[3] derivatives, cannot be recovered by steam distillation. In addition, phenols with *para* substituents do not give a colour reaction with the 4-aminoantipyrine reagent used in spectrophotometric determination. As a consequence, the results of such a determination might be low.

Incineration is the usual procedure for eliminating organic wastes composed of deteriorated oil and emulsions used in metal manufacturing. However, burning wastes containing significant amounts of phenols can result in dangerous gaseous pollutants, so careful determination of phenol species prior to incineration is needed. As the spectrophotometric determination of phenols in water–oil mixtures is difficult and of low precision, and the complexity of the samples together with low individual phenol concentrations prevents direct gas chromatographic (GC) determination, this paper reports an attempt to solve the problem of the determination of phenol by extraction and GC.

EXPERIMENTAL

A Spectra-Physics 7100 research gas chromatograph equipped with a flame ionization detector, an autosampler adjusted to inject 2 nl and an integrator was employed. A fused-silica 20 m × 0.23 mm I.D. Supelco SPB 5 capillary column and purified hydrogen as carrier gas were used throughout. The following chromatographic conditions provided a baseline separation of fourteen standard phenols: initial temperature 40°C for 10 min, increased at 5°C/min to 70°C, held for 1 min, a second ramp at 8°C/min to 200°C and isothermal operation for the next 10 min. All

0021-9673/89/$03.50

the phenols were eluted in 35 min, but the final ramp of 15°C/min and the hold of 10 min were necessary to elute heavy components from the oil extracts. The column head pressure was maintained at 40 kPa and the injector was operated at 250°C in the splitless mode for 0.5 min, then the splitting ratio automatically regained its original value of 1/200.

Fig. 1a shows the separation of the standard phenol mixture. Depending on the type of the phenol analysed, and with the instrument operating at maximum sensitivity, the detection limits varied from 2 to 5 mg/l in direct determinations.

Materials

All the organic compounds were of analytical-reagent grade and used as received. For recovery experiments, doubly distilled water was used. Phenols were used without further treatment; the stock solutions in ethanol were kept refrigerated. No noticable deterioration of the constituents was observed during a period of 4 weeks.

Stock standard solutions

A stock solution containing approximately 100 ppm of each of the phenols was prepared by mass, and for detector calibration diluted portions (10, 20 and 50 ppm) were used. The following phenols were used (in order of elution): 2-chlorophenol, phenol, 2-methylphenol, 2-nitrophenol, 2,4-dichlorophenol, 2,4-dimethylphenol, hydroquinone, 4-chloro-3-methylphenol, 2,4,6-trichlorophenol, 2,4-dinitrophenol, 3-nitrophenol, 4-nitrophenol, 2,3-dinitrophenol and benzylphenol. The plot of detector response *vs.* individual phenol concentration was linear, with a regression coefficient exceeding 0.99.

RESULTS AND DISCUSSION

Liquid wastes originating from a car engine factory contained two phases: a grey aqueous layer, apparently a fine water-oil emulsion, and a dark oil overlayer. In addition, considerable amounts of insolubles and graphite particles were present. The existence of phenols in both phases seemed very probable, especially as the aqueous phase was close to neutral, enabling water-soluble phenates to be formed.

Direct GC analysis of phenols present in such an oil sample is complicated for several reasons. First, a specimen displaying several hundred partially resolved peaks is too complex to permit confident component identification based on GC measurements only. Second, it is likely that some of the heavy components of the wastes are retained permanently in the capillary column, resulting in rapid column deterioration. Finally, the column might be easily clogged with particles from the used oil. Obviously, prior to the determination of phenols, they must be extracted from the complex sample such as a water–oil emulsion, various types of competitive adsorptions may occur and cause interferences. As an alternative, we used an extraction–concentration step and at the same time a clean-up procedure for treating the samples.

Extraction step

Extraction was performed in separating funnels as follows. (1) With the oil layer, the phenols were transferred into the aqueous phase as phenates using equal

volumes of oil and 2.5% sodium hydroxide solution, followed by phase separation. (2) The aqueous water phase, either from the sample or oil extract produced as indicated above was acidified using phosphoric acid. Phosphoric acid was selected rather than hydrochloric or nitric acid. For acidification of the aqueous, as the latter acids may cause oxidation or phenol degradation[4]. (3) The final step consists in phenol extraction with the chosen extractant, phase separation and drying of the organic layer prior to GC analysis using a few pellets of calcium chloride.

To verify the procedure, fresh unused motor oil was employed. GC analysis under the selected conditions (see Experimental) showed that all the phenols are eluted well before the first component of the oil. Prior to the experiments, fresh motor oil was washed with alkali to remove phenols possibly present. The purified oil was then used to study the recovery of phenols from a new oil and the water–oil phase.

Recovery from the oil phase

New oil was doped with known amounts of phenols and the above extraction scheme was followed.

Following step 1, the aqueous phase containing the phenols as phenates was washed twice with equal volumes of light petroleum (b.p. 40–70°C) to remove any residual oil hydrocarbon. In step 3, diethyl ether, benzene and butyl acetate were selected as extractants. As the extraction of phenols with organic solvents is dependent on the degree of dissociation, *i.e.*, the pH of the aqueous phase, experiments on the extraction of phenols with various acidities of the aqueous phase were performed. In the pH range 1.2–5.2 the extraction of phenols with the above solvents was nearly complete, with recoveries from 95 to 102%, except for 2-chlorophenol (78%) and phenol (76%). The percentage extraction is independent of the extractant applied, varying by only 2% about the average. This was calculated to be the overall precision of the extraction–chromatographic procedure.

Recovery of phenols from water–oil emulsion

To prepare a synthetic water–oil emulsion, 10 ml of alkali-washed fresh oil was added to 500 ml of distilled water and mixed vigorously with a mechanical stirrer until an emulsion with slow phase separation was obtained. The prepared sample was enriched with 5–10 ppm of 2-methylphenol, 2-chlorophenol, 2-nitrophenol, 2,4-dinitrophenol, 2,4-dichlorophenol, 2,3-dinitrophenol, 4-nitrophenol and benzylphenol, made alkaline and washed three times with light petroleum to remove the added oil. The first portion of the light petroleum wash was saved for subsequent GC analysis. The water layer was acidified and extracted with 20 ml of diethyl ether (organic to aqueous phase ratio 1 : 25 and the extract was analysed for phenols recovery.

The resulting chromatogram of the diethyl ether extract is shown in Fig. 1b, revealing the absence of benzylphenol and the recovery of all other components with 95–102% efficiency. A similar efficiency was reported by Abrahamsson and Xie[5] for the extraction of numerous phenols from water with *n*-hexane. A high recovery is maintained provided that the phase ratio does not exceed approximately 1 : 30; at higher phase ratios the extraction is poorer[6].

Fig. 1c shows the chromatogram of the first light petroleum wash with an easily recognized benzylphenol peak, the only phenol extracted with light petroleum from aqueous alkali media.

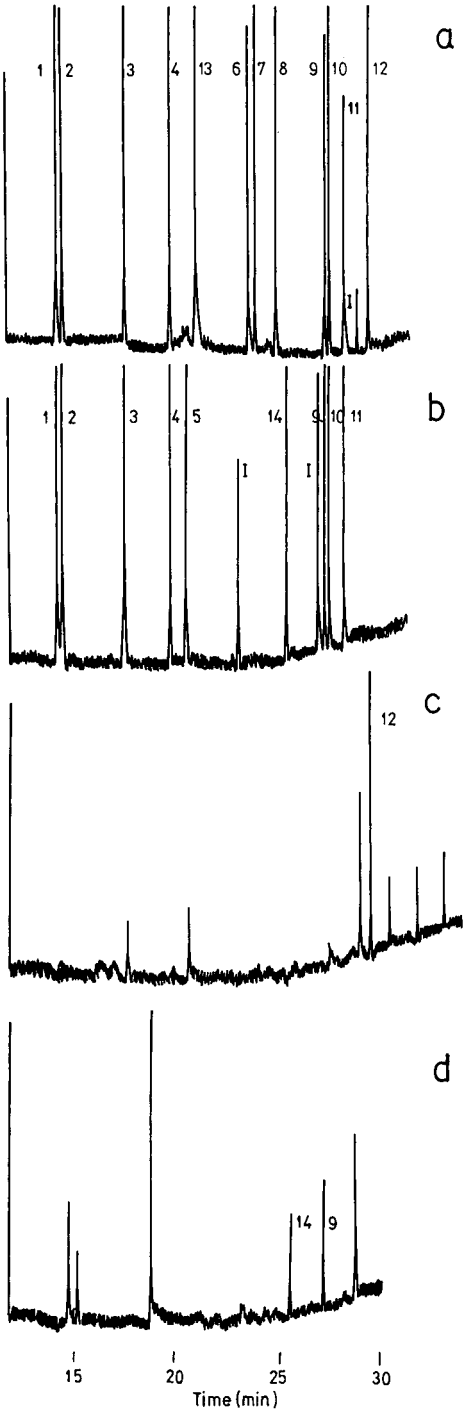

Fig. 1. Chromatograms of (a) standard phenols (50 ppm of each), (b) diethyl ether extract from synthetic water–oil emulsion, (c) light petroleum wash and (d) diethyl ether extract of water–oil emulsion sample I. Detector, flame ionization, $1 \cdot 10^{-12}$ a.u.f.s.; chart speed, 0.1 cm/min from 0 to 14 min, then 1 cm/min. Phenols: 1 = 2-chloro-; 2 = phenol; 3 = 2-methyl-; 4 = 2-nitro-; 5 = 2,4-dichloro-; 6 = hydroquinone; 7 = 4-chloro-3-methyl-; 8 = 2,4,6-trichloro-; 9 = 3-nitro-; 10 = 4-nitro-; 11 = 2,3-dinitro-; 12 = benzyl-; 13 = 2,4-dimethyl-; 14 = 2,4-dinitro-.

TABLE I

DETERMINATION OF PHENOLS (ppm) IN WASTE OIL–WATER EMULSION USING VARIOUS EXTRACTANTS

Phenol	*Sample I*			*Sample II*		
	Diethyl ether	*Benzene*	*Butyl acetate*	*Diethyl ether*	*Benzene*	*Butyl acetate*
3-Nitro-	0.4	18.6	17.9	0.7	17.7	18.0
2,4-Dinitro-	1.7				0.5	0.4
2,4-Dimethyl-	1.7	33.9	29.2	1.2	22.1	20.2
Benzyl-		0.2	0.4			0.4
2,4,6-Trichloro-			0.4			1.1
4-Nitro-			3.2			1.6
Total phenols	2.1	52.7	51.1	1.9	40.3	41.7
Spectrophotometric determination of total phenol content (mg/l)		0.42			0.64	

Sample analysis

The waste samples were split into an emulsion phase (here termed aqueous) and an oil phase, each treated independently according to the previously described procedure. GC analysis of the oil extracts using diethyl ether, benzene or butyl acetate as extractant did not reveal any of the phenols studied here. However, the chromatograms were too complicated in every instance, even with diethyl ether, showing a large number of peaks. Evidently they represent water-soluble organics such as alcohols and acids, and some of the hydrocarbons retained in the aqueous phase owing to poor phase separation and especially to the presence of small organic droplets in water, residual film on the funnel walls, etc. Hence, a positive identification of phenols in oil samples remains a difficult task requiring more sophisticated techniques such as GC combined with mass spectrometry.

After the light petroleum pre-wash of the alkaline water–oil emulsion, the aqueous phase was acidified and divided into three 100-ml portions and further extracted with 3 ml of diethyl ether, benzene and butyl acetate, respectively. The chromatograms of the extracts differ greatly in complexity. When diethyl ether was used, eight baseline-resolved peaks were recorded (Fig. 1d, sample I). Two peaks were identified by their retention times as 2-nitrophenol and 2,3-dinitrophenol. The same pattern was obtained for two waste samples analysed, here labelled I and II. The benzene extracts are significantly more complex, and those of butyl acetate exhibit only a 4–5-fold reduction in the number of peaks in comparison with the chromatogram of the new oil phase. With such a large number of peaks, one has to be careful with the assignment. Here, only those peaks coinciding within ± 0.03 min (2 s) with the retention time of the standard were identified as the corresponding phenols. The value of 0.03 min was selected as it had been found that this value approximated to the daily instrumental drift of the retention times of standard phenols.

Table I presents the results of the analysis of two waste water–oil liquids. Unrealistically high phenol concentrations when benzene or butyl acetate was selected as

the extractant indicate poor integrator peak assignment, a result of the complexity of the extract. The 4-amino antipyrine spectrophotometric method resulted in total phenol content of 0.42 and 0.64 mg/l for samples I and II, respectively, which agree well with the results of the GC analysis of the diethyl ether extracts. A similar agreement between the spectrophotometric and GC results was reported by Folke and Lund[6] for the analysis of phenols in municipal waste waters. The higher GC values can be ascribed to incomplete steam distillation of nitrophenols[3].

CONCLUSION

This work was partly aimed at studying the use of benzene and butyl acetate as extractants for phenols in acidic water media. The choice was made on the basis of literature information[7–9] on these two extractants, which are far superior to *n*-hexane and diethyl ether. Our experiments indicate that the benzene extraction of standard phenols from neutral water exhibits a low concentration factor, in accordance with the reported lower distribution coefficient for phenols[7–10]. To gain a desired concentration of phenols in the organic phase and to improve the GC detection limit, a benzene : water phase ratio exceeding 1 : 30 is used, and this has the drawback of a reduced extraction efficiency[6]. Butyl acetate, with distribution coefficients for phenols two orders of magnitude greater than those with benzene[7–10], completely extracts phenols in a single step, and the pre-concentration is easily carried out. Hence, butyl acetate is recommended for the extraction of trace amounts of phenols from organic samples. Unfortunately, butyl acetate is also a strong, non-selective extractant for non-phenolic species, so that in a system with hundreds of unknown components, it is almost impossible to resolve phenols from the maxtrix using GC analysis alone.

The extraction of phenols from a water–oil phase having a pH lower than 6 with diethyl ether is suitable for the determination of phenols in complex organic mixtures. The confident determination of phenols in crude waste oils is a future concern on which we hope to report soon.

ACKNOWLEDGEMENT

We are grateful to the U.S. Environmental Protection Agency, Cincinnati, OH, for supplying the standard phenols.

REFERENCES

1 L. D. Rossemyr, *J. Chromatogr.*, 170 (1979) 463.
2 M. J. Taras, A. E. Greenberg, R. D. Hoan and M. C. Rand (Editors), *Standard Methods for the Examination of Water and Wastewaters*, American Public Health Association, Washington, DC, 1971, p. 501.
3 G. Norwitz, N. Nataro and P.N. Keiliher, *Microchem. J.*, 35 (1987) 240.
4 C. D. Chriswell, R. C. Chang and J. S. Fritz, *Anal. Chem.*, 47 (1975) 1325.
5 K. Abrahamsson and T. M. Xie, *J. Chromatogr.*, 279 (1983) 199.
6 J. Folke and U. Lund, *J. Chromatogr.*, 279 (1983) 189.
7 Yu. I. Korenman, *Russ. J. Phys. Chem.*, 46 (1972) 77.
8 Yu. I. Korenman, *Russ. J. Phys. Chem.*, 46 (1972) 2254.
9 Yu. I. Korenman, *Russ. J. Phys. Chem.*, 46 (1972) 2617.
10 D. S. Abrams and J. M. Prausnitz, *J. Chem. Thermodyn.*, 7 (1975) 61.

Journal of Chromatography, 462 (1989) 398–405
Elsevier Science Publishers B.V., Amsterdam — Printed in The Netherlands

CHROM. 21 059

Note

Stability-indicating high-performance liquid chromatography assay for bepridil hydrochloride drug substance and drug products

NED L. RENZI*, MICHAEL E. FRONHEISER, HANG T. DUONG and DEBORAH J. FULTON
McNeil Pharmaceutical, Welsh and McKean Roads, Spring House, PA, 19477-0776 (U.S.A.)
and
MICHAEL RABINOWITZ
Wallace Laboratories, Division of Carter-Wallace Inc., Half Acre Road, Cranbury, NJ 08512 (U.S.A.)
(First received August 29th, 1988; revised manuscript October 18th, 1988)

Bepridil hydrochloride (I), β-[(2-methylpropoxy)methyl]-N-phenyl-N-(phenylmethyl)-1-pyrrolidineethanamine monohydrochloride monohydrate, is a new calcium-channel blocker currently undergoing clinical evaluation for the treatment of angina pectoris. Its antianginal properties have been demonstrated in animal studies[1–5] and in clinical studies[6,7].

Various analytical methods have been reported for determining the bepridil concentration in plasma. These methods are both sensitive and selective and range from gas chromatography (GC) with nitrogen-specific detection[8,9] to GC–mass spectrometry (MS)[10] to high-performance liquid chromatography (HPLC)[11]. These methods focus on very low limits of detection of bepridil in biological media, and thus are not appropriate for assaying drug substance and drug product for product release and stability, since they are not designed to detect and quantitate process impurities and degradation products.

In this paper, a stability-indicating HPLC assay method capable of monitoring the purity of bepridil hydrochloride drug substance and drug product (tablet, capsule and injection solution) is described.

Experiments were performed and data generated establishing the linearity, specificity, ruggedness, precision, sensitivity and accuracy of the method.

EXPERIMENTAL

Equipment

The HPLC system consists of a DuPont (Wilmington, DE, U.S.A.) Model 850 liquid chromatograph equipped with a DuPont automatic sampler, a 20-μl loop, a fixed-wavelength 254 nm detector and a Spectra-Physics (San Jose, CA, U.S.A.) Model 4270 integrator. The column employed is μBondapak™ C_{18}, 10 μm particle size, 30 cm × 4.6 mm (Waters Assoc., Milford, MA, U.S.A.), thermostated at 35°C. A flow-rate of 1.3 ml/min is used throughout the study.

0021-9673/89/$03.50

Reagents

HPLC-grade water and acetonitrile, analytical-reagent grade glacial acetic acid (Fisher Scientific, Fairlawn, NJ, U.S.A.) and chromatography grade 1-heptanesulfonic acid sodium salt (Eastman Kodak, Rochester, NY, U.S.A.) are used to prepare the mobile phase. N-Benzylaniline (II) is used as a resolution test compound (Aldrich, Milwaukee, WI, U.S.A.). Bepridil hydrochloride standard and debenzylated bepridil (III) are obtained from McNeil Pharmaceutical (Spring House, PA, U.S.A.). Benzaldehyde and benzoic acid analytical-reagent grade, were used without further purification (Aldrich).

Solutions

Paired ion. Dissolve 1.1 g of 1-heptanesulfonic acid sodium salt in 405 ml of water. Using a pH meter adjust the pH to 2.37 with glacial acetic acid (approximately 15 ml will be needed).

Mobile phase. Acetonitrile–paired ion (580:405).

Sample solvent. Acetonitrile–paired ion (580:405) for drug substance; acetonitrile for drug product.

Standard. Accurately weigh about 37 mg of standard into a 50-ml volumetric flask and dilute to volume with sample solvent.

Drug substance sample. Same as standard.

Drug product sample. Accurately weigh an amount of triturated capsule or tablet granulation theoretically equivalent to 150 mg of bepridil hydrochloride into a 200-ml volumetric flask and add 150 ml of acetonitrile. Shake for 30 min and dilute to volume with acetonitrile. Shake well and filter about 20 ml through prepleated filter paper of 0.22 mm thickness (Schleicher and Schüll, grade 588).

Resolution test mixture. Weigh about 44 mg of bepridil hydrochloride and about 2 mg of debenzylayed bepridil and 10 mg of N-benzylaniline for drug substance and drug product, respectively, into the same 50-ml volumetric flask and dilute to volume with mobile phase.

Diluted resolution test mixture. Accurately dilute a portion of the resolution test mixture in half with sample solvent.

System suitability

Prior to running the system suitability check, the column should be equilibrated for at least 15 min with the mobile phase flowing through the system. An injection of the sample solvent is made to obtain a blank chromatogram. The system suitability is determined by evaluating the resolution solution, injection precision and detector linearity. The resolution mixture is injected and the resolution (not less than 1.6 between peaks) calculated using the standard resolution equation found in the *United States Pharmacopoeia*[12]. The precision is determined using the relative standard deviation of the response factors (area/μg) of injections of the standard solutions. The relative standard deviation (R.S.D.) should be less than 2.0%. An injection of the diluted resolution mixture is chromatographed and the integrated area for the bepridil peak should be within 48–52% of that in the resolution mixture to meet the detector linearity criteria. Acceptable results for system suitability tests are required before samples are analyzed.

TABLE I

STRUCTURE, RETENTION TIMES AND DETECTION LIMITS OF BEPRIDIL HYDROCHLORIDE, ITS PROCESS IMPURITIES AND DEGRADATION PRODUCTS

Compound	*Structure*	*Approximate retention time (min)*	*Detection limit*		
			Percent	*μg*	*Sensitivity factor*
Benzoic acid (degradation product of benzaldehyde)	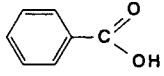	2.6	0.13	0.020	0.17
Benzaldehyde (process impurity)	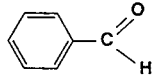	3.2	0.02	0.003	2.76
Debenzylated bepridil · HCl (III) (process impurity)	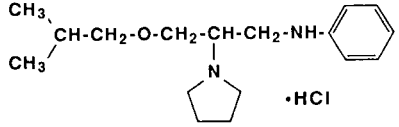	4.2	0.09	0.013	0.44
N-Benzylaniline (II) (process impurity)	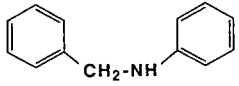	5.0	0.07	0.010	1.27
Bepridil · HCl (I)	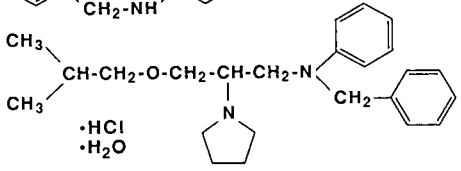	6.8	—	0.01	1.00

Calculations

To determine percent assay, the following equation is used:

$$\% \text{ (w/w) bepridil hydrochloride} = \frac{R_x P_s}{R_s}$$

where R_x is equal to the response factor of the peak area of the corresponding bepridil peak per μg sample injected, R_s is the response factor of the peak area of the bepridil peak per μg standard injected, and P_s is the percent purity of the bepridil hydrochloride standard. Percent impurities are calculated in a similar manner using a sensitivity factor as described in the Results and discussion section. Unknown impurities are assigned a sensitivity factor of 1.0.

RESULTS AND DISCUSSION

Specificity and stability-indicating ability

The process impurities and degradation products (Table I) are separated from bepridil hydrochloride and from each other as shown in Fig. 1. The assay value for drug substance in samples spiked with all the impurities listed in Table I at the 3.0% level was not effected (data given in Table II). In the case of drug product, the placebo granulation did not produce any interfering peaks or affect the quantitation of any peaks of interest.

Sensitivity

The process impurities and degradation products listed in Table I can be quantitated down to at least the 0.2% level for drug substance and drug product. A sensitivity factor was also determined for each impurity. This was accomplished by analyzing samples of these compounds under normal analytical conditions, measuring the resulting peak areas, and dividing by the amount of compound injected. The ratio of the response factors (peak area/μg injected) of the impurity to bepridil hydrochloride is labeled the sensitivity factor in Table I. The sensitivity factor allows the conversion of area percent to weight percent by normalizing the difference in sensitivity between bepridil hydrochloride and the impurity of interest.

Precision

The precision of the system was evaluated by preparing four portions of the same reference standard and injecting each of them in duplicate. The assay results are given in Table II which show that the relative standard deviation for this set of solutions was 0.22%.

Linearity

Solutions containing from 0 to 400% of the normal amount of bepridil hydrochloride and from 0 to at least 6.0% of each impurity were analyzed. All calibration plots were linear when using area and intersected near the origin. The regression curve for the bepridil hydrochloride plot gave a slope of 0.603, y-intercept of -0.019 and a correlation coefficient of 0.9999. Regression equations for benzoic acid, benzaldehyde, debenzylated bepridil and N-benzylaniline were $y = 0.097x + 0.001$;

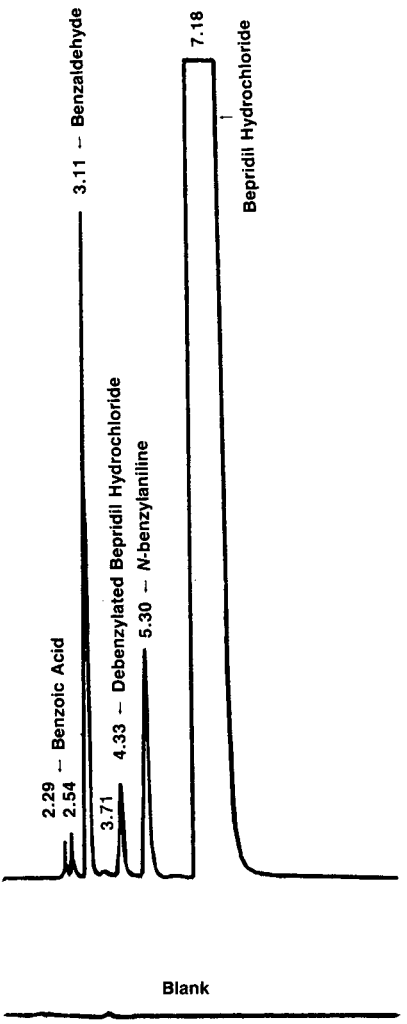

Fig. 1. Liquid chromatogram of the bepridil hydrochloride reference standard spiked with 0.5% levels of benzoic acid, benzaldehyde, debenzylated bepridil and N-benzylaniline using the procedures described herein. Numbers indicate retention times in min.

$y = 1.92x + 0.011$; $y = 0.404x + 0.003$; and $y = 0.917x + 0.001$, respectively. The correlation coefficients were 0.9999 in all cases.

Accuracy

The recovery of bepridil hydrochloride from the drug product was evaluated by spiking placebo granulation with 80% to 120% of the normal amount of bipridil hydrochloride. The recovery of bepridil hydrochloride from these mixtures ranges from 99.2% to 100.1% (Table III).

TABLE II

PRECISION DATA OBTAINED FROM FOUR BEPRIDIL HYDROCHLORIDE REFERENCE STANDARD SOLUTIONS

Sample No.	*Beprimil · HCl (mg)*	*Impurities* (mg)*	*Recovery (%)**, Bepridil · HCl*
1	100.0	0.5	100.5
2	100.0	1.0	100.3
3	100.0	2.0	100.1
4	100.0	3.0	100.0
		Mean	100.2
		R.S.D.	0.22%

* Demonstrates that impurities at concentrations up to 3% do not interfere with the recovery of bepridil hydrochloride.

** The number given is the mean of two determinations per sample.

Ruggedness

The ruggedness of the HPLC system has been demonstrated by obtaining accurate quantitation of bepridil hydrochloride and some potential impurities in a spiked reference standard solution (Table IV) when different flow-rates, column temperatures, columns, mobile phases (pH and composition), instruments and analysts were used. However, benzoic acid and debenzylated bepridil hydrochloride are somewhat affected by the parameter changes.

System suitability

System suitability tests are performed each time the method is run in order to ensure that the entire system is working properly. The resolution is checked by calculating the resolution between the bepridil and N-benzylaniline or debenzylated bepridil in the analysis of drug substance and drug product samples. The linearity of the detector is evaluated by comparing the area of the bepridil peaks of the resolution

TABLE III

RECOVERY DATA OBTAINED FOR BEPRIDIL HYDROCHLORIDE USING THE ASSAY PROCEDURE DESCRIBED

NA = Not applicable; ND = none detected.

Bepridil content (%)		*Recovery (%)*
Actual	*Determined*	
Placebo	ND	NA
80% Spike	79.4	99.3
100% Spike	100.1	100.1
120% Spike	119.4	99.5
	Mean	99.6
	R.S.D.	0.34%

TABLE IV

QUANTITATIVE RESULTS (%, w/w) FOR A SPIKED BEPRIDIL HYDROCHLORIDE REFERENCE STANDARD SOLUTION USING VARIOUS CONDITIONS, INSTRUMENTS AND ANALYSTS

*Conditions instrument and analyst**	*Bepridil · HCl*	*Benzoic acid*	*Benzaldehyde*	*Debenzylated bepridil · HCl*	*N-Benzylaniline*
	Known % (w/w)				
	100.0	*0.50*	*0.50*	*0.50*	*0.50*
(a)	100.5	0.47	0.55	0.54	0.48
(b)	100.3	0.70	0.54	0.54	0.46
(c)	100.2	0.51	0.53	0.48	0.47
(d)	99.9	0.43	0.51	0.31	0.47
Mean	100.2	0.53	0.53	0.47	0.47
S.D.	0.37	0.12	0.02	0.11	0.01

* (a): Flow-rate 1.3 ml/min, column temperature 35°C, column 1, mobile phase acetonitrile–paired ion solution–acetic acid (580:405:15), instrument 1, analyst 1. (b): Flow-rate 1.0 ml/min, column temperature 40°C, column 2, mobile phase acetonitrile–paired ion solution–acetic acid (580:402:18), instrument 2, analyst 2. (c): Flow-rate 1.5 ml/min, column temperature ambient, column 3, mobile phase acetonitrile–paired ion solution–acetic acid (570:415:15), instrument 3, analyst 3. (d): Flow-rate 1.4 ml/min, column temperature ambient, column 4, mobile phase acetonitrile–paired ion solution–acetic acid (590:398:13), instrument 4, analyst 4.

test mixture and the diluted resolution test mixture. The bepridil hydrochloride concentration of the resolution test mixture is 120% of the normal concentration in order to provide a safety factor for linearity. Finally, the precision is checked by calculating the percent relative standard deviation of the bepridil peak areas of the standards bracketing the samples.

CONCLUSION

The results of thus study indicate that the HPLC method presented is specific, stability-indicating, linear, precise, sensitive and accurate. This method has been found

TABLE V

ANALYSIS OF BEPRIDIL HYDROCHLORIDE DRUG SUBSTANCE FOR RELEASE USING HPLC ASSAY

ND = None detected.

Drug substance lot number	*Assay values (expressed as %, w/w)*				
	Bepridil · HCl	*Benzoic acid*	*Benzaldehyde*	*Debenzylated bepridil · HCl*	*N-Benzylaniline*
8506963	100.8	ND	ND	0.07	ND
8304091	100.9	ND	ND	0.08	ND

suitable for the analysis of bepridil hydrochloride, process impurities and degradation products in both drug substance (see Table V) and drug products (tablets and capsules at 100, 200, 300 and 400 mg; injection solution at 4.0 mg/ml.

REFERENCES

1 D. Cosnier, P. Duchene-Marullaz, G. Riospat and G. Streichenberger, *Arch. Int. Pharmacodgn. Ther.*, 225 (1977) 133.
2 M. T. Michelin, M. Cheuche and P. Duchene-Marullaz, *Therapie*, 32 (1977) 485.
3 P. Piris, M. Beaughard, D. Cosine and C. Labrid, *Arch. Int. Pharmacodgn.*, 235 (1978) 147.
4 C. Chassaing, N. Moins, J. Lavarenne and P. Duchene-Marullaz, *J. Pharmacol.*, 8 (1977) 503.
5 M. Boucher and P. Duchene-Merullaz, *Arch. Int. Pharmacodgn. Ther.*, 233 (1978) 65.
6 J. C. Canicave, J. Deu and F. X. Lesbre, *Lyon Med.*, 243 (1980) 107.
7 D. Granatelli, D. Germa and L. Tatibouef, *Quest. Med.*, 15 (1981) 1041.
8 J. Vink, H. J. M. van Hal, J.-F. Pognat ans J.-L. Bouquet Des Chaux, *J. Chromatogr.*, 272 (1983) 87.
9 M. L. Holland and K. T. Ng, *J. Chromatogr.*, 374 (1986) 87.
10 J. Vink, H. J. M. van Hal, F. M. Kaspersen and H. P. Nijnand, *Int. J. Mass Spectrom. Ion Phys.*, 48 (1983) 217.
11 K.-T. Ng, J. A. Plutte and L. J. Galante, *J. Chromatogr.*, 309 (1984) 125.
12 *United States Pharmacopoeia*, United States Pharmacopeial Convention, Rockville, MD, 25th revision, 1985, p. 1229.

Journal of Chromatography, 462 (1989) 406–410
Elsevier Science Publishers B.V., Amsterdam — Printed in The Netherlands

CHROM. 21 005

Note

High-performance liquid chromatographic determination of citrinin in cereals using an acid-buffered silica gel column

B. ZIMMERLI*, R. DICK and U. BAUMANN
Laboratory of Food and Radiochemistry, Division of Food Control, Office of Public Health, CH-3000 Berne 14 (Switzerland)
(Received September 1st, 1988)

Since the mid seventies, reversed-phase chromatography had developed to become the most dominant branch of high-performance liquid chromatography (HPLC), while normal-phase chromatography, most popular in classical column liquid chromatography, has lost its leading role. This paper describes the successful normal-phase HPLC of trace amounts of the acid compound citrinin on a acid-buffered silica gel column as recently described by Schwarzenbach[1]. By treating the silica gel with a buffer salt, virtually insoluble in the mobile phase, an environment is created on the surface of the adsorbent that permits tail-free elution of very polar compounds[1].

Citrinin (IUPAC: (3*R*,4*S*)-4,6-dihydro-8-hydroxy-3,4,5-trimethyl-6-oxo-3H-2-benzopyran-7- carboxylic acid; C.A. 518-75-2), a fungal metabolite, is produced by several Aspergillus and Penicillium species. It has been reported to demonstrate antibiotic, antifungal, antiprotozoal and bacteriostatic properties as well as to cause nephrotoxicity in several animal species. Citrinin-producing fungi grow on grains and fruits which are stored in high humidity as well as on mould-fermented sausages; however, the presence of the fungus does not necessarily indicate the presence of the mycotoxin[2,3]. In order to evaluate possible health risks, an estimate of its daily intake by the population is needed. This implies a reliable quantitative method for the determination of citrinin in food.

Several methods to determine citrinin have been published, primarily based on thin-layer chromatography (TLC), but relatively low sensitivities in the range of 10–50 ng/g at best have been reported in recent reviews[2–4]. On the other hand, HPLC has been applied to the analysis of citrinin in grains and biological fluids[5–9]. Mostly reversed-phase chromatography was performed using acidic mobile phases and fluorescence[5,8,9] or UV[6] detection; the ion-pair technique with UV detection has also been applied[7]. The stated detection limits were comparable to those reached by TLC.

Unfortunately, neither of the described HPLC conditions, except ion-pair chromatography, worked well in our hands. Seriously distorted peaks and extremely low sensitivities resulted with several commercially available reversed-phase columns using appropriate acidic eluents. However, reversed-phase ion-pair HPLC[7] provided good peak forms, but the fluorescence of citrinin was completely lost. Thereby the sensitivity and selectivity of the detection method was diminished. This drawback had

0021-9673/89/$03.50

been overcome by acidifying the eluate of the HPLC column before entering the fluorescence detector.

A much easier and more elegant procedure is the buffered silica gel separation technique[1] which, as far as we know, is not widely applied at the moment. However, it seems to be very effective for the chromatographic separation of polar compounds. In any case we were very successful with citrinin at the first go.

EXPERIMENTAL

Chemicals and reagents

Citrinin was obtained from Sigma (St. Louis, MO. U.S.A.). For HPLC a working standard in chloroform (0.5 μg/ml) was used. All reagents, except chloroform, which was distilled, were p.a. grade and were used without any further treatment. Deionized water was used throughout this study.

Apparatus

The chromatographic system consisted of a Model 100A pump (Altex, Berkeley, CA, U.S.A.), a Model U6K sample injection valve (Waters, Milford, MA, U.S.A.) and a Model 650–109 fluorescence spectrometer (Perkin-Elmer, Norwalk, CI, U.S.A.) equipped with a flow-cell (excitation 360 nm, emission 500 nm, slits 10–20 nm). For the measurement of peak areas, a Model D-2000 Chromato-Integrator (Merck-Hitachi, Tokyo, Japan) was applied. All chromatographic columns (300 mm × 4.6 mm I.D.) used were commercially prepacked with microparticulates and made from stainless steel.

Preparation of buffered silica gel column[1]

A prepacked LiChrospher® Si 100 column [mean particle size 5 μm, specific surface area 420 ±30 m^2/g, specific pore volume 1.25 ± 0.05 ml/g (ref. 10), 300 mm × 4.6 mm] supplied by Merck (Darmstadt, F.R.G.) was rinsed with about 200 ml of methanol, followed by about 200 ml of water. Then about 400 ml of aqueous buffer solution (0.2 *M* citric acid, adjusted to pH 2.5 with a saturated disodium hydrogenphosphate solution) were pumped through the column. It was connected to a nitrogen source and, after all the remaining buffer solution had been removed in a gentle stream of nitrogen (5–10 ml/min) at room temperature, the column was heated at 80°C for about 30 h. After cooling to room temperature, the column was equilibrated with about 100 ml of the mobile phase.

Chromatographic conditions

The mobile phase consisted of *n*-hexane–chloroform (typically 60:40, v/v), and a flow-rate of 1 ml/min was applied (room temperature). Typical injection volumes were 10 μl. The retention time of citrinin under the conditions described (buffered silica gel column) was 10 to 15 min. For quantification, peak areas were measured and compared to those of standard solutions.

Extraction and clean-up

To a 40-g ground sample of cereal (or flour), 150 ml chloroform and 20 ml 0.1 *M* phosphoric acid were added, mixed for 5 min, using a Polytron PCU-2 (Kinema-

tica, Luzerne, Switzerland) and then centrifuged (*ca.* 3000 *g*) for 10 min. Tapping down carefully the formed cake of flour with a spatula makes it easier to withdraw an aliquot of the chloroform extract.

A 7-g amount of Extrelut® (Merck) was uniformly impregnated with 10 ml of a an aqueous 1% sodium bicarbonate solution in a beaker. After packing the thus prepared alkaline adsorbent into an Extrelut® column (shortened by *ca.* 4.5 cm and equipped with an additional stopcock), 100 ml of chloroform extract (corresponding to 26.7 g sample) were added to the column; after elution the column was rinsed with 2 × 40 ml chloroform, and the eluates were discarded. After blowing out with air the rest of the chloroform (balloon), a mixture of 30 ml chloroform and 1 ml formic acid (100%) was added to the column (without piston, stopcock closed) and thoroughly mixed with the column material (glass rod); the drain was collected. After reinstallation of the piston and light compression of the column material, the rest of the citrinin was eluted with 2 × 40 ml chloroform. The eluate was evaporated to dryness (Rotavapor®, Büchi, Switzerland, 40°C), and the residue was dissolved in 1 ml distilled chloroform for HPLC analyses. For recovery purposes the citrinin standard solution in chloroform was distributed uniformly (syringe) on the ground sample.

RESULTS AND DISCUSSION

It might be expected that the analysis of citrinin in food be facilitated by its acid and fluorescence properties. However, several difficulties have been described in the analysis of citrinin, *e.g.*, poor repeatability and/or recovery, tendency to be retained by glassware and syringes, sensitivity to light and temperature[11–16].

Fig. 1A–D demonstrates the good peak form of citrinin, the sensitivity of the chromatographic system and the acceptable separation from coextractives. In the tested range of 1–20 ng the detector signal was linearly related to the amount of citrinin injected. Without specially optimizing the excitation and emission wavelengths the minimum detectable amount of standard citrinin was about 0.1 ng (three

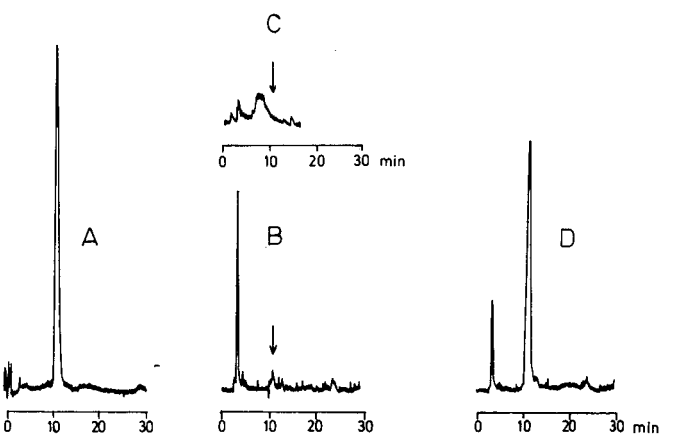

Fig. 1. Chromatograms of citrinin. (A) 5.3 ng standard; (B) brown flour (wheat naturally contaminated) *ca.* 0.8 ng/g; (C) wheat bran < 0.2 ng/g; (D) brown flour (wheat) spiked with 15 ng/g. Chromatographic conditions as described, injection volumes each 10 μl.

times the noise). Preliminary results have shown that filling the cell of the fluorescence detector with a similar acid-buffered silica gel as used in the column enhances the detector response for citrinin in about the same way as it has been demonstrated for aflatoxins[17,18].

The mean recovery of citrinin in brown wheat flour in the concentration range of 1–30 ng/g was 85.2% with a standard deviation of 7.4% ($n = 9$) and a range of 77.1–99.5%. With injection volumes of, *e.g.*, 40 μl of the extract, corresponding to 1.07 g sample, a limit of quantification of about 0.1 ng/g is achievable. The extraction procedure and the solid phase clean-up resulted in acceptable recoveries and chromatograms. However, the efficiency of different potential extraction procedures has not been tested with naturally contaminated samples. In 14 of a total of 38 analyzed samples of cereals from the retail level, citrinin has been detected in the range of 0.2–1 ng/g; details are given elsewere[19].

Although the batch procedure to prepare a buffered silica gel column has been mentioned to be much more reliable than the *in situ* coating of prepacked silica gel columns[1], we have applied with acceptable success the latter procedure. Since a 0.1 *M* solution leads to a coating of approximately 1.5–2.5% (m/m) of silica gels with a specific surface area of about 400m^2/g (ref. 1), we can assume a load in the range of 3–5% (m/m) for our column.

Probably because the water content of the eluate mixture was not under strict control, some variation of the retention time of citrinin from one day to the next has been observed occasionally. By slightly changing the ratio of hexane to chloroform, the retention of citrinin may be adjusted.

After prolonged use of the column, the retention time of citrinin became shorter and shorter and the number of theoretical plates decreased. By pumping about 50 ml of a mixture of 5% (v/v) methanol in chloroform through the system the chromatographic properties were restored, probably by removing polar coextractives from the column. After these treatments the retention time of citrinin increased, *e.g.*, from about 6 to 14 min.

After the column had once been accidentally eluted with about 100 ml of methanol, no chromatographic separation could be achieved. However, by repeating the coating procedure (without water, 100 ml ethanol instead of 200 ml methanol, and 200 ml buffer solution), the original properties of the column were completely restored.

CONCLUSIONS

Although reversed-phase HPLC is mostly used today because of its advantages over conventional normal-phase HPLC, our results show that the latter on modified silica gels, *e.g.*, buffered silica gel, is a remarkable alternative, especially in trace analysis of very polar compounds.

The procedure described for the determination of citrinin in cereals, based on an alkaline/acid partition step on Extrelut and HPLC on an acid-buffered silica gel column with fluorescence detection, has been successfully applied to durum and soft wheat, wheat bran, rice, barley, corn, oat, oat groats and pastas. A limit of quantification of about 0.1 ng/g is achievable.

ACKNOWLEDGEMENT

We thank our colleague Dr. R. Gerber for his helpful support in the preparation of this manuscript.

REFERENCES

1 R. Schwarzenbach, *J. Chromatogr.*, 334 (1985) 35.
2 V. Betina, in V. Betina (Editor), *Mycotoxins–Production, Isolation, Separation and Quantification* (*Developments in Food Science*, Vol. 8), Elsevier, Amsterdam, Oxford, New York, Tokyo, 1984, pp. 217–236.
3 *IARC Monographs on the Evaluation of the Carcinogenic Risk of Chemicals to Humans*, 40, International Agency for Research on Cancer (IARC), Lyon, 1986, pp. 67–82.
4 V. Betina, *J. Chromatogr.*, 334 (1985) 211.
5 L. R. Marti, D. M. Wilson and B. D. Evans, *J. Assoc. Off. Anal. Chem.*, 61 (1978) 1353.
6 R. D. Phillips, A. W. Hayes and W. O. Berndt, *J. Chromatogr.*, 190 (1980) 419.
7 T. Nakagawa, T. Kawamura, Y. Fujimoto and T. Tatsuno, *J. Food Hyg. Soc. Jpn.*, 23 (1982) 297.
8 P. Lepom, *J. Chromatogr.*, 355 (1986) 335.
9 D. L. Orti, R. H. Hill, Jr., J. A. Liddle, L. L. Needham and L. Vickers, *J. Anal. Toxicol.*, 10 (1986) 41.
10 K. F. Krebs and W. Jost, *Kontakte*, No. 2 (1986) 13.
11 L. Stoloff, *J. Assoc. Off. Anal. Chem.*, 65 (1982) 316.
12 L. Stoloff, *J. Assoc. Off. Anal. Chem.*, 66 (1983) 355.
13 P. M. Scott, *J. Assoc. Off. Anal. Chem.*, 67 (1984) 366.
14 P. M. Scott, *J. Assoc. Off. Anal. Chem.*, 68 (1985) 242.
15 P. M. Scott, *J. Assoc. Off. Anal. Chem.*, 69 (1986) 240.
16 P. M. Scott, *J. Assoc. Off. Anal. Chem.*, 70 (1987) 276.
17 B. Zimmerli, *Chimia*, 30 (1976) 497.
18 B. Zimmerli, *J. Chromatogr.*, 131 (1977) 458.
19 R. Dick, U. Baumann and B. Zimmerli, *Mitt. Gebiete Lebensm. Hyg.*, 79 (1988) 159.

Journal of Chromatography, 462 (1989) 411–418
Elsevier Science Publishers B.V., Amsterdam — Printed in The Netherlands

CHROM. 21 078

Note

Characterization and purification of iron porphyrins by high-performance liquid chromatography and column chromatography

DABNEY WHITE DIXON*, LOUISA AMIS and MIN SOOK KIM
Department of Chemistry and Laboratory for Microbial and Biochemical Sciences, Georgia State University, Atlanta, GA 30303 (U.S.A.)
and
JON CALLAHAN*
Department of Chemistry, Washington University, St. Louis, MO 63130 (U.S.A.)
(First received April 6th, 1988; revised manuscript received October 25th, 1988)

Iron porphyrins are important as biological cofactors and regulatory signals. In addition to serving as a prosthetic group for many enzymes[1–3], iron porphyrins regulate many biosynthetic pathways[4–16].

Many workers have investigated the high-performance liquid chromatographic (HPLC) characterization of iron-containing natural porphyrins[17–25]. Lim *et al.*[18] were able to achieve excellent separation of *meso* and protoporphyrins and their corresponding Fe(III) derivatives using a SAS-Hypersil (C_1) column with a methanol–1 *M* ammonium acetate gradient; Bonkovsky *et al.*[19] have used a reversed-phase C_{18} column and similar solvent conditions. Tangerås[20] has separated protoporphyrin and protohemin (**1**) using a reversed-phase C_{18} column and tetrabutylammonium hydrogen sulfate in a water–methanol mixture. Protohemin and protoporphyrin have also been separated on a silica column using methanol–acetonitrile–acetic acid–pyridine as the mobile phase[21]. HPLC techniques have been used to quantitate protoporphyrin and protohemin in mitochondria of mice with porphyria induced by griseofulvin[22] and to analyze levels of heme synthesis in mitochondria[23]. There has been far less study of non-biological iron-containing porphyrins although it has been found that Fe(III) tetrakis(N-methyl-4-pyridyl)porphyrin chloride gives a sharp peak on a LiChrosorb RP-18 column using acetone[24] or ethanol[25] as the mobile phase.

As described above, most of the HPLC methods development work to date centers on protohemin and related iron porphyrins, because these are the most important *in vivo*. However, there is a need to extend this work to a larger variety of iron-containing porphyrins for two reasons. First, there is a good deal of current work involving the isolation and characterization of hemes from a variety of proteins which would be aided by improved isolation and characterization techniques[26–30]. Second, there is an increasing interest in the reconstitution of heme proteins with iron-containing porphyrins to probe structure-function relationships in these proteins. Studies include those of cytochrome b_5[31,32], myoglobin[33], hemoglobin[34], cyto-

* Present address: Department of Chemistry, University of Washington, Seattle, WA 98195, U.S.A.

0021-9673/89/$03.50

chrome *c* peroxidase[35,36] and horseradish peroxidase[37,38]. Finally, the use of positively-charged porphyrins for imaging *in vivo*[39,40], as DNA complexing agents[41] and as electron transfer agents in model systems for photosynthesis and energy storage[42,43] has led us to investigate the purification of these species.

In this paper we report the HPLC characteristics of a variety of ferric porphyrins, both natural (derived from protoporphyrin IX) and synthetic (derived from tetraphenylporphyrin).

EXPERIMENTAL

Apparatus

Chromatography was performed with Beckman 110A/110B solvent delivery modules equipped with a Beckman 160 UV absorbance detector (visible lamp operating at 405 nm), an Axxion 710 HPLC controller, a Hewlett-Packard 3392A integrator and Econosphere silica gel 5-μm or C_8 5-μm columns (150 × 4.4 mm I.D., Alltech). All HPLC solvents were filtered and degassed. The mobile phase flow-rate was 1 ml/min. Sephadex LH-20-100 was from Sigma, 25–100 μm. Optical spectra were taken on a Varian DMS 200 spectrometer.

Porphyrins

Protohemin (**1**) was obtained from Aldrich. The Fe(III) bismethyl esters of the natural hemins were made by inserting iron into the commercially available porphyrins (Midcentury) using the $FeCl_2$–propionic acid method[44]. The Fe(III) bis(glycine ethyl ester) (**3**), biscyclohexylmethyl ester (**4**), cyclic ester (**5**) and monomethyl ester (**6**)[35] protohemin derivatives were made from protohemin with pivaloyl chloride as the condensing reagent[45]. The bispositively-charged porphyrin (**8**) was synthesized by condensing protohemin and $H_2NCH_2CH_2CH_2N(CH_3)_2$ using carbonyldiimidazole to give **7** followed by alkylation of **7** with methyl iodide. Details of the syntheses will be described elsewhere[46]. All compounds based on the protoporphyrin ring system were characterized by thin-layer chromatography (TLC) and NMR[47–49]. Tetrakis (N-methyl-4-pyridyl)porphyrin (TMPyP) tosylate, Fe(III)TMPyP chloride and *trans*-5,10-diphenyl-15,20-di-(N-methylpyridyl)porphyrin chloride (Midcentury) were used as received. The other Fe(III) tetraphenylporphyrin (TPP) derivatives were

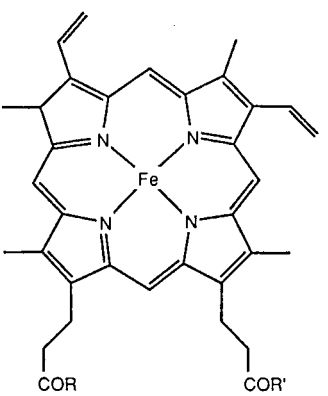

1 R = R′ = OH
2 R = R′ = OCH_3
3 R = R′ = $NHCH_2COOC_2H_5$
4 R = R′ = CH_2-cyclo-C_6H_{11}
5 R - R′ = OCH_2CH_2O
6 R = OH, R′ = OCH_3
7 R = R′ = $NH(CH_2)_3N(CH_3)_2$
8 R = R′ = $NH(CH_2)_3N^+(CH_3)_3$

either purchased from Midcentury Chemicals or synthesized by pyrrole–benzaldehyde condensation in a propionic acid reflux[50]. Iron was inserted using $FeCl_2$ in dimethylformamide[51].

RESULTS AND DISCUSSION

Analysis of hemin esters and Fe(III)TPP derivatives

Some hemins separate well on silica columns. Following earlier work of Bauer and Fornnarino[21], we used an acetonitrile–methanol–acetic acid–pyridine (240:240:1:40) solvent mixture on the silica column. The pyridine in this solvent mixture serves to ligate the positively charged iron; ligation appears to be necessary to move the Fe(III) porphyrins off the column. For complexes with propionic acid side chains, it is necessary to add acid to the eluent to protonate the CO_2^- groups of the porphyrin. Acetic acid served well, retention times decreased (and peaks sharpened) as the amount of acetic acid was increased. The effect of acetic acid on retention time was general, however, and observed also for Fe(III) porphyrins without acid side chains. Loss of iron under HPLC conditions was not observed for any of the compounds investigated. Table I gives the retention times for ferric porphyrins under these conditions.

For protohemin, the longer the complex remained on the column, the broader the peak, as expected for a system undergoing protonation/deprotonation. Under the conditions described in this paper, iron porphyrin diacids remaining on the column longer than about 20 min gave peaks that were so broad as to be almost indistinguishable from baseline. Design of an individual separation scheme must balance the better peak separation at longer times with the increased broadening. Fig. 1 shows the separation of protohemin(**1**) and protohemin bismethyl ester (**2**) under gradient conditions.

Although the acetic acid is necessary to protonate any porphyrin acid side chains in the mixture, it must be noted that the acetic acid can add itself, or promote

TABLE I

RETENTION TIMES OF Fe(III) PORPHYRINS ON SILICA WITH ACETONITRILE–METHANOL–ACETIC ACID–PYRIDINE (240:240:1:40, v/v) MOBILE PHASE

Fe(III) Porphyrins	*Retention time (min)*
Natural Fe(III) porphyrins	
Protohemin bismethyl ester, **2**	19.2
*Meso*hemin bismethyl ester	18.8
Deuterohemin bismethyl ester	20.1
Protohemin bis(glycine ethyl ester), **3**	9.4
Protohemin bis(cyclohexylmethyl) ester, **4**	18.4
Protohemin cyclic ester, **5**	20.4
Tetraphenyl Fe(III) porphyrins	
Tetraphenylporphyrin	18.2
(4-Methyl) tetraphenylporphyrin	17.1
(4-Isopropyl) tetraphenylporphyrin	14.5
(4-Methoxy) tetraphenylporphyrin	16.7
Tetraphenylporphyrin μ-oxodimer	18.5

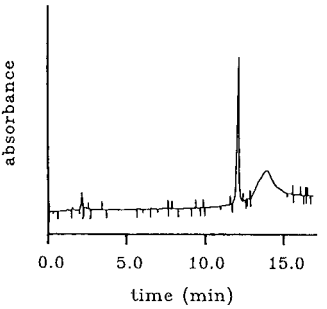

Fig. 1. HPLC trace of Fe(III) protoporphyrin (**1**, 13.7 min) and the corresponding bismethyl ester (**2**, 11.8 min). The solvent system was acetonitrile–methanol–acetic acid–pyridine, held at a ratio of 240:240:1:40 for 5 min and ramped to a ratio of 45:45:10:5 over a 5-min period.

the addition of methanol, to the vinyl groups at the 2 and/or 4 positions. Addition is most easily verified by taking the optical spectrum of a reduced sample in a solution containing enough pyridine to ligate the Fe(II) center fully. These pyridine hemochrome spectra show shifts of the bands that are characteristics of the extent of delocalization of the ring system with the vinyl side chains[52].

The extent of addition of nucleophiles to the heme vinyl groups depends both on the compound and on sample preparation. The vinyl groups of protohemin itself remained intact even after storage of the compound in the HPLC solvent (acetonitrile–methanol–acetic acid–pyridine, 240:240:1:40) for many days (Table II). Protohemin bismethyl ester, however, added one, but not two, nucleophiles during storage in the HPLC solvent (Table II). This type of addition has been observed before[53,54]. When a freshly prepared sample of protohemin bismethyl ester in acetonitrile was subjected to HPLC, the vinyl groups remained intact for the 30 min that the compound remained on the column, as shown by the maxima at 415.6 and 555.6 nm in the visible spectrum of the pyridine hemochrome. Addition of the solvent to the vinyl groups can on occasion make interpretations of results difficult. Changes in substituent at the 2 and 4 positions of the heme periphery can be visualized by HPLC in some instances, *e.g.* deuteroporphyrin bismethyl ester and *meso*porphyrin bismethyl ester can be differentiated readily (Fig. 2).

TABLE II

UV–VIS SPECTRAL CHARACTERISTICS OF SELECTED Fe(III) PORPHYRINS

Compounds	α	β	*Soret*
Freshly prepared protohemin*	555.6	522.8	416.7
Protohemin solution**	554.5	522.8	416.7
Freshly prepared protohemin bismethyl ester*	555.6	522.8	415.6
Protohemin bismethyl ester after HPLC***	555.6	522.8	415.6
Protohemin bismethyl ester solution**	550.8	520.3	413.5
*Meso*hemin bismethyl ester solution**	545.8	516.7	410.1

* Solvent acetonitrile–methanol–acetic acid–pyridine (240:240:1:40, v/v).
** Solid sample dissolved in acetonitrile.
*** Sample in HPLC solvent for 5 days or more.

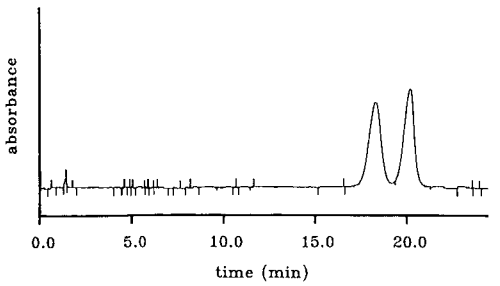

Fig. 2. HPLC trace of Fe(III) *meso*porphyrin bismethyl ester (18.9 min) and Fe(III) deuteroporphyrin bismethyl ester (20.1 min). The solvent system was acetonitrile–methanol–acetic acid–pyridine (240:240:1:40).

Another concern in the ferric porphyrin series is that these molecules can exist either associated with a counterion (*e.g.* chloride) or in an oxygen-bridged dimer, the μ-oxo dimer. Treatment of the ferric porphyrin with acid gives the former species; treatment with aqueous base gives the latter species. We observed no difference in retention time between the Fe(III)Cl and μ-oxo dimer complex of tetraphenylporphyrin, probably because one is converting to the other on the column. Table I gives the retention times for selected derivatives of Fe(III)TPP.

Separation of protohemin, the monoacid monomethyl ester and bismethyl ester

Because the role of the 6- and 7-propionic acid side chains in heme proteins continues to be of interest[31–38,55–57], we were especially interested in using HPLC to characterize the monoacid monomethyl esters of protohemin, **6**. These can be synthesized either by partial esterification of protohemin or by partial hydrolysis of the protohemin bismethyl ester[45]. Either of these techniques gives a mixture of protohemin, the two monoacid monoester derivatives (the 6,7 and 7,6 positional isomers) and the bismethyl ester. All three were separated cleanly using a reversed-phase column, as shown in Fig. 3. No separation of the 6,7 positional isomers were observed on either the silica or reversed-phase columns.

Purification of positively-charged porphyrins and hemins

Initial studies were performed with 5,10-diphenyl-15,20-di-(N-methylpyridyl) porphyrin chloride because this porphyrin has only two positive charges and no central metal. No clear peak was seen on the C_8 column with a gradient between

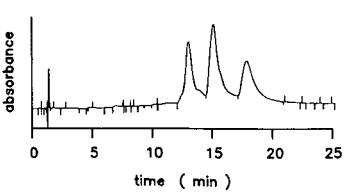

Fig. 3. Separation of protohemin (**1**, 12.9 min), the monoacid monomethyl esters (**6**, 14.9 min) and bismethyl ester (**2**, 17.7 min) on a C_8 5-μm column. A solution of methanol–0.1 *M* ammonium phosphate (30:70) adjusted to pH 3.5 (using concentrated phosphoric acid) was run in a 15-min gradient to 100% methanol and held at 100% methanol for 15 min.

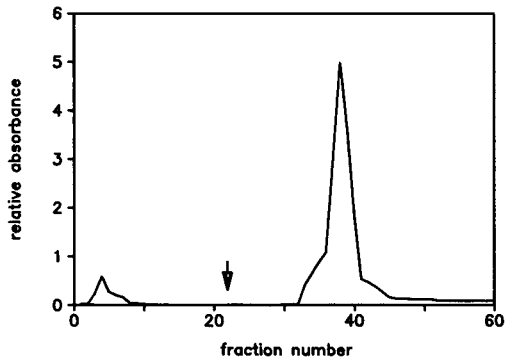

Fig. 4. Separation of a mixture of TMPyP and Fe(III)TMPyP on a Sephadex LH-20 column. Methanol was used as the eluent for the first 22 fractions (elution of TMPyP); saturated aqueous $NaHCO_3$–methanol (15:85) thereafter [elution of Fe(III)TMPyP]. The absorbance was measured at 420 nm. The maximum absorbances for TMPyP and Fe(III)TMPyP are 420.7 nm and 424.4 nm (methanol), respectively.

solution A containing 0.1 *M* potassium acetate adjusted to pH 3.0 with formic acid and solution B containing equal amounts of acetonitrile and water[39] nor with a gradient between aqueous ammonium phosphate and methanol[19]. Similar negative results were obtained using water–acetic acid (50:50) containing 0.35 *M* sodium dodecyl sulfate[58]. A gradient of water–acetic acid (9:1) to water–acetic acid (3:1) ramped over 15 min again gave the same results not only for this porphyrin but also for TMPyP and Fe(III)TMPyP.

Excellent results were obtained, however, using Sephadex LH-20 in standard column chromatography. This has been reported to work very well for TPP quaternized with 1–4 hexadecyl chains[42] and for mixtures derived from the self-condensation of hematoporphyrin[59], but poorly for TMPyP and InTMPyP[39]. We have achieved very good separation of positively charged porphyrins eluting with mixtures of methanol and saturated aqueous $NaHCO_3$. For example, Fig. 4 shows the elution profile of a mixture of the tetrapositively charged TMPyP and its corresponding Fe(III) chelate eluted with 15% saturated aqueous $NaHCO_3$ in methanol; baseline separation is observed, with the porphyrin eluting first. It should be noted that TMPyP can chelate metals and that reproducible results necessitate metal-free solvents.

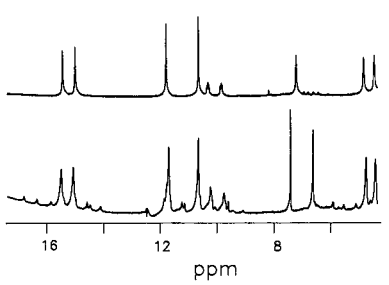

Fig. 5. ^1H NMR of the reaction of **7** with methyl iodide to give the bispositively charged **8**. (Bottom) Reaction mixture after purification by column chromatography on Sephadex LH-20 using only methanol as the eluent. (Top) Reaction mixture after purification on Sephadex LH-20 as described in the text. Spectra were taken of the low-spin biscyano complexes in dimethyl sulfoxide-d_6.

Sephadex LH-20 chromatography is also very useful in purifying positively-charged derivatives of natural porphyrins. For example, methylation of **7** to give **8** is expected to give the protohemin bearing two quaternary ammonium side chains. However, if methylation is incomplete, some of the compound bearing one $-N(CH_3)_3^+$ and one $-N(CH_3)_2$ will be formed. Because there are two positional isomers (6,7 and 7,6 substitution), the ^1H NMR of the methyl region of the low-spin Fe(III) complex shows eight methyl peaks, four each for the two isomers. The bottom trace of Fig. 5 shows a reaction mixture after alkylation and one attempt at purification. The four methyl singlets of the desired bisquaternary salt are seen between 10 and 16 ppm but other peaks in this region indicate the presence of other hemin derivatives as well. The top trace of Fig. 5 shows the same sample after passage though a Sephadex LH-20 column eluting first with methanol and then with 20% saturated aqueous $NaHCO_3$ in methanol; the presence of only four methyl peaks indicates that only the desired bisquaternary salt is present.

ACKNOWLEDGEMENTS

We thank the National Institutes of Health for support of this work (DK 38826). D.W.D. thanks the National Science Foundation for a Career Advancement Award (NSF CHE 8707447).

REFERENCES

1 T. L. Poulos and B. C. Finzel, *Peptide and Protein Reviews*, Vol. IV, Marcel Dekker, New York, 1984, p. 115.
2 P. R. Ortiz de Montellano, *Acc. Chem. Res.*, 20 (1987) 289.
3 F. S. Mathews, *Prog. Biophys. Molec. Biol.*, 45 (1985) 1.
4 M. R. Moore, K. E. L. McColl, C. Rimington and A. Goldberg, *Disorders of Porphyrin Metabolism*, Plenum Medical Book Company, New York and London, 1987.
5 J. Ross and D. Sautner, *Cell*, 8 (1976) 513.
6 S. C. Lo, R. Aft and G. C. Mueller, *Cancer Res.*, 41 (1981) 864.
7 D. N. Ishii and G. M. Maniatis, *Nature (London)*, 247 (1978) 373.
8 J. J. Chen and I. M. London, *Cell*, 26 (1981) 117.
9 K. Tsutsui and G. C. Mueller, *Biochem. Biophys. Res. Commun.*, 149 (1987) 628.
10 A. Verma, J.S. Nye and S. H. Snyder, *Proc. Natl. Acad. Sci. U.S.A.*, 84 (1987) 1.
11 S. H. Snyder, A. Verma and R. R. Trifiletti, *FASEB J.*, 1 (1987) 282.
12 V. J. Dwarki, V. N. K. Francis, G. J. Bhat and G. Padmanaban, *J. Biol. Chem.*, 262 (1987) 16958.
13 G. J. Bhat and G. Padmanaban, *Biochem. Biophys. Res. Commun.*, 151 (1988) 737.
14 R. D. Viestra and M. L. Sullivan, *Biochemistry*, 27 (1988) 3290.
15 T. Yoshida, P. Biro, T. Cohen, R. M. Müller and S. Shibahara, *Eur. J. Biochem.*, 171 (1988) 457.
16 I. Z. Ades, T. M. Stevens and P. D. Drew, *Arch. Biochem. Biophys.*, 253 (1987) 297.
17 L. J. DeFilippi and D. E. Hultquist, *Biochim. Biophys. Acta*, 498 (1977) 395.
18 C. K. Lim, J. M. Rideout and T. J. Peters, *J. Chromatogr.*, 317 (1984) 333.
19 H. L. Bonkovsky, S. G. Wood, S. K. Howell, P. R. Sinclair, B. Lincoln, J. F. Healy and J. F. Sinclair, *Anal. Biochem.*, 155 (1986) 56.
20 A. Tangerås, *J. Chromatogr.*, 310 (1984) 31.
21 J. Bauer and J. Fornnarino, *J. Chromatogr.*, 283 (1984) 378.
22 A. Tangerås, *Biochim. Biophys. Acta*, 882 (1986) 77.
23 A. Tangerås, *Biochim. Biophys. Acta*, 843 (1985) 199.
24 K. Saitoh, M. Kobayashi and N. Suzuki, *J. Chromatogr.*, 243 (1982) 291.
25 N. Suzuki, T. Takeda and K. Saitoh, *Chromotographia*, 22 (1986) 43.
26 M. J. Chatfield, G. N. La Mar and R. J. Kauten, *Biochemistry*, 26 (1987) 6939.

27 L. L. Bondoc, M. H. Chau, M. A. Price and R. Timkovich, *Biochemistry*, 25 (1986) 8458.
28 C. K. Chang, R. Timkovich and W. Wu, *Biochemistry*, 25 (1986) 8447.
29 W. A. Oertling, H. Hoogland, G. T. Babcock and R. Wever, *Biochemistry*, 27 (1988) 5395.
30 A. W. Nichol, L. A. Angel, T. Moon and P. S. Clezy, *Biochem. J.*, 247 (1987) 147.
31 M. R. Mauk, A. G. Mauk, P. C. Weber and J. B. Matthew, *Biochemistry*, 25 (1986) 7085.
32 M. R. Mauk, A. G. Mauk, P. C. Weber and J. B. Matthew, *Biochemistry*, 26 (1987) 974.
33 S. Neya and N. Funasaki, *J. Biol. Chem.*, 262 (1987) 6725.
34 K. Miki, Y. Ii, M. Yukawa, A. Owatari, Y. Hato, S. Harada, Y. Kai, N. Kasai, Y. Hata, N. Tanaka, M. Kakudo, Y. Katsube, K. Kawave, Z. Yoshida and H. Ogoshi, *J. Biochem. (Tokyo)*, 100 (1986) 269.
35 T. Asakura and Y. Yonetani, *J. Biol. Chem.*, 244 (1969) 4573.
36 S. L. Edwards, N. H. Xuong, R. C. Hamlin and J. Kraut, *Biochemistry*, 26 (1987) 1503.
37 T. Araiso and H. B. Dunford, *Arch. Biochem. Biophys.*, 211 (1981) 346.
38 A. Shinohara, T. Kamataki, T. Iizuka, Y. Ishimura, H. Ogoshi and K. Okuda, *Jpn. J. Pharmacol.*, 45 (1987) 107.
39 G. A. Duff, S. A. Yeager, A. K. Singhal, B. C. Pestel, J. M. Ressner and N. Foster, *J. Chromatogr.*, 416 (1987) 71.
40 G. D. Robinson, A. Alavi, R. Vaum and M. Staum, *J. Nucl. Med.*, 27 (1986) 239.
41 J. A. Strickland, D. L. Banville, W. D. Wilson and L. G. Marzilli, *Inorg. Chem.*, 26 (1987) 3398; and references therein.
42 Y. Okuno, W. E. Ford and M. Calvin, *Synthesis*, (1980) 537.
43 J. Davila, A. Harriman, M.-C. Richoux and L. R. Milgrom, *J. Chem. Soc., Chem. Commun.*, (1987) 525; and references therein.
44 C. K. Chang, R. K. DiNello and D. Dolphin, *Inorg. Synth.*, 20 (1980) 147.
45 T. G. Traylor, C. K. Chang, J. Geibel, A. Berzinis, T. Mincey and J. Cannon, *J. Am. Chem. Soc.*, 101 (1979) 6716.
46 D. W. Dixon and M. S. Kim, in preparation.
47 A. Shirazi, M. Barbush, S. B. Ghosh and D. W. Dixon, *Inorg. Chem.*, 24 (1985) 2495.
48 D. W. Dixon, M. Barbush and A. Shirazi, *Inorg. Chem.*, 24 (1985) 1081.
49 G. N. La Mar, G. R. Eaton, R. H. Holm and F. A. Walker, *J. Am. Chem. Soc.*, 95 (1973) 63.
50 A. D. Adler, F. R. Longo, J. D. Finarelli, J. Goldmacher, J. Assour and L. Korsakoff, *J. Org. Chem.*, 32 (1967) 476.
51 A. D. Adler, F. R. Longo and V. Varadi, *Inorg. Synth.*, 16 (1976) 213.
52 J. H. Fuhrhop and K. M. Smith, in J. H. Fuhrhop and K. M. Smith (Editors), *Porphryins and Metalloporphyrins*, Elsevier, New York, 1975, p. 804.
53 P. S. Clezy, T. T. Hai, R. W. Henderson and L. van Thuc, *Aust. J. Chem.*, 33 (1980) 585.
54 R. Bonnett, R. J. Ridge, P. A. Scourides and M. C. Berenbaum, *J. Chem. Soc., Perkin Trans. 1*, (1981) 3135.
55 N. K. Rogers and G. R. Moore, *FEBS Lett.*, 228 (1988) 69.
56 P. P. Tamburini and J. B. Schenkman, *Arch. Biochem. Biophys.*, 245 (1986) 512.
57 A. J. Mathews and T. Brittain, *Biochem. J.*, 243 (1987) 379.
58 S. Igaraski, M. Nakano and T. Yotsuyanagi, *Bunseki Kagaku*, 32 (1983) 67; *C.A.*, 98 (1983) 155516a.
59 D. Kessel, *Photochem. Photobiol.*, 44 (1986) 193.

Journal of Chromatography, 462 (1989) 419–425
Elsevier Science Publishers B.V., Amsterdam — Printed in The Netherlands

CHROM. 21 056

Note

Confirmation of domoic acid in molluscan shellfish by chemical derivatization and reversed-phase liquid chromatography

JAMES F. LAWRENCE*, CLAUDETTE F. CHARBONNEAU, B. DENIS PAGE and GLADYS M. A. LACROIX

Food Research Division, Bureau of Chemical Safety, Food Directorate, Health Protection Branch, Ottawa, Ontario K1A 0L2 (Canada)

(Received October 4th, 1988)

Domoic acid (Fig. 1), a neurotoxic amino acid originally isolated from the red alga, *Chondria armata*[1,2] was found to be the toxic substance in contaminated mussels from Prince Edward Island in eastern Canada[3].

Analytical methodology employed for its determination at low μg/g levels has involved either hot acid or water extraction of the sample followed by dilution, filtration and chromatographic analysis using reversed-phase liquid chromatography (LC)[4,5]. Detection of the substance was by UV absorption at 242 nm, the absorbance maximum of the compound. Under the conditions employed, less than 1 μg/g of domoic acid could be detected in mussels, clams and oysters. However, confirmation of positive results are often necessary particularly if the levels are high enough to be a health concern. To date the only means of confirming domoic acid is either to collect the isolated substance by LC and perform mass spectrometric (MS) analysis or to use a diode array detector to obtain a complete UV spectrum of the eluting peak. The latter does not provide an unequivocal identification since many compounds have absorption maxima near 242 nm. Also, few laboratories are equipped with this type of detector.

An alternative approach is to prepare a chemical derivative and reanalyse the sample with comparison to a known standard carried through the same reaction procedure. The present work evaluates two derivatization techniques for domoic acid and applies them to mussel tissue. One involves the formation of the phenyl isothiocyanate (PITC) derivative of the amino moiety and the other, an esterification of the three carboxylic acid groups.

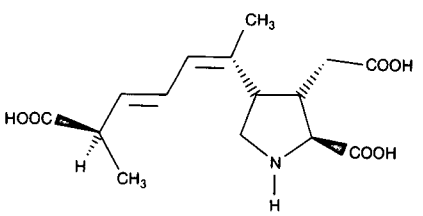

Fig. 1. Structure of domoic acid.

0021-9673/89/$03.50

EXPERIMENTAL

Reagents

Domoic acid was obtained from the National Research Council's Atlantic Research Laboratory (Halifax, Canada). Solutions were prepared in twice deionized water (Milli-Q, Millipore, Bedford, MA, U.S.A.). Phenyl isothiocyanate was obtained from Pierce. Triethylamine was obtained from Aldrich (99+%, Gold Label). Acetonitrile was HPLC-grade. All other solvents and chemicals were analytical reagent grade materials. All standard and sample solutions were refrigerated when not in use. Acetyl chloride (Gold Label) was obtained from Aldrich.

Preparation of derivatization reagent solutions

The PITC reagent was prepared fresh daily as for normal amino acid analysis by mixing 200 μl of methanol, 50 μl triethylamine, 50 μl water and 20 μl PITC.

The esterification reagent was prepared as described earlier[6] by adding 10 ml of isopropanol into a 30-ml headspace vial which was then sealed with a silicone septum. A disposable syringe needle was inserted through the septum and left as a vent. The contents were cooled in an ice bath, then 3 ml acetyl chloride added slowly using a 5-ml glass-bodied syringe, swirling the mixture during addition. The vent, seal and septum were removed and immediately loosely replaced with a new seal and septum. The headspace was briefly flushed with nitrogen and the container quickly sealed. This solution was used for the derivatization.

Liquid chromatography

The direct LC determination of domoic acid was carried out isocratically exactly as described earlier[5]. The LC system consisted of a Model 110B pump (Beckman) a 20-μl loop injector (Beckman), a Supelcosil LC-18 column (15 cm × 4.6 mm I.D., 5 μm), a variable-wavelength UV detector (Micrometrics) set to 242 nm and an integrating recorder (Varian). The mobile phase was acetonitrile–water (12:88, v/v) adjusted to pH 2.5 with 2% (v/v) orthophosphoric acid, degassed and filtered before use. The flow-rate was 1.0 ml/min.

The same system was employed for the PITC derivatives but using a mobile phase of acetonitrile–water (32.5:67.5) at pH 2.5. Reagent peaks were eluted from the column by washing the column using a step gradient of 99.8% acetonitrile from 10 to 16 min, then reequilibrating for 5 min before the next analysis. For the ester derivatives, gradient elution was used with a Supelcosil LC-18 column (as above) with an initial mobile phase of 0.02 *M* phosphate buffer, pH 3, containing 0.02% triethylamine changing linearly to 100% acetonitrile from 0 to 15 min.

Sample extraction

Mussel tissue was extracted by boiling the homogenized sample with an equal weight of 0.1 *M* hydrochloric acid for 5 min. The mixture was quickly cooled and centrifuged. An aliquot of the clear supernatant was diluted with water for direct LC analysis. Details of this procedure are published elsewhere[5].

Clean-up procedure for derivatization

Both derivatization procedures required additional sample clean-up before car-

rying out the reactions. The reason for this was to remove the abundance of coextracted amino acid and other proteinaceous material in the initial sample extracts. These substances interfered in the determinations of the derivatives by producing an intractable tar, consuming reagent and/or yielding interfering peaks in the resulting chromatograms.

The clean-up was carried out by passing 1 ml of undiluted clear supernatant from the extraction above, through a 1-ml phenylsulfonic acid strong cation-exchange solid phase extraction cartridge (Baker). (The cartridge was preconditioned with 6 ml of methanol followed by 6 ml of 0.1 *M* hydrochloric acid.) The sample effluent was discarded and the cartridge rinsed with 3 ml of water which was also discarded. The cartridge was then dried by aspiration. The domoic acid was eluted with two 3-ml volumes of 0.5 *M* hydrochloric acid, the first 3 ml being allowed to remain in the cartridge for 5 min before elution. The last drops of hydrochloric acid were forced from the cartridge by pushing air through it. The 0.5 *M* hydrochloric acid was collected and further cleaned up as follows.

A 1-ml octadecyl (3 ml reservoir) cartridge (Baker) was conditioned with 6 ml of methanol followed by 6 ml of water and finally 6 ml of 0.5 *M* hydrochloric acid ensuring that the cartridge did not run dry after the last wash. The combined acid fraction from the phenylsulfonic acid cartridge was transferred to the octadecyl cartridge and passed through at *ca.* 2 ml/min. The effluent was discarded. The cartridge was then washed with 3 ml of water which was discarded and all remaining water forced from the column with air. The domoic acid was eluted with 2 ml of 20% acetonitrile in water (1% acetic acid) after allowing it to remain in the cartridge for 1 min. After this another 2 ml were passed through the cartridge and collected, forcing out the last few drops with air. These fractions were combined and used for derivatization.

Phenyl isothiocyanate derivatization

A 0.2–1.0 ml aliquot of the cleaned up extract (enough to yield 1–10 μg domoic acid) was evaporated to dryness in a 2-ml culture tube under nitrogen, in a water bath at 50°C. After this, 50 μl of PITC derivatization solution were added and the tube swirled to ensure that the reagent wets the residue. The contents were permitted to react at room temperature for 20 min, swirling the tube after 10 min. The contents were then evaporated to dryness in a water bath at 40°C under nitrogen for about 20 min to ensure that excess reagent was evaporated. The residue was dissolved in 1 ml of water by strirring on a vortex mixer for 1 min. The solution was filtered (0.45 μm) before injection into the LC system.

Esterification

A 1-ml aliquot of the cleaned up extract was evaporated to dryness in a 15-ml graduated centrifuge tube, under nitrogen, at 50°C. A 1.0-ml volume of methylene chloride was added and evaporated to dryness to remove the last traces of water. After this, 0.6 ml of esterification solution was added using a syringe. The tube was stoppered tightly with a plastic cap, vortexed for 1 min to dissolve or suspend the residue and heated for 30 min at 100°C in an oil bath with the liquid level of the bath at that of the tube contents. The tube was then cooled to room temperature and the contents evaporated just to dryness under nitrogen at 35°C (higher temperatures and

unnecessarily long evaporation times led to derivative losses). The residue was dissolved in 1 ml of acetonitrile–water (1:1), filtered (0.45 μm) and analysed by LC.

RESULTS AND DISCUSSION

The PITC derivatization was found to work well for domoic acid. Although structural confirmation by MS was not carried out it is most probable that the PITC reacts with domoic acid in an analogous fashion to other amino acids[7]. However, under the conditions employed, several large reagent peaks were always present in the chromatograms and eluted after the domoic acid derivative.

Fig. 2 compares results obtained for a cleaned up mussel extract, before and after PITC derivatization, employing gradient elution to enable the detection of both free and derivatized domoic acid on the same chromatogram. (Conditions, 10–64% acetonitrile in water, pH 3, from 0 to 12 min; 64–99.8% acetonitrile in water from 12 to 16 min.) It can be seen that the original domoic acid peak (6 min) has disappeared and the derivative peak is observed at *ca.* 10.5 min. Quantitatively, the conversion to the derivative was always greater than 90% under the reaction conditions used. For routine confirmation of domoic acid in mussel tissue, an isocratic system was employed as described in the experimental section. Fig. 3 shows chromatograms obtained under isocratic conditions for a reagent blank, a mussel blank and a mussel tissue spiked with 19 ppm domoic acid, all after derivatization. The derivatized compound can be clearly observed at this level. The confirmation limit was estimated to be 2–5 μg/g domoic acid in mussel tissue depending upon quantity of extract injected. The absolute sensitivity of the detector to the derivative is the same as for domoic acid itself since the chromophoric group responsible for the absorption at 242 nm is unchanged.

During the investigation of the esterification reaction; a series of alcohols were evaluated. Fig. 4 shows a chromatogram of the separation of a mixture of the trialkyl-

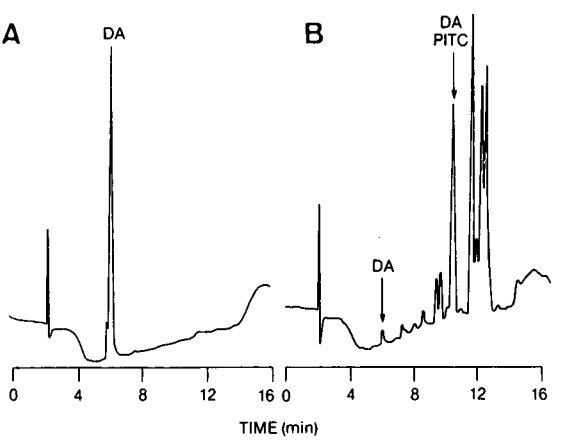

Fig. 2. Chromatograms of domoic acid in contaminated mussel tissue (380 μg/g) before (A) and after (B) PITC derivatization. Gradient conditions as described in the text. Detector, 242 nm, 0.16 absorbance units full scale. Chromatogram A, 126 ng domoic acid injected. Chromatogram B, 95 ng equivalent domoic acid injected.

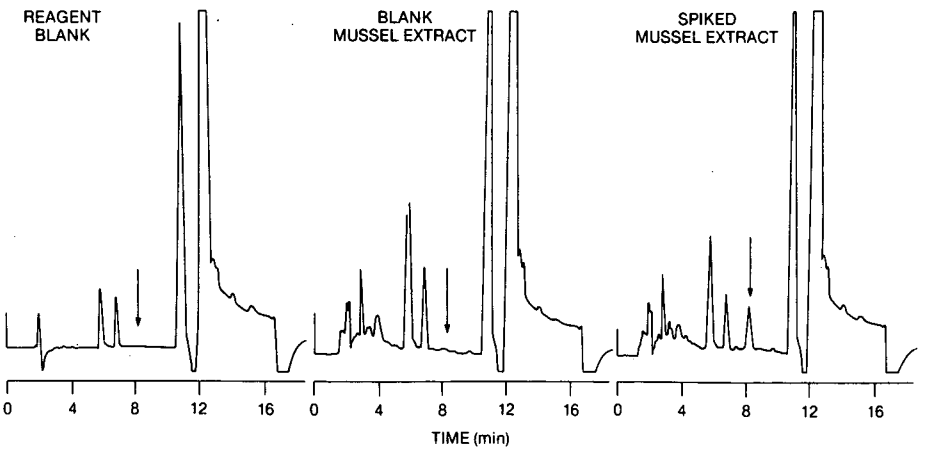

Fig. 3. Isocratic chromatograms of a reagent blank, a control mussel extract and the same extract spiked at 19 μg/g domoic acid, after PITC derivatization. The arrow indicates retention time of domoic acid. Mobile phase as described in the text. Other conditions as in Fig. 2.

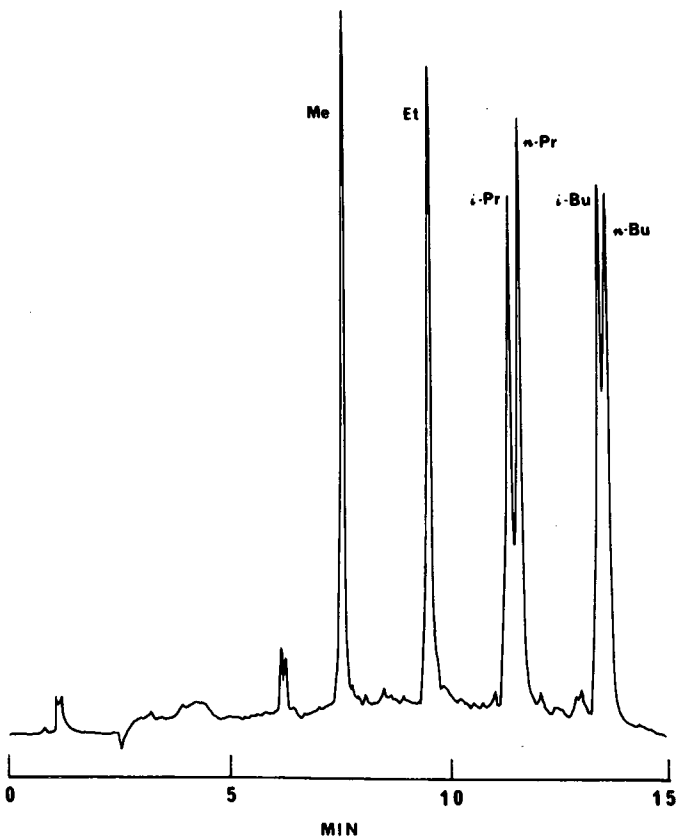

Fig. 4. Chromatogram of a mixture of trialkyl ester derivatives of domoic acid. Methyl (Me), ethyl (Et), isopropyl (i-Pr), *n*-propyl (*n*-Pr), isobutyl (i-Bu) and *n*-butyl (*n*-Bu) derivatives. Conditions as described in the text. Detector, 242 nm, underivatized domoic acid elutes at 4.5 min.

esters obtained using six different alcohols. The trialkyl derivatives were confirmed by gas chromatography–MS after formation of the N-trifluoracetyl derivative[6]. For routine work, the isopropyl triester was employed although the others would also be suitable.

Fig. 5 shows the application of the esterification to the confirmation of domoic acid in mussel tissue at 308 μg/g after the solid phase extraction clean-up. The triisopropyl ester is easily observed at this concentration. A small amount of triethylamine was required in the mobile phase to produce reproducible chromatography. Once the carboxylic acid groups are esterified the molecule becomes basic, thus necessitating the amine to prevent tailing. The detection limit under these conditions was estimated to be in the low μg/g range, similar to underivatized domoic acid. The absolute detector response of the derivative was similar to the parent domoic acid both in terms of molar absorbtivity and UV spectra. All trialkyl derivatives had spectra virtually identical to the undervatized domoic acid. (Determined using an LKB diode array detector under identical chromatography conditions.) This is ex-

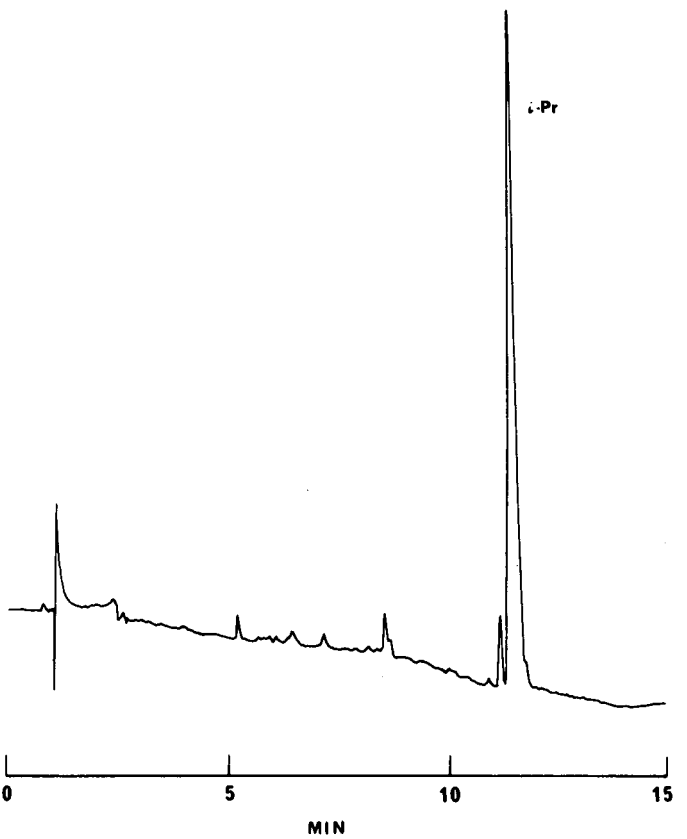

Fig. 5. Chromatogram of an extract of contaminated mussel (308 μg/g) after clean-up and esterification hydrochloric acid–isopropanol. Conditions as described in the text. i-Pr = Isopropyl.

pected since the chromophoric group is not appreciably affected by the esterification. Thus the actual detection limits should be similar to the parent domoic acid.

The above described derivatization procedures offer two independent means (derivatives at the –N or –COOH moiety) of confirming domoic acid residues in mussel extracts. The procedure should be applicable to other molluscan shellfish after solid phase extraction clean-up of the extracts.

REFERENCES

1 T. Takemoto, K. Daigo, Y. Kondo and K. Kondo, *Yakugaku Fasahi,* 86 (1966) 874.
2 M. Maeda, T. Kodama, T. Tanaka, H. Yoshizumi, T. Takemoto, K. Nomoto and T. Fujita, *Chem. Pharm. Bull.,* 34 (1986) 4892.
3 J. L. C. Wright, R. K. Boyd, A. S. W. de Freitas, M. Falk, R. Foxall, W. D. Jamieson, M. V. Laycock, A. W. McCulloch, A. G. McInnes, P. Odense, V. Pathak, M. A. Quilliam, M. Ragan, P. G. Sim, P. Thibault, J. A. Walter, M. Gilgan, D. Richard and D. Dewar, *Can. J. Chem.*, submitted for publication.
4 M. A. Quilliam P. G. Sim, A. W. McCulloch and A. G. McInnes, *Int. J. Environ. Anal. Chem.*, submitted for publication.
5 J. F. Lawrence, C. F. Charbonneau, C. Ménard, M. A. Quilliam and P. G. Sim, *J. Chromatogr.*, 462 (1989) 349.
6 R. W. Zumwalt, J. Desgres, K. C. Kuo, J. E. Pautz and C. W. Gehrke, *J. Assoc. Off. Anal. Chem.*, 70 (1987) 253.
7 B. A. Bidlingmeyer, S. A. Cohen, T. L. Tarvin and B. Frost, *J. Assoc. Off. Anal. Chem.*, 70 (1987) 241.

Journal of Chromatography, 462 (1989) 426–429
Elsevier Science Publishers B.V., Amsterdam — Printed in The Netherlands

CHROM. 21 033

Note

Determination of morpholinosulphenylbenzothiazole by high-performance liquid chromatography

M. PETRO* and K. ĎULÁK
Research Institute of Chemical Technology, 836 03 Bratislava (Czechoslovakia)
(Received October 3rd, 1988)

Morpholinosulphenylbenzothiazole (BT-S-MOR) is an important industrially produced vulcanization accelerator (rubber adjuvant) available commercially under names as Vulcafor MBS, Sulfenamid M, Santocure MOR, etc.

Non-selective methods for the determination of this compound in the technical product have been reported[1,2]. We have found that BT-S-MOR can be determined by acidimetric titration (unpublished work). Although high-performance liquid chromatographic (HPLC) methods have been described for the determination of BT-S-MOR and its most frequently occuring impurities[3,4], HPLC is not applicable to the study of the formation of this compound in aqueous medium without previous modification of the sample.

The development of reversed-phase liquid chromatographic columns for the separation of closely related compounds led us to investigate a new method for the determination of BT-S-MOR and by-products. The method can be used for checking the waste water and the composition of solid waste during the production process.

EXPERIMENTAL

Chromatographic equipment

All separations were carried out using a Varian Model 2210 isocratic system, which includes a Model 2010 pump, Model 2050 variable-wavelength UV detector, Model 2081 column/valve mounting module and a Rheodyne injector. Retention data and peak areas were measured and calculated by a Model SP 4200 computing integrator (Spectra-Physics).

Chemicals

The chemicals were of analytical-reagent grade. Solvents were freshly distilled before use and were purified by recommended methods[5]. The standards used (Table I) were prepared by the Division of Organic Chemistry in this Institute according to standard procedures. Their purities and structures were established by elemental analysis and standard physico-chemical techniques.

Mobile phase

The mobile phase was acetonitrile–ammonium acetate solution (65:35, v/v).

0021-9673/89/$03.50

The solution of ammonium acetate was prepared by dissolving 6 g of anhydrous ammonium acetate in water and diluting to 1 l.

Standard solutions

Standard solutions were prepared in the range 1–10 mg per 50 ml. Stock solutions of BT-SH, BT-SO-MOR, BT-SO_2-MOR, BT-MOR, BT-S-MOR and BT-S-S-MOR were first prepared by dissolving 100 mg of the appropriate compound in 50 ml of acetonitrile, then working standards were prepared by dilution of the stock solutions. The stock solutions were stable for up to 10 days when stored in a refrigerator. The refrigerated standards were brought to room temperature prior to their injection into the chromatograph.

Sample solution

For the analysis of accompanying compounds in technical BT-S-MOR, a 500-mg sample was accurately weighed into a 50-ml volumetric flask, dissolved and diluted to volume with acetonitrile. Waste water was injected directly, without dilution. All sample solutions were filtered through a 20-μm syringe filter (Nalgene Labware) before injection on to the column.

Chromatographic procedure

The separations were performed in the isocratic mode at ambient temperature at a flow-rate of 0.8 ml/min (inlet pressure *ca.* 200 atm). Volumes of 10 μl of the solutions were introduced on to the column with a constant-volume loop injector. The detector was operated at 280 nm (1.28 a.u.f.s.) and the chart speed was 0.25 cm/min.

Calculation

Calibration graphs were generated by plotting the peak-height ratio *versus* the concentration of standard substances in the concentration range 20–200 μg/ml. In all instances the calibration graphs were linear with a correlation coefficient of 0.998 and passed through the origin. Values of unknown sample concentrations were determined by comparison with the calibration graph.

RESULTS AND DISCUSSION

Combinations of methanol, acetonitrile and water were evaluated as mobile phases. A solvent containing acetonitrile and aqueous ammonium acetate (65:35) was found to be the most successful. This mobile phase allowed the isocratic elution of the compounds listed in Table I well within 18 min. A representative chromatogram of synthetic mixture is shown in Fig. 1.

In contrast to the most frequently occuring impurities BT-MOR and BT-SO-MOR, BT-SH[6–15] has its absorption maximum at 325 nm. Therefore, to achieve the maximum detectability of BT-SH it is advantageous to use dual- or variable-wavelength detection. Under the conditions used, as little as 1 mg/l of BT-S-MOR, BT-SO-MOR, BT-MOR and BT-SH can be determined in waste water without previous treatment of the sample.

In order to evaluate different analytical procedures, we compared the proposed

TABLE I

NAMES AND STRUCTURES OF STANDARDS USED

Name	*Structure*	*Abbreviation*	*Retention time (min)*
2-Mercaptobenzothiazole	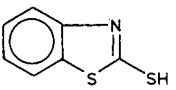	BT-SH	4.46
Morpholinosulphinylbenzothiazole	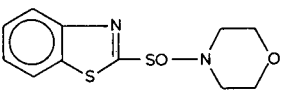	BT-SO-MOR	5.27
Morpholinosulphonylbenzothiazole	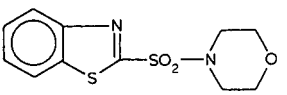	BT-SO_2-MOR	6.06
Morpholinobenzothiazole	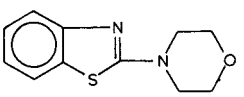	BT-MOR	7.01
Morpholinosulphenylbenzothiazole	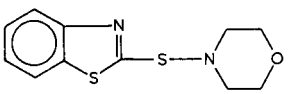	BT-S-MOR	10.49
Morpholinodithiobenzothiazole	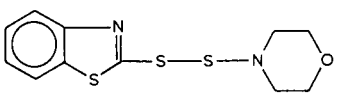	BT-S-S-MOR	16.23

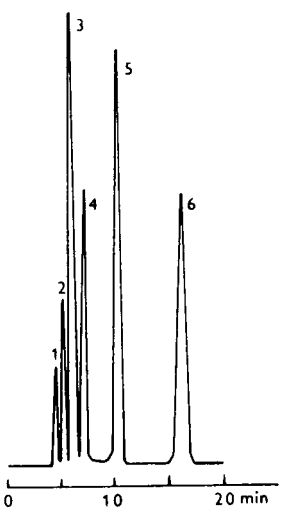

Fig. 1. High-performance liquid chromatogram of a synthetic mixture. Column, 300 × 4 mm I.D. Micro-Pak MCH-5-N-Cap; eluent, acetonitrile–ammonium acetate solution (65:35, v/v); flow-rate, 0.8 ml/min; detection, UV (280 nm). Peaks: 1 = BT-SH; 2 = BT-SO-MOR; 3 = BT-SO_2-MOR; 4 = BT-MOR; 5 = BT-S-MOR; 6 = BT-S-S-MOR.

HPLC method with the titrimetric method. The latter method gave higher results.

Although the proposed method is simple, sensitive and reliable for the analysis of the technical product, of the reaction mixture in morpholine–water medium and for checking technological wastes (filtrates, distillation residues, waste water, etc.), it is not suitable for the determination of benzothiazyl disulphide (BT-S-S-BT) because of its poor solubility in polar solvents.

REFERENCES

1 N. N. Mikhailova, Z. K. Timokhina and L. A. Panova, *Zh. Anal. Khim.*, 26 (1971) 2248.
2 *Technical Service Report, No. LR 73/52*, Monsanto, St. Louis, MO, 1973.
3 S. Vertalier, M. C. Caude and J. L. Millet, *Analusis*, 7 (1979) 441.
4 T. F. Petrova, M. P. Ivanova and A. A. Lapschova, *Kauch. Rezina*, 12 (1983) 29.
5 J. A. Riddick and W. B. Burger, *Techniques of Chemistry, Vol. II, Organic Solvents*, Wiley-Interscience, New York, 3rd ed., 1970.
6 W. R. Biggs and J. C. Fetzer, *J. Chromatogr.*, 260 (1983) 137.
7 H. Henke, *J. Chromatogr.*, 254 (1983) 296.
8 J. Shinohara, R. Shinohara, S. Eto and T. Hori, *Bunseki Kagaku*, 27 (1978) 716.
9 S. Eto, R. Shinohara, A. Kido and T. Hori, *Bunseki Kagaku*, 29 (1980) 213.
10 D. P. Lopes and J. A. Galoway, *J. Chromatogr. Sci.*, 20 (1982) 533.
11 C. B. Airando, A. Assaf, A. Gayte-Sorbier, G. Salmona and E. J. Vincent, *Anal. Chim. Acta*, 166 (1984) 221.
12 G. Blosczyk and H. J. Doemling, *Lebensmittelchem. Gerichtl. Chem.*, 36 (1982) 90.
13 J. S. Warner, T. M. Engel and P. J. Mondron, *Report, 600/4-85/026*, U.S. Environmental Protection Agency, 1985.
14 A. B. Sullivan, E. Morita and R. I. Leib, *Rubber World*, 195 (1986) 21.
15 R. N. Datta and D. K. Basu, *Rubber Chem. Technol.*, 59 (1986) 27.

Journal of Chromatography, 462 (1989) 430–434
Elsevier Science Publishers B.V., Amsterdam — Printed in The Netherlands

CHROM. 21 035

Note

High-performance liquid chromatographic determination of ethiofencarb and its metabolic products

PAOLO CABRAS*, MARCO MELONI and ANTONIO PLUMITALLO
Istituto di Chimica Farmaceutica Tossicologica ed Applicata, Viale A. Diaz 182, 09100 Cagliari (Italy)
and
MARA GENNARI
Istituto di Chimica Agraria, Via P. Giuria 15, 10126 Torino (Italy)
(Received September 29th, 1988)

Ethiofencarb (I) is a systemic insecticide with a specific action against aphids; it is mainly adsorbed by roots and translocated to the aerial part of the plant[1], where it is quickly converted into its sulphoxide (II) and, more slowly, sulphone (III) derivatives (Fig. 1). The same metabolic pathway is observed in soil, whereas in water it is mainly (90%) transformed into the corresponding phenol (IV) by hydrolysis of the carbamic group[2]. Phenolic derivatives, produced by hydrolysis of the carbamic

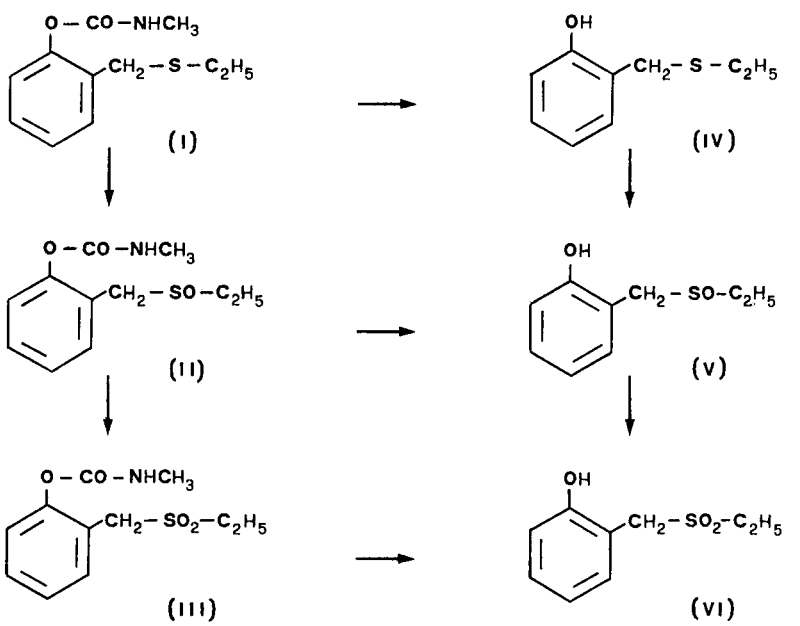

Fig. 1. Metabolic pathway of ethiofencarb in plant, soil, water and animals.

0021-9673/89/$03.50

group, have also been found in animals; the major metabolites are the phenol sulphoxide (V) and phenol sulphone (VI)[3].

Residues of ethiofencarb and its metabolites have been determined by chromatography, by oxidation of the active ingredient and its sulphoxide to the sulphone[4] and by thin-layer chromatography of labelled products[5]. The Drager method was optimized, which allowed the individual determination of ethiofencarb and the sulphoxide and sulphone after separation of the active ingredient from its metabolites with different solvents (light petroleum for ethiofencarb and chloroform for the metabolites). The same oxidative process was used for their determination[6]. Wuest and Meier[7] determined ethiofencarb by capillary chromatography, without any derivatization. A high-performance liquid chromatographic (HPLC) method with electrochemical detection[8] was applied to the determination of the active ingredient after alkaline hydrolysis of its carbamic group to give the phenol derivative (IV).

In this paper the HPLC determination of ethiofencarb and its metabolites (II–VI) without any derivatization or solvent fractioning is described.

EXPERIMENTAL

Apparatus

A Varian (Varian, Palo Alto, CA, U.S.A.) Model 5020 liquid chromatograph equipped with a variable-wavelength UV 100 UV–VIS detector, a Rheodyne injector (50-μl loop) and a Hewlett-Packard 3390A reporting integrator was used.

Chromatography

Hibar RP-18 (Merck, Darmstadt, F.R.G.), Erbasil 10 C_8/H (Carlo Erba, Milan, Italy) and Violet RP-2 (Violet, Rome, Italy) columns (250 × 4.0 mm I.D., 10 μm) were employed. The mobile phase was water–acetonitrile at a flow-rate of 1.0 ml/min. Based on the UV spectra, 190 nm was chosen for the simultaneous determination of all compounds.

Chemicals

Acetonitrile and dichloromethane were HPLC grade solvents (Carlo Erba); water was distilled twice and filtered throughout a Milli-Q apparatus (Millipore, Milan, Italy) before use. Ethiofencarb (2-[(ethylthio)methyl]phenyl methylcarbamate) was an analytical standard purchased from Eherenstorfer (Augsburg, F.R.G.). The 2-[(ethylsulphinyl)methyl]phenyl methylcarbamate (sulphoxide) and the 2-[(ethylsulphonyl)methyl]phenyl methylcarbamate (sulphone) were synthesized by oxidation of the technical active ingredient (extracted by the commercial formulation Croneton 10 Granulare, Bayer AG, containing 10% ethiofencarb) using hydrogen peroxide as oxidizing agent. The sulphoxide was obtained by performing the reaction with stirring at room temperature in methanol for 3 h in the presence of catalytic amounts of ammonium molybdate; the sulphone was obtained in the same way, but with refluxing for 2 h in methanol. Then the reaction mixture was diluted with water and extracted with chloroform. The chloroform layers were dried and evaporated to give the crude sulphone or sulphoxide.

2-[(Ethylthio)methyl]phenol (phenol), 2-[(ethylsulphinyl) methyl]phenol (phenolsulphoxide) and 2-[(ethylsulphonyl)methyl]phenol (phenolsulphone) were ob-

tained by hydrolysis of the corresponding N-methylcarbamate with 3% methanolic potassium hydroxide solution.

All the products (carbamates and phenols) were purified by chromatography on a column of silica gel eluted with suitable benzene–acetone mixtures and their identities were confirmed by IR and ^{1}H NMR spectroscopy.

Extraction procedure

After trituration and homogenization, 25 g of lettuce sample were weighed in a 250-ml screw-capped flask, 50 ml of dichloromethane (or methanol for the phenol IV) were added and the mixture was agitated in a flask-shaker (Stuart Scientific) for 30 min. The organic layer was separated and dehydrated with sodium sulphate; 2 ml were then dried in a thermo-ventilated stove at 30°C, taken up in 1 ml of eluent and injected for HPLC analysis.

RESULTS AND DISCUSSION

A good separation of ethiofencarb (I) and the sulphoxide (II) and sulphone (III) derivatives was achieved using an RP-18 column with water–acetonitrile (50:50, v/v) as eluent (Table I). The separation of the active ingredient and the metabolites was improved by increasing the water content to 60%; only the peaks of the sulphone (III) and the phenol sulphone (VI) derivatives were not enough separated. A further increasing in the water content (to 70%) gave a better separation of metabolites II, III, V and VI, but the retention times of I and IV were too long and their peaks were not sharp enough.

A reduction in retention times was obtained by replacing water with a 10^{-3} *N* sulphuric acid (pH 3.0) in the eluent, but the separation was not improved. The use of methanol instead of acetonitrile in the eluent mixture reversed the elution order of the sulphoxides (II and V) and sulphones (III and VI), but the peaks were less sharp than

TABLE I

RETENTION TIMES OF ETHIOFENCARB (I) AND ITS METABOLITES (II–VI) USING DIFFERENT COLUMNS AND MOBILE PHASE COMPOSITIONS

Column	*Water–acetonitrile composition*	*Retention time (min)*					
		II	*V*	*III*	*VI*	*I*	*IV*
RP-18	50:50	2.45		2.88		6.06	
	60:40	2.65	2.97	3.27	3.40	9.02	10.66
	70:30	3.36	3.76	4.40	4.67	20.02	24.46
C_8/H	60:40	3.32	3.55	4.03	4.23	9.86	11.32
	65:35	3.58	3.88	4.56	4.84	14.09	16.51
	70:30	4.01	4.43	5.39	5.80		
RP-2	60:40	3.52	3.52	3.71	3.92		
	70:30	3.84	4.11	4.48	4.89		
	80:20	4.79	5.55	6.03	6.99		

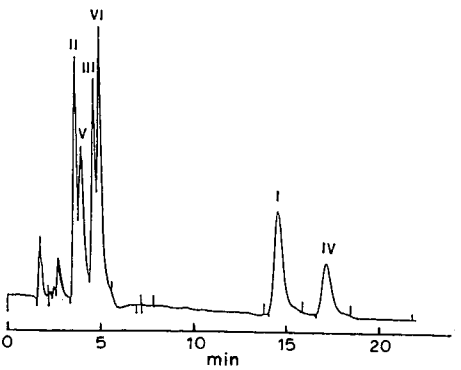

Fig. 2. Chromatography of ethiofencarb (I) and its metabolites: sulphoxide (II), sulphone (III) phenol (IV), phenol sulphoxide (V) and phenol sulphone (VI), on an C_8/H column. Mobile phase, water–acetonitrile (65:35, v/v); flow-rate, 1.0 ml/min; detection, UV (190 nm).

with acetonitrile. This reversal of the peak elution order between sulphones and sulphoxides could be valuable in confirmatory assays.

On a C_8/H column using the same chromatographic conditions the retention times increased, improving the separation, particularly of the sulphone (III) and phenol sulphone (VI). The best conditions for satisfactory separation and good peak sharpness were achieved using water–acetonitrile (65:35, v/v) as eluent (Fig. 2). An increase of only 5% in the water content is sufficient to produce poorer peak sharpness, to increase the retention time differences and to produce worse separations.

The retention times also increased when an RP-2 column was used under the same chromatographic conditions, but a worse separation of metabolites II, III, V and VI was achieved. In order to obtain a better separation it was necessary to increase the percentage of water in the eluent, but this produced a poorer peak sharpness.

Calibration graphs for each compound were constructed by plotting concentrations *vs.* peak areas; good linearities were achieved in the range 0–2.5 ppm, with correlation coefficients between 0.9952 and 0.9977.

Under the optimum conditions the detection limit was 0.02 ppm for all the

TABLE II

RECOVERIES OF ETHIOFENCARB (I) AND ITS METABOLITES (II–VI) BY DICHLOROMETHANE EXTRACTION FROM LETTUCE

Results are means of four experiments.

Compound	*Fortification level (ppm)*	*Recovery ± R.S.D. (%)*
Ethiofencarb (I)	1.50	90.3 ± 5.7
Sulphoxide (II)	1.50	96.4 ± 5.1
Sulphone (III)	1.50	103.1 ± 4.8
Phenol (IV)	1.50	34.9 ± 2.1
Phenol sulphoxide (V)	1.50	93.1 ± 6.7
Phenol sulphone (VI)	1.50	102.4 ± 4.2

compounds. This technique was used to determine ethiofencarb and its metabolites in lettuce. In the extraction procedure, with several organic solvents (benzene, cyclohexane, chloroform and light petroleum) part of the ethiofencarb co-distilled with the solvent during evaporation, making its quantitative determination impossible. Dichloromethane was found to be the only solvent tested that allowed the quantitative extraction of all compounds, except the phenol IV, without any problem of co-distillation and interferences. A good recovery of the phenol IV (>87%) was carried out with methanol as the extraction solvent, using the same procedure as with dichloromethane.

Considering the FAO/WHO specifies the sum of the active ingredient and metabolites II and III as the maximum residue limit allowed in food, the described procedure allows the determination of residues and the study of the metabolites.

REFERENCES

1 B. Homeryer, *Pflanzenschutz-Nachr.*, 29 (1976) 255.
2 G. Drager, *Pflanzenschutz-Nachr.*, 30 (1977) 18.
3 *Pesticides Residues in Food: 1977 Evaluations*, FAO/WHO, Rome, 1978, pp. 187–221.
4 G. Drager, *Pflanzenschutz-Nachr.*, 27 (1974) 144.
5 D. E. Nye, H. E. Hurst and H. W. Dorough, *J. Agric. Food Chem.*, 24 (1976) 371.
6 N. Aharonson, I. Neubauer, I. Ishaaya and B. Raccah, *J. Agric. Food Chem.*, 27 (1979) 265.
7 O. Wuest and W. Meier, *Z. Lebensm.-Unters.-Forsch.*, 177 (1983) 25.
8 M. Olek, F. Blanchard and G. Sudraud, *J. Chromatogr.*, 325 (1985) 239.

Journal of Chromatography, 462 (1989) 435–441
Elsevier Science Publishers B.V., Amsterdam — Printed in The Netherlands

CHROM. 21 028

Note

Dosage du dihydrosafrole dans le butoxyde de pipéronyle par chromatographie liquide haute performance

J. PASTOR*, A. M. PAULI et E. SCHREIBER-DETURMENY
Laboratoire de Chimie Analitique, UFR de Pharmacie, 27 Bd Jean Moulin, 13005 Marseille (France)
(Reçu le 20 juillet 1988, manuscrit modifié reçu le 4 octobre 1988)

Le butoxyde de pipéronyle (BOP) est utilisé comme synergiste de nombreux insecticides entrant dans la composition de quelques préparations pharmaceutiques ou cosmétiques. Le BOP se prépare à partir du chlorométhyldihydrosafrole[1]; le dihydrosafrole (DHS) est un produit intermédiaire de la synthèse et aurait des propriétés cancérigènes[2,3].

L'administration quotidienne de DHS per os à des rats, pendant plusieurs mois, a provoqué l'apparition de tumeurs de l'oesophage chez 75% des animaux; quelques tumeurs du foie ont également été observées, mais en trop petit nombre pour être significatives[2]. Le même mode d'administration à des souris a induit des cancers du foie et des poumons chez plus de la moitié des animaux traités, les tumeurs du foie ne touchant que les mâles alors que les poumons étaient atteints de la même manière chez les mâles et les femelles[3].

Beaucoup de travaux sont relatifs au dosage du safrole par chromatographie gazeuse (CPG) équipée d'un détecteur à ionisation de flamme[4,5], ou par chromatographie en phase liquide à haute performance (CLHP) avec détection en ultra violet à 289 nm[6] ou à 282 nm[7], ou encore par fluorimétrie avec des longueurs d'onde d'excitation et d'émission respectivement de 295 et 323 nm[8], ou 290 et 325 nm[9]. Le plus souvent, le safrole est dosé dans les boissons alcooliques ou non[4–6,9], dans certains aliments[5,7] ou dans les parfums[8].

En revanche, les publications relatives au dosage du DHS sont peu nombreuses et traitent seulement de la CPG. Larry[4] propose une détermination semiquantitative du DHS dans les boissons non alcooliques, avec détection en ionisation de flamme et étalonnage interne (*m*-tolyl-acétate). Decsy[10] étudie les intermédiaires dans les synthèse du BOP et les sépare par CLHP. Leur dosage est effectué par CPG, et dans le cas du DHS, l'étalon interne utilisé est le Safrole.

Le but de notre travail est de proposer une méthode sensible pour le dosage du DHS dans le BOP. En effet, les teneurs en DHS varient beaucoup selon l'origine des butoxydes.

Il est donc utile pour les industriels de connaître la concentration en DHS dans cette matière première dont la qualité sera d'autant plus appréciée qu'elle contiendra moins de DHS.

Par ailleurs, il serait souhaitable d'établir des normes pour la dose maximale admissible (DMA).

0021-9673/89/$03.50

La CLHP avec gradient d'élution et détection par fluorimétrie nous a permis d'atteindre une bonne sensibilité. Cette dernière peut être encore augmentée en procédant à un isolement préalable du DHS par passage de l'échantillon, en solution dans de l'hexane, sur Sep-Pak silice. Le BOP fortement retenu par la silice sera donc séparé du DHS que l'on retrouvera dans l'éluat accompagné de quelques impuretés du BOP. La prise d'essai initiale pourra donc être augmentée sans pour autant introduire dans la colonne du BOP dont l'élution totale demanderait trop de temps. La méthode proposée est une méthode par chromatographie de partage en phase inverse avec utilisation d'un étalon interne le safrole.

EXPERIMENTATION

Appareillage et conditions opératoires

Les spectres de fluorescence du safrole et du DHS en solution dans la phase mobile (méthanol à 35% d'eau bidistillée) ont été réalisés sur un spectrofluorimètre Aminco-Bowman, American Instrument Company.

L'isolement du DHS se fait par passage des butoxydes sur Sep-Pak silice (Waters, Réf. 51900). Le solvant d'élution est le mélange hexane–éther éthylique (95:5, v/v).

Le chromatographe est équipé de deux pompes (Beckman 114 M et 110 M), d'un mélangeur et d'une colonne μBondapak C_{18} (Waters, Réf. 27334) de 30 cm × 3,9 mm I.D. L'injecteur (Beckman 340 organizer) est muni d'une boucle de 20 μl. La programmation du gradient d'élution est assurée par un microprocesseur (Altex 421 controller).

La phase mobile est obtenue par mélange de deux solvants: le solvant A (méthanol à 35% d'eau bidistillée) et le solvant B (méthanol pur). Dans la phase initiale, seul le solvant A est pompé (élution du Safrole et du DHS) et dans la phase terminale seul le solvant B est pompé, (élution des impuretés du butoxyde) le débit étant constamment de 1 ml min^{-1}.

Le détecteur est un fluorimètre Shimadzu RF 530, la longueur d'onde d'excitation est réglée à 292 nm et celle d'émission à 325 nm, l'appareil étant utilisé au maximum de sensibilité.

L'enregistreur (Kipp & Zonen) est réglé à 10 mV pleine échelle. La vitesse de déroulement du papier est de 5 mm min^{-1} lors de la sortie des pics intéressants et passe à 2 mm min^{-1} lors de la phase d'élution des impuretés.

Réactifs

Nous avons utilisé alcool méthylique RS-ACS pour spectrophotométrie (UV) (Carlo Erba); *n*-hexane RPE (Carlo Erba); éther éthylique RPE (Carlo Erba); safrole "purum" (Fluka, Buchs, Suisse, Réf. 84130); dihydrosafrole, préparé par hydrogénation catalytique du safrole; butoxyde de pipéronyle redistillé sous vide (2 mm de mercure). On ne retient que le produit de coeur.

Préparation de la gamme d'étalonnage

Toutes les solutions sont préparées à 20°C dans de l'hexane, à partir de deux solutions "mères" à 4 g l^{-1}, l'une de safrole et l'autre de DHS. Elles sont préparées dans des ballons jaugés de 50 ml par pesées exactes de 200 mg de chacune des deux substances. Puis on prépare les solutions "stock" à 20 mg l^{-1} par dilution au 1/200 des solutions "mères".

Enfin, les solutions "étalons" sont à 0,5 mg l^{-1} pour le DHS et à 2 mg l^{-1} pour le safrole. A partir de ces solutions, on prépare les points de gamme renfermant 50, 100, 200 et 300 μg l^{-1} de DHS et dans chaque cas, 200 μg l^{-1} de safrole.

Les solutions de BOP étant de 5 g l^{-1}, la solution "gamme" à 50 μg l^{-1} de DHS correspond donc à 10 ppm de DHS dans le butoxyde.

Préparation des échantillons de BOP

Des solutions renfermant le BOP seul ou avec l'étalon interne (safrole) sont préparées dans l'hexane. Elles contiennent, par litre, 5 g de BOP additionné ou non de 200 μg de safrole. On prépare en général 50 ml de solution.

La solution contenant le butoxyde seul permet de contrôler l'absence d'impuretés de temps de rétention voisin de celui du safrole et d'avoir une première approximation de la teneur en DHS. Si celle-ci est trop élevée (hauteur de pic supérieure à celle du dernier point de gamme) des solutions moins concentrées en BOP sont préparées.

Toutes les solutions (DHS, Safrole et BOP) sont conservées au réfrigérateur dans des flacons bouchants émeri.

Mode opératoire

Séparation sur Sep-Pak. Les Sep-Pak sont chargés avec 1 ml des solutions de BOP ou de la gamme d'étalonnage précédemment préparées. L'élution est faite avec 3 ml du mélange hexane–éther éthylique (95:5, v/v) à la vitesse de 1 ml min^{-1}. L'étude de l'éluat fractionné a montré que le DHS et le safrole se retrouvent dans le 3ème millilitre. La méthode consiste donc à éliminer les deux premiers millilitres et à injecter une fraction (20 μl) du troisième millilitre. Cette injection est faite immédiatement aprés élution. Dans le cas contraire, l'éluat est conservé au réfrigérateur dans des flacons bouchés émeri. Nous nous sommes assurés qu'en aucun cas le BOP n'est élué en même temps que le DHS ou le Safrole. Si l'on désire récupérer le BOP, il convient de procéder ultérieurement à une élution par le méthanol.

Des essais préliminaires réalisés sur les solutions de la gamme d'étalonnage avec passage sur Sep-Pak ou sans passage nous ont montré que les rapports des hauteurs de pics du DHS à celles du Safrole étaient identiques. Il est toutefois indispensable de traiter les solutions étalons dans des conditions identiques à celles des solutions de BOP.

CLHP. Vingt microlitres du 3ème millilitre provenant de l'élution des "Sep-Pak" sont injectés en tête de colonne.

Le gradient d'élution est le suivant: solvant A pur, 18 min; passage du solvant A au solvant B, 5 min; solvant B, 20 min; retour au solvant A, 10 min; solvant A seul, 5 min. Puis nouveau cycle.

Le débit de la phase mobile est dans tous les cas de 1 ml min^{-1}. Dans les conditions opératoires précédemment décrites, le temps de rétention du safrole est de l'ordre de 600 s, celui du DHS de 780 s. Des exemples de chromatogrammes obtenus avec un point de gamme et avec un BOP sont reproduits Figs. 1 et 2.

La teneur en DHS est calculée par rapport à une droite d'étalonnage construite en portant en abscisse la concentration en DHS dans le butoxyde exprimée en ppm, et en ordonnées le rapport de la hauteur du pic de DHS à celle du pic de safrole.

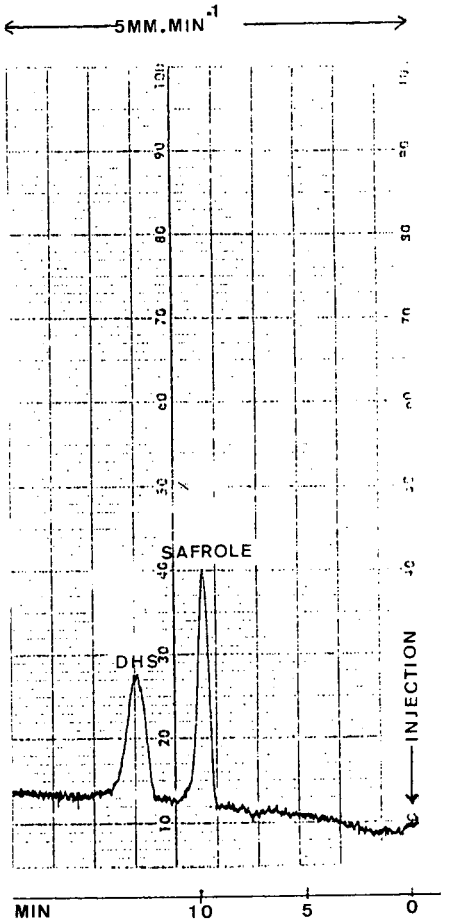

Fig. 1. Chromatogramme provenant de l'injection de 20 µl de la solution dans l'hexane du point de gamme à 40 ppm (soit 4 ng de DHS et 4 ng de safrol dans 20 µl d'hexane).

RÉSULTATS ET DISCUSSION

Choix de l'étalon interne

Nous avons choisi comme étalon interne le safrole car son affinité pour la silice du Sep-Pak est voisine de celle du DHS; de plus, ces deux composés en solution dans la phase mobile (méthanol à 35% d'eau bidistillée) présentent des spectres de fluorescence identiques. Nous avons constaté que tous les échantillons de BOP ne renfermaient pas de safrole. Comme nous l'avons dit ci-dessus, un essai préliminaire sur solution de butoxyde permet de s'assurer de l'absence de safrole.

Avantages du gradient d'élution

Il serait tout à fait possible d'obtenir avec le solvant A, sans gradient d'élution, une séparation convenable du safrole et du DHS. Mais l'élution ultérieure des

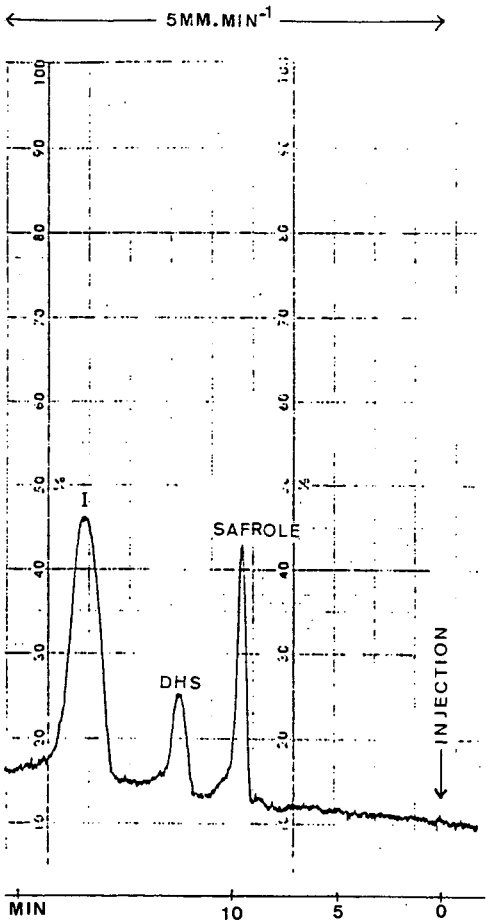

Fig. 2. Chromatogramme provenant de l'injection de 20 μl du 3ème millilitre d'éluat d'un Sep-Pak chargé avec 0,5 mg d'un BOP additionnée de 200 ng de safrole. Le pic "I" provient d'une impureté du butoxyde.

impuretés du butoxyde serait excessivement longue et rendrait la méthode peu intéressante par la durée d'une analyse. C'est pourquoi nous avons été amenés à utiliser un gradient d'élution conduisant très rapidement à un solvant ne renfermant que du méthanol, solvant permettant d'éluer les impuretés précitées en une vingtaine de minutes, alors qu'avec le solvant initial, l'élution complète des impuretés demandait environ 2 heures.

Valeur de la méthode

Linéarité. La réponse est linéaire entre 10 et 80 ppm, l'équation de la droite de régression étant:

$$Y = 0{,}0125\,X + 0{,}0271, \quad r = 0{,}9972, \quad p < 0{,}01$$

$$Y = \frac{\text{hauteur du pic DHS}}{\text{hauteur du pic safrole}}$$

X = mg de DHS par kg de BOP

Pourcentage de récupération. Nous avons procédé à des expériences de charge en ajoutant dans un BOP renfermant initialement 18 ppm de DHS, des quantités croissantes et connues de ce dernier. Nous donnons dans le Tableau I les résultats obtenus.

A l'exception de la charge à 10 ppm, le pourcentage de récupération est compris entre 97 et 103%. La marge d'erreur correspond sensiblement à la précision de la méthode.

Précision de la méthode. La reproductibilité a été étudiée à deux niveaux: celui de la reproductibilité des hauteurs de pics en injectant 10 fois successivement le même éluat après passage sur Sep-Pak (cet éluat provient d'un BOP contenant 33 ppm de DHS). Nous avons obtenu $m = 33{,}7$; $\sigma = 0{,}717$ et CV% $= 2{,}13\%$. Puis, afin de juger de la reproductibilité de l'élution sur Sep-Pak, nous avons fait passer sur onze Sep-Pak différents la même solution de butoxyde en procédant à une seule injection pour chaque éluat. Nous avons obtenu dans ce cas $m = 31{,}8$; $\sigma = 1{,}124$ et CV% $= 3{,}42\%$.

Limite de détection. Pour déterminer la limite de détection nous avons calculé l'écart type des variations observées sur la ligne de base (après agrandissement photographique de cette dernière) et nous avons retenu comme limite de détection la valeur qui correspond à 3 fois l'écart type. Cette limite de détection est de 3 ppm.

Résultats

La méthode a été appliquée à la détermination de la teneur en DHS dans plusieurs BOP. Les résultats sont présentés dans le Tableau II; les concentrations en DHS, exprimées en ppm et en micromoles kg^{-1}, sont extrêmement variables et s'échelonnent de quelques ppm à plusieurs milliers.

Il est à remarquer que la distillation est un bon moyen de purifier les butoxydes présentant une forte teneur en DHS. Nous avons procédé à une distillation sous vide (2 mm de mercure) du butoxyde "A" qui renfermait 315 ppm de DHS. Le produit distillé ne renferme plus que 9 ppm de DHS.

TABLEAU I

ÉTUDE DU POURCENTAGE DE RÉCUPÉRATION EN AJOUTANT DANS UN BOP RENFERMANT INITIALEMENT 18 ppm DE DHS, DES QUANTITÉS CROISSANTES ET CONNUES DE CE DERNIER

Quantité de DHS ajoutée (ppm)	*Quantité de DHS retrouvée (ppm)*	*Pourcentage de recuperation*
10	9	90
20	19,4	97
40	40	100
60	61,6	103

TABLEAU II

CONCENTRATIONS EN DHS DÉTERMINÉS DANS LES BOP ANALYSÉS

BOP analysés	*DHS en ppm*	*DHS en µmol kg*$^{-1}$
A distillé	9	55
B	16	98
C	27	165
D	55	335
E	128	780
F	305	1860
A	315	1920
G	3662	22 329

CONCLUSION

La technique que nous proposons permet de doser le DHS dans le butoxyde de pipéronyle avec une limite de détection égale à 3 ppm. La méthode est reproductible (CV% de l'ordre de 3,5%). Elle est relativement simple et permet d'effectuer une détermination en une heure environ.

Il est indispensable de procéder à un dosage avec étalon interne car il est impossible de concentrer les éluats par évaporation, car au cours de cette dernière, le DHS se volatilise.

L'utilisation simultanée d'une séparation préalable sur Sep-Pak et d'une détection spectrofluorimétrique permet d'évaluer très rapidement le DHS à des concentrations minimes de l'ordre de 5 ppm.

BIBLIOGRAPHIE

1 O. Repasy, R. Csikos, R. Soos, G. Baktay, Z. Decsy, J. Bodor, J. Bathory, T. Varga et A. Starcsevics, *Hung. Teljes*, H434, 452, (Cl. C 07D317/54), 28 Mar. 1985, Appl. 83/388, 4 Feb. 1983.
2 E. C. Hagan, P. M. Jenner, W. I. Jones, O. G. Fitzhugh, E. L. Long, J. G. Brouwer et W. K. Webb, *Toxicol. Appl. Pharmacol.*, 7 (1965) 18.
3 J. R. M. Innes, B. M. Ulland, M. G. Valerio, L. Petrucelli, L. Fishbein, E. R. Hart, A. J. Pallota, R. R. Bates, H. L. Falk, J. J. Gart, M. Klein, I. Mitchell et J. Peters, *J. Nat. Cancer Inst.*, 42 (1969) 1101.
4 D. Larry, *J. Assoc. Off. Anal. Chem.*, 54 (1971) 900.
5 F. Grundschober, *Int. Flavours Food Addit.*, 8 (1977) 27.
6 G. Mazza, *Riv. Soc. Ital. Sci. Aliment.*, 12 (1983) 159.
7 A. W. Archer, *J. Chromatogr.*, 438 (1988) 117.
8 H. H. Wisneski, R. L. Yates et H. M. Davis, *J. Chromatogr.*, 255 (1983) 455.
9 P. Curro, G. Micali et F. Lanuzza, *J. Chromatogr.*, 404 (1987) 273.
10 Z. Decsy, *Magy. Kem. Foly.*, 84 (1978) 420.

Journal of Chromatography, 462 (1989) 442–447
Elsevier Science Publishers B.V., Amsterdam — Printed in The Netherlands

CHROM. 21 008

Note

Assay for the main phallotoxins in *Amanita phalloides* Fr. by direct fluorimetry on thin-layer plates

F. ENJALBERT*
Laboratoire de Botanique, Phytochimie et Mycologie, Faculté de Pharmacie, Avenue Charles Flahaut, 34060 Montpellier Cedex (France)
M. J. BOURRIER
Laboratoire Interrégional de la Répression des Fraudes, 2 Rue Saint-Pierre, 34024 Montpellier Cedex (France)
and
C. ANDARY
Laboratoire de Botanique, Phytochimie et Mycologie, Faculté de Pharmacie, Avenue Charles Flahaut, 34060 Montpellier Cedex (France)
(First received May 16th, 1988; revised manuscript received September 23rd, 1988)

As phallotoxins are not taken up by intestinal epithelial cells, they do not play a role in poisoning by the death cap mushroom. The toxic effects after eating the mushroom are caused solely by amatoxins[1,2]. However, like amatoxins, phallotoxins have become important tools in biochemical and biological research. They inhibit the conversion of actin F into actin G and disturb the dynamic equilibrium of these forms which are necessary in cell functions[3]. In addition, when taken up selectively by hepatocytes, they cause cholestasis by interaction with the polymerization of hepatocellular actin and are used as hepatotoxic substances[4,5].

Phalloidin was the first phallotoxin isolated from *Amanita phalloides*. Other toxins derived from this structure were then characterized. Phallotoxins are dicyclic heptapeptides which are divided into two groups. The first group consists of neutral molecules: phalloin (PHN), phalloidin (PHD), phallisin (PHS) and prophalloin (PPN). The second consists of the acid molecules phallacin (PCN), phallacidin (PCD) and phallisacin (PSC). The presence of an hydroxyl group on proline makes these molecules toxic. The LD_{50} of PPN, for example, which has lost this OH, is ten times as great[6].

Knowledge of the locations of phallotoxins in the mushroom was hindered by the lack of sufficiently sensitive and reliable methods of detection. The isolation techniques proposed use thin-layer or column chromatography. After separation of the toxins, identification was carried out using UV absorption spectophotometry or colorimetric reactions[7–9]. High-performance liquid chromatography (HPLC) was applied mainly to biological liquids[10]. Assaying was carried out using chemical or biological methods. The first methods include the evaluation of gammalactones derived from amino acids resulting from the hydrolysis of toxins and separated by column chromatography[7] and fluorimetric detection of cyclopeptides before and after hydro-

0021-9673/89/$03.50

lysis[11]. Biological techniques make use of the affinity of phallotoxins for muscle actin which is a target protein. One biological assay uses the polymerizing effect of [^{3}H]dimethylphalloin on rabbit muscle actin[12]. Another more sensitive assay is based on the protective effect of PHD on the inhibition of a pancreatic desoxyribonuclease by actin[13]. Biological assaying is of great value since its high sensitivity (detection limit 6.3 ng) has made it possible to detect phallotoxins in other species of the genus *Amanita* such as *A. vera, A. suballiacea, A. mutabilis* and *A. rubescens*[13].

However, these biological techniques result in an overall assay of these molecules and are thus ineffective in a search for the locations of the various neutral and acid phallotoxins in the mushroom. A sensitive, reproducible assaying technique is therefore proposed for the main phallotoxins present in *A. phalloides*. It was used to determine these toxins in each part of the mushroom (cap, stipe and volva).

MATERIALS AND METHODS

Extraction

A fragment of each organ of fresh mushroom (0.5 to 1.5 g) was crushed and extracted with methanol–water–0.01 *M* hydrochloric acid (5:4:1). Three extractions were carried out ultrasonically at 40°C using 7 ml of extraction medium for each extraction. The samples were rinsed twice in 5 ml of solvent, pooled, filtered and concentrated in a rotary evaporator at 35°C until a dry residue was obtained. This was then resuspended in methanol–water (8:2) to obtain a 20% extraction solution for the assays.

Thin-layer chromatography (TLC)

The following materials and reagents were employed: silica gel plates. Ref. 5721 (Merck, Darmstadt, F.R.G.); "Gold label" microcaps (Drummond, Broomal, PA, U.S.A.); calibration solution of phalloidin (Boehringer, Mannheim, F.R.G.); $1 \cdot 10^{-4}$g/ml in methanol–water (10:90); tank lined with filter-paper at room temperature (20 ± 2°C); solvent chloroform–methanol–28% ammonia (60:40:10).

F-detection two solutions were used: (a) 2.5% (w/v) 4-dimethylaminobenzaldehyde (PDAB) (Fluka, Buchs, Switzerland) in methanol; (b) 2 ml of concentrated sulphuric acid (Prolabo, Paris, France) added gradually while shaking to 10 ml of methanol–glycerol (6:4). An UV chromatographic analyser, Farrand Vis 2 (Optical, New York, NY, U.S.A.) with two monochromators, operating by fluorescence and by reflection (excitation at 325 nm, emission at 480 nm) was employed.

Procedure

A 15- to 20-μl volume of 20% mushroom extract and 0.5, 1, 3, 5 and 7 μl of phalloidin solution, corresponding to 50, 100, 300, 500 and 700 ng of toxin were placed on a silica gel plate with a micropipette. The plate was placed in the tank, which was saturated with solvent vapour, and developed to an height of 16 cm (duration 100 min). After drying under cold air to remove the alkaline residue and traces of developing solvent, the chromatogram was visualized by spraying with solution (a) followed by drying. This operation was carried out three times. Solution (b) was then sprayed on to the plate which was subsequently dried in an oven at 115°C for 10 min. After removal from the oven the chromatogram was covered with a glass plate until it was completely cold.

Phallotoxins were visible as white fluorescent spots after exposure to UV light at 360 nm. Levels were determined by referring to a calibration line representing the variation of peak area of the PHD standard as a function of concentration.

RESULTS AND DISCUSSION

Extraction

The extraction method was chosen in accordance with the literature. Most of the tests were carried out with alcohol: ethanol or methanol[14] or a mixture of alcohol and water (1:1)[8,9] or methanol–ammonia[7]. Methanol–water (1:1) treatment was effective, although methanol–water–0.01 *M* hydrochloric acid (5:4:1) was preferred as the yield of PHD was greater. A slightly acid pH appeared to enhance the stability of the toxins[8]. Most authors[7–9,11] then purified the extracts; this involved long operations which inevitably resulted in loss of toxins. This was avoided in the present work by the use of raw extracts obtained using this simple and reproducible extraction method.

The advantage of carrying out these tests on fresh material should also be noted. Drying causes considerable degradation of phallotoxins, which are comparatively thermolabile molecules. Up to 30% loss of toxins was observed in assays carried out in parallel on fresh material and dried material from the same cap.

The reproducibility of this method of extraction was verified by carrying out several assays on extracts from the same organ. The average deviation between the levels of the various toxins was of the order of 3%.

Assays

Solvents. Several eluting agents recorded in the literature were tested[7,8,15,16]. One of them[16] gave good separation of the neutral toxin group (PHN, PHD, PHS) but the gap between the R_F values of PCD and PSC was too small to permit photodensimetric assay.

A more polar solvent was therefore devised: chloroform–methanol–28% ammonia (60:40:10). This gave better separation of the five phallotoxins from each other and from other spots. Chromatograms with well defined, well separated spots perfectly suitable for photodensimetric assay were obtained. The mean R_F values of the main phallotoxins in this solvent are shown in Table I.

TABLE I

MEAN R_F VALUES IN SILICA GEL TLC OF THE MAIN PHALLOTOXINS IN *AMANITA PHALLOIDES*

Solvent: chloroform–methanol–28% ammonia (60:40:10).

Phallotoxin	R_F *(mean ± S.E.M., n = 3)*
PHN	0.60 ± 0.03
PHD	0.50 ± 0.02
PHS	0.44 ± 0.03
PCD	0.21 ± 0.02
PSC	0.14 ± 0.01

Detection. Sensitive, stable resolution was desired which would enable direct assay on a chromatoplate. A fluorimetric detection method was used first with phosphoric acid at 80°C recommended for resolution of α-amanitin[17]. This led to several trials with different acids: sulphuric acid, perchloric acid and trichloroacetic acid at between 80 and 100°C. Sulphuric, phosphoric and perchloric acids reacted with approximately the same sensitivity but the fluorescence was fugacious. In order to improve this medium sensitivity, we tested the addition of several aldehydes (cinnamaldehyde, anisaldehyde, *p*-dimethylaminobenzaldehyde and *p*-dimethylaminocinnamaldehyde). A mixture of PDAB and sulphuric acid gave better sensitivity but the reaction was not sufficiently stable for assays. The stability of fluorescence was considerably improved by the addition of glycerol to the acid mixture. In this procedure the reagent was used in two steps and the chromatogram was protected with a glass plate until it had cooled completely; this made it possible to fix the reaction. Phallotoxin fluorescence resolved in this way remained stable for several hours and permitted fluorodensimetric assaying with a sensitivity of 25 ng per spot on the chromatograms.

Sensitivity, validation and precision

The resolution method generally used is based on the colorimetric reaction produced by contact of cinnamic aldehyde with hydrochloric acid vapour. Phallotoxins appeared on the chromatogram in the form of blue-grey spots and disappeared very rapidly. The limit of detection was of the order to 500 ng per spot[6]. The resolution was 20 times as sensitive when the PDAB–sulphuric acid based reagent was used. The results reported in Fig. 1 indicate that the validation of the method is satisfactory

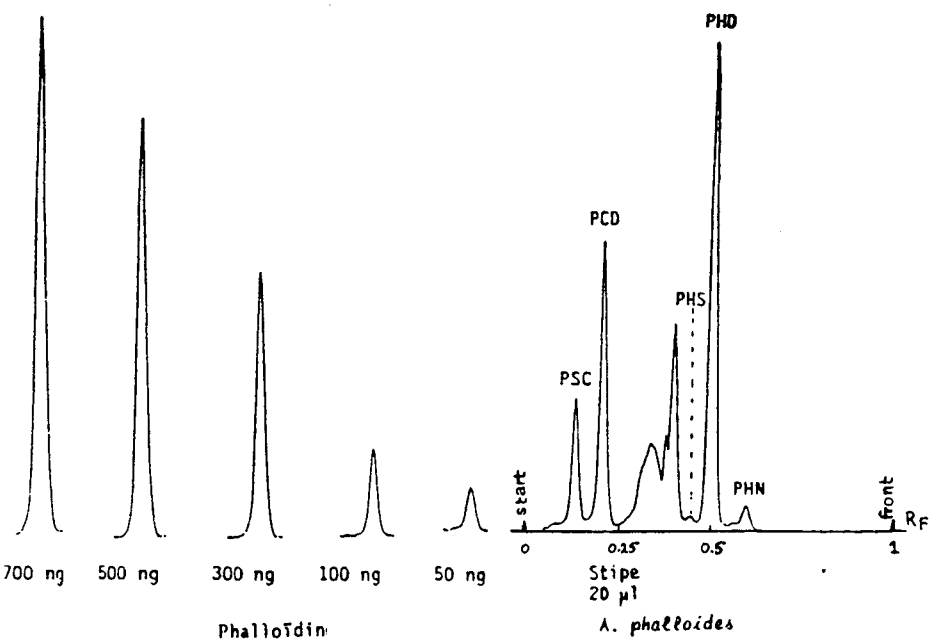

Fig. 1. Graphic plotting after fluorodensitometric reading (excitation at 325 nm, emission at 480 nm) of the spots in silica gel TLC of a calibration range of phalloidin and an extract of *Amanita phalloides* stipe.

since the calibration graph for PHD is linear from 50 to 700 ng (coefficient of correlation, $r = 0.9996$). The regression equation indicating the peak area (mm^2) *versus* the PHD concentration is as follows: $s = 0.223[PHD] - 2.11$, with standard deviations of slope and intercept of 0.004 and 1.42 respectively. The quantification limit is 8 μg of toxin per g of fresh material. The inter-assay precision was verified by subjecting the same extract (accompanied in each case by the same series of standard solutions) to three assays (Table II). The coefficient of variation (standard deviation/mean) calculated for PHD, PCD and PSC was found to be 5%. It was not calculated for PHN since the values were too small.

The technique recommended can be used to measure the amounts of five phallotoxins in the various organs (cap, stipe and volva) of an *Amanita phalloides*. PHN, PHD, PHS, PCD and phallisacin PSC were characterized using the reference substances kindly provided by Professor H. Faulstich. In the absence of a PCN standard, it was not possible formally to locate and assay this acid molecule on the chromatograms. However, it is noted that in previous work PCN was found only in very small amounts in a single specimen (less than 1/30 of PCD content)[18]. In addition, the low toxicity of PPN led to its exclusion from the study[6].

For practical reasons, all assays are expressed in mg of PHD per g of fresh organ. Indeed, phalloidin (commercially available) was the only pure toxin in our possession.

Fig. 1 shows the graphic plotting of the chromatographic spots of an organ (stipe) extract of *A. phalloides* prepared using the method described together with the calibration range. As the plot is linear from 50 to 700 ng, it was possible to assay the five toxins using the same preparation. Table II shows the amounts of each phallotoxin and total (T) in each organ (cap, stipe and volva); the last column gives the concentrations for the whole mushroom calculated from the respective weights of the three organs.

According to these results, the volva is the organ richest in phallotoxins and the stipe is the poorest. These data are in perfect agreement with Faulstich's observa-

TABLE II

MEAN PHALLOTOXIN CONTENT IN mg/g OF FRESH SPECIMEN IN THE VARIOUS ORGANS OF A SINGLE SPECIMEN OF *AMANITA PHALLOIDES* (MEAN ± S.E.M., $n = 3$) AND PHALLOTOXIN CONTENT OF THE WHOLE MUSHROOM CALCULATED USING THE RESPECTIVE WEIGHTS OF THE THREE ORGANS

C = cap; S = stipe; V = volva; W = whole fungus. T = All toxins. S.E.M. values of PHN and PSC are corrected to three decimal places.

Toxins	*C* *(30.073 g)*	*S* *(11.1 g)*	*V* *(1.006 g)*	*W* *(42.179 g)*
Neutral				
PHN	0.008 ± 0.001	0.008 ± 0.001	0.008 ± 0.001	0.008
PHD	0.141 ± 0.004	0.114 ± 0.003	0.275 ± 0.008	0.137
PHS		Traces		
Acidic				
PCD	0.059 ± 0.002	0.055 ± 0.002	0.069 ± 0.002	0.056
PSC	0.022 ± 0.001	0.022 ± 0.001	0.024 ± 0.001	0.022
T	0.298 ± 0.004	0.275 ± 0.004	0.448 ± 0.008	0.295

tions[6]. With regard to the distribution of toxins in each organ, it will be noted that the major toxin was PHD, followed by PCD and PSC. The amounts of PHN were very small and traces of PHS were found only in the stipe. PHD and PCD were thus the main toxins of the neutral and acid phallotoxin groups respectively. This was also a feature of the assays carried out previously by other authors[8,9,18]. However, the contents of each of the two molecules are very different to those in the literature; our results show that PHD was predominant whereas the dominance of PCD had always been noted[8,9,18].

The rapidity of the method means that it can be applied to a large number of specimens to measure the variations in the levels of these toxins as a function of the ecology and age of the fungus.

ACKNOWLEDGEMENT

The authors thank Professor H. Faulstich for kindly providing phallotoxin standards not commercially available: phalloin, phallisin, phallacidin and phallisacin.

REFERENCES

1 H. Faulstich and K. Munter, *Klin. Wochenschr.*, 64, suppl. VII (1986) 66.
2 T. Wieland, *Naturwissenschaften*, 74 (1987) 367.
3 T. Wieland, *Int. J. Pept. Protein Res.*, 22 (1983) 257.
4 H. Faulstich, K. Munter and D. Mayer, *Falk Symp.*, 38 (1984) 183.
5 M. Frimmer, *Toxicol. Lett.*, 35 (1987) 169.
6 T. Wieland and H. Faulstich, in R. F. Keller and A. T. Tu (Editors), *Handbook of Natural Toxins*, Vol. I, Marcel Dekker, New York, 1983, Ch. 18, p. 585.
7 H. Faulstich, D. Georgopoulos and M. Bloching, *J. Chromatogr.*, 79 (1973) 257.
8 R. R. Yocum and D. M. Simons, *Lloydia*, 40 (1977) 178.
9 J. A. Beutler and A. H. Der Marderosian, *J. Natl. Prod.*, 44 (1981) 422.
10 G. Caccialanza, C. Candini and R. Ponci. *J. Pharm. Biomed. Anal.*, 3 (1985) 179.
11 M. C. Little and J. F. Preston, *J. Natl. Prod.*, 47 (1984) 93.
12 J. A. Schäfer and H. Faulstich, *Anal. Biochem.*, 83 (1977) 720.
13 J. E. Mullersman and J. F. Preston, *Anal. Biochem.*, 119 (1982) 266.
14 T. Stijve and R. Seeger, *Z. Naturforsch.*, 34C (1979) 1133.
15 C. Andary, F. Enjalbert, G. Privat and B. Mandrou, *J. Chromatogr.*, 132 (1977) 525.
16 S. H. A. Malak, *Planta Med.*, 29 (1976) 80.
17 Y. Plancke, J. P. Henichart and J. L. Bernier, *Z. Naturforsch.*, 35C (1980) 516.
18 H. Faulstich, D. Georgopoulos, M. Bloching and T. Wieland, *Z. Naturforsch.*, 29C (1974) 86.

Journal of Chromatography, 462 (1989) 448–453
Elsevier Science Publishers B.V., Amsterdam — Printed in The Netherlands

CHROM. 21 010

Note

Determination of cholinesterase-inhibiting pesticides and some of their metabolites in cases of animal poisoning using thin-layer chromatography

P. E. F. ZOUN* and Th. J. SPIERENBURG
Central Veterinary Institute, Department of Analytical Chemistry and Toxicology, P.O. Box 65, 8200 AB Lelystad (The Netherlands)
(First received June 3rd, 1988; revised manuscript received September 26th, 1988)

In veterinary practice one is regularly confronted with incidents involving unwanted side-effects, abuse or —more frequently— misuse of agrochemicals. Domestic animals and wildlife, especially birds, may be affected. Annually 100–250 cases of suspected acute pesticide intoxication in animals need to be diagnosed, the majority of them being caused by cholinesterase-inhibiting compounds. Hence a rapid screening method for representatives of this group in gizzard and gastrointestinal contents as well as in baits, food and environmental samples was necessary.

A thin-layer chromatographic (TLC) method for qualitative and semiquantitative analysis of some hundred pesticides and metabolites was developed, most of them belonging to the class of organophosphates. Although less relevant in veterinary practice from a diagnostic point of view, the present method includes (thio-)carbamates, carbamoyloximes, dithiocarbamates and ureas too. These compounds exhibit cholinesterase-inhibiting properties *in vitro*, by which they may interfere during analysis.

Principle of the method

Samples were ground with anhydrous sodium sulphate and extracted with dichloromethane. In general, the pesticides extracted were subjected to TLC without additional cleaning. The extracts were spotted on silica gel HPTLC plates and developed with either xylene, di-*n*-butyl ether, *n*-butyl acetate or methyl isobutyl ketone. After evaporation of the solvent and, if necessary, an activation of the spots by bromine vapour, the plates were sprayed and incubated with bovine liver suspension. To detect cholinesterase inhibition, the plates were sprayed with the substrate 2-naphthyl-acetate and Fast Blue B salt as the chromogenic agent.

EXPERIMENTAL

Chemicals

All chemicals were of analytical grade from E. Merck (Darmstadt, F.R.G.) unless specified otherwise.

0021-9673/89/$03.50

Pesticide standard solutions

Pesticide reference standards of >99% purity were obtained from the U.S. Environmental Protection Agency, and from Lamers & Pleuger ('s-Hertogenbosch, The Netherlands). For TLC, standard solutions were prepared in dichloromethane (residue analytical quality). Both reference standards and standard solutions were stored at 4°C.

HPTLC plates

Ready to use HPTLC glass plates 20 cm × 10 cm, coated with silica gel 60 F_{254} (Merck), were employed.

Preparation of enzyme solution

A 20-g amount of fresh beef liver was homogenized in a Sorvall Omni Mixer with 200 ml of 0.05 *M* Tris–HCl buffer pH 8.2 containing 0.1% (v/v) Triton X-100 followed by centrifugation for 5 min at 150 *g*. Aliquots of 4 ml of the supernatant were transferred to plastic tubes and freezed at –20°C. Prior to use, portions were each diluted in 12 ml of distilled water. One portion suffices for the spraying of two 20 cm × 10 cm plates.

Preparation of substrate solution

Solution A: 1.25 g/l 2-naphthyl acetate (biochemical grade) in ethanol. Solution B: 1.56 g/l Fast Blue B (for microscopy) in water. Immediately before use, 4 ml of solution A were mixed with 16 ml of solution B. This suffices for the spraying of four 20 cm × 10 cm plates.

Sample extraction

Amounts of 5–10 g of gizzard or gastrointestinal content, bait, food or environmental sample were ground in a mortar with anhydrous sodium sulphate (residue analytical quality) and sea-sand to a free flowing powder. The powder was extracted with 10–25 ml of dichloromethane (residue analytical quality) in a conical flask by mechanical shaking for 1 h, followed by filtration through Whatman No. 41 paper.

TLC

Aliquots of extracts and different concentrations of pesticide standard solutions were spotted on the HPTLC plates using micropipettes (5 × 1 μl). The plates were developed in either xylene, di-*n*-butyl ether (spectroscopic grade), *n*-butyl acetate or methyl isobutyl ketone in an unsaturated chamber to a distance of about 6 cm from the origin. After evaporation of the solvents, the plates were exposed to bromine vapour for 30 s and kept in a ventilated hood for 10 min in order to evaporate the excess of bromine. The plates were then uniformly sprayed with 6 ml of enzyme solution and placed for 30 min in an incubator with 80–85% relative humidity at 37°C. Next, the plates were sprayed with freshly prepared substrate solution and left at room temperatue. White spots appeared on a magenta background after some minutes and were marked with a pencil. Subsequently, hR_F values were calculated.

RESULTS AND DISCUSSION

The present method is a modification of that by Ackermann[1–4]. Dichloromethane was preferred to chloroform as the extraction solvent: due to its higher volatility, it evaporates faster during spotting, resulting in smaller spot areas at the origin, thus enhancing resolution and sensitivity. For all the pesticides tested, the solubility in dichloromethane was $\geqslant 1$ mg/ml. Although chloroform might be a more efficient extraction solvent for some pesticides with high polarity, dichloromethane suffices for the present application of acute intoxications with high levels of pesticides. No significant differences were observed between chloroform or dichloromethane extracts as judged from interfering spots resulting from matrix components. Moreover, dichloromethane is less toxic.

The enzyme solution needed a Tris–HCl buffer of pH 8.2. Unbuffered homogenization resulted in severe loss of activity. Furthermore, Triton X-100 was added in order to achieve a better disposition of the esterases involved, resulting in an increased activity.

Table I shows the mean hR_F values of some hundred cholinesterase inhibiting

TABLE I

hR_F VALUES OF CHOLINESTERASE-INHIBITING PESTICIDES AFTER HPTLC ANALYSIS

Values are means from at least three experiments.

Compound	hR_F			
	Solvent			
	Xylene	*Dibutyl ether*	*Butyl acetate*	*Methyl isobutyl ketone*
Acephate	5	35	95	98
Aldicarb	0	2	47	74
Aldicarbsulfone	0	0	8	30
Aldicarbsulfoxide	0	0	0	0
Asulam	0	0	41	75
Azamethiphos	0	0	42	59
Azinphosmethyl	3	17	81	91
Bendiocarb	0	13	79	92
Benomyl	0	20	89	ns*
Bromophos	82	92	96	97
Bromophosethyl	86	96	97	98
Butocarboxim	0	0	43	70
Butoxycarboxim	0	0	7	27
Butylate	15	80	97	98
Carbaryl	2	18	80	92
Carbetamide	0	1	30	67
Carbophenothion	78	96	98	98
Carbofuran	0	5	70	87
Chlorbromuron	4	18	75	90
Chlorbufam	32	87	97	98
Chlorphenvinphos	0	7	70	81

TABLE I (*continued*)

Compound	hR_F			
	Solvent			
	Xylene	*Dibutyl ether*	*Butyl acetate*	*Methyl isobutyl ketone*
Chlorpropham	29	81	95	ns*
Chlorpyriphos	81	95	98	98
Chlorpyriphoxon	0	10	74	90
Chloroxuron	0	0	32	67
Chlortoluron	0	0	39	73
Coumaphos	7	54	92	95
Coumaphoxon	0	0	33	69
Cycloate	9	67	94	98
Demeton-S-methyl	0	0	30	64
Demeton-S-methylsulfon	0	0	6	22
Diallate	44	91	98	98
Diazinon	3	40	88	92
Diazoxon	0	0	6	12
Dibrom	0	11	67	82
Dichlofenthion	82	94	97	97
Dichlorvos	0	5	48	68
Difenoxuron	0	0	28	64
Diflubenzuron	4	32	89	ns*
Dimethoate	0	0	17	46
Diuron	0	0	43	73
Eptam	12	74	91	98
Ethiophencarb	0	15	80	92
Ethephon	0	0	0	0
Ethoprophos	0	10	68	87
Etrimfos	9	67	98	98
Fenitrothion	43	72	93	96
Fenoxycarb	2	22	84	94
Fenthion	51	82	94	97
Fonofos	54	89	96	97
Fonofoxon	0	3	51	56
Formothion	3	8	82	92
Glyphosate	0	0	0	0
Heptenofos	0	0	47	68
Isofenphos	9	75	97	97
Isoproturon	0	2	34	66
Jodfenphos	80	91	97	98
Linuron	4	14	75	93
Malaoxon	0	0	48	73
Malathion	5	37	92	96
Methabenzthiazuron	0	4	43	71
Methamidophos	0	0	5	12
Methidathion	10	39	92	96
Methiocarb	3	20	79	92
Methomyl	0	0	22	57
Metobromuron	3	15	7	89
Metoxuron	0	0	27	59

(*Continued on p. 452*)

TABLE I (*continued*)

Compound	hR_F			
	Solvent			
	Xylene	*Dibutyl ether*	*Butyl acetate*	*Methyl isobutyl ketone*
Mevinphos	0	0	18–32–40**	37–55–62**
Mevinphos-*cis*-isomer	0	0	18–32**	37–55**
Monolinuron	3	15	74	91
Omethoate	0	0	0	4
Oxamyl	0	0	4	22
Oxydemetonmethyl	0	0	0	0
Paraoxon	0	2	48	77
Paraoxonmethyl	0	0	34	62
Parathion	47	83	96	96
Parathionmethyl	39	71	94	97
Pencycuron	2	24	97	97
Phosalone	21	61	93	97
Phosphamidon	0	0	10–32**	36–65**
Phosmet	7	26	87	95
Phoxim	52	85	96	98
Pirimicarb	0	1	36	69
Pirimiphosmethyl	16	75	97	98
Propetamphos	7	66	96	98
Propoxur	0	10	77	93
Pyrazophos	1	28	90	94
Sodam	0	0	0	0
Sulfotep	41	86	96	96
Temephos	30	71	96	97
Terbufos	60	97	98	98
Tetrachlorvinphos	2	11	78	87
Thiofanox	0	3	59	82
Thiometon	47	83	94	96
Thiram	4	19	83	93
Tolclofosmethyl	69	87	95	96
Triallate	51	91	98	98
Triazophos	0	17	87	95
Trichlorphon	0	0	13	32
Trichloronate	84	94	97	97
Vamidothion	0	0	2	9

* No spots visible.
** Multiple spots.

compounds. The means are based on at least three observations. In contrast to other reports[1–8], in which low-boiling solvent mixtures were employed, hR_F values of excellent long-term reproducibility were obtained using single solvent systems with relatively high vapour pressures. Deviations of the mean hR_F values were often not more than 3 units at the most. Consequently, preliminary identification of spots proceeded more quickly and with greater confidence. Further decrease of the analysis time was

achieved by employing HPTLC plates in stead of normal TLC plates. Since HPTLC plates have an higher number of plates per unit length, shorter development times were feasible. A skilled analyst is able to perform 20 or more analyses per day.

Identification of inhibiting spots of extracts was mainly based on comparison of hR_F values with those of reference compounds with and without derivatization with bromine vapour prior to development of the plates. Bromine vapour oxidizes the P=S bond, present in most cholinesterase-inhibiting pesticides, to a P=O bond. If for example paraoxon, the oxidized derivative of parathion, is detected on a plate exposed to bromine vapour prior to development, additional evidence is obtained for an intoxication by parathion. Treatment of plates with bromine after development results in a better detection limit of most pesticides, because oxidized organophosphorus compounds are stronger cholinesterase inhibitors than their sulphur analogues. Limits of detection (per spot) are in the range of 0.2–20 ng, with the exception of dimethoate (200 ng), ethephon (2000 ng), ethoprophos (2000 ng), glyphosate (2000 ng), pirimicarb (100 ng) and sulfotep (200 ng). In intoxications with juridical aspects or doubtful TLC results, confirmatory evidence was obtained using gas or liquid chromatography.

In conclusion, the present method provides efficient analysis of cholinesterase-inhibiting pesticides. It was demonstrated to be a valuable diagnostic tool in veterinary toxicology.

REFERENCES

1 H. Ackermann, *J. Chromatogr.*, 36 (1968) 309–317.
2 H. Ackermann, *J. Chromatogr.*, 44 (1969) 414–418.
3 H. Ackermann, B. Lexow and E. Plewka, *Arch. Toxicol.*, 824 (1969) 316–324.
4 H. Ackermann, *Nahrung*, 10 (1966) 273–374.
5 O. Antoine and G. Mees, *J. Chromatogr.*, 58 (1971) 247–256.
6 B. Bajer-Rapic, E. R. Schmid, E. Juenger and K. Pollak, *Nahrung*, 19 (1975) 551–555.
7 C. F. Ernst, C. Pieterse and L. J. H. Martens, *J. Chromatogr.*, 133 (1977) 245–251.
8 S. N. Tewari and R. Singh, *Fresenius' Z. Anal. Chem.*, 294 (1979) 287.

Journal of Chromatography, 462 (1989) 454–457
Elsevier Science Publishers B.V., Amsterdam — Printed in The Netherlands

CHROM. 21 053

Note

Preparative separation of the enantiomers of the cholecystokinin antagonist (3*S*)-(±)-N-(2,3-dihydro-1-([$^3H_3$]methyl)-2-oxo-5-phenyl-1H-1,4-benzodiazepine-3-yl)-1H-indole-2-carboxamide by high-performance liquid chromatography

JON F. DENISSEN

Biotransformation Section, Drug Metabolism Department, Abbott Laboratories, Abbott Park, IL 60064 (U.S.A.)

(Received September 14th, 1988)

(3*S*)-(−)-N-(2,3-dihydro-1-methyl-2-oxo-5-phenyl-1H-1,4-benzodiazepine-3-yl)-1H-indole-2-carboxamide (L-364,718; **I**) (Fig. 1) is a potent, non-peptidal antagonist of the peptide hormone and proposed neurotransmitter cholecystokinin[1] possessing high peripheral cholecystokinin receptor selectivity.[2] Tissue binding studies have shown the (−)-3*S* enantiomer of compound **I** to be approximately 100 times more biologically active than the (+)-3*R* enantiomer[3] and optically pure (−)-I has been prepared on a multigram scale by a resolution-racemization sequence involving compound **I** precursor[4,5]. In order to obtain (+) and (−) enantiomers of the drug in high optical purity for use in radioligand receptor binding assays, a procedure that would resolve commercially available (±)-[N-methyl-$^3H_3$]-**I** was desired. An high-performance liquid chromatographic (HPLC) system employing a chiral stationary phase was developed to separate microgram amounts of the enantiomers of [$^3H_3$]-**I** without the need for chemical derivatization.

EXPERIMENTAL

Chemicals

n-Hexane (Fisher Scientific), chloroform (EM Science), and absolute ethanol (Midwest Solvents of Illinois) were filtered through a Millipore Durapore 0.45 μm membrane filter and degassed before use. (±)-[N-methyl-$^3H_3$]-**I** (87 Ci/mmol) was purchased from New England Nuclear Research Products in ethanol solution (0.0047

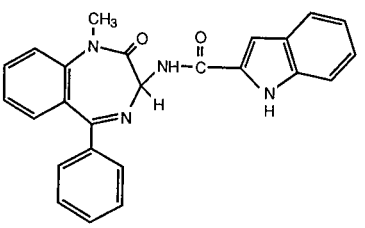

Fig. 1. Structure of (±)-**I**.

0021-9673/89/$03.50

mg/ml). A reference sample of (−)-**I** was obtained from Merck Sharp & Dohme Research Laboratories (West Point, PA, U.S.A.).

High-performance liquid chromatography

Separations were carried out using a Waters 6000 A solvent delivery system, a Rheodyne 7125 injector, and a Kratos Spectroflow 757 variable-wavelength absorbance detector operated at 290 nm. The chiral HPLC column used was a YMC (Mt. Freedom, NJ, U.S.A.) A-K03 250 × 4.6 mm I.D. column packed with a (+)-naphthylethylamine polymer bonded to spherical silica (particle size 5 μm). A mobile phase consisting of *n*-hexane–chloroform–ethanol (75:22:3) at a flow-rate of 1 ml/min was used.

Injection volumes of the drug in ethanol ranged from 10–30μl corresponding to sample amounts of 0.5–1 μg. Enantiomeric purity estimates based on chromatography peak integrations are ±3%.

RESULTS AND DISCUSSION

The enantiomers of [N-methyl-$^3H_3$]-**I** were resolved on a YMC A-K03 chiral column as shown in the chromatogram in Fig. 2a. The (+) enantiomer was eluted first at 8.9 min and was followed by the (−) enantiomer at 9.5 min, a retention time identical to that of authentic (−) enantiomer standard. A number of different solvent system combinations of *n*-hexane–chloroform, ethyl acetate, ethylene dichloride, methylene chloride, or *tert.*-butyl methyl ether–ethanol or isopropanol were examined; however, none surpassed the partial separation (α = 1.08; R_s = 0.8) achieved with *n*-hexane–chloroform–ethanol (75:22:3). It should be noted that a Resolvosil (Macherey-Nagel) bovine serum albumin chiral column was also used to partially resolve the [$^3H_3$]-**I** enantiomers [α = 1.38, (−) enantiomer eluted first]. However, the high organic content of the methanol–0.1 *M* monobasic potassium phosphate (15:85)

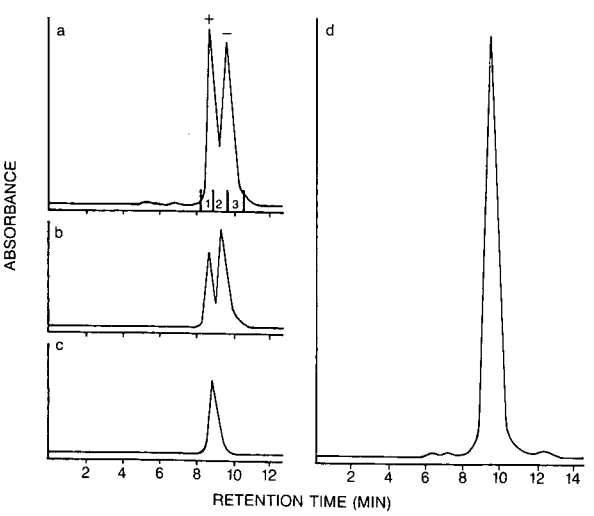

Fig. 2. Preparative HPLC of [N-methyl-$^3H_3$]-**I**. (a) Racemic mixture; (b) 65:35 (+)/(−) mixture; (c) (+) enantiomer; (d) (−) enantiomer.

mobile phase required for resolution caused significant column stationary phase denaturation after only two preparative sequences.

In order to obtain research quantities of the [$^3H_3$]-**I** enantiomers, twelve *ca.* 20-μl injections (1.829 mCi total) of radiochemically pure racemic drug were performed and three fractions were collected for each injection. As indicated in Fig. 2a, fraction 1 was collected from the beginning of the elution of the first peak, the (+) enantiomer, to the peak apex while fraction 2 was then collected to the apex of the second peak. Fraction 3, consisting primarily of the pharmacologically active (−) enantiomer was collected from the apex of the second peak until drug elution ceased. The enantiomeric purity, as determined by rechromatography, and total radioactivity for each of these fractions are listed in row A of Table I. Mixed fraction 2A, consisting of 65% of the (−) enantiomer as shown by the chromatogram in Fig. 2b, was further purified by a second round of chromatography (five *ca.* 20-μl injections). Once again, three fractions were collected with fraction 2 consisting of a mixed fraction collected between the peak apices. As detailed in row B of Table I, fraction 1B was essentially pure (+) enantiomer as shown in the chromatogram in Fig. 2c. Fraction 3B contained 95% of the (−) enantiomer. Fraction 3B and fraction 3A from the first injection series, containing 90% of the (−) enantiomer, were obtained and further purified by rechromatography (six *ca.* 20-μl injections). Three fractions were collected as usual with mixed fraction 2C between peak apices. Fraction 3C (row C, Table I) consisted of essentially 100% of the (−) enantiomer as shown by the chromatogram in Fig. 2d. A final total of 542 μCi of [^3H]$_3$-(−)-**I** was obtained, corresponding to an overall recovery of 60% from the amount of (−) enantiomer present in the racemic mixture.

In conclusion, the simple preparative procedure described above allows isolation of microgram quantities of (−)- and (+)-[N-methyl-$^3H_3$]-**I** in high enantiomeric purity and good yield for cholecystokinin antagonist studies. Although attention was directed at maximization of the yield of the pharmacologically active (−) enantiomer, the yield of the inactive (+) enantiomer could easily be increased by rechromatography of mixed fractions 1A, 2A and 2B. The number of replicate injections required could be reduced by the use of a larger, semi-preparative chiral column. Additionally,

TABLE I

CHROMATOGRAPHY DATA FROM PREPARATIVE RESOLUTION OF (+)-[N-METHYL-$^3H_3$]-**I**

		Fraction 1	*Fraction 2*	*Fraction 3*	*Recovery (%)*
A	Chromatography of racemic [$^3H_3$]-**I**	704 μCi 90% (+) 10% (−)	661 μCi 35% (+) 65% (−)	454 μCi 10% (+) 90% (−)	1.829 μCi injected 1.819 μCi recovered 99%
B	Rechromatography of mixed fraction 2A	116 μCi 100% (+)	230 μCi 40% (+) 60% (−)	279 μCi 5% (+) 95% (−)	661 μCi injected 625 μCi recovered 95%
C	Rechromatography of fractions 3A + 3B	39 μCi 62% (+) 38% (−)	72 μCi 35% (+) 65% (−)	542 μCi 100% (+)	733 μCi injected 653 μCi recovered 89%

a chiral column consisting of the analogous (−)-naphthylethylamine polymer stationary phase (currently not commercially available) would be expected to elute the desired (−) enantiomer first, potentially increasing the yield of the active enantiomer and reducing the number of replicate injections.

ACKNOWLEDGEMENTS

The author would like to thank Dr. John Bauer of Abbott Laboratories for initial development of the Resolvosil column chromatographic resolution and Merck Sharp & Dohme Laboratories for providing a sample of and (−)-**I**.

REFERENCES

1 B. E. Evans, M. G. Bock, K. E. Rittle, R. M. DiPardo, W. L. Whittier, D. F. Veber, P. S. Anderson and R. M. Freidinger, *Proc. Natl. Acad. Sci. U.S.A.*, 83 (1986) 4918.
2 R. S. L. Chang and V. J. Lotti, *Proc. Natl. Acad. Sci. U.S.A.*, 83 (1986) 4923.
3 R. S. L. Chang, V. J. Lotti, T. B. Chen and K. A. Kunkel, *Mol. Pharmacol.*, 30 (1986) 212.
4 P. J. Reider, P. Davis, D. L. Hughes and E. J. J. Grabowski, *J. Org. Chem.*, 52 (1987) 955.
5 M. G. Bock, R. M. DiPardo, B. E. Evans, K. E. Rittle, D. F. Veber, R. M. Freidinger, J. Hirshfield and J. P. Springer, *J. Org. Chem.*, 52 (1987) 3232.

Journal of Chromatography, 462 (1989) 458–460
Elsevier Science Publishers B.V., Amsterdam — Printed in The Netherlands

CHROM. 21 071

Note

Resolution of *rac*-1,2-halohydrins by chiral complexation gas chromatography

N. N. JOSHI and M. SREBNIK*
H. C. Brown and R. B. Wetherill Laboratories of Chemistry, Purdue University, West Lafayette, IN 47907 (U.S.A.)
(First received July 12th, 1988; revised manuscript received October 25th, 1988)

One of the important requisites in asymmetric synthesis is the determination of enantiomeric excess (ee) by a simple and suitable analytical technique. During the course of our studies aimed at the asymmetric synthesis of 1,2-halohydrins[1], we required a rapid and reliable method to determine %ee of the synthesized compounds. In this regard, capillary gas chromatography (GC) affords a high degree of precision and reproducibility. Surprisingly, there is no report in the literature describing the resolution of 1,2-halohydrins by GC[2].

Initially we attempted the resolution on capillary GC through the standard chiral derivatizing agents, (+)- or (–)-α-methoxy-α-(trifluoromethyl)phenylacetyl chloride (MTPA)[3], (–)-menthyl chloroformate (MCF)[4] and (–)-N-(trifluoroacetyl) prolyl chloride (TPC)[5], on the following columns of increasing polarity: methyl silicone (50 m × 0.25 mm I.D.), SPB-35 (30 m × 0.25 mm I.D.) and Supelcowax (15 m × 0.25 mm I.D.). However, only a few chlorohydrins could be moderately resolved and most compounds did not resolve at all. In addition, retention times for the iodo derivatives were excessively long with concommitant peak broadening. Recently, chiral metal complexation chromatography has emerged as an efficient method for resolving various classes of compounds[6]. Roush has further extended the scope of this method to include homoallylic alcohols as their methyl ethers[7]. We, therefore, decided to investigate the feasibility of separating, 1,2-halohydrins by complexation GC.

EXPERIMENTAL

Separations were performed on a 25 × 0.25 mm I.D. fused-silica Ni-R-Cam column purchased from Capillary Columns Complexation Chromatography (Kirchentellinsfurt, F.R.G.), with a Hewlett-Packard Model 5890 gas chromatograph and monitored with a Hewlett-Packard Model 3392A integrator. Helium was used as the carrier gas.

A microscale procedure for the derivatization was performed as follows: to a solution of acetyl chloride (0.15 mmol, 1.0 *M* in carbon tetrachloride) the halohydrin (0.1 mmol) was added, followed by pyridine (0.15 mmol, 1.0 *M* in carbon tetrachloride). After stirring at room temperature for 1 h, the reaction mixture was diluted with diethyl ether (20 ml) and washed successively with 2 *M* hydrochloric acid, water,

0021-9673/89/$03.50

saturated aqueous $NaHCO_3$ and water. After drying over sodium sulfate the solution was filtered through a short pad of neutral alumina (grade I), and an aliquot (0.2–0.4 μl) was injected in the column.

RESULTS AND DISCUSSION

We first examined underivatized chlorohydrins on an Ni-R-Cam column (25 m × 0.25 mm I.D.). Unfortunately the resolution was marginal, and the retention times were unacceptably long. In addition, thermally labile bromo- and iodohydrins could not be analysed directly. It is generally known that the introduction of π-donor systems (aromatic, carbonyl and nitrogen containing groups) enhances the chiral recognition on metal complex chiral columns. We therefore examined the corresponding acetates. Gratifyingly, the results were impressive (Table I). Excellent resolutions were obtained for all the halohydrins (Cl, Br, I) examined, cyclic as well as acyclic. In general, the separation factor (α) was greater in the case of cyclic compounds than for the corresponding acyclic analogues. Also for each series of halohydrins, resolution was in the order, Cl < Br < I. An important finding was the fact that the (1*R*,2*R*) enantiomers always eluted first on the Ni-R-Cam column[1]. A typical chromatogram is shown in Fig. I.

TABLE I

RESOLUTION OF 1,2-HALOHYDRINS (AS THEIR ACETATES) ON NI-R-CAM

Entries 1–6: carrier gas, helium; head pressure, 207 kPa. Entries 7–12; carrier gas, helium; head pressure, 137 kPa.

Entry	*Compound*	*X*	*Temperature (°C)*	t_R *(min)**	*Absolute configuration*[1]	α**
1	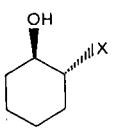	Cl	100	11	1*R*,2*R*	1.16
2		Br	105	11.8	1*R*,2*R*	1.18
3		I	110	12.3	1*R*,2*R*	1.19
4	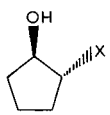	Cl	85	9.9	1*R*,2*R*	1.14
5		Br	95	10.7	1*R*,2*R*	1.15
6		I	100	11.9	1*R*,2*R*	1.17
7		Cl	80	10.97	1*R*,2*R*	1.06
8		Br	85	10.7	1*R*,2*R*	1.10
9		I	90	12.7	1*R*,2*R*	1.11
10	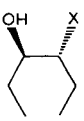	Cl	85	12.47	1*R*,2*R*	1.04
11		Br	90	16.4	1*R*,2*R*	1.07
12		I	95	17.5	1*R*,2*R*	1.07

* Retention time for the first eluting enantiomer.

** Defined as $[(t_{R2}-t_0)/(t_{R1}-t_0)]$, where t_{R1} is the retention time for the first eluting enantiomer, t_{R2} for the second, and t_0 for the unretained solvent.

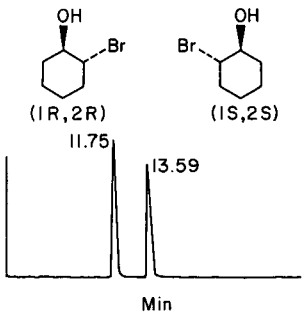

Fig. 1. Enantiomeric resolution of (±)-*trans*-1-bromocyclohexanol (as the acetate) on an Ni-R-Cam column (25 m × 0.25 mm I.D.) at 100°C and 207 kPa. Carrier gas:.helium.

Thus, we have demonstrated the efficacy of complexation GC for the enantiomeric analysis of 1,2-halohydrins. Since optically active halohydrins are potentially important synthons, the present method, which is both rapid and unequivocal, should find wide applicability.

ACKNOWLEDGEMENTS

We would like to thank the National Institutes of Health (Grant No. GM 10937-25) for financial support of this work, and Professor H. C. Brown for fruitful discussions.

REFERENCES

1 N. N. Joshi, M. Srebnik and H. C. Brown, *J. Am. Chem. Soc.*, 110 (1988) 6246.
2 W. A. König, *The Practice of Enantiomer Separation by Capillary Gas Chromatography*, Hüthig Verlag, Heidelberg, 1987.
3 J. A. Dale, D. L. Dull and H. S. Mosher, *J. Org. Chem.*, 34 (1969) 2543.
4 J. W. Westley and B. Halpern, *J. Org. Chem.*, 33 (1968) 3978.
5 E. A. Hoopes, E. T. Peltzer and J. L. Bada, *J. Chromatogr. Sci.*, 16 (1978) 556.
6 V. Schurig, *Kontakte (Darmstadt)*, 1 (1986) 3.
7 R. L. Halterman, W. R. Roush and L. K. Hoong, *J. Org. Chem.*, 52 (1987) 1152.

Journal of Chromatography, 462 (1989) 461–466
Elsevier Science Publishers B.V., Amsterdam — Printed in The Netherlands

CHROM. 21 079

Note

Analysis of vanilla essences by high-performance liquid chromatography

ALAN W. ARCHER
Division of Analytical Laboratories, New South Wales Department of Health, P.O. Box 162, Lidcombe, New South Wales 2141 (Australia)
(Received October 20th, 1988)

Vanilla essence is prepared by the extraction of vanilla beans, the cured and dried fruit pods of *Vanilla planifolia* Andrews, grown in Madagascar and Indonesia, and *V. tahitensis* Moore, grown in Tahiti. Essences may be prepared by direct extraction of the beans with aqueous ethanol or by dilution of concentrated extracts or vanilla oleoresins. The authenticity of vanilla essences has been assessed by a variety of procedures[1,2] including stable-isotope ratio analysis[3]. The use of the vanillin/*p*-hydroxybenzaldehyde ratio has been proposed[4] for this purpose and it has been suggested that the other minor compounds present in vanilla extracts could also give an indication of authenticity[5]. Vanillin and related compounds present in vanilla beans have been determined by a variety of techniques[6] including high–performance liquid chromatography (HPLC)[5,7–12]; the published HPLC methods are summarised in Table I. Only two of these methods use an internal standard and both of the compounds used as internal standards are far from ideal as ethyl vanillin may occur as an artificial additive in vanilla essences and 3,4-dihydroxybenzaldehyde occurs naturally in vanilla[5]. This note describes the separation and determination of vanillin and related compounds in vanilla essences using an aqueous–organic mobile phase with a C_{18} stationary phase and phenoxyacetic acid as an internal standard.

EXPERIMENTAL

Chromatography

The apparatus used consisted of an Altex Model 321 liquid chromatograph with a Rheodyne 7125 sample injector fitted with a 10-μl loop, and an Erma Model ERC-7210 variable-wavelength detector set at 275 nm and 0.08 absorbance units. A Microsorb C_{18} reversed-phase column, 150 × 4.6 mm I.D., 5 μm particle size, Rainin, cat. No. 80-215, with a Brownlee RP-18 5-μm, 3-cm guard column, was used with a flow-rate of 1 ml/min. The mobile phase was a mixture of 50 ml of methanol, 100 ml of acetonitrile and 10 ml of acetic acid, diluted to 1 l with filtered, de-ionised water. All organic solvents were HPLC grade and acetic acid was analytical-reagent grade.

Reagents

Ethyl vanillin, vanillyl alcohol and *p*-hydroxybenzyl alcohol were purum grade

0021-9673/89/$03.50

TABLE I

CHROMATOGRAPHIC CONDITIONS USED FOR THE DETERMINATION OF VANILLIN AND RELATED COMPOUNDS

Column	*Particle size (μm)*	*Mobile phase*		*Detector wavelength (nm)*	*Flow-rate (ml/min)*	*Internal standard*	*Ref.*
		Aqueous phase modifier	*Organic component*				
Micropak MCH	10	Orthophosphoric acid	Methanol 10–100%	280	2	No	5
μBondapak Phenyl	10	Orthophosphoric acid	Methanol 25%	280	3	No	7
RP-18 Merck	10	Acetic acid	Methanol 8–48%	275	1	No	8
C_{18}	–	Orthophosphoric acid	Methanol 25%	254	–	2,4-Dihydroxybenzaldehyde	9
LiChrosorb C_{18}	5	Buffer, pH 2.4	Methanol 35%	254	1	Ethyl vanillin	10
LiChrosorb C_8	10	Acetic acid	Methanol 10%	254	2.5	No	11
μBondapak C_{18}	5	Nil	Methanol 40%	275	1	No	12
Microsorb C_{18}	5	Acetic acid	Methanol 5%, acetonitrile 10%	275	1	Phenoxyacetic acid	This work

(Fluka), vanillin was Unilab grade (Ajax Chemicals, Sydney, Australia), vanillic acid, *p*-hydroxybenzoic acid, *p*-hydroxybenzaldehyde, coumarin and 3,4-dihydroxybenzaldehyde were from Tokyo Kasei; phenoxyacetic acid was from Merck. Methanol for the standard and internal standard solutions was analytical-reagent grade from May and Baker.

A standard solution was prepared to contain 100 mg of vanillin, 10 mg vanillic acid, 10 mg *p*-hydroxybenzaldehyde and 5 mg of *p*-hydroxybenzoic acid in 100 ml of methanol. The internal standard solution contained 250 mg phenoxyacetic acid in 1 litre of methanol–water (50:50, v/v).

Procedure

Vanilla essences contain about 0.1% (w/v) vanillin and were analysed without further dilution; concentrates and oleoresins were diluted with methanol–water (50:50) to give a vanillin concentration of about 0.1% vanillin. Add 1 ml of standard solution to 10 ml of internal standard solution, mix, inject 10 μl and determine the peak area ratios of vanillin, *p*-hydroxybenzaldehyde, vanillic acid and *p*-hydroxybenzoic acid to phenoxyacetic acid. Add 1 ml of vanilla essence, or diluted concentrate, to 10 ml of internal standard solution and inject 10 μl. From the peak area ratios of vanillin, *p*-hydroxybenzaldehyde, vanillic acid and *p*-hydroxybenzoic acid to phenoxyacetic acid, calculate the concentration of these compounds in the sample.

RESULTS AND DISCUSSION

Vanilla essences contain vanillin as the major aromatic compound and this is accompanied by smaller concentrations of vanillic acid, vanillyl alcohol, *p*-hydroxybenzaldehyde, *p*-hydroxybenzoic acid, *p*-hydroxybenzyl alcohol and 3,4-dihydroxybenzaldehyde. Ethyl vanillin, a synthetic vanillin analogue, may be present as an additive in vanilla essences. The major compound vanillin has a UV absorption maximum in the mobile phase at 275 nm and this was chosen as the detector wavelength. Adequate separation of the compounds of interest was obtained with an aqueous mobile phase containing both methanol and acetonitrile. A number of aromatic acids were examined for use as an internal standard; phenoxyacetic acid has a suitable retention time and uv absorption spectrum, with a maximum in the mobile phase at 275 nm. It was necessary to dilute the samples before analysis and this was done by adding the sample to the internal standard solution. Vanilla essences may contain caramel as an added colouring and it was found that a precipitate was produced if these essences were added to the internal standard dissolved in 100% methanol. When this solvent was replaced with methanol–water (50:50), no precipitation occured. The separation of reference compounds is shown in Fig. 1A. Typical retention times (in minutes) were: *p*-hydroxybenzyl alcohol, 4.1; vanillyl alcohol, 4.9; *p*-hydroxybenzoic acid, 7.3; vanillic acid, 8.8; *p*-hydroxybenzaldehyde, 10.4; vanillin, 13.5; phenoxyacetic acid, 21.8; ethyl vanillin, 28.8. Coumarin, retention time 39.2 min, was not detected in the vanilla extracts, essences and oleoresins examined. In practice, the two earlier eluting compounds were not quantitated as interfering compounds with similar retention times are present in vanilla essences, as shown in Fig. 1B. The small peak X (Fig. 1B), retention time 6.2 min, was identified by co-chromatography as 3,4-dihydroxybenzaldehyde. The detector response for vanillin, *p*-hy-

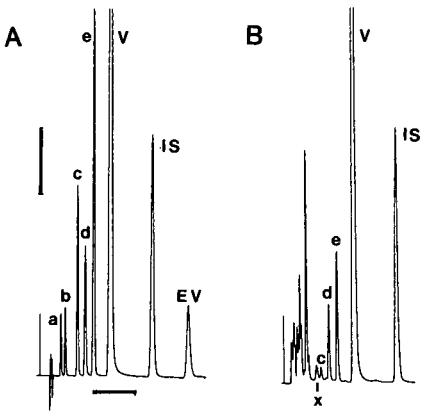

Fig. 1. HPLC traces of (A) reference compounds and (B) laboratory-prepared extract of vanilla beans. Peaks: a = *p*-hydroxybenzyl alcohol; b = vanillyl alcohol; c = *p*-hydroxybenzoic acid; d = vanillic acid; e = *p*-hydroxybenzaldehyde; V = vanillin; IS = phenoxyacetic acid, EV = ethyl vanillin; x = 2,4-dihydroxybenzaldehyde. Vertical bar = 0.01 a.u.; horizontal bar = 10 min. For chromatographic conditions see text.

TABLE II

HPLC ANALYSIS OF VANILLA OLEORESINS, VANILLA EXTRACTS AND RETAIL VANILLA ESSENCES

	p-Hydroxy-benzoic acid	*Vanillic acid*	*p-Hydroxy-benzaldehyde*	*Vanillin*
Retail vanilla essences (mg/100 ml)				
1	0.14	0.50	6.23	79.3
2	0.17	0.97	9.46	128.2
3	1.27	2.34	2.09	82.6
4	1.51	4.27	5.52	100.4
5	2.57	8.62	8.34	115.5
Vanilla extracts (mg/100 ml)				
1 Bourbon beans	1.33	3.49	6.49	85.4
2 Bourbon beans	0.90	3.90	5.90	85.7
3 Bourbon beans	1.77	7.04	7.38	129.3
4 Bourbon beans	1.63	7.16	7.83	134.0
5 Bourbon beans	1.85	9.30	11.2	163.2
6 Java beans	2.43	7.95	7.48	81.9
Vanilla oleoresins (%, w/w)				
1	0.028	0.089	0.093	1.58
2	0.058	0.192	0.183	3.32
3	0.009	0.017	0.305	3.98

TABLE III

RATIOS OF CONCENTRATIONS OF MINOR COMPOUNDS TO VANILLIN

	Ratio (mg compound/g vanillin)		
	p-Hydroxy-benzoic acid	*Vanillic acid*	*p-Hydroxy-benzaldehyde*
Retail vanilla essences			
1	2	6	78
2	1	8	73
3	15	28	25
4	15	42	55
5	22	75	72
Vanilla extracts			
1	16	41	76
2	11	46	69
3	14	55	57
4	12	53	58
5	11	57	69
6	30	97	91
Vanilla oleoresins			
1	18	57	59
2	17	58	55
3	2	4	77
U.S.A. values*	5–21	27–82	57–90 (n = 13)
F.R.G. values**	–	–	54–92 (n = 40)

* Calulated from the results in ref. 11.
** Calulated from the results in ref. 4.

droxybenzaldehyde, vanillic acid and *p*-hydroxybenzoic acid was linear up to concentrations of 150, 12, 10 and 5 mg/100 ml, respectively, in the sample. The recoveries of compounds added to a diluted vanilla essence to give concentrations within the linear response range were: vanillin 99.8–101%, vanillic acid 100.5–102%, *p*-hydroxybenzaldehyde 100.9–108.5% and *p*-hydroxybenzoic acid 99.0–100.7%

Samples of vanilla oleoresins, extracts of vanilla beans prepared in the laboratory with ethanol–water (50:50, v/v) and retail samples of vanilla essences were examined; the results are shown in Table II. Although the concentrations of all compounds vary widely, the ratios of the concentrations of the minor compounds to that of vanillin, expressed as mg of compound/g of vanillin, show less variation and these ratios can be used to assess the authenticity of vanilla extracts. These ratios are shown in Table III. The ratios for the three compounds present in the genuine, laboratory prepared vanilla extracts are similar to those calculated from the reported concentrations found in vanilla extracts by HPLC[11]. The ratio of vanillin to *p*-hydroxybenzaldehyde has been used to determine the authenticity of vanilla extracts and a range of 10.9–18.4 g vanillin/g *p*-hydroxybenzaldehyde was reported[4]. This is equivalent to a range of 54–92 mg *p*-hydroxybenzaldehyde/g vanillin, similar to those calculated from the U.S.A. results and the range of ratios found for the laboratory prepared

vanilla extracts (Table III). The following ranges of ratios (mg compound/g vanillin) are suggested for genuine vanilla essences: *p*-hydroxybenzoic acid, 5–30; vanillic acid, 27–97; *p*-hydroxybenzaldehyde, 54–92. The *New South Wales Pure Food Regulations*[13] require vanilla essence to contain "the quantity of soluble substances in their natural proportions that are extracted by an aqueous alcoholic solution", the ethanol content of which is 50–55% (v/v). A comparison of the results obtained from the retail samples of vanilla essences and the ratios proposed above, suggest that these requirements[13] are met only by retail essences 4 and 5.

ACKNOWLEDGEMENTS

The author is grateful to Bush Boake Allan Australia Ltd., Melbourne, Australia, Givaudan Pty. Ltd., Sydney, Australia and Allied Industries Pty. Ltd., Sydney, Australia, for gifts of vanilla beans and oleoresins and acknowledgement is made to the Director, Division of Analytical Laboratories, New South Wales Department of Health, for permission to publish this paper.

REFERENCES

1 G. E. Martin, M. W. Etheridge and F. E. Kaiser, *J. Food Sci.*, 42 (1977) 1580.
2 M. Ishiguro, S. Nanba and A. Nakatsu, *Kazei Chuo Bunseikishoho*, 26 (1986) 61.
3 G. E. Martin, F. C. Alfonso, D. M. Figert and J. M. Burggraff, *J. Assoc. Off. Anal. Chem.*, 64 (1981) 1149.
4 U. Jürgens, *Lebensmittelchem. Gerichtl. Chem.*, 35 (1981) 97.
5 F. Dalang, E. Martin and J. Vogel, *Mitt. Geb. Lebensmittelunters. Hyg.*, 73 (1982) 371.
6 J. S. Pruthi, *Spices and Condiments: Chemistry, Microbiology, Technology*, Academic Press, New York, 1980, p. 146.
7 U. Jürgens, *Deut. Lebens. Rundschau*, 77 (1981) 211.
8 A. Herrmann and M. Stöckli, *J. Chromatogr.*, 246 (1982) 313.
9 N. Arnaud, J. C. Bayle and M. Derbesy, *Parfums, Cosmet. Aromes*, 53 (1983) 99; *Chem. Abstr.*, 100 (1984) 101716b.
10 D. Fraisse, F. Maquin, D. Stahl, K. Suon and J. C. Tabet, *Analusis*, 12 (1984) 63.
11 P. A. Guarino and S. M. Brown, *J. Assoc. Off. Anal. Chem.*, 68 (1985) 1198.
12 R. D. Thompson and T. J. Hoffmann, *J. Chromatogr.*, 438 (1988) 369.
13 *New South Wales Pure Food Regulations*, 1937, regulation 49 (6), vanilla essences.

Journal of Chromatography, 462 (1989) 467–470
Elsevier Science Publishers B.V., Amsterdam — Printed in The Netherlands

CHROM. 21 047

Note

Chromatographic separation of cholesteryl acetate and its chloro analogues

HARI K. BHAT and G. A. S. ANSARI*

Department of Human Biological Chemistry and Genetics and Department of Pathology, University of Texas Medical Branch, Galveston, TX 77550 (U.S.A.)

(First received July 20th, 1988; revised manuscript received October 12th, 1988)

Cholesterol is esterified by long chain fatty acids for storage, transport and maintenance of cholesterol homeostasis in the body. Enzymes responsible for the formation of cholesterol esters are present both in the cell as well as in plasma[1–7].

Recently, it has been shown that xenobiotics containing free carboxylic functional groups or those which are converted to carboxylic acid during their metabolism result in the formation of cholesteryl esters[8–12]. These xenobiotic cholesteryl esters behave differently than the normally occurring long chain cholesteryl esters[10,11] and possess specific toxicity[13].

In order to study the formation and behavior of xenobiotic cholesteryl esters resulting from mono-, di- and tri-chloroacetic acids, we have synthesized and characterized mono-, di- and tri-chloroacetates of cholesterol. For the purpose of analysis of these cholesteryl chloroacetates in various tissues and fluids, we have developed chromatographic procedures which are described in this communication.

MATERIALS AND METHODS

Reagents

Cholesterol was purchased from MCB (Cincinnati, OH, U.S.A.). Cholesteryl acetate was obtained from Sigma (St. Louis, MO, U.S.A.). Chloroacetyl chloride, dichloroacetyl chloride and trichloroacetyl chloride were bought from Aldrich (Milwaukee, WI, U.S.A.).

Thin-layer chromatography (TLC) plates coated with silica gel were purchased from Analtech (Newark, DE, U.S.A.). Silica gel was purchased from E. Merck (Cherry Hill, NJ, U.S.A.). Solvents (HPLC-grade) were purchased from Fisher Scientific (Houston, TX, U.S.A.).

Purification of cholesterol and cholesteryl acetate

Cholesterol was purified by column chromatography over silica gel 60 (70–230 mesh) and eluted with hexane–ethylacetate (19:1, v/v). Fractions of 5 ml were collected and monitored by TLC as described later. Fractions corresponding to cholesterol were pooled and crystallized from methanol. Cholesteryl acetate was purified by crystallization from a hexane–acetone (1:5, v/v) mixture.

0021-9673/89/$03.50

Synthesis of mono-, di- and tri-chloroacetates of cholesterol

Cholesteryl monochloroacetate was prepared by dissolving 10 g of purified cholesterol in 14 ml of dry pyridine, to which 2.72 g of monochloroacetyl chloride were added. The reaction mixture was heated at 60°C for 4 h, cooled and poured into ice-cold water. The solid mass thereby formed was filtered, dried over anhydrous calcium chloride and recrystallized from hexane–acetone (1:1, v/v). Cholesteryl dichloro- and trichloroacetates were similarly prepared by using 3.67 g of dichloroacetyl chloride and 5.60 g of trichloroacetyl chloride, respectively. The structures of these compounds were confirmed by NMR and mass spectrometry (data not shown).

High-performance liquid chromatography (HPLC)

The chromatographic analysis was conducted on a Beckman Model 334 liquid chromatograph connected with an Ultrasphere ODS column (5 μm particle size, 25 cm × 4.6 mm I.D.) Altech Assoc. (Deerfield, IL, U.S.A.); a Beckman 165 variable-wavelength detector and a Perkin-Elmer 023 recorder.

Thin-layer chromatography

TLC was performed on silica gel G (250 μm) glass plates in a presaturated chromatographic chamber. The plates were air dried, sprayed with 50% sulfuric acid and heated at 120°C for 5 min, to detect cholesteryl esters.

Stock solutions

Stock solutions of standards were prepared by dissolving 20 mg in 10 ml of chloroform and stored at 4°C. A stock solution of the mixture was prepared by dissolving cholesteryl acetate (58.0 μmol), cholesteryl monochloroacetate (54.0

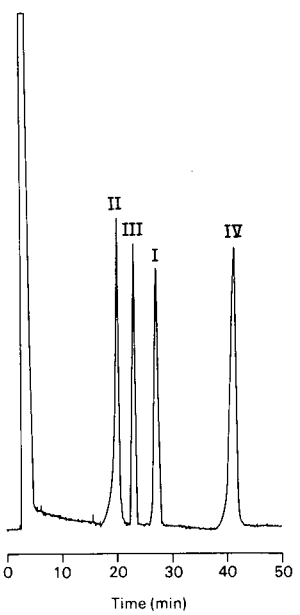

Fig. 1. Separation of cholesteryl acetate and its chloro analogues by HPLC. Injection volume 100 μl; detection at 210 nm; 0.300 a.u.f.s.

TABLE I

STANDARD CURVE OF CHOLESTERYL ESTERS

The data presented are averages of three experiments ± standard deviation.

Concentration (μg)	*Peak area (mm^2)*			
	I	*II*	*III*	*IV*
2.0	1.51 ± 0.31	1.44 ± 0.17	1.76 ± 0.13	1.83 ± 0.09
4.0	2.72 ± 0.49	2.48 ± 0.40	3.71 ± 0.54	3.54 ± 0.06
6.0	3.38 ± 0.47	3.20 ± 0.39	5.51 ± 0.34	5.83 ± 0.72
8.0	4.08 ± 0.24	4.90 ± 0.91	5.90 ± 0.44	5.94 ± 0.09
10.0	5.86 ± 0.11	6.29 ± 0.28	8.14 ± 0.74	7.61 ± 1.25
Correlation coefficient	0.990	0.984	0.983	0.976

μmol), cholesteryl dichloroacetate (50.30 μmol), and cholesteryl trichloroacetate (47.0 μmol) in 10 ml chloroform. Dilutions were made from the stock solutions of standards and mixture to estimate the detection limit.

RESULTS AND DISCUSSION

Cholesteryl acetate (I), cholesteryl monochloroacetate (II), cholesteryl dichloroacetate (III), and cholesteryl trichloroacetate (IV) can be resolved by HPLC using hexane–methanol (1:32, v/v) at a flow-rate of 1 ml/min in 42 min (Fig. 1). Under these conditions cholesteryl monochloroacetate eluted first (19.8 min) and cholesteryl trichloroacetate last (41.6 min). Cholesteryl acetate had a retention time higher than

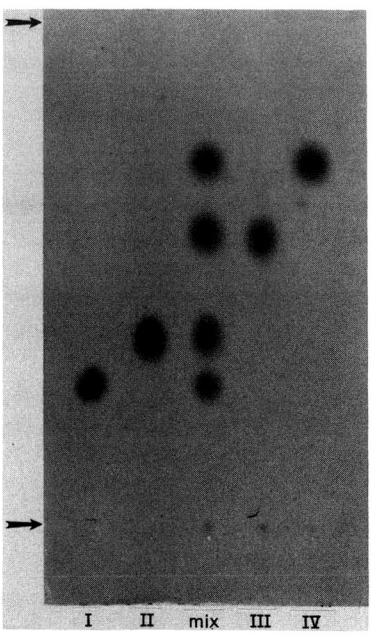

Fig. 2. Separation of cholesteryl acetate and its chloro analogues by TLC.

TABLE II

R_F VALUES RELATIVE TO CHOLESTERYL ACETATE, USING DIFFERENT RATIOS OF HEXANE AND ETHYL ACETATE

R_F values of cholesteryl acetate were: 0.66, 0.55, 0.37, 0.35 and 0.29 using hexane–ethyl acetate 4:1, 9:1, 19:1, 24:1 and 66:1 (v/v), respectively.

Solvent system: hexane–ethyl acetate (v/v)	*Relative R_F*		
	II	*III*	*IV*
4:1	1.06	1.14	1.18
9:1	1.13	1.27	1.36
19:1	1.24	1.73	2.02
24:1	1.26	1.77	2.14
66:1	1.29	1.95	2.41

cholesteryl dichloroacetate and lower than cholesteryl trichloroacetate. Similar resolution was achieved by using hexane–methanol (1:19, v/v) in 35 min (I, 23.24; II, 17.80; III, 20.12; IV, 34.8 min). The standard curve for each ester was determined (Table I) and was found to be linear between 2–10 μg at 0.05 a.u.f.s. Under these conditions, cholesteryl palmitate, cholesteryl stearate and cholesteryl oleate have a much longer retention time (>90 min).

Fig. 2 shows that compounds I–IV could be resolved on a silica gel TLC plate, using hexane–ethyl acetate (66:1, v/v) as the mobile phase. Table II summarizes the relative R_F values relative to compound I, using different solvent systems. As evident from Table II, the solvent system for the best separation of these halogenated esters of cholesterol is hexane–ethyl acetate (66:1, v/v). Cholesterol does not move in this solvent system. If we use only hexane as a solvent, compound I does not move and compound II barely moves (R_F 0.02). If hexane and ethyl acetate are used in the ratio of 4:1 (v/v) a poor resolution of compound III and IV is obtained.

ACKNOWLEDGEMENTS

This research was supported by grants ES 04815 awarded by the National Institute of Environmental Health Sciences and DK 27135 awarded by the National Institute of Diabetes, Digestive and Kidney Diseases.

REFERENCES

1 A. A. Spector, S. N. Mathur and T. L. Kauce, *Prog. Lipid Res.*, 18 (1979) 31.
2 A. H. Lichtenstein and P. Brecher, *J. Biol. Chem.*, 255 (1980) 9098.
3 A. J. Day and R. K. Tume, *Biochim. Biophys. Acta*, 176 (1969) 367.
4 D. Kritchevsky and H. V. Kothari, *Biochim. Biophys. Acta*, 326 (1973) 489.
5 D. S. Goodman, D. Keykin and T. Shiratori, *J. Biol. Chem.*, 239 (1964) 1335.
6 J. A. Glomset, *J. Lipid Res.*, 9 (1968) 155.
7 Y. L. Marcel, *Adv. Lipid Res.*, 19 (1982) 85.
8 G. B. Quistad, L. E. Staiger and D. A. Schooley, *J. Agric. Food Chem.*, 24 (1976) 644.
9 G. B. Quistad, L. E. Staiger and D. A. Schooley, *J. Agric. Food Chem.*, 26 (1978) 60.
10 R. Fears, K. H. Baggaley, P. Walker and R. M. Hindley, *Xenobiotica*, 12 (1982) 427.
11 P. O. Gunnarsson, S. A. Johansson and L. Svensson, *Xenobiotica*, 14 (1984) 569.
12 H. Kaneko, M. Matsuo and J. Miyamoto, *Toxicol. Appl. Pharmacol.*, 83 (1986) 148.
13 Y. Okuno, T. Seki, S. Ito, H. Kaneko, T,. Watanabe, T. Yamada and J. Miyamoto, *Toxicol. Appl. Pharmacol.*, 83 (1986) 157.

Journal of Chromatography, 462 (1989) 471–474
Elsevier Science Publishers B.V., Amsterdam — Printed in The Netherlands

CHROM. 21 004

Note

Sensitive detection of unsaturated disaccharides from chondroitin sulphates by thin-layer chromatography as their dansylhydrazine derivatives

KAZUFUSA SHINOMIYA, YUKIKO HOSHI and TOSHIO IMANARI*
Faculty of Pharmaceutical Sciences, Chiba University, 1-33, Yayoi-cho, Chiba-shi, Chiba, 260 (Japan)
(First received May 27th, 1988; revised manuscript received September 23rd, 1988)

Paper chromatography[1] has been used for the analysis of unsaturated disaccharides after the digestion of chondroitin sulphates (ChS) by chondroitinase ABC or AC. Thin-layer chromatography (TLC) on cellulose plates has also been used by many workers[2–4]. Recently, high-performance liquid chromatography (HPLC) has been used for the determination of unsaturated disaccharides[5–12], but TLC is still useful as a simple analytical method.

Shimada and co-workers reported the application of TLC on silica gel for the separation of hyaluronate oligosaccharides[13] and unsaturated chondroitin sulphate disaccharides[14]. However, colorimetric detection on TLC plates with a carbazole reagent is not sensitive enough.

In this paper, we describe the TLC separation of small amounts of unsaturated disaccharides as their dansylhydrazine [1-naphthalenesulphonyl-5-(dimethylamino) hydrazide] derivatives, which have been used in fluorimetric precolumn derivatization in HPLC[10,11].

EXPERIMENTAL

Reagents and materials

The standard unsaturated disaccharides 2-acetamido-2-deoxy-3-O-(β-D-gluco-4-enepyranosyluronic acid)-D-galactose (ΔDi-0S), 2-acetamido-2-deoxy-3-O-(β-D-gluco-4-enepyranosyluronic acid)-4-O-sulpho-D-galactose (ΔDi-4S), 2-acetamido-2-deoxy-3-O-(β-D-gluco-4-enepyranosyluronic acid)-6-O-sulpho-D-galactose (ΔDi-6S), 2-acetamido-2-deoxy-3-O-(2-O-sulpho-β-D-gluco-4-enepyranosyluronic acid)-D-galactose (ΔDi-UA2S), 2-acetamido-2-deoxy-3-O-(2-O-sulpho-β-D-gluco-4-enepyranosyluronic acid)-4-O-sulpho-D-galactose (ΔDi-diS$_B$), 2-acetamido-2-deoxy-3-O-(2-O-sulpho-β-D-gluco-4-enepyranosyluronic acid)-6-O-sulpho-D-galactose (ΔDi-diS$_D$), 2-acetamido-2-deoxy-3-O-(β-D-gluco-4-enepyranosyluronic acid)-4,6-di-O-sulpho-D-galactose (ΔDi-diS$_E$), 2-acetamido-2-deoxy-3-O-(2-O-sulpho-β-D-gluco-4-enepyranosyluronic acid)-4,6-di-O-sulpho-D-galactose (ΔDi-triS), 2-acetamido-2-deoxy-3-O-(β-D-gluco-4-enepyranosyluronic acid)-D-glucose (ΔDi-HA) and chondroitinase ABC were purchased from Seikagaku Kogyo (Tokyo, Japan) and dansylhydrazine from Fluka (Buchs, Switzerland). All other chemicals were of analytical-reagent grade.

0021-9673/89/$03.50

Kieselgel 60 thin-layer plates (plastic plate, 0.2 mm thickness) were obtained from Merck (Darmstadt, F.R.G.).

A UV lamp (Model UVGL-15 Mineralight Lamp; San Gabriel CA, U.S.A.) was used to detect the spots on the developed TLC plates.

Separation of glycosaminoglycans in rabbit plasma and urine

Plasma glycosaminoglycans (GAGs) were separated according to the method of Emura and Mukuda[15] with a 100-μl sample plasma.

Urinary GAGs were separated according to Poulsen's method[16].

Enzymatic digestion

Aliquots of 10 μl each of 0.2 *M* Tris–HCl buffer (pH 8.0) and an aqueous solution of 0.1 U chondroitinase ABC were added to 20 μl of plasma or a urinary GAG solution. The mixture was incubated at 37°C for 3 h and then lyophilized. The residue was dissolved in 10 μl of water. This solution was used for dansylhydrazine derivatization.

Fluorescent derivatization of unsaturated disaccharides

Aliquots of 20 μl of a 0.75% (w/v) solution of trichloroacetic acid in ethanol and 20 μl of a 1.0% (w/v) solution of dansylhydrazine in ethanol were added to 10 μl of an aqueous solution of unsaturated disaccharides produced enzymatically from plasma or urinary GAGs. The mixture was incubated at 40°C for 150 min, then cooled to room temperature. An aliquot of 5 μl of the resulting solution was submitted to TLC.

RESULTS AND DISCUSSION

Separation of unsaturated disaccharides

The separation of dansylhydrazine derivatives of unsaturated disaccharides was examined under various conditions using commercial silica plates. It was found that ΔDi-0S, ΔDi-4S, ΔDi-6S, ΔDi-UA2S, ΔDi-diS_B, ΔDi-diS_D, ΔDi-diS_E, ΔDi-triS and ΔDi-HA could be resolved satisfactorily with *n*-propanol–isopropanol–*n*-butanol–water (30:45:5:20, v/v) containing 0.04 *M* sodium chloride and 0.01 *M* ammonia (Table I).

The detection limits of ΔDi-0S, ΔDi-4S and ΔDi-6S were 90 pmol with observation under UV light with the naked eye.

TABLE I

R_F VALUES OF DANSYLHYDRAZINE DERIVATIVES OF UNSATURATED DISACCHARIDES

Unsaturated disaccharide	R_F	*Unsaturated disaccharide*	R_F
ΔDi-0S	0.72	ΔDi-diS_D	0.52
ΔDi-4S	0.56	ΔDi-diS_E	0.41
ΔDi-6S	0.61	ΔDi-triS	0.30
ΔDi-UA2S	0.66	ΔDi-HA	0.75
ΔDi-diS_B	0.47		

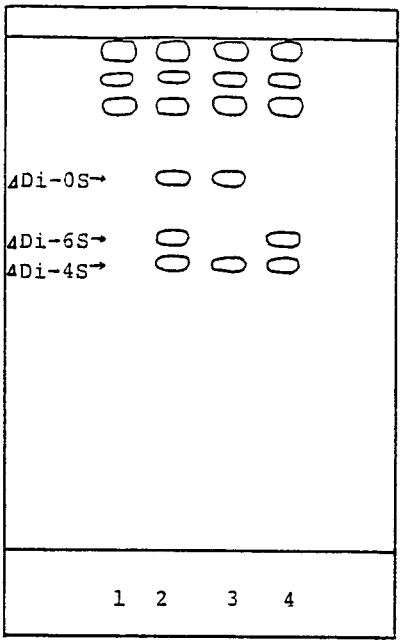

Fig. 1. Chromatogram of dansylhydrazine derivatives of unsaturated disaccharides produced from plasma and urinary chondroitin sulphates: 1 = blank; 2 = mixture of ΔDi-0S, ΔDi-4S and ΔDi-6S; 3 = plasma ChS; 4 = urinary ChS. Conditions: TLC plate, silica gel 60; developing solvent, *n*-propanol–isopropanol–*n*-butanol–water (30:45:5:20, v/v) containing 0.04 *M* sodium chloride and 0.01 *M* ammonia.

Although the TLC of ΔDi-0S, ΔDi-4S and ΔDi-6S has been studied previously[2–4,14], the separation of oversulphated unsaturated disaccharides such as ΔDi-diS_B, ΔDi-diS_D, ΔDi-diS_E and ΔDi-triS has not been reported. Using the method described here, all unsaturated disaccharides produced enzymatically from ChS can be separated satisfactorily with development under isocratic conditions.

Identification of unsaturated disaccharides from ChS in rabbit plasma and urine

The proposed method was applied to the identification of unsaturated disaccharides produced enzymatically from ChS in rabbit plasma and urine. Fig. 1 shows the chromatogram of dansylhydrazine derivatives of unsaturated disaccharides from rabbit plasma and urinary GAGs obtained by digestion with chondroitinase ABC.

ΔDi-0S and ΔDi-4S were detected in plasma ChS and ΔDi-4S and ΔDi-6S in urinary ChS.

In conclusion, the proposed method is useful for the identification of the unsaturated disaccharides produced from GAGs such as ChS by chondroitinases, and can be used for their structural characterization and as a screening test for ChS in biological samples because of its high sensitivity.

REFERENCES

1 H. Saito, T. Yamagata and S. Suzuki, *J. Biol. Chem.*, 243 (1968) 1536.
2 L. Wasserman, A. Ber and D. Allalouf, *J. Chromatogr.*, 136 (1977) 342.
3 Y. Mikuni-Takagaki and B. P. Toole, *J. Biol. Chem.*, 254 (1979) 8409.
4 A.-M. Säämänen and M. Tammi, *Anal. Biochem.*, 140 (1984) 354.
5 K. Murata and Y. Yokoyama, *Anal. Biochem.*, 146 (1985) 327.
6 J. Macek, J. Krajíčková and M. Adam, *J. Chromatogr.*, 414 (1987) 156.
7 K. Murata and Y. Yokoyama, *J. Chromatogr.*, 415 (1987) 231.
8 T. Gherezghiher, M. C. Koss, R. E. Nordquist and C. P. Wilkinson, *J. Chromatogr.*, 413 (1987) 9.
9 C. Kodama, N. Ototani, M. Isemura and Z. Yosizawa, *J. Biochem.*, 96 (1984) 1283.
10 K. Shinomiya, I. Koshiishi, T. Imanari, M. Takeda, M. Maeda and A. Tsuji, *Chem. Pharm. Bull.*, 34 (1986) 4887.
11 K. Shinomiya, S. Yamanashi and T. Imanari, *Biomed. Chromatogr.*, 2 (1987) 169.
12 H. Toyoda, K. Shinomiya, S. Yamanashi, I. Koshiishi and T. Imanari, *Anal. Sci.*, 4 (1988) 381.
13 E. Shimada and G. Matsumura, *J. Biochem.*, 96 (1984) 721.
14 E. Shimada, N. Kudoh, M. Tomioka and G. Matsumura, *Chem. Pharm. Bull.*, 35 (1987) 1503.
15 Y. Emura and T. Mukuda, *Seikagaku*, 45 (1973) 30.
16 J. H. Poulsen, *Scand. J. Clin. Lab. Invest.*, 41 (1981) 367.

Journal of Chromatography, 462 (1989) 475–477
Elsevier Science Publishers B.V., Amsterdam — Printed in The Netherlands

CHROM. 21 052

Book Review

Methods in molecular biology, Vol. 3, New protein techniques and *Vol. 4, New nucleic acid techniques*, edited by J. M. Walker, Humana Press, Clifton, NJ, 1988, 512 (Vol. 3) and 576 (Vol. 4) pp., price US$ 49.50 per volume, ISBN 0-89603-126-8 (Vol. 3), 0-89603-127-6 (Vol. 4).

This series of volumes has set itself a very laudable task: "... many of the new techniques in molecular biology are relatively easy to master, it is often difficult for a researcher to obtain all the relevant information necessary for setting up and successfully applying a new technique. Information is of course available in the research literature, but this often lacks the depth of description that the new user requires".

In other words it was thought that a series of volumes should be created analogous to *Organic Syntheses* which gives a detailed description of new techniques.

"Each method is described by an author who has regularly used the technique in his or her own laboratory". The series differs here from *Organic Syntheses* in that the method and its description were not checked by another group. It also makes evident the major draw-back of these volumes. The "chapters", *i.e.* methods are described by somebody who has used it for some time. Will he be the right person to explain it to a worker who has no knowledge of it? Will he not forget to mention items which have become obvious to him through long practise but are not obvious to beginners?

Let us take a typical method (p. 53, Vol. 3) on N-terminal amino acids:

N-Terminal Amino Acids 53

5. Centrifuge briefly to ensure that reagents are at the bottom of tube.
6. Cover the tubes with parafilm to minimize evaporation, and incubate at approximately 20°C for 35 min in the dark.
7. Add 2 μL of ethylammonium chloride solution, and centrifuge briefly.
8. After 1 min incubation, dry in the centrifugal concentrator.
9. Add 50 μL of HCl and seal the tube in a oxygen/butane flame by twisting and drawing out when hot.
10. Incubate at 105°C for 8 h. Crack open the tubes by prescoring with the diamond tip pen, and dry off the HCl under vacuum.

3.2. Separation of Derivatives

1. Equilibrate the HPLC column at 39°C in 93% buffer

A/7% buffer B at a flow rate of 1.2 mL/min for 5 μm packing or 1.0 mL/min for 3 μm packings.
2. Add 4 μL of dry methanol to each of the sample and standard tubes and dry in the centrifugal concentrator. Repeat this procedure once more. This step ensures removal of all volatile contaminants.
3. Redissolve the samples and standards in a suitable volume to enable injection of 5 μL of solution containing 50–200 pmol of Dns-amino acid(s).
4. The derivatives are eluted with a gradient of buffer B. The exact gradient required will vary from column type to column type; that used for the LKB SuperPac column is shown in Fig. 2.
5. The eluate is monitored for absorbance at 254 nm, or for more sensitive detection for fluorescence

Point 8. How critical is the 1-min incubation?
Point 10. How critical are 105°C for 8 h?

For the separation:

Point 1. Equilibrate the HPLC column at 39°C ... How critical is that?
Point 4. The derivatives are eluted with a gradient of buffer B. The exact gradient required will vary from column type to column type.

This is hardly an exact description, nor are data provided that would help in the decision.

There are "notes" which deal with some of the points but certainly not all. So the reader will have to look up the original paper in the hope of finding further details.

In Chapter 20 on "Computer analysis of 2-D electrophoresis gels" one reads:

2. System Overview

The computing hardware for abstracting protein spot data from a 2-D gel image comprise the CLIP4S array computer and a LSI11-23™ minicomputer. Apart from controlling the operations and data movements in and out of the array computer, the minicomputer also provides the tools and environment for software developments under the UNIX™ operating system. Mass data storage is provided by magnetic disks.

Briefly a 2-D gel is back-illuminated from a lightbox with a Vidicon television camera mounted directly above it. The television signals of the 2-D gel image are converted into a digitized image of 512 x 512 picture elements (pixels): each pixel can have one of 256 (8 bits) gray values or intensity (0 = black, 255 = white).

The CLIP4S array computer consists of a 512 x 4 strip of processing cells. Each processing cell is a simple computer in its own right, and each cell is connected to its eight nearest neighbors, as shown in Fig. 1, so that information can be passed between them. The array com-

> puter operates on successive strips of 512 x 4 pixels in the gel image, starting from the top of the image and working downward. This scanning process is completely automatic. The processing power of the array computer comes from the design; all available 2048 processing cells operate on their assigned pixels simultaneously. For example, 2048 additions can be completed in the

This is surely not very explanatory for a worker who is not in the computer field and perhaps of little use to one who is. The discussion concludes that "The success of the computerized 2-D gel analysis depends on close collaboration between research workers working on computer development and those in the laboratory". This is eminently correct, but does it help those in the laboratory?

Another chapter on "Chromatofocusing" is fine, but does not offer anything that cannot be found in the original papers by Sluyterman *et al.*, which are much more readable.

To sum up: The series aims to help the research worker. How successful it is in each case will depend on the level of formation of the individual worker and on whether there is a good library within reach or not. Hence the volumes cannot be recommended without reservations.

Journal of Chromatography, 462 (1989) 478
Elsevier Science Publishers B.V., Amsterdam — Printed in The Netherlands

CHROM. 21 074

Book Review

Chromatography '87 (Symposia Biologica Hungarica, Vol. 37), edited by H. Kalász and L. S. Ettre, Akadémiai Kiadó, Budapest, 1988, XI + 539 pp., price US$ 54.00, ISBN 963-05-4988-3.

Though the preface mentions that due to the tardy publication of previous volumes, two symposia were combined into a single volume, this does not appear to have solved all problems. The 43 camera-ready manuscripts are to a large extent in alphabetical order and hence it is impossible to ascertain which papers stem from the 1986 and which from the 1987 meeting. This hinders an overview of the publications as to actuality or precedence.

Without wanting to carp unduly, it would have been preferable if the editors could have evened out some incoherences, perhaps by the addition of footnotes. There is the case of the paper by Edward-Inatimi, which presents a chromatogram for the analysis of soils, showing five adjacent peaks of Cu, Ni, Pb, Co and Mn complexes obtained by extracting with diethylammonium diethyldithiocarbonate, but where no hint is given where the other metals such as Fe, Zn, Cd, Tl etc. would be found if present and whether they would interfere with these peaks. Then the paper by Yegazar'yants on the group separation of different petroleum fractions by high-performance liquid chromatography gives no references to previous work, oddly enough as excellent pioneering work was done in the laboratory of one of the editors of this volume.

The book is attractively produced and offers a list of contributors, unfortunately with some incomplete addresses, and also a subject index.

Author Index

Erratum

J. Chromatogr., 452 (1988) 309–316
p. 312, eqn. 8 should read:

$$\alpha = \frac{k'_{A_R}}{k'_{A_S}} = \frac{k''_{A_R}}{k''_{A_S}} \cdot \frac{1 + K^m_{A_S\mathrm{CuB}}[\mathrm{CuB}^m]}{1 + K^m_{A_R\mathrm{CuB}}[\mathrm{CuB}^m]}$$

$$= \frac{1 + K^m_{A_S\mathrm{CuB}}[\mathrm{CuB}^m]}{1 + K^m_{A_R\mathrm{CuB}}[\mathrm{CuB}^m]}$$

Vol. 462

journal of chromatography news section

NEW BOOKS

Practical high performance liquid chromatography method development, by L.R. Snyder, J.L. Glajech and J.J. Kirkland, Wiley, Chichester, New York, 1988, *ca.* 288 pp., price *ca.* US$ 65.00, ISBN 0-471-62782-8.

High performance liquid chromatography, edited by P.R. Brown and R.A. Hartwick, Wiley, Chichester, New York, 1988, *ca.* 550 pp., price *ca.* US$ 87.50, ISBN 0-471-84506-X.

Principles and practice of chromatography, by B. Ravindranath, Wiley, Chichester, New York, 1988, *ca.* 380 pp., price *ca.* £ 103.00, ISBN 0-7458-0296-6.

Computerized multiple input chromatography, by M. Kaljurand and E. Küllik, Ellis Horwood, Chichester, 1988, *ca.* 200 pp., price *ca.* US$ 72.10, ISBN 0-7458-0120-X.

Chromatographic enantioseparation: methods and applications, edited by S.G. Allenmark, Ellis Horwood, Chichester, 1988, 224 pp., price £ 38.50, ISBN 0-85312-988-6.

Ion chromatography in water analysis, by O.A. Shpigun and Yu. A. Zolotov, Ellis Horwood, Chichester, 1988, 188 pp., price £ 32.50, ISBN 0-7458-0020-3.

Analytical isotachophoresis, by P. Boček, M. Deml, P. Gebauer and V. Dolnik, VCH, Weinheim, 1988, XVIII + 237 pp., price DM 156.00, £ 57.00.

Natural products isolation, separation methods for antimicrobials, antivirals and enzyme inhibitors, edited by G.H. Wagman and R. Cooper, Elsevier, Amsterdam, Oxford, New York, Tokyo, 1988, XII + 618 pp., price Dfl. 285.00, U.S.A. and Canada US$ 139.00, ISBN 0-444-87147-0.

Die Chemische Industrie und ihre Helfer, Ausgabe 1988–1989, edited by Edition Selka, Industrieschau Verlagsgesellschaft mbH, 1988, *ca.* 550 pp., price DM 53.50, ISBN 3-7790-0198-5.

Hauswirtschaftliche Briefe, by F.R. Runge, VCH, Weinheim, 1988, XIV + 546 pp., price DM 49.00.

AWARDS

DAL NOGARE AWARD

The Dal Nogare Award will be presented to Professor Phyllis R. Brown. This award has been given by the Chromatography Forum of the Delaware Valley annually since 1972. This year the award will be presented to Professor Brown by Mary Ellen McNally, President of the Chromatography Forum of the Delaware Valley on Tuesday Afternoon, March 7, 1989.

Professor Brown received a B.S. degree from George Washington University and Ph.D. from Brown University. At Brown University she did postdoctoral work in the Pharmacology Section. She was a visiting professor at the Hebrew University in Israel in 1979 and 1983. She received a Fulbright Fellowship for study in Israel in 1987. In 1983 she was given the Excellence in Research Award from the University of Rhode Island. Currently, she is Professor in the Chemistry Department at the University of Rhode Island.

Professor Brown is a pioneer in the applications of high-performance liquid chromatography (HPLC) to biomedical research. She has published over 110 research articles and 30 review articles or chapters in books. She wrote the first book on the biomedical and biochemical applications of HPLC and co-authored the first book on Reversed-Phase HPLC. Currently, she is also a co-author of the series *Advances in Chromatography* and serves on the Editorial Board of *Journal of Chromatography, Biomedical Applications*. Her current research interests involve the use of computers in the optimization of chromatographic separations of nucleotides, nucleosides and their bases, preparative HPLC for biologically samples for use in medical research and the clinical laboratory. At present, work is in progress on the separation of nucleic acids, catecholamines, and long chain unsaturated fatty acids.

1989 AMERICAN CHEMICAL SOCIETY AWARD

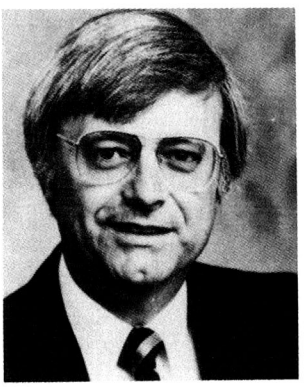

The recipients of the 1989 American Chemical Society Awards have been selected. Professor Fred E. Regnier of Purdue University will receive the ACS Award in chromatography, sponsored by Supelco. The award honors outstanding contributions to the field of chromatography.

Professor Regnier has made major contributions toward the high-performance liquid chromatographic separation of biopolymers such as proteins and nucleic acids. He received a B.S. degree from Nebraska State College (1960) and a Ph.D. degree from Oklahoma State University (1965). After completing postdoctoral research at Oklahoma State University (1966), the University of Chicago (1967), and Harvard University (1968), he joined the faculty at Purdue University in 1969.

Regnier's current research interests include the preparative and production scale separation of biopolymers and development of macroporous rigid microparticulate stationary phases. He was the recipient of the David B. Hilme Award (1982) and the Stephen Dal Nogare Award (1987) and is Editor of *Preparative Chromatography*.

The award will be presented in April 1989 at the 197th ACS Spring National Meeting in Dallas, TX, U.S.A.

KEENE P. DIMICK AWARD

Professor Herbert H. Hill, Jr. will receive the second Keene P. Dimick Award at the 40th Pittsburgh Conference. This Award is administered by the Society for Analytical Chemists of Pittsburgh and sponsored by Keene P. Dimick. Professor Herbert H. Hill was born in Helena, AR, U.S.A. on November 25, 1945. He received a B.S. degree in chemistry from Rhodes College, Memphis, TN, U.S.A. in 1970. He received a M.S. degree in biochemistry at the University of Missouri, Columbia, MO, U.S.A. in 1973 and a Ph.D. in chemistry from Dalhousie University, Halifax, Canada in 1975. At Dalhousie University he was awarded the Izaak Walton Killam Memorial Scholarship for Advanced Study. He performed postdoctoral research from 1975 to 1976 at the University of Waterloo under the direction of Professor F.W. Karasek. He joined the chemistry department at Washington State University, Pullman, WA, U.S.A. in 1976 where he is now Professor. In addition, from 1982 to the present, he has held a joint appointment in the Program of Pharmacology and Toxicology. During 1983–1984 he spent a year as guest professor of chemistry at Kyoto University, Kyoto, Japan. He has also served as Director of the Office of Research and Development at Washington State University from 1985–1987.

Professor Hill's research has been focused in the area of trace organic analysis of environmental and biomedical samples using chromatography. His work involves ambient pressure ionization detection methods for capillary gas chromatography, supercritical-fluid chromatography and high-performance liquid chromatographic detection. His work has involved fundamental and practical research in flame ionization, photo-ionization, chemical ionization, corona ionization and radioactive ionization as detection processes after chromatography. His recent work involves investigating the potential of ion mobility spectrometry for the detection of high-molecular-weight compounds after supercritical-fluid and liquid separation processes. Professor Hill has published over 70 papers in the area of chromatography and chromatographic detection methods.

1989 PITTSBURGH CONFERENCE MEMORIAL NATIONAL COLLEGE GRANTS AWARD PROGRAM

The Pittsburgh Conference on Analytical Chemistry and Applied Spectroscopy, Inc., and its co-sponsoring technical societies, the Spectroscopy Society of Pittsburgh (SSP) and The Society for Analytical Chemists of Pittsburgh (SACP), announce the 16th year of funding of the Pittsburgh Conference Memorial National College Grants Award Program.

Awards are made to small colleges for the purchase of scientific equipment, audio-visual or other teaching aids, and/or library materials for use in the teaching of science at the undergraduate level. Based on submitted proposals, at least ten colleges will be selected to receive awards (U.S.$ 3000.00 maximum).

To be eligible for an award, schools must meet the following criteria:

(1) Enrollment must not exceed 2500 students.
(2) No more than 25% of operating budgets may come from national or state governments. Two-year community colleges sponsored by political subdivisions of a state are not bound by criteria 1 and 2.
(3) Requests for materials to be used only for research purposes shall not be funded.
(4) Awards may be used as a part of a "Matching Grant" program for undergraduate studies as described above. Generating "Matching Funds" is recommended.
(5) Previous awardee schools are not eligible for an award for a three-year period following receiving a PCMNCG award (example, the 1986, 1987, and 1988 awardee schools are not eligible for the 1989 program).

Interested faculty members are urged to participate by completing an application form and submitting it along with a proposal (original and three copies of each), by March 1, 1989 to John A. Queiser, The Pittsburgh Conference, Inc., 12 Federal Drive, Pittsburgh, PA 15235, U.S.A.

Announcement of the award-winning schools will be made by May 1, 1989. These schools will join the list of 91 previous award-winners who have participated in the program since its inception in 1974.

For application/proposal forms write to Pittsburgh Conference at address above.

ANNOUNCEMENTS OF MEETINGS

9th INTERNATIONAL SYMPOSIUM ON HIGH-PERFORMANCE LIQUID CHROMATOGRAPHY OF PROTEINS, PEPTIDES AND POLYNUCLEOTIDES, PHILADELPHIA, PA, U.S.A., NOVEMBER 6–8, 1989.

The 9th ISPPP will be held at the Wyndham Franklin Plaza Hotel in Philadelphia, PA, U.S.A., November 6–8, 1989.

The three-day programme will include both oral and poster presentations organized into different sessions. Recognized authorities will review current trends and future perspectives in various topics, including: electrokinetic separations; column technology and support materials; protein conformation and chromatographic behaviour; polypeptide structural studies; protein purity and QC of recom-

binant proteins; polynucleotides; polysaccharides; membrane proteins; affinity chromatography; analytical applications; sample preparation; preparative chromatography of biopolymers; high-resolution electrophoresis; integrated purification systems; biospecific detectors; process monitoring; recovery of recombinant proteins. The scientific committee welcomes suggestions for additional topics to be covered.

Abstracts (one original and five copies) describing original research in any of the above or related areas, should be mailed to the secretariat. The deadline for submission is June 15, 1989. It is anticipated that complete manuscripts submitted at the time of the symposium will, subject to normal review procedures, be published in a complete, collected proceedings volume of the *Journal of Chromatography*.

The advance registration fee will be US$ 350 which covers all scientific and social events. Students will be eligible for a reduced rate of US$ 250 (a copy of the proceedings is not included).

Abstract forms, registration information and full details of the symposium can be obtained by contacting the Secretariat: Barr Enterprises, P.O. Box 279, Walkersville, MD 21793, U.S.A. Tel.: 301-898-3772; telefax: 301-898-5596.

2nd INTERNATIONAL SYMPOSIUM ON MICROCOLUMN SEPARATION METHODS, BADEN-BADEN, F.R.G., NOVEMBER 8–10, 1989

The 2nd International Symposium on Microcolumn Separation Methods will be held in the Congress Centre of Baden-Baden, F.R.G., November 8–10, 1989. A first event in this direction has been organized with the conference on microcolumn separation methods held in Bloomington, IN, U.S.A., October 10–11, 1988. The symposium now planned continues the tradition started in 1984.

Words such as "microbore", "miniaturization", "high speed", "low dispersion", have turned up already many years ago reflecting a trend in reduction of volumes of components in chromatographic systems. Not only in gas chromatography but also in liquid phase separation techniques this trend has become quite significant which prompted us already in January 1984 in Amsterdam to stage a Workshop emphasizing miniaturization in liquid chromatography. In the meantime these developments have become sufficiently important to urge the formation of a forum for information exchange in microcolumn separation techniques with emphasis on liquid chromatography, supercritical-fluid chromatography, electrophoresis and hyphenated techniques in the microcolumn separation field.

New columns, instrumentations, applications will be featured via lectures and posters and international leaders in the field will be invited to participate in the scientific programme. The symposium proceedings are planned for publication in a special issue of *Journal of Chromatography*. The scientific committee consists of: R.W. Frei (Amsterdam, The Netherlands), K. Jinno (Japan), J.W. Jorgenson (U.S.A.), M.L. Lee (Brigham Young University, U.S.A.), M.V. Novotny (Indiana University, U.S.A.), D. Westerlund (Uppsala, Sweden), and F. Yang (Salt Lake City, U.S.A.).

An exhibition of instruments and literature is planned.

Two days prior to the symposium (November 6–7, 1989) a short course will be held in the Congress Centre.

For further details contact: Workshop Office IAEAC, Ms. M. Frei-Hausler, Postfach 46, CH-4123 Allschwil, Switzerland.

PUBLICATION SCHEDULE FOR 1989

Journal of Chromatography and Journal of Chromatography, Biomedical Applications

MONTH	J	F	M	
Journal of Chromatography	461 462 463/1	463/2 464/1	The publication schedule for further issues will be published later	
Bibliography Section		486/1		
Biomedical Applications	487/1	487/2	488/1 488/2	

INFORMATION FOR AUTHORS

(Detailed *Instructions to Authors* were published in Vol. 445, pp. 453–456. A free reprint can be obtained by application to the publisher, Elsevier Science Publishers B.V., P.O. Box 330, 1000 AH Amsterdam, The Netherlands.)

Types of Contributions. The following types of papers are published in the *Journal of Chromatography* and the section on *Biomedical Applications:* Regular research papers (Full-length papers), Notes, Review articles and Letters to the Editor. Notes are usually descriptions of short investigations and reflect the same quality of research as Full-length papers, but should preferably not exceed six printed pages. Letters to the Editor can comment on (parts of) previously published articles, or they can report minor technical improvements of previously published procedures; they should preferably not exceed two printed pages. For review articles, see inside front cover under Submission of Papers.

Submission. Every paper must be accompanied by a letter from the senior author, stating that he is submitting the paper for publication in the *Journal of Chromatography*. Please do not send a letter signed by the director of the institute or the professor unless he is one of the authors.

Manuscripts. Manuscripts should be typed in double spacing on consecutively numbered pages of uniform size. The manuscript should be preceded by a sheet of manuscript paper carrying the title of the paper and the name and full postal address of the person to whom the proofs are to be sent. Authors of papers in French or German are requested to supply an English translation of the title of the paper. As a rule, papers should be divided into sections, headed by a caption (*e.g.*, Summary, Introduction, Experimental, Results, Discussion, etc.). All illustrations, photographs, tables, etc., should be on separate sheets.

Introduction. Every paper must have a concise introduction mentioning what has been done before on the topic described, and stating clearly what is new in the paper now submitted.

Summary. Full-length papers and Review articles should have a summary of 50–100 words which clearly and briefly indicates what is new, different and significant. In the case of French or German articles an additional summary in English, headed by an English translation of the title, should also be provided. (Notes and Letters to the Editor are published without a summary.)

Illustrations. The figures should be submitted in a form suitable for reproduction, drawn in Indian ink on drawing or tracing paper. Each illustration should have a legend, all the *legends* being typed (with double spacing) together on a *separate sheet*. If structures are given in the text, the original drawings should be supplied. Coloured illustrations are reproduced at the author's expense, the cost being determined by the number of pages and by the number of colours needed. The written permission of the author and publisher must be obtained for the use of any figure already published. Its source must be indicated in the legend.

References. References should be numbered in the order in which they are cited in the text, and listed in numerical sequence on a separate sheet at the end of the article. Please check a recent issue for the layout of the reference list. Abbreviations for the titles of journals should follow the system used by *Chemical Abstracts*. Articles not yet published should be given as "in press" (journal should be specified), "submitted for publication" (journal should be specified), "in preparation" or "personal communication".

Dispatch. Before sending the manuscript to the Editor please check that the envelope contains three copies of the paper complete with references, legends and figures. One of the sets of figures must be the originals suitable for direct reproduction. Please also ensure that permission to publish has been obtained from your institute.

Proofs. One set of proofs will be sent to the author to be carefully checked for printer's errors. Corrections must be restricted to instances in which the proof is at variance with the manuscript. "Extra corrections" will be inserted at the author's expense.

Reprints. Fifty reprints of Full-length papers, Notes and Letters to the Editor will be supplied free of charge. Additional reprints can be ordered by the authors. An order form containing price quotations will be sent to the authors together with the proofs of their article.

Advertisements. Advertisement rates are available from the publisher on request. The Editors of the journal accept no responsibility for the contents of the advertisements.